THE ACKLEY HIGH-SILICA MAGMATIC/ METALLOGENIC SYSTEM AND ASSOCIATED POST-TECTONIC GRANITES, SOUTHEAST NEWFOUNDLAND

C. JOHN TUACH

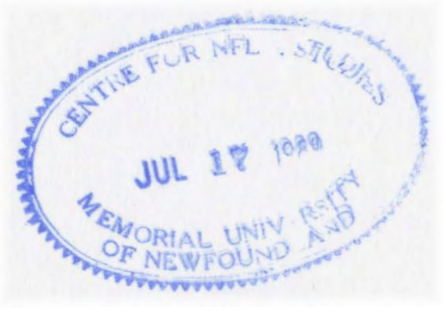
CENTRE FOR NFL. STUDIES
JUL 17 1980
MEMORIAL UNIV ERSITY
OF NEWFOUND AND

NOTICE

The quality of this microform is heavily dependent upon the quality of the original thesis submitted for microfilming. Every effort has been made to ensure the highest quality of reproduction possible.

If pages are missing, contact the university which granted the degree.

Some pages may have indistinct print especially if the original pages were typed with a poor typewriter ribbon or if the university sent us an inferior photocopy.

Previously copyrighted materials (journal articles, published tests, etc.) are not filmed.

Reproduction in full or in part of this microform is governed by the Canadian Copyright Act, R.S.C. 1970, c. C-30.

AVIS

La qualité de cette microforme dépend grandement de la qualité de la thèse soumise au microfilmage. Nous avons tout fait pour assurer une qualité supérieure de reproduction.

S'il manque des pages, veuillez communiquer avec l'université qui a conféré le grade.

La qualité d'impression de certaines pages peut laisser à désirer, surtout si les pages originales ont été dactylographiées à l'aide d'un ruban usé ou si l'université nous a fait parvenir une photocopie de qualité inférieure.

Les documents qui font déjà l'objet d'un droit d'auteur (articles de revue, tests publiés, etc.) ne sont pas microfilmés.

La reproduction, même partielle, de cette microforme est soumise à la Loi canadienne sur le droit d'auteur, SRC 1970, c. C-30.

THE ACKLEY HIGH-SILICA MAGMATIC/METALLOGENIC SYSTEM AND ASSOCIATED POST-TECTONIC GRANITES, SOUTHEAST NEWFOUNDLAND.

by

C John Tuach, B.Sc, M.Sc.

A thesis submitted to the School of Graduate Studies in partial fulfillment of the requirements for the degree of Doctor of Philosophy

Department of Earth Sciences
Memorial University of Newfoundland
January 1987

St. John's
Newfoundland

ISBN 0-315-43354-X

COLOUR PHOTOGRAPHS SHOULD NOT BE USED. THEY WILL APPEAR AS GREY OR BLACK. WE RECOMMEND THAT THE COPY OF THE THESIS SUBMITTED FOR MICROFILMING INCLUDE BLACK AND WHITE PHOTOGRAPHS REPRINTED FROM THE COLOUR PHOTOGRAPHS BY A PHOTOGRAPHER IF NECESSARY.

LORSQUE MICROFILMEES, LES PHOTOGRAPHIES EN COULEUR PARAISSENT GRISES OU NOIRES. NOUS RECOMMANDONS QUE L'EXEMPLAIRE DE LA THESE A MICROFILMER SOIT ACCOMPAGNE PLUTOT DE PHOTOGRAPHIES EN NOIR ET BLANC PRODUITES A PARTIR DES PHOTOGRAPHIES EN COULEURS PAR UN PHOTOGRAPHE, SI NECESSAIRE.

FRONTISPIECE

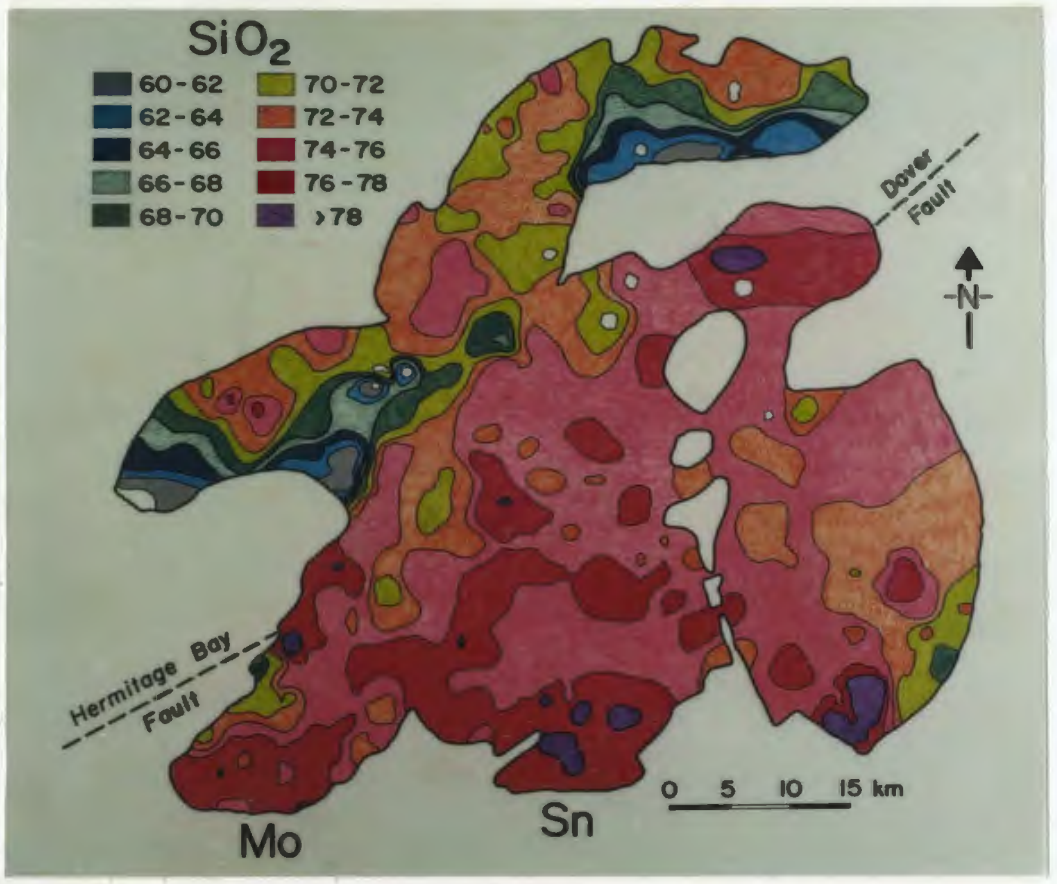

SiO_2 distribution in post-tectonic granite.

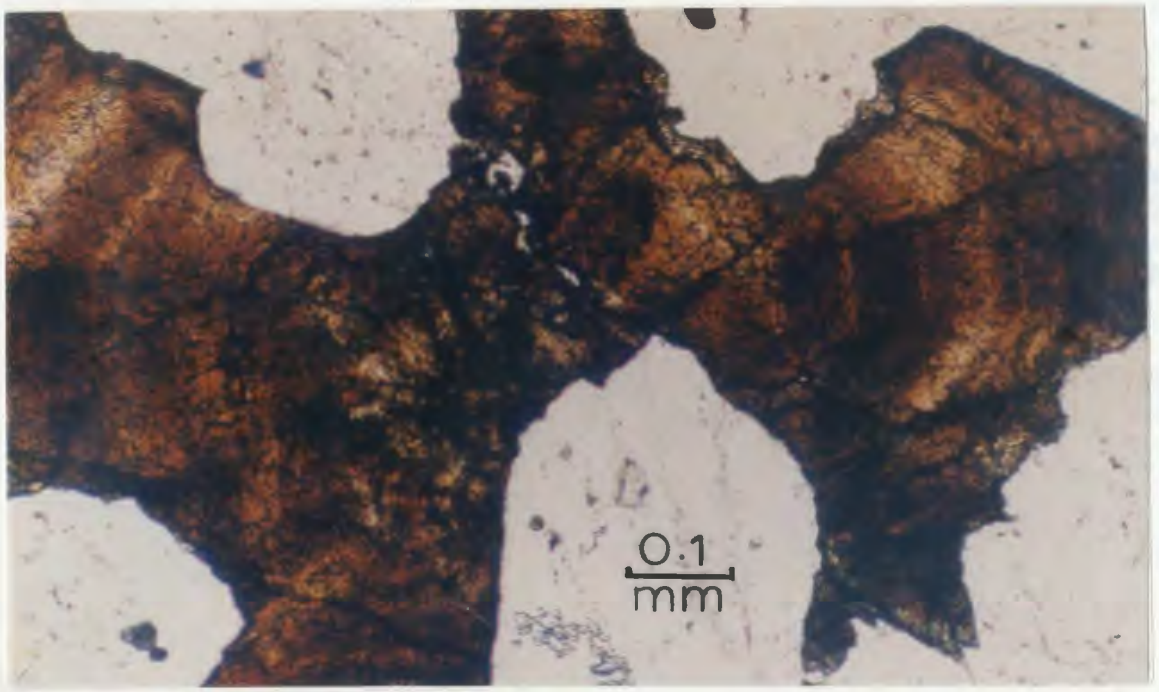

Zoned cassiterite from the Esso Prospect.

ABSTRACT

The Ackley Granite Suite occupies 2,415 km^2 in southeastern Newfoundland, and intruded across the boundary between the Avalon and Gander tectonostratigraphic terranes. An Rb-Sr whole rock age of 355 ± 9 Ma is younger than $^{40}Ar/^{39}Ar$ ages around 370 ± 5 Ma. Two calc-alkaline granodiorite-granite plutons to the west and northeast of the Ackley Granite Suite provided an Rb-Sr whole rock age of 427 ± 12 Ma, in agreement with an $^{40}Ar/^{39}Ar$ biotite age of 410 ± 4 Ma.

Much of the Ackley Granite Suite exhibits geochemical signatures of A-type granites, and a muscovite-bearing phase occurs in the north. Geochemical enrichment/depletion trends culminate at significant, endocontact, spatially separate, aplite-pegmatite Mo deposits at Recontre Lake, and quartz-topaz-Sn greisen deposits at Sage Pond. Hydrothermal muscovites from the deposits provide almost identical $^{40}Ar/^{39}Ar$ ages, indistinguishable from $^{40}Ar/^{39}Ar$ ages of biotite in granites. The granites and the mineralized areas have high-temperature, magmatic, oxygen isotope signatures, with minor evidence for high-temperature meteoric hydrothermal activity at the prospects, and evidence for low temperature subsolidus exchange with meteoric fluids through much of the Ackley Granite Suite. The data confirm previous interpretations that large areas of the Ackley Granite Suite were rapidly cooled, and together with fluid inclusion data, provide evidence for the contemporaneity of magmatic and mineralizing processes.

The southern Ackley Granite Suite is the frozen equivalent of high-silica, chemically zoned, magma chambers responsible for the formation of large ash flows. Convective fractionation may have operated to produce the observed chemical zonations. An emplacement model based on available geophysical data indicates stoping of large (20 km x 10 km) blocks from the upper to middle crust in response to regional crustal extension and lower crustal melting.

The H_2O content and the degree of trace element enrichment in the magma appear to have been important controls on mineralization. The Mo deposits formed from fluids evolved from a relatively H_2O-rich magma while Sn mineralization formed from F-rich fluids evolved from a more specialized, relatively anhydrous magma. A genetic trend from Mo-mineralization to Sn-mineralization during development of the high-silica upper magma layer is suggested.

Keywords: Ackley Granite Suite, granite, high-silica, post-tectonic, tin, molybdenum, chemical zonation, metallogenesis, isotopes, geochemistry, pluton emplacement.

ACKNOWLEDGEMENTS

The opportunity to perform this study was only possible through wholehearted support and encouragement from my wife Ruth. I am extremely fortunate to have such a marvelous and understanding companion.

I am indebted to Dave Strong for friendship and advice over the past years, and for supervision of this work.

The rock collection and geochemical data base from the study area which was established by Dr. Lawson Dickson (Newfoundland Department of Mines and Energy) provided the essential foundation for this work, and Lawson's encouragement and assistance are gratefully acknowledged. Lawson suggested many improvements to this manuscript.

The staff of the Mineral Development Division at the Newfoundland Department of Mines and Energy are thanked for their support. Paul Dean initiated the logistical support for this project, and provided continuing discussion and interest. Peter Davenport showed exemplary patience while providing a great deal of advice and assistance on data analysis. The professional and technical staff at the Mines Branch provided assistance, encouragement, and advice from time to time, and their collective help is acknowledged.

Drs. H. Longerich and B.J. Fryer, and Patricia Finn are thanked for assistance with analyses at Memorial University, and Drs. Fryer, G. Jenner and J. Welhan are thanked for reviews and discussion. D.F.G. Taylor provided field assistance to the author during the 1984 field season.

Dr. R. Kerrich of the University of Western Ontario provided oxygen isotope analyses, Dr. D. Kontak performed $^{40}Ar/^{39}Ar$ analyses at Queen's University, and Dr. R.P. Taylor performed neutron attivation analyses for rare earth elements at Université de Montreal. All are thanked for their support and interest in this project.

Funding for the period April 1983 to April 1984 was obtained through contract 83-00036 with the Geological Survey of Canada, under the Canada-Newfoundland Mineral Agreement, 1982-1984.

Additional support was obtained from a Memorial University fellowship, and from NSERC operating grant No. A7975 to Dave Strong.

Last but not least, I have benefited from my association with the "mature" graduate school at Memorial University :- Jack Botsford, Scott Swinden, Tom Lane, and Scott Schillereff are cited for their social efforts.

TABLE OF CONTENTS

CHAPTER 6

RARE EARTH ELEMENT CHEMISTRY

CHAPTER 9

FLUID INCLUSION STUDIES

CHAPTER 10

THE ACKLEY MAGMATIC/METALLOGENIC SYSTEM

LIST OF TABLES

LIST OF FIGURES

LIST OF PLATES

CHAPTER 1 - INTRODUCTION

1-1 BACKGROUND

The study of granitoid rocks provides information on crustal and magmatic processes (e.g. Chappell and White, 1974; Hildreth, 1979, 1981) and on associated "granophile" mineral deposits (e.g. Strong, 1980, 1981). Metallogenic and petrogenetic investigations have tended to be independent but are now beginning to converge, and many investigators consider magma generation, magma evolution and ore generation as a continuum of processes.

Major outstanding problems of granitoid mineralization as expressed at an international conference on granite-related mineral deposits (Taylor and Strong, 1985) were identified as follows; (1) what are the parent granites like; (2) what are the ore deposits like; and (3) how can the observed variabilty be explained? Current controversy centers around magma source-materials, magma generation and fractionation processes, temporal and genetic relationships of ores to associated granites and late magmatic to magmatic-hydrothermal processes.

Granitoid plutons associated with tin mineralization, "specialized" granites of Tischendorf (1977), are commonly high in silica ($>72\%$ SiO_2) and the large-ion lithophile (LIL) elements, and low in Ba and Sr (e.g. Tischendorf, 1977; Lenthall and Hunter, 1977; Olade, 1980; Hudson and Arth, 1983; Chatterjee et al., 1983). Comparable geochemical signatures have been documented for granite-molybdenum systems, especially of the

Climax-type (Mutschler et al., 1981; Westra and Keith, 1981; White et al., 1981) and several of these authors have commented on the similarities between tin-bearing and molybdenum-bearing granite systems.

Most studies of granophile ore generation have concentrated on small areas surrounding or defined by mines and prospects. Reasons for this localization are: (a) many deposits are associated with small granite cupolas which are apparently spatially, geologically or geochemically distinct from associated large batholiths; and (b) logistical problems and financial restrictions commonly prevent large, systematic, integrated programmes of study on major magmatic systems associated with mineralization.

Hildreth (1981) and Mutschler et al. (1981) emphasized the need for extensive evaluation of granitoid systems. This must involve the collection of a large and representative data set for each pluton of interest, an exercise which has seldom been undertaken, even for batholiths associated with the exceptionally productive Climax-type deposits in Colorado.

The study area in southeast Newfoundland (Fig. 1) is predominantly composed of post-tectonic, high-level, high-silica, Devonian granitoid rocks (Strong et al., 1974; Whalen, 1976; Dickson, 1983). Spatially separated aplite-pegmatite molybdenite deposits and cassiterite-wolframite-bearing quartz-topaz greisen deposits occur in granite along the southern contact of the study area, and extensive geochemical enrichment/depletion patterns culminate in areas of known mineralization

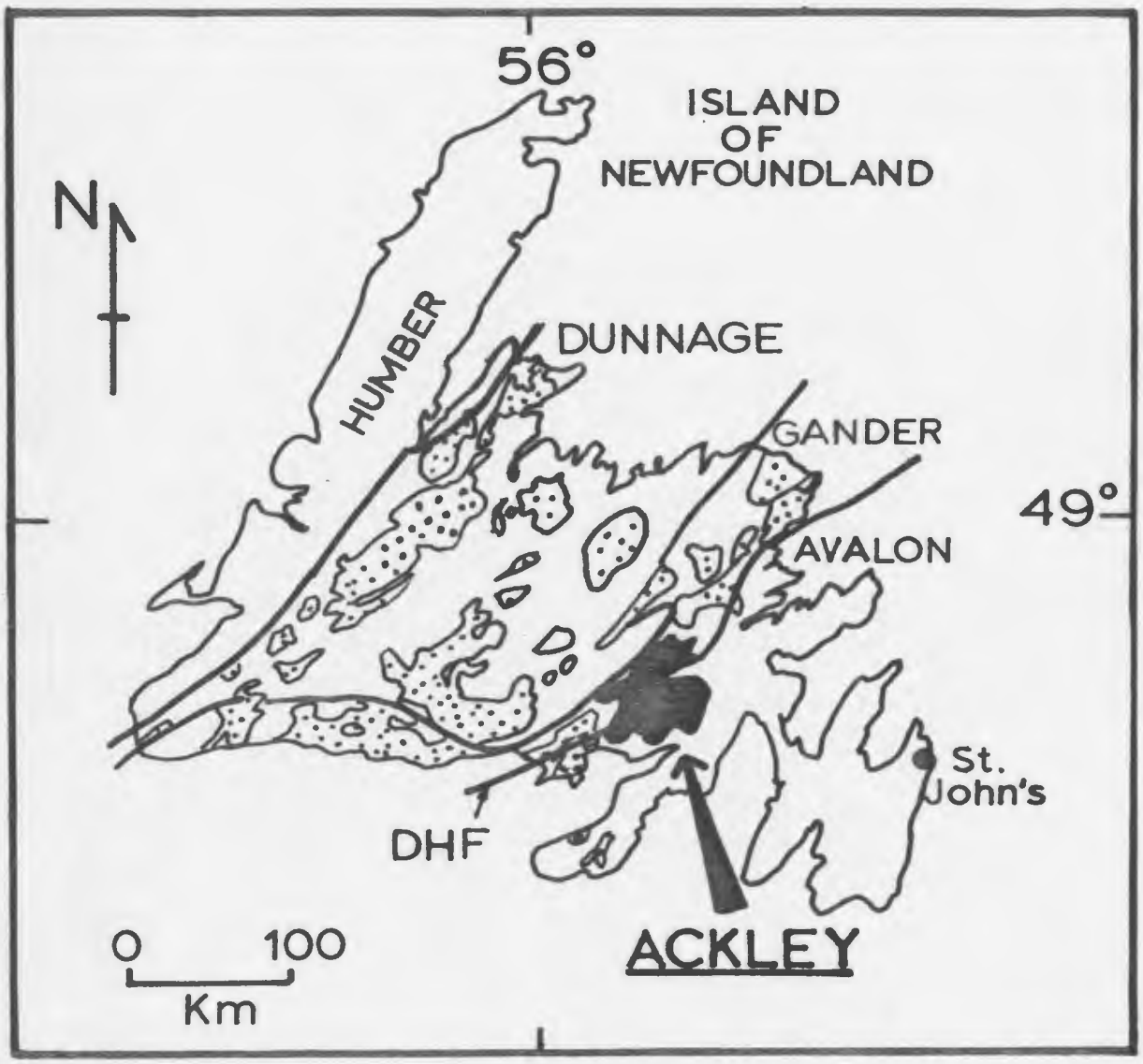

Figure 1: Location of the study area (shaded) with respect to other Paleozoic granitoid plutons in Newfoundland (dotted). Also shown are major terranes and their boundaries (Williams and Hatcher, 1983). DHF - Dover-Hermitage Bay Fault zone.

(Davenport et al., 1984). The granites in the southeastern part of the study area have been interpreted to represent a solidified, high-silica, chemically zoned magma chamber (Tuach et al., 1986). These rocks intruded across a major tectonostratigraphic boundary between the predominantly Precambrian metavolcanic Avalon Terrane and the predominantly Lower Paleozoic metasedimentary Gander Terrane of the Newfoundland Appalachians (Williams and Hatcher, 1983).

The area provides a unique opportunity to investigate: (1) the relationship of the separate types of mineralization to the host granites, (2) the potential influence of source rock on magma composition and ore formation, (3) the nature and extent of magmatic processes associated with mineralization, and (4) the nature of the fluids involved in ore formation and in sub-solidus recrystallization. The study was facilitated by the large library of rock samples, powders, thin sections and geochemical analyses, maintained by the Newfoundland Department of Mines and Energy.

1-2 OBJECTIVE

The objective of this work was to investigate the nature and extent of the magmatic/metallogenic system(s) responsible for formation of mineral deposits in the southern part of the study area, using a combination of petrological, geochemical, isotopic and fluid inclusion studies. Problems of particular interest are: (1) definition of the magmatic systems in the study area, (2) the influence of potential source compositions on the chemical patterns preserved in the granites,

(3) the nature and extent of the fluid phase and its relationship to mineralization, and (4) definition of the controls over tin-tungsten and molybdenum mineralization in high-silica granitic systems.

1-3 THESIS PRESENTATION

Following the introductory chapter, a review of mineral deposits and metallogenic concepts associated with granite is presented in Chapter 2. This review is necessary since there is considerable overlap and confusion in terminology, particularly between different geographic areas of the world. Furthermore, it outlines the concepts and alternative hypotheses that are discussed in Chapters 10 and 11.

The results of specific techniques of investigation are presented in Chapters 3 to 9, and direct conclusions from the data are presented and discussed in the relevant Chapter. The results and conclusions of the various investigations are integrated and discussed in Chapter 10, where an attempt is made to define the magmatic/metallogenic systems in the study area. The final Chapter discusses the significance of the data and conclusions from the study area, with respect to magmatic and metallogenic systems in general.

Nomenclature, analytical techniques, analytical precision and accuracy, results of microprobe analyses, whole rock geochemical analyses, tables of correlation coefficients and fluid inclusion data are presented in Appendices. Small data tables are included in the relevant Chapters.

1-4 NOMENCLATURE OF GRANITOID ROCKS IN THE STUDY AREA

The post-tectonic granitoid rocks which are the subject of this thesis have been commonly referred to as Ackley Batholith, Ackley City Batholith, Ackley Granite and Ackley City Granite. Petrological, geochemical, geochronological, and geophysical work, performed as part of this study, require revision of unnamed subdivisions (units 9 to 15) proposed by Dickson (1983) for these rocks, and a formal nomenclature system will facilitate description in this thesis.

The proposed nomenclature is presented in Figure 2 and is summarized in Table 1. A review of previously used names and formal proposals for abandoning some names, for boundary revision, for rank elevation, and for new names, are presented in Appendix A.

Introduction of new names at the beginning of the thesis, as opposed to performing the required changes in mid-thesis where the supporting data are presented, is a practical procedure which allows continuity of description. Nevertheless, references will be made to the lithological subdivisions of Dickson (1983) in Chapters 3 to 8. These references are necessary to illustrate the discrepancies between the new information and the former subdivisions and to substantiate the local redefinition of boundaries.

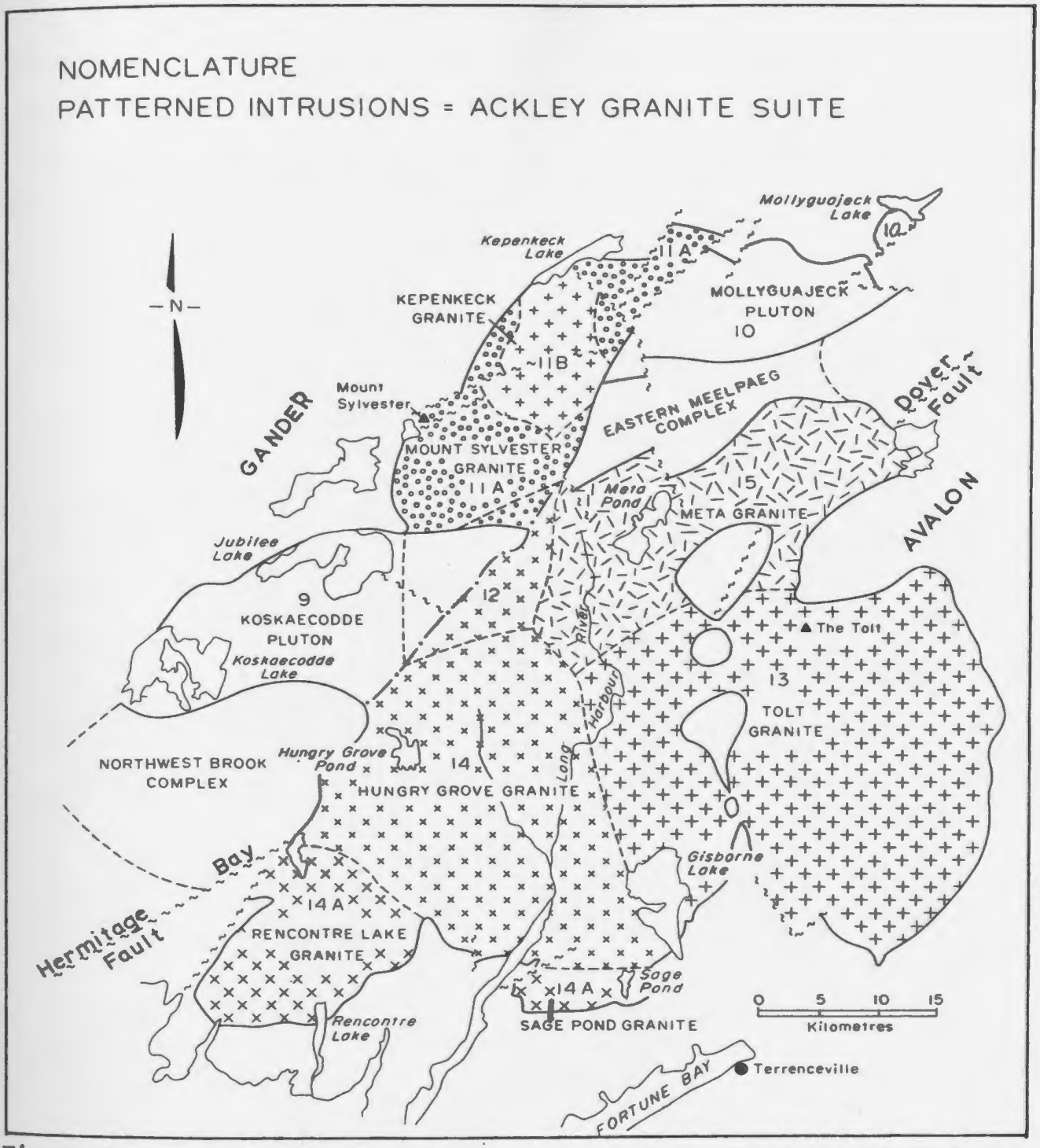

Figure 2: Nomenclature in the study area. Units of Dickson (1983) are shown by numbers and are bounded by dashed lines. The position of the Dover-Hermitage Bay Fault which separates the Gander and Avalon tectonostratigraphic terranes is shown. Significant molybdenum and tin prospects along the southern margin of the granites are located at Rencontre Lake and Sage Pond, respectively.

Table 1: Area and general description of intrusive rocks

ACKLEY GRANITE SUITE (biotite-bearing)	UNIT (Dickson, 1983)	GENERAL DESCRIPTION	AREA (sq.km.)
Mount Sylvester Granite	11 + 12	Massive, equigranular, coarse grained.	= 220
Kepenkeck Granite	11A	As above, with muscovite.	= 85
Tolt Granite	13	Massive, porphyritic, coarse grained.	= 880
Hungry Grove Granite	14 + 12	Massive, equigranular, coarse grained.	= 635
Rencontre Lake Granite	14A	Fine to medium grained, miarolitic.	= 190
Sage Pond Granite	14A	As above.	= 30
Meta Granite	15	Undivided, coarse grained, massive.	= 375
Total area of Ackley Granite Suite			=2,415
OTHER			
Koskaecodde (Granodiorite - Granite) Pluton	9 + 12	Massive porphyritic medium to coarse-grained, biotite and hornblende granodiorite.	= 290
Mollyguajeck (Granodiorite - Granite) Pluton	10	Massive equigranular, coarse grained.	= 160
Area of Intrusive Rocks Studied			=2,865

Geographic References:

Northwest = Koskaecodde + Mollyguajeck + Mount Sylvester.
Southeast = Hungry Grove, + Tolt + Meta + Rencontre Lake + Sage Pond.
Eastern = Meta + Tolt.

1-5 PREVIOUS WORK

Detailed summaries of previous work in and around the Ackley Granite Suite are presented by Whalen (1976), Dickson (1983) and by O'Brien et al. (1984). Results of geological mapping have been reported by Bradley (1962), Jenness (1963), Anderson (1965), O'Driscoll and Hussey (1978), Anderson and Williams (1971), Williams (1971), O'Brien et al. (1980a,b), Swinden and Dickson (1981), Dickson (1980, 1982, 1983) and O'Brien et al. (1984).

Geochemical analyses from the Ackley Granite Suite were included in a reconnaisance report by Strong et al. (1974). Dickson (1983) presented results of a regional mapping, petrographic and geochemical survey over the study area which was undertaken on a 4 km^2 grid. A total of 357 stations were sampled and 482 samples including station duplicates and analytical splits were analysed for 11 major and 21 trace elements. Field and analytical data listings and CIPW norms of these samples were included in reports by Colman-Sadd et al. (1981) and Dickson (1983).

Aplite-pegmatite molybdenum mineralization has long been known in the Rencontre Lake area (White, 1939, 1940; Fig. 2). The geology, geochemistry and exploration history of these deposits were recently described in detail by Whalen (1976, 1980, 1983), Dickson and Howse (1982) and Dickson (1983).

Cassiterite-bearing quartz-topaz greisen veins were identified in the Sage Pond area (Fig. 2) by Esso Minerals Limited (O'Sullivan, 1982,

1983) and by the Newfoundland Department of Mines and Energy (Dickson, 1982; Dickson and Howse, 1982). Additional descriptions of these veins were provided by Tuach (1984a,b,c) and the local presence of tungsten mineralization was noted by Tuach (1984c).

Recent mineral exploration projects in the Ackley Granite Suite have resulted from the release of geochemical data obtained in government-sponsored lake sediment surveys (Butler and Davenport, 1979a,b) and have concentrated on the molybdenum or tin potential (Saunders, 1980; McKenzie, 1980; Burns, 1981, 1982; O'Sullivan, 1982, 1983). Geochemical studies of surficial deposits have been reported by McConnell (1984).

Gravity surveys were performed by Weaver (1967) and by Miller (1986a; Fig. 3). These indicate that much of the Ackley Granite Suite is steep sided, with the largest Bouguer anomalies occurring in a north-south trend through the east part of the Ackley Granite Suite.

Whalen (1983) noted similarities between geochemical patterns in a 10 km^2 portion of the Rencontre Lake Granite in the Rencontre Lake area and geochemical trends defined by Hildreth (1979, 1981) in the Bishop Tuff. He suggested that either crystal-liquid or liquid state magmatic fractionation models can account for the observed geochemical patterns in his study area. Results of recent geochronological studies have been published by Bell et al. (1977) and by Dallmeyer et al. (1983) and these gave ages of 355 ± 10 Ma.

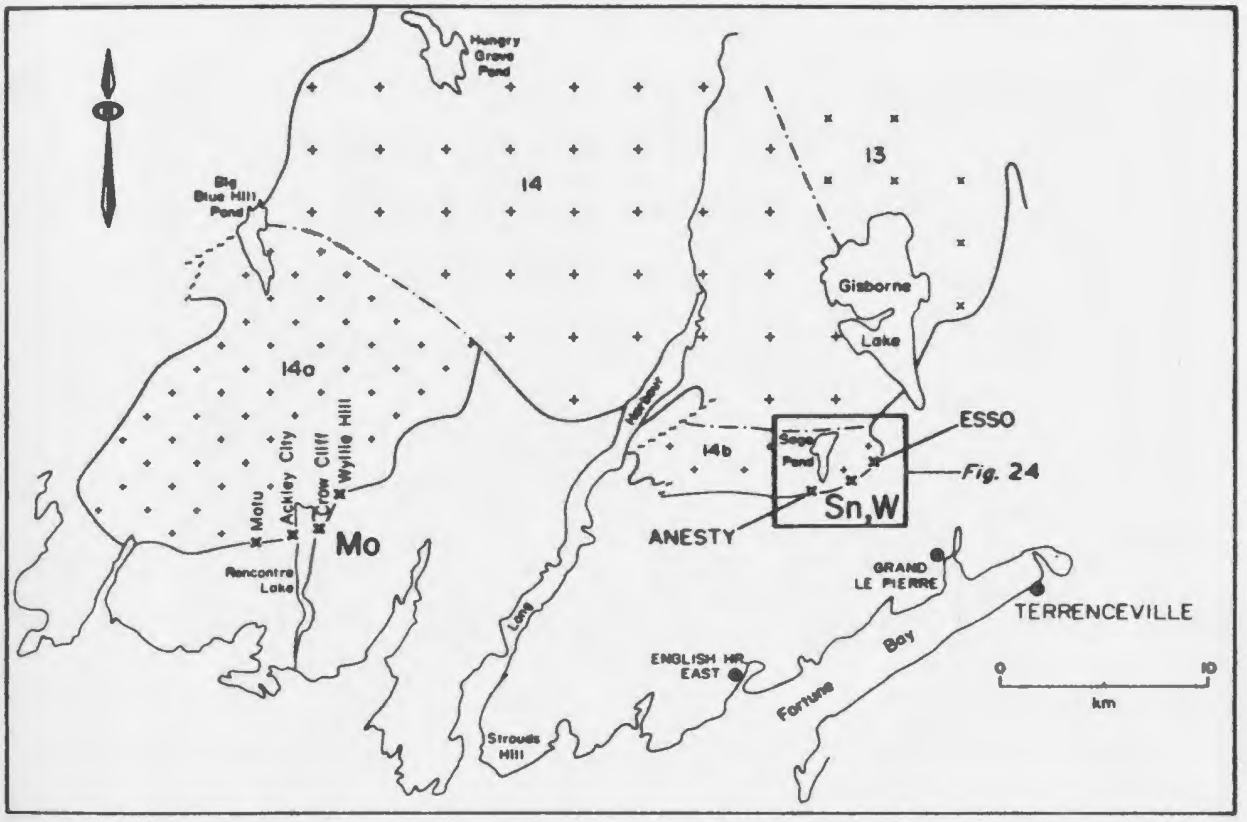

Figure 4: Geological map of the southern portion of the study area. The names and locations of the significant mineral prospects are shown. An area of more detailed study is outlined. 13 - Tolt Granite; 14 - Hungry Grove Granite; 14A - Rencontre Lake Granite; 14B - Sage Pond Granite.

1-6 GEOLOGICAL SETTING OF THE ACKLEY GRANITE SUITE

The Devono-Carboniferous Ackley Granite Suite intruded across the fault zone boundary (Fig. 1) between the Avalon and Gander tectonostratigraphic terranes of the Newfoundland Appalachians (Williams and Hatcher, 1983). This boundary is known as the Dover-Hermitage Bay Fault (Blackwood and O'Driscoll, 1976) and represents a zone of sinistral strike slip movement in the middle Paleozoic (Hanmer, 1981; Blackwood, 1985). Movement on this Fault ceased after the Acadian Orogeny prior to emplacement of the Ackley Granite Suite (Blackwood and O'Driscoll, 1976; Dickson, 1983). The late Devonian-Carboniferous environment was one of continental rift-controlled basins (Williams and Hatcher, 1983).

In the Avalon Terrane, the Ackley Granite Suite intruded Late Precambrian rocks of the Long Harbour, Love Cove and Musgravetown groups (Bradley, 1962; Jenness, 1963). These are predominantly subaerial, siliciclastic, and silicic volcanic rocks with lesser volumes of basic volcanic rocks, which have been subject to low greenschist facies metamorphism. The assemblages have been correlated with Pan-African Late Precambrian sequences in North Africa (O'Brien et al. 1983). The Ackley Granite Suite also intruded Early Cambrian gabbroic rocks of the Cross Hills Plutonic Suite (Tuach, 1984a; and unpublished data) and Cambrian or older sedimentary rocks of the Youngs Cove Group (Williams, 1971). The Cross Hills Plutonic Suite may be correlated with widely dispersed Late Pan-African peralkaline activity in northern Africa and Arabia (cf. Drysdall et al. 1984),

In the Gander Terrane, the Ackley Granite Suite intruded: (1) Lower Paleozoic, predominantly marine, metasedimentary and metavolcanic rocks of the Gander and Baie d'Espoir groups which have been subject to middle greenschist to lower amphibolite facies metamorphism (McGonigal, 1973; Colman-Sadd, 1976), (2) undated, strongly foliated, granitoid plutons and unseparated, high grade metamorphosed sediments of the North West Brook and Eastern Meelpaeg complexes (Dickson, 1983), (3) unfoliated granodiorite to granite intrusions which are named the Koskaecodde and Mollyguajeck plutons in this thesis. The Lower Paleozoic sedimentary and volcanic rocks are thought to represent a clastic wedge formed at the eastern margin of the Iapetus ocean (Kennedy and McGonigal, 1972) and are part of the Appalachian Orogen. The tectonic settings of the high grade plutonic-metamorphic complexes and of the granodiorite-granite plutons have not been ascertained, although they are confined to the Gander Terrane of the Appalachian Orogen. The plutonic-metamorphic complexes may have been generated in a megashear environment related to the Dover-Hermitage Bay Fault (Strong, 1980; Hanmer, 1981).

Roof pendants in the Avalon Terrane consist of metamorphosed felsic and mafic volcanic rocks of the Love Cove and Belle Bay formations (O'Brien et al., 1984). Roof pendants in the Gander Terrane consist of rocks similar to those of the North West Brook and Eastern Meelpaeg complexes.

Metamorphic aureoles related to the Ackley Granite Suite are narrow and generally less than 500 m wide (Dickson, 1983) indicating a shallow depth of intrusion.

1-7 GEOLOGY OF THE ACKLEY GRANITE SUITE

The Ackley Granite Suite underlies an area of approximately 2415 km^2, in southeast Newfoundland (Figs. 1 and 2, Table 1). It generally lies at an elevation between 200 and 300 m, with maximum topographic relief of about 300 m exposed in coastal cliff sections in Fortune Bay.

It is a high level, cross-cutting pluton, with narrow thermal aureoles. Whole rock dating by Rb/Sr (Bell et al., 1977) and step-heating of biotite and hornblende with $^{40}Ar/^{39}Ar$ analyses (Dallmeyer et al., 1983), gave ages around 355 ± 10 Ma. The Rb/Sr age was obtained from six samples collected from the Hungry Grove, Meta, Tolt and Mount Sylvester granites. The $^{40}Ar/^{39}Ar$ analyses were performed on samples from the eastern margin of the Tolt Granite.

Geochronological data presented in Chapter 7 have confirmed the Rb-Sr isochron of 355 ± 10 Ma. However, $^{40}Ar/^{39}Ar$ ages of 370 ± 5 Ma are slightly older.

Following work by Dickson (1983), seven member granites are recognized in the Ackley Granite Suite on the basis of variations in mineralogy and texture (Fig. 2, Table 1). Geological boundaries between the granites have not been identified in the field because of poor outcrop, or the presence of gradational boundaries in areas of good exposure (Dickson, 1983). The Kepenkeck and Mount Sylvester granites consist of coarse grained, biotite-orthoclase granite and medium grained, biotite-muscovite-orthoclase granite respectively.

The Meta, Tolt, Hungry Grove, Rencontre Lake and Sage Pond granites are composed of coarse grained, equigranular to porphyritic, biotite granite. The southern portion of the Hungry Grove Granite may contain miarolitic cavities. The Rencontre Lake and Sage Pond granites contain abundant fine to medium grained, equigranular to porphyritic, biotite granite and are highly variable in texture. Giant (to 50 cm. across) quartz crystals and blebs, pegmatite patches, quartz-lined miarolitic cavities, granophyres, and gas breccias, occur throughout the hornblende-free portion of the Rencontre Lake Granite. Small quartz-lined miarolitic cavities and local gas breccias are present in the Sage Pond Granite, but pegmatite patches and giant quartz crystals are rare. Whalen (1980) and Dickson (1983) considered the fine grained marginal granites to represent the roof zone of the Ackley magma chamber.

Aplite dikes and bodies are present in all units of the Ackley Granite Suite and internal intrusive contacts are common. Geochemical variation between textural varieties in any local area is minor to absent.

Dickson (1983) described a single, thin, mafic dike in the Tolt Granite. Minor small (< 20 cm), oval-shaped, fine grained, diorite xenoliths or enclaves occur in outcrops of the Tolt Granite at and near the Burin Highway (Route 210) and can contain isolated large feldspar phenocrysts. These are the only recognized mafic plutonic phases which may be genetically related to the Ackley Granite Suite.

The author has observed abundant xenoliths and large rafts or roof pendants of semipelitic schist near the western margin of the Rencontre Lake Granite. Bradley (1962) and Dickson (1983) have mapped and described large roof pendants in the Ackley Granite Suite in the Avalon and the Gander terranes.

1-8 MINERALIZATION IN THE ACKLEY GRANITE SUITE

Known areas of significant mineralization are confined to the southern margin of the Ackley Granite Suite (Fig. 4). Elsewhere, mineralization consists of minor disseminations and blebs (predominantly molybdenite) in thin and isolated quartz veins.

Endocontact, aplite-pegmatite type deposits occur in the Rencontre Lake Granite at the contact of the fine grained margin or roof zone with Precambrian silicic volcanic rocks (Whalen 1976, 1980; Dickson and House, 1982). A maximum of 10^5 tonnes grading 0.3% MoS_2 and 10^6 tonnes grading 0.14% MoS_2 have been indicated by exploration drilling of the Ackley City and Wyllie Hill prospects respectively (McKenzie, 1981).

Cassiterite-wolframite-bearing (± sericite and/or kaolinite) greisen occurs in easterly trending, steeply dipping veins and pods within the Sage Pond Granite and as larger pods (maximum 200 * 60 m) at the granite contact in the Sage Pond area. Greisen veins are generally less than 10 * 1 m in plan view and are found at or near the granite contact for 15 km between Long Harbour and Gisborne Lake (Fig. 4). Pyrite, fluorite, rutile and hematite are accessories in the greisen and minor molybdenite is present (Dickson, 1983; Tuach, 1984a, b, c).

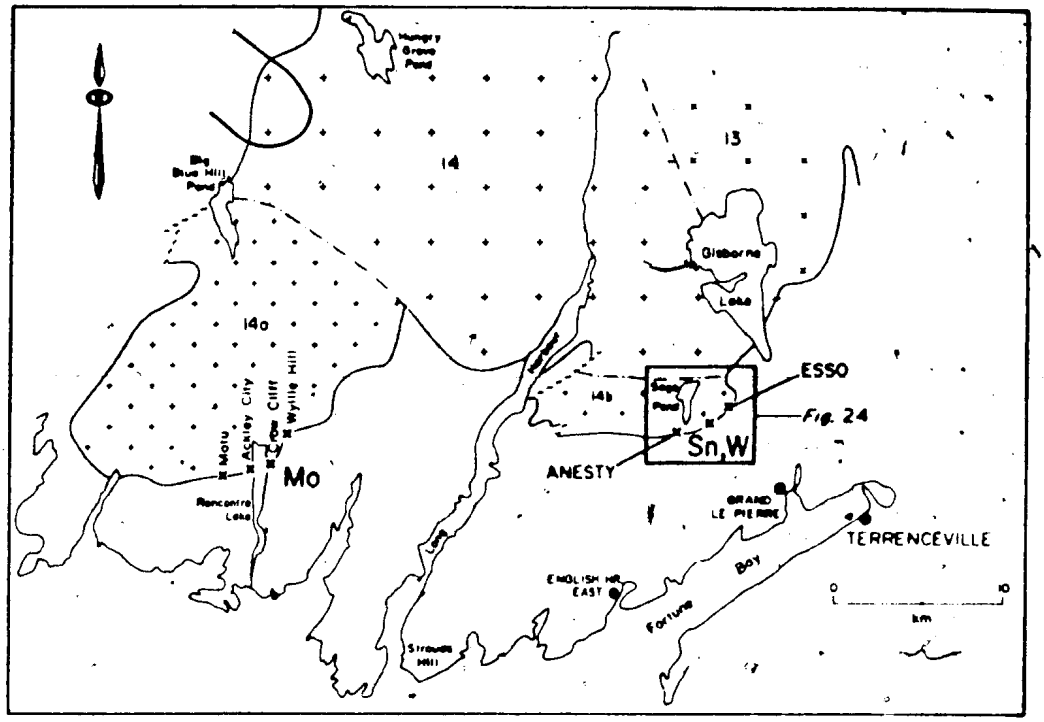

Figure 4: Geological map of the southern portion of the study area. The names and locations of the significant mineral prospects are shown. An area of more detailed study is outlined. 13 - Tolt Granite; 14 - Hungry Grove Granite; 14A - Rencontre Lake Granite; 14B - Sage Pond Granite.

CHAPTER 2 - GRANITOID ROCKS: THEIR MINERAL DEPOSITS AND ASSOCIATED METALLOGENIC CONCEPTS

2-1 INTRODUCTION

The purpose of this Chapter is to review current definitions and concepts relating to mineral deposits associated with granites. This is necessary since there is some confusion and overlap in the literature concerning deposit characteristics and definitions, and there is considerable confusion with respect to granite nomenclature. This review will form a background against which the discussion Chapters (10 and 11) will be presented.

Plutonic rocks of granitic composition occupy 40% of the continental crust. Ore deposits associated with granitic bodies contain the world's major economic reserves of Sn, W, Mo, Bi, Nb, Ta, F, Be, Li, Zr, Hf, Ti, Sb, Ga and rare-earth elements, significant portions of the world's Cu, and variously contribute to world requirements for Zn, Pb, P, Al, Rb, Th and U. Many of these elements are of vital importance and are considered by governments to be "strategic and critical minerals". In particular, increasing world demand is projected for Nb, Ta, Zr and rare-earth elements to fuel the development of the computer and space age. A major demand for new primary tin is also anticipated, as production declines from secondary placer deposits (Pollard and Taylor, 1985).

Felsic plutonic rocks are commonly classified according to relative modal content of quartz, alkali feldspar and plagioclase. Field boundaries erected by an international committee on nomenclature and presented by Streckeisen (1976; see Fig. 8), are accepted by most workers. These rocks are divided into an oversaturated (with modal or normative quartz) series of voluminous extent in the earths crust and a spatially restricted undersaturated (modal or normative feldspathoids) or alkaline series. Oversaturated rocks are further classified as calcic, calc-alkalic, alkali-calcic and alkalic on the basis of $(Na_2O+K_2O)/CaO$ ratios (Shand, 1950), and as peraluminous, metaluminous, subaluminous and peralkaline on the basis of $(Na_2O+K_2O+CaO)/Al_2O_3$ ratios (Peacock, 1931).

Granitoid rocks contain 5-60% modal quartz. Granophile mineral deposits are defined as those with 5-60% modal quartz in the host or parent pluton (Strong, 1980).

2-2 MAJOR FAMILIES OF GRANITOID MINERALIZATION

2-2-1 Introduction

There are four popular descriptions of granitoid mineralization in the literature. These are porphyry copper (± Au ± Mo), Climax-type (Mo ± Sn, ± W; also termed granite-molybdenite systems), granophile (Sn, W, Mo, Sb, Bi, ± U, ± Ta) and skarn (W, Cu, ± Zn, ± Pb) deposits. Peralkaline deposits (Be, Zr, Nb, Ta, Th, Sn, F and rare-earth elements) have recently been added by Taylor and Fryer (1983). Major deposits of Fe, Cu, Nb, Ta, Mo, P and rare-earth elements are

associated with alkaline series rocks but are excluded from this discussion. Abundant overlap is present between recognized families and competing classification and nomenclature schemes have been variously based on plate tectonics, inferred depth of formation, host rock composition, associated rock alteration, contained economic mineralization and morphology.

"Porphyry" is synonomous with "stockwork" and has genetic overtones which imply that a "fossil" hydrothermal system is present. A basic implication of porphyry is that deposits are of large tonnage and low grade. Sutherland-Brown (1976) defines porphyry as "pervasive primary mineralization, spatially distributed on fracture or veinlet stockworks, breccias, or as disseminations, that are intimately associated with felsic plutons which almost invariably display porphyritic texture to some degree. Mineralization and alteration are distributed in either intrusive or host rocks in zonal patterns related to intrusive architecture". This definition is applicable to a wide variety of important mineral deposits containing one or more of Cu, Mo, W, Sn, Au, Ag, Sb and subeconomic Pb-Zn mineralization.

2-2-2 Porphyry Copper

The economic significance of "porphyry copper" mineralization was initially recognized as a result of the application of bulk mining techniques to low grade disseminated mineralization surrounding bonanza ore shoots of Cu, Au and Ag, at Bingham, Utah, in 1906. At present, this type of deposit is estimated to contain approximately half of the world

copper reserve and significant Au, Mo and Ag production is currently achieved. Porphyry coppers are concentrated in Mesozoic and younger orogenic belts. Cordilleran (Cu, Cu-Mo) and island-arc (Cu-Au-Ag) sub-classifications primarily reflect differences between a continental and an oceanic setting (Taylor and Van Leeuvan, 1980).

These deposits consist of disseminations and fracture fillings of chalcopyrite, bornite and pyrite. They are spatially and genetically related to basic to intermediate igneous, epizonal, generally porphyritic, multiple intrusions, dyke swarms and breccias. The deposits are commonly associated with small stocks or plugs which are thought to relate to more extensive under lying calc-alkaline magma chambers, but they may also be found in large magmatic bodies (e.g. Highland Valley in the Guichon Creek Batholith; Olade, 1980). Host rocks for individual deposits can vary from pluton to country rock to co-magmatic extrusive equivalents. Alteration is widespread, exhibiting lateral zonation, ideally from a potassic core, outwards through phyllic, argillic and propylitic alteration (Figure 5). Mineralization is often concentrated at the interface between potassic and phyllic alteration (Fig. 5). Most deposits diverge from the 'ideal' patterns and massive ore bodies or veins can occur within or outside of the porphyry system. Later supergene oxidation can greatly enhance the economic potential of these deposits.

Porphyry copper systems emplaced into carbonate rocks give rise to stockwork and manto copper skarn deposits. These deposits are generally of higher grade than accompanying porphyry mineralization and exhibit

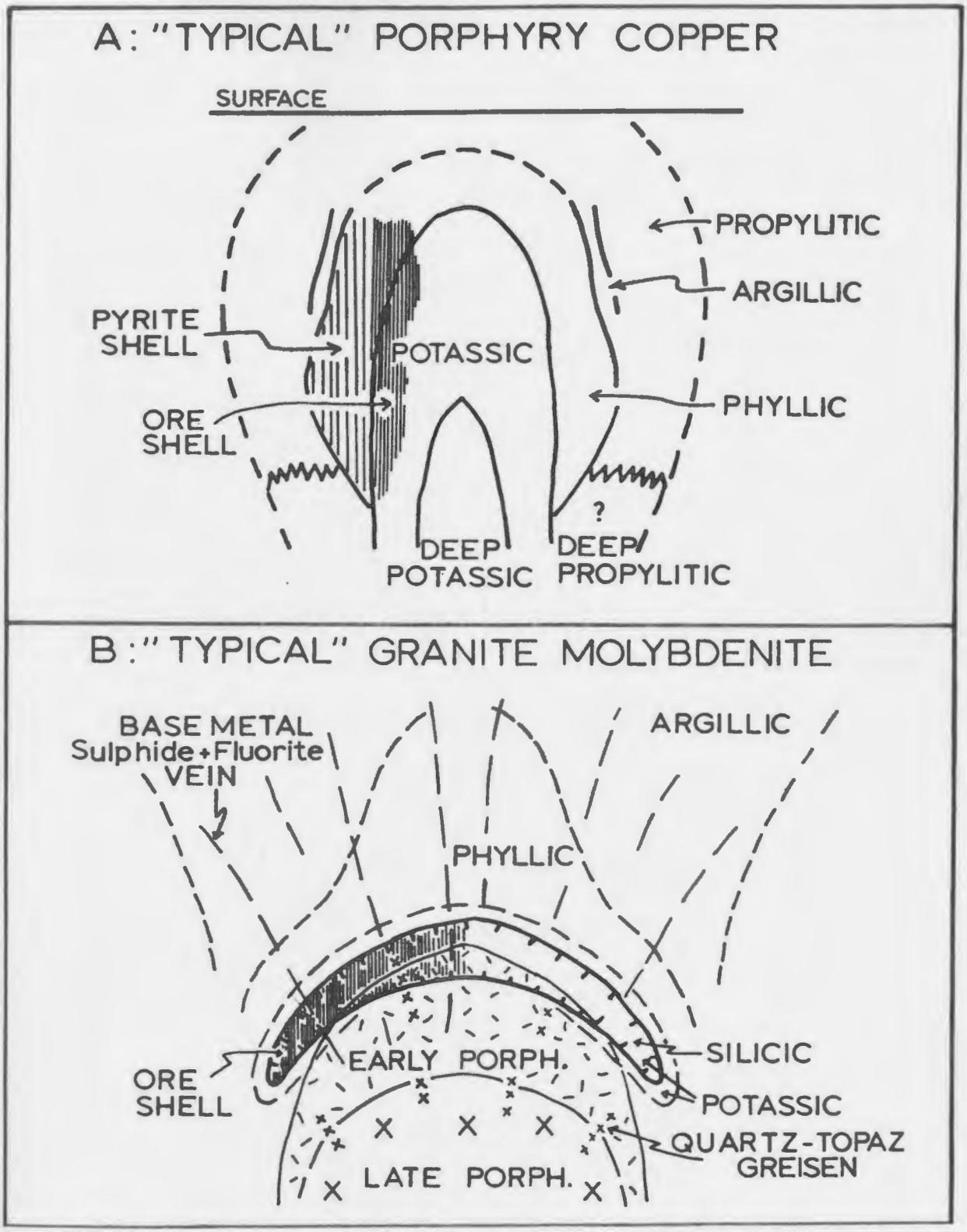

Figure 5: Idealized models for major deposit 'types' showing zoned hydrothermal mineral assemblages.
A: 'typical' porphyry copper deposit (Beane, 1982).
B: 'typical' granite molybdenite system (Climax type), from Mutschler et al. (1981).

different morphology and alteration mineralogy, due to fluid reaction with carbonate rock at higher PCO_2 (Einaudi et al., 1981).

A spectrum of important deposits from porphyry copper to "porphyry" (or stockwork) molybdenum is associated with basic to intermediate calc-alkaline plutons (White et al., 1981). Molybdenite is the dominant economic sulphide phase in the latter deposits. In copper-molybdenum deposits, molybdenite is found internally with respect to copper in the cylindrical ore shell.

Tungsten (scheelite) may be present and may be the only economic metal (Westra and Keith, 1981). Important skarn deposits of tungsten may be associated with porphyry systems.

The common feature of all the deposits described above is the association with low fluorine and relatively high Ba, Sr, Cu, calc-alkaline, mafic to intermediate plutons of peraluminous affinity (Mutschler et al., 1981). Porphyry copper-molybdenum deposits related to alkaline plutons are recognized as a separate subgroup (Barr et al., 1976; Westra and Keith, 1981).

2-2-3 Climax-Type

Climax-type deposits have also been described as Granite-molybdenite systems by Mutschler et al. (1981) and as stockwork molybdenum systems. They are commonly subclassified, or confused with diorite-granodiorite related porphyry copper-molybdenum deposits.

These deposits have attained prominance in the past two decades and produce 50% of the world molybdenum requirements. They are associated with highly differentiated multiple intrusions of high-level (2.5 km depth), peraluminous to metaluminous,, aplite and/or rhyolite porphyry and/or granite stocks and plugs with silica content of greater than 73%, i.e. they are associated with plutonic rocks of granitic composition (Mutschler et al., 1981; Westra and Keith, 1981; White et al., 1981). Hydrothermal breccia pipes are common features of these systems.

The idealized economic deposit (White et al., 1981) is elliptical in plan, arcuate-concave downwards in section and is centered on the apex of a plug shaped intrusion (Fig. 5). The deposit either overlaps or is found 'in excess' of 100 m above the parent intrusive body. Several overlapping ore shells relating to separate intrusive phases may occur (Seedorf, 1985). Molybdenite, associated with pyrite and accessory fluorite in stockwork veins and sheet veins, is the dominant economic mineral. Tungsten mineralization (hubnerite-wolframite, or rarely scheelite) occurs above the molybdenite ore zone, and anomalous tin (probably cassiterite) may coincide with the tungsten halo or may occur with anomalous base metals (Zn, Pb, Cu, Sb) well above the ore zone. Alteration patterns in the outer portions of the Climax-type system are similar to those associated with porphyry copper deposits. However, the ore zone is hosted by a quartz-magnetite-topaz-fluorite (± biotite, ± chlorite) assemblage and late greisen veins occur in and beneath the ore zone.

Molybdenum-tungsten-tin skarn deposits are formed when Climax-type systems interact with carbonate rocks. A continuum from granite-related Climax molybdenum to diorite-granodiorite -related porphyry copper environments has been described (Westra and Keith, 1981; Mutschler et al., 1981).

A striking similarity between major and trace element compositions in zoned rhyolite tuffs and unaltered host plutons to the Climax-type deposits was noted by Mutschler et al. (1981). These authors suggested that magmatic diffusion processes (Hildreth, 1979, 1981) are important controls on primary ore metal concentration if the host pluton does not vent to surface during initial emplacement. In addition Mutschler et al. (ibid.) noted similarities between element patterns associated with Climax-type 'plutons' and those patterns reported from tin-bearing granophile deposits (Tischendorf, 1977).

Climax-type deposits are generally found in Mesozoic and younger orogenic belts and are best defined in the western United States. Canadian examples of probable Climax-type, associated with leucocratic granitic and alaskitic granite plutons, include Endako, Glacier Gulch and Adanac (Drummond and Godwin, 1976). The huge Quartz Hill molybdenite deposit in Alaska has been described by Hudson and Arth (1983). Recent studies of tin and molybdenum mineralization associated with Proterozoic rapakivi granites have indicated a Climax-type affinity (Haapala, 1985).

2-2-4 Granophile Deposits

Granophile (or granite associated) deposits containing tin have been the worlds major source of this metal since the bronze age and

approximately half of current world tungsten production is obtained from deposits which can be placed in this category. Bi, Mo, Sb and more recently U, were and have been extensively mined in the Old World. These deposits have been the subject of much study, resulting in models which have dominated metallogenic and geological concepts outside North America (Fig. 6).

Granophile deposits are defined by Strong (1980) as "typically hosted by quartz-rich leucocratic granitoids (granites, sensu stricto; 72% SiO_2) enriched in the so called granophile elements". These granophile elements include the Large Ion Lithophile (LIL) and incompatible elements Sn, W, U, Mo, Be, B, Li, P and F are of major importance, and significant concentrations of Nb, Ta, Bi and Ag may occur. The parent granites are peraluminous and generally contain biotite and muscovite. Tourmaline and fluorite are common accessory minerals.

The various forms of granophile deposits are summarized schematically in Figure 6 (after Pollard and Taylor, 1985). Based on the historical and economic preference to mine high grade vein material, granophile deposits have been classified into quartz, greisen, or pegmatite bodies. These deposits can occur as single veins, or vein swarms over large areas. Recently, important massive carbonate replacement deposits and skarn deposits have been discovered (Pollard and Taylor, 1985). Stockwork "porphyry" fracture fillings and disseminated Sn and Sn-Ag systems have been recognized as important economic targets in or above subvolcanic plutons (Sillitoe et al., 1975; Grant et al., 1977). Other large tonnage-low grade deposits, e.g. East

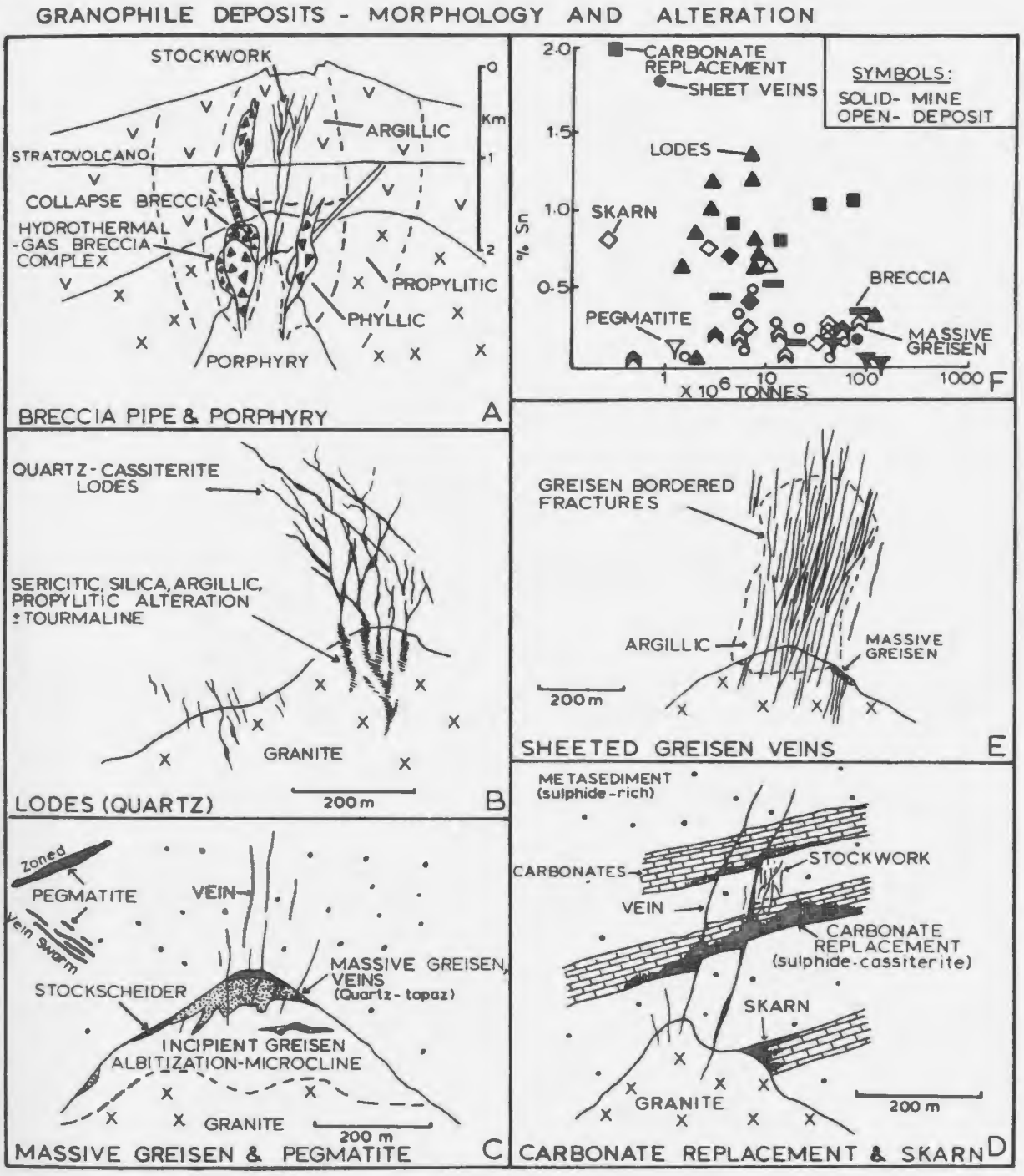

Figure 6: Styles of granophile mineralization with emphasis on tin, summarized from Pollard and Taylor (1985). Note that the tonnage-grade diagram (F) has Sn only on the Y-axis; other metals may contribute to the economic viability of the deposit.

Kemptville, Nova Scotia (Richardson et al., 1982), consist of sheets of greisen veins.

Deposits are often associated with plugs or cupolas on the upper surface of large granitic bodies. In addition, these deposits are commonly found at or near the margins of large negative gravity anomalies which may represent subsurface granitic bodies. Mineralization can be located within the host pluton (endocontact) or outside of it (exocontact). Textural, lithogeochemical, mineralization and alteration patterns commonly parallel or are strongly influenced by the granite margin. Metal zonation is highly variable but shows a general outward or down-temperature gradient from W-Mo-Sn to Cu-U to Pb-Zn-Ag (e.g., Taylor, 1979). Cassiterite and wolframite are the most important tin and tungsten minerals.

Widespread accessory mineral phases consisting of one or more of fluorite, topaz, lepidolite and tourmaline may be present in the host granite, and these are generally considered to be secondary subsolidus minerals. These minerals form greisen veins or borders to quartz greisen veins. Topaz-quartz greisen forms as high-temperature replacement of original granite (Kleeman, 1985) and muscovite-quartz greisen borders are common to veins formed by filling of open fractures.

In many mineralized systems, spatially extensive hydrothermal alteration features are not present in host rocks to high grade veins. Albitites or syenogranites, formed by high temperature sodium metasomatism, are associated with granophile deposits and often occur

adjacent to uranium mineralization (Chatterjee et al., 1983). Zoned sericitic, argillic and silicic alteration has been described from "porphyry" tin deposits by both Sillitoe et al. (1975) and by Grant et al. (1977).

Extensive kaolinite deposits (argillic alteration) may be present, of which the china clay ore bodies in southwest England are the most important. This clay alteration has overprinted greisen features related to tin and tungsten mineralization, causing controversy over the temporal and spatial relationship of alteration to granite emplacement and metal deposition (see review by Stone and Exley, 1985). The current consensus is that extensive low temperature hydrothermal circulation systems were periodically established over long time intervals in the granite, due to high initial content of radiogenic elements (U, Th, K) and led to extensive kaolinization (Allman-Ward, 1985).

The similarity between host plutons, morphology, major and trace element geochemistry, alteration assemblages and metal content, indicates that Climax-type and granophile mineral deposits have a comparable genetic history. Many granophile deposits are located in Paleozoic to Mesozoic orogenic belts. These belts have generally been eroded to deeper levels than the younger Mesozoic to Tertiary belts which contain Climax-type deposits.

2-2-5 Skarn Deposits

Granitoid skarn deposits are exocontact concentrations of metallic mineralization derived from or by, emplacement of plutons into carbonate

rocks. The mineralization is commonly massive, but disseminated, vein or stockwork zones are present. Skarns are characterized by Fe-Mg-Mn bearing silicates formed by metasomatism and replacement of impure carbonate rocks due to passage of pluton-related magmatic or meteoric hydrothermal fluids. Skarn is classified on the basis of mineral assemblage present, while skarn deposits are classified on the basis of the contained economic minerals (Einaudi et al., 1981).

Scheelite-bearing skarn deposits associated with granodiorite or quartz monzonite plutons contain 50% of the world tungsten reserve (Einaudi et al., 1981) and significant Fe, Cu, Zn-Pb, or Mo deposits may be present. Minor quantities of W, Au, Ag, Sn, Be and Bi have been produced from skarn deposits associated with leucocratic plutons, although significant tin-skarn deposits may occur (see Fig. 6F; Pollard and Taylor, 1985).

Tungsten skarns are generally stratiform showing selective alteration and deposition in preexisting beds. The major deposits do not contain dyke swarms, tuffisites, or breccias and alteration in granite is restricted to a narrow zone of clinopyroxene-plagioclase-epidote adjacent to the contact. In contrast to tungsten skarns, copper skarn deposits may exhibit zonal alteration comparable to that of porphyry copper deposits and are interpreted to have formed at shallower depth than tungsten skarns (Einaudi et al., 1981).

2-2-6 Peralkaline Granite

Taylor and Fryer (1983) have suggested that Zr, Nb, Ta, Be, F, U, Th, Sn, rare earth element-rich concentrations associated with peralkaline granites form a major class of granitoid mineralization. Those metals are used in high technology industries and have generally been obtained as by-products from other types of deposits. Their increasing importance will probably result in development of new mines for primary production. Relatively few major deposits related to peralkaline granites have been mined, with the exception of the St. Lawrence fluorspar veins (Strong et al., 1984).

These deposits vary considerably in their mineralogy and morphology. One or more of zircon, monazite, bastinaesite, pyrochlore, xenotime, gittinsite and many other comparatively rare minerals may form ore assemblages. Fluorite and barite are commonly present and may form ore. Tin, uranium and thorium may occur. Mineralization varies from magmatic-pneumatolytic to hydrothermal (Sorenson, 1974). Deposits may occur as single or multiple veins, shears, vertical or flat lying pegmatite sheets, greisens, or as enriched layers in highly differentiated granite. They are generally associated with small, high level plutons which are commonly (not always) located in more extensive provinces of alkali volcanism and plutonism. These provinces are thought to represent areas of crustal tension or mantle upwelling (Bailey, 1974; Taylor, 1979).

Extensive albitization, locally with disseminated mineralization is described from many mineralized areas. Fluorite, K-feldspar, aegirine and carbonate alteration may occur in many of the vein systems. Other deposits, particularly late magmatic deposits and open fracture-fill deposits, may not show obvious alteration features, although a high iron content and a red-brown colour are distinctive of highly differentiated peralkaline granite.

Included in this group are the Sn-Zn-Ta-Nb deposits of Nigeria described as pegmatite and greisen veins and disseminated stockworks associated with sodium metasomatism (Jacobsen et al., 1958, Kinnaird et al., 1985); the fluorite deposits at St. Lawrence, Newfoundland (Teng and Strong, 1976; Strong et al., 1984), consisting of open fracture-filling fluorite with little obvious associated alteration, Be-Nb-Ta-Y-U-Th deposits at Thor Lake, North West Territories (Davidson, 1978; Trueman et al., 1985) which are located in quartz-albite-fluorite-carbonate breccia zones, the Strange Lake Zr-Y-F-Nb deposits in Quebec-Labrador (Currie, 1985), and similar deposits in Saudi Arabia (Drysdall et al., 1984; Jackson et al., 1985). These Zr-Y-F-Nb deposits are associated with late magmatic, relatively unaltered phases of peralkaline granites and with related aplite, pegmatite and hydrothermal breccia.

2-2-7 Models of Ore Formation

Models for the formation of porphyry copper mineralization are based on the study of deposits in the southwestern United States. These

models are centered around the separation by retrograde boiling and vertical rise of high salinity, metal-rich, magmatic fluids from a porphyritic stock or plug, during and after emplacement and crystallization of the carapace of the magma chamber. Metals are precipitated from these magmatic fluids. The magmatic fluids may interact with an external, convecting system of meteoric fluids, generated by heat from the intrusion (Henley and McNabb, 1978; Burnham, 1979). Variable interaction between the magmatic and meteoric fluids, in time and space, causes differences in observed alteration and economic sulphide distributions and can result in concentration of metalliferous proto-ore which was precipitated from magmatic fluids (Henley and McNabb, 1978; Taylor and Fryer, 1983). Variation of hydrogen, sodium and potassium cation activity in hydrothermal fluids is an important control on mineralization and alteration patterns developed. Possible reaction paths for fluid evolution in these hydrothermal systems are discussed by Beane (1982).

Models for the genesis of Climax-type deposits are similar to those erected for porphyry copper systems and are based mainly on studies of the Climax and Urad-Henderson deposits in Colorado (White et al., 1981; Stein and Hannah 1985). These envisage concentration of volatiles and ore elements in a late magmatic phase by crystal fractionation and/or liquid state diffusion, followed by separation of a fluid phase and partitioning of fluorine and ore metals into the evolved fluid. Brecciation is caused by fluid overpressure and the characteristic ore-elements are precipitated as a stockwork deposit. The spatial and temporal overlap of several separate intrusive phases and associated

mineral-rich hydrothermal systems, accompanied by the interplay between magmatic plume and meteoric convective systems may cause variations on the main alteration theme (Seedorf, 1985). Interaction of the mineralized system with convecting meteoric waters is thought to lead to the formation of the late greisen veins and base metal mineralization. The chemical controls of the hydrothermal systems are less understood than those for the porphyry copper environment; the activity of fluorine is thought to be of primary importance and hydrogen and potassium cation exchange may be significant factors (Burt, 1981).

The genesis of granophile mineralization has been discussed by Burnham (1979) and Strong (1980, 1981) and is comparable to that of the Climax systems. These authors envisage magmatic concentration of volatiles, followed by fluid separation and ore deposition, at or near the carapace of the magma chamber. The widespread relationship of breccia pipes and stockschieder to areas of tin and tungsten mineralization imply a close genetic link between crystallization, devolatilization of the parent magma and mineralization.

Magmatic concentration of ore elements and volatile phases, accompanied by high level pluton emplacement again seem to be important controls in the peralkaline environment. Important components of the fluid phase are F^-, CO_3^{2-} and Na^+ (Taylor and Fryer, 1983).

Aplite-pegmatite, massive greisen deposits, and magmatic deposits are generally considered to represent deeper levels of ore formation (Strong, 1980). Veins and breccias are considered to form under lower confining pressures (Pollard and Taylor, 1985)

2-3 MAGMATIC-METALLOGENIC CONCEPTS

2-3-1 Introduction

The granitoid magmatic-metallogenic-volcanogenic system, as conceived by most authors, can be considered as part of a continuum of physical and chemical processes in three main environments. These three environments are: 1) the Source Regions, where discrete magma bodies form through coalescence of material derived through partial melting of a source rock, or where silicic magma forms through fractionation processes from larger, less evolved magmatic systems. These processes may operate extensively in the lower crust or upper mantle at depths greater than 20 km and fractionation processes may produce relatively minor granite bodies at depths of less than 20 km; 2) Ascent and Emplacement predominantly involves vertical rise of magma through diapirism or stoping. The liquid may be partly or completely separated from its parent rock and crystallization and fractionation processes may operate extensively in this environment; 3) Final Crystallization and/or Fractionation where the magma system 'freezes'. If the magma collects in large chambers at high crustal levels, and is maintained as magma by a large thermal input to higher crustal levels, then extensive chemical fractionation may occur. This environment may be dominated by crystal or liquid-state physico-chemical fractionation processes and be strongly influenced by fluid phases in the magma. Physical processes related to volcanism and possible caldera formation may be be important.

The tendency for the recognized types of ore deposits (Porphyry copper versus Climax and Granophile) to occur in associations with

plutons of specific characteristics implies an important petrogenetic control over the metallogeny. Magma ascent to high crustal levels (generally less than 5 km) appears to be important for the development of large granitoid ore deposits. Therefore, depth or pressure and/or height of the magma column in the crust requires consideration. In addition, some investigators suggest that the main or only role of the pluton is to provide a heat source to form convecting meteoric water systems. In these convecting systems, metals from the granite or from the host rock are leached out and may be precipitated as granophile deposits.

Source rocks and/or fractionation processes are considered by most authors (cf. Strong and Chatterjee, 1985) to be the most significant factors in controlling metallogenic processes in granitoid rocks. Some major features of recent concepts are reviewed below.

2-3-2 Source Concepts

Partial melting of lower continental crust or upper mantle protolith in continental environments may form extensive bodies of granitic magma. A diverse range of potential source compositions is provided by three main continental tectonic environments which are; (1) Subduction Zones (Hamilton, 1969; Atherton et al., 1979); (2) Megashear accompanied by tectonic thickening (Arthaud and Matte, 1977; Strong, 1980; Strong and Hanmer, 1981); (3) Crustal Extension accompanied by mafic underplating (Hildreth, 1981; Thompson et al., 1984).

Additional source rocks are present in the oceanic environment. Trondjhemitic granitic magmas may form in ophiolitic suites and in island arcs developed over subduction zones in oceanic crust (White, 1979). Minor volumes of felsic plutonic rocks, commonly with alkaline affinities, form in oceanic islands.

An important development in the understanding of granitoid rocks has been the classification of plutons in terms of their probable source or protolith (Table 2). Chemical characteristics of plutons derived from a crustal igneous protolith (I-type) and from a crustal sedimentary protolith (S-type) were initially proposed for examples in eastern Australia by Chappell and White (1974) where the possibility of a significant parent component or 'restite' fraction was identified and chemically evaluated. Subsequently, the concept of Anorogenic or A-type granitoid bodies, derived by a second stage of melting from a previously melted crustal source was proposed by Loiselle and Wones (1979) and Collins et al. (1982). Characteristics of the I-, S-, and A-type plutons were summarized by White and Chappell (1983). White (1979) introduced M-type, or mantle derived plutons which are tonalitic-trondjhemitic-dioritic bodies associated with ophiolitic environments and oceanic island arcs. Pitcher (1983) identified the Caledonian I-type pluton, associated with post orogenic environments in relatively stable tectonic regimes (Table 2).

Pitcher (1983) discussed the tectonic significance of these classifications. He suggested that they are useful in determining the nature and polarity of major orogenic events.

Table 2: Granite types (summarized after Pitcher, 1983)

Type	M	I-Cordilleran	I-Caledonian	S	A
Dominant Lithology	Plagiogranite -gabbro	Tonalite, diorite-monzogranite (53-76% SiO_2)	Granodiorite-granite Assoc. with minor diorite and gabbro	Granite (65-74% SiO_2)	Biotite granite alkalic granite syenite
Initial $^{87}Sr/^{86}Sr$	0.704	0.706	0.705-0.709	0.708	0.708-0.712
Al/(Na+K+Ca/2)		1.1, often 1	c.a. 1	1.05	Not all peralkaline
Morphology	Small, complete	Multiple linear batholiths, composite cauldrons	Isolated complexes multiple plutons, sheets	Multiple batholiths and sheets-diapiric	Multicentered cauldron complexes
Volcanism	Island Arc	Andesite-dacite	Basalt-andesite plateau lavas	Generally rare	Alkalic lavas Calderas
Duration	Short, sustained	Long, episodic plutonism	Short, sustained, post kinematic	Moderate, syn. and post kinematic	Short
Tectonic Setting	Ocean Island-Arc	Andinotype-marginal continental arc	Caledonian-post closure uplift	Hercinotype continental collison + shear belts	Post-orogenic to anorogenic
Mineralization	Porphyry-Cu, Au	Porphyry-Cu, Mo	Rarely strong mineralization	Sn + W greisen + veins	Columbite, cassiterite, fluorite

Ultimately, a mantle source is envisaged for many batholiths, particularly for the Cordilleran batholiths (e.g. Atherton et al., 1979; DePaolo, 1981). Tindle and Pearce (1981) and DePaolo (1981) envisage a process whereby fractional crystallization of mantle-derived hydrous mafic magmas trapped in hot crust, together with progressive assimilation of sialic material, gives rise to the granitic magmas.

Underplating of the continental crust (cf. Hildreth, 1981) may take place due to mantle convection. A more sophisticated model has been proposed by Thompson et al. (1984). These authors envisage that the thickened subcontinental lithospheric mantle root of a collisional orogen subducts, or falls off. This permits upwards flow of the 'fertile' ocean island basalt source-mantle (relatively rich in incompatible elements). Abundant melting of this mantle is accompanied by fractional crystallization and melting of sialic rocks and gives rise to incompatible element-rich (A-type) anorogenic magmas and ultimately to peralkaline magmas.

Many authors have linked mineral deposits to the A-, S-, I-classification scheme, thus implying an important source control on metallogenesis. S-type plutons are considered to be associated with granophile Sn-W oxide mineralization and I-type plutons are considered to be associated with Cu-Mo porphyry, sulphide deposits (e.g. White et al., 1977; Beckinsale, 1979). Significant Sn, Nb, F, and rare earth mineralization may be associated with A-type plutons (Collins et al., 1982; Taylor et al., 1985), and the host rocks to the Climax-type deposits have A-type affinities. The Proterozoic rapakivi granites also

have A-type affinities (Haapala, 1985). Porphyry Cu and Cu-Au deposits are associated with M-type plutons and significant mineralization is not considered to develop in association with Caledonian I-type bodies (Pitcher, 1983).

Calc-alkaline granitoid rocks in Japan were divided into a magnetite-series of rocks associated with Cu + Mo sulphide deposits and an ilmenite-series associated with Sn + Mo oxide deposits by Ishihara (1981). This classification, which is based largely on petrographic and petrochemical criteria, does not compare directly to the S vs I scheme of Chappell and White (1974) and has not been widely accepted.

Enlarging on the work of Brown and Fyfe (1970) and Burnham (1979) Strong (1980) emphasized that the ability of a granitoid melt to ascend from its depth of formation to high crustal levels is dependant on water and volatile content of the magma in addition to source composition and degree of melting. The water and volatile content of the magma may in turn be controlled by water and possibly volatile content of the source region (cf. Collins et al., 1982). Mafic magmas with low water content would be able to rise to high crustal levels prior to crystallization (intersection of the solidus by the magma) and hydrous, volatile-rich, felsic plutons will also rise to high crustal levels due to suppression of the granite-solidus by volatile complexing in the liquid-silicate phase. In addition, Strong (op. cit.) pointed out that plutons formed with intermediate dissolved H_2O and low LIL content will crystallize at intermediate depths. Significant ore deposits will not form in this environment due to the absence of convecting meteoric fluids, except under special circumstances (Strong, 1980).

Source composition strongly influences the chemistry of derived granitoid bodies, their ability to ascend in the crust and consequently their ability to form ore deposits. In addition, limited partial melting would enrich the magma in LIL elements (Strong, 1980) which in turn would depress the granite-solidus and decrease viscosity (see Dingwell, 1985). LIL element-enriched magmas have greater potential to rise to high crustal levels and to form associated ore deposits.

A classification system based on perceived genetic source (A vs I vs S) does not provide a sound basis for detailed study of granitoid deposits. The subdivision of major stockwork molybdenite deposits into Granite and Granodiorite (Diorite) systems by Mutschler et al., (1981) is both empirical and can be explained in genetic terms (e.g. Strong, 1980, 1981). This terminology could be expanded to provide a primary subdivision for all granitoid deposits (e.g. Table 3). The term porphyry has gained such widespread application that it has become redundant as a useful genetic or descriptive term. Porphyry copper ores associated with more mafic plutons would best be called granodiorite-copper stockwork deposits; Climax, porphyry tin and peralkaline would be related via their association with silicic magmatism and all termed granite-systems. Many deposits are spatially removed from the parent body (particularly veins and pegmatites) such that identification of the associated granitoid composition may be impossible. However, emphasis on this factor may be fundamental to achieving a full understanding of the metallogenesis of these deposits.

Table 3: Description and classification of mineralization associated with granitoid rocks based on empirical and genetic observations (an enlargement of proposals by Mutschler et al., 1981).

SYSTEM DESCRIPTION		MAIN QUALIFYING DESCRIPTIONS		
PARENT	ORES	MORPHOLOGY	ALTERATION	TECTONIC SETTING
	OXIDE			
	Zircon			
(-peralkaline-)			Tourmalinite	
	Yttrium	Breccia	Albitite	Peralkaline or
	Rare Earths	Stockwork	Greisen	Post Orogenic (= Caled.I?)
	Thorium	Massive	Potassic	
GRANITE	Niobium	Vein	Sericitic	
	Uranium	Lode	Argillic	Anorogenic (= A-type)
	Molybdenum	Sheet	Propylitic	
	Tin	Disseminated	also	Continental (= S-type)
	Tungsten	Skarn	Chloritic	Collision
	Antimony		Clay	
	Bismuth			
	SULPHIDE			
	Tungsten			
GRANODIORITE	Molybdenum			Pacific (= I-type)
	Copper (Gold)			Margin
(Diorite)	Copper			
	Gold			Island Arc (= M-type)

e.g. granodiorite-tungsten skarn deposit or granite-tin stockwork deposit.

2-3-3 Fractionation Processes

The processes which affect the petrological and chemical variation in the magma after its separation from the source region include fractional crystallization and filter pressing (McCarthy and Hasty, 1976), volatile phase transport in the magmatic stage (Burnham, 1979), thermo gravitational diffusion and large scale magma convection (Shaw et al., 1976; Hildreth, 1979, 1981) and convective fractionation (Rice, 1981; Sparks et al., 1984). The above processes may be influenced by changes in melt structure (Hess, 1980). Restite unmixing, crustal assimilation and magma mixing may strongly affect compositional trends in magma series and may also contribute to the LIL element enrichment process.

The process of crystal-liquid fractionation has traditionally been considered to be dominant. This model proposes that elements in the silicate melt are selectively removed by the stable crystallizing phases (predominantly feldspar and quartz, with lesser biotite, hornblende and pyroxene in granitoid systems) with resulting enrichment of the less compatible elements in the inter-crystal melt. Extensive geochemical variation in granitic systems is attributed to physical removal of the crystalline phases by cumulate or adcumulate processes and/or separation and upward coalescence of the incompatible element enriched interstitial magma from a 'crystal mush' (Filter pressing: McCarthy and Hasty, 1976). Michael (1983) and Mittlefehldt and Miller (1983) have recently supported the fractional crystallization model.

Shaw et al. (1976) and Hildreth (1979, 1981), amongst others, have suggested that liquid state processes of convective overturn and diffusion are responsible for large scale chemical variation in granitoid magmas. Hildreth (1979, 1981) has argued that fractional crystallization processes are inadequate to account for observed chemical zonation in many large, crystal-poor ash flows. His model of thermogravitational diffusion suggests that an upper gravitationally stable, lower density, possibly depolymerized magma (Hess, 1980), overlies a slightly denser convecting magma body in the typical magma chamber (Fig. 7). Diffusion of elements across the interface between the two magma types and within the upper, less dense magma is driven by thermal and possibly gravitational gradients. In addition, Hildreth (1981) suggested that significant thermally driven diffusion may take place towards the walls of the magma chamber.

Sparks et al. (1984) accepted the concept of a chemical and density stratified magma chamber, but suggested a process called Convective Fractionation i.e. "any fractionation process involving convection of fluids away from crystals" is responsible for magma zonation. They pointed out that as crystals grow in a closed system the adjacent fluid is depleted in its denser components so that the resulting less dense fluid would rise convectively. The less dense fluid would accumulate at the top of the magma chamber and would retain its identity due to gravitational stability and low diffusivity of chemical components. They emphasized that such a process would be particularly effective at the walls of the magma chamber where cooling was fastest and would allow for the effective fractionation of large proportions of

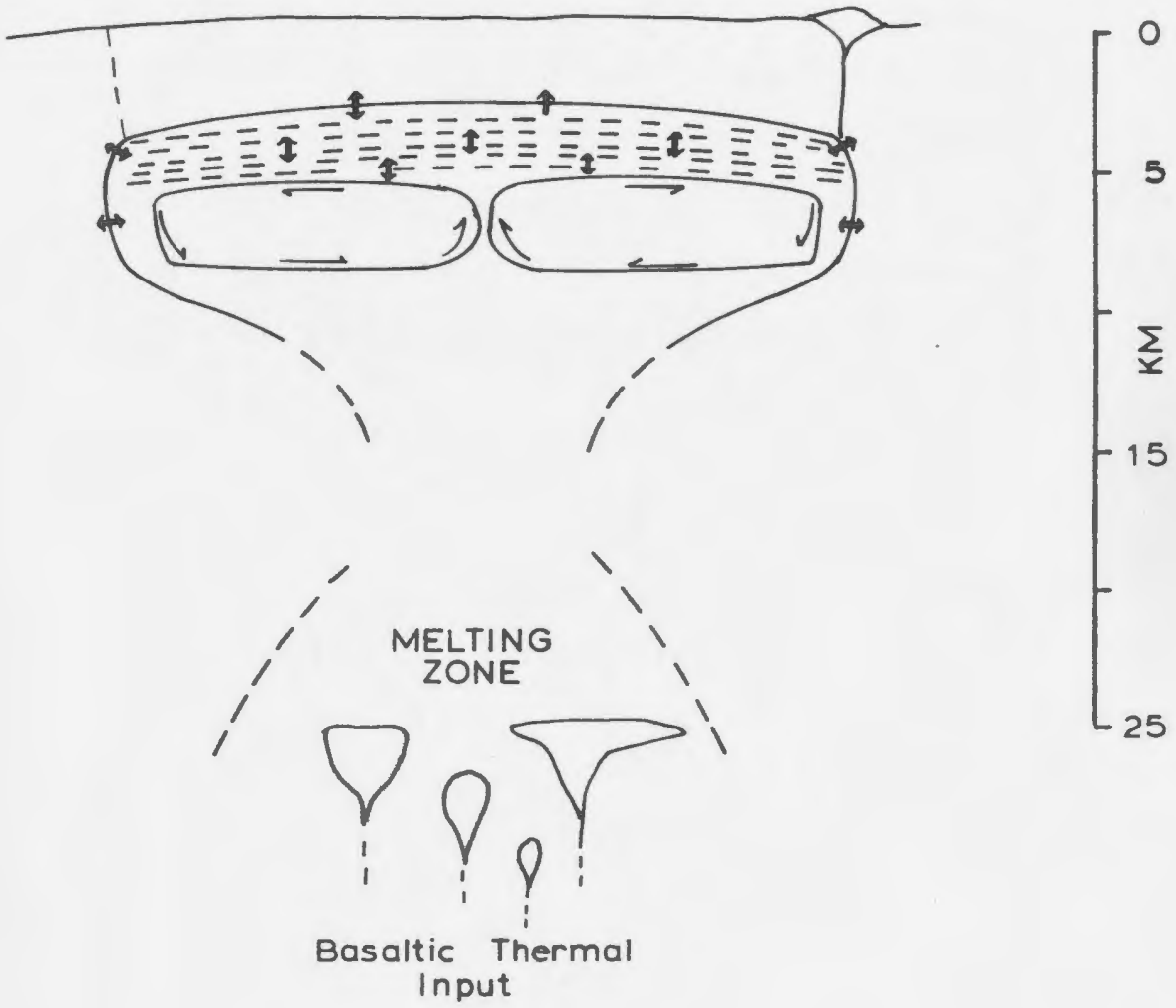

Figure 7: Conceptual model of a convecting high-level chamber of magma formed by crustal melting due to heating by basaltic input in the lower crust (Hildreth, 1981). Double arrows indicate directions of element diffusion. Single arrows indicate convection cell.

crystals (predominantly feldspars in granitoid systems) at the boundary layer to produce major changes in the resulting liquid.

The thermogravitational diffusion and the convective fractionation models account for large chemical variations in a predominantly liquid silicate body, whereas fractional crystallization models require large (commonly 50%) proportions of crystals in the system. Many geological observations on flow structures, immiscibility, magma mixing, lack of phenocrysts in major eruptive units and the origin of mafic enclaves (i.e. Vernon, 1984), suggest that the liquid phase predominates in high level silicic magma chambers. These observations support the more dynamic models.

CHAPTER 3 - PETROGRAPHY AND MINERAL CHEMISTRY OF THE POST-TECTONIC GRANITES

3-1 INTRODUCTION

The objectives of this Chapter are to describe the distribution, texture and composition of minerals in the study area. These features were investigated without reference to the boundaries established by Dickson (1983). Representative modal analyses presented by Dickson (1983) are summarized in Table 4 and in Figure 8. This approach was adopted since reconnaisance work indicated that many of the petrographic and petrochemical features transcend the previously defined internal unit boundaries and these boundaries were recognized as approximate by Dickson (1983). The observed features are classified in terms of primary magmatic and secondary sub-solidus origin at the end of the chapter.

The results of microprobe analyses are presented in Appendix C. The textures and mineralogy of granite and greisens observed in a detailed study area in the Sage Pond Granite are described in Chapter 4.

The macroscopic features show coarse grained and feldspar porphyritic lithotypes in the northwestern (Koskaecodde, Mollyguajeck, Mount Sylvester and Kepenkeck) and eastern (Meta and Tolt) granitoids. The Hungry Grove Granite is coarse to medium grained and becomes finer grained towards its southern boundary. Minor fine grained granite and aplite may be present throughout the area. Quartz, feldspars, biotite and locally muscovite are the only minerals which can be recognized in

TABLE 4: Summary of modal analyses of representative samples of the various units in the Ackley Granite (from Dickson, 1983). x = Mean, s = standard deviation. See Figure 2 for location of units.

Unit No.	9		10		11A		11B		12		13		14		14A		14B*		15	
No. of samples	8		8		7		6		6		33		16		3		8		8	
	x	s	x	s	x	s	x	s	x	s	x	s	x	s	x	s	x	s	x	s
Quartz	23.4	7.57	26.0	9.06	31.75	7.13	28.8	7.19	33.45	15.70	32.7	12.27	36.9	7.42	33.3	5.15	42.4	6.18	43.0	7.59
K-feldspar	31.3	19.1	25.0	12.0	22.8	7.68	32.8	8.57	36.35	12.30	51.8	13.42	46.7	10.72	49.7	2.97	44.5	7.02	30.7	8.65
Plagioclase	32.5	12.3	35.8	7.28	38.5	13.5	32.4	2.31	24.2	7.12	11.95	10.09	12.7	6.8	14.3	3.29	10.4	6.76	22.8	9.29
Biotite	11.3	7.42	11.2	4.73	6.3	4.23	4.41	2.11	5.43	3.40	3.05	2.49	3.3	2.03	2.4	2.21	2.07	0.93	2.2	1.37

Individual minerals were noted if they composed greater than 0.5 percent. In the following list, the number of samples for which data is recorded is noted followed by the maximum percentage of the mineral observed.

Hornblende	2, 1.2	4, 4.2	--	--	--	--	--	--	--	--
Muscovite	--	--	--	6, 2.5	--	--	--	--	--	--
Sericite	--	1, 0.5	--	--	1, 0.8	--	1, 0.9	--	2, 1.2	--
Epidote	1, 0.5	1, 1.3	2, 0.6	1, 0.5	--	1, 0.7	2, 0.6	--	1, 0.3	5, 1.0
Opaques	1, 3.0	5, 1.0	2, 1.2	3, 0.7	2, 0.8	2, 1.2	1, 0.9	1, 0.6	2, 0.5	4, 1.8
Sphene	2, 1.8	--	2, 0.6	--	--	--	1, 0.6	--	1, 0.7	2, 0.5

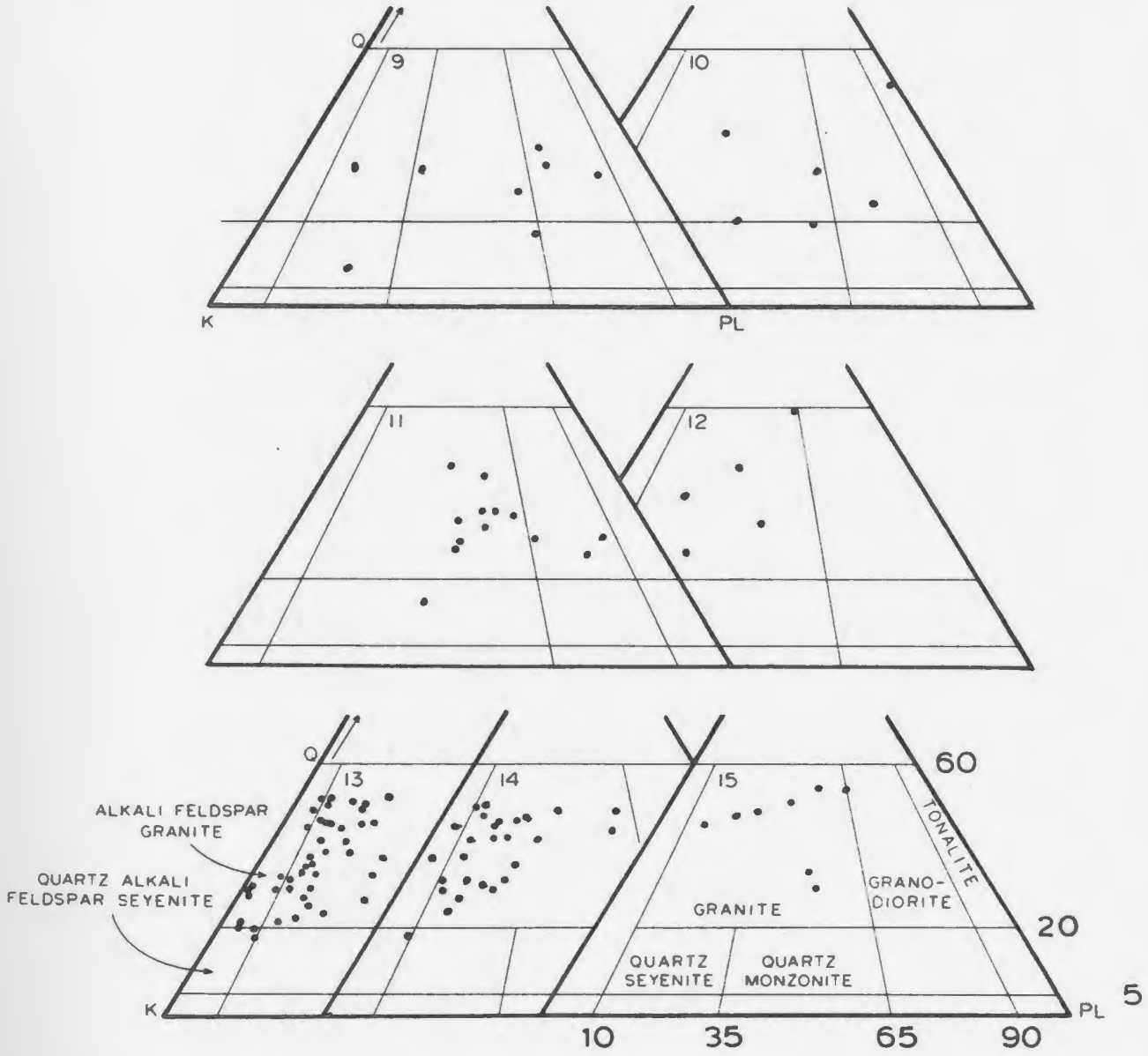

Figure 8: Modal quartz (Q) - alkali feldspar (A) - plagioclase (PL) in the granitoid units from the study area (from Dickson, 1983). Granite classification from Streckeisen (1976). Numbers in triangles refer to units of Dickson (1983).

outcrop and in hand specimen on a regional basis. Poorly developed rapakivi texture is locally present in the Tolt, Meta and Hungry Grove granites.

Fine grained, quartz-feldspar porphyritic granite, granophyre and microgranite may be present in the southern part of the Hungry Grove Granite and in the Rencontre Lake and Sage Pond granites. These granites have a pronounced orange colour due to exsolution of hematite from K-feldspar. This colour is darker towards the south. Miarolitic cavities containing small terminated quartz crystals are locally developed in the southern part of the Hungry Grove Granite and in the Tolt Granite. They are common in the Rencontre Lake and Sage Pond granites. Alkali feldspar megacrysts are present within and across the margin of minor rounded quartz diorite enclaves located at the eastern margin of the Tolt Granite. A single thin diabase sheet is reported by Dickson (1983) to occur in this Granite.

3-2 PETROGRAPHY

3-2-1 Introduction

Quartz, K-feldspar and plagioclase are present in all samples. Biotite, or chlorite pseudomorphs after biotite are present in all but two samples located in close proximity to greisen veins in the Sage Pond Granite. Hornblende is a minor mineral in the more mafic granites and in granodiorite. Chlorite is variably developed as an alteration product from biotite. Minor epidote may be associated with the chlorite and locally with sericitic alteration of feldspar. Coarse sericite is

present in the Kepenkeck Granite and in the Sage Pond Granite and a trace of sericite is common throughout the study area. Sphene, apatite, magnetite, allanite, zircon and ilmenite are present as accessory minerals. Minor fluorite was noted in the Rencontre Lake and Sage Pond granites and tourmaline was noted in two samples from the Sage Pond Granite.

3-2-2 Quartz

Quartz occurs as anhedral to subhedral grains, as spherical frosted phenocrysts up to 1 cm in diameter, and as finer interlocking grains in the matrix to coarser quartz and feldspar crystals. Quartz also occurs as small euhedral to anhedral inclusions in the other main silicate phases. Graphic intergrowths of quartz with feldspar are common in the finer interstitial granitic material, in aplitic phases and in the southern finer grained granite. In the southeastern granites (Hungry Grove, Tolt, Meta, Rencontre Lake and Sage Pond), the phenocrysts and crystals commonly exhibit embayed margins (Plate 1), and locally show evidence of strong resorption and possible disintegration prior to crystallization of K-feldspar (Plate 2). Weak to moderate undulose extinction is present and is more pronounced in the Koskaecodde and Mollyguajeck plutons, where distinct deformation domains have developed.

3-2-3 Plagioclase

Plagioclase is an integral part of the granular matrix of all units of the granite. Anhedral phenocrysts of plagioclase, up to 4 cm long,

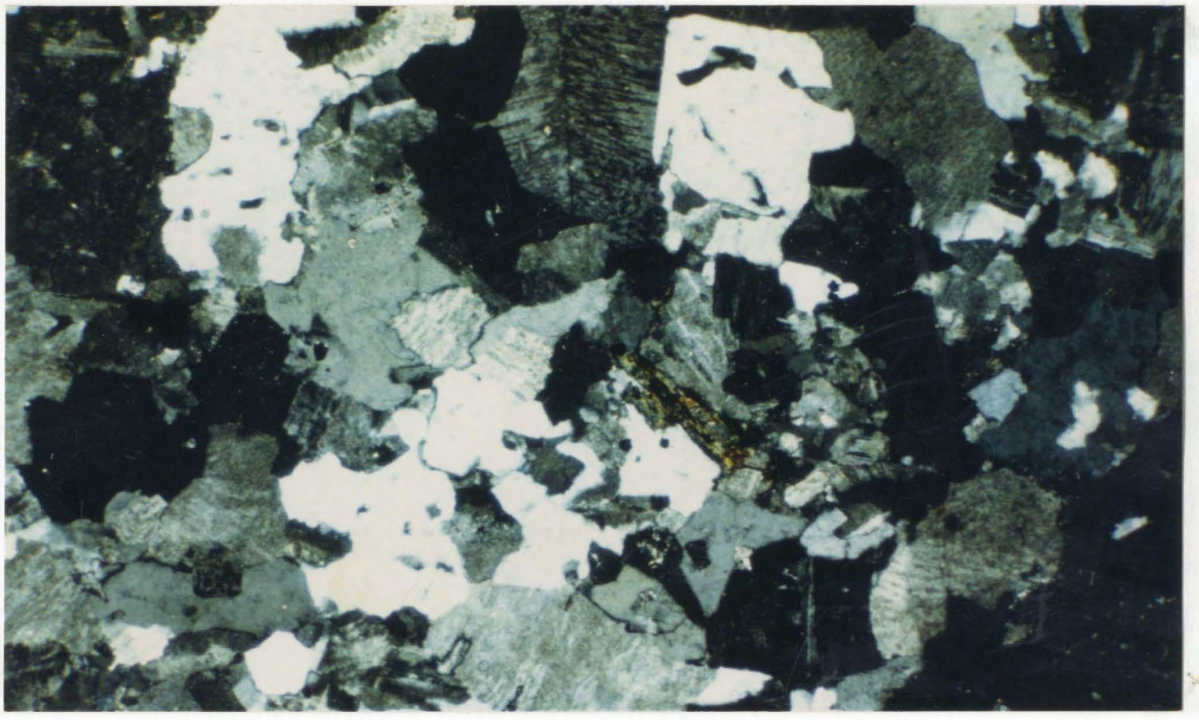

Plate 1: Equigranular microgranite showing strongly embayed quartz, perthite, minor twinned plagioclase, and an intergranular flake of chloritized biotite. Meta Granite. LD-119. XNic.

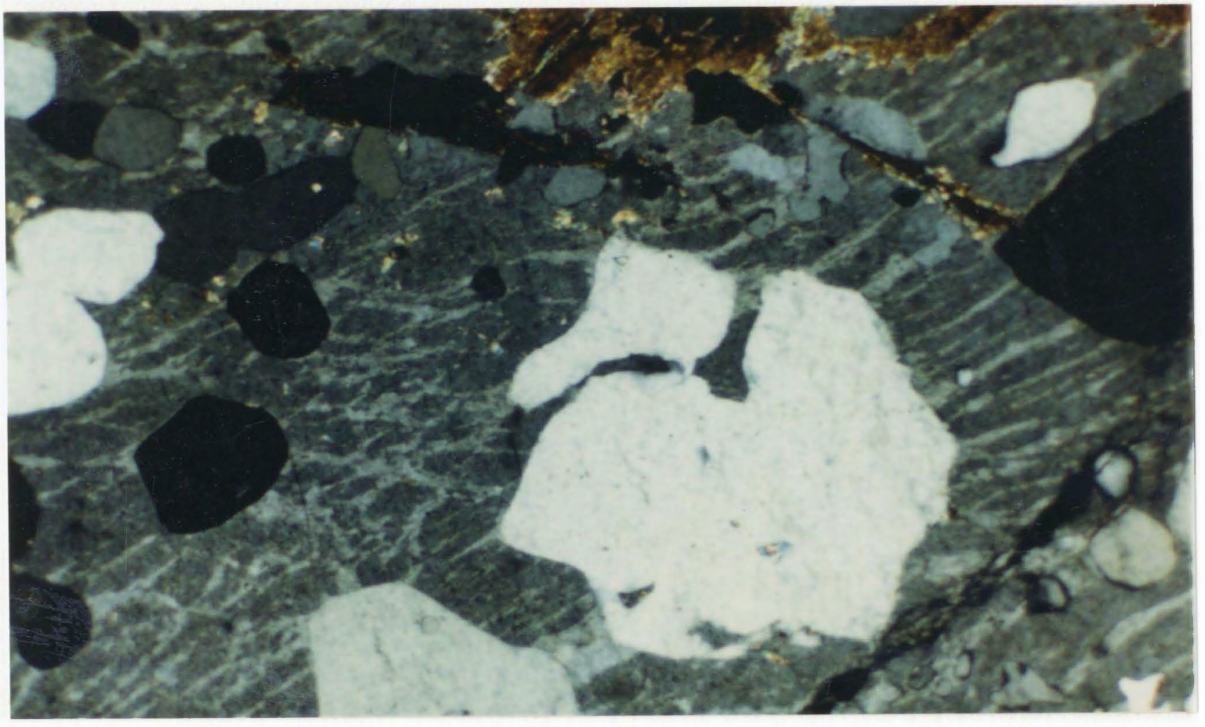

Plate 2: Quartz crystal in perthite exhibiting embayed margins, resorption, and partial disintegration. Smaller sub-hedral quartz grains are present as inclusions on left of photo. Ragged bronze, biotite in upper center with minor marginal sericite alteration. Fracture at lower right. Hungry Grove Granite. LD-451. XNic.

are present in the Mount Sylvester and Kepenkeck granites and locally in the Meta and Tolt granites. Minor subhedral to euhedral plagioclase is common as inclusions in alkali feldspar phenocrysts, particularly in the Koskacodde and Mollyguajeck plutons. In the Rencontre Lake, Sage Pond, Tolt and Hungry Grove granites, albite may be present as a thin rim round alkali feldspar (rapakivi texture). Perthitic albite exsolution lamellae are common, and are abundant in Rencontre Lake, Sage Pond and southern Hungry Grove granites.

The plagioclase exhibits characteristic albite twinning and weak to moderate, normal and locally oscillatory zoning. The biotite- and hornblende-bearing rocks in the northwestern granitoids (Koskaecodde, Mollyguajeck, Mount Sylvester and Kepenkeck) have plagioclase cores of sodic andesine zoned to oligoclase rims (An_{35}-An_{15}) and the more felsic rocks have weakly zoned oligoclase crystals. The southeastern granites have a restricted plagioclase composition which ranges from sodic oligoclase (An_{20}) in the more mafic rocks to albite (An_{0-10}) in the vicinity of the mineral prospects.

In the northwestern granitoids, the more calcic cores are commonly strongly altered to fine sericite and rarely to epidote. Minor muscovite crystals, up to 1 mm long, are locally developed as an alteration product. The sericite cores often have sharp boundaries with surrounding more sodic plagioclase and they locally display well developed internal tabular crystal outlines.

In the southeastern granites, plagioclase shows weak to moderate alteration to fine grained sericite and locally to epidote, particularly in the more calcic cores. There appears to be an increase in the intensity of plagioclase alteration to sericite in the northeastern granitoids which may in part reflect the tendency for the more calcic compositions to occur in this area. However, felsic granites with less calcic plagioclase are also more altered in the northwest.

3-2-4 Alkali Feldspar

The porphyritic phases of the granitoid rocks contain perthitic alkali feldspar crystals, up to 5 cm long, as the main phenocryst phase. Perthitic alkali-feldspar also occurs in the groundmass and forms large irregular crystals interlocking with quartz and plagioclase in generally hypidiomorphic textured, equigranular granite. The phenocrysts and the grains in equigranular granite, contain inclusions of quartz, plagioclase and biotite. These inclusions are more prevalent in the Koskaecodde and Mollyguajeck plutons and are commonly orientated within the alkali feldspar lattice.

The outer margins of the phenocrysts and of larger grains in equigranular granites have a complex interference pattern with the other phases present and locally contain large numbers of inclusions with the development of poikilitic textures (Plate 3). Graphic intergrowths with quartz are common in the outer half of individual alkali feldspar crystals in the Tolt, Rencontre Lake, Sage Pond and southern Hungry Grove granites. At least two stages of graphic intergrowth are indicated

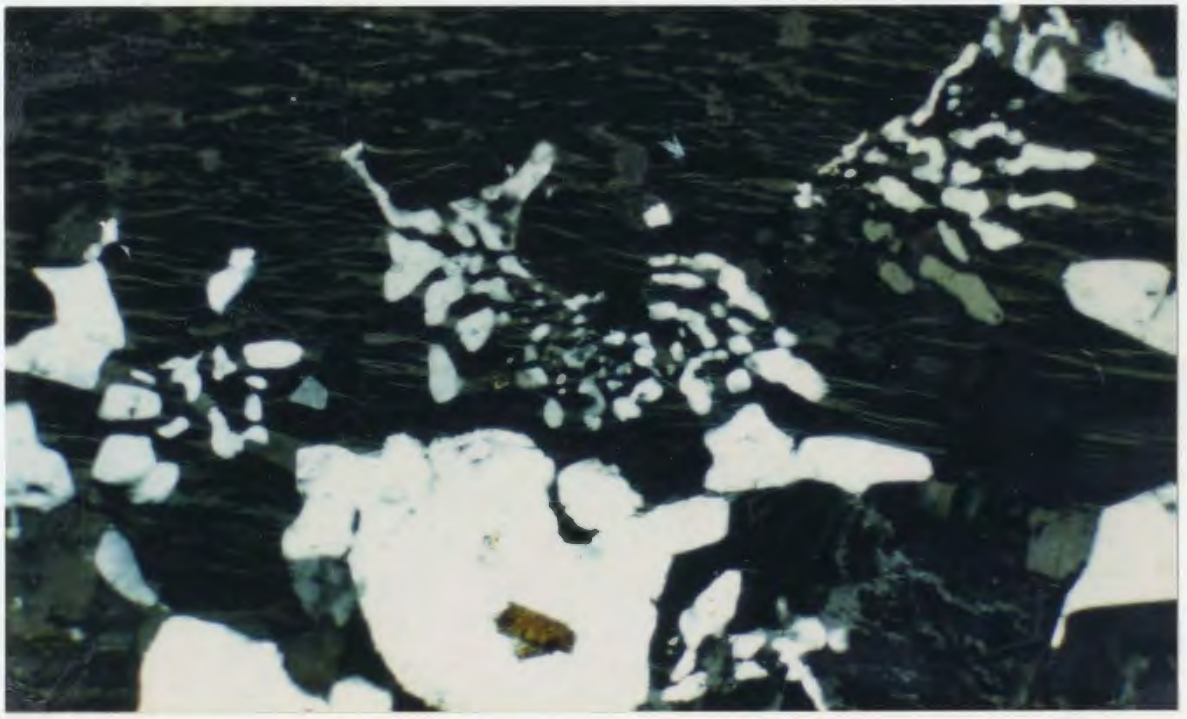

Plate 3: Graphic intergrowth of quartz and K-feldspar in a large (2 cm) optically continuous poikolitic crystal. Braided perthitic exsolution lamellae are present in the K-feldspar. A quartz crystal in the lower center has embayed margins and contains a biotite inclusion. Hungry Grove Granite. LD-451. XNic.

by individual alkali feldspar crystals (Plate 3). Albite rims (rapakivi texture) up to 2 mm wide, are locally present on alkali feldspar grains in the southeastern granites. The dominant alkali feldspar is orthoclase perthite with microcline and orthoclase perthite co-existing in the Mollyguajeck Pluton, and microcline perthite prevailing in the Koskaecodde Pluton. Microcline in the Koskaecodde Pluton is grid-twinned.

In the Rencontre Lake, Sage Pond and southern Hungry Grove granites, albite exsolution lamellae (Plates 4, 5, 6), commonly twinned, demonstrate a wide variety of textures from fine stringers to coarse braid, vein, and patch textures. The exsolution features become coarser and more abundant to the south and the more felsic granites in the south contain up to 20% exsolved albite near the mineralized areas. The granodiorites in the Koskaecodde and Mollyguajeck plutons may exhibit only minor perthite exsolution.

3-2-5 Biotite

Biotite (or chlorite pseudomorphs of biotite) is present in all thin sections of granitoid rocks within the study area, with the exception of two hydrothermally altered samples collected near greisen veins at the southern edge of the Sage Pond Granite. An estimate of the amount of biotite (Fig. 9) was obtained by calculating normative biotite (after Barth, 1959, 1961). Biotite is the only magnesium-bearing phase present in most samples. In hornblende-bearing rocks (Fig. 11), the amount of hornblende is generally less than 1%. There is close agreement between normative biotite and modal biotite content.

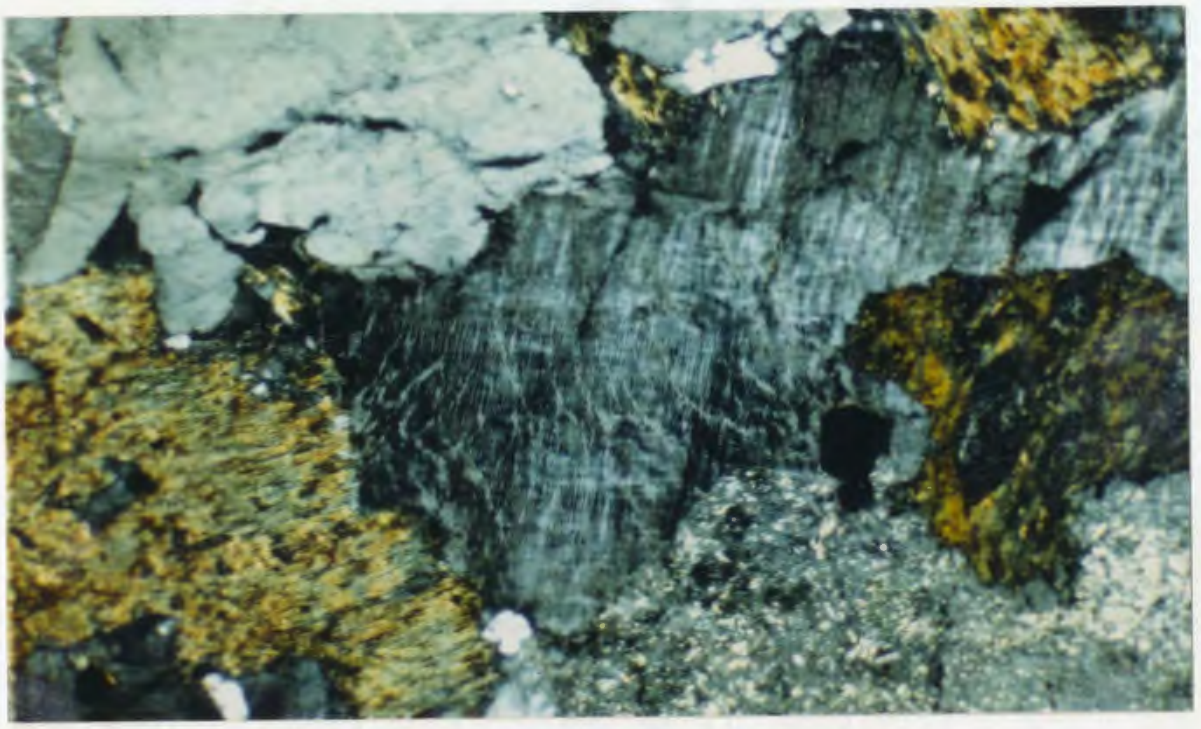

1.0
mm

Plate 4: Perthite with parallel rib lamellae cut by later braid and string lamellae. Quartz crystal with embayed margin at upper left. Strongly altered plagioclase at lower right. Ragged to subhedral strongly chloritized biotite, with biotite as brown areas and laminar domains of chlorite replacement as blue gray colors. Euhedral opaque in right center. Mollyguajeck Pluton. LD-075. XNic.

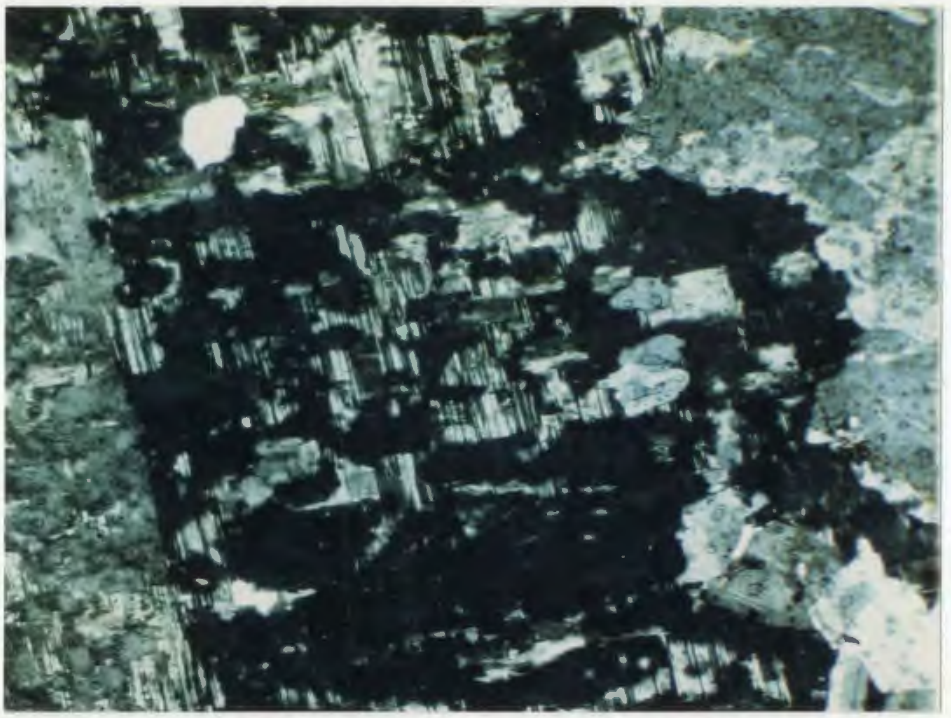

Plate 5: Coarse patch perthite. Hungry Grove Granite. LD-179. XNic.

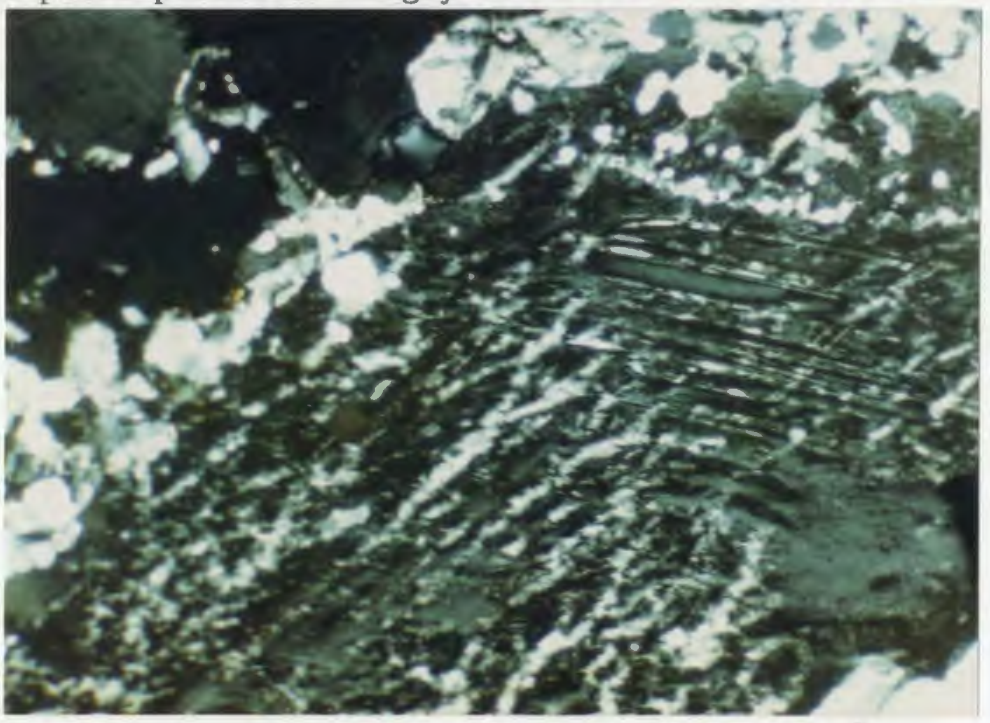

Plate 6: Growth zoning in alkali feldspar cut by string and braid exsolution lamellae. Graphic intergrowth at upper margin of crystal. Hungry Grove Granite. LD-421. XNic.

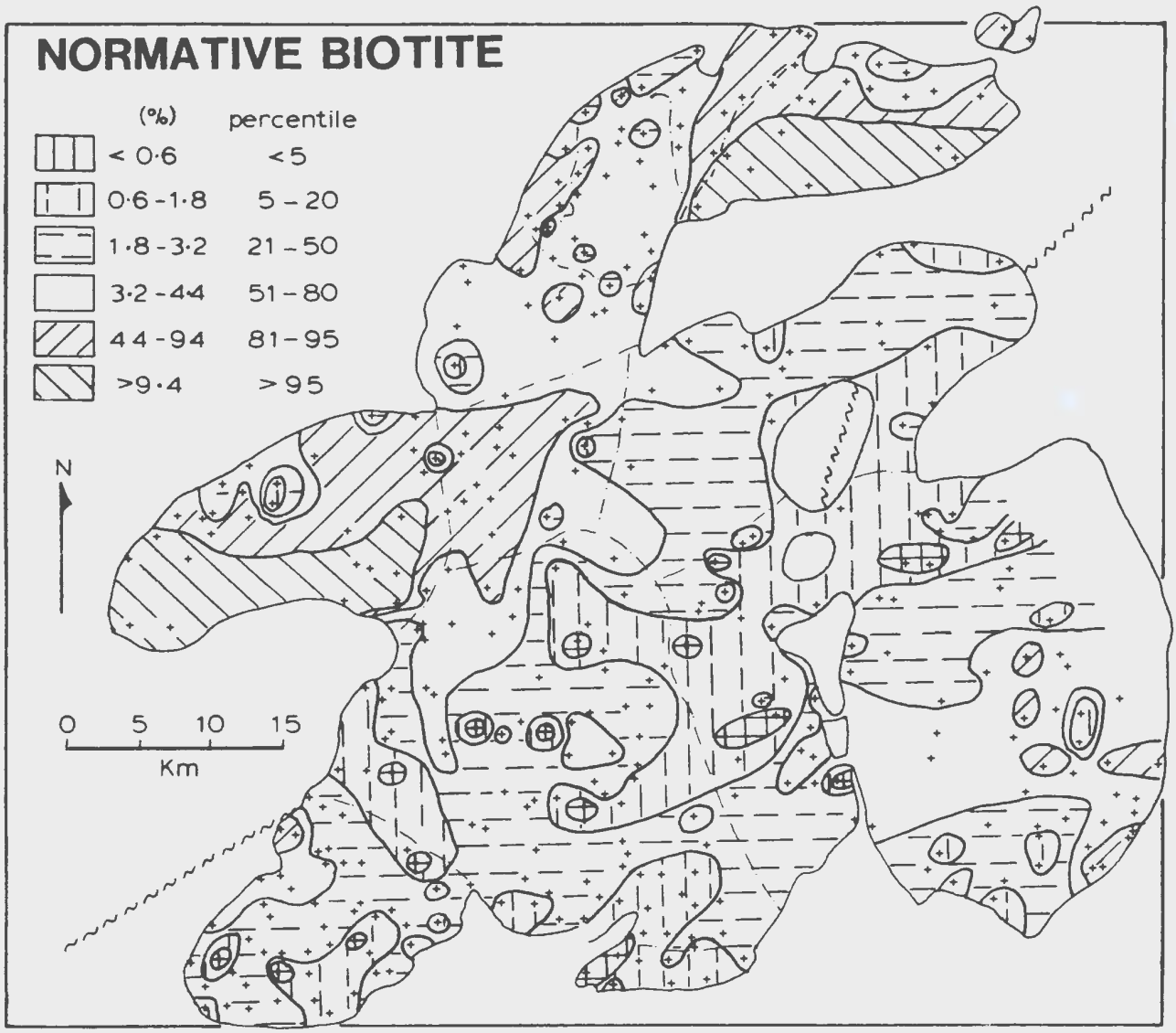

Figure 9: Distribution of wt. % normative biotite in the study area (calculated after Barth, 1959, 1961). Sample locations are indicated by small crosses. Dashed lines are boundaries of Dickson (1983).

The main textural variations displayed by biotite are 1) coarse phenocrysts, 2) fine intergranular grains and flakes, and 3) fine grained biotite or biotite-rich aggregates. These varieties commonly occur within a single specimen and a complete gradation between the three designated end-member textures may be present.

Most biotite exists as coarse, dark brown, ragged-edged phenocrysts or books which rarely attain 1 cm across (Plate 7). Subhedral to euhedral hexagonal basal sections are common. Locally these coarse grained biotites form clusters in the granite. Biotite in the southern exposures is bronze to black (Plate 8).

Intergranular, finer grained individual flakes and irregular grains of biotite are present between quartz and feldspar crystals (Plates 1, 2). This variety generally accounts for a minor proportion of the biotite.

Fine grained aggregates of biotite or biotite + quartz + feldspar (Plates 9, 10) are common in approximately 20% of samples in the Koskaecodde and Mollyguajeck plutons. These aggregates also occur in the Hungry Grove Granite and may occur throughout the study area (Fig. 10). In the eastern part of the Koskaecodde Pluton, this is the dominant biotite texture. Many of these aggregates occurs in local areas of graphic intergrowths between fine grained quartz and feldspar. In the Koskaecodde Pluton, the biotite clusters have associated fine grained hornblende on the margins. In the quartz-biotite clusters, some of the biotite grains have a dendrititic or poikilitic texture.

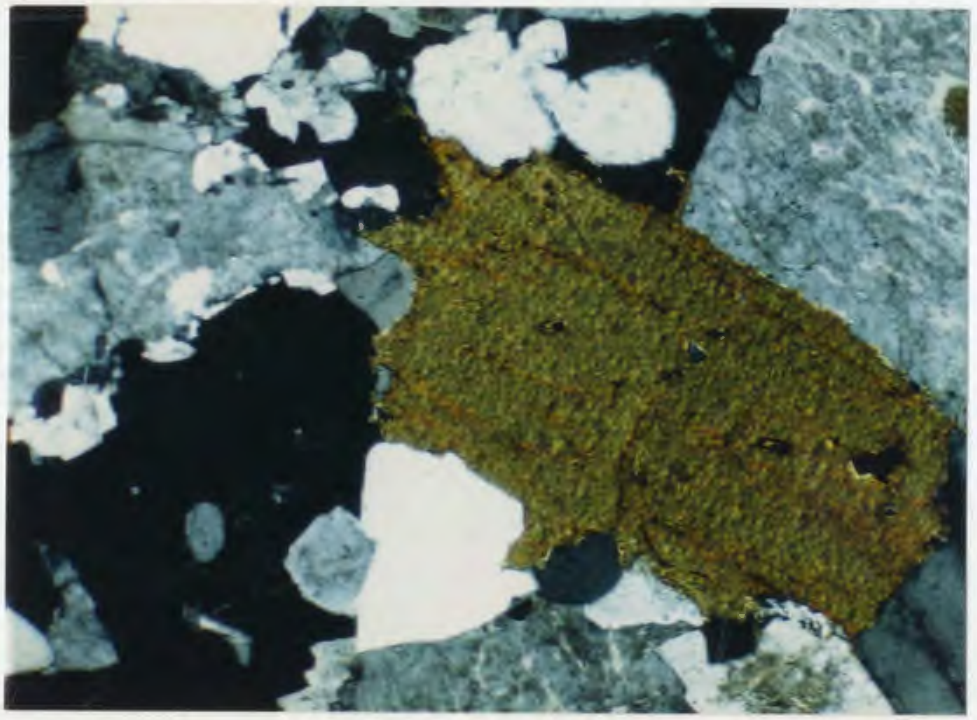

Plate 7: Fresh subhedral biotite. Hungry Grove Granite. LD-453. XNic.

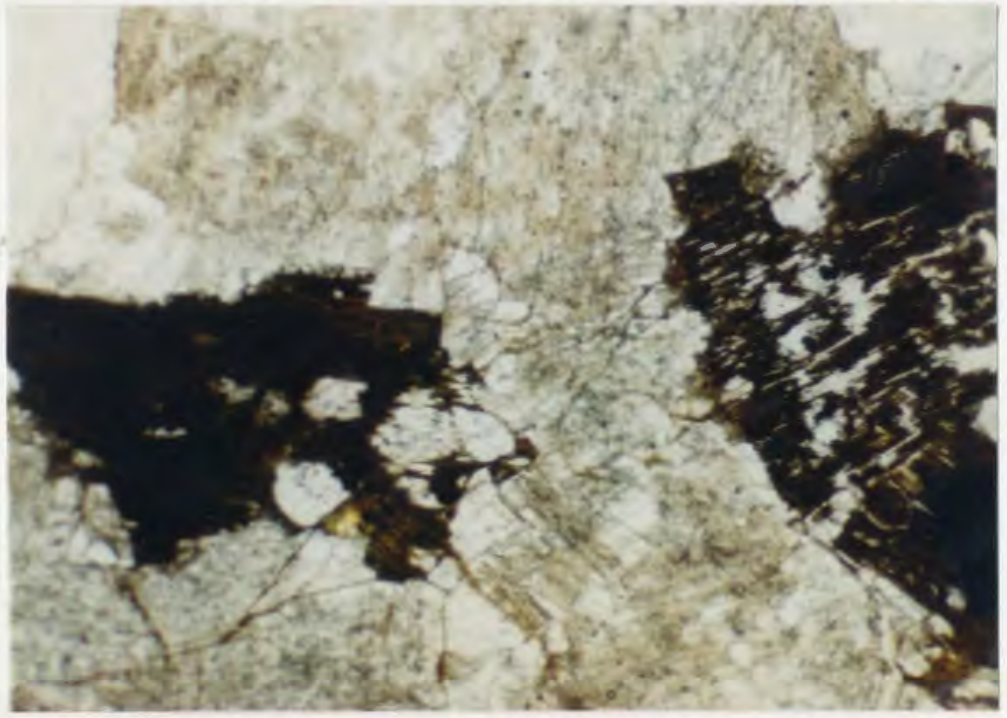

Plate 8: Bronze to black biotite with tendency to skeletal texture. Hungry Grove Granite. LD-695. Plain Light.

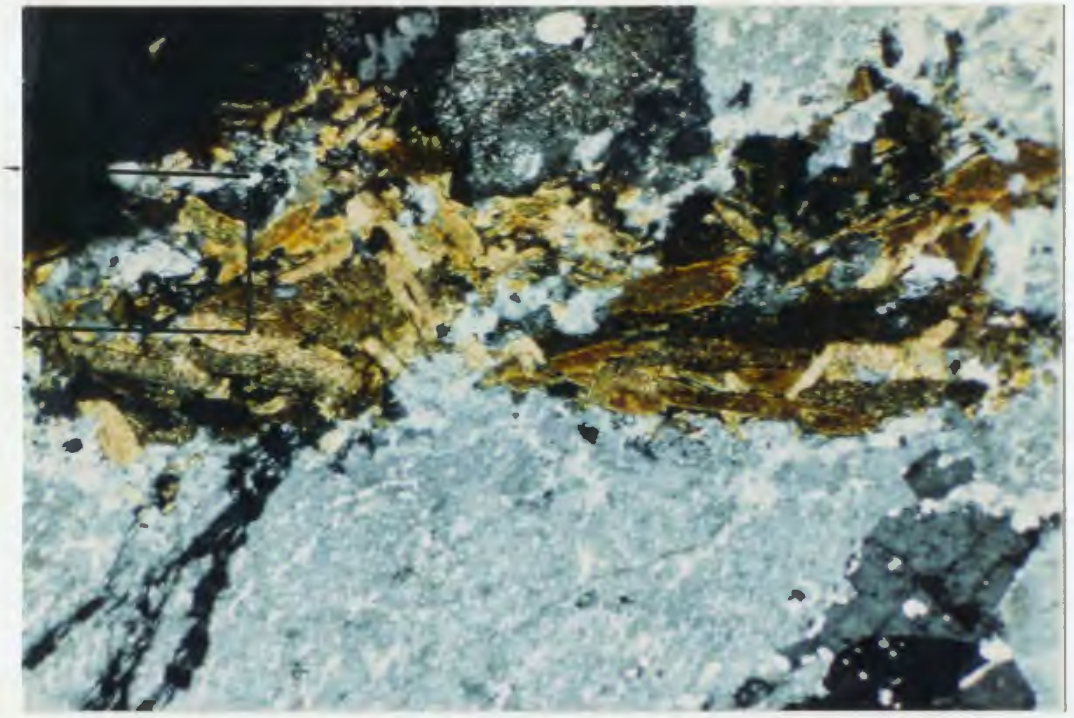

Plate 9: Fine grained biotite aggregates. Area outlined is enlarged in Plate 10. Mollyguajeck Pluton. LD-348. XNic.

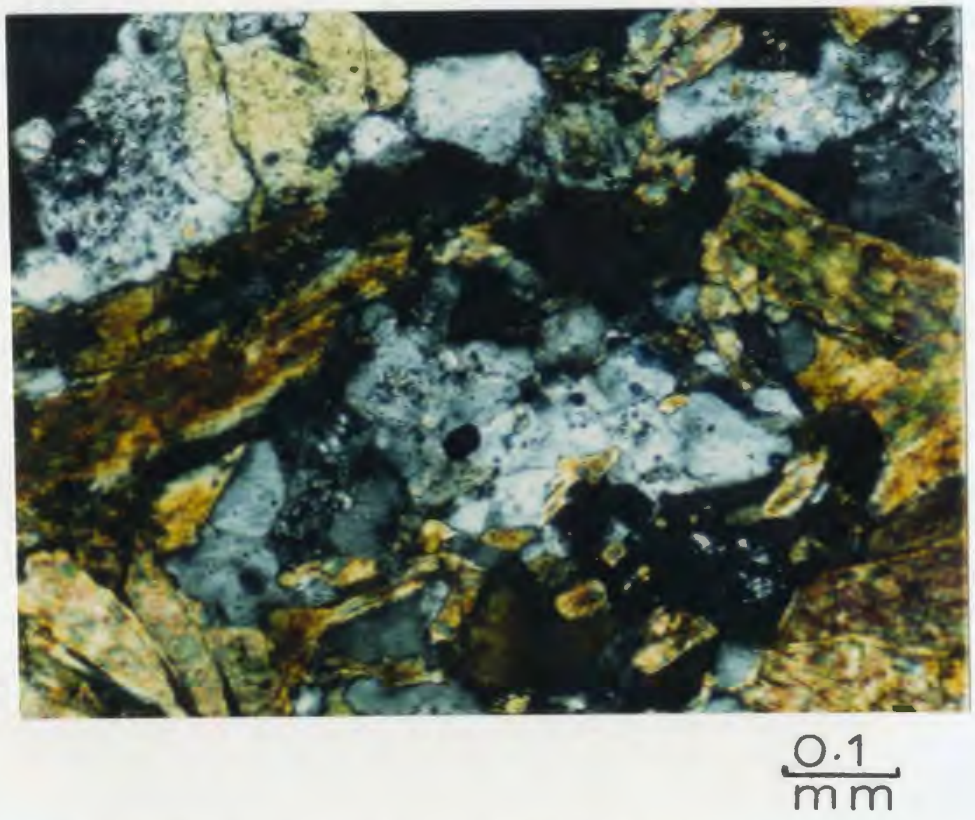

Plate 10: Detail of area outlined in Plate 9. Mollyguajeck Pluton. LD-348. XNic.

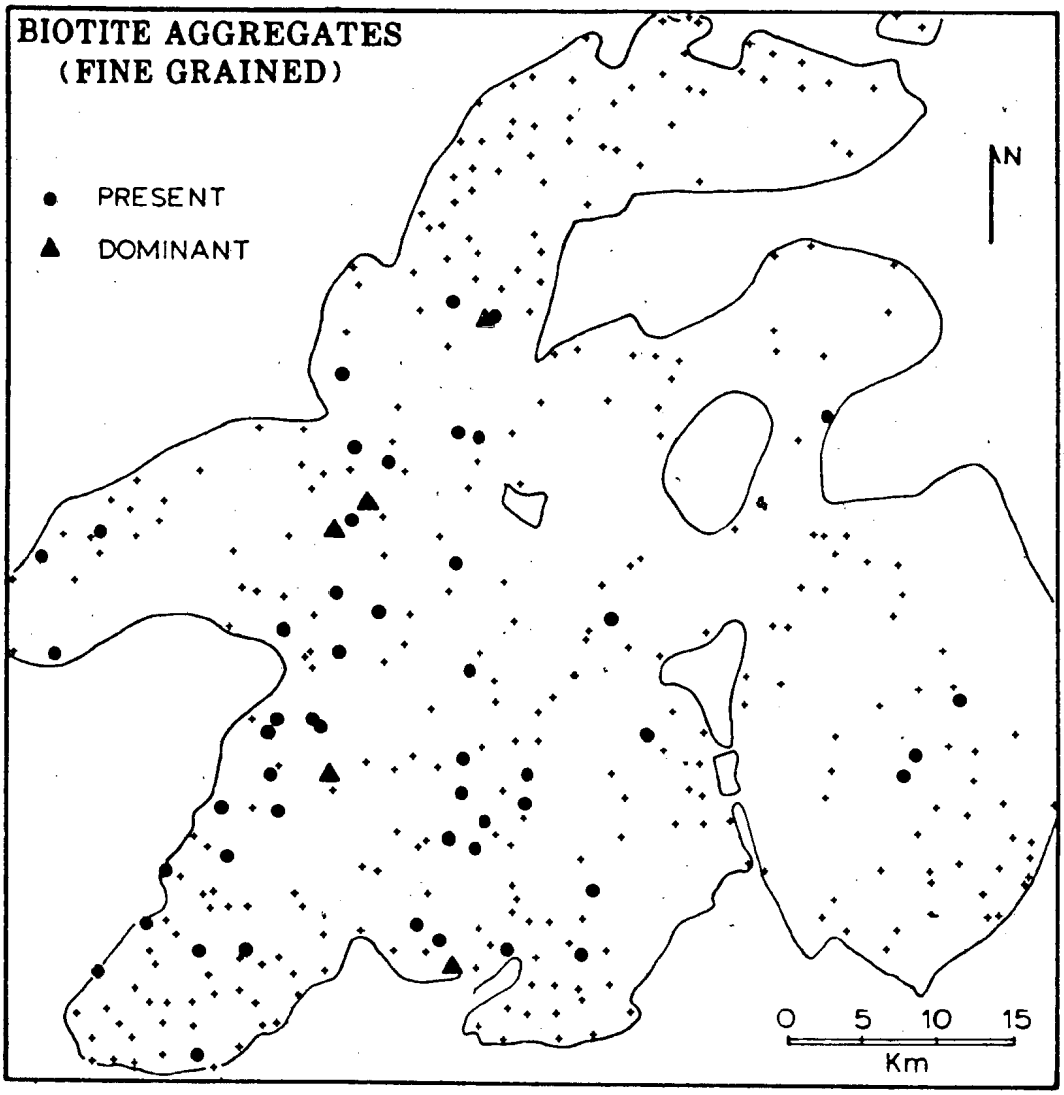

Figure 10: Distribution of fine biotite aggregates in the study area. Crosses represent sample sites in which aggregates were not observed.

In addition to the three main modes of occurrence, small anhedral biotite inclusions are present in the other coarser silicate phases (Plate 3). Skeletal biotite (Plate 11) is common in fine grained aplitic rocks, particularly towards the southern margins of the study area.

In the northwestern granitoids, biotite is pleochroic from light to dark brown. In much of the southeastern granites, dark brown, bronze, and black colours are dominant and are most pronounced near mineralized areas in the Rencontre Lake and Sage Pond granites (Plate 8).

Biotite in the study area is variably altered to chlorite. This feature is described below.

3-2-6 Hornblende

Hornblende generally constitutes less than 1% (when present) and has not been observed in hand specimen. The distribution of samples containing hornblende is shown in Figure 11. This mineral tends to occur in a linear belt on the southeast sides of the Koskaecodde and Mollyguajeck plutons. In addition, it occurs in the more mafic rocks present in the southeastern granites.

Euhedral to anhedral, pleochroic, green hornblende crystals (maximum length 3 mm) occur in association with clusters of coarse biotite grains, opaque minerals and sphene (Plates 12, 13). The hornblende is commonly fresh in appearance.

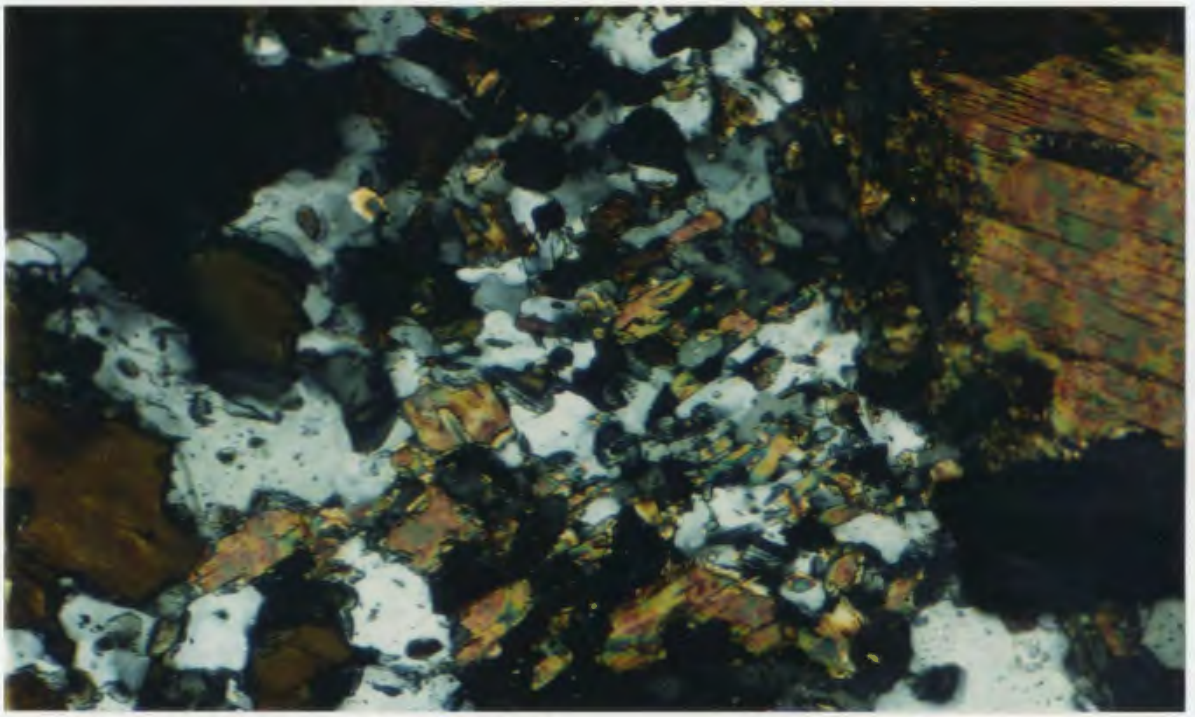

Plate 11: Fine grained skeletal aggregate of biotite, quartz, opaque minerals, and plagioclase, surrounded by coarser biotite. Tolt Granite. LD-017. XNic.

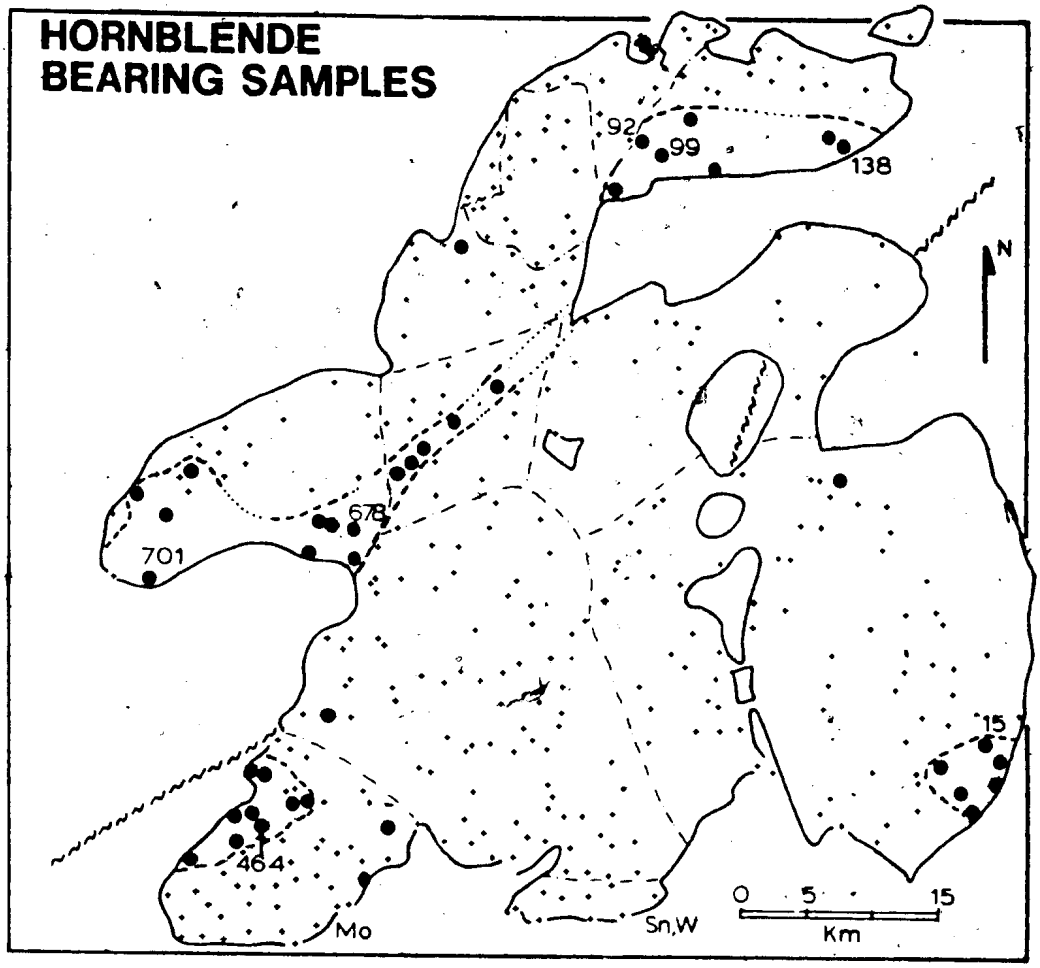

Figure 11: Distribution of samples with minor hornblende in thin section (dots) from the study area. Crosses represent samples in which hornblende was not observed. Dashed lines are internal boundaries of Dickson (1983).

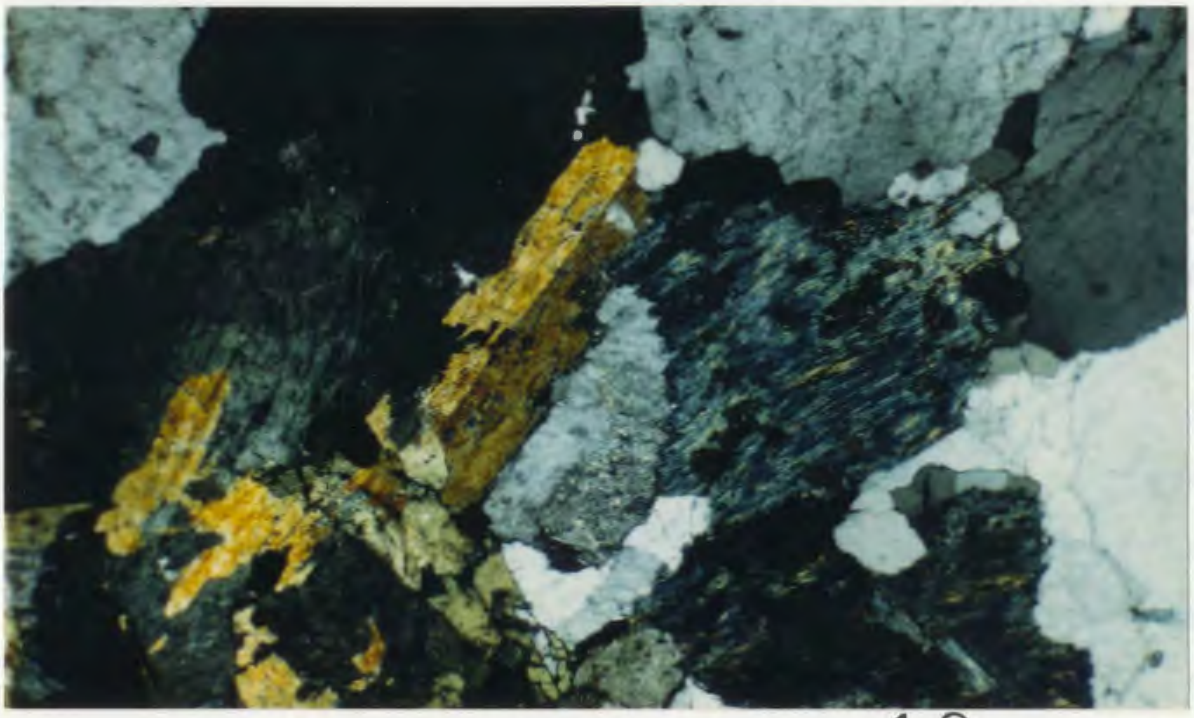

Plate 12: Twinned hornblende crystals associated with strongly chloritized biotite (blue-gray). Relict patches of biotite (brown). Mollyguajeck Pluton. LD-084. XNic.

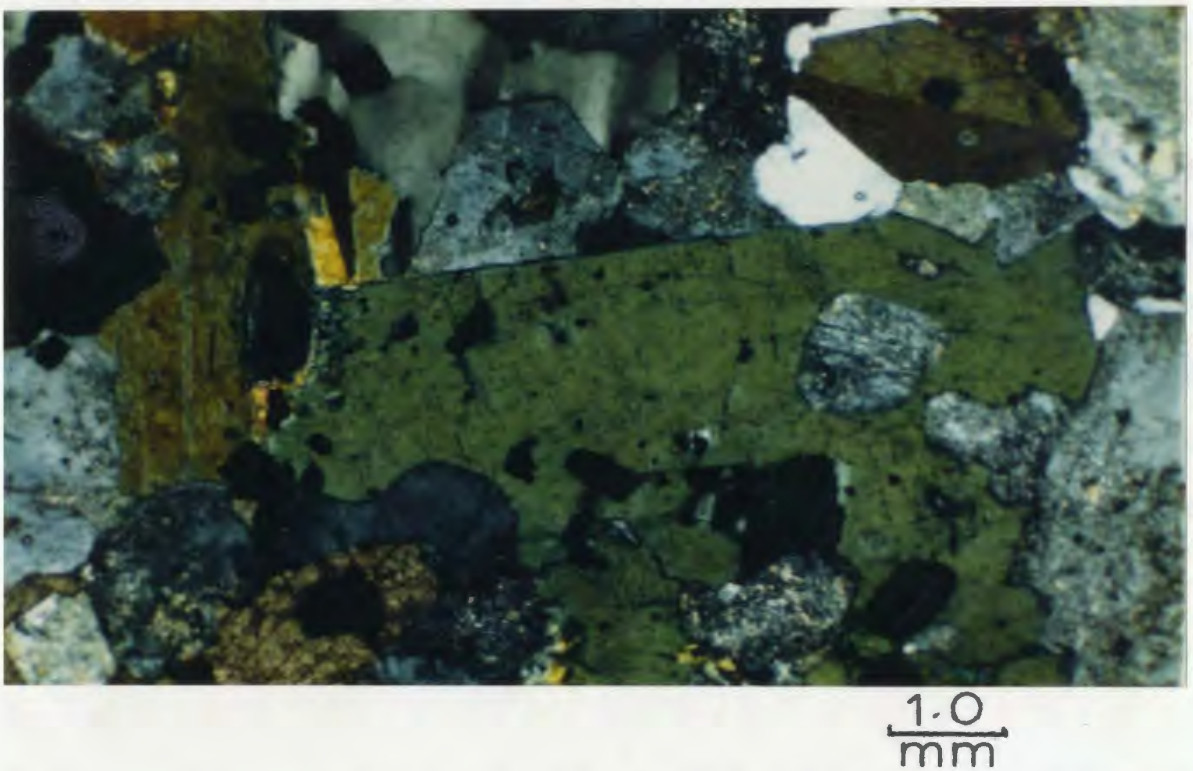

Plate 13: Hornblende crystals in saussuritized plagioclase. Abundant subhedral opaque minerals. Sphene with opaque inclusion at bottom left, and inclusions of plagioclase in hornblende. Mollyguajeck Pluton. LD-103. XNic.

3-2-7 Chlorite

Chlorite is developed as an alteration product after biotite (Fig. 12). In samples with low chlorite content, fine interstitial biotite grains are partly or totally altered and chlorite rims form around coarser biotite grains. As the amount of chlorite increases, individual chlorite lamellae or zones in the biotite are developed. Abundant chlorite is formed by total replacement of fine and coarse biotite grains (Plates 4, 12). Locally, chlorite is developed along kink bands and fractures in the parent biotite. Totally chloritized and completely fresh, coarse biotite grains are found in a single thin section and relict biotite cores may be present even in the most altered samples. Penninite is common in the northwestern granitoids.

The distribution of the chlorite in thin section suggests an inhomogeneity of the chloritization process on the microsopic and larger scales. Nevertheless, in the northwestern granitoids, the relative percentage of chlorite to biotite in thin section is greater, and chlorite is more widespread. There is no correlation between chlorite alteration and areas of tin-tungsten mineralization in the Sage Pond Granite. The Rencontre Lake Granite contains a relatively large proportion of chlorite throughout, although there is no direct correlation with the known areas of molybdenum mineralization.

3-2-8 Muscovite/Sericite

The estimated percentage of muscovite and sericite in thin sections from the study area is presented in Figure 13. Well-formed crystals and

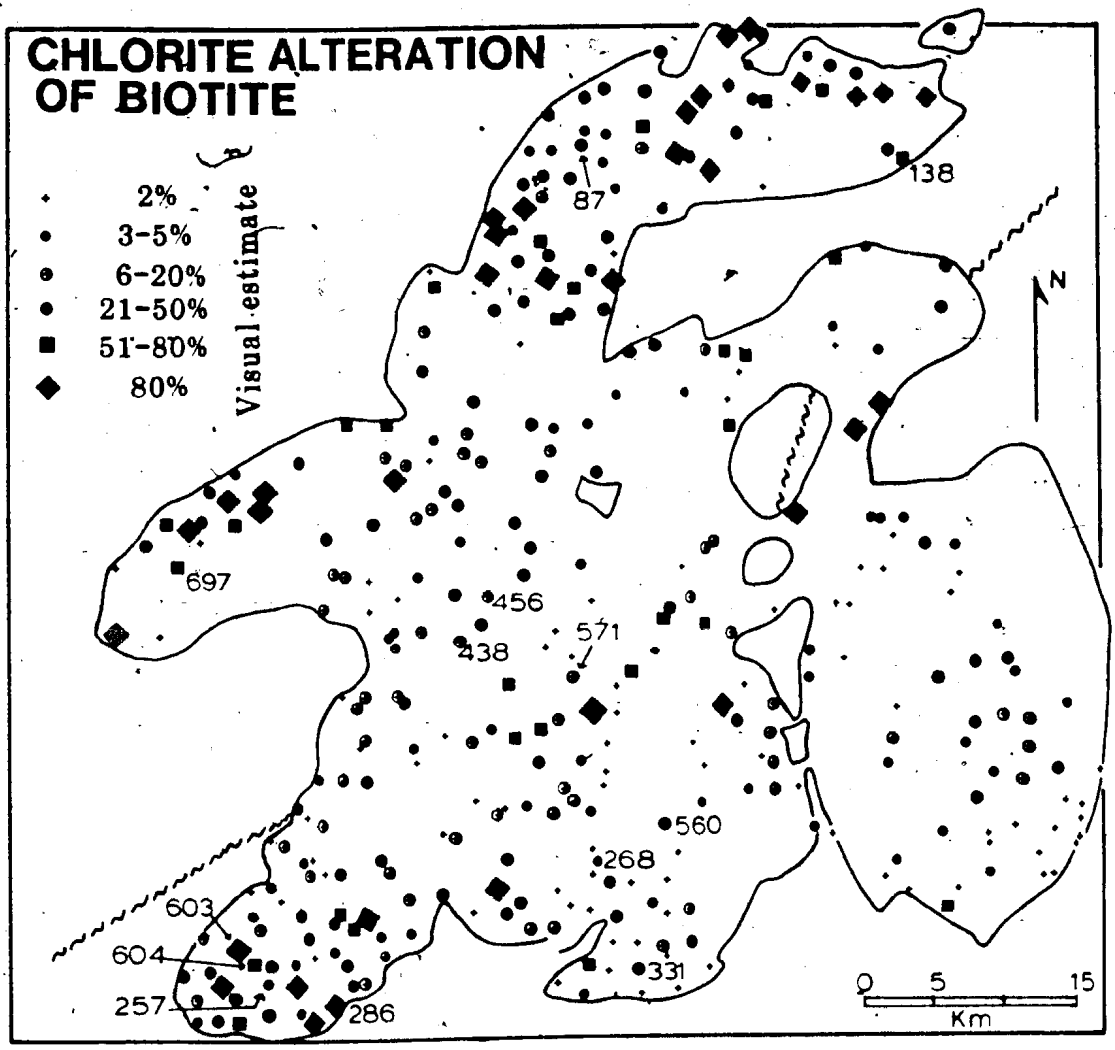

Figure 12: Visual estimate of percentage chlorite alteration of biotite in thin section. The locations of analyzed chlorite samples are also shown.

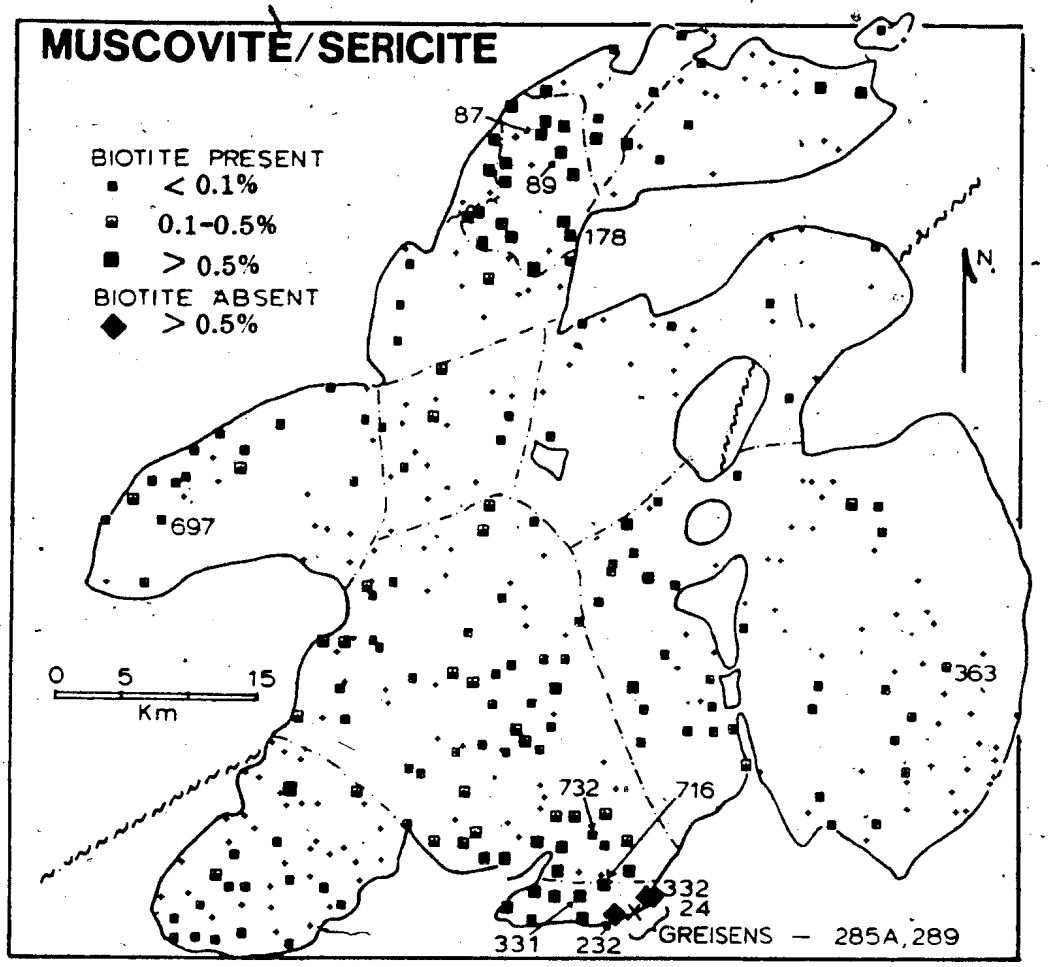

Figure 13: Muscovite/sericite in the study area. This is a visual estimate of the amount of muscovite or coarse sericite grains in thin section. A value of > 0.1% indicates that there are no individual grains present. A value of > 0.5% indicates that there are coarse (> 0.1 mm) flakes in thin section.

flakes of muscovite (to 4 mm) were considered by Dickson (1983) to be a characteristic of the Kepenkeck Granite and occur along with finer interstitial grains. Most of the coarser grains occur marginal to, or within, coarse grained plagioclase crystals (Plate 14) and also occur as overgrowths or alteration products of biotite (Plate 15). Dickson (1983) suggested that some of the coarse muscovite in this granite may be of primary magmatic origin. The finer grained crystals are obviously present as an alteration product after both plagioclase and biotite.

A halo of sericite is present to the north of the greisen-mineralized area in the Sage Pond Granite, and in the Hungry Grove Granite. Coarse flakes up to 3 mm may be present if the sericite content is greater than 0.2 %. The grains in the latter area are obviously secondary, replacing both feldspars and biotite.

Traces of sericite may be present throughout the study area and are commonly associated with turbid alteration of feldspar cores. Sericite is also present as inclusions in quartz, and locally occurs in fractures.

3-2-9 Accessory Minerals

Sphene, apatite, zircon and opaque iron-titanium minerals occur in most samples, and allanite is common. Minor epidote may be present as an alteration of feldspar. Traces of fluorite were noted in the Rencontre Lake Granite; minor tourmaline and fluorite were noted in samples from the Sage Pond Granite.

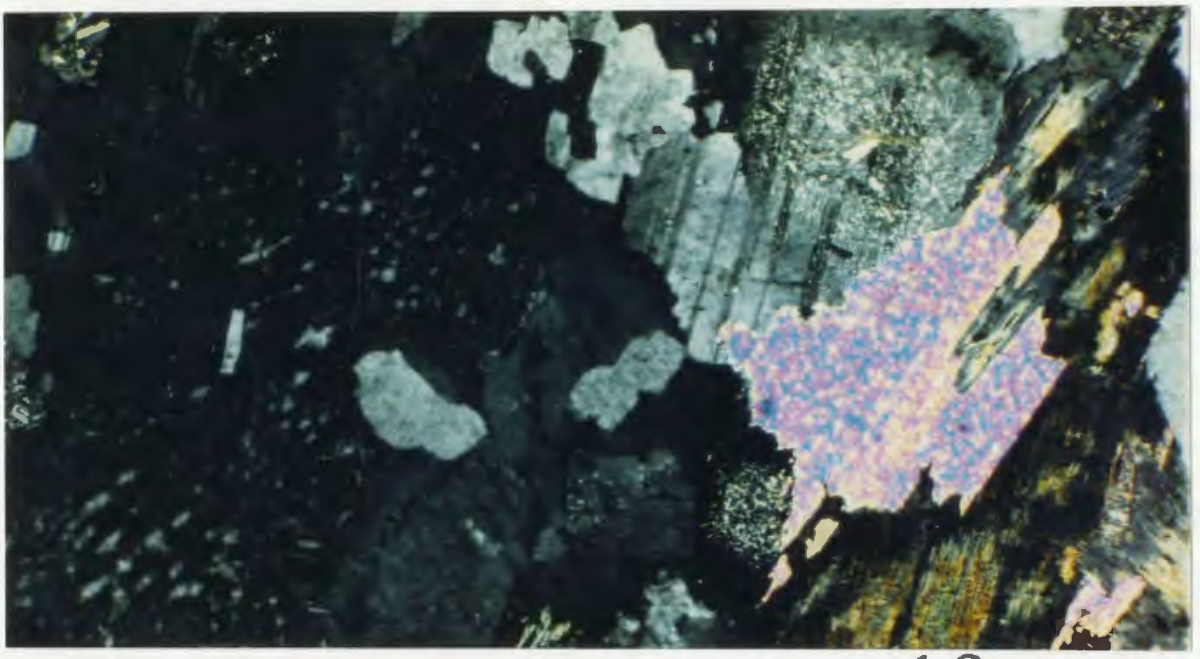

Plate 14: Irregular flake of muscovite associated with strongly chloritized biotite. Altered plagioclase grain above muscovite. Large perthite crystal at left with patch exsolution and with irregularly orientated plagioclase inclusions. Kepenkeck Granite. LD-176. XNic.

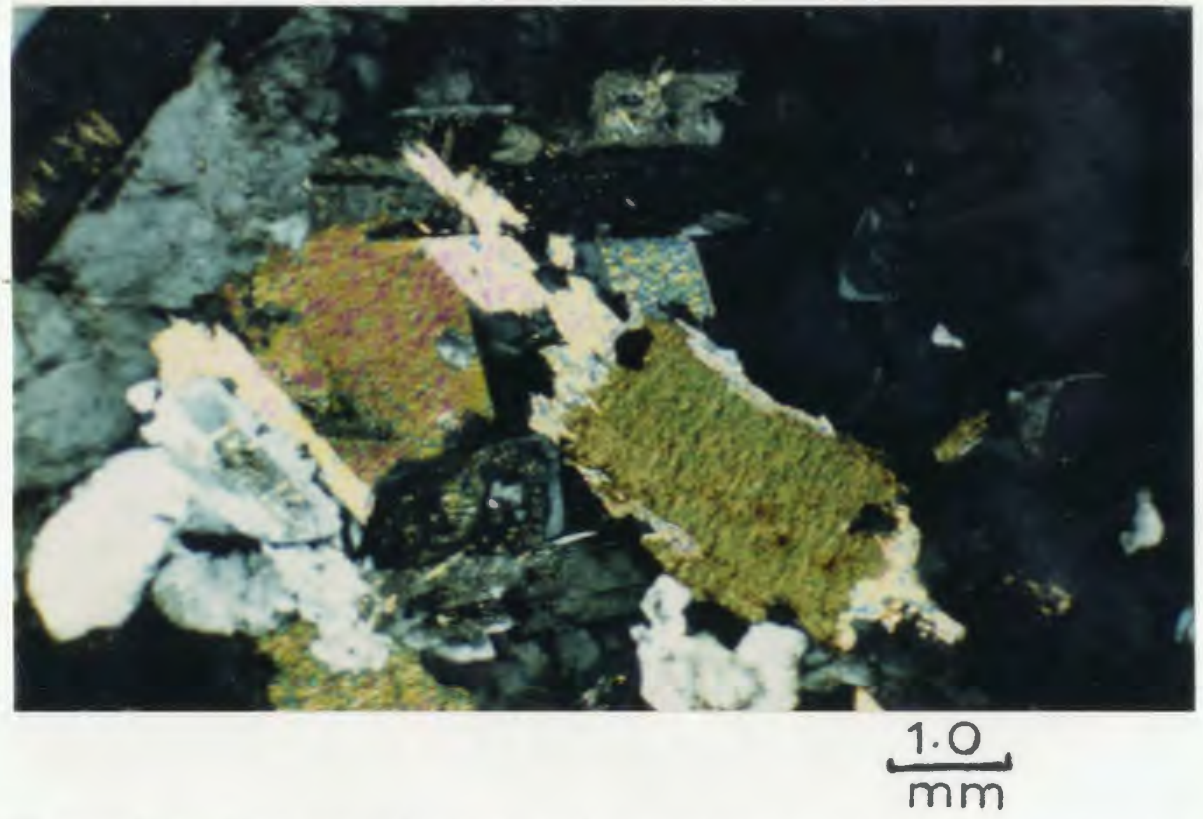

Plate 15: Muscovite rims on biotite and individual flakes of muscovite in perthite and plagioclase. Kepenkeck Granite. LD-095. XNic.

Euhedral to subhedral crystals and local rosettes of sphene, up to 3 mm long (Plate 16), occur throughout the study area and are often associated with coarse grained biotite or biotite-hornblende clusters in the more mafic rocks. These grains may form more than 1% of the thin section. In addition, minor sphene is associated with opaque minerals and chlorite and formed during the alteration of biotite.

Apatite is ubiquitous and forms euhedral crystals up to 1 mm. It occurs as inclusions in feldspars (see Plate 20), biotite and locally in hornblende.

Euhedral zircon crystals, which are commonly zoned, occur in biotite. These zircons are surrounded by typical dark radiation halos (see Plate 18).

Light to dark brown, subhedral allanite crystals up to 3 mm in diameter (Plate 17) were noted in many samples. These crystals are isolated and zoned and appear to be an early crystallizing phase.

Subhedral to anhedral epidote grains up to 1 mm in diameter, occur sporadically in association with strongly altered feldspars and altered biotite. The epidote is more abundant in the Koskaecodde and Mollyguajeck plutons.

Magnetite is the dominant opaque phase in the granite. It generally occurs as euhedral to subhedral grains in association with coarse biotite clusters or biotite-hornblende clusters. Skeletal magnetite may

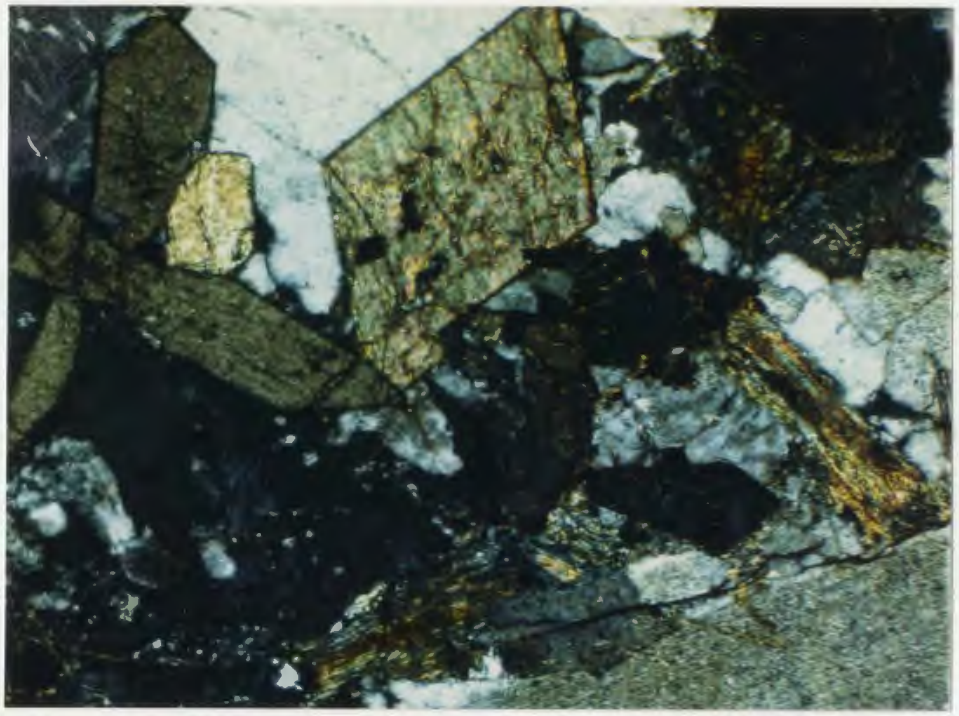

Plate 16: Euhedral sphene crystals in perthite. Chloritized biotite grain present. Hungry Grove Granite. LD-192. XNic.

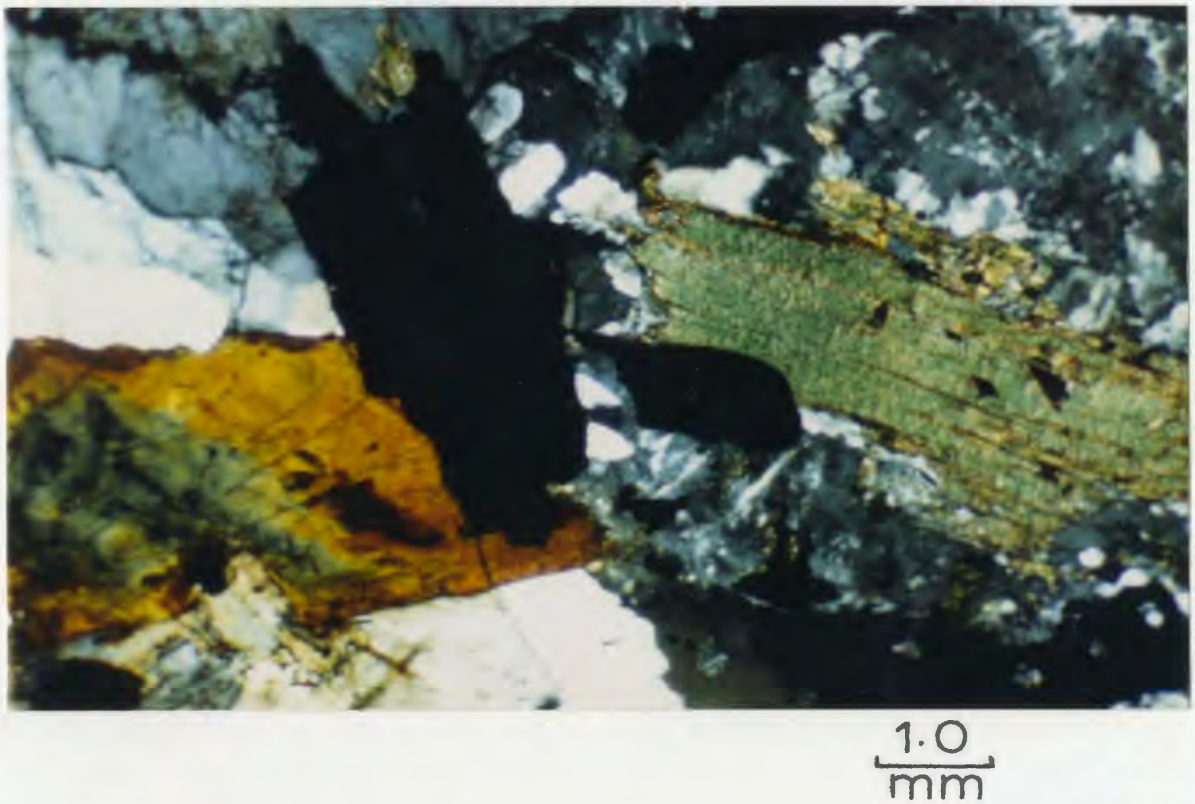

Plate 17: Zoned allanite on left. Bent biotite crystal on right. Meta Granite. LD-165, XNic.

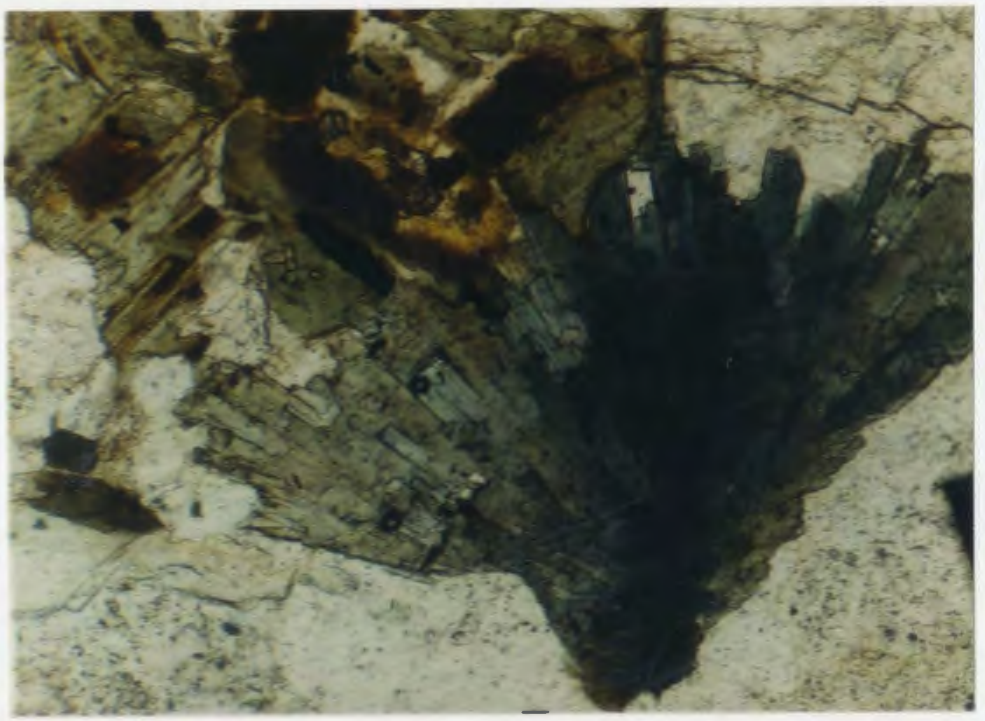

Plate 18: Tourmaline rosette. Sage Pond Granite. Zircon halos are present in biotite at upper left. Host to tourmaline is quartz. LD-712. Plain light.

be present in the southern portions of southeastern granites and fine grained irregular grains are common in biotite, partially altered biotite, and in chlorite pseudomorphs after biotite.

Trace of fluorite is present in several samples from the Rencontre Lake and Sage Pond granites, as irregular interstitial grains and in fractures.

Rosettes of tourmaline (Elbaiite?, Plate 18) were noted in the Sage Pond Granite. Minor tourmaline was also noted in a few thin sections of rock samples from the mineralized area at Rencontre Lake.

3-3 MINERAL CHEMISTRY

3-3-1 Feldspar

Representative microprobe analyses plotted in Figure 14 (data in Appendix C) show the range of feldspar composition.

Plagioclase exhibits a sodium enrichment trend towards areas of mineralization on the southern margin. Sample JT-24 is a 'fresh' granite between mineralized veins collected from drill core in the Sage Pond area, samples 232 and 237 were collected approximately 100 m and 200 m north of the Anesty Greisen respectively. Most alkali feldspar analyses are of almost pure orthoclase and are not presented in Appendix C.

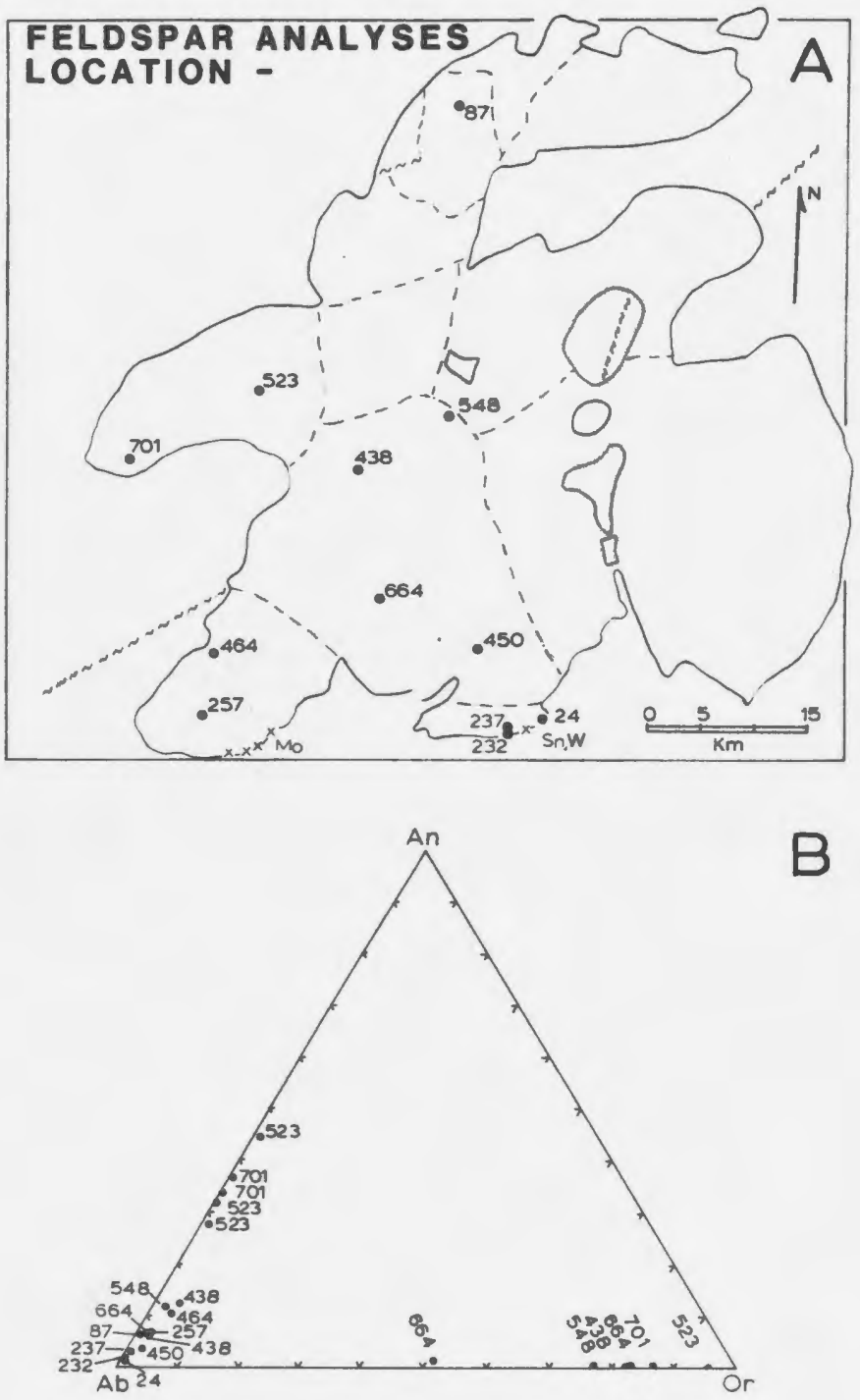

Figure 14: Feldspar analyses from the study area. Dashed lines are internal boundaries of Dickson (1983).
A: Location of analyzed samples.
B: Orthoclase - albite - anorthite plot of representative samples.

3-3-2 Biotite

There is a marked divergence in the correlation trends in the various chemical plots (Figs. 15, 16, 17, 18) between the samples from the Koskaecodde and Mollyguajeck plutons and the samples from the Ackley Granite Suite. These differences occur across a line located 10 to 15 km west of, and subparallel to, the trace of the Dover-Hermitage Bay Fault zone (see Fig. 16). Hornblende constitutes less than 1% of the mafic minerals when present, therefore, the different trends cannot be ascribed solely to the co-existence of hornblende and biotite in the more mafic rocks.

Biotite has a relatively constant composition in the Koskaecodde and Mollyguajeck plutons (SiO_2 range from 60 to 75%) with an annite ratio (FeO(total)/(FeO(total)+MgO)) of 0.45 to 0.51 (Figs. 16, 17). The three samples from the Kepenkeck Granite have annite ratios of 0.50 to 0.52 and plot at the lower end of the trend defined by the southeastern granites. Analyses of core to rim transects in individual biotite grains (Table 5) did not show any consistent trends in the biotite composition in these granitoid rocks.

In the southeastern granites (SiO_2 range from 60 to 79%), annite ratios exhibit strong Fe-enrichment with values from 0.43 to 0.98. The Fe-rich samples occur towards the southern margins and mineralization (Figs. 16, 17). This trend is accompanied by an increase in SiO_2 and a decrease in TiO_2 and MgO in whole rock (Figs. 17, 18). Analyses of core-rim pairs from biotite grains in the southeastern granites (Table

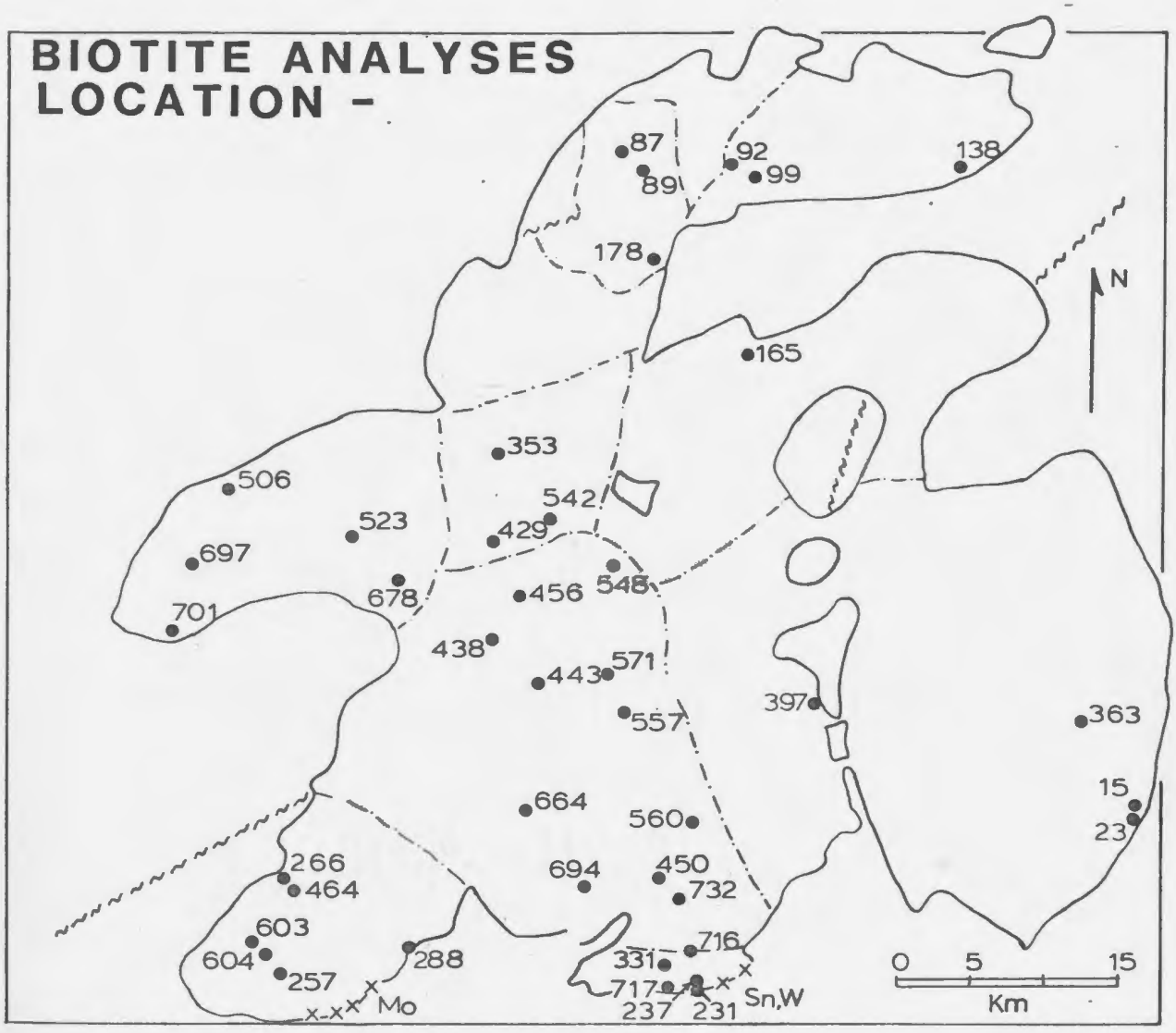

Figure 15: Location of analyzed biotite in the study area. Dashed lines are internal boundaries of Dickson (1983). Samples 231 and 237 preceded by 7040 . Other samples preceded by 220 .

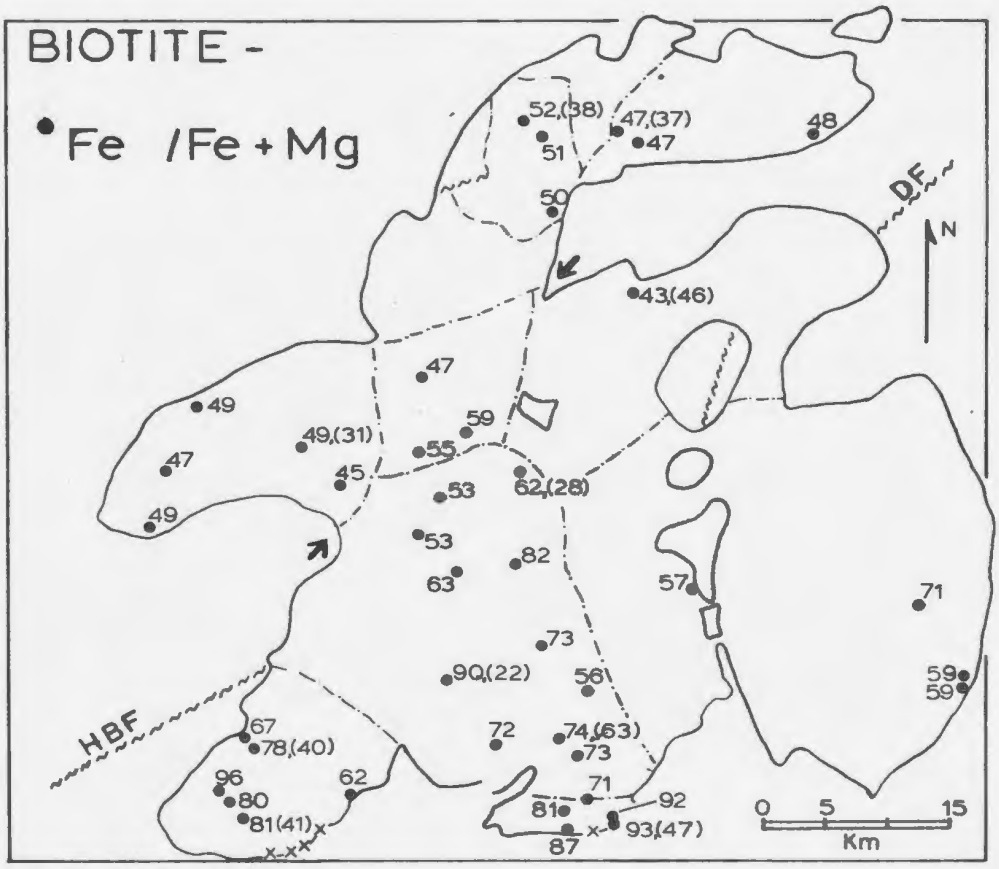

Figure 16: Ratios of Fe(total)/(Fe(total)+Mg) * 100 in biotite. The numbers in brackets are ferric/ferrous ratios from selected biotite samples (refer to Table 6). Dashed lines are internal boundaries of Dickson (1983). HBF - Hermitage Bay Fault, DF - Dover Fault. Arrows indicate position of boundary between areas with biotite showing different petrochemical trends.

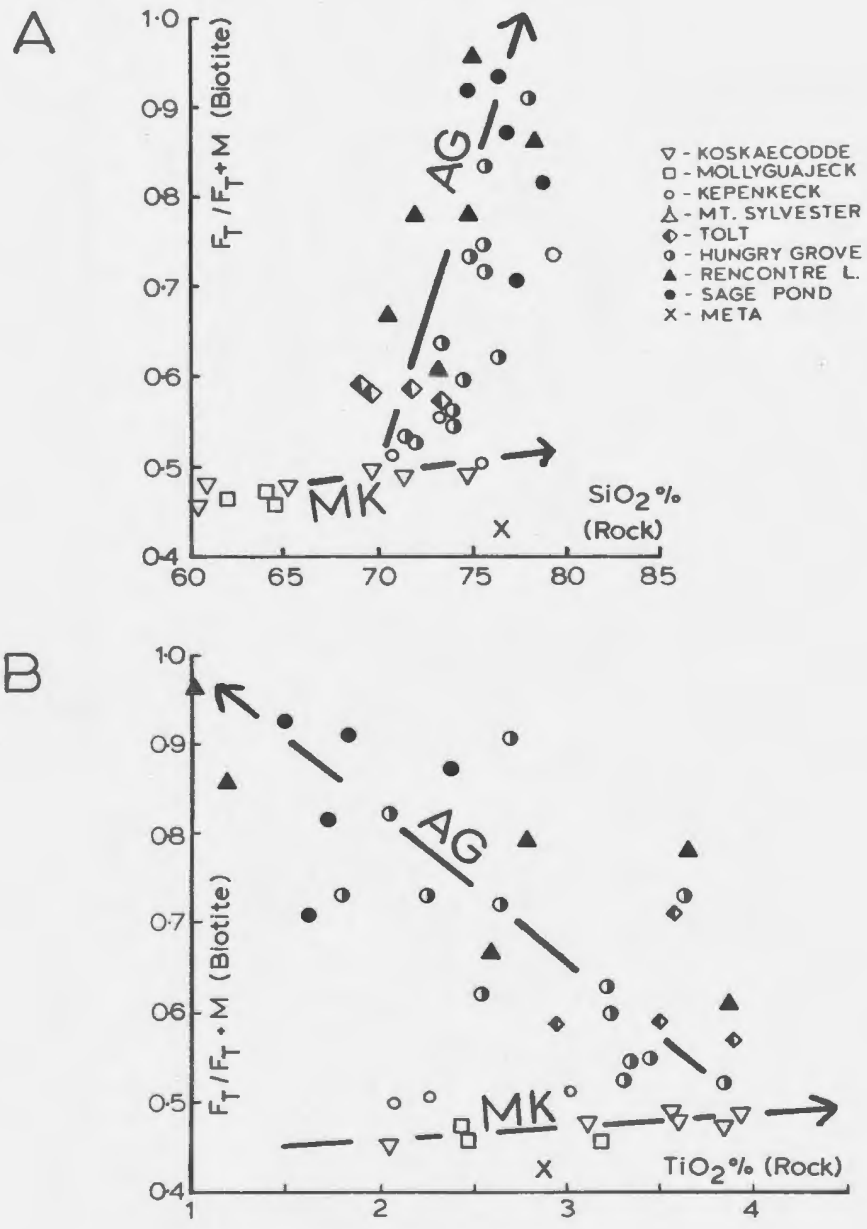

Figure 17: Bivariate plots of whole rock analyses and Fe/Fe+Mg in biotites.
A: Fe(total)/(Fe(total)+Mg) versus SiO_2.
B: Fe(total)/(Fe(total)+Mg) versus TiO_2. MK - trend observed in the Mollyguajeck and Koskaecodde plutons, AG - trend in Ackley Granite Suite.

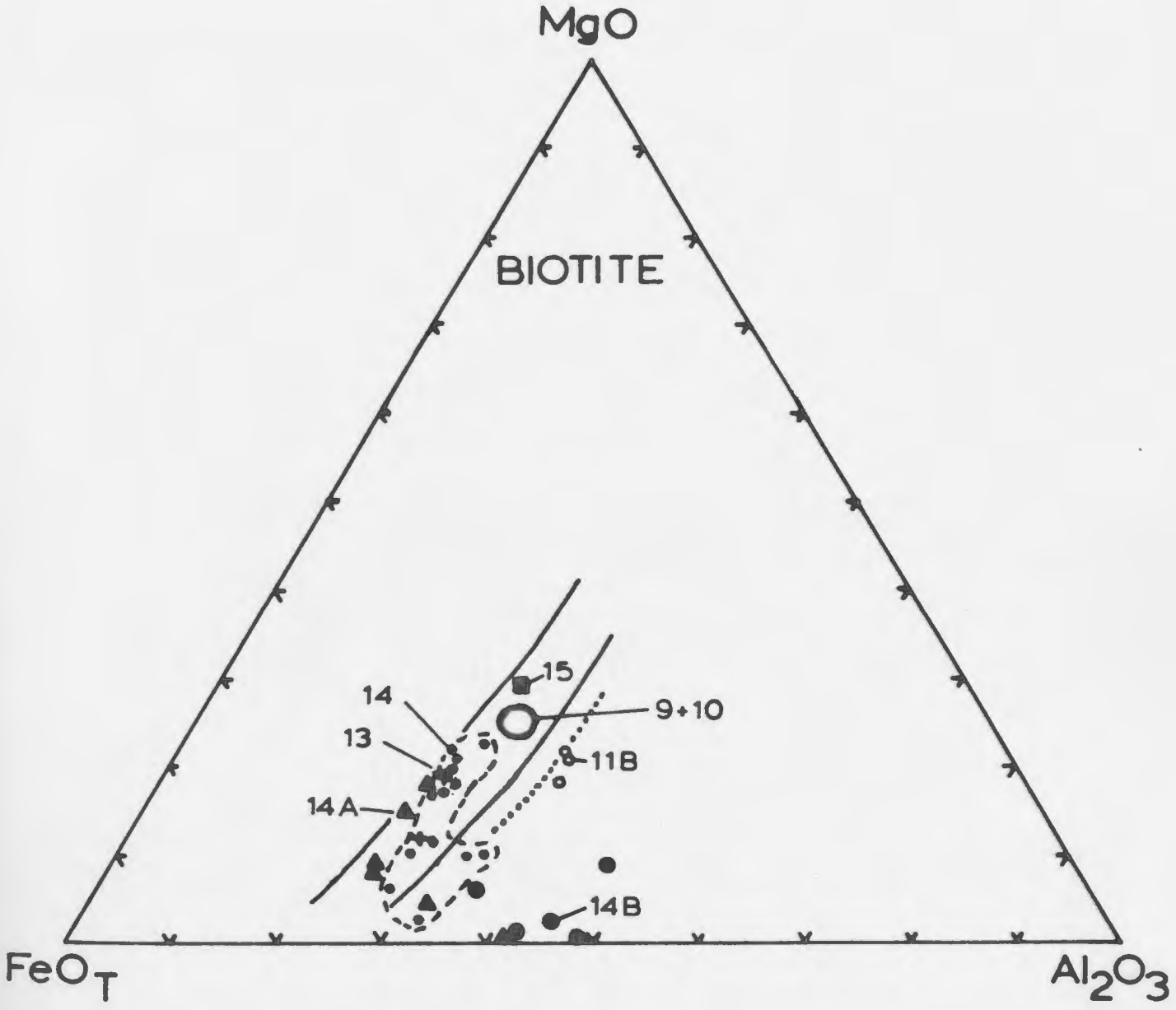

Figure 18: MgO - FeO - Al_2O_3 plot for analyzed biotite from study area. Solid lines outline field of igneous biotite drawn by Nockolds (1947). b/bm is dividing line between field of biotite and biotite-muscovite bearing granites in northern Portugal (de Albuquerque, 1975). 9 - Koskaecodde; 10 - Mollyguajeck; 11B - Kepenkeck; 13 - Tolt; 14 - Hungry Grove; 14A - Rencontre Lake; 14B - Sage Pond; 15 - Meta.

5) show slight increases in FeO and Al_2O_3 and a slight decrease in TiO_2 towards the crystal rim with no consistent trend observed in MgO.

Most of the samples plot within the field of normal magmatic biotites as defined by Nockolds (1947) on the Mgo-FeO(total)-Al_2O_3 plot in Figure 18, with the samples from the Koskaecodde and Mollyguajeck plutons in a tight grouping. The three samples from the Kepenkeck Granite are relatively enriched in Al_2O_3 and plot in the field of muscovite-biotite bearing granites as defined by de Albuquerque (1975). The compositional trend in the biotites of the southeastern granites is also well displayed in this diagram. Samples from the southern portion of the Hungry Grove Granite, the Sage Pond Granite, and sample 604 from the Rencontre Lake Granite (this sample is partially chloritized) plot to the Al_2O_3 side of the magmatic trend. The biotites from the Rencontre Lake Granite and are slightly enriched in iron relative to the other samples in the field of normal igneous biotite.

Ferric/ferrous ratios in biotite were determined on ten pure biotite separates (Table 6, Figs. 15 and 16). The ferric/ferrous ratios of the molybdenum mineralized Rencontre Lake Granite and the tin-tungsten mineralized Sage Pond Granite are comparable. Insufficient data was collected to define significant trends.

The fluorine content of biotite from the ten selected samples (Table 6) is presented in Figure 19. Biotites from the Hungry Grove and Sage Pond granites contains between 1.67 and 1.96% F. In contrast, the

Table 5: Core/Rim compositional variation (microprobe analysis) in biotite (cation proportions). Sample locations on Figure 15.

Sample No.		Si	Ti	Al	Fe	Mn	Mg	Na	K
JT231	Core	43.01	1.04	24.89	15.96	1.23	1.28	0.57	11.97
"	Rim	42.12	0.91	25.07	17.41	1.19	1.25	0.06	11.91
JT237	Core	38.62	1.61	22.32	22.68	1.16	1.89	0.33	11.37
"	Mid	39.20	1.56	22.54	21.83	1.36	1.79	0.47	11.21
"	Rim	39.64	1.30	23.26	21.08	1.27	1.97	0.18	11.24
220226	Core	37.74	2.45	13.76	23.31	0.59	11.54	0.35	10.24
"	Rim	37.50	2.34	14.03	23.14	0.64	11.52	0.16	10.62
220332	Core	42.56	0.98	22.20	13.69	0.44	8.21	0.60	11.32
"	Rim	41.38	1.01	22.43	13.99	0.34	8.63	0.76	11.44
220353	Core	36.35	2.62	15.38	16.59	0.57	17.89	0.21	10.31
"	Mid1	37.36	2.72	15.18	15.91	0.47	17.82	0.00	10.52
"	Mid2	37.34	2.74	15.19	16.13	0.26	18.19	0.16	9.99
"	Mid3	37.37	2.64	15.48	15.98	0.49	18.26	0.25	9.47
"	Mid4	36.63	2.80	15.22	16.36	0.50	17.59	0.25	10.57
"	Rim	35.49	2.6	15.73	16.67	0.55	18.11	0.23	10.53
"	Mid1	37.18	2.81	15.44	15.63	0.49	17.83	0.09	10.47
"	Core	37.46	2.67	15.75	15.34	0.51	17.78	0.34	10.06
220438	Core	37.81	3.03	13.72	17.28	0.62	15.76	0.33	11.42
"	Rim	37.62	2.66	14.85	17.17	0.65	16.01	0.22	10.67
220523	Core	36.36	3.06	16.17	17.02	0.04	16.43	0.23	10.65
"	Rim	36.93	2.21	16.97	16.16	0.60	17.40	0.06	9.61
220701	Core	36.43	2.31	16.83	16.07	0.19	16.73	0.19	11.21
"	Mid1	36.96	2.50	16.74	16.04	0.26	16.04	0.08	11.30
"	Rim	37.05	1.89	16.40	15.88	0.37	17.40	0.19	10.78

Table 6: Analyses of biotite separates. Sample locations on Figure 15. Analyses as per Appendix B-3.

Sample No.	87	92	165	237*	257**	450	464***	523	548	664
Major Oxides (Weight Percent)										
SiO_2	35.9	35.8	36.5	39.3	29.6	36.1	34.7	36.9	37.9	35.8
Al_2O_3	18.0	15.5	14.9	19.2	15.8	14.9	12.7	14.7	13.1	16.1
Fe_2O_3	5.51	5.40	5.95	7.27	10.51	10.52	9.03	4.66	5.71	5.82
FeO	14.55	14.54	12.85	15.34	25.89	16.61	22.36	14.88	20.19	26.83
MgO	9.06	12.23	13.43	1.18	3.10	4.80	5.09	11.18	8.09	1.80
CaO	0.10	1.14	0.60	0.10	0.00	0.26	1.08	0.68	0.24	0.06
Na_2O	0.12	0.09	0.20	0.30	0.11	0.19	0.16	0.11	0.17	0.16
K_2O	8.92	7.84	7.06	8.84	1.38	7.54	5.25	8.60	7.96	7.58
TiO_2	2.47	2.89	2.62	2.03	2.25	2.80	3.56	3.50	2.97	2.58
MnO	0.88	0.42	0.88	1.28	1.20	1.06	0.67	0.67	0.81	0.88
P_2O_5	0.02	0.13	0.21	0.00	0.00	0.01	0.09	0.20	0.13	0.04
LOI	4.41	4.53	5.36	3.79	9.11	4.92	6.15	3.74	4.74	4.70
TOTAL	99.9	100.5	100.6	98.6	99.0	99.5	100.8	99.8	100.0	99.7
F (ppm)	7710	3695	17012	19575	3198	17332	4405	5070	19575	16690

* Sample preceeded by 7040___ . All other samples preceeded by numbers 220___.
** Strong chloritization of sample.
*** Moderate chloritization of sample.

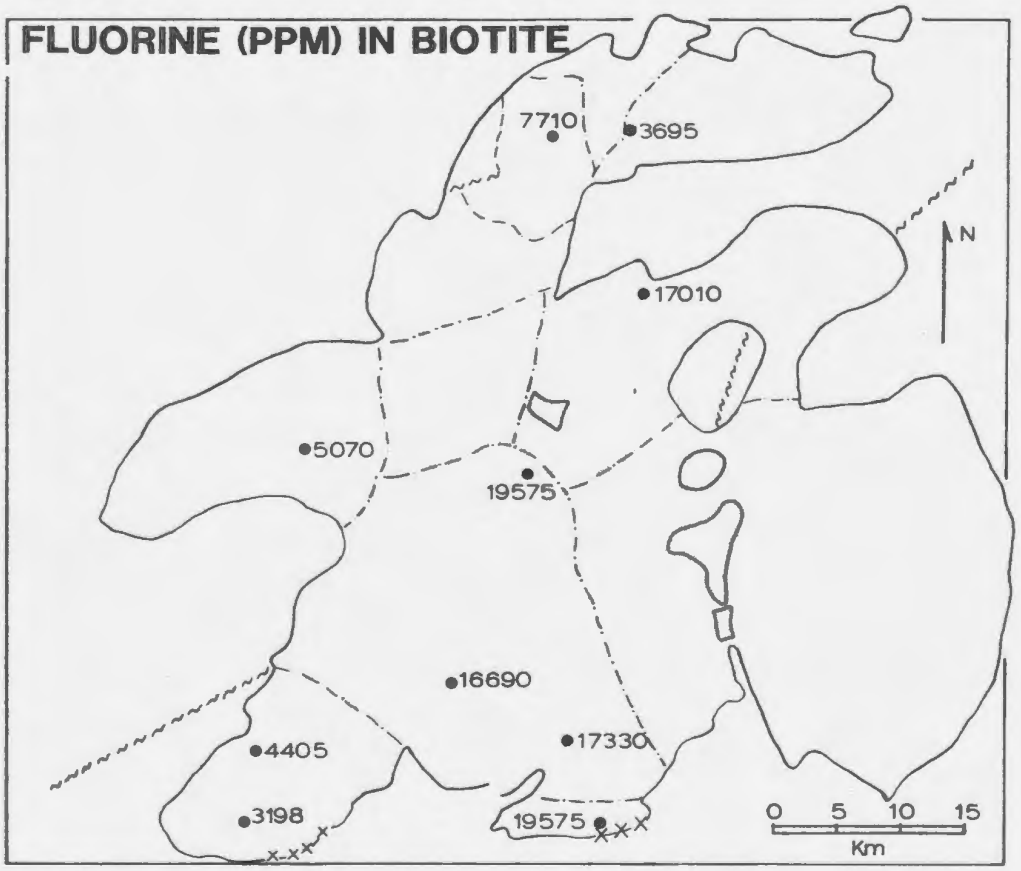

Figure 19: Distribution of fluorine (ppm) in biotite from selected samples in the study area. Sample locations shown on Fig. 15.

fluorine content of biotite in the Rencontre Lake Granite is much lower (0.31 to 0.44%); the biotites from this area are chloritized (Table 6, and see Fig. 20), The fluorine content of biotite in the northwestern granitoids ranges from 0.37 to 0.775%.

3-3-3 Hornblende

Analyzed hornblende crystals from the southeastern granites have a higher iron content than those from the northwestern granitoids (see Appendix C).

3-3-4 Chlorite

Chlorite analyses (Fig. 20) indicate a trend of iron enrichment in the chlorite parallel to that observed in biotite. The correlation coefficient of FeO(tot)/(FeO(tot)+MgO) between coexisting chlorite and biotite is 0.98.

3-3-5 Muscovite/Sericite

Muscovite analyses (Fig. 21A) show significant iron and magnesium and plot towards the celadonite position in the $MgO-Al_2O_3-FeO$ diagram. Two of the samples from the Kepenkeck Granite plot in the field of predominantly primary plutonic muscovite as outlined by Miller et al. (1981) in a plot of Ti-Mg-Na cation ratio (Fig. 21B). However, two samples from muscovite-bearing topaz greisen in the Sage Pond Granite also plot in the field of plutonic muscovite.

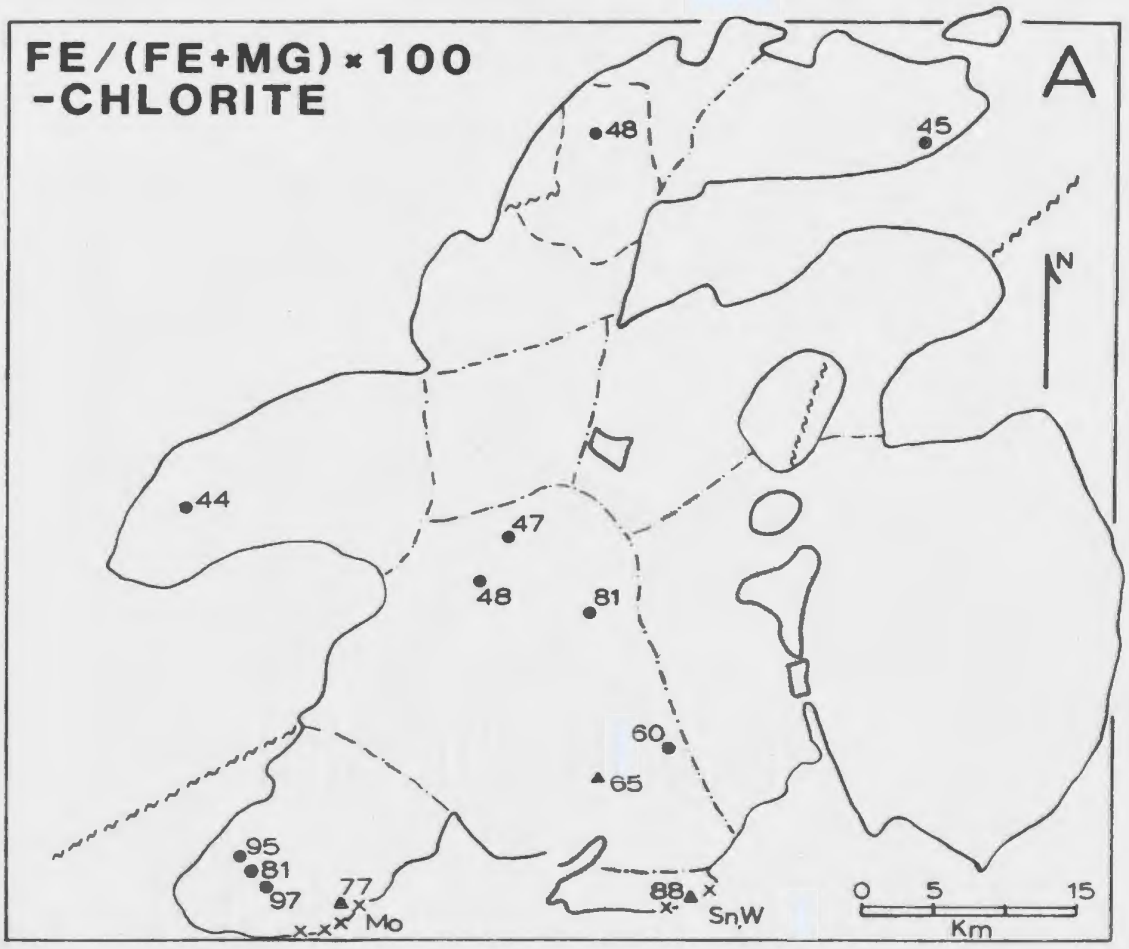

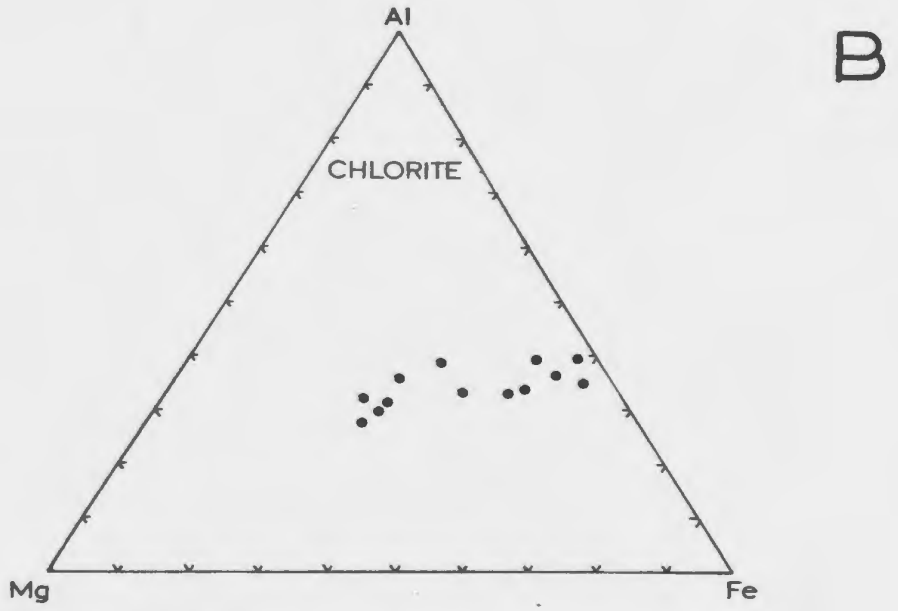

Figure 20: Chlorite analyses. Sample numbers shown on Figure 12.
A: Distribution of Fe/(Fe(total)+Mg).
B: Plot of Al - Fe - Mg cation proportions.

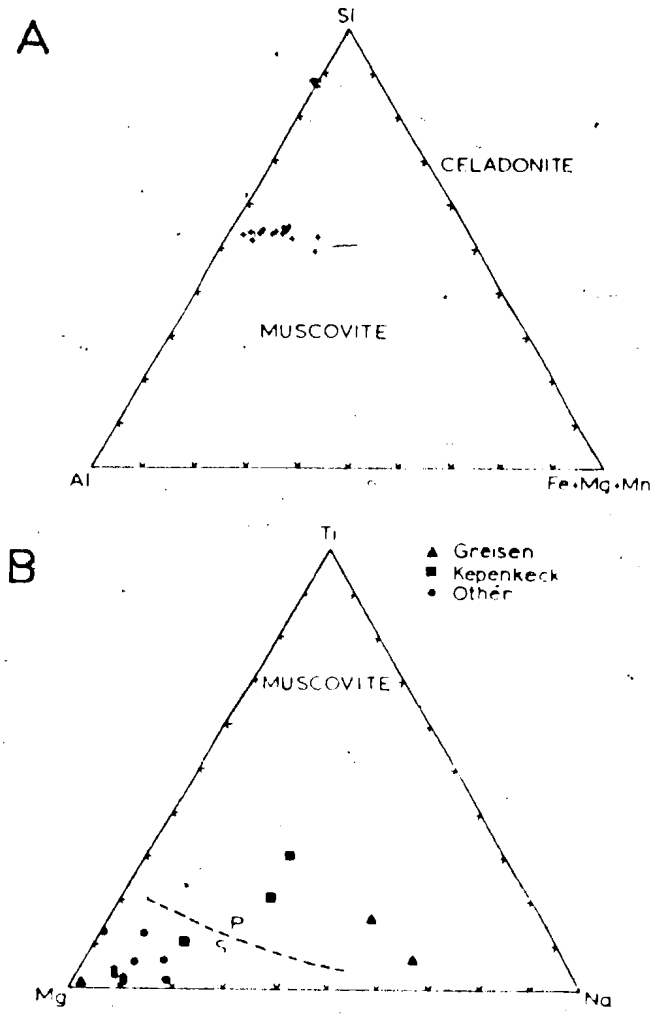

Figure 21: Muscovite analyses from the study area. Location of analyzed samples shown on Figure 22.
A: Plot of cation proportions Si - Al - (Fe+Mg+Mn).
B: Plot of cation proportions Ti - Mg - Na. P and S refer to primary and secondary composition fields suggested by Miller et al. (1981).

3-4 INTERPRETATION

3-4-1 Primary Magmatic Textures

The dominant textural features observed in the post-tectonic granitoid rocks are interpreted as resulting from primary magmatic crystallization.

The following observations indicate a relatively rapid crystallization history at high crustal levels near the southern contact in the Rencontre Lake and Sage Pond granites and in the southern part of the Hungry Grove Granite: a) the abundance of fine to medium grained granite and associated aplite and microgranite; b) the presence of miarolitic cavities; c) seriate and irregular grain boundary contacts; d) graphic and myrmekitic granophyric intergrowths; e) strong resorption of quartz crystals; f) general lack of well formed crystals or grain boundaries; g) the local presence of dendritic magnetite and biotite crystals; and h) the abundance of inclusions of various phases in K-feldspar. All of these features may indicate quenching of a predominantly liquid magma (Hibbard, 1965, 1979; Cherry and Trembath, 1978; Vernon, 1986). A progressive coarsening in grain size northwards in the Hungry Grove Granite and eastwards in the Tolt Granite may be related to a progressively longer cooling history in the latter areas, which may in turn be interpreted to relate to progressively deeper levels of crystallization. The slower cooling at deeper levels may relate to higher heat flux from below, or thermal and pressure-insulation at deeper levels due to crystallization of the carapace of the magma chamber. Discrete phenocryst phases have not been identified

in the coarser northern portions of the Hungry Grove Granite (although their early presence may be hidden by textures related to the later stages of crystallization) and it is impossible to assess their potential contribution to a process of crystal-liquid fractional crystallization.

There is a general lack of miarolitic cavities in the northwestern granitoids, in the northern part of the Hungry Grove Granite, and in the east part of the Tolt Granite. This suggests that these granites crystallized at deeper levels relative to the southern granites (Hungry Grove, Rencontre Lake, and Sage Pond). However, the northern Hungry Grove and the eastern Tolt granites also contain aplite, microscopic, fine grained intergranular material and locally, most of the textural features outlined above. The presence of a narrow thermal aureole in the northwest (Swinden and Dickson, 1981) also indicates emplacement at relatively high crustal levels.

The widespread occurrence of inclusions in alkali feldspar and the common presence of graphic intergrowths on the margins of the alkali feldspar crystals, particularly in the southwestern granites, are indicative of relatively rapid crystal growth (Hibbard, 1965, 1979). It is also possible that some of the dendritic biotite aggregates may represent a quench texture.

The sequence of crystallization of the various phases in the magma chamber and possible areal variations in relative appearance of phases is difficult to assess with certainty from textural evidence. Biotite

is present locally as small inclusions in quartz and remained a stable phase throughout the crystallization of the pluton. Alkali feldspar exhibits abundant evidence of late crystallization. However, it is impossible to determine the relative timing of the appearance of this mineral on the liquidus. Similarly, the relative timing of the appearance of plagioclase cannot be determined.

The distribution of hornblende indicates: a) that mineral isopleths can be drawn within a magma chamber, or b) that separate intrusive phases are present.

The microscopic and textural features of the post-tectonic granitoid rocks in the study area indicate intrusion at high crustal levels with progressively shallower levels exposed towards the southern margin of the southeastern granites (Whalen, 1976, 1980, 1983; Dickson, 1983). This southern margin represents a rapidly cooled or quenched carapace.

3-4-2 Subsolidus Recrystallization Textures

Perthite formation, microclinization, albitization, sericitization and saussuritization of alkali feldspar and plagioclase, recrystallization of biotite and alteration of biotite to chlorite, and less commonly to muscovite, are all features of subsolidus recrystallization which are observed. The presence of an H_2O-rich fluid phase at submagmatic temperatures is essential to permit recrystallization and nucleation of the secondary mineral phases. Thus,

the abundance and distribution of secondary mineral phases and textures provide an index to the relative activity of the fluids which migrated through the rocks after solidification of the magma chamber.

Microcline is the dominant alkali feldspar in the Koskaecodde and Mollyguajeck plutons and probably formed as an inversion product from orthoclase. This feature, coupled with the presence of abundant biotite aggregates in the eastern part of the Koskaecodde pluton, suggests that these plutons may have suffered a relatively low-temperature metamorphic event prior to, or contemporaneous with, the intrusion of the Ackley Granite Suite.

Perthite exsolution occurs throughout the study area. In the southeastern granites, lamellae become progressively coarser, and more abundant towards the southern part of the Hungry Grove Granite and in the Rencontre Lake and Sage Pond granites. Up to 20% coarse patches of albite may be exsolved in the latter two granites. This texture (along with the Na-rich albite compositions) is indicative of the large and widespread sub-solidus migration and reaction of fluids with the primary mineral phases in the southeastern granites and also indicates that fluid reactions were progressively more advanced to the south.

The normal interpretation of fine grained biotite aggregates is that they result from secondary recrystallization of primary biotite during low temperature hydrothermal alteration. The widespread occurrence of biotite aggregates, the lack of association of biotite aggregates with mineralization and areas exhibiting the more pronounced

physical evidence for subsolidus fluid reactions, the location of many aggregates in matrix material, and the local dendritic and poikilitic biotite texture may suggest an origin due to rapid crystallization during final quenching of the magma for some of this biotite texture. However, the location of abundant biotite aggregates in the eastern part of the Koskaecodde Pluton supports the suggestion by Dickson (1983) that the textures in this area may have developed due to contact metamorphism as a result of the Hungry Grove Granite intruding the cooled Koskaecodde Pluton.

A fluid phase was essential to the formation of the greisen veins and vein swarms in the Sage Pond Granite. The halo of microscopic sericite alteration identified for a distance of up to 20 km to the north of the mineralized area (Fig. 13) could possibly be related or independant of this event (i.e. a fluid related to magmatic devitalization and a second related to mineralization). It should be noted that sericite alteration is not extensively developed throughout the Rencontre Lake Granite (Mo mineralization) although a zone of less than 1 km^2 surrounding the Wyllie Hill prospect has abundant secondary sericite (Whalen, 1976).

Chloritic alteration of biotite appears to be more abundant in the northwestern granitoids, and is also concentrated in the Rencontre Lake Granite. There is no spatial association of chlorite alteration with the mineralized areas. Chlorite growth in kink bands in biotite indicates that chlorite alteration at least in part post-dated fracturing of biotite.

Alteration of plagioclase is concentrated in the northwestern granitoids and particularly in the Koskaecodde and Mollyguajeck plutons, which may in part reflect the more calcic compositions in this area. The local presence of extremely altered euhedral cores which have sharp boundaries with surrounding weakly altered plagioclase may suggest that the cores reacted with a fluid phase prior to final crystallization of the magma.

Fluorite and tourmaline, which are present near the southern margin of the study area, are generally considered to form from a subsolidus fluid phase (cf. Manning and Pichivant, 1985).

In summary, the Koskcaecodde and Mollyguajeck plutons exhibit greater evidence of regional metamorphism and subsolidus reaction with fluids than the Ackley Granite Suite. This is indicated by chloritization and recrystallization of biotite, alteration of plagioclase, perthite formation and microclinization. Muscovite in the more aluminous rocks of the Kepenkeck Granite may by secondary. The southeastern granites exhibit a coarsening and increase in abundance of perthite texture to the south, which can be interpreted to indicate an increase in activity of fluids towards the roof of the Ackley Granite Suite in this area. The sericite halo surrounding the tin-tungsten mineralization may be indicative of the importance of these fluids to the mineralizing process. Finally the absence of a large sericite halo in association with molybdenite mineralization in the Rencontre Lake Granite and the presence of chlorite alteration in the latter unit may relate to a fundamental difference in the metallogenic evolution

(particularly fluid development) of the two mineralized areas on the southern margin of the Ackley Granite Suite.

3-4-3 Deformation Textures

Perhaps the most important aspect of the granitoid rocks in the study area is the absence of penetrative schistosities or lineation textures which relate to any regional deformation. In addition, the Ackley Granite Suite cuts across the trace of the major tectonic boundary between the Avalon and Gander tectonostratigraphic terranes, and no evidence of strong fracturing or of mylonitic textures has been reported. Quartz vein swarms and minor brecciation of the Hungry Grove Granite were noted by the author along the trace of the Dover-Hermitage Bay Fault at the north end of Big Blue Hill Pond (Fig. 4). However, these deformation features are weak and may indicate very minor adjustment on this boundary after granite crystallization. The granitoid rocks in the study area display abundant microscopic evidence for post crystallization fracturing and minor deformational adjustments.

Late stage fractures are common and are locally filled with sericite. Kink bands were noted locally in plagioclase and in biotite (Plate 21) (Plates 20). Quartz invariably displays weak undulose extinction which may develop into deformation lamellae in the Koskaecodde and Mollyguajeck plutons. It is possible to interpret these textures as resulting from stress related to phase transitions or crystallization in the deeper layers of the the pluton, or to subsolidus fluid pressures in the upper parts of the granite, or to mild regional deformation.

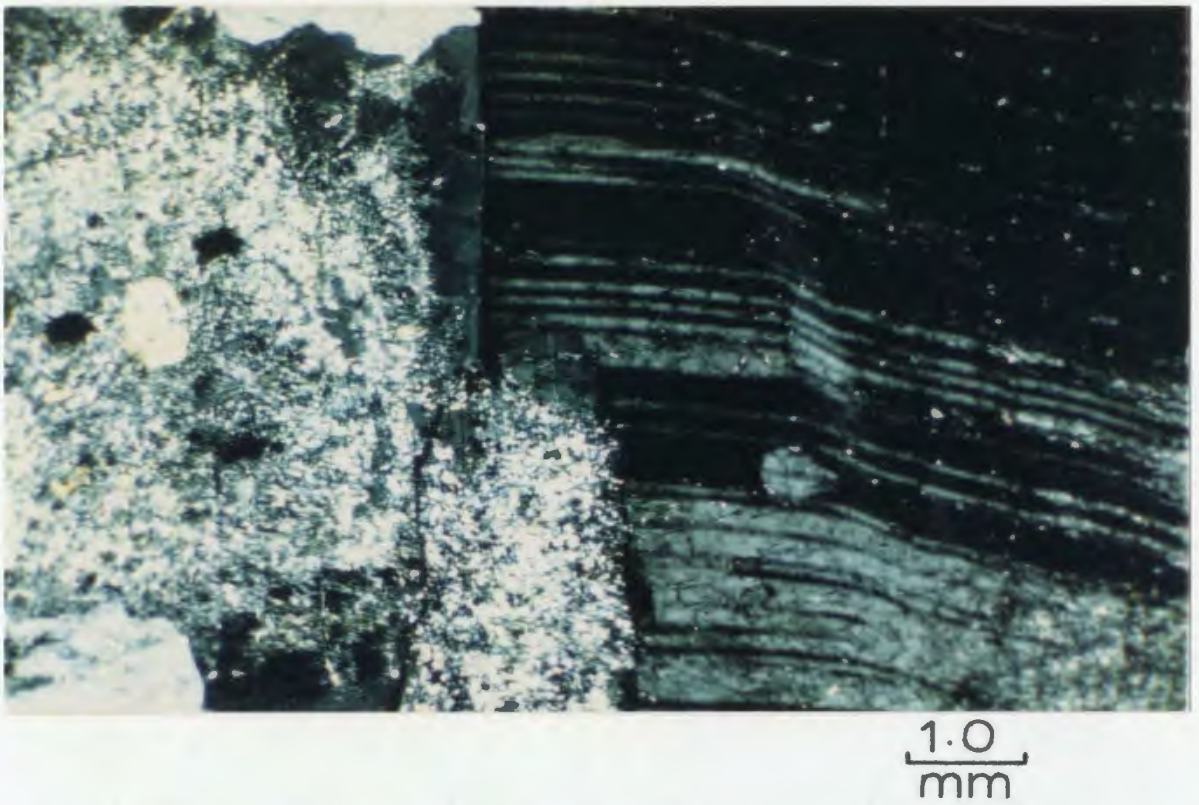

Plate 19: Kink band in plagioclase. Strong alteration of plagioclase grain at left. Mount Sylvester Granite. LD-084. XNic.

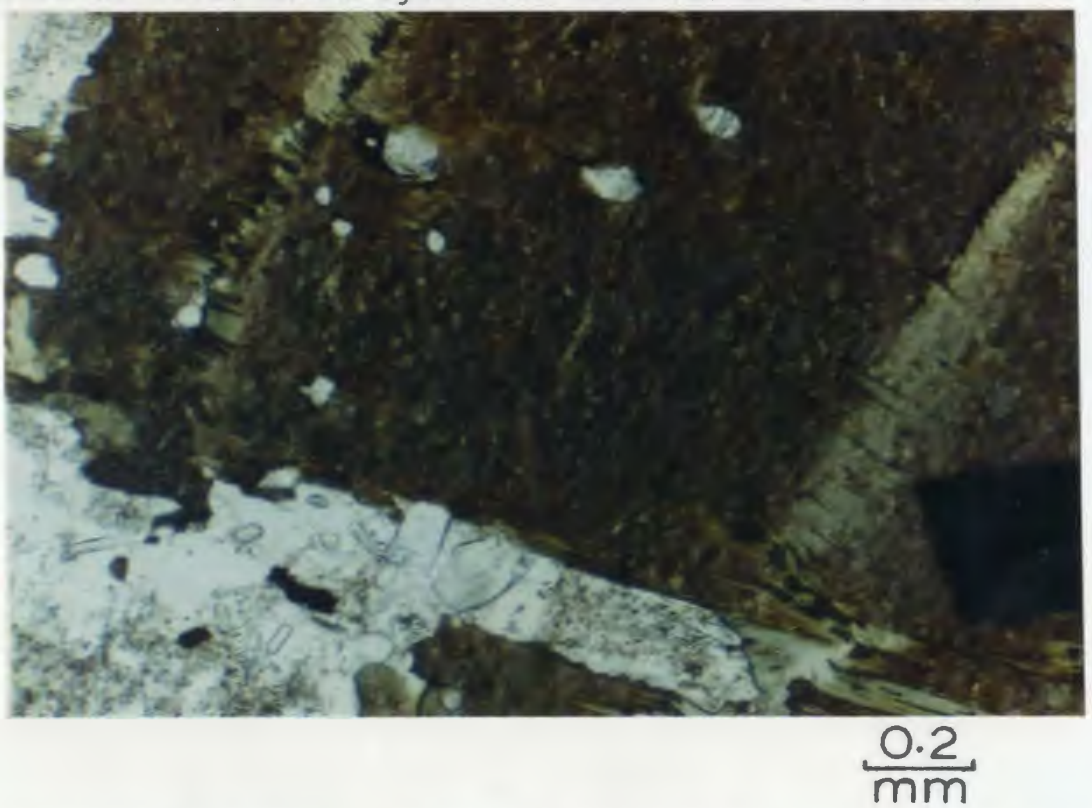

Plate 20: Kink band in biotite. Euhedral apatite crystals (high relief) in feldspar at bottom left. Mollyguajeck Pluton. LD-353. Plane light.

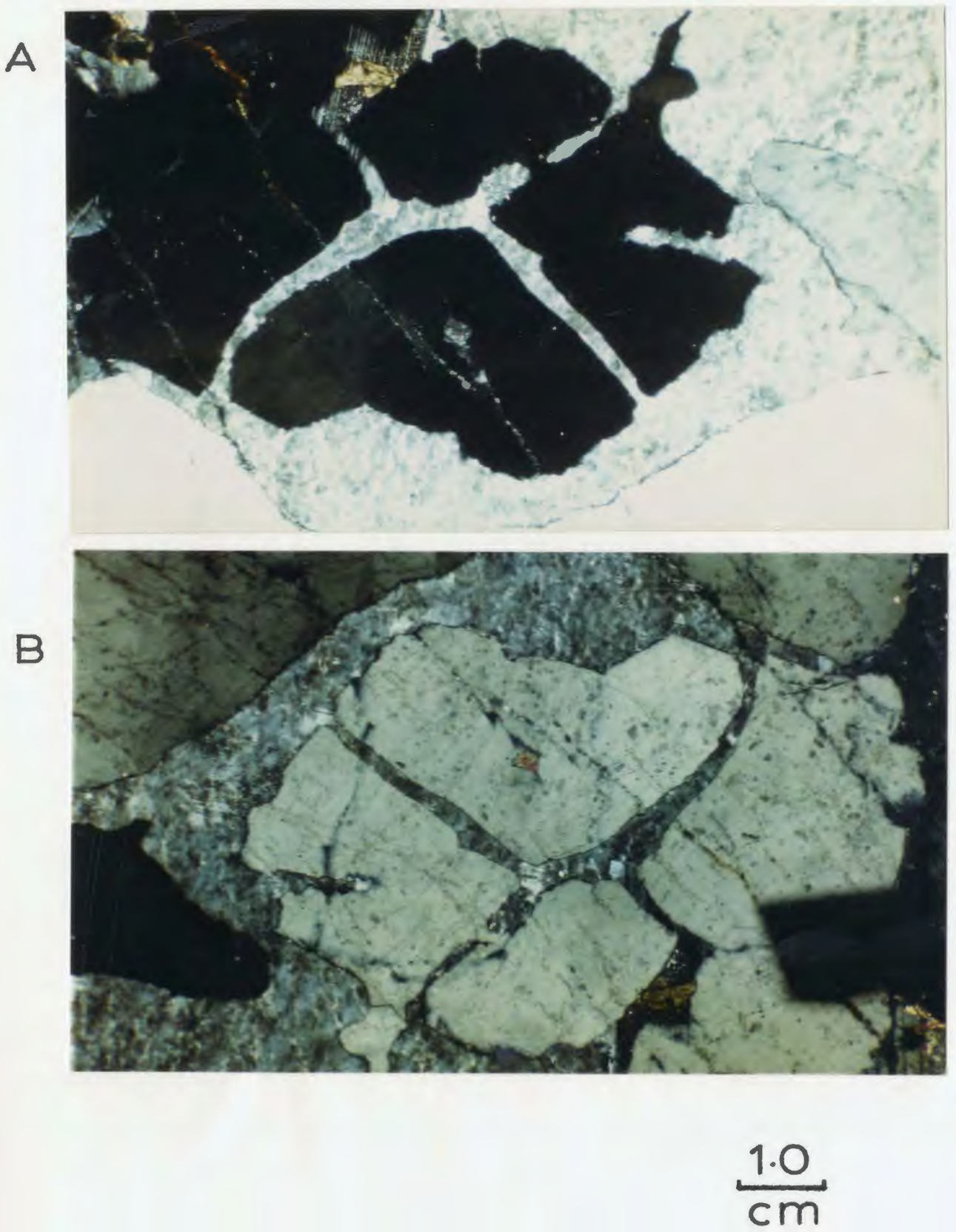

Plate 21: Rounded quartz phenocryst in perthite and plagioclase showing resorption and disaggregation. The quartz has weak undulose extinction, and some of the sericite filled fractures do not cut across perthite. Small biotite grains are present (brown). Tolt Granite. LD-421. A is a plane light; B is XNic.

The distribution of greisen in the Sage Pond area is controlled in part by large joints or fractures near the granite margin (see Chapter 4). Widespread jointing of the granite may relate to release of pressure during uplift and erosion.

Quartz grains and phenocrysts in the southeastern granites exhibit evidence of disaggregation prior to crystallization of the surrounding perthite and albite (Plate 21).

3-4-4 Mineral Chemistry: Magmatic Trends

The iron enrichment trend in biotite, displayed by the southeastern granites, is interpreted to represent a magmatic compositional trend (cf. Volkov and Gorbacheva, 1980).

The biotite data indicate a similarity in petrogenetic process in the southeastern granites which results in Fe-enrichment in biotite. In contrast, the consistency of the relatively low annite ratios in the Koskaecodde and Molyguajeck plutons indicates that these rocks are petrogenetically distinct from the Ackley Granite Suite. The inherent differences in the structure of biotite between these granitoid rocks is emphasized by the divergence of trends in a plot of the cation proportion of magnesium in biotite versus the MgO content of the whole rock (Fig. 22).

The lack of corresponding trends in the ferric/ferrous ratios from the biotite mineral separates suggests that fO_2 was buffered throughout

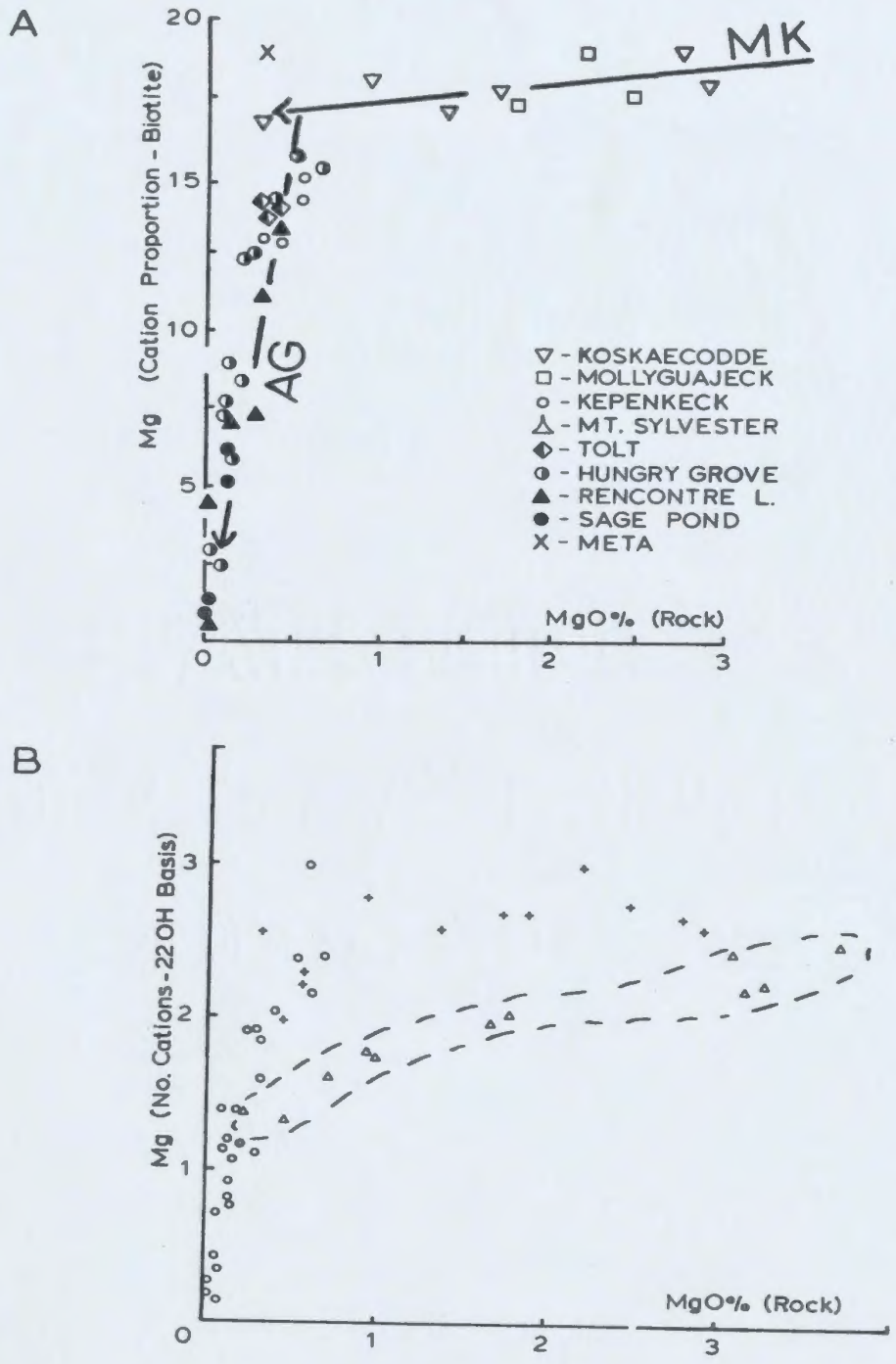

Figure 22: Plots of Mg-cation proportion of biotites versus the MgO (wt. %) content of the whole rock samples. A: Mg in biotite versus MgO of whole rock. B: Comparison of data to those of de Albuquerque (1975). Crosses are Mollyguajeck and Koskaecodde plutons; open circles are Ackley Granite Suite; open triangles are data of de Albuquerque.

the magma system. In addition, the ferric/ferrous ratios in the molybdenum-mineralized Rencontre Lake Granite and the tin-mineralized Sage Pond Granite are identical, suggesting that fO_2 was not a significant factor in isolating molybdenum from tin. Alternatively, the ferric/ferrous ratios may be buffered by the presence of fine hematite or magnetite in the biotite which may relate to subsolidus alteration.

The distribution of fluorine values in biotite indicates that magmatic fluorine concentration and activity was relatively constant in the Sage Pond and Hungry Grove granites. In contrast, the lower fluorine concentration in the Rencontre Lake Granite may reflect a lower magmatic concentration in this area. Similarly, the intermediate fluorine concentrations in the biotites from the northwestern granitoids may indicate intermediate and variable fluorine concentration during biotite crystallization. Biotites in high-silica systems can contain up to 4% F (Manning, 1981), this may suggest that the Ackley magma system was undersaturated with respect to fluorine.

A plot of tetrahedral alumina against annite composition in biotite (Fig. 23) compares data from the study area to data from mineralized granitic rocks in Nova Scotia (Strong and Chatterjee, 1985). There is a wide range of values in the data presented here compared to the relatively tight data clusters for mineralized areas in Nova Scotia. The differences are probably due to scale since the Ackley data are from representative samples over the study area (2700 km^2). The Nova Scotia samples were collected from relatively small areas proximal to mineralization and probably reflect rather restricted ranges of magmatic

evolution. Analyses of closely-spaced samples in the study area have similar values, suggesting that samples from restricted areas would give tight groupings of data.

Biotite compositions in the southeastern granites trend from an approximate value of 2.3 for Al IV and 0.5 annite, to 2.1 for Al IV and 0.9 for annite. The higher Al IV values probably reflect fluid interaction and tetrahedral alumina substitution in biotite. Thus the tendency for the data trends in mineralized areas to parallel the Al IV axis probably reflect alteration processes in mineralized areas suggesting that mineralizing processes can develop at any stage during the annite crystallization (e.g. within the magmatic evolution of high-silica systems), and are due to devolatilization during crystallization.

The presence of relatively Fe-rich hornblende in the more mafic rocks of the southeastern granites is in accordance with the more extensive Fe-rich biotite compositions and also indicates a different genetic regime compared to the Mollyguajeck and Koskaecodde plutons. Thus it is probable that a mineral isopleth can be drawn round the areas containing hornblende in the southeastern granites and also within the Koskaecodde and Mollyguajeck plutons. However, the eastern boundary of the hornblende-bearing rocks in the Koskaecodde Pluton is probably an intrusive contact as indicated by the textural evidence of biotite aggregates and microcline recrystallization in the pluton.

The correlation between Fe/Mg ratios of biotite and chlorite indicates that the chlorite inherits its Fe/Mg composition from biotite,

i.e. that there has not been significant metasomatism. This contrasts with hydrothermal systems in which Fe/Mg changes as a result of fluid reactions.

Dickson (1983) considered that the muscovite in the Kepenkeck Granite may be of primary magmatic origin. This view is supported by the location of several analyses on the Ti-Mg-Na plot in Fig. 21B. However, muscovite crystals may also have a composition comparable to some of the secondary sericite associated with mineralization in the Sage Pond Granite and these muscovite and sericite may be secondary in origin. It is relevant that the Al_2O_3 content of whole rocks is highest in the Kepenkeck Granite, with most samples having peraluminous compositions, and the compositional field of muscovite stability is probably greatest in these higher-alumina rocks. In addition, it is possible that muscovite which replaces biotite may inherit the high Ti (and possibly Fe and Mg) of the parent biotite. Thus the origin of the muscovite in the Kepenkeck Granite is ambiguous and may represent both primary and secondary crystallization.

CHAPTER 4 - GEOLOGY OF MINERALIZED AREAS IN THE SAGE POND AND RENCONTRE LAKE GRANITES

4-1 INTRODUCTION

The objectives of this Chapter are to describe the geology and mineralization of the significant mineral prospects in the Sage Pond and Rencontre Lake granites. The descriptions are oriented to highlight the similarities and differences between style and type of mineralization in the two areas. Semiquantitative microprobe studies were performed to identify the mineral species in the greisen veins. The textural and petrographic features described in Chapter 3 indicate that the host granites to mineralization form part of the much larger, possibly cogenetic, Ackley Granite Suite.

The most significant mineralization occurs at the southern contact of the Ackley Granite Suite in the Rencontre Lake (molybdenite) and Sage Pond (tin) granites (Fig. 4; Table 7). In addition, numerous small occurrences of molybdenite in quartz veins have been reported by Dickson (1983) and include the Franks Pond molybdenite occurrence (Whalen, 1976, 1980; see Fig. 68). Tuach (1984a) reported narrow (10 cm wide) tin- and tungsten-bearing greisen veins and a quartz pocket with some coarse beryl crystals at two separate localities southeast of Big Blue Hill Pond in the Hungry Grove Granite (Fig 4).

Table 7: Mineral prospects in the Ackley Granite Suite. All significant mineral deposits occur at the granite margin within miarolitic granite. Data on the Rencontre Lake area from Whalen (1976) and Dickson (1983).

Prospect	Commodity	Accessory Minerals	Dimension (Meters) Length, Width, Plunge Length	Tons/Grade or Assays	Style of Mineralization	Alteration	Associated Features	Classification
RENCONTRE LAKE AREA								
Moto	Molybdenite		175, 10, 30	Too erratic and low grade.	Coarse rosettes and fine disseminated in aplite or granite. Occasionally in miarolitic cavities and in quartz veins.	Very minor sericite?	Hematite stain.	Aplitic-magmatic.
Ackley City	Molybdenite	Py, F, Ba, Ct, ± Sp, cp, Po	42, 12, 50	80,000/0.6% MoS_2	Disseminated, fracture coatings in quartz pods, veins and pegmatite.	Occasional minor muscovite greisen.	Quartz + pegmatite segregations to 1 m long. Stockwork of pyrite-lined fractures in rhyolite.	Aplitic - magmatic. Minor stockwork features.
Crow Cliff-Dunphy Brook	Molybdenite	-	Individual areas to 10 meter diameter. Along 1 km of contact.	Too erratic and low grade.	Rosettes in large quartz-pegmatite crystals and disseminated in aplite.	Occasional minor fracture with quartz-sericite halo.	Tuffisite.	Pegmatite - magmatic.
Wyllie Hill	Molybdenite	Py, F, ± Sp, Gn, U, Au.	2 bodies, each 370, 120, 500	1,000,000/ 0.15% MoS_2.	Fracture coatings (stockwork), disseminated in quartz veins, pods and pegmatite.	Abundant sericite plus saussuritized feldspar.	Pegmatite. Pyritic nodules in altered zone. Post mineralization quartz-feldspar porphyry dike. Minor fracture stockwork and abundant quartz veins in rhyolite with very minor sulphides.	Stockwork - hydrothermal. Some magmatic features.
SAGE POND AREA								
Esso	Cassiterite	Py, F, Hem, Ru, W	50, 20	Too erratic and low grade. Best assay 0.79% Sn over 0.5 m.	Disseminated in fractures and vugs.	Quartz-topaz sericite, kaolinite.	Numerous small greisen veins in area.	Massive topaz greisen underlain by sheet greisen.
Amoco	Cassiterite	Py, F, Ru, W	160, 50	Too erratic and low grade. Best assay 0.4% Sn over 1 m.	Disseminated in fractures and vugs.	Quartz-topaz, sericite, kaolinite.	Numerous small greisen veins in area.	Massive topaz greisen

Py - pyrite; F - fluorite; Ba - barite; Ct - calcite; Sp - sphalerite; Cp - chalcopyrite; Po - pyrrhotite; Gn - galena; U - uraninite; Au - gold; Hem - hematite; Ru - rutile; W - wolframite.

4-2 THE SAGE POND AREA

4-2-1 Granite

4-2-1-1 Intrusive relationships: The Sage Pond Granite intrudes both the Precambrian Belle Bay Formation (Bradley, 1962) and the Cambrian Cross Hills Plutonic Suite (Bradley, 1962; O'Brien et al., 1984; Tuach, unpub. data). In the Sage Pond area, the attitude of the granite contact varies from vertical to gentle southerly, with possible roof pendants west of Anesty Hill and east of Moulting Pond (Fig. 24).

In the Sage Pond Granite, gradational to abrupt variation in grain size and texture are common, both in outcrop and in drill core. Finer grained phases locally intrude the coarser granite. Limited outcrop in the area (< 10%) precludes construction of a detailed textural map.

The contact between the Hungry Grove Granite and the Sage Pond Granite is gradational. Finer grained, variable rocks are progressively more abundant to the south, across a 500 m wide zone.

4-2-1-2 Lithology: The Hungry Grove Granite (Figs. 4, 24) consists of medium to coarse-grained, equigranular, biotite granite. Minor alkali-feldspar phenocrysts (1-2 cm) occur locally. The Sage Pond Granite is sandy weathering, friable, orange, equigranular to quartz-feldspar porphyritic, fine to medium grained. Phenocryst content averages 10-20%, but up to 50% phenocrysts are present in granite which hosts the quartz-topaz greisen veins southeast of Moulting Pond.

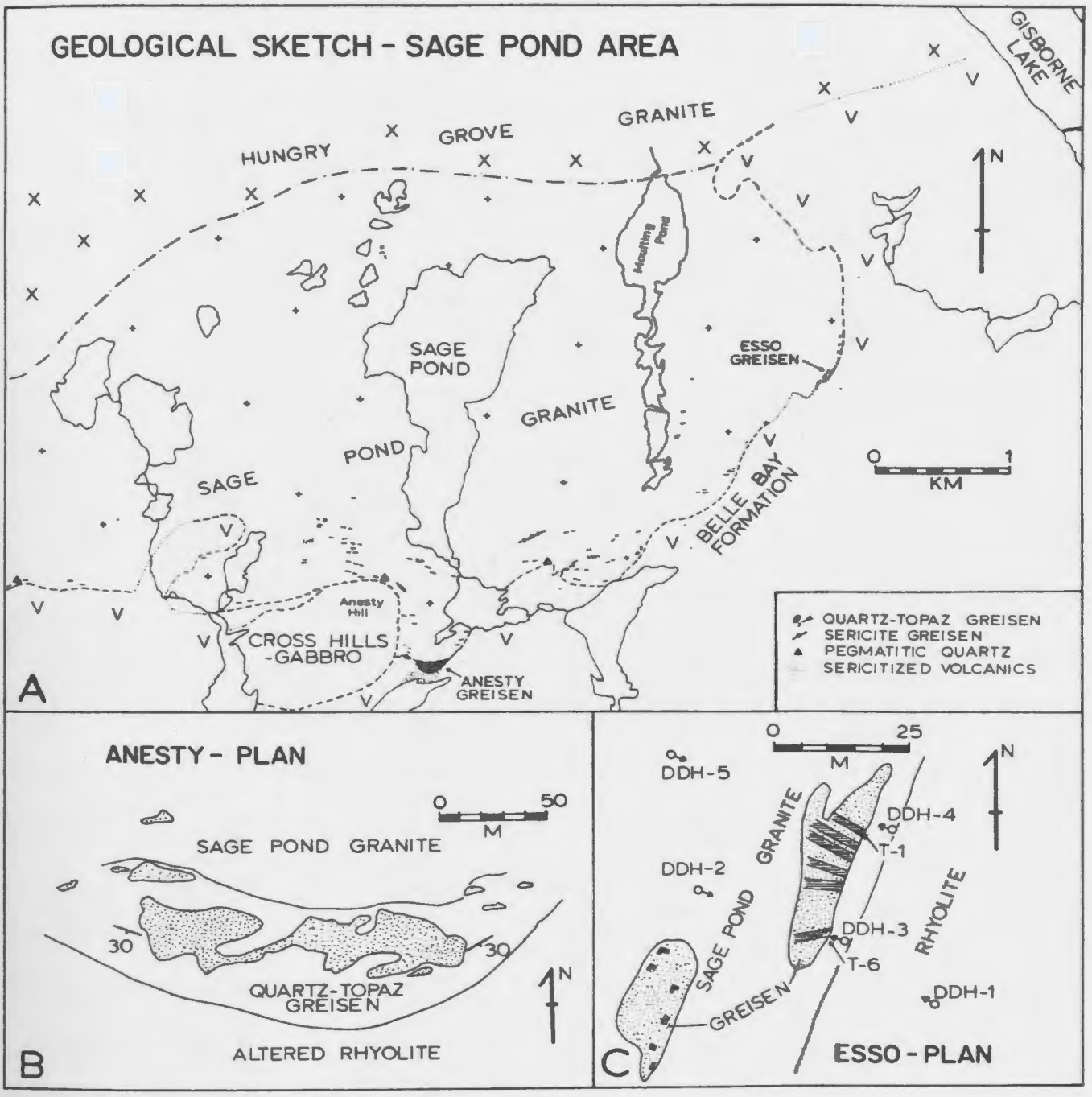

Figure 24: Geological sketch maps from the Sage Pond area.
A: General geology and distribution of greisen.
B: Outcrop pattern of the Anesty greisen (stippled). Dip strike symbol is attitude of greisen.
C: Outcrop pattern and location of trenches (lined areas) and drill holes (DDH).

Gas breccias (tuffisite) and miarolitic cavities are common in fine grained granite at Long Harbour (Dickson, 1983). In the Sage Pond area, these textures are rare and contain minor fluorite in the breccia matrix and in associated fractures. Small pegmatite patches (crystals less than 3 cm long) occur locally and large quartz crystals (to 20 cm across) were noted at three localities at the granite contact (Fig. 24).

4-2-1-3 Petrography: Seriate and granophyric texture is ubiquitous in both the Hungry Grove and the Sage Pond granites. Quartz commonly shows embayed margins and alkali feldspar crystals locally contain zones of graphic intergrowth with quartz.

The Hungry Grove Granite contains perthitic alkali feldspar, quartz, plagioclase, biotite and minor magnetite. Accessory minerals are zircon, allanite and sphene. Interstitial granophyric and graphic intergrowths are common. Alkali feldspars contain up to 20% coarse strings and patches of albite. Plagioclase displays weak normal zonation in the albite composition range and cores may be weakly saussuritized. Minor interstitial biotite (2%) occurs as 1-4 mm flakes and shows local alteration to chlorite, sericite and magnetite. Magnetite is locally altered to hematite.

The Sage Pond Granite has comparable mineralogy to the Hungry Grove Granite. It contains coarse patch perthite and less than 5% weakly zoned plagioclase crystals with a composition range of Ab_{90} to Ab_{100}. Biotite has ragged outlines and is bronze to black due to exsolution of opaque oxides. Accessory fluorite is present. Locally, topaz and tourmaline

occur. Biotite is a minor phase near the southern contact and is absent in the immediate host rocks to the larger greisen veins where muscovite, topaz and fluorite are accessory phases.

Fine to coarse sericite is part of an extensive halo (in thin section) which focuses on the quartz-topaz greisen veins in the Sage Pond area (see Fig. 13). The sericite forms after feldpsar and biotite. Towards the southern contact and the larger greisen veins, coarse sericite has a weak to moderate brown pleochroism.

4-2-1-4 Mineral Chemistry: The compositions of albite and biotite in the Sage Pond area plot as end members of trends which are present over much larger areas in the southeastern granites. The albite content reaches a maximum adjacent to large greisen bodies at the granite contact (see Fig. 14) and the biotite analyses give an annite ratio of 0.71 to 0.93 (Fig. 16). Sericite has celadonite-rich compositions (MgO-, FeO-bearing; Fig. 21).

4-2-2 Alteration and Mineralization

4-2-2-1 Introduction: Tin and tungsten values (Table 7) of economic interest have been reported from the Anesty and Esso prospects (O'Sullivan, 1982, 1983; Tuach, 1984b,c). Significant tin mineralization in smaller greisen veins is confined to the eastern part of the area near the Esso prospect (O'Sullivan, 1982). The minerals of economic interest (cassiterite and wolframite) are generally not visible in outcrop. Scheelite fluorescence under ultraviolet light was not

observed at the Esso or Anesty propects. The Anesty area was originally considered as a molybdenite prospect (Ricketts and Bumgarner, 1954).

4-2-2-2 Distribution and General Description: A major concentration of quartz-topaz (topazite) greisen veins and pods occurs in the Sage Pond area, at and near the southern contact of the Sage Pond Granite. The larger greisen form gray nobs of outcrop or suboutcrop in weathered granite till or subcrop. Fresh greisen is not available due to an intense limonite stain on broken surfaces. Isolated veins of green muscovite-rich greisen are present.

Quartz-topaz veins have been noted as far west as Long Harbour (over a total distance of 15 km) and have been observed within granite up to 3 km from its margin. They increase in concentration and size southwards, with the largest quartz-topaz outcrops at convex undulations of the granite contact. Rare, narrow veins less than 10 cm wide may occur in rhyolite up to 5 m south of the granite contact.

Veins follow joints and fractures in the granite are podiform-elongate with a predominant easterly trend and are generally less than 10 m * 2 m. Several localities were noted at which small veins (1-2 m * 0.5-1 m) trending 020-040 degrees are arranged 'en-echelon' in a main trend of 120 to 140 degrees. These have the appearance of gash veins. Most veins are vertical to subvertical. Subvertical layering and laminae defined by grain size, relative proportion of quartz, topaz, hematite, or pyrite content may parallel central fractures in the veins.

The two largest greisen occurrences are described below:

A) The Esso prospect: A 50 m * 6 m outcrop of massive quartz-topaz greisen located to the southeast of Moulting Pond at the granite contact (Fig. 24) was drilled by Esso Resources Limited in 1982 (O'Sullivan, 1983). Subparallel quartz-topaz (with pyrite and/or hematite and/or fluorite) vein swarms, ranging from fracture-fillings to veins 3 m wide underlie the massive outcrop (Plate 22A). Sericitization and bleaching (commonly with accessory pyrite) of the host granite is limited to within 1 m of individual veins and is generally narrower than vein width (Plate 22A). Gray-green muscovite-quartz-topaz greisen (Plate 22B) occurs marginal to massive quartz-topaz and can occur as individual veins. Pyrite-bearing fracture networks containing up to 2% fine grained disseminated pyrite are present in the unaltered granite. Fracture networks are also present in the adjacent rhyolite and contain minor epidote, quartz, pyrite and isolated grains of molybdenite.

B) The Anesty prospect: This massive quartz-topaz greisen body outcrops over an area of 200 m * 60 m within a convex south lobe of the granite (Fig. 24). The greisen exhibits both gently dipping (20-40 degrees to the south) and contorted layering which is defined by grain size variation and by variation in relative proportions of quartz and topaz. Up to 10% disseminated pyrite, minor fluorite and rare small grains of molybdenite occur. Vugs (to 2 cm) and narrow open fractures in the greisen are lined with quartz and lesser amounts of fluorite. Coarse rosettes of molybdenite occur in green muscovite greisen over an area of 6 m * 2 m at the west side.

A

B

Plate 22: A: Greisen veins and alteration halos in drill core from the Esso greisen. Length of core box is 1.52 m.
B: Close-up of area outlined in A. From top to bottom shows brown gossan, green sericite greisen, massive blue-white quartz-topaz greisen with minor pyrite, bleached altered granite, and relatively fresh granite. Scale in inches (1 inch = 2.5 cm).

Rhyolite outcropping immediately south and west of the Anesty greisen is strongly sericitized. A 3 cm wide quartz vein containing rosettes of molybdenite up to 1 cm in diameter, outcrops 10 m southeast of the greisen contact and a biotite-rich pegmatite vein (80 cm * 5 cm) was noted near the southwest contact.

4-2-2-3 Quartz-Topaz Greisen: This rock is white, medium to coarse grained (1-4 mm), equigranular to weakly porphyritic. Locally, coarse quartz crystals impart a porphyritic appearance texturally comparable to the host granite. Green muscovite and white kaolinite may be associated with the topazite. Vugs, small open cavities, and fractures are ubiquitous in generally massive greisen. These open spaces are lined with crystals of quartz, dark blue to black fluorite, hematite, sericite and kaolinite. Colour banding, due to hematite stain, locally occurs parallel to hair-line fractures. Greisen veins located in the north of the area generally contain less sericite and kaolinite is absent.

Up to 10% pyrite occurs as disseminations and in fractures in the greisen. Isolated grains of molybdenite are common. Malachite stain and minor fine disseminated bornite were observed in a 20 cm, rounded, greisen boulder on the east side of Sage Pond. However, copper mineralization was not observed in outcrop.

Cassiterite crystals (0.1 - 1.0 mm diameter) are visible in hand specimen at the Esso prospect, along with dark blue to black fluorite and fine grained hematite. These minerals are disseminated in darker patches in the greisen matrix or are concentrated in dark, subvertical

bands. However, cassiterite is generally too fine grained to be observed in outcrop.

The quartz-topaz greisen consists of quartz (80-95%), topaz (5-20%), sericite-muscovite (0-5%), kaolinite (0-5%), fluorite (0-5%) and opaque minerals. The opaque minerals are predominantly pyrite (0-15%), and hematite (0-5%). Fine grained cassiterite (0.1 mm) occurs locally and minor rutile occurs as individual grains or as coarse intergrowths with cassiterite. Tourmaline (elbaite) was observed in one thin section.

Quartz varies in grain size from 0.5 mm to 2 mm and exhibits serrated grain boundaries. Phenocrysts or 'porphyrocrysts' of quartz up to 6 mm in diameter are common. Weak undulose extinction may be present and the quartz grains are locally fractured.

Topaz occurs as interstitial euhedral to anhedral aggregates between quartz grains or in fractures. Grain size is less than 0.2 mm (Plates 23, 24). Variation in the amount and grain size of topaz is responsible for the subtle layering observed in the Anesty and other greisen.

Sericite is very fine grained (0.1 mm). It is associated with the topaz and is common in fractures and vugs. Most sericite has a weak, brown pleochroism. Minor white non-pleochroic sericite is also present.

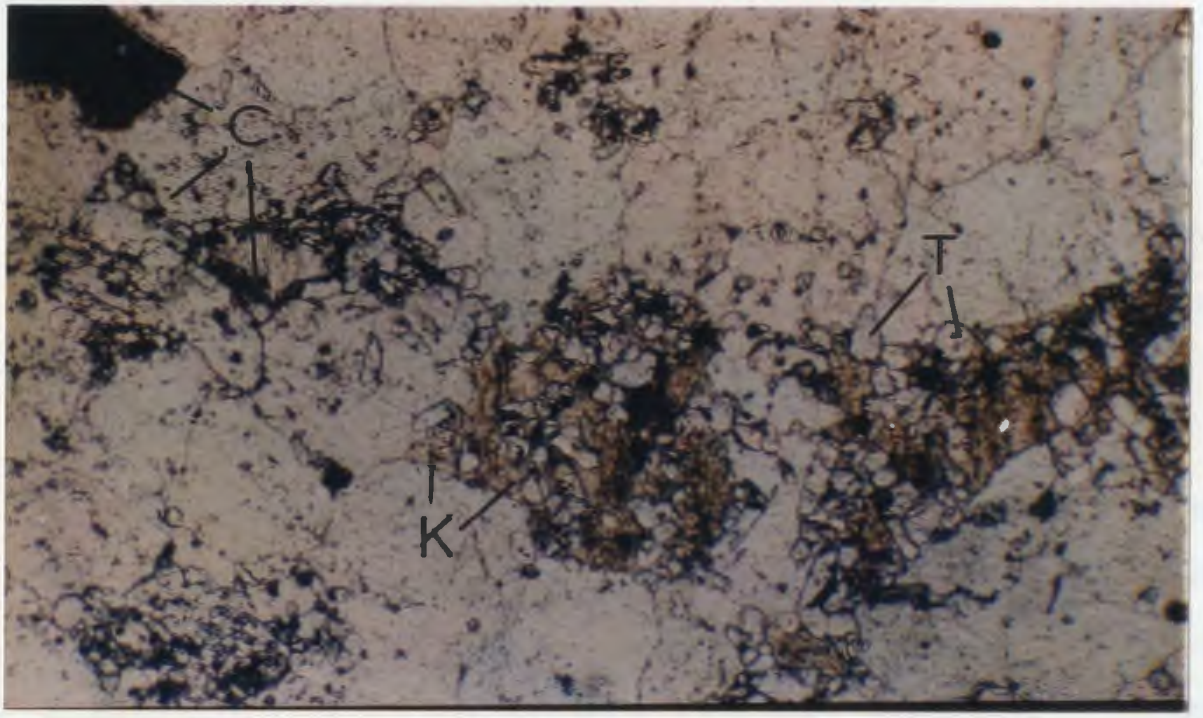

Plate 23: Topaz (T), cassiterite (C), kaolinite (K) in quartz. JT-239. Plain light.

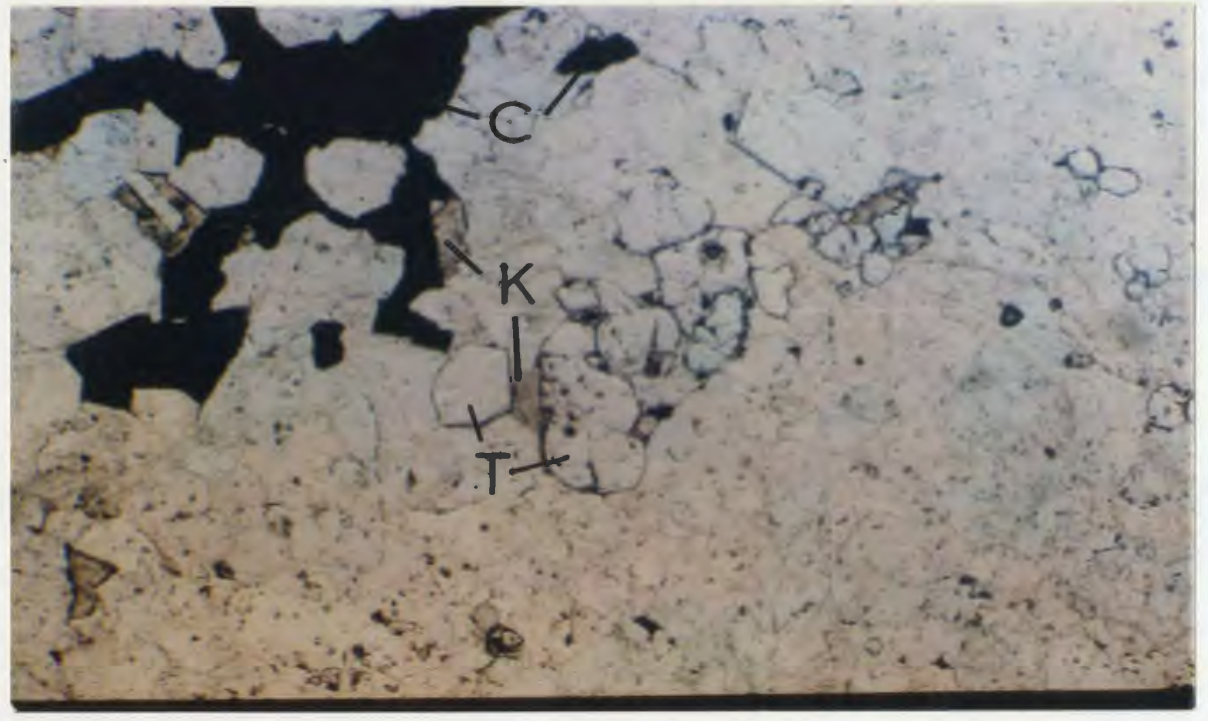

Plate 24: Topax (T), kaolinite (K), and opaque minerals in fracture. JT-239. Plain light.

Kaolinite (Plates 23, 24) is very fine grained and occurs interstitially to quartz, in fractures, and in vugs. It is associated with sericite and topaz.

Fluorite is common as late irregular interstitial grains or as aggregates in fractures. It is dark blue to black and varies in grain size up to 1 mm.

Cassiterite is erratically distributed and generally very fine grained (0.05 mm), although larger euhedral crystals up to 1 mm have been observed in vugs in the greisen. The cassiterite is red-brown and a pronounced zonation is evident in the coarser grains (Frontispiece). It occurs as interstitial grains to quartz, as aggregates in fractures and is associated with topaz and sericite (Plate 24).

Red-brown rutile occurs as small (<0.05 mm) grains and as complex intergrowths with cassiterite.

Pyrite is present as subhedral to euhedral grains up to 2 mm and occurs as interstitial disseminated grains and in fractures.

Hematite occurs as irregular interstitial grains, as intergranular coatings, as coatings in fractures and vugs, and locally as dendritic grains. It may also occur as coarser grains (to 1 mm) in cavities.

A single dendritic crystal of tourmaline (elbaite) was observed in thin section from sample 285B.

4-2-2-4 Mineral Chemistry in greisen: Two varieties of sericite occur in the greisen. One variety has a significant iron and minor magnesium content (the brown pleochroic variety), while the second variety has the composition of pure muscovite (compare samples 285A and 289 in Appendix C).

Topaz was identified by x-ray diffraction (XRD) and electron microprobe analyses. The composition is similar to that listed in Deer et al. (1962).

Kaolinite was identified by XRD and electron microprobe analyses. The location of the X-ray peaks and the high-alumina content of the probed grains indicates that the variety of kaolinite present is halloysite.

Cassiterite was identified by XRD and by scanning electron microscope (SEM) analyses (Plate 25). It contains up to 2% FeO and TiO_2 with a trace of Al_2O_3. Trace element content is variable (Fig. 25). Niobium and tantalum peaks were not observed on three separate microprobe spectral scans. The cassiterite commonly has complex and intimate intergrowth pattern with rutile (Plate 26) and the rutile may contain up to 5% SnO_2. Minor discrete tin-silicate grains up (to 10 micrometers diameter) are present as inclusions in cassiterite (Fig. 26).

Wolframite is extremely fine grained and has not been identified in hand specimen or optically in thin section. It was detected by electron

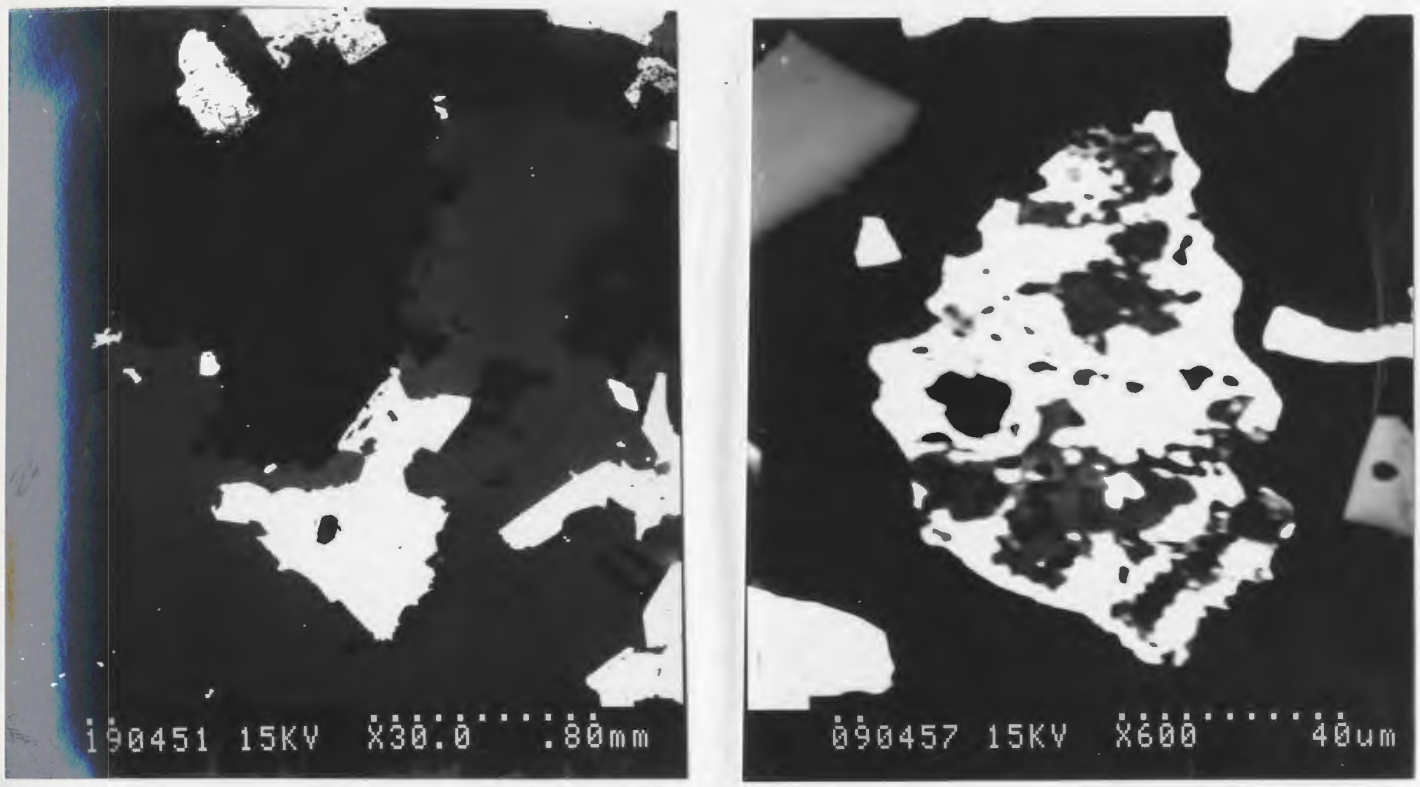

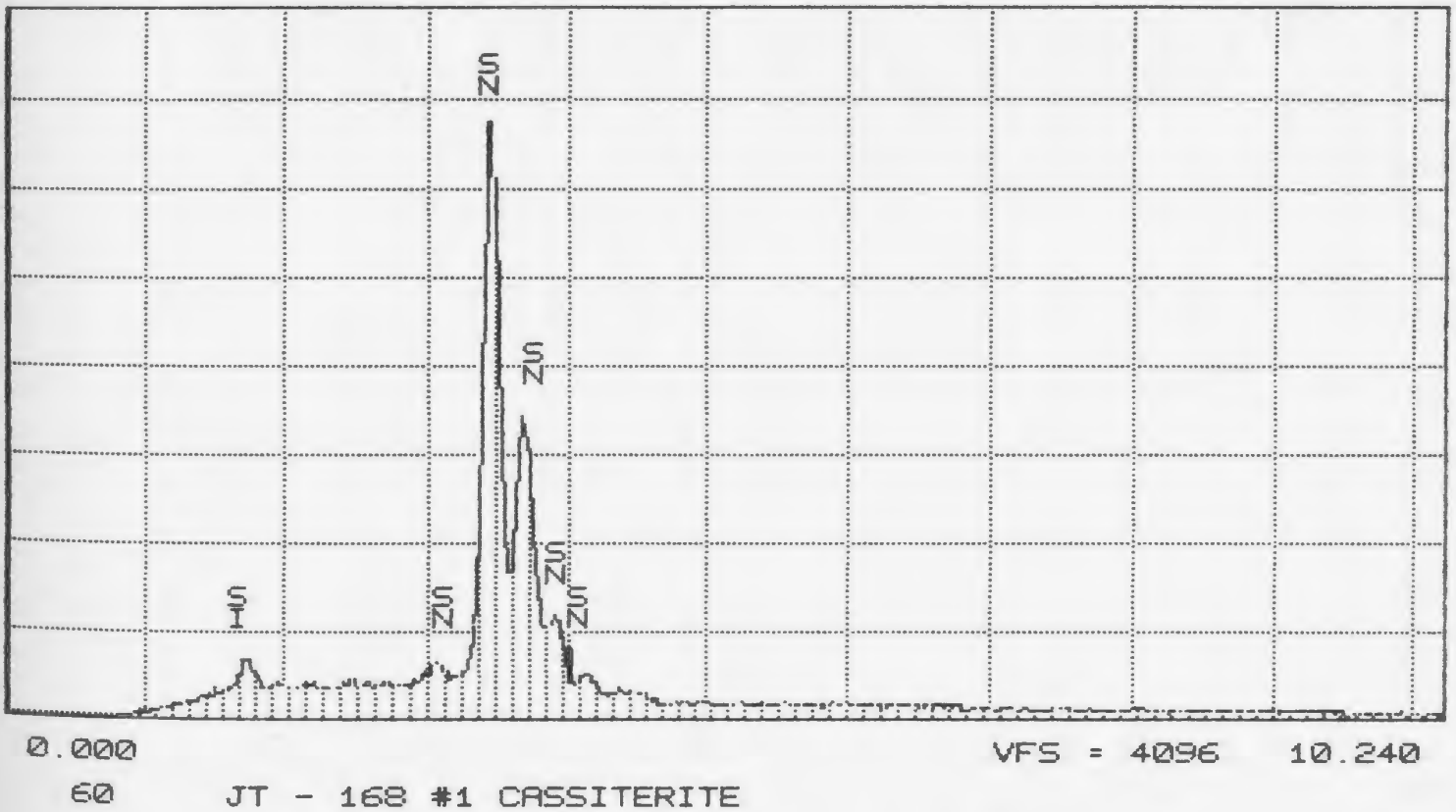

Plate 25: Scanning electron microscope images of cassiterite (white) in greisen, and spectral scan of cassiterite grain. JT-168. Bar on photograph is 0.8 mm.

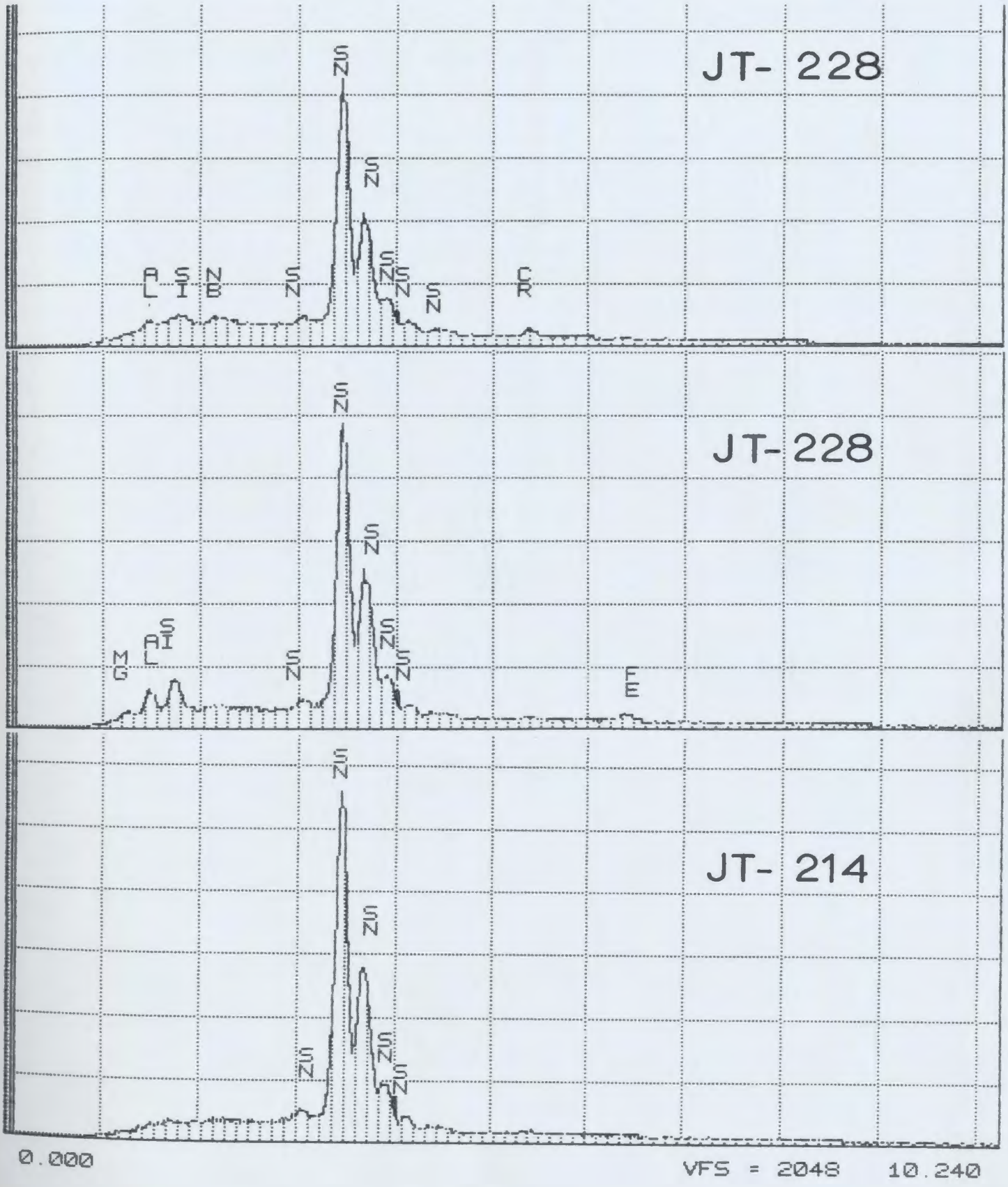

Figure 25: Scanning electron microscope spectral scans from cassiterite showing variable minor element content.

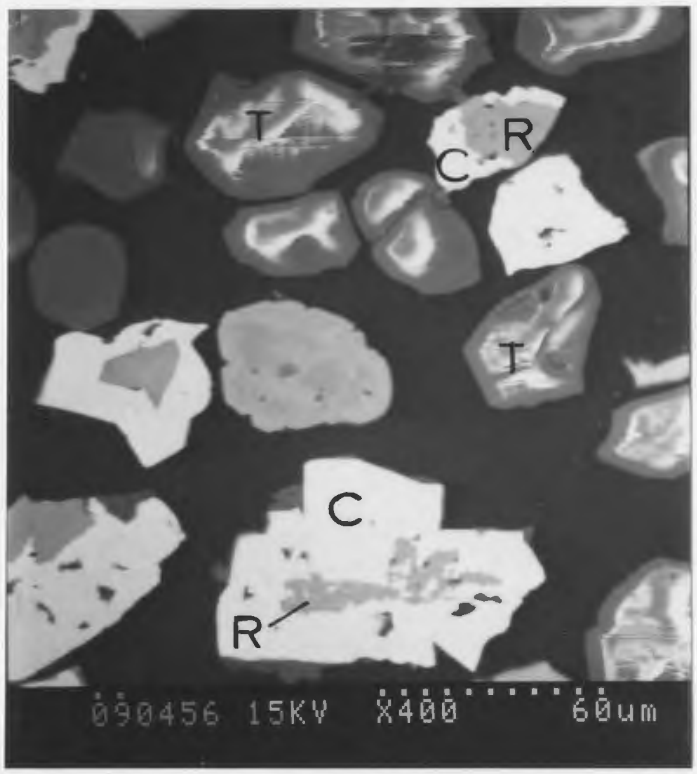

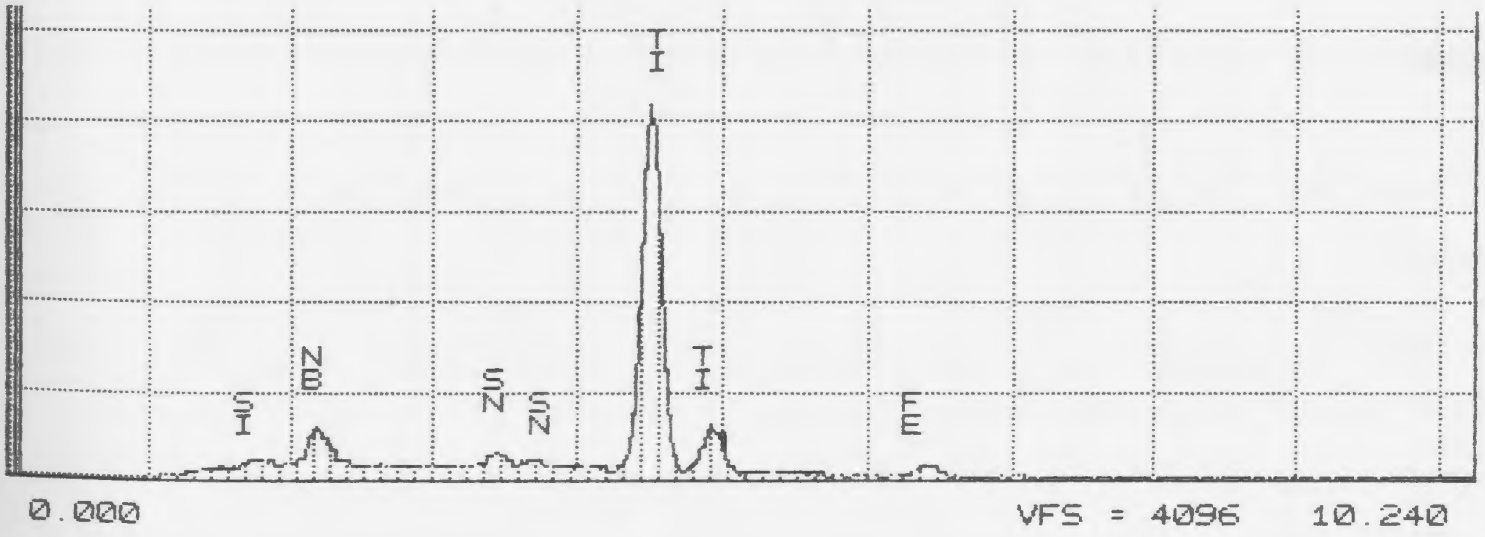

Plate 26: Scanning electron microscope image of cassiterite (C) intergrown with rutile (R). The light gray grains with white halos are topaz (T). From mounted heavy mineral concentrate. JT-228. Scale shown on photograph. Lower diagram is a spectral scan of rutile.

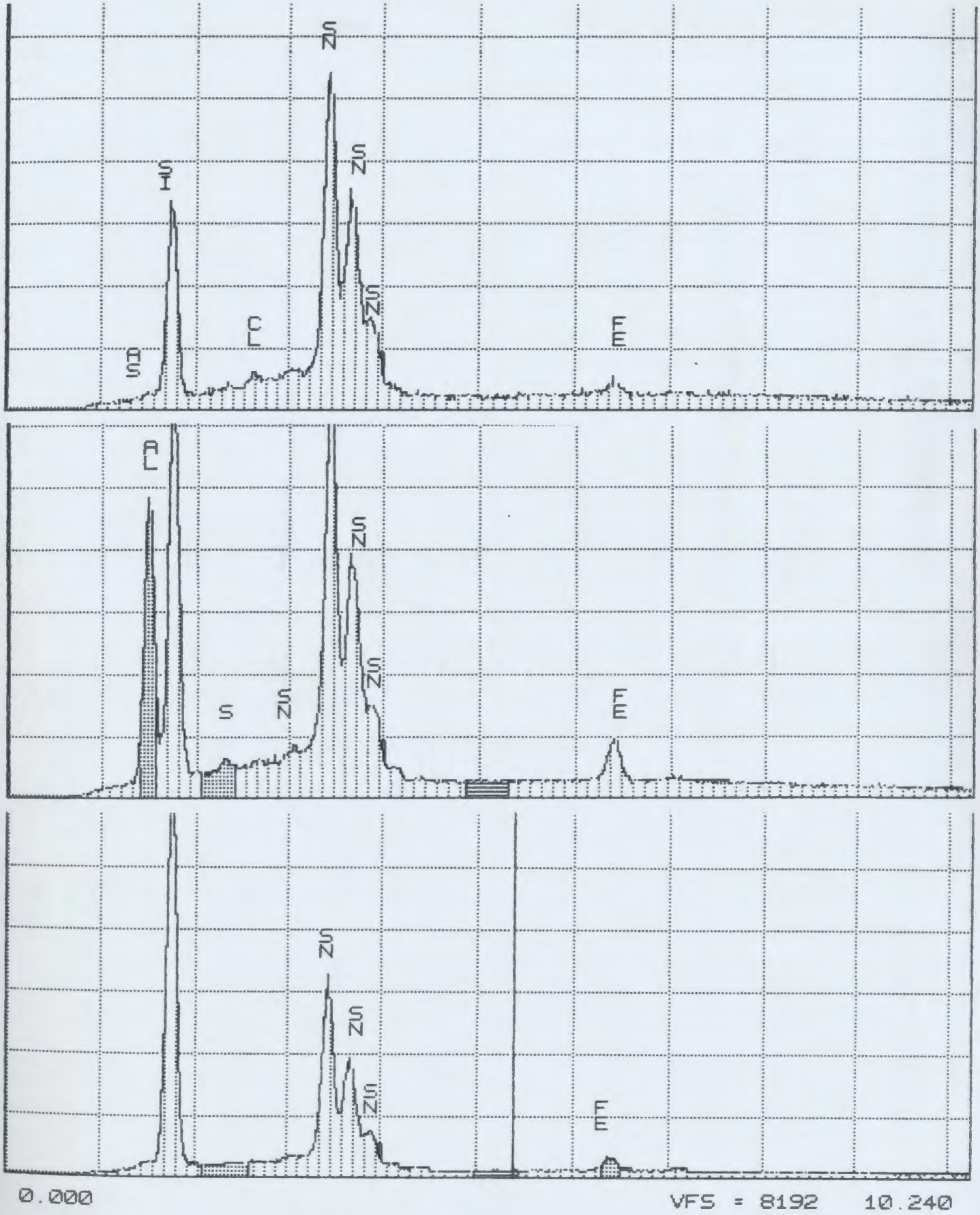

Figure 26: Scanning electron microscope spectral scans of small (5 - 10 microns) silicate inclusions in cassiterite from sample JT-228.

microprobe in polished sections of mounted heavy mineral separates from samples known to contain tungsten from assay data. The probed wolframite has a FeO/MnO ratio of 2.0 to 2.2 and contains up to 0.3% TiO_2.

Rutile contains up to 5% SnO_2 and significant niobium may be present. One sample contained 1.1% WO_3, although most samples analysed did not contain tungsten.

The hematite contains trace amounts amounts of TiO_2 and WO_3.

A zirconium-cerium oxide (approximately 20 micrometers in diameter) was noted during electron backscatter imaging of a mounted and polished heavy mineral concentrate of sample 214 (Fig. 27).

4-3 THE RENCONTRE LAKE AREA

4-3-1 Granite in the Rencontre Lake Area

4-3-1-1 Intrusive Relationships: The Rencontre Lake Granite in the immediate vicinity of the molybdenum prospects intrudes rhyolites (banded, possibly welded, ash-flow tuffs) of the Precambrian Belle Bay Formation (Bradley, 1962). Contacts between the various granite lithologies are commonly gradational. Finer aplitic units may intrude coarser grained rocks. North trending, porphyritic, aplite dikes intrude the Belle Bay Formation and the Rencontre Lake Granite.

4-3-1-2 Lithology: The Lithologies have been described in detail by Whalen (1976, 1980). Maps showing the distribution of lithologies with

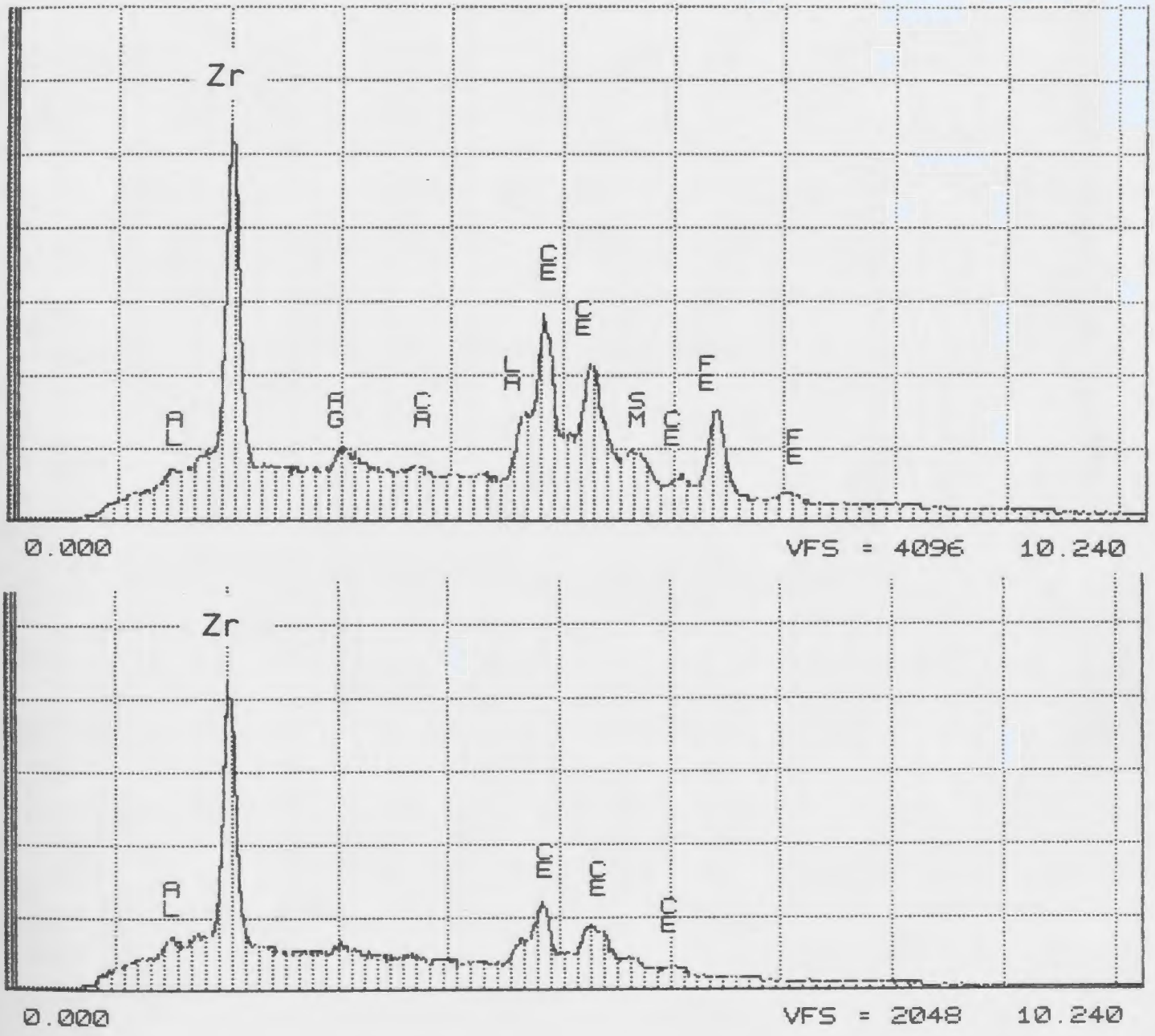

Figure 27: Scanning electron microscope spectral scans of zirconium oxide from sample JT-214.

respect to the surficial location of molybdenite mineralization are presented in Figure 28 (after Whalen, 1976, 1980).

These rocks consist of variably textured, fine to coarse grained, orange to red, equigranular to porphyritic granite with abundant pegmatite patches, quartz segregations and miarolitic cavities. Miarolitic cavities and quartz-pegmatite pockets are common. Whalen (1976) emphasized an abundance of quartz segregations in the vicinity of the Ackley City prospect and tuffisite veins near the Crow Cliff-Dunphy Brook prospect.

4-3-1-3 Petrography: The mineralogy and textures have been summarized in Chapter 3 and are similar to those of the Hungry Grove and Sage Pond Granites. The finer grained rocks commonly exhibit graphic and granophyric intergrowths, quartz is embayed and strained, alkali feldspar is strongly perthitic and commonly poikilitic. Normal zoned plagioclase is albitic and may show minor sericite alteration. Biotite is dark coloured, ragged and variably chloritized. Accessory zircon, allanite, fluorite and tourmaline are common.

4-3-1-4 Mineral Chemistry: The mineral chemistry of the rocks in the vicinity of the molybdenite prospects was not investigated in detail. However, biotite has annitic composition (Fig. 16). Fe-enrichment is also indicated by the high Fe/Mg ratios of chlorite (Fig. 20).

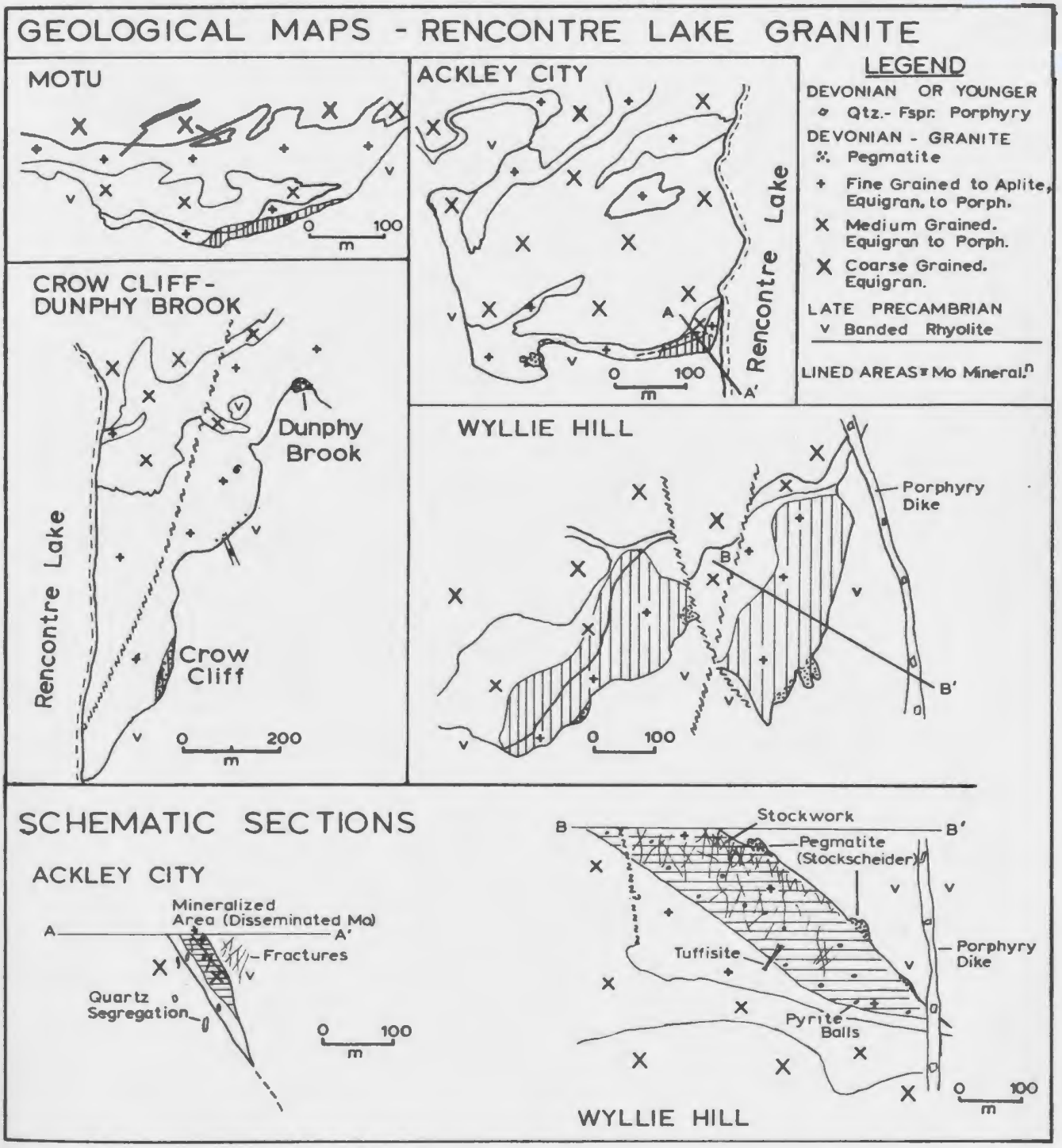

Figure 28: Generalized geology of the molybdenum prospects in the Rencontre Lake area (after Whalen, 1976).

4-3-2 Alteration and Molybdenite Mineralization

4-3-2-1 Introduction: Molybdenum is the only commodity of economic interest reported from the the prospects in the Rencontre Lake Granite (Table 7). Molybdenite is visible at all of the prospects.

4-3-2-2 Description of the Molybdenite Prospects: Four granite-hosted molybdenite deposits are located at the granite contact in the Rencontre area. From west to east, these are known as the Motu, the Ackley City, the Crow Cliff-Dunphy Brook and the Wyllie Hill prospects (Figs. 4, 28). A summary description is presented in Table 7. The reader is referred to Whalen (1976) and to Dickson (1983) for more specific details. The material presented below is summarized from Whalen (1976, 1980).

A) The Motu prospect is described as a sheet dipping 30 degrees to the south, adjacent to the granite-rhyolite contact. Molybdenite occurs predominantly as fine disseminated intergranular grains and as rosettes in quartz filled miarolitic cavities. Minor molybdenite occurs in thin quartz veins. The host granite is pink to orange, and predominantly fresh in appearance, though weak hematite stain and minor sericite alteration of the feldspar is locally present. Whalen (1976) described bead-perthite, variable chlorite alteration of biotite, and plagioclase dusted with sericite and locally altered to clay minerals. Concentrations of muscovite, greisenized granite, and kaolinite were reported in drill logs (Nolan, 1969).

B) The Ackley City prospect occurs at the granite contact and has a steep southerly dip (Fig. 28). Molybdenite occurs predominantly as 2-5 mm disseminated flakes and is also common in miarolitic cavities, in

quartz and pegmatite segregations, in muscovite greisen pods, in quartz veins, and on fracture surfaces (Plate 27). Up to 2% pyrite was noted in some slightly bleached samples on the adit dump. However, pyrite is generally rare to absent. Fluorite may occur as disseminated grains in the granite or on fracture surfaces. Trace amounts of sphalerite, chalcopyrite and pyrrhotite have been reported (White, 1939). The prevalent feature attributed to alteration is an abundance of quartz segregations up to 1 m in diameter. Muscovite alteration of feldspar and pods of coarse grained muscovite are also common. Secondary biotite may be present near quartz veins. The intruded rhyolite is cut by stockworks of pyrite-chlorite-filled fractures for a distance of 100 m to the south of the prospect.

C) The Crow Cliff - Dunphy Brook prospects are the largest of a series of coarse, quartz-alkali feldspar, pegmatite sheets (stockscheider) in granite, which outcrop over 1 km at and near the contact (Fig. 28). The contact dips from 60 degrees E at Crow Cliff in the south to 15 degrees E at Dunphy Brook in the north. Pegmatite sheets (to 1 m thick) at Crow Cliff and Dunphy Brook have been exposed over a length of 60 m and 20 m, respectively. Molybdenite occurs predominantly in pegmatite-quartz crystals as isolated coarse clusters and rosettes (to 3 cm diameter), or as zones of coarse crystals and rosettes. Minor fine disseminated molybdenite is locally present in the aplitic host to the pegmatite bodies. Rare fractures in granite contain sparse chalcopyrite, galena and sphalerite mineralization associated with narrow sericite alteration zones.

Plate 27: Collection of samples from the Ackley City molybdenite prospect showing style of mineralization. These are disseminated, fracture controlled, quartz vein fill, and in quartz pods.

Plate 28: Coarse pegmatitic quartz from the Dunphy Brook prospect.

Quartz crystals are commonly very coarse, reaching 50 cm perpendicular to the c-crystallographic axis (Plate 28). These crystals have vertical orientation with downward pointing terminations. Parallel sheets of pegmatite (stockscheider) with intervening aplite are present. D) The Wyllie Hill prospect (Fig. 28) outcrops in two zones of white, altered aplite and fine grained granite, separated by northerly trending faults. Several areas of pegmatite and stockscheider occur at the granite contact. A post-mineralization quartz-feldspar porphyry dike is present to the east of the deposit.

Mineralization consists of molybdenite and pyrite coatings on fractures and joint surfaces (Plate 29) and of fine disseminated pyrite and molybdenite (pyrite/molybdenite = 10). Pyrite-rich aggregates up to 3 cm are common and locally contain molybdenite. These aggregates attain a density of 4-5/m^2 and form rusty-weathering nodules. The most abundant mineralization is best described as a stockwork system. Minor sphalerite, galena and a trace of gold-bearing pitchblende were reported by Whalen (1976). A maximum tin content of 30 ppm was reported by Dickson (1983).

The mineralized aplite is white to buff and grades northwards into normal orange-red granite at a distance of 50-100 m from the granite contact. The heavily mineralized stockworks are accompanied by sericite zones round the fractures, and kaolinite is locally present. The aggregates of pyrite are locally accompanied by abundant muscovite. Whalen describes a unit of quartz-aplite consisting of aplite with abundant ameoboid quartz bodies up to 0.5 cm * 2.0 cm. Abundant barren

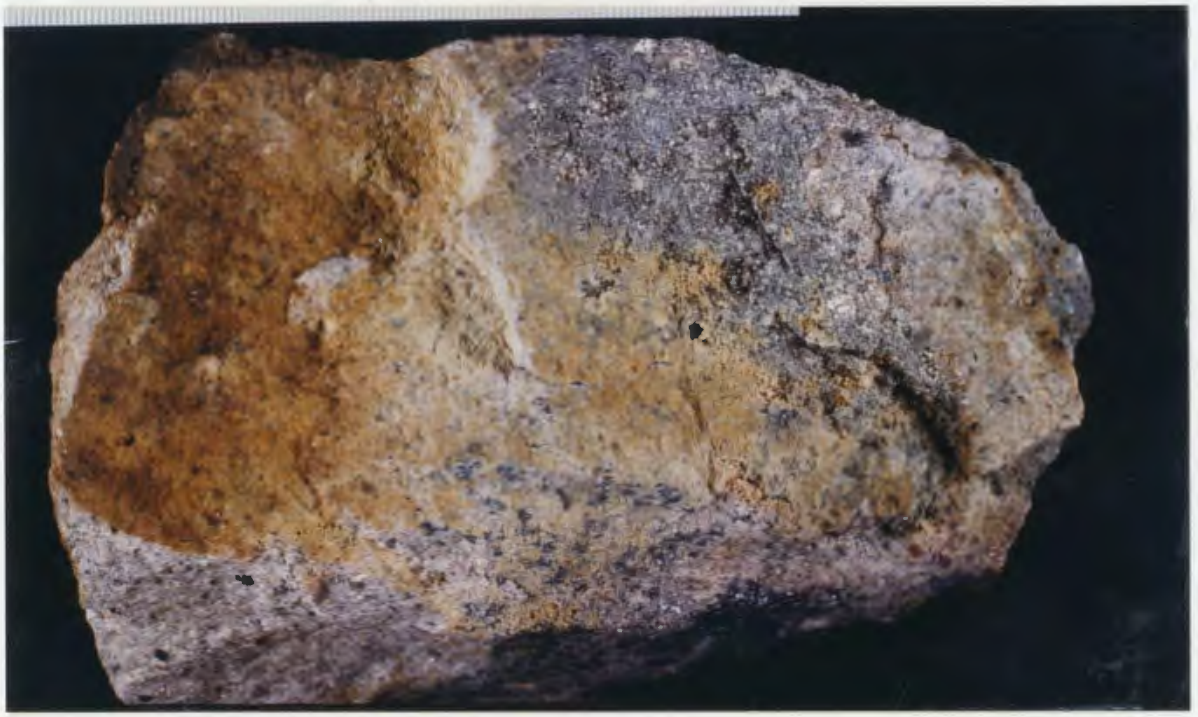

Plate 29: fracture controlled mineralization and alteration at the Wyllie Hill molybdenite prospect.

quartz veins occur in the rhyolite adjacent to the mineralized zone. These veins have variable attitudes, pinch and swell, and are up to 0.5 m wide. Minor pyrite and molybdenite occurs in fractures in the rhyolite.

4-3-2-3: Lithology: The coarse to fine grained granites at the prospects (Fig. 28) are comparable to those of the host granite (see section 4-3-1) and have been described by Whalen (1976, 1980). In general, mineralization is present in finer grained rocks and areas of abundant coarse pegmatite are associated with the Ackley City, Crow Cliff-Dunphy Brook and Wyllie Hill prospects. However, these lithologies are not confined to mineralized areas but may occur throughout the Rencontre Lake Granite. Muscovite-greisen pods at the Ackley City prospect do not form mappable features but are presumably related to mineralization. The bleached aplite which hosts the Wyllie Hill deposit is the only distinctive, exposed, lithology associated with molybdenite in the Rencontre Lake Granite. White mica alteration is abundant adjacent to veins and fractures in the most heavily mineralized parts of the Wyllie Hill prospect.

4-3-2-4 Petrography: This has been described by Whalen (1976, 1980; see section 4-3-1). At the Ackley City prospect, microcline is the dominant alkali feldspar in granite. This contrasts with orthoclase at the other prospects and throughout the Rencontre Lake Granite. Feldspars contain abundant fine grained hematite. In addition, calcite, barite, and fluorite have been reported from veins and fractures at the Ackley City prospect.

The area of bleached feldspar at the Wyllie Hill prospect contrasts with the normal pink to orange colour. The feldspar does not exhibit pervasive alteration to sheet silicates, but minor saussuritization is present.

4-3-2-5 Mineral Chemistry: The molybdenite polytype $2H_1$ occurs at all four prospects and slightly disordered orthoclase is the pegmatitic alkali feldspar at the Ackley City, Crow Cliff-Dunphy Brook and Wyllie Hill prospects (Whalen, 1976).

4-4 THE ENVIRONMENT OF CRYSTALLIZATION AND METALLIZATION

4-4-1 The Geological Environment

The variable, coarse to fine grained rocks in the Rencontre Lake and Sage Pond granites have been considered to represent the marginal, or roof, facies of the Ackley Granite Suite (White, 1939; Whalen, 1976, 1980; Dickson, 1983; Tuach 1984a). Rapid variations in grain size and texture, along with pegmatite, are interpreted to reflect rapid changes in nucleation rates and crystal growth rates which occurred in response to local variation in vapour pressure and/or cooling rates at the roof and margin of the granite. These textural variations collectively define the roof facies of the granite, but individually have little direct influence on the locale of mineralization. The internal intrusive contacts in the granites are not considered to be temporally or genetically significant and individual textural facies have no direct correlation with mineralization.

4-4-2 Formation of the Molybdenite Deposits

The main prospects occur in shallower dipping concave features on the generally steeply dipping contact of the Rencontre Lake Granite. Thus they represent areas where mineral bearing fluids or magmatic precursors to mineralization were trapped against the contact (White, 1939; Whalen, 1976, 1980). The deposits have been classified (Whalen, 1976, 1980) as aplite-pegmatite 'type', collectively exhibiting features which represent the transition from molybdenite deposition in the magmatic environment (Motu and partly Ackley City), to the pneuomatolytic environment (Crow Cliff-Dunphy Brook) to the dominantly hydrothermal environment (Wyllie Hill and parts of Ackley City). The magmatic environment is texturally indicated by the granular disseminated molybdenite and a lack of low temperature alteration features, the hydrothermal environment is characterized by secondary alteration and the stockwork mineralization (Whalen, 1976, 1980).

The miarolitic cavities and the pegmatite indicate that the magmatic environment was fluid saturated at the four sites of mineral deposition, a feature in common with large areas of the Rencontre Lake Granite. The quartz pods which are most abundant at the Ackley City prospect have margins of quartz-feldspar and may simply reflect an excess of silica in the final stages of crystallization of the fluid-rich magma. The downward termination of quartz crystals in the Crow Cliff-Dunphy Brook area indicate downward-growth from the rhyolite roof (Whalen, 1976), or from early chilled marginal aplite phases near the roof. Parallel sheets of stockscheider with intervening aplite may be

developed, indicating rapid variations in fluid pressure in the roof zone during crystallization, with the pegmatite formed under high fluid pressure and the aplite formed by pressure-quenching due to loss (through fracturing?) of vapour (Jahns and Burnham, 1969).

The low temperature alteration features (muscovite and sericite alteration) at the Ackley City and Wyllie Hill prospects indicate a continuum of higher to lower temperature alteration as the granite cooled. The stockwork alteration and mineralization at the Wyllie Hill prospect indicate a low temperature overprint (possibly by meteoric) of magmatic features. Bleaching of feldspar in the Wyllie Hill area has been attributed to leaching of iron from the feldspars to form pyrite (White, 1939) and to reduction of ferric to ferrous iron by addition of sulphur to the rock (Whalen, 1976). The bleaching is also partly due to fine sericite alteration of feldspar.

Whalen (1980) suggested that the aplites intruded the coarser grained granite and that the aplite and associated mineralizing fluids were a final product of liquid-crystal fractional crystallization processes (cf. McCarthy and Hasty, 1976). Whalen (1983) suggested that liquid-state magmatic diffusion processes (Hildreth, 1979, 1981) could have also been important in the generation of the molybdenite prospects.

4-4-3 Formation of the Sage Pond Greisen

The predominant subvertical E-W trend of the smaller greisen veins, the presence of en echelon sets of veins and the internal vertical

layering in these small veins, indicate that the mineralizing fluids rose along pre-existing fractures in a solid granite body. The presence of quartz phenocrysts in adjacent greisen and host granite suggest that these veins formed by alteration of pre-existing granite. Stockworks of hair-line fractures in the Granite with minor alteration and mineralization, indicate that the process of hydraulic fracturing (Burnham, 1979) may have assisted in formation of the larger fractures and mineralized veins. The relative absence of kaolinite and sericite in small greisen veins from the north part of the Sage Pond Granite, suggest that temperatures of vein formation were higher in this area, or that low temperature modification of high temperature veins did not occur.

The largest greisen are located in outward (southwards) convex lobes of the granite contact and the presence of shallow southerly-dipping quartz-topaz layering at the Anesty prospect suggests that this greisen formed from a fluid ponded in an embayment at the granite margin. Alteration of the intruded rhyolite to the south of the Anesty prospect suggests that the greisen forms a sheet or body which extends under the rhyolite.

The erratic distribution of minerals of economic interest is typical of many granophile deposits (Pollard and Taylor, 1985). The difficulty in identification of the tungsten-bearing phase in the Sage Pond area is thought to be due to its erratic distribution and its fine grained habit. Significant concentrations of tungsten were not recorded during analyses of the other mineral phases.

A model is envisaged in which fluorine-tin-tungsten-bearing magmatic fluids evolved from a rapidly crystallizing, highly fractionated, high level marginal phase of the Ackley Granite Suite and rose along predominantly E-W trending fractures in the solidified granite carapace to collect in embayments at the granite margin and roof. Comparable models have been presented for Sn-W granitoid mineralization in many parts of the world (eg. Richardson et al., 1982; Eadington, 1983; Kleeman, 1985).

Most authors accept that topaz-rich greisens form by hydrothermal alteration caused by aqueous solutions, although Eadington (1983) argued that massive topazite greisens in eastern Australia formed from residual fluorine-rich silicate magmas. This latter proposal was opposed by Kleeman (1985) on the basis of field evidence. The greisens in the Sage Pond area provide ample field evidence for hydrothermal alteration of the host granite and are considered to have formed by hydrothermal alteration of the parent rock.

4-4-4 Comparison Between the Sage Pond and Rencontre Lake Areas

The similarities in lithology, petrography, and texture of the host granites to mineralization in the Rencontre Lake and Sage Pond granites are striking. In addition, the deposits all occur at the granite contact in convex lobes, with the most widespread mineralization located at areas of shallow dip of the rhyolite-granite contact. These features indicate that the petrogenetic and crystallization history of the separate granites and mineral deposits are similar and that the large

scale controls over location and morphology of the different deposits are identical.

Differences between the Rencontre Lake and Sage Pond granites are minor. The Sage Pond granite contains relatively fewer miarolitic cavities and pegmatite. Muscovite alteration of biotite and feldspar is widespread in the Sage Pond area, while chlorite alteration of biotite is dominant in the Rencontre Lake Granite. The textural differences may be related to the degree of water saturation or pressure of crystallization of the solidifying magma. Differences in alteration mineralogy reflect differences in the subsolidus history which may be controlled by different fluid composition and temperature.

There is also a difference in the style of mineralization between the two areas. Small Sn-W greisen veins occur throughout the Sage Pond Granite, with the largest mineralized greisen at the granite margin. In contrast, molybdenite mineralization and associated alteration in the Rencontre Lake Granite are generally confined to the granite margin. However, isolated, small quartz veins are present over large areas of the Rencontre Lake Granite and may be an equivalent to the smaller greisen veins in the Sage Pond Granite.

CHAPTER 5 - MAJOR OXIDE AND TRACE ELEMENT GEOCHEMISTRY

5-1 INTRODUCTION

This chapter: (1) defines regional geochemical trends based on the data of Dickson (1983), (2) describes the geographic relationship of these trends to areas of known mineralization and to textural and mineralogical variations in the study area, (3) summarizes and compares geochemical data from the mineralized rocks and host granite at Sage Pond and at Rencontre Lake and (4) compares the geochemistry of the study area to that of granites associated with significant mineralization and to high-silica volcanic systems in other parts of the world.

Dickson (1983) presented analytical data for the major oxides and 21 trace elements from 357 samples collected systematically on a grid of 4 km spacing over the study area (Appendix B-1). These data were collected as part of a regional 1:50,000 scale mapping programme currently being undertaken by the Newfoundland Department of Mines and Energy. A major advantage of the large body of systematically collected data is that it can be used to show statistically valid geographic trends in the geochemical variation, both for the body as a whole and for the individual lithological units. Much of the data analysis was performed on sample groups outlined by Dickson (1983). Therefore, reference is made to the original units in some of the data presentation, particularly where significant features diverge from them.

Instrumental neutron activation analyses (INNA) for rare-earth elements (REE), As, Co, Cs, Hf, Sb, Sc, Ta, Th, U and W were performed on 20 samples from throughout the study area (Appendix B). These data are listed in Appendix F and the rare-earth element data are discussed in Chapter 6. In addition, the 357 samples collected by Dickson were analyzed for H_2O, S and CO_2 at the Newfoundland Department of Mines and Energy Laboratory.

5-2 AREAL PATTERNS OF GEOCHEMICAL VARIATION

5-2-1 Regional Variations

The average compositions of the sample groups, or lithological units, recognized by Dickson (1983) are presented in Table 8 and summarized in Figures 29 and 30. These figures show the sample groups plotted in order of increasing mean SiO_2 content from left to right, an arrangement which mimics their geographic distribution from west to east. Silica content throughout the southeastern granites is very high. The five lowest-silica sample groups occur in the Gander Terrane to the west of the projected trace of the Dover-Hermitage Bay Fault zone. The other groups either overlap the Fault zone (Meta Granite) or occur in the Avalon Terrane. The different terranes are also reflected in the other major oxides which are higher in the northwest than in the southeast. The concentrations of V, Zn, Sr and Ba are significantly higher in the granitoid rocks intruding the Gander Terrane, while Rb, Y, Nb, Th and U are highest in the granites intruding the Avalon Terrane. Other trace elements (Li, Be, F, Cu, Pb, Ga, Zr, Sn and Mo) do not exhibit systematic variations with respect to the Fault zone.

Table 8: Mean Composition of the lithological units recognized by Dickson, (1983).

Pluton	Total Popn.		Koskaecodde		Mollyguajeck	
Unit			9		10	
No. Samples	357		29		22	
Statistic	x	s	x	s	x	s
Oxide wt.%						
SiO_2	73.7	3.8	68.4	5.5	68.9	4.6
Al_2O_3	13.11	1.30	14.53	1.54	14.44	1.27
Fe_2O_3	0.53	0.42	0.95	0.62	0.84	0.66
FeO	1.09	0.68	2.09	1.13	1.81	0.96
MgO	0.45	0.51	1.31	0.86	1.15	0.82
CaO	0.92	0.76	2.10	1.20	1.93	1.17
Na_2O	3.45	0.37	3.17	0.55	3.09	0.26
K_2O	5.00	0.52	4.90	0.71	5.02	0.86
TiO_2	0.39	0.18	0.56	0.29	0.46	0.25
MnO	0.05	0.02	0.08	0.03	0.06	0.03
P_2O_5	0.06	0.06	0.16	0.10	0.23	0.10
LOI	0.83	0.32	1.18	0.46	1.32	0.51
Element g/t						
Li	43	22	37	17	38	14
Be		6	3	4	1	No Analyses
F	737	548	769	359	498	238
V	20	26	56	40	52	36
Cu	3	3	4	3	5	5
Zn	16	16	31	20	22	20
Ga	17	3	15	3	16	3
Rb	274	95	232	51	217	48
Sr	112	134	167	96	198	103
Y	55	28	44	15	29	9
Zr	159	58	185	70	159	64
Nb	34	18	23	8	16	7
Mo	4	5	3	1	4	3
Sn	2	13	1	1	1	0
Ba	308	243	504	328	521	246
Pb	27	10	29	8	32	11
Th	40	14	28	12	22	11
U	.4	3	4	2	3	1

Table 8: (Cont.d)

Pluton	Sylvester		Kepenkeck		N.A.	
Unit	11A		11B		12	
No. Samples	28		20		15	
Statistic	x	s	x	s	x	s
Oxide wt.%						
SiO_2	71.5	2.0	72.4	1.5	70.6	4.3
Al_2O_3	13.75	0.79	14.11	0.50	14.09	2.25
Fe_2O_3	0.67	0.55	0.50	0.28	0.69	0.40
FeO	1.14	0.39	1.06	0.28	1.62	0.43
MgO	0.63	0.29	0.56	0.26	0.86	0.42
CaO	1.16	0.36	1.16	0.32	1.53	0.80
Na_2O	3.53	0.28	3.68	0.25	3.20	0.27
K_2O	4.69	0.56	4.62	0.34	5.21	1.02
TiO_2	0.35	0.10	0.38	0.09	0.45	0.15
MnO	0.06	0.02	0.06	0.01	0.06	0.02
P_2O_5	0.09	0.04	0.09	0.02	0.01	0.06
LOI	1.01	0.37	1.01	0.78	0.96	0.25
Element g/t						
Li	50	20	78	21	51	19
Be	6	1	7	3	5	2
F	626	365	538	169	707	251
V	29	12	23	12	41	27
Cu	4	5	2	1	2	0
Zn	19	14	18	6	25	15
Ga	16	3	17	2	18	5
Rb	234	65	222	22	295	117
Sr	230	128	297	68	119	52
Y	36	14	22	5	45	16
Zr	146	35	114	22	184	59
Nb	24	10	18	3	28	10
Mo	4	2	4	1	4	1
Sn	1	1	1	0	1	1
Ba	420	158	579	129	384	186
Pb	28	6	29	3	36	29
Th	26	10	30	10	30	10
U	4	2	5	2	5	2

Table 8: (Cont.d)

Pluton	Tolt		Hungry Grove		Rencontre Lake	
Unit	13		14		14A	
No. Samples	80		84		49	
Statistic	x	s	x	s	x	s
Oxide wt.%						
SiO_2	74.6	2.5	75.7	2.2	75.5	2.3
Al_2O_3	12.78	1.08	12.40	0.79	12.65	0.82
Fe_2O_3	0.47	0.30	0.42	0.28	0.33	0.26
FeO	0.91	0.49	0.89	0.40	0.90	0.44
MgO	0.29	0.15	0.22	0.16	0.16	0.12
CaO	0.77	0.38	0.52	0.23	0.49	0.29
Na_2O	3.34	0.31	3.49	0.26	3.77	0.23
K_2O	5.21	0.44	5.01	0.29	4.9	0.27
TiO_2	0.26	0.11	0.21	0.11	0.18	0.11
MnO	0.04	0.01	0.04	0.02	0.04	0.01
P_2O_5	0.04	0.03	0.04	0.03	0.03	0.03
LOI	0.67	0.15	0.70	0.14	0.71	0.11
Element g/t						
Li	40	15	46	19	30	13
Be	5	1	7	3	5	2
F	675	365	1022	697	533	412
V	11	7	13	23	9	19
Cu	3	3	2	2	2	2
Zn	10	10	12	16	20	18
Ga	16	3	18	3	18	3
Rb	255	60	334	88	263	76
Sr	93	192	63	68	47	54
Y	54	21	70	28	75	24
Zr	153	57	168	56	164	71
Nb	31	11	46	18	44	20
Mo	5	8	4	3	4	2
Sn	2	1	2	1	3	2
Ba	293	180	206	216	175	182
Pb	24	8	27	7	26	11
Th	28	14	40	13	32	9
U	4	2	7	3	7	3

Table 8: (Cont.d)

Pluton	Sage Pond		Meta		Whalen 1976	
Unit	14B		15		Part of 14A	
No. Samples	9		21		31	
Statistic	x	s	x	s	x	s
Oxide wt.%						
SiO_2	76.9	0.8	75.1	2.2	76.5	1.9
Al_2O_3	11.99	0.22	12.93	0.85	12.25	0.67
Fe_2O_3	0.39	0.37	0.50	0.34	1.17	0.42
FeO	0.55	0.33	0.67	0.31	-	(TOT)
MgO	0.10	0.04	0.31	0.13	0.20	0.13
CaO	0.33	0.11	0.61	0.25	0.43	0.19
Na_2O	3.52	0.18	3.57	0.42	3.44	0.44
K_2O	4.98	0.14	5.06	0.45	4.80	0.16
TiO_2	0.11	0.03	0.24	0.10	0.22	0.22
MnO	0.03	0.01	0.04	0.01	0.05	0.02
P_2O_5	0.01	0.00	0.04	0.03	-	
LOI	0.77	0.09	0.76	0.15	-	
Element g/t						
Li	87	31	23	9	-	
Be	12	5	3	1	-	
F	2016	987	328	162	-	
V	5	0	9	7	-	
Cu	2	0	2	1	4	11
Zn	12	11	12	10	25	37
Ga	21	2	13	2	-	
Rb	556	46	207	48	313	61
Sr	11	3	93	46	60	40
Y	96	42	32	12	-	
Zr	154	17	141	48	176	52
Nb	76	12	23	4	-	
Mo	5	2	4	1	-	
Sn	29	80	1	0	-	
Ba	56	24	295	178	138	86
Pb	35	9	25	7	-	
Th	65	7	23	6	-	
U	14	4	4	1	-	

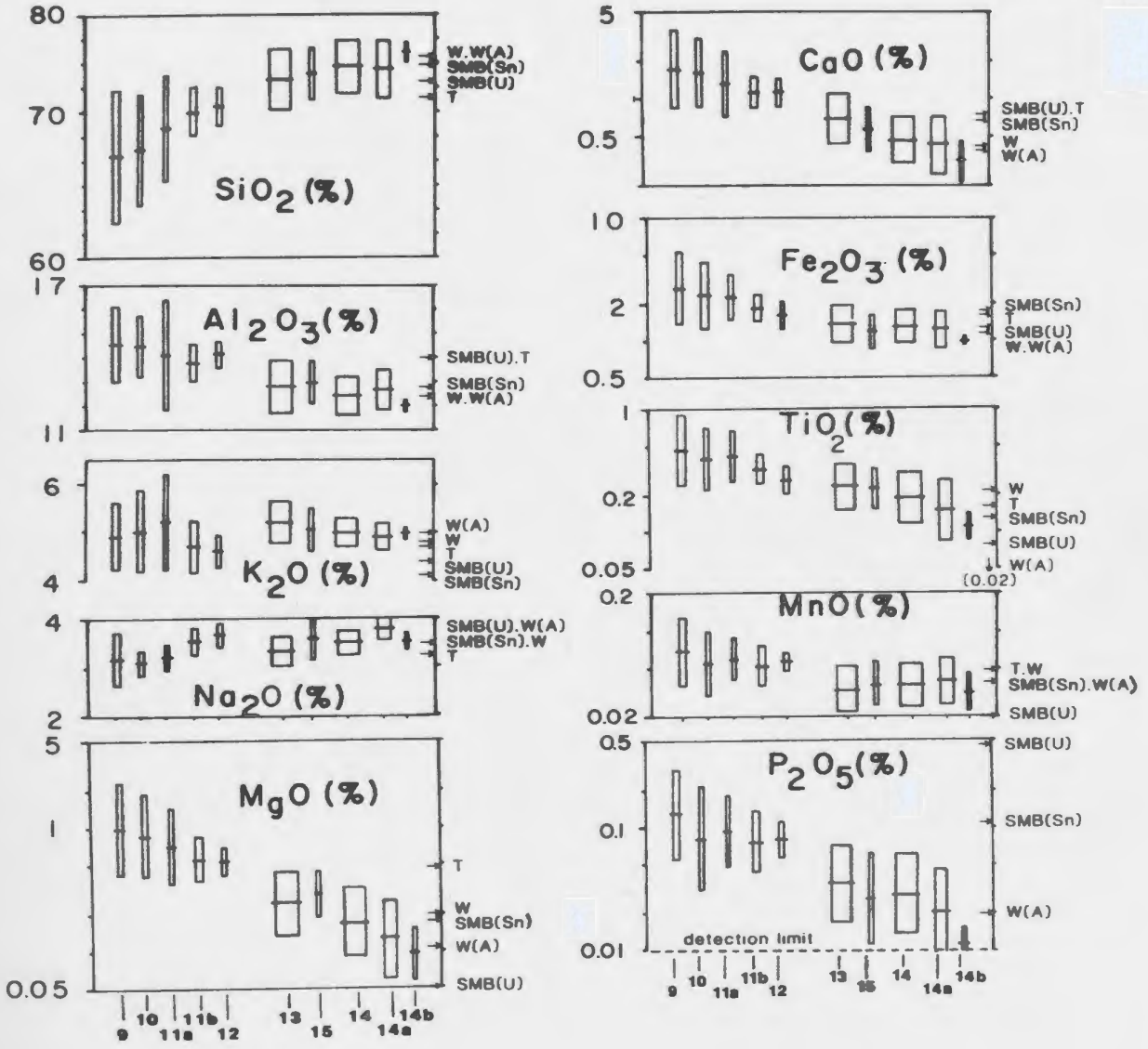

Figure 29: Major element distribution in the study area based on the units of Dickson, (1983). Horizontal line is mean, vertical range is one standard deviation, and width of box is proportional to number of samples in the unit. Unit numbers are shown on the horizontal axis of the plots. Arrows on right of diagrams are means of other data sets for comparison: W - Whalen (1976); W(A) - Whalen (1980); T - Tischendorf (1977); SMB(U) and SMB(Sn) - Chatterjee and Strong (1983).

Figure 30: Trace element distribution in the study area based on the units of Dickson (1983). Diagram explained in caption to Figure 29.

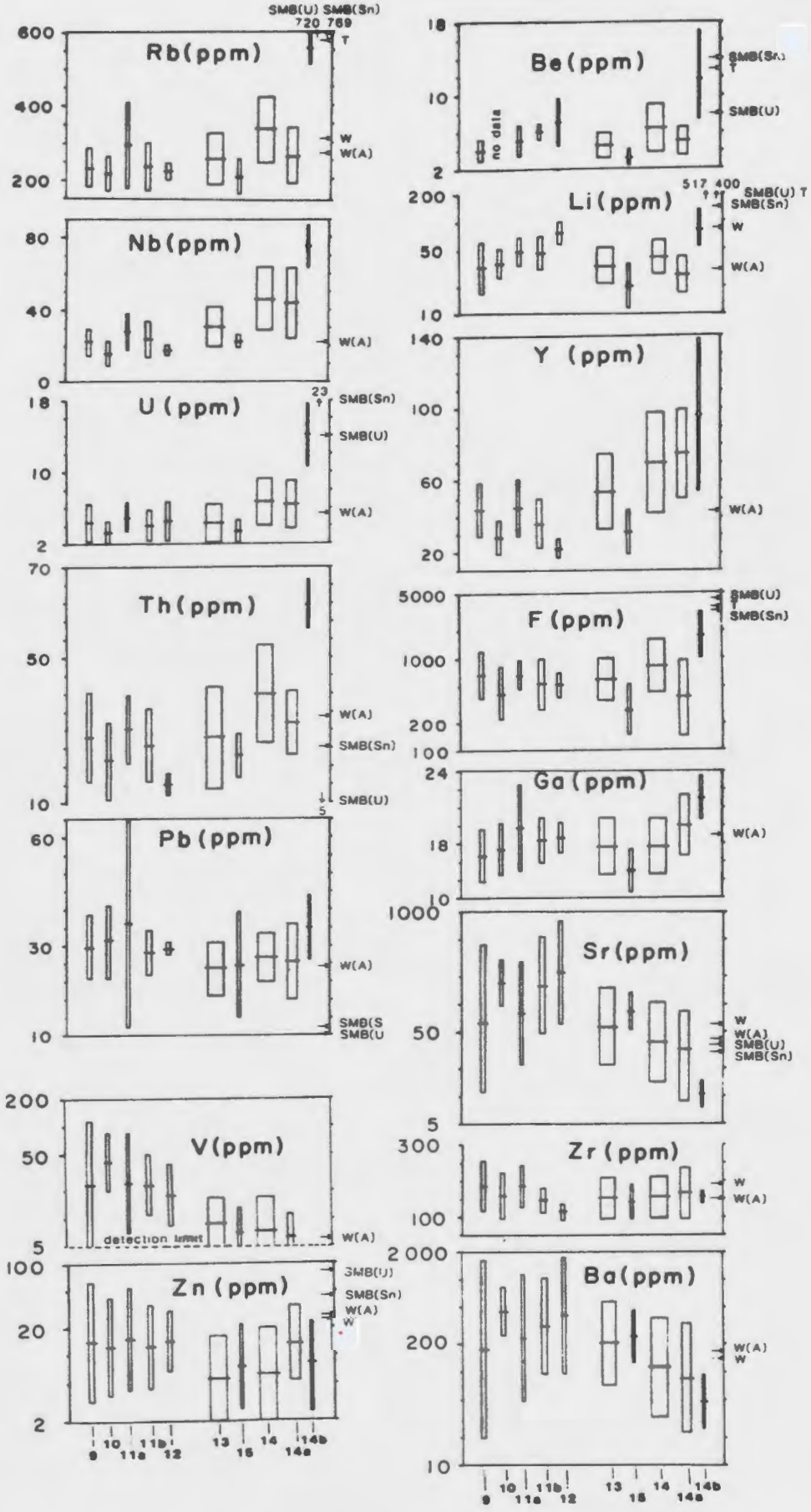
Rb(ppm)
SMB(U) SMB(Sn)
720 769
T
W
W(A)
Nb(ppm)
W(A)
U (ppm)
23
SMB(Sn)
SMB(U)
W(A)
Th(ppm)
W(A)
SMB(Sn)
SMB(U)
Pb(ppm)
W(A)
V(ppm)
detection limit
W(A)
Zn (ppm)
SMB(U)
SMB(Sn)
W(A)
W
Be(ppm)
no data
SMB(U)
Li(ppm)
517 400
SMB(U) T
SMB(Sn)
W
W(A)
Y (ppm)
W(A)
F (ppm)
SMB(U)
SMB(Sn)
Ga (ppm)
W(A)
Sr(ppm)
W
W(A)
SMB(U)
SMB(Sn)
Zr (ppm)
W
W(A)
Ba(ppm)
W(A)
W
9
10
11a
11b
12
13
15
14
14a
14b

There are also some clear differences displayed in Figures 29 and 30 between the Sage Pond Granite and the other granites in the southwest. It has highest silica content and has higher concentrations of Rb, Nb, Th and U. The concentrations of Be, Ga, F and Li are double those of all other units.

The geochemical differences between the granitoid rocks in the northwest with lower silica and higher Ca-Femic oxides and those in the southeast with higher silica and lower Ca-Femic oxides, are seen in Figures 31 and 32 to occur across a line located approximately 10-15 km northwest of the projected trace of the Dover-Hermitage Fault zone. The projected trace is not highlighted by the chemical maps, nor are there distinct differences across this line. These features suggest that the magmatic systems indigenous to the Avalon Terrane overlapped onto the Gander Terrane.

The main chemical boundary between the northwest and southeast granitoids bisects unit 12 established by Dickson (1983). This boundary is also indicated from the petrographic data by the presence of hornblende on the northwest side and by changes in compositional trends of biotite across this line. The distribution of Al_2O_3, Li, F, Nb, Rb and Th (Figs. 31, 34, 35, 36), indicates that the southeast half of unit 12 forms part of the Hungry Grove Granite and the major oxide maps (Fig. 31, 32) indicate that the granitoid rocks in unit 12 immediately west of the chemical boundary belong to the Koskaecodde Pluton.

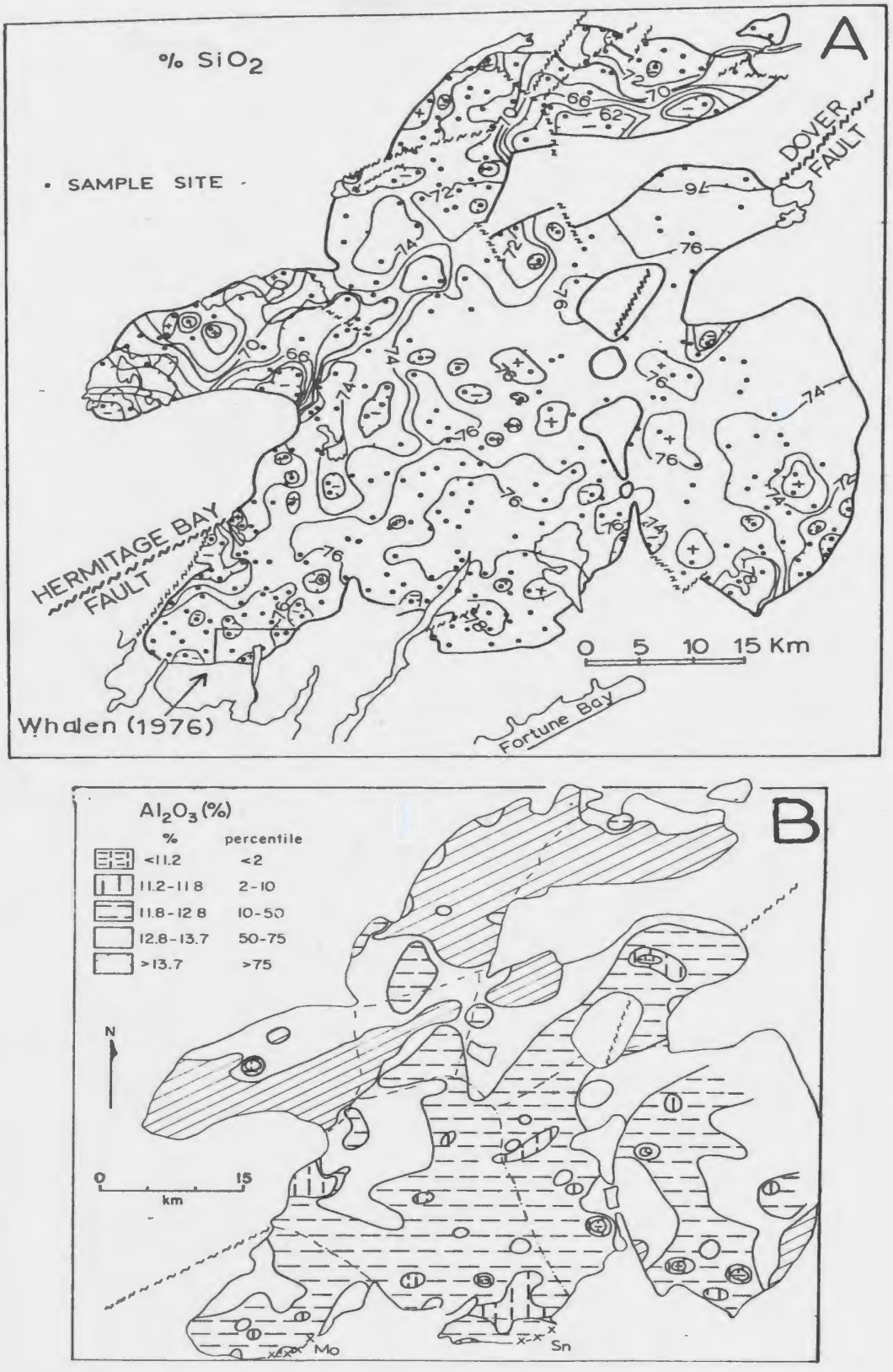

Figure 31: A: Sample location map and computer contoured map of silica in the study area. The area studied by Whalen (1976, 1980, 1983) is outlined (see frontispiece).
B: Map distribution of Al_2O_3 in the study area. Hand contoured, computer plotted data for sample stations illustrated on A.

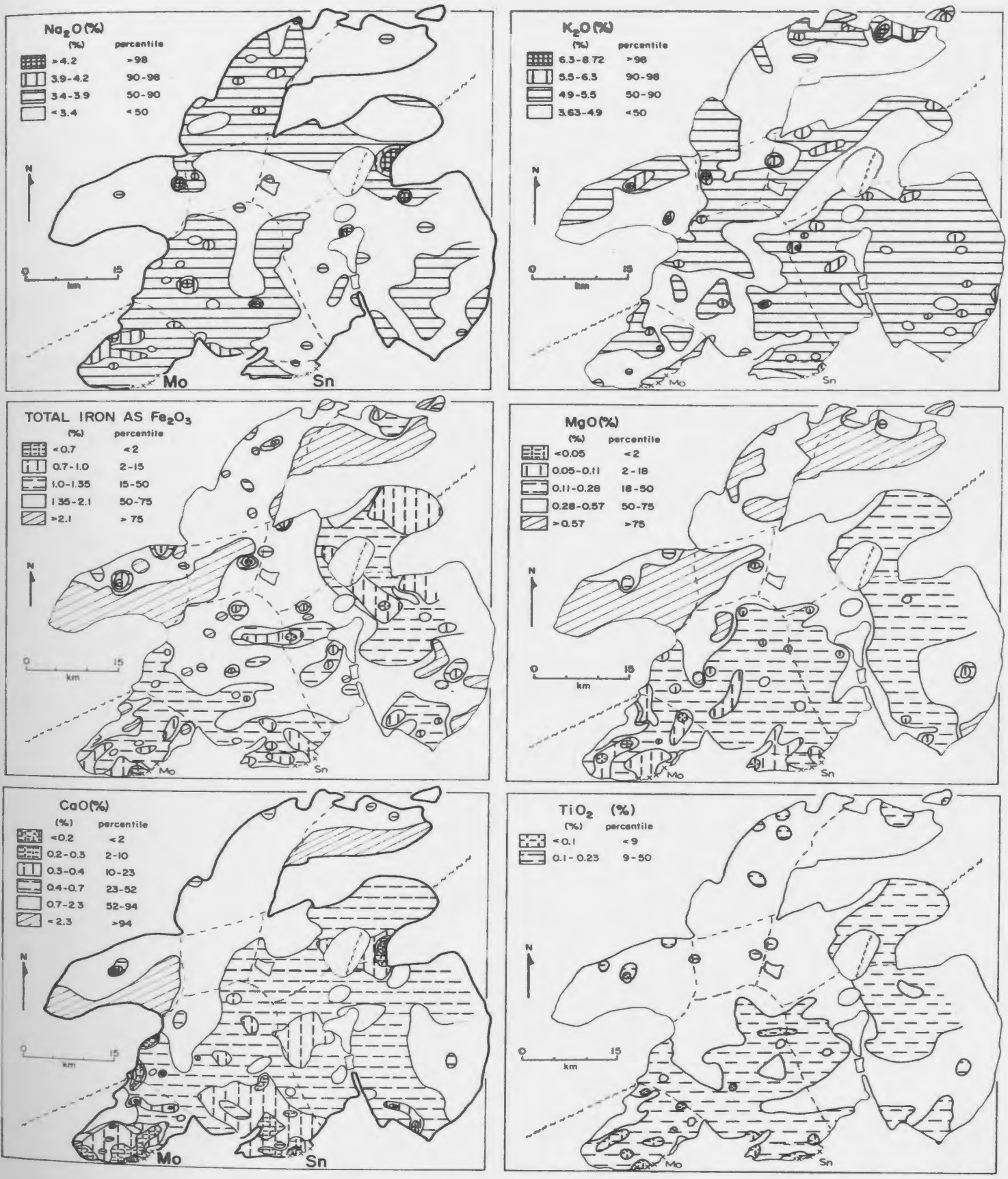

Figure 32: Map distribution of Na_2O, K_2O, Fe_2O_3, MgO, CaO and TiO_2 in the study area. Details as on Figure 31B.

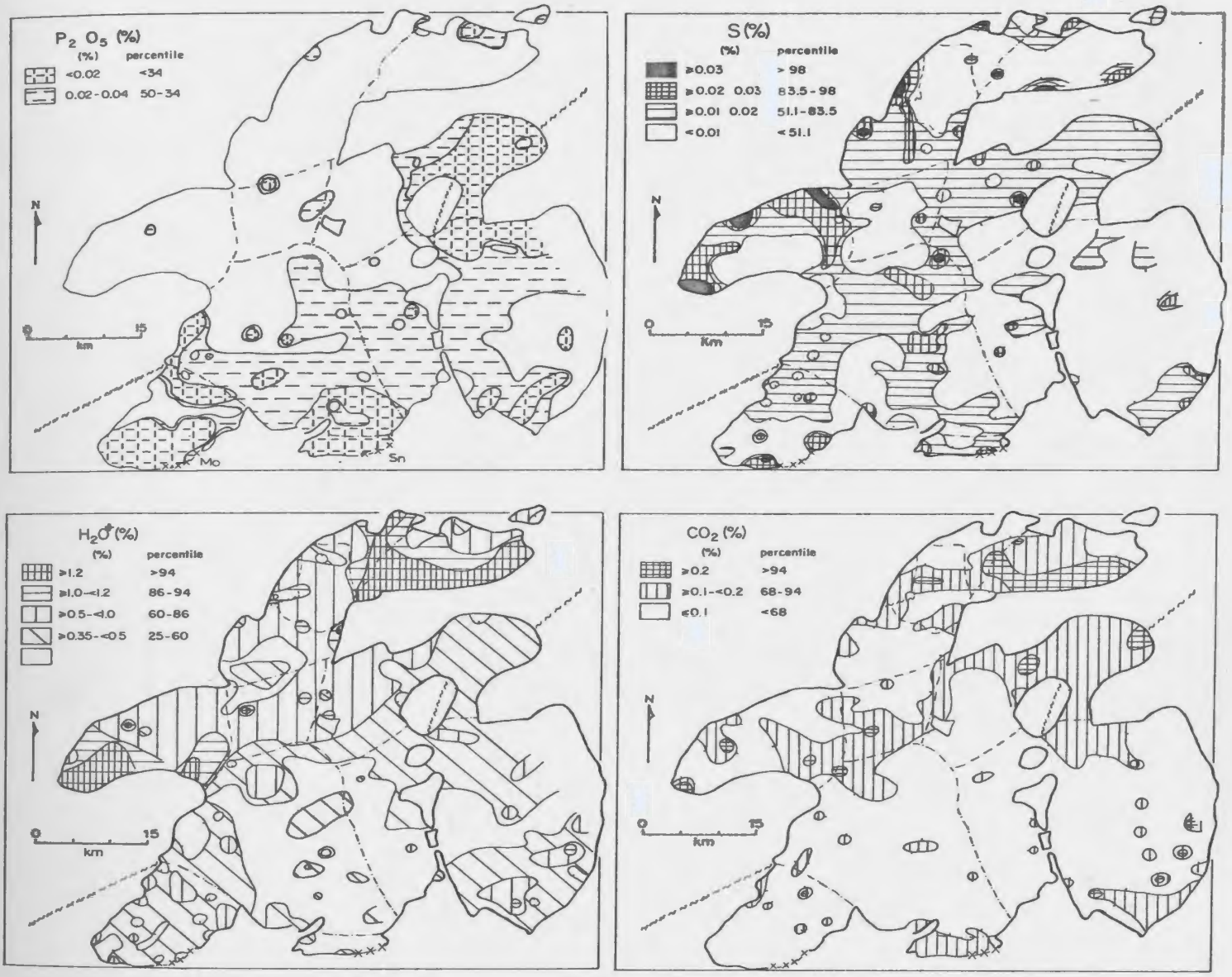

Figure 33: Map distribution of P_2O_5, S, H_2O^+ and CO_2. Details as Figure 31B. Clear areas have lower values than those shown in legends.

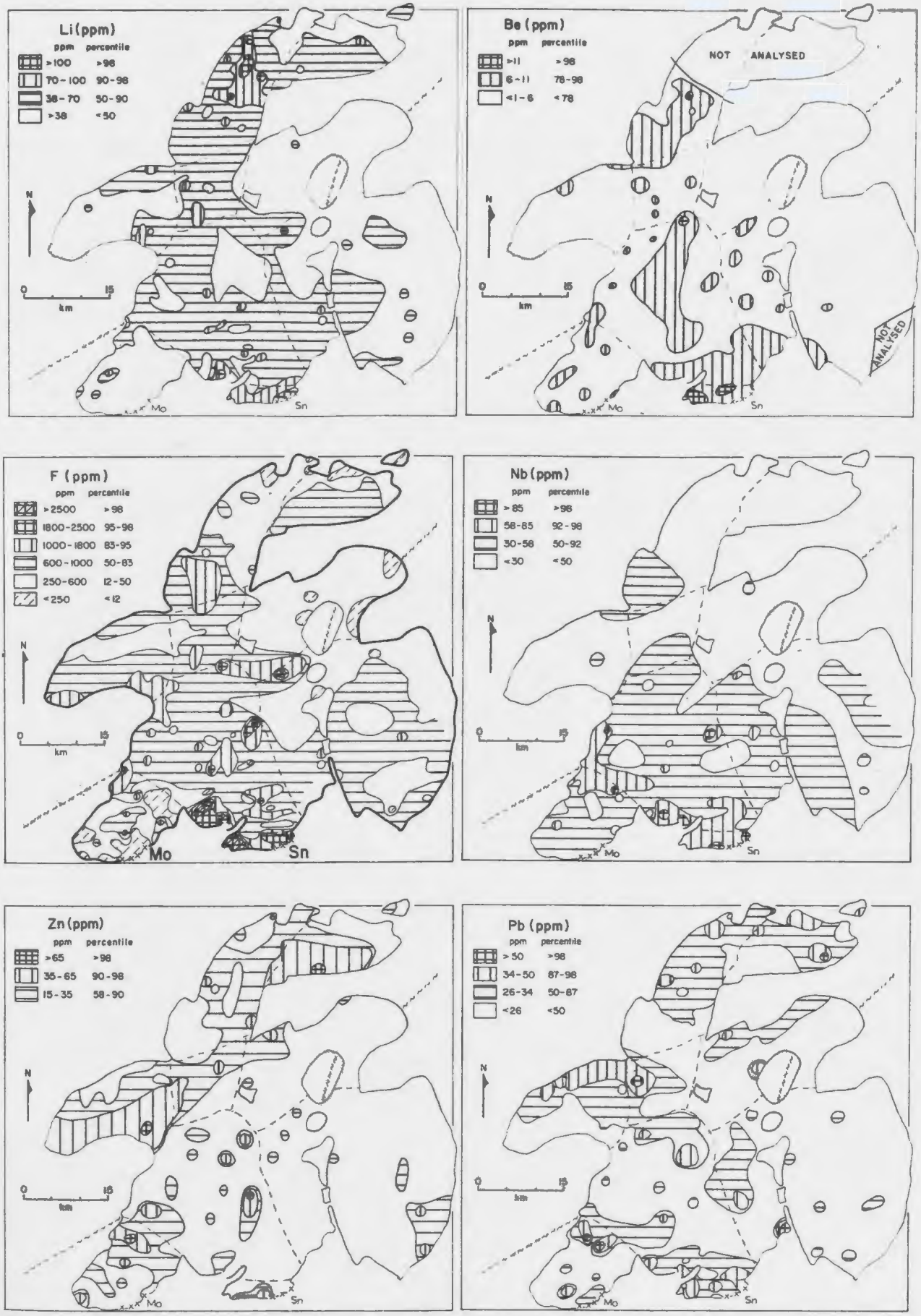

Figure 34: Map distribution of Li, Be, F, Nb, Zn and Pb in the study area. Details as on Figure 31B.

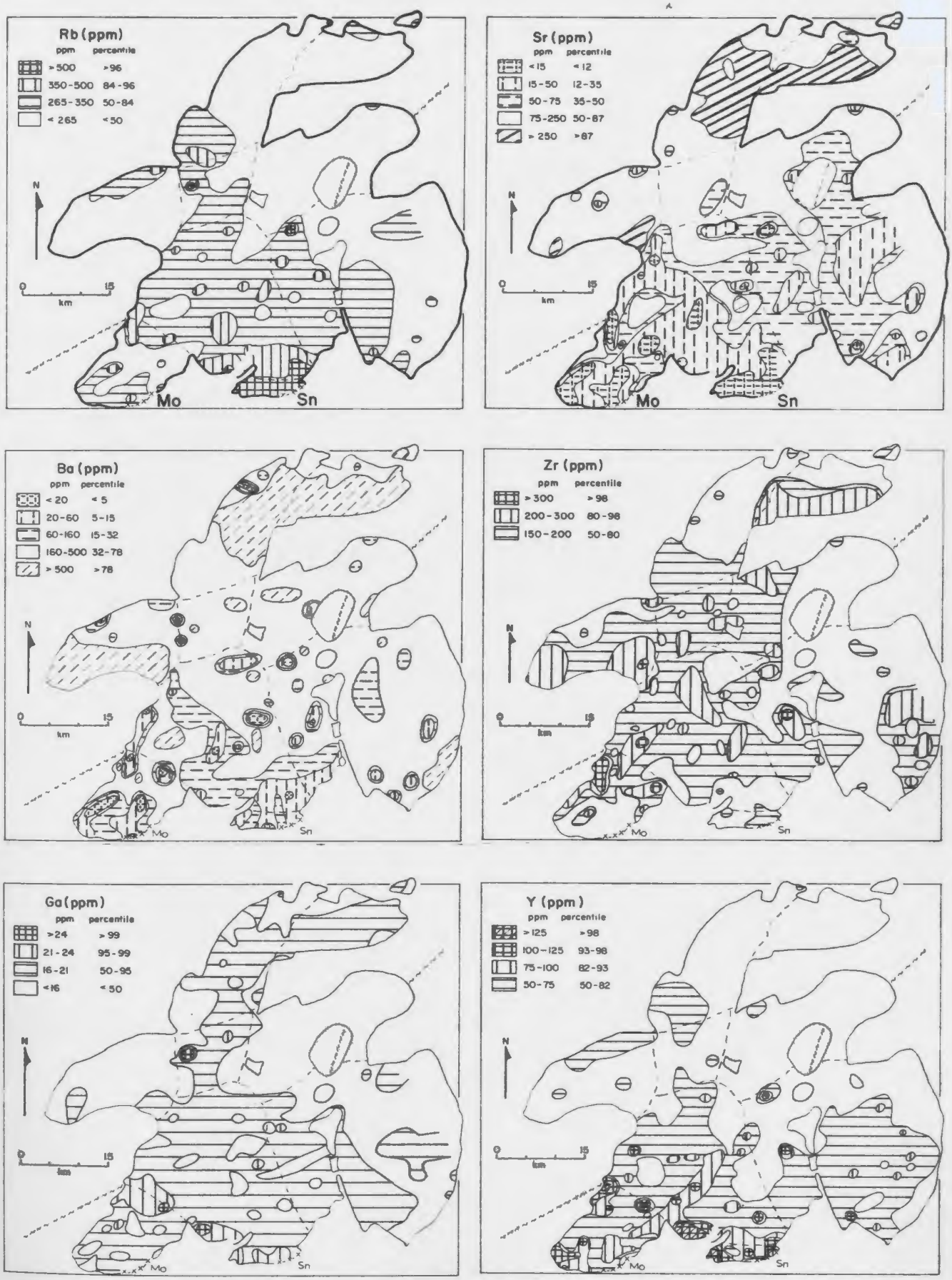

Figure 35: Map distribution of Rb, Sr, Ba, Zr, Ga, and Y in the study area. Details as on Figure 31B.

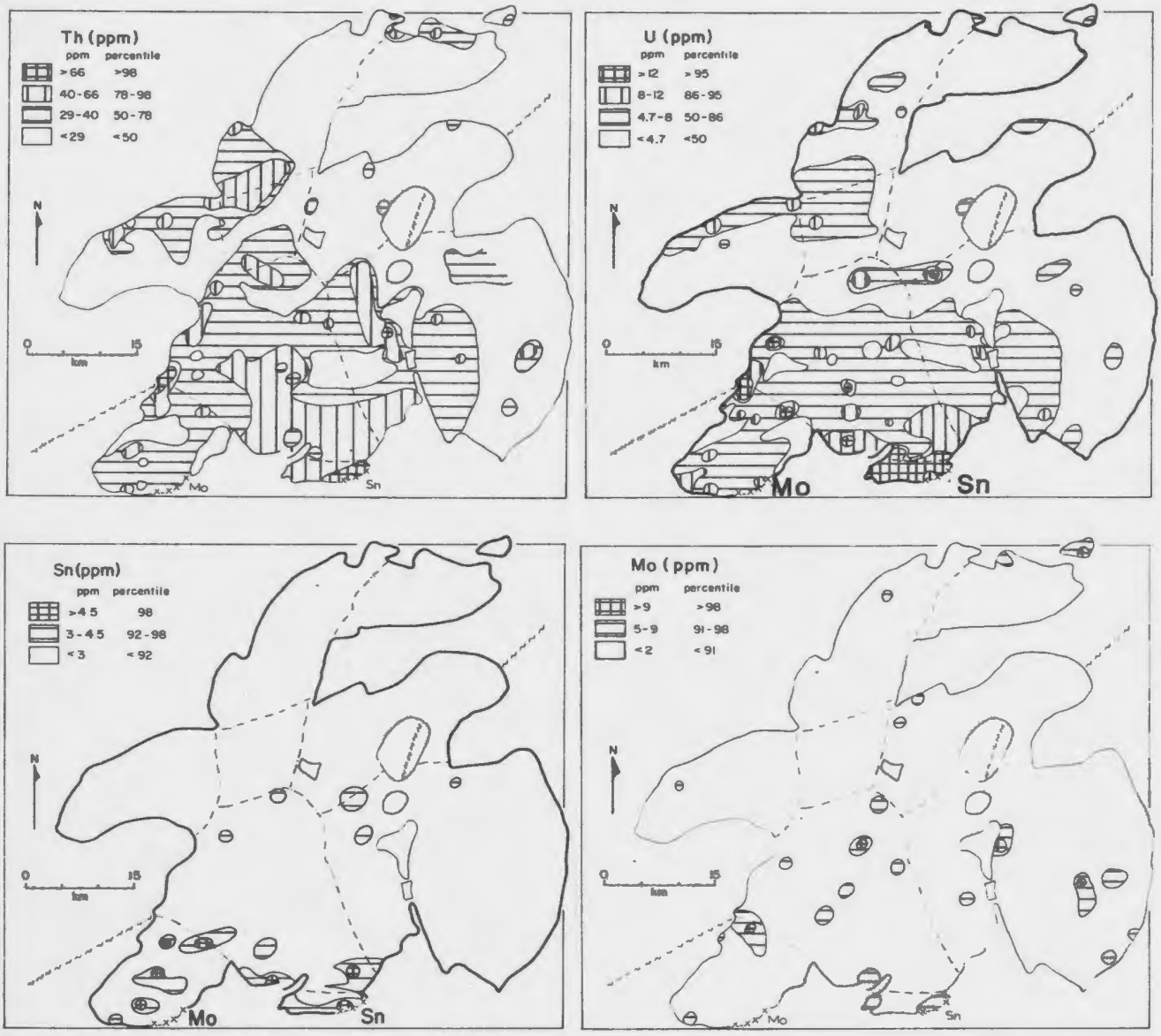

Figure 36: Map distribution of Th, U, Sn and Mo in the study area. Details as on Figure 31B.

Maps of Na_2O and K_2O do not exhibit clear trends with respect to the other oxides and elements. There is a tendency for Na_2O to have higher values in the northern and southwestern Ackley Granite Suite. There is no evidence for extensive albitization (Na-metasomatism) or K-Feldspar alteration associated with the main mineralized areas. Highest values for H_2O (Fig. 33) occur in the biotite-rich, relatively mafic rocks and slightly higher values occur in the Rencontre Lake Granite relative to the Sage Pond Granite. Carbon dioxide is highest in the mafic portion of the Mollyguajeck Pluton (unit 10) and is elevated along the trace of the northwest margin of the Hungry Grove Granite and in the Meta Granite; elevated values also occur in the Sage Pond Granite and in the southeast part of the Toit Granite. Sulphur values are erratic and are highest in the Koskaecodde Pluton.

In the northwest granitoids, values for SiO_2 are lower, and for other major oxides are higher, in the granodioritic parts of the Koskaecodde and Mollyguajeck plutons. These rocks have correspondingly low values for most large ion lithophile (LIL) trace elements (F, Ga, Rb, Y, Zr, Nb, Mo, Sn, Th and U) and higher values for Ba. Strontium is higher in the Mollyguajeck Pluton relative to the Koskaecodde Pluton (Table 8). Strontium and Ba values in the more felsic rocks of the Kepenkeck Granite are at a comparable level, or slightly higher, than values in mafic rocks of the Koskaecodde and Mollyguajeck plutons and are significantly higher than those for the latter plutons at the same SiO_2 levels (Dickson, 1983; Figs. 31, 35). This latter feature implies that the Kepenkeck Granite is genetically unrelated to the granodiorite-granite plutons.

Within the southeastern granites, there is a trend to higher values of LIL trace elements (enrichment trend) and to lower values of CaO, MgO, Ba and Sr (depletion trend) which culminates at the areas of known mineralization at Sage Pond and Rencontre Lake. The concentrations of Mo and Sn (Fig. 36) are generally at or below the analytical detection limit and it is not possible to map their regional distribution. Nevertheless, the higher concentrations of Sn occur in the Rencontre Lake, Sage Pond and southern Hungry Grove granites.

The elements Be, F, Ga, Rb, Y, Nb, Th and U are shown in Figures 34, 35 and 36 to be distinctly higher in the Sage Pond Granite compared to the other granites. This is also apparent from the geochemical maps, but the enrichment of these elements can be seen as part of a broad trend which includes all of the Hungry Grove Granite and the western parts of the Tolt and Meta granites. Several of the element trends (particularly F, Rb and Li) continue into the northwestern granitoids.

The values and patterns of major elements, Ba, Sr and Y are similar in the Rencontre Lake Granite and in the Sage Pond Granite. However, there are significant differences in other trace element concentrations. Rubidium, Nb, Th and U have elevated background values in the Rencontre Lake Granite but do not show the strong enrichment trends which are apparent in the Hungry Grove and Sage Pond granites. Fluorine is relatively depleted in the Rencontre Lake Granite and strongly enriched in the southern Hungry Grove and Sage Pond granites.

The trace element enrichment/depletion trends do not correspond exactly with silica enrichment and major element trends. High-silica rocks of the Meta Granite and the east part of the Tolt Granite are not enriched in the LIL elements or depleted in Ba and Sr. Contour lines and major oxide and trace element trends, clearly cross the defined lithological boundaries and there is a greater complexity of distribution of the trace elements relative to major oxides. These features indicate a form of trace element-cryptic layering throughout the southeastern granites.

5-2-2 Distribution of Element Ratios

The distribution of Rb/Sr ratios, shown in Figure 37, demonstrates the extremely differentiated (Rb/Sr $\geq$ 50) nature of the southern part of the Ackley Granite Suite and shows a trend of increasing values towards the main mineralized areas. K/Ba ratios (Fig. 37) also show the extreme differentiation. Both the Rb/Sr and the K/Ba are relatively high throughout the southeast granites.

U/Th ratios do not form a trend in association with mineralization and do not indicate U-specialization in the study area (cf. Chatterjee et al., 1983). These elements have a strong correlation and both show strong enrichment towards the Sage Pond area.

Ferric/ferrous ratios are erratic, although those in the Sage Pond Granite are higher than those associated with molybdenite in the Rencontre Lake Granite. Some of the highest values occur to the north of the tin-tungsten mineralized area at Sage Pond.

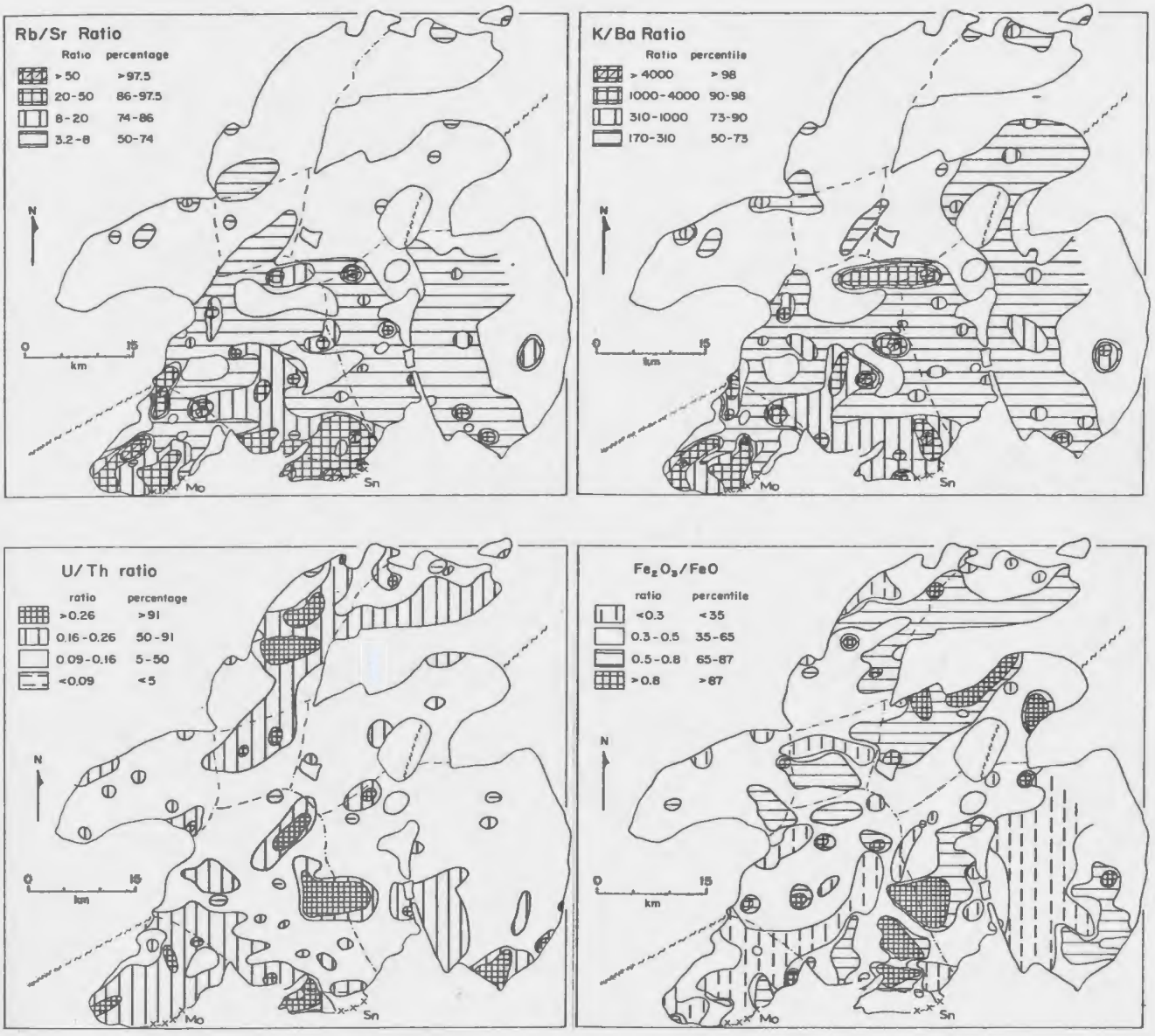

Figure 37: Map distribution of ratios of Rb/Sr, K/Ba, U/Th and Fe_2O_3 in the study area. Clear areas - Rb/Sr and K/Ba photos have values lower than those in legends.

5-3 STATISTICAL ANALYSIS OF GEOCHEMICAL DATA

5-3-1 Introduction

The data has been subject to statistical treatment to assess its accuracy and precision and estimates of these parameters were presented by Dickson (1983), and are summarized in Appendix B. Examination of data from duplicate and replicate samples and from resampling by the author indicates that the results are highly reproducible. The SPSS package (version 9.0; Nie et al., 1975) was used for the data analysis.

The range of data in many of the bivariate plots could be considered to result from problems associated with the coarse-grained nature of many of the rocks. However, the large samples collected (2 Kg), the scale of the sampling project and the reproducibility of the data in small areas indicate that the poor covariation between many element pairs is due to inherent variability in the chemical processes which operated to produce the granite compositions. Any trends which are evident from the large body of data are therefore considered to be real.

The results of three of the statistical procedures used to analyze the data are presented and discussed below. Spearman non-parametric correlation matrices were constructed to assess the co-variation of elements. R-mode factor analysis was chosen in order to summarize the large numbers of variables in the data file. Discriminant function analysis was selected to assist in classifying the granitoids in areas of ambiguity.

5-3-2 Spearman Correlations

Spearman non-parametric rank correlations were calculated for selected groupings of the data. This technique was selected since some element distributions are neither normal or lognormal and spurious values in a small sample population may strongly influence the apparent population distribution and the calculated covariance. This latter feature may affect comparison of data between sample populations of different size. The covariance values for the Spearman and the more commonly used Pearson correlations vary within a range of 10% for the larger groupings of samples.

The covariance of elements in the Rencontre Lake Granite and the Hungry Grove and Sage Pond granites are presented in two separate correlation matrices in Appendix E-1 and E-2 respectively. Correlation coefficients at less than the 90% confidence level have been omitted from these tables for clarity. The observed element covariances are considered normal for evolving granitic magma systems with a negative correlation between SiO_2 and the Ca-Femic oxides and a positive correlation between SiO_2 and the LIL trace elements; these element associations are generally stronger in the Rencontre Lake Granite than in the Hungry Grove Granite. K_2O and Na_2O have weak covariances in both matrices and are either independent or show a only weak covariance with the other elements in the Hungry Grove and Sage Pond granites. However, there is a moderate negative correlation of both of these oxides with SiO_2 and the LIL incompatible trace elements and a moderate positive correlation with the compatible trace elements (Ba, Sr) in the Rencontre Lake Granite.

A subsidiary correlation matrix based on 14 samples for which REE and INAA analyses are available is presented in Appendix E-3. The samples were selected as representative of the southeastern granites; data from the Rencontre Lake Granite was omitted since there are significant differences in trace element concentrations (Figs. 34, 35, 36).

The covariance of many elements in the main table (Appendix E-2) and in the subsidiary table are of similar sign and intensity, while other elements show significant differences. For example, SiO_2 has covariances with most other elements in the main table and does not show significant covariance with FeO, CaO, K_2O, TiO_2, F, Rb, Y, Nb, Th, or U in the subsidiary Table. In addition, F and Li are independent of the other variables in the subsidiary data-set while showing weak to moderate covariances with other trace elements in the main data. These features, resulting from the differences in size of the populations, may mean that the subsidiary sample set is inadequate to realistically characterize the geochemical variations in the Hungry Grove and Sage Pond granites. Nevertheless, there are some notable features.

The elements Li and F are commonly considered to be retained in the melt during magmatic differentiation, to partition into late aqueous phases, and to be concentrated via hydrothermal fluids (Strong, 1980, Manning and Pichivant, 1985). Thus the independent behavior of these elements from the other LIL elements and from each other in the subsidiary matrix may reflect their behavior in the magmatic system. The larger data base may reflect the compatible behavior of Li and F in the

magmatic stage, while the subsidiary data base, which is weighted with samples in proximity to mineralized areas, reflects the hydrothermal and therefore erratic, concentration of these elements.

Significant covariance of the light REE (La, Ce, Nd) and significant covariance of the light REE with other variables is not evident. A moderate negative covariance of Nd with CaO, V and Sr is present. This latter feature is unusual since the trivalent REE are thought to substitute most readily for Ca (cf. Taylor and Fryer, 1983), as does Sr. In contrast, the heavy REE (Tb to Lu) and Sm exhibit some of the strongest inter-element covariances and correlate strongly with most other LIL elements. The heavy REE also have a positive covariance with K_2O, a negative covariance with FeO, MgO, CaO, TiO_2, MnO and P_2O_5 and are independent of Na_2O. These features suggest that the controls over the distribution of the light REE are more complex than the controls over the heavy REE.

Tantalum and Hf, as expected, have a strong positive correlation with the elements Rb, Y, Th, U and As, while Co and Sc correlate positively with the compatible elements Sr and Ba, and with the Ca-Femic oxides. W shows a moderate covariance with both Li, F and As and has a negative covariance with K_2O and MnO.

5-3-3 Factor Analysis

5-3-3-1 A Factor Model: The statistical technique of R-mode factor analysis provides a method of combining the chemical data into a smaller

number of correlated variables ("factors") which can be calculated for each sample and thus assessed in terms of their spatial distribution. This technique, using principle component analysis requires no a priori assumptions about the underlying structure of, or relationship between, the variables.

The results of a four-factor model for the sample suite from the study area are shown in Table 9. The elements Sn, Mo and Be have been omitted from this model because a large proportion of the values for these elements are at or below the analytical detection limits. Communalities for each variable are also shown in Table 9 from which it can be seen that the model accounts well for the variance of all elements except Cu, which is near the analytical detection limit.

Together the four factors of the model account for 72% of the combined variance in the data. Factor 1, which accounts for almost half the variance, has high loadings for all the major oxides except K_2O and Na_2O, with the loading for silica being opposite in sense to that of the other oxides. This factor summarizes the trends shown in Figure 29 and in the map distributions of the major oxides (Figs. 31, 32, 33). The trace elements V, Sr, Ba, Zn, Zr and Cu all have positive loadings greater than 0.4 and Nb, Pb, Th and U negative loadings less than -0.4. Therefore, these elements contribute significantly to this factor. Factor 1 can be interpreted to represent the oxide and element correlation and associations related to crystallization of the major silicate phases in the granitoid rocks.

Table 9: The first four principal components (factors) for all lithogeochemical data (after VARIMAX rotation). Oxides and elements with factor loadings ≤ 0.4 are omitted.

Variable	Factor 1	Factor 2	Factor 3	Factor 4	Communality	
MgO	0.91				0.92	MgO
SiO_2	-0.90				0.87	SiO_2
TiO_2	0.90				0.88	TiO_2
CaO	0.90				0.86	CaO
Fe(tot.)	0.89				0.82	Fe(total)
P_2O_5	0.89				0.83	P_2O_5
Al_2O_3	0.83				0.89	Al_2O_3
MnO	0.81				0.71	MnO
V	0.86				0.77	V
Sr	0.75	-0.50			0.82	Sr
Ba	0.72	-0.47			0.74	Ba
Zn	0.68				0.61	Zn
Zr	0.57				0.60	Zr
Cu	0.41				0.22	Cu
Nb	-0.41	0.78			0.84	Nb
Rb	-0.42	0.76			0.85	Rb
U	-0.41	0.72			0.72	U
Th	-0.44	0.72			0.72	Th
Y		0.70			0.72	Y
F		0.63			0.59	F
Li		0.61			0.52	Li
Ga		0.52		0.51	0.57	Ga
Pb			0.79		0.72	Pb
K_2O			0.68		0.50	K_2O
Na_2O				0.82	0.68	Na_2O
percent variance	44.4%	14.6%	6.9%	6.0%		

Whereas major element oxide loadings of magnitude greater than 0.4 are associated solely with Factor 1, some trace elements are associated with two factors. Factor 2 is a positive association of the trace elements which are thought to be characteristically enriched in magmas during crystallization, together with a negative association of Sr and Ba. The fact that all of these elements (except Y, F and Li) are significant contributers to both Factors 1 and 2, which are by definition independent of each other, suggests that there are at least two distinct processes which account for the main geochemical variations in the granitoid rocks.

Factors 3 and 4 are much less important in accounting for the overall variance and demonstrate the independent behavior of K_2O and Na_2O, both from each other and from the other oxides. The association of Pb with K_2O and Ga with Na_2O suggests a substitution of Pb for K in alkali feldspar and Ga for Na in plagioclase respectively.

5-3-3-2 Factor Scores and Areal Distribution: From the factor model presented in Table 9, factor scores have been computed for each sample for each of the four factors, which can be mapped as shown in Figure 38. The relatively smooth patterns observed were obtained by hand-contouring and succinctly summarize the major and trace element trends in Figures 29 to 37.

Factor 1 is generally low (less than median value) in the southeastern granites. The enrichment in the LIL trace elements in the Sage Pond Granite and the southern Hungry Grove Granite is clearly shown

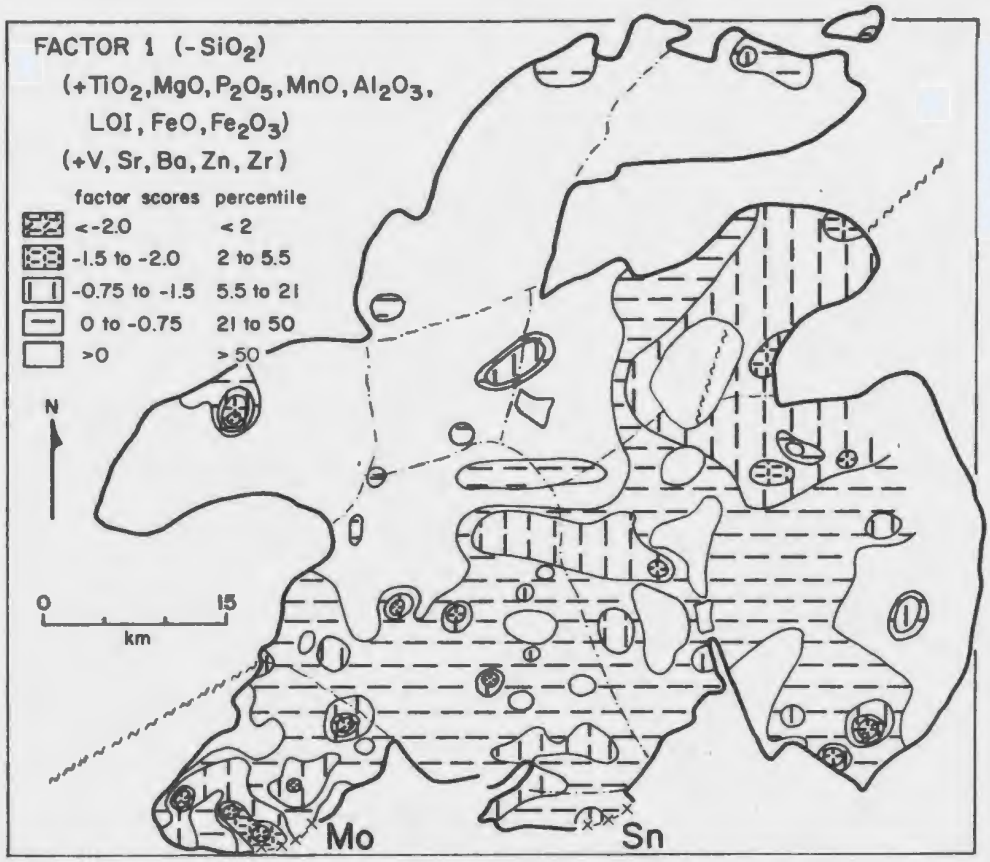

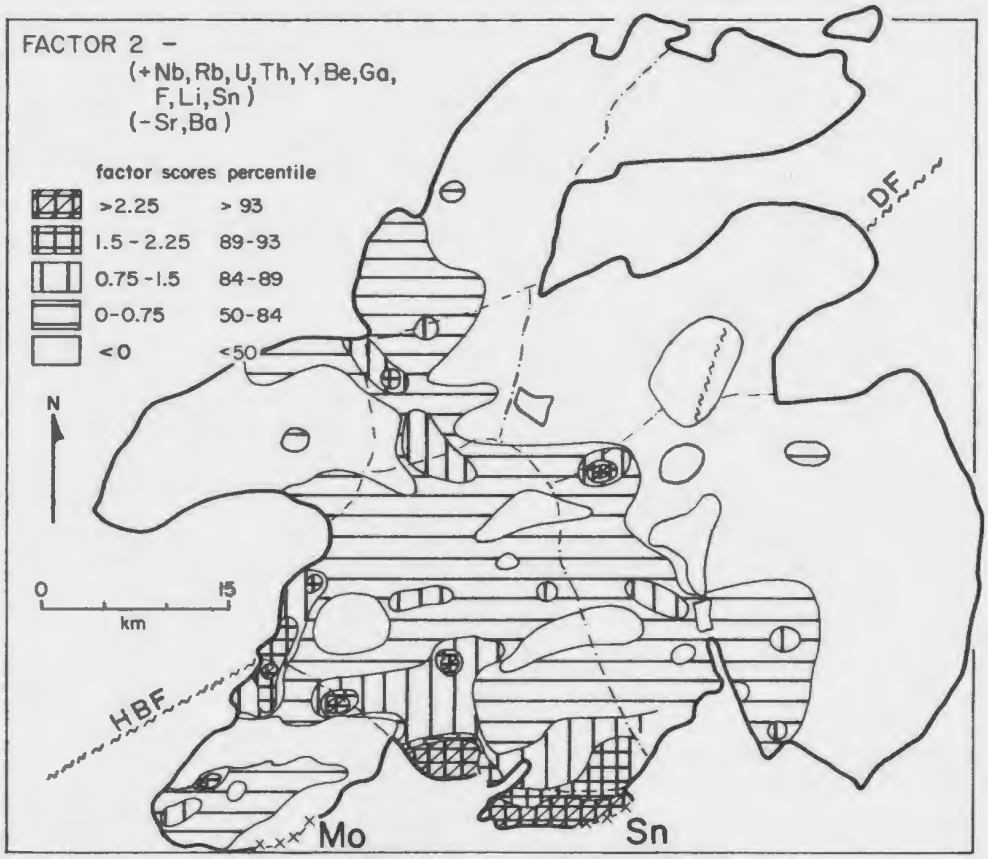

Figure 38: Map distribution of Factor 1 and Factor 2 scores for samples in the study area.

by Factor 2 in Figure 38. Another feature of the areal distribution of Factor 2 is that it shows little relation to the area of low Factor 1 values. In particular, the high Factor 2 values trend in a northwesterly direction across the fault zone, almost at right angles to the Factor 1 trend. The difference in Factor 2 scores between the Rencontre Lake Granite and the Sage Pond Granite reflects the lesser enrichment in the former in incompatible trace elements and its depletion in fluorine, although both granites show depletion trends in Ba and Sr.

5-3-3-3 Enrichment/Depletion trends: The dominant control over the relative enrichment or depletion of elements during differentiation in magmatic systems may be partitioning of trace elements between crystals and liquid (Hanson, 1978), or alternatively, relative diffusion rates for the elements (Hildreth, 1979, 1981), or relative density contrast between silicate-melt-polymers and crystals (Sparks et al., 1984). A quantitative estimate of the degree of element enrichment and depletion may be useful in assessing the relative importance of the mechanisms noted above.

A problem with the evaluation of enrichment/depletion factors lies in the subjectivity in choice of parameters used to measure them. For example Hildreth (1979) was able to use physical boundary conditions, based on the assumption that the lowest (earliest) material erupted in the Bishop Tuff represents the uppermost parts of the source magma chamber and that the upper (later) erupted material came from correspondingly deeper parts. Whalen (1983) selected a few samples which he considered to be "representative chemical data" and his enrichment/

depletion diagram is based on the ratio of analysis of chemically evolved granite divided by least evolved granite.

The factor loadings which have been calculated and mapped provide an index of the enrichment and depletion of the range of elements. Quasi-enrichment/depletion diagrams can be constructed for the data which are analogous to early/late enrichment/depletion diagrams presented by Hildreth (1979) and such a diagram is shown in Figure 39. This is a plot of the element loadings for Factor 2, arranged as positive above and negative below a zero line. The patterns are remarkably similar to those observed by Hildreth (Fig. 39).

Element loadings (Fig. 39) were also calculated for the Rencontre Lake Granite which is associated with molybdenite mineralization, and for the combined data for the Hungry Grove and Sage Pond granites associated with tin-tungsten mineralization. Comparison of the two sets of loadings shows most of the features described from the geochemical maps. Manganese and F are depleted and Zr is slightly enriched in the Rencontre Lake Granite compared to the Hungry Grove and Sage Pond granites. Most of the other elements show the expected contrasts in degree of enrichment, with the Rencontre Lake Granite exhibiting a lesser degree of enrichment in the LIL elements and a lesser depletion in Ba and Sr. Sodium exhibits an enrichment trend in the Hungry Grove and Sage Pond granites and K_2O exhibits a strong depletion trend in the Rencontre Lake Granite. These latter features are not readily apparent from the map distribution of these elements.

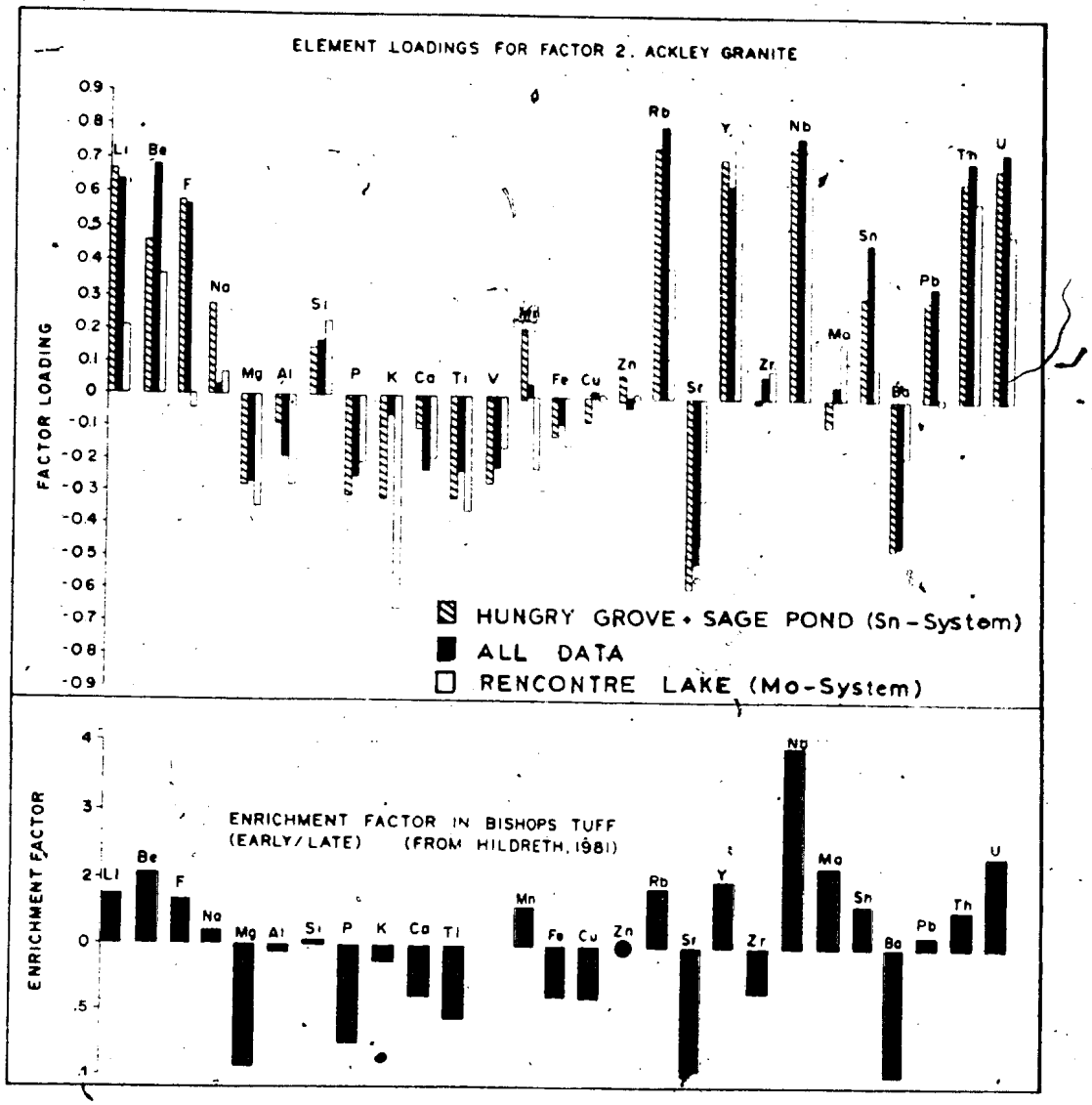

Figure 39: A: Relative enrichment and depletion of elements in the study area based on element loadings for Factor 2. Hatched bars are Hungry Grove and Sage Pond granites (Sn-system), solid bars are all data, and open bars are Rencontre Lake Granite (Mo-system).
B: Shows enrichment-depletion factors calculated for the Bishop Tuff (Hildreth, 1979).

The similarity between patterns based on factor scores and those based on physical boundary conditions suggest that factor analysis may provide a powerful means of quantifying and comparing enrichment/depletion processes as well as trends in granitoid systems. This approach summarizes the inherent trends in the whole body of data under consideration and requires few assumptions and no bias. Comparison of data between different granites may be facilitated by comparing trends between specified silica levels, or between specified levels of differentiation as defined by various differentiation indices.

5-3-4 Discriminant Function Analysis

It became apparent from the geochemical maps and from the petrographic features described in Chapter 3 that some revision of the boundaries and geological units erected by Dickson (1983) is required. Unit 12 in particular is comprised of rocks which are characteristic of the surrounding plutonic bodies. In addition, it is a useful exercise to test the internal geochemical consistency of the individual granitoid bodies. Discriminant function analysis was applied to the problem of classification in order to determine if the plutons and their boundaries could be consistently defined.

The discriminant functions were calculated using all the geochemical variables for seven specified 'training sets' of samples which were considered to unambiguously represent individual granitoid bodies. These training sets are illustrated by the small symbols in Figure 40. The Kepenkeck and Sage Pond granites were considered to be

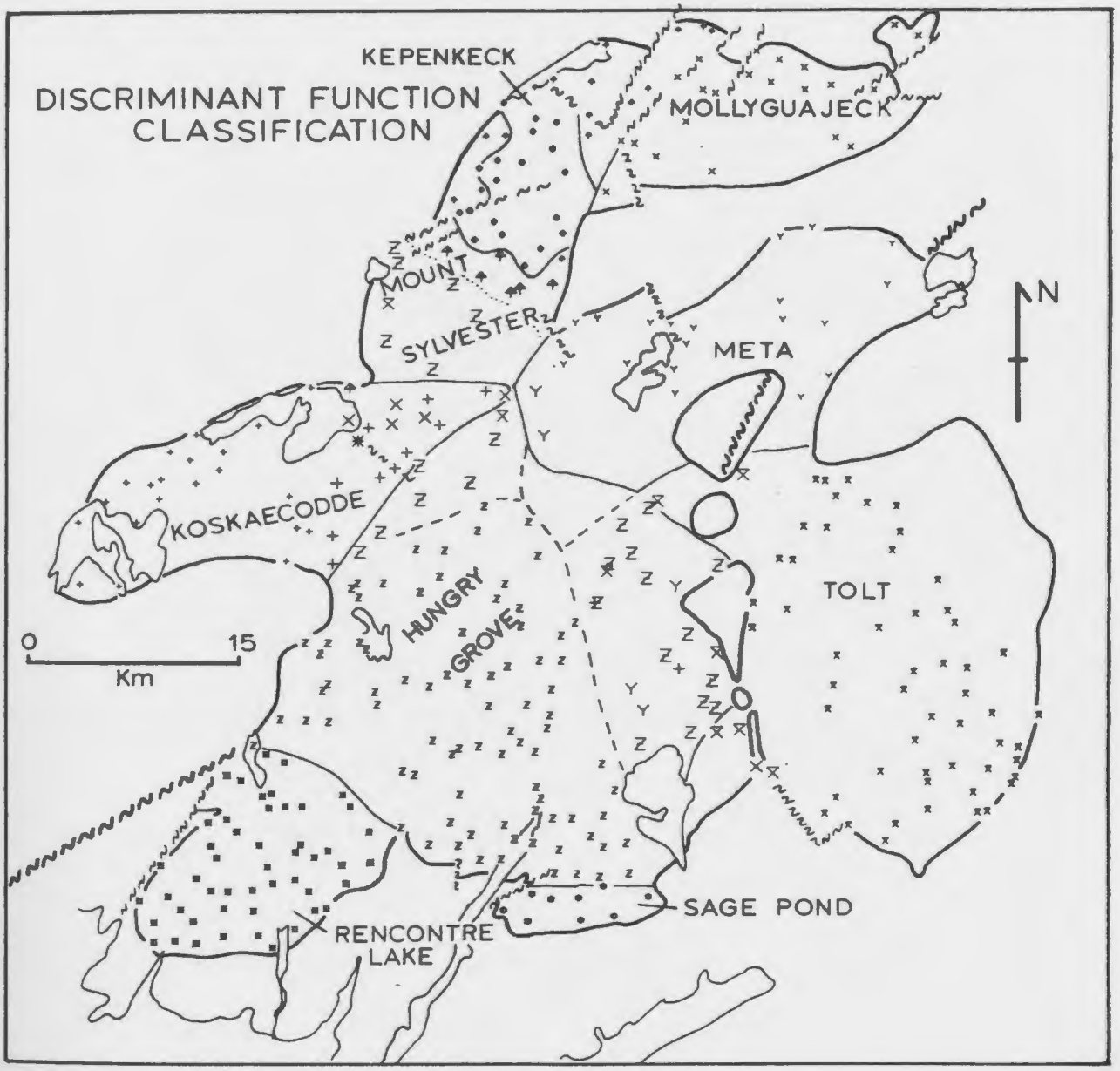

Figure 40: Classification of the granitoid rocks in the study area based on discriminant function analyses. Small symbols are selected 'training groups'; large symbols are assigned units based on the discriminant analyses. Dashed lines are boundaries of Dickson (1983). Solid lines are boundaries indicated by discriminant function analyses.

well defined and not in need of revision and were omitted from the analysis. Samples from problematical areas which were not included in the training sets were subsequently assigned to one or other of the training sets using the calculated discriminant functions. These assigned samples are shown by the larger symbols in Figure 40.

The method of analysis used was difect, whereby all the variables were entered simultaneously and required no assumptions. Stepwise methods were also tried and gave similar results, as did other functions which were calculated using all of the units recognized by Dickson (1983).

Six discriminant functions were calculated using the seven training sets. The oxide and element correlations with each of the six functions are presented in Table 10, along with the percentage of the variance described by each function. A "territorial map" of the data based on the first two functions (which account for 58.31% of the variance) is presented in Figure 41 and shows a clear separation between the southeastern granites (Tolt, Meta, Hungry Grove and Rencontre Lake) and the Koskaecodde, Mollyguajeck and Mount Sylvester plutons. The group centroids also show this cluster effect (Table 11).

The results of the internal classification of samples in the discriminant function analysis are shown in Table 12. Overall, 85% of the training sets were classified back into the correct units. Most of the mis-classification occurred within the two major territorial associations described above and results from the gross internal

Table 10: Rotated correlations between discriminating variables and canonical discriminant functions (Variables ordered by size of correlation within function).

	Function 1	Function 2	Function 3	Function 4	Function 5	Function 6
MgO	0.51824*	-0.03917	-0.03304	-0.07743	-0.05262	0.16192
P_2O_5	0.49084*	-0.04580	0.02587	0.00460	-0.05427	-0.05599
CaO	0.42843*	0.01392	-0.12575	0.06801	-0.20245	0.19982
FeO	0.41480*	-0.05157	0.01605	0.18570	-0.11321	0.11196
TiO_2	0.39211*	-0.02741	-0.05002	-0.03044	-0.13076	-0.03295
SiO_2	-0.37449*	-0.08977	0.12462	-0.06590	0.04821	-0.12918
MnO	0.37087*	-0.01420	0.01553	0.04169	0.16449	-0.04525
V	0.36707*	0.02143	0.08980	0.00793	0.01625	0.16899
Al_2O_3	0.29611*	0.09165	-0.18251	-0.00342	0.03986	0.05699
Zn	0.26549*	-0.05414	-0.01679	0.13970	0.16425	-0.07115
Fe_2O_3	0.22327*	0.02224	0.01794	-0.07872	0.00498	0.01383
Ba	0.17046*	0.12874	-0.13376	-0.06073	-0.07402	-0.03329
Sr	0.02409	0.30851*	-0.08352	-0.03015	0.07783	-0.03264
Rb	-0.07388	0.00605	0.59497*	0.04871	0.01699	0.07468
Th	0.00350	-0.12384	0.53878*	0.03673	0.05894	0.02648
U	0.00699	-0.13126	0.47144*	0.16621	0.18707	0.07939
Nb	-0.06857	-0.11302	0.45563*	0.27219	0.11593	-0.01744
F	-0.00491	0.03522	0.44260*	0.06730	-0.12346	-0.01614
Li	-0.06797	0.35476	0.41885*	0.06111	0.08364	-0.01492
Y	0.00275	-0.07938	0.30764	0.54710*	-0.02988	-0.13963
Ga	-0.04059	0.14992	0.26597	0.39427*	0.18111	0.12020
Zr	0.10242	-0.09379	0.09690	0.13257*	-0.03349	0.03646
Na_2O	-0.22809	-0.02252	-0.05830	0.06695	0.46493*	-0.10987
K_2O	0.01742	-0.11879	-0.06627	-0.00666	-0.28855*	0.00644
Pb	0.12837	0.06314	0.16210	-0.07633	0.21730*	0.14572
Cr	0.22189	-0.12652	0.09373	-0.01109	-0.07573	0.36413*
% variance	37.6	20.95	13.74	11.24	11.16	5.55

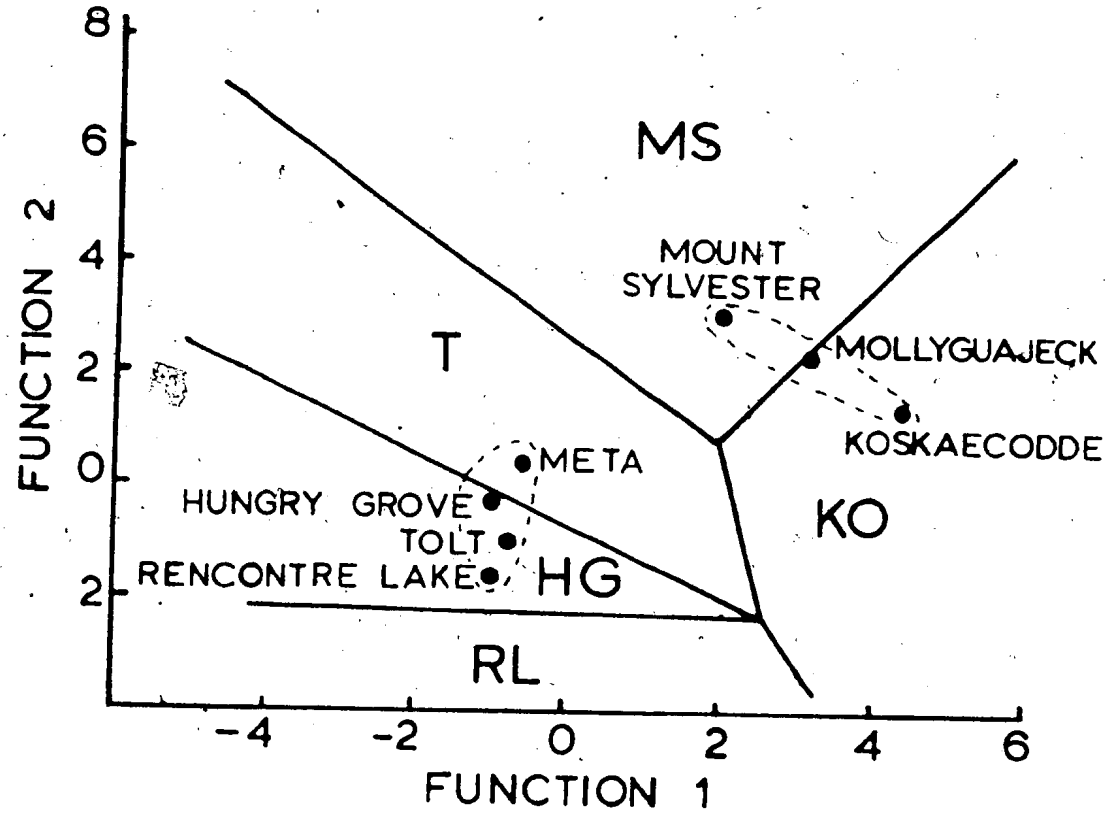

Figure 41: Territorial map of group centroids assuming all but the first two functions are 0. Lines are vertical projections to the plane of section of best fit boundaries between the groups.

Table 11: Canonical discriminant functions evaluated at Group Means (Group Centroids). Func = Function. Group 9 - Koskaecodde; Group 10 - Mollyguajeck; Group 11 - Kepenkeck; Group 13 - Meta; Group 14 - Hungry Grove; Group 15 - Tolt; Group 17 - Kepenkeck.

Group	Funct 1	Funct 2	Funct 3	Funct 4	Funct 5	Funct 6
9	4.37920	1.29139	-0.10590	-1.05734	-0.93475	-0.02611
10	3.25867	2.31562	-1.00749	-1.02819	-0.52392	2.20079
11	2.03595	2.99447	-0.95448	-1.24330	1.33954	-0.13210
13	-0.55464	0.27510	-0.72844	0.17191	-1.24899	-0.47110
14	-1.02611	-0.48862	1.53969	0.04848	-0.10329	-0.15880
15	-0.89124	-0.85294	-1.36368	-1.62775	0.43425	-0.19917
17	-1.07294	-1.61792	-0.41710	1.58868	1.46462	-0.08438

Table 12: Classification results for cases selected for use in the analysis - group numbers as in Table 10.

Actual Group	No. of Cases	Group Membership 9	10	11	13	14	15	17
Group 9	18	14 77.8%	2 11.1%	1 5.6%	0 0.0%	0 0.0%	1 5.6%	0 0.0%
Group 10	22	0 0.0%	18 81.8%	3 13.6%	0 0.0%	0 0.0%	1 4.5%	0 0.0%
Group 11	16	0 0.0%	2 12.5%	14 87.5%	0 0.0%	0 0.0%	0 0.0%	0 0.0%
Group 13	53	0 0.0%	0 0.0%	0 0.0%	45 84.9%	6 1.3%	2 3.8%	0 0.0%
Group 14	81	0 0.0%	0 0.0%	1 1.2%	2 2.5%	67 82.7%	5 6.2%	6 7.4
Group 15	19	0 0.0%	0 0.0%	1 5.3%	1 5.3%	0 0.0%	17 89.5%	0 0.0%
Group 17	50	0 0.0%	0 0.0%	0 0.0%	0 0.0%	2 4.0%	2 4.0%	46 92.0%

Percent of "Grouped" Cases Correctly Classified: 85.33%

Ungrouped Cases	62	8 12.9%	6 9.7%	7 11.3%	9 14.5%	26 41.9%	5 8.1%	1 1.6%

similarities in these two fields. Mis-classification across these fields is minor.

There is a clear distinction between the Rencontre Lake Granite and the other southeast granites, since only 4 samples were misclassified. The major differences between the Rencontre Lake Granite and the Hungry Grove Granite are in function 4 (Table 11) which is dominated by Y, Ga and Zr. There is also a heavier loading for function 5 which is dominated by Na_2O and K_2O and a relatively smaller influence from function 3 (incompatible element-dominated) in the Rencontre Lake Granite.

The results of the classification of the unassigned samples is shown in Figure 40. The southeastern part of unit 12 of Dickson (1983) has been reassigned to the Hungry Grove Granite and the northwestern half has been reassigned to the Koskaecodde and Mollyguajeck plutons. The functions for these two plutons are very similar (Table 10). Thus the rocks formerly described as the northwest part of unit 12 are regarded as part of the Koskaecodde Pluton. The reclassification of unit 12 using discriminant function analysis is considered to be a better method than the arbitrary definition of boundaries using element contours or isolated petrographic criteria.

Six samples from the southern part of unit 11A (Dickson, 1983) were classified with the Hungry Grove Granite and one sample was classified with the Tolt Granite. This suggests that unit 11A is composite, with the northern part related to the Koskaecodde-Mollyguajeck plutons and

the southern part associated with the southeastern granites of the Ackley Granite Suite. The author considers that further work is required to substantiate this possibility and therefore unit 11A (Dickson, 1983) was simply renamed the Mount Sylvester Granite.

Most of the samples located between the training sets for the Hungry Grove Granite and the Tolt Granite (Fig. 40) were assigned to the Hungry Grove Granite (three samples were assigned to the Meta Granite). The geochemical signature ascribed to the Hungry Grove Granite therefore crosses the textural boundary between the porphyritic Tolt Granite and the equigranular Hungry Grove Granite. The functions for the two training sets are similar (Table 11), with the exception of function 3 which is dominated by the elements F, Li, Rb, Th and U (Table 9). Thus the discriminant function analysis also supports the argument that the boundaries within the southeastern part of the Ackley Granite Suite are gradational. The boundary between the Hungry Grove and Tolt Granites as defined by Dickson (1983) for units 13 and 14 has been retained since it is based on textural differences observed in the field.

5-4 VARIATION DIAGRAMS

5-4-1 Introduction

Bivariate plots, identifying individual units of all the major oxides and trace elements plotted against the Thornton-Tuttle Differentiation Index (TTDI; Thornton and Tuttle 1960), were presented by Dickson (1983). Covariance of elements is summarized in the correlation tables presented in Appendix E and is briefly discussed in

Section 5-3. Selected diagrams to illustrate previously unrecognized features of the data are presented below.

5-4-2 Harker Diagrams

Plots of total alkalis against SiO_2 are presented in Figure 42. In the data from the Koskaecodde and Mollyguajeck plutons, there is no significant correlation between total alkalis and silica. This contrasts with the data from the higher-silica, Rencontre Lake, Meta and Tolt granites, where there is a strong to moderate negative correlation of alkalis with SiO_2. The cluster of data from the Hungry Grove and Sage Pond granites does not show convincing trends.

The variations of K_2O and Na_2O with increasing SiO_2 in selected parts of the study area are illustrated in Figure 43. The Koskaecodde and Mollyguajeck plutons have a strong positive correlation of K_2O with SiO_2 and no correlation is evident for Na_2O and SiO_2. The Rencontre Lake Granite has a strong negative correlation of both alkalis with SiO_2 and a weak negative association is evident from the Meta and Tolt granites. As with the plot of total alkalis, the Hungry Grove and Sage Pond Granites do not show any clear trends. The trends observed in the Koskaecodde and Mollyguajeck plutons could be ascribed to plagioclase fractionation, while those in the Rencontre Lake, Meta and Tolt granites may be interpreted to result from K-feldspar fractionation, but where does the K-feldspar go? Alternatively, the trends of the alkalis in the latter granites may be simply derived by SiO_2 dilution in the upper part

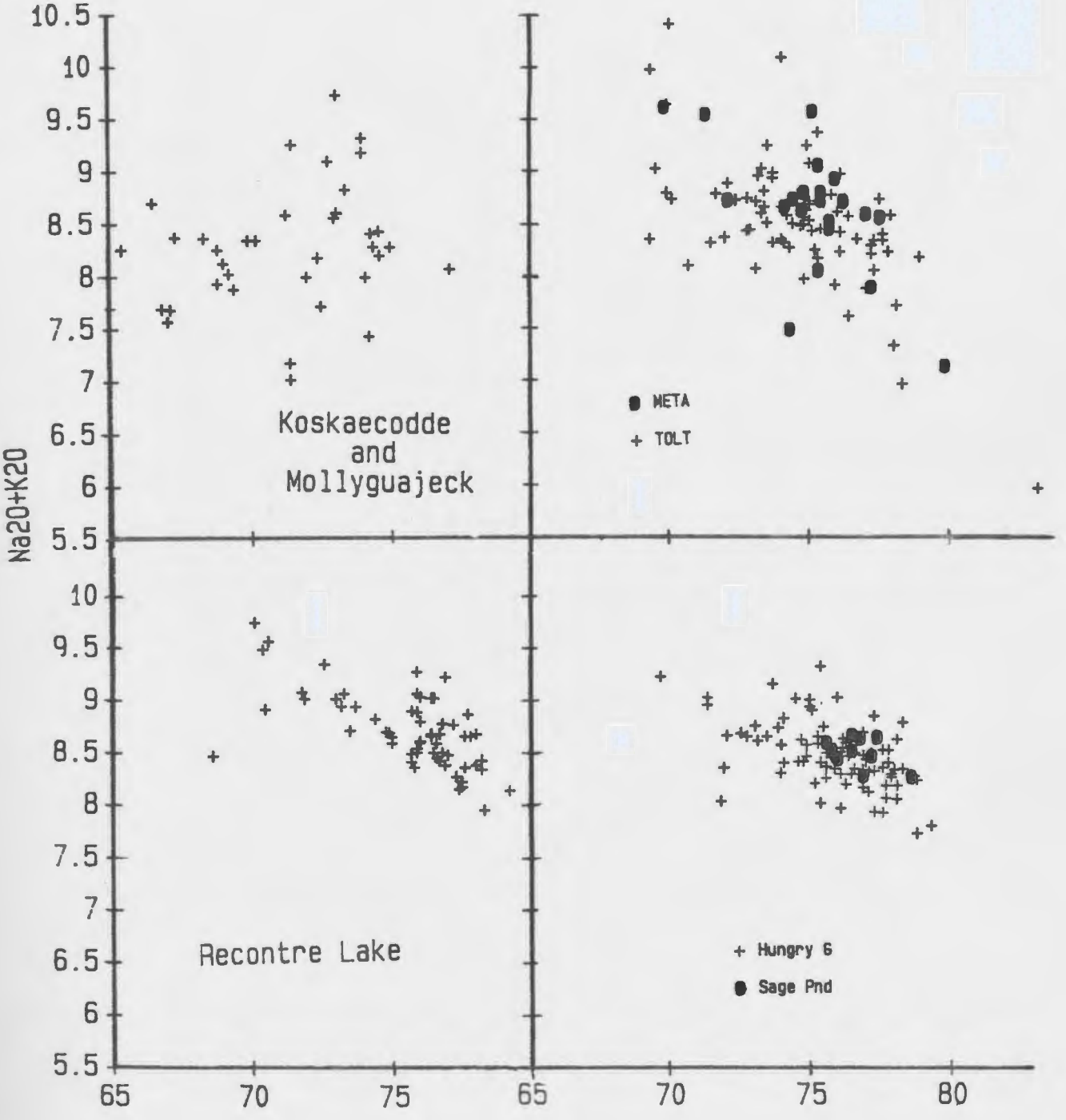

Figure 42: Plots of total alkalis versus SiO_2.

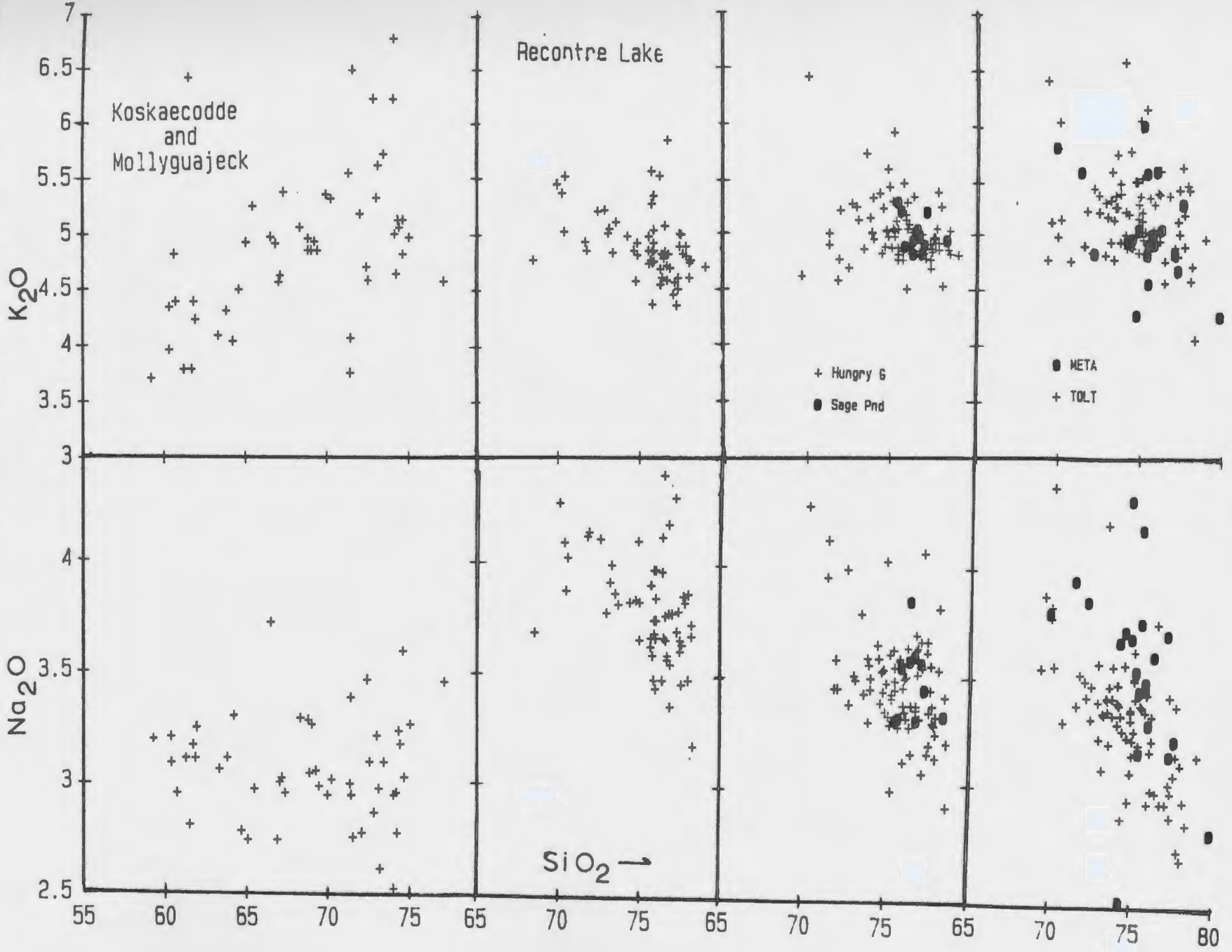

Figure 43: Plots of Na_2O and K_2O versus SiO_2.

of the magma chamber. However, the variations in concentrations of the other major oxides indicate that processes other than simple dilution were taking place. The lack of trends in the alkalis in the Hungry Grove and Sage Pond granites may be partly due to the restricted range of SiO_2 observed over much of the area and an inherent geochemical variation over the large area sampled.

Figure 44 shows that for the whole study area and also for the data from the Hungry Grove, Rencontre Lake and Sage Pond granites, there is greater variability and higher concentrations of Rb at above 74% SiO_2. Similar patterns are present at above 74% SiO_2 for the elements Be, Ga, Y, Nb, Th and U. A trend to lower values is evident at above 74% SiO_2 in Sr and Ba (e.g. Fig. 45). Fluorine shows a trend to enrichment in the Hungry Grove and Sage Pond granites and a trend to depletion in the Rencontre Lake Granite at above 74% SiO_2. The differences in element concentrations above and below 74% SiO_2 suggest that the same process caused the extreme Sr and Ba depletion as caused the LIL enrichment and also led to mineralization associated with the high-silica rocks.

Although 74% SiO_2 seems to be a critical value separating specialized (LIL enriched) from unspecialized rocks in the Ackley Granite Suite, there is no a priori reason why this should be so. For example, Tischendorf (1977) suggests a value of 72% SiO_2 as a critical minimum value for tin-specialized granites.

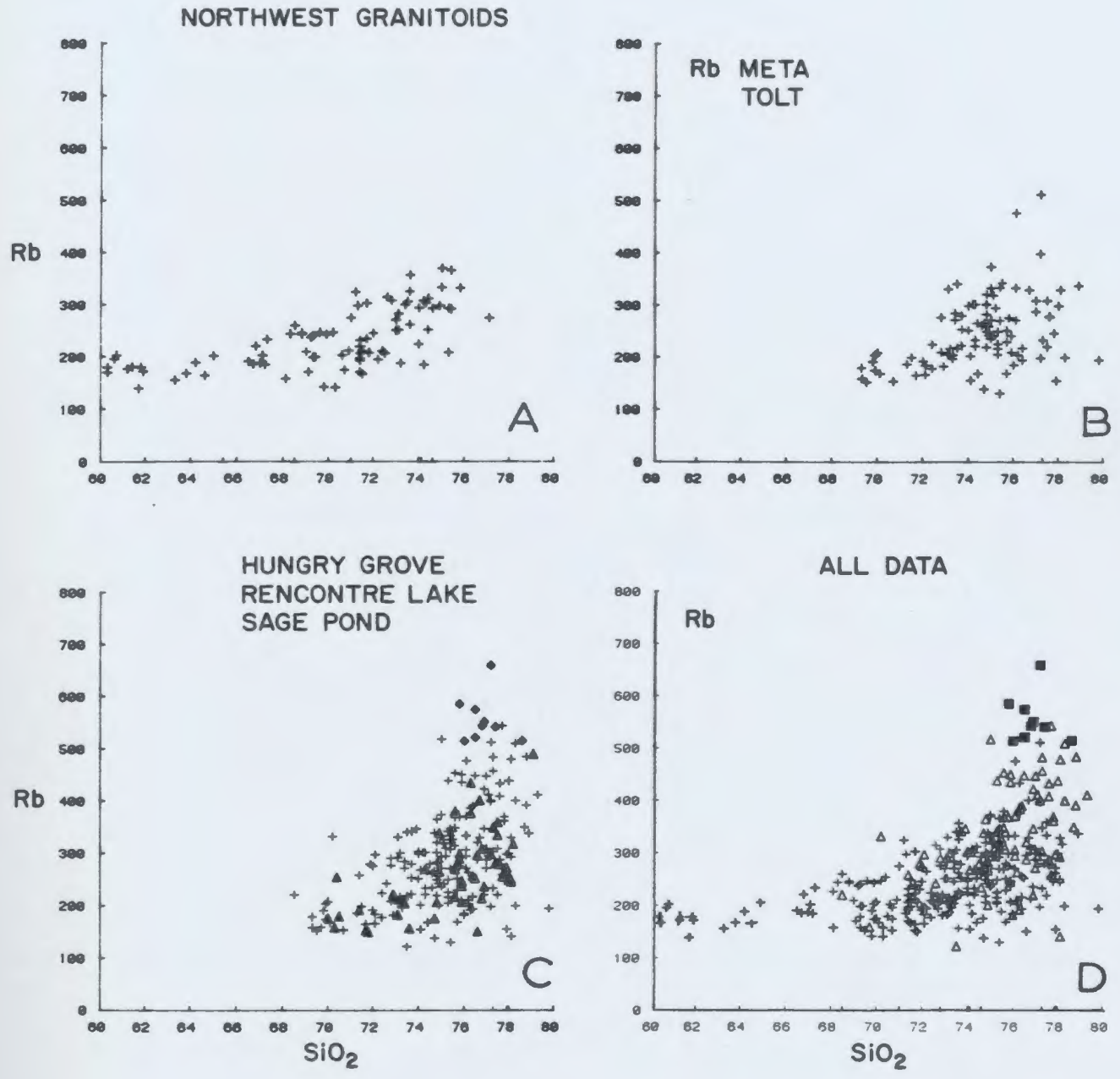

Figure 44: $Rb-SiO_2$ diagrams for:
A: Northwest granitoids (Mollyguajeck, Koskaecodde, Mt. Sylvester, Kepenkeck).
B: Meta and Tolt granites.
C: Crosses - Hungry Grove Granite; triangles - Rencontre Lake Granite; diamonds - Sage Pond Granite.
D: Squares - Sage Pond Granite, triangles - Rencontre Lake Granite, crosses - rest of data from the Ackley Granite Suite.

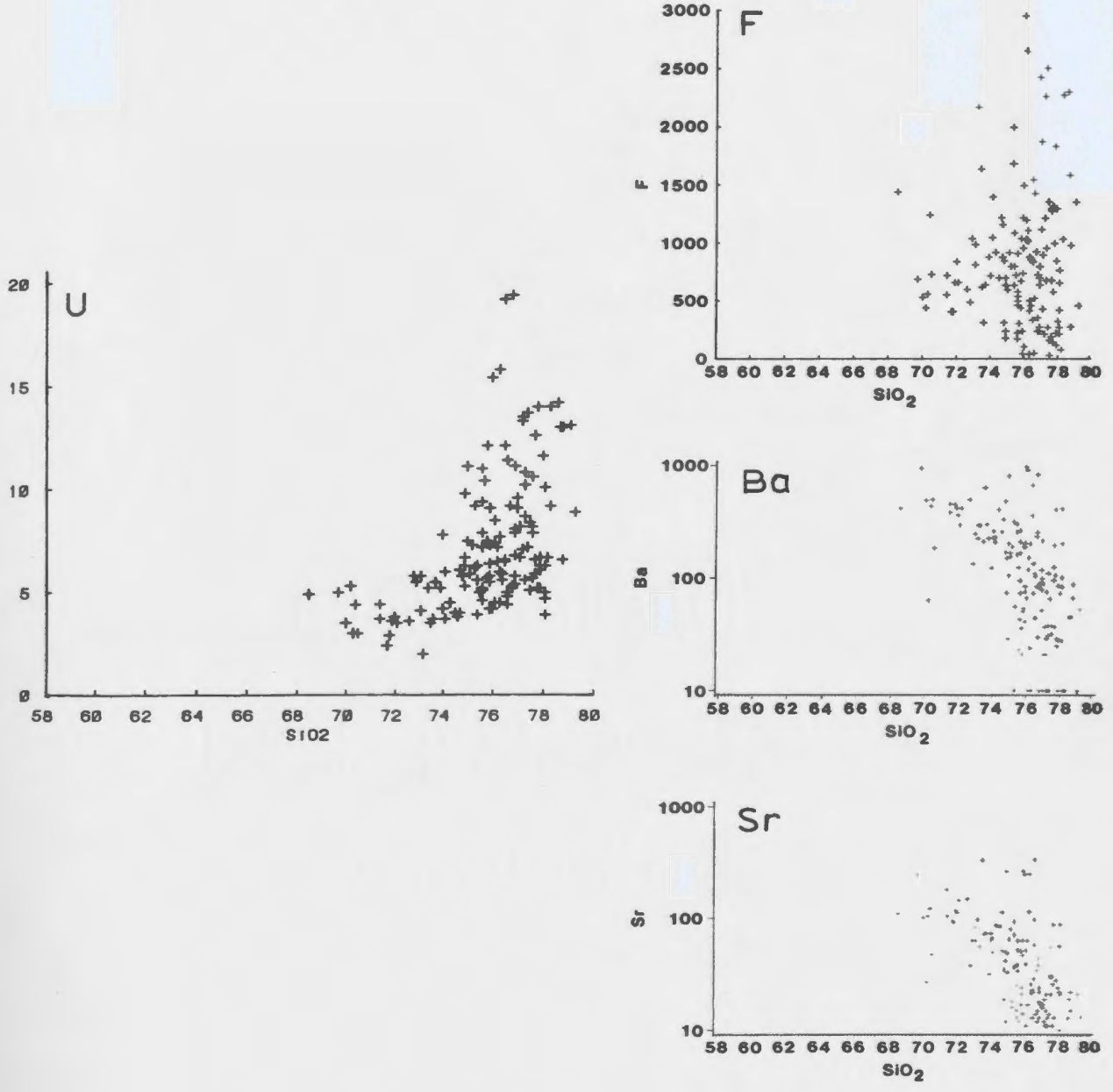

Figure 45: Harker diagrams of Sr, Ba, F and U for the Hungry Grove, Rencontre Lake and Sage Pond granites.

5-5 GEOCHEMISTRY IN MINERALIZED AREAS

5-5-1 Sage Pond Area

5-5-1-1 The Sage Pond Granite: The locations of 21 samples analyzed from the Sage Pond Granite are shown on Figure 46 and analytical results are listed in Appendix D-2. Six of the samples are of relatively fresh granite between greisen veins and were obtained from drill core at the Esso drill site. These data are summarized in Table 13 and compared to the mean of 8 previous analyses from the same granite (Dickson, 1983; unit 14B). Values obtained for the two sample sets are remarkably similar, indicating that the data are reproducible. Petrochemical features are similar to those described by Dickson (1983), with agpaitic indices ranging from 0.89 to 0.96.

Background radioactivity in the granite increases towards the southern contact and is highest in the vicinity of the Anesty greisen where scintillometer counts are 1.5 to 2 times those observed in the north of the study area. Anomalous radioactivity up to 5 times background was noted in local patches (maximum 5 m diameter) in soil in the Anesty area, and probably reflect surficial concentration of uranium leached from the granite. Greisen has a radioactive response comparable to or lower than the host granite.

The map distribution of elements from both the samples analyzed during this work and samples analyzed by Dickson (1983) are illustrated in Figures 47 and 48. The regional depletion trends of MgO, CaO, Sr, Ba and possibly Pb continue and become more extreme towards the main

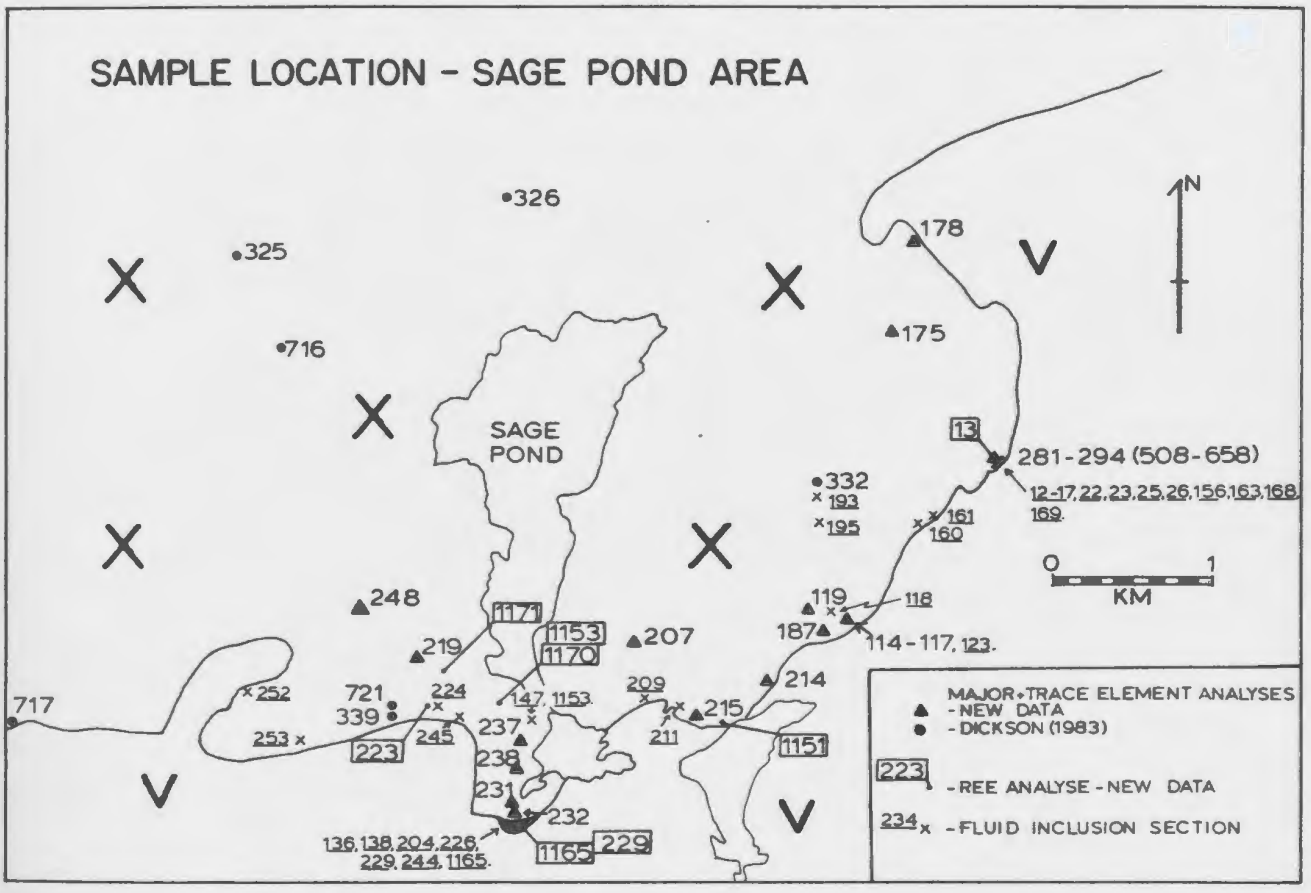

Figure 46: Sample locations (solid symbols) in the Sage Pond area. The locations of analyzed samples (in boxes) and samples used for fluid inclusion studies (small x) are also shown. X - Sage Pond Granite; v - Precambrian volcanic rocks.

Table 13: Summary of geochemical data, from the Sage Pond Granite.

	FINE GD GRANITE		JT-83-175 TUFFISITE	JT-83-180 VEIN MARGIN ALT. GRAN	UNIT 14A DICKSON 1983
	$\bar{x}$ N = 21	s	N = 1	N = 1	N = 8
Oxide wt.%					
SiO_2	76.5	1.1	81.0	76.5	76.9
Al_2O_3	12.0	0.4	9.1	11.6	12.0
Fe_2O_3	0.45	0.37	0.08	1.72(TOT)	0.30
FeO	0.46	0.29	0.38	-	0.62
MgO	0.46	0.03	0.05	0.08	0.11
CuO	0.30	0.18	0.10	0.47	0.32
Na_2O	3.52	0.37	2.61	2.33	3.51
K_2O	4.93	0.59	3.94	4.97	4.99
TiO_2	0.17	0.03	0.16	0.18	0.11
MnO	0.03	0.01	0.03	0.02	0.03
P_2O_5	0.02	0.01	0.01	0.01	0.01
LOI	0.78	0.19	0.68	1.56	0.77
TOTAL	99.2	0.7	98.1	99.4	99.7
Element g/t					
Li	87	44	52	171	87
Be	12	9	2	49	8
F	2491	1507	2263	4648	2162
V	5	2	-	5	5
Cr	2	0	1	24	5
Ni	-	-	3	1	-
Cu	-	-	13	22	2
Zn	20	8	20	43	12
Ga	21	2	-	16	21
Rb	572	150	5	569	560
Sr	7	4	1	8	11
Y	80	31	-	58	99
Zr	152	14	-	126	154
Nb	79	16	-	58	76
Mo	-	-	-	-	5
Ag	0	0	1	0	-
Ba	29	25	3	69	57
La	44	17	-	63	
Ce	176	63	-	175	
Pb	19	10	15	31	35
Th	71	15	49	67	66
U	11	5	5	-	15

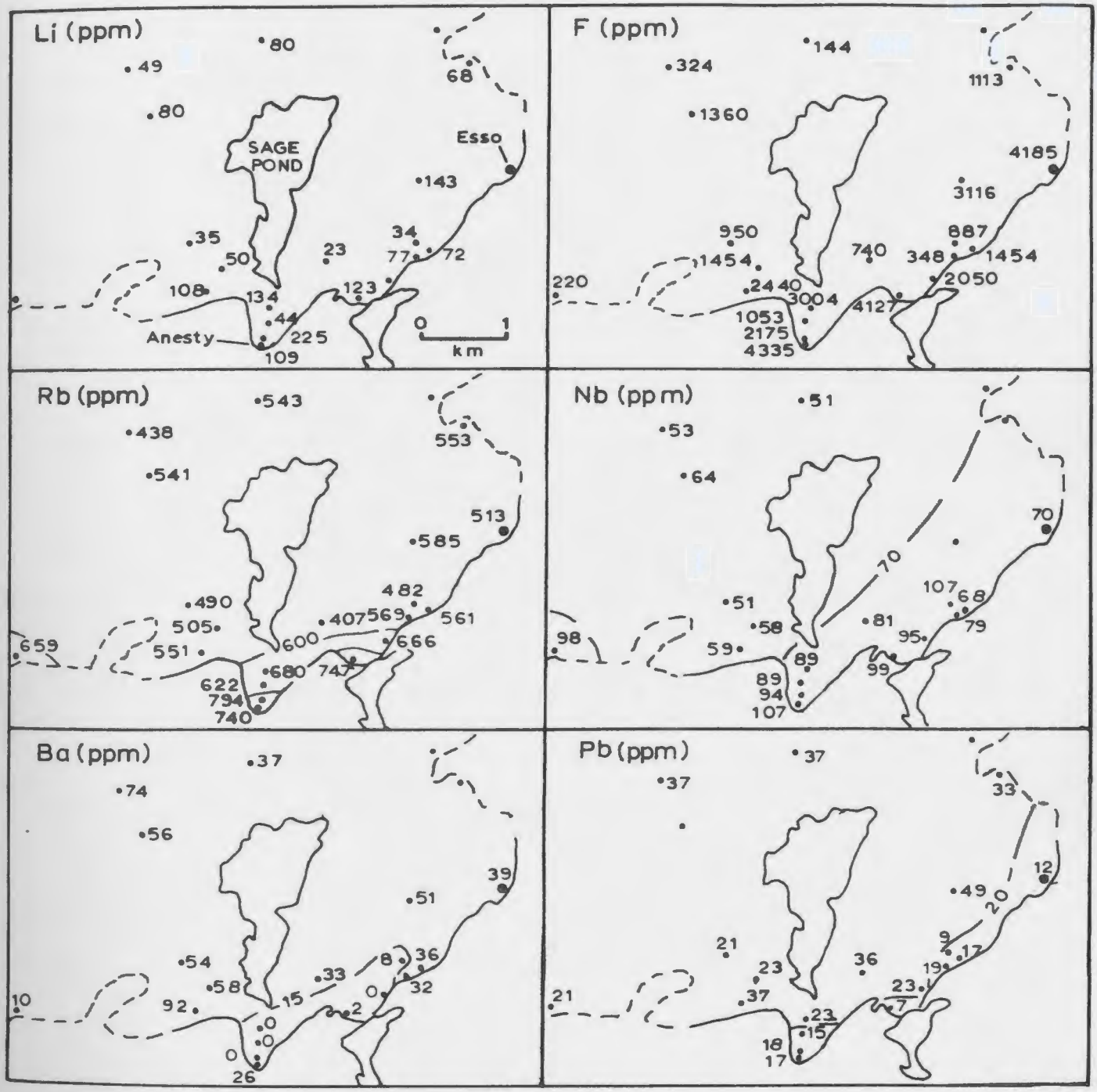

Figure 48: Map distribution of Li, F, Rb, Nb, Ba and Pb in the Sage Pond area. Dots - sample location.

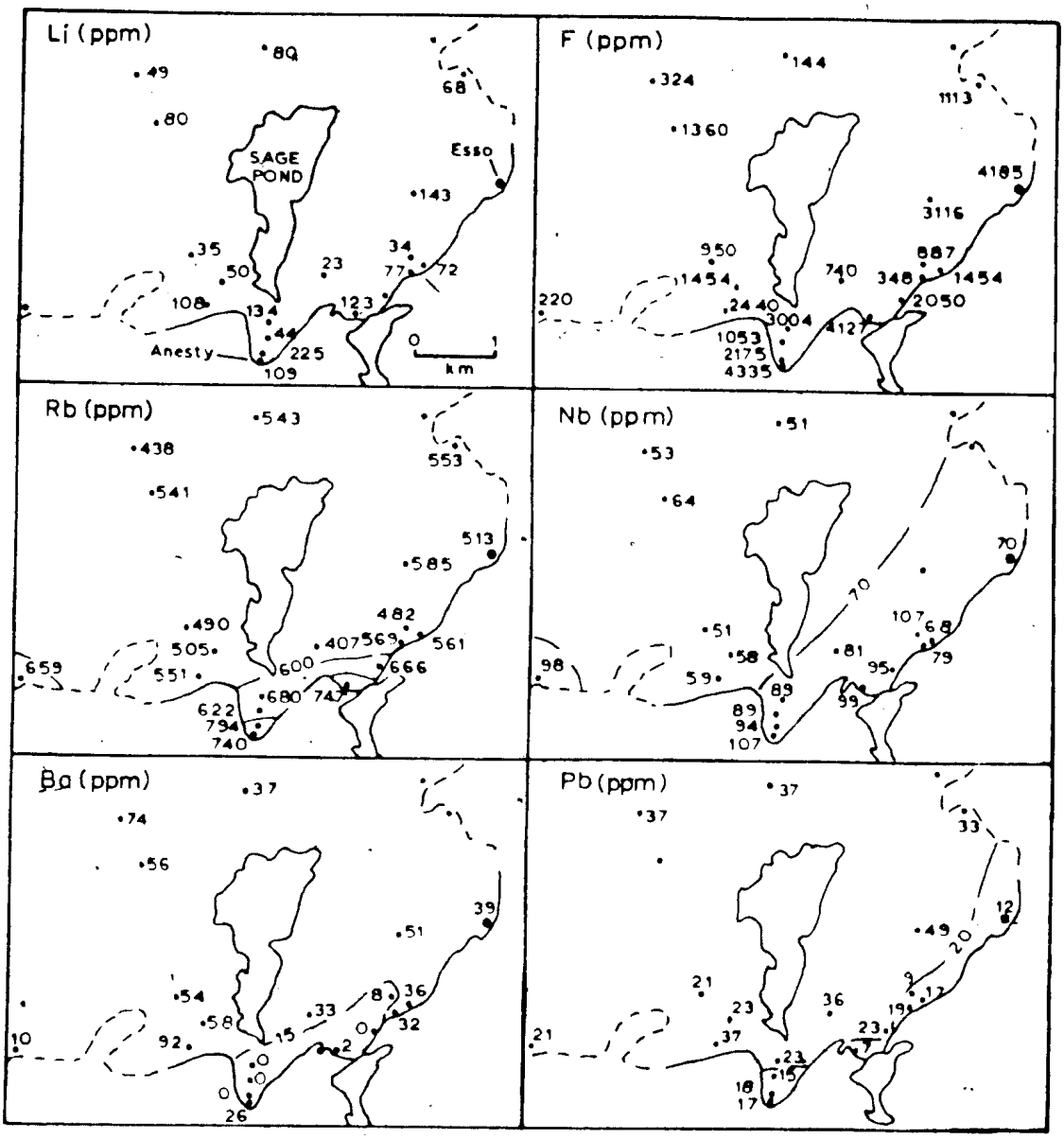

Figure 48: Map distribution of Li, F, Rb, Nb, Ba and Pb in the Sage Pond area. Dots - sample location.

greisen outcrops. Notable enrichment trends in Rb and F highlight the areas of known mineralization. Nb and Li are also enriched close to the greisen. Sodium has slightly higher values around the Anesty greisen. Other elements do not show clear contourable trends and are not presented in plan form.

These features demonstrate that the chemical enrichment/depletion noted by Dickson (1983) and Davenport et al. (1984) and described in detail above, focus directly on areas of known tin-tungsten mineralization. These trends are a form of cryptic chemical variation which must be related to the mineralization process.

5-5-1-2 Greisen: Geochemical analyses of 23 samples from greisen veins are summarized in Table 14. Dickson (1983) and McConnell (1984) have reported 19 of these analyses and 4 samples were analyzed by the author (Appendix D-2). Four sets of averages of data are presented in Table 14, these are: 1) from the Esso greisen, 2) from the Anesty greisen, 3) from 'other' greisen where mineralization is not indicated and 4) from muscovite-rich greisen.

Enrichment/depletion of elements in the greisen relative to the mean of the 21 fresh samples of Sage Pond Granite are shown in Figure 49. Most samples consist predominantly of SiO_2 and Al_2O_3 with minor CaO and F reflecting the quartz-topaz-fluorite-kaolinite mineralogy. Samples with K_2O contain sericite. Samples from the greisen veins drilled by Esso and from the Anesty outcrop, are higher in iron (due to the presence of pyrite) than samples which are not associated with

Table 14: Summary of geochemical analyses of greisen in the Sage Pond Granite.

	Esso N = 6		Anesty N = 3		Other N = 11		Muscovite N = 3	
	$\bar{x}$	s	$\bar{x}$	s	$\bar{x}$	s	$\bar{x}$	s
Oxide (wt.%)								
SiO_2	82.4	5.2	82.8	7.0	83.3	3.6	80.0	4.3
Al_2O_3	11.43	3.05	8.96	4.44	12.06	3.21	10.42	1.51
Fe_2O_3	1.77	1.73	2.37	1.88	0.41	0.49	2.10	0.80
FeO	0.11	0.14	1.70	1.83	0.20	0.16		
MgO	0.05	0.06	0.03	0.01	0.04	0.04	0.16	0.07
CaO	0.38	0.54	0.88	1.40	0.89	1.18	0.86	0.75
Na_2O	0.02	0.01	0.03	0.03	0.04	0.01	0.20	0.20
K_2O	0.33	0.30	0.19	0.15	0.28	0.19	3.16	0.60
TiO_2	0.14	0.05	0.17	0.10	0.16	0.07	0.15	0.08
MnO	0.02	0.01	0.02	0.0	0.02	0.01	0.25	0.17
P_2O_5	0.03	0.02	0.02	0.01	0.01	0.0	0.01	0.01
LOI	1.84	1.60	2.96	1.21	1.27	0.70	2.28	0.95
TOTAL	98.6	1.5	99.5	1.50	98.7	0.7	99.8	0.8
Element (g/t)								
F	20063	9124	10224	3566	13657	4715	9970	11085
Li	13	10	5	2	32	28	106	35
Be	1	0*	1	0*	6	10	28	37
V	4	1	4	1	5	2	5	1
Ni	2	1	1	0*	1	0*	3	
Cu	11	6	7	4	10	5	15	7
Zn	14	4	15	8	10	4	64	27
Ga	3	5	4	0*	3	1*	16	0*
Rb	37	28	23	19	52	34	629	286
Sr	2	2	5	6	4	3	6	3
Y	21	12*	42	-	36	3*	74	
Zr	145	26*	-	-	13	0*	166*	
Nb	91	61	80	-	71	13*	95	
Mo	113	98*	190	232	59	65*	28	24*
Sn	1440	2976	513	588	23	30	359	415
W	658	1119*	5	2*	6	5	10	4*
Ag	0	0	7	0	0	0	0	0
Ba	7	11	26	9	30	27	37	46
Pb	15	16	8	6	12	22	13	9
U	3	0	5	0	3	1	-	-
Th	27	34	11	0	10	7	-	-

* Incomplete data set

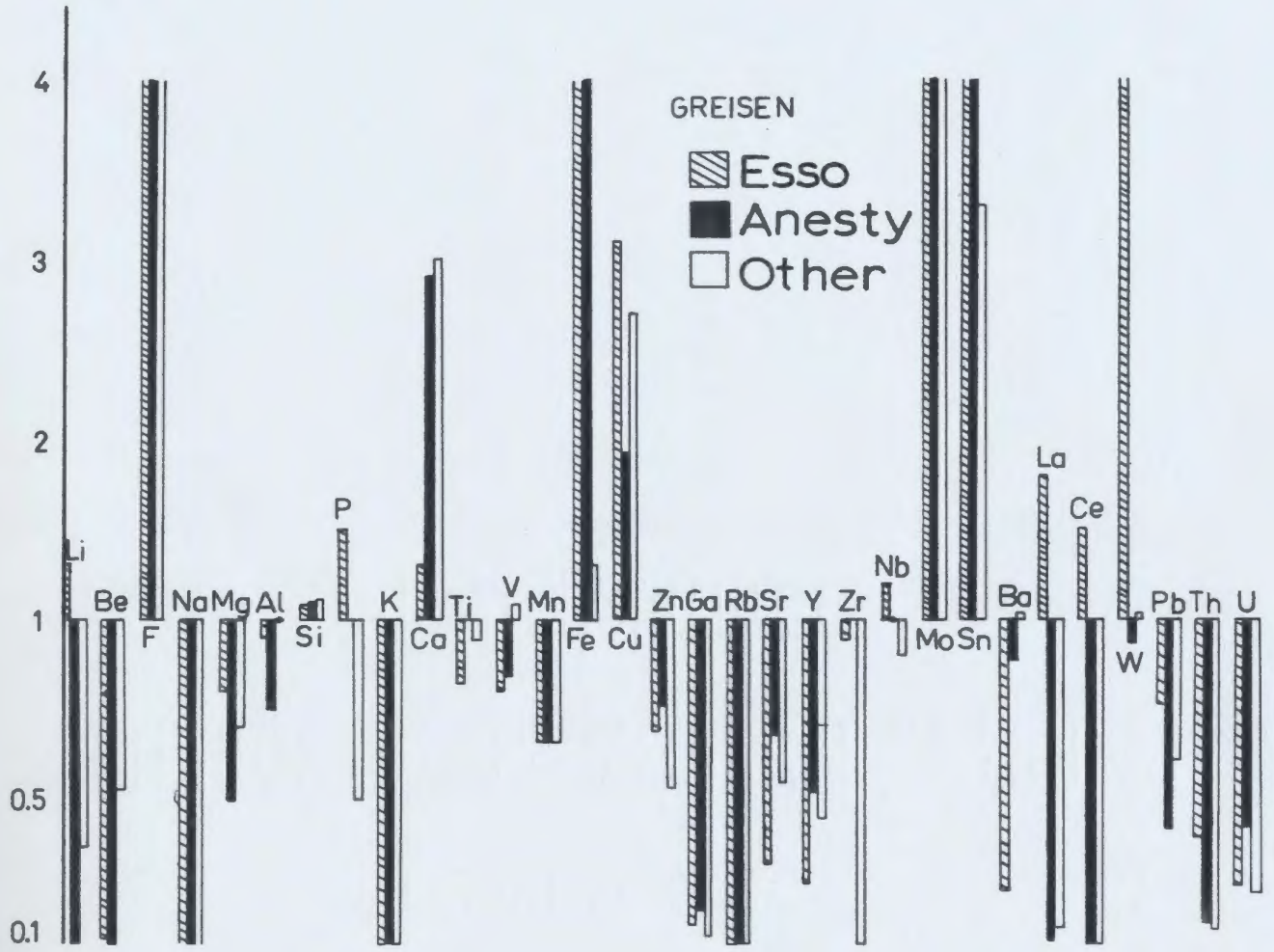

Figure 49: Enrichment and depletion of elements in greisen relative to the mean of the data for 21 unaltered samples in the Sage Pond area.

mineralization. The samples from the Anesty greisen do not contain significant tungsten, which probably reflects the erratic distribution of fine grained wolframite in the outcrop. Fluorine enrichment is strongest in the tin bearing greisens. The data do not suggest any significant differences in the processes which formed the different quartz-topaz greisen.

5-5-2 Rencontre Lake Area

Geochemical data presented by Whalen (1976, 1980, 1983) were obtained from an area of approximately 10 km^2 around the molybdenite prospects in the Rencontre Lake Granite (Fig. 31A) and averages of Whalen's data are presented in Figures 29 and 30 and in Table 8. These data show strong chemical gradients which culminate at molybdenite-mineralized areas (Fig. 50).

Allowing for the fact that the regional samples from the Rencontre Lake Granite represent an area of 190 km^2 and Whalen's results are from a small area with steep chemical gradients, there is good agreement in the data sets, with the exception of Y. Analysis of samples from approximately the same locality which belong to the separate data sets also demonstrates good agreement.

5-5-3 Belle Bay Formation

A summary of analyses of representative rocks from the predominantly volcanic Belle Bay Formation is presented in Table 15,

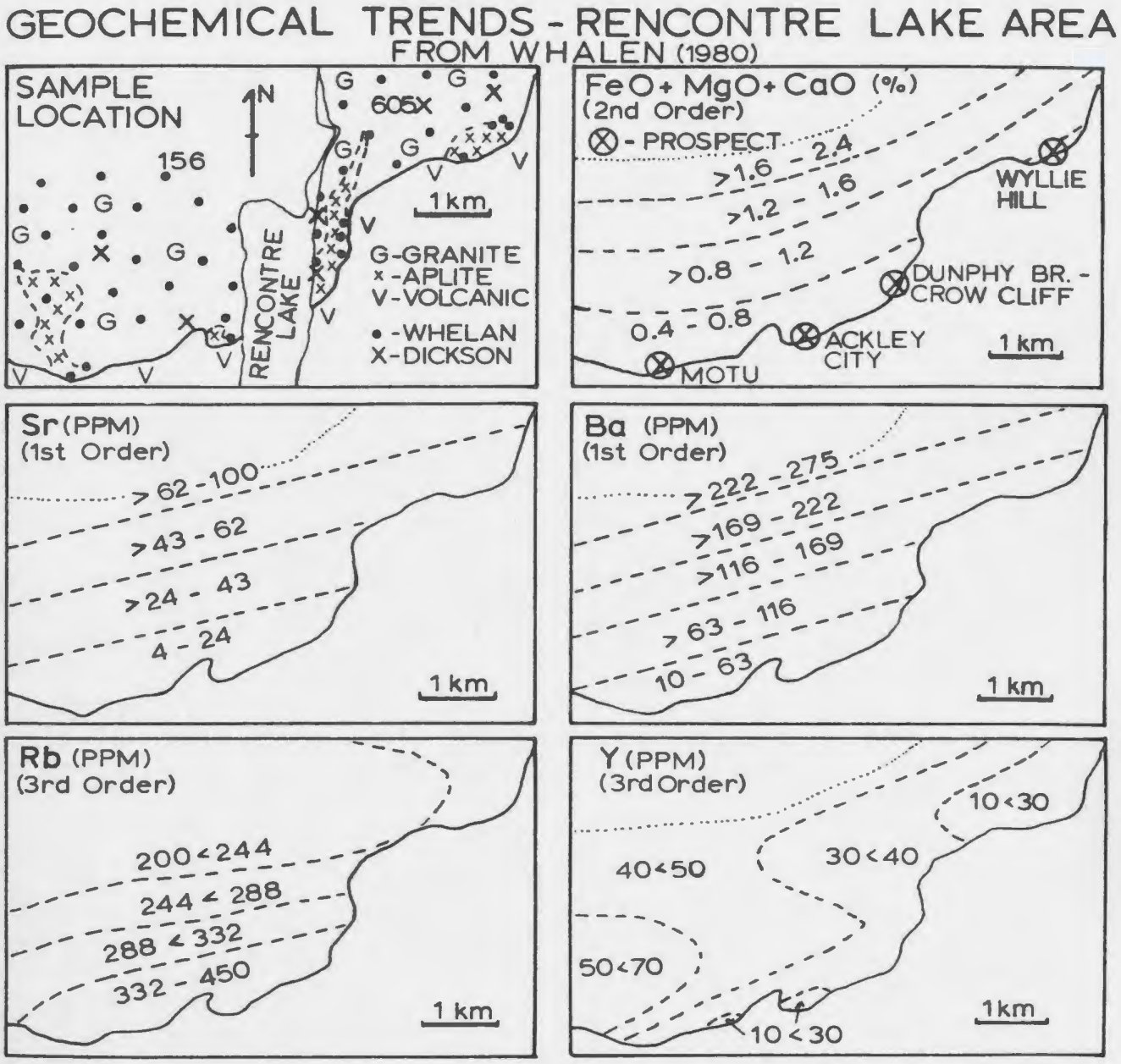

Figure 50: Sample locations (dots), and trend surface maps of geochemical variations in the Rencontre Lake area from Whalen (1980). The locations of samples analyzed by Dickson (1983) are shown by an x. Numbered samples are those for which REE analyses are available (see Chapter 6).

Table 15: Summary of geochemical data from the Belle Bay Formation in the Sage Pond area, and comparison to data from the Rencontre Lake area (Whalen, 1976).

	MAFIC ROCKS N = 3		RHYOLITE N = 4		FELDSPAR PORPHYRY N = 1	TUFF N = 13		RHYOLITES (WHALEN 1976) N = 44	
	$\bar{x}$	$\bar{s}$	$\bar{x}$	$\bar{s}$		$\bar{x}$	$\bar{s}$	$\bar{x}$	$\bar{s}$
Oxide (wt.%)									
SiO_2	45.9	2.5	79.0	0.9	70.1	69.9	2.4	76.0	2.2
Al_2O_3	13.65	1.32	11.12	1.02	14.3	14.48	1.43	11.76	1.39
Fe_2O_3	4.97	1.61	0.84	0.24	2.34	2.31	0.98	2.12	1.05
FeO	7.49	0.96	0.56	0.10	1.16	0.81	0.39	0.58	0.36
MgO	7.52	2.21	0.15	0.09	0.78	0.72	0.42	0.08	0.07
CaO	2.67	1.42	1.29	1.47	1.75	1.71	0.78	0.14	0.21
Na_2O	2.83	0.97	1.56	0.82	5.41	4.10	0.86	3.64	1.13
K_2O	1.16	0.58	4.14	0.97	2.18	3.41	1.18	4.55	0.92
TiO_2	2.19	0.68	0.17	0.02	0.47	0.54	0.17	0.22	0.08
MnO	0.26	0.05	0.04	0.02	0.10	0.08	0.02	0.06	0.04
P_2O_5	0.42	0.10	0.02	0.01	0.13	0.10	0.06		
LOI	1.41	0.29	1.00	0.47	0.95	1.34	0.47	0.59	0.42
TOTAL	99.0	0.7	98.8	0.4	99.7	99.5	0.5	99.7	
Element (g/t)									
Li	45	18	239	19	15	24	19		
Be	3	1	4	2	2	3	1		
F	1298	382	461	263	225	393	210		
V	345	79	8	6	30	35	15		
Zn	115	35	31	16	68	64	21	112	105
Ga	21	5	19	5	15	17	4		
Rb	142	69	171	73	52	122	40	174	48
Sr	331	81	79	69	210	207	97	24	40
Y	45	21	66	23	47	56	28	145	45
Zr	166	82	335	160	215	314	137	945	334
Nb	10	1	29	11	12	18	8	50	25
Mo	-	-	8	0	-				
Ag	0	0	0	0	0	0	0		
Ba	68	92	160	164	536	833	346	191	218
Pb	1	0	50	65	5	25	38	41	29
Th	7	2	24	7	7	15	3		
U	-	-	4	2	-	3	0		

along with data presented by Whalen (1976) from the Rencontre Lake area. The volcanic rocks from the Sage Pond area have considerably higher values for Ba, Sr, Zn and Zr and have significantly lower values for the incompatible elements Li, Be, F, Rb, Nb, Th and U than the Sage Pond Granite and the Ackley Granite Suite. No areal chemical trends were observed in the volcanic rocks in relationship to the contact of the Sage Pond Granite.

The observed chemical features in the country rock and adjacent Ackley Granite Suite do not indicate any contamination of the Ackley magma chamber by the country rocks either through bulk assimilation or element exchange. Comparable conclusions were reached by Whelan (1976, 1983) for the rocks in the Rencontre Lake area.

5-5-4 Comparison between the Sage Pond and Rencontre Lake Areas

The chemical patterns in the Rencontre Lake Granite are similar to trends in the Sage Pond area. However, there are some differences.

The enrichment trends of the LIL elements recognized in the Hungry Grove and Sage Pond granites are areally much more extensive than those in the Rencontre Lake Granite and can be recognized up to 15 km from the mineralized area (Figs. 34, 35, 36). Those in the Rencontre Lake area occur within 2-3 km of the contact and are not detectable for most elements on a regional scale. On a local scale, enrichment is less extreme in the Rencontre Lake area. For example, values of Rb in proximity to mineralization in the Rencontre Lake area range from 332 to

450 ppm while those in the Sage Pond area range from 500 to 800 ppm. Both mineralized areas exhibit Ba and Sr depletion, but the depletion is extreme in the Sage Pond area. There is also a trend to low Y values (10-30 ppm) in the Rencontre Lake area compared to average values of 80 ppm in the Sage Pond area.

5-6 INTERPRETATION OF GEOCHEMICAL DATA

Three distinct geochemical suites have been defined. These are: 1) The Mollyguajeck and Koskaecodde plutons with relatively lower SiO_2 and LIL elements and higher Ca-Femic oxides, 2) The Kepenkeck Granite with higher Al_2O_3 and Sr concentrations, and 3) The southern Ackley Granite Suite with relatively high SiO_2 and LIL concentrations. The southern Ackley Granite Suite exhibits remarkably similar geochemical signatures over an area of approximately 2100 km^2 and was intruded across the trace of the Dover-Hermitage Bay Fault zone.

Regional trends in enrichment and depletion of elements culminate at the Sn-mineralized greisen in the Sage Pond Granite and at the Mo prospects in the Rencontre Lake Granite. These trends are best developed in the Hungry Grove-Sage Pond granites. However, in both areas, the steepest geochemical gradients are developed at the margin of the granite around mineralization. These signatures are interpreted to reflect large, magmatic, geochemical systems involved in the primary ore-forming process.

The Rencontre Lake Granite when compared to the Hungry Grove-Sage Pond Granite exhibits comparable major element geochemistry but more erratic LIL concentrations. In addition, LIL enrichment trends and trends to low values in Sr and Ba are less extreme. Thus significant differences in trace element signatures of the granites hosting mineralization are present and may be related to the processes of mineralization.

5-7 GEOCHEMISTRY OF OTHER HIGH-SILICA SYSTEMS

Published geochemical analyses from selected, mineralized granites and high-silica volcanic and subvolcanic rocks are presented in Table 16. In addition, the means for specialized granites (Tischendorf, 1977) and for granitic rocks associated with mineralization in the South Mountain Batholith of Nova Scotia (Chatterjee et al., 1983) are plotted in Figures 29 and 30.

The important features of the chemistry of the mineralized granite systems are the high-silica content, relatively high sodium and potassium values, low values for Ca-Femic oxides, Ba, Sr and K/Rb and high values for incompatible trace elements. The most important variable is Al_2O_3 which is highest in peraluminous, muscovite-rich, tin- and tungsten-bearing, S-type granites.

The southeastern Ackley Granite Suite shows almost identical major and trace element values to relatively unaltered granites associated with the major Climax-type ore deposits which are increasingly

Table 16: Averages of published geochemical analyses from selected high-silica systems.

	Quartz Hill[1] Climax-type		'A' Type[2] Mumballa Batholith	'I' Type[2] (Bega)	SMB (Sn)[3]	
	$\bar{x}$	$\bar{s}$	$\bar{x}$	$\bar{x}$	$\bar{x}$	$\bar{s}$
Oxide (wt.%)						
SiO_2	73.8	1.7	77.2	76.0	75.8	2.4
Al_2O_3	13.30	0.54	11.79	12.14	12.65	1.37
Fe_2O_3	0.84	0.41	0.36	0.46	0.39	0.19
FeO	0.62	0.25	0.85	0.70	1.21	0.31
MgO	0.30	0.22	0.04	0.24	0.18	0.11
CaO	0.85	0.30	0.39	0.80	0.67	0.27
Na_2O	3.45	0.30	3.08	3.43	3.41	0.83
K_2O	4.67	0.52	5.00	4.46	4.08	0.82
TiO_2	0.21	0.02	0.13	0.11	0.13	0.12
MnO	0.05	0.02	0.03	0.03	0.04	0.05
P_2O_5	0.05	0.03	0.02	0.02	0.11	0.03
Element (g/t)						
Li					146	64
Be					14	70
F					3318	1042
V			2	6		
Cu			9	2	7	26
Zn	28	5	122	20	43	14
Ga			20	14		
Rb	145	44	242	212	700	122
Sr	175	122	43	67	31	112
Y			90	46		
Zr	156	47	170	95		
Nb			19	11		
Sn					50	60
Ba			575	331	73	60
Pb			37	24	7	4
Th	23	8	26	25	25	6
U	9	3	6	6	23	4
N =	7		8	20	94	

[1] Hudson *et al.*, 1981
[2] Collins *et al.*, 1982
[3] Chatterjee *et al.*, 1983. SMB - South Mountain Batholith.

Table 16: (Cont.d)

	Erzgebirge[4] most evolved phase	'S' Type[5] Koskiusko Batholith		'S' Type[6] Cornubian Batholith	
	$\bar{x}$	$\bar{x}$	$\bar{s}$	$\bar{x}$	$\bar{s}$
Oxide (wt.%)					
SiO_2	74.5	73.9	1.4	71.44	.47
Al_2O_3		13.03	.57	14.98	.55
Fe_2O_3		0.36	0.29	1.06	.37
FeO		1.28	1.05	.85	.35
MgO	0.13	.55	.35	.44	.02
CaO	0.40	1.49	.48	.73	.08
Na_2O	3.5	2.62	0.12	2.72	.21
K_2O	4.6	4.25	.37	5.46	.19
TiO_2	0.06	.24	0.07	.24	.04
MnO		.04	.02	.04	.01
P_2O_5		.11	.02	.24	.02
Element (g/t)					
Li	600			95	27
Be	11				
F	7000				
V	2				
Cu		5	3		
Zn		36	16		
Ga	32				
Rb	1200	214	39	465	190
Sr		92	37	86	21
Y		31	3		
Zr		116	41	86	18
Nb					
Sn	35				
Ba		343	146		
Pb					
Th		15	4	21	3
U		3	1		
N =		5		5	

[4] Tischendorf, 1977
[5] Hines et al., 1978
[6] Alderton et al., 1980

Table 16: (Cont.d)

	'Peralkaline'[7] Granite	Bishop Tuff[8] E	Bishop Tuff[8] L	Tin Bearing[9] Rhyolites	
	$\bar{x}$	$\bar{x}$	$\bar{s}$	$\bar{x}$	$\bar{s}$
Oxide (wt.%)					
SiO_2	74.4	74.4	75.5	76.2	0.9 (13)
Al_2O_3	11.7	12.3	13.0	13.00	0.40
Fe_2O_3	1.8			1.41	0.28
FeO	1.6	0.7	1.1	0.16	0.24
MgO	0.1	0.01	0.25	0.11	0.08
CaO	0.6	0.45	0.95	.46	0.25
Na_2O	4.2	3.9	3.35	3.29	0.46
K_2O	5.1	4.8	5.55	5.16	0.45
TiO_2	0.4	0.07	0.21	0.12	0.07
MnO		0.04	0.02	0.03	0.01
P_2O_5	0.1	0.01	0.06	0.01	0.02
Element (g/t)					
Li				2590 (2 samples)	
Be					
F	789				
V					
Cu					
Zn	141	38	40		
Ga					
Rb	255	190	95	545	216 (11)
Sr	20	40	110	27	32
Y	95	25	12		
Zr	715	85	140	181	137
Nb	65	725	25		
Sn					
Ba	154	10	465	99	73+(10)
Pb					
Th	23	21	13	48	13
U		7	3	15	5
N =	37	1	1		15

[7] Hill and Thomas, 1983
[8] Hildreth, 1979. E - Early erupted tuff; L - late erupted tuff.
[9] Huspeni et al., 1984. Bracketed numbers are number of analyses.

recognized as A-Type granites (Mutschler et al., 1981; Taylor et al., 1985; Stein and Hannah, 1985). Peralkaline granites, which have still lower alumina values, have comparable to extreme LIL enrichment trends. Allowing for the inherent variability in any data set and system analyzed, there is a remarkable consistency in data between the different 'types' of high-silica granites.

As noted by Strong (1980), Hildreth (1981) and Mutschler et al. (1981) comparison of data from high-silica ash-flows with those from high-silica, mineralized, granite systems implies a strong genetic association between magma chambers responsible for major ash-flows and for significant mineral deposits. There is also a remarkable similarity between data from the high-fluorine topaz-bearing rhyolites (Burt et al., 1982; Huspeni et al., 1984), from the Ackley Granite Suite, and from the A-type mineralized granites in general. Included in the A-type suite of granites are the Proterozoic rapakivi granites (Haapala, 1985).

There is a large scatter in the data from the study area which makes direct comparison of the granitic and volcanic systems difficult. Nevertheless, there is some consistency in the data, and Figure 51 shows that the Ta-Th values are similar to, and also higher than, the tuffaceous systems described by Hildreth (1981). The granitic environment presumably enhanced the LIL enrichment trends due to retention of volatiles in the magma, whereas the volcanic rocks may have erupted prior to onset of significant LIL enrichments (cf. Hildreth, 1981).

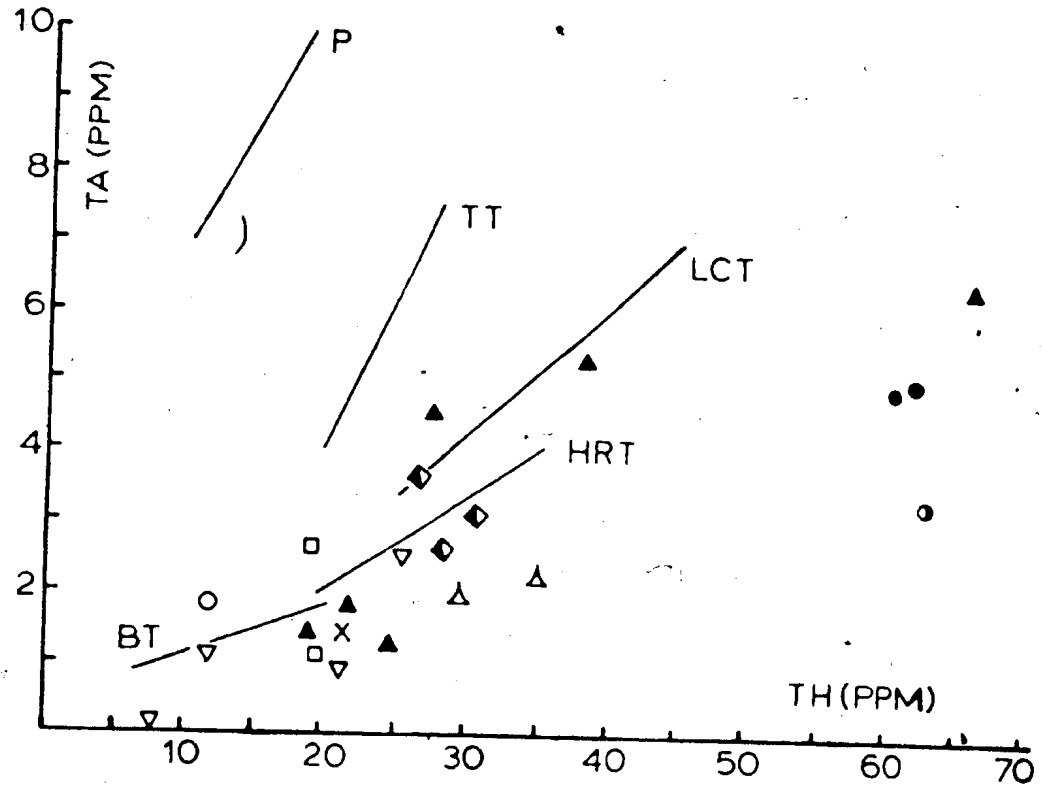

Figure 51: Plot of Ta against Th for samples from the study area. Symbols are described in Figure 17 or Figure 53. BT - Bishop Tuff, HRT - Huckleberry Ridge Tuff, LCT - Lava Creek Tuff, TT - Tala Tuff, P - Pantalleria Tuff (Hildreth, 1981).

CHAPTER 6 - RARE EARTH ELEMENT GEOCHEMISTRY

6-1 INTRODUCTION

The objectives of this Chapter are to summarize the distribution of the rare earth elements (REE) in the study area and to discuss the significance of these variations. Modelling of the REE data in terms of crystal fractionation has been done by Whalen (1983) and was not repeated during this study. Conceptual and philisophical problems which are discussed in Chapter 10 (ie. non-equilibrium due to extra degree of freedom as result of density contrasts) prevent realistic modelling. REE analyses are available for 41 samples (35 new analyses in Appendix F, and 6 from Whalen, 1983). All of the available data are discussed below. The REE analyses obtained by Whalen are indicated by W on the diagrams and are similar to those presented here for samples from the same general area, a feature which promotes confidence in the data.

Results and conclusions from the investigation of specific topics (ie. regional variations, molybdenum-mineralized area, and tin-mineralized area) are presented separately. A detailed discussion section at the end of the chapter draws conclusions from comparisons between the different study areas.

The distribution of samples from the regional surveys for which REE analyses are available is shown in Figure 52. All of the REE patterns in the following diagrams were normalized using the chondritic values of Taylor and Gorton (1977).

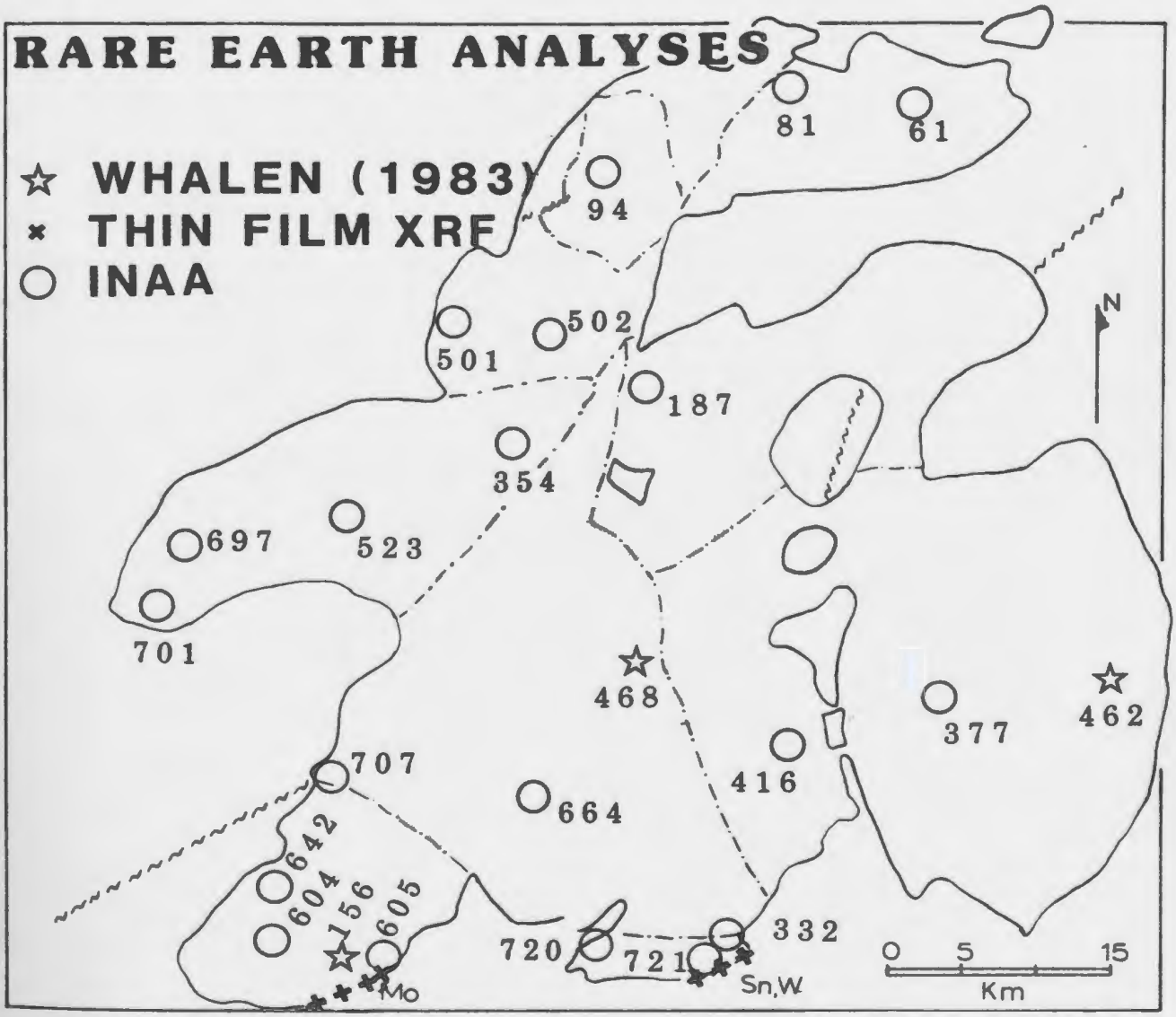

Figure 52: Location of rare earth element (REE) analyses. Circles are new instrumental neutron activation analyses (INAA), crosses are thin film - XRF data, and stars are INAA data of Whalen (1983). Additional samples from the mineralized areas are not numbered.

The relative enrichment of REE lighter than europium (LREE) and REE heavier than europium (HREE) within and between rock samples is considered to be an important index to the processes and controls over the REE distribution (e.g. Hanson, 1978; Taylor and Fryer, 1983)). Values for the more abundant HREE, Gd and Dy were not obtained by INAA and values for Tb and Ho are too low to be accurately determined by the thin-film XRF technique. Therefore, comparison of variation between total LREE and total HREE is not possible. The plot of La (ppm) versus Yb (ppm) shown in Figure 53 allows some comparison of the relative enrichment and depletion of LREE and HREE within samples. The plot is also an approximation of the relative concentrations of REES between analyzed samples. The enrichment or depletion of Eu relative to the trend of the other REE in the normalized REE pattern describes the Eu anomaly (Eu/Eu*), where:

Eu/Eu* = Actual Normalized Eu/Expected Normalized Eu

Expected normalized Eu is obtained by averaging the normalized values for Sm and Gd. By convention, the anomaly is positive if the ratio is $>$ 1 and negative if the ratio is $<$ 1.

6-2 REES IN THE KOSKAECODDE AND MOLLYGUAJECK PLUTONS

6-2-1 Results

Chondrite normalized REE patterns from the Koskaecodde Pluton have a steep negative slope and a small but variable Eu anomaly (Fig. 54). Sample 701 is the least differentiated (60.3% SiO_2) and has a slight positive Eu anomaly (Eu/Eu* = 1.12). Samples 697 (65% SiO_2) and 354 (69.3% SiO_2) have a weak negative Eu anomaly (Eu/Eu* = 0.54 and 0.31

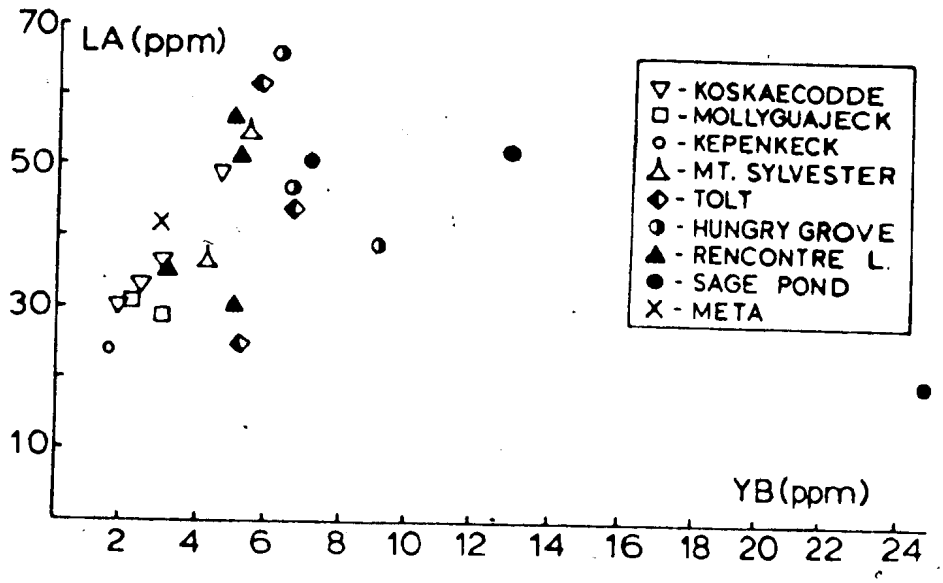

Figure 53: Plot of La against Yb.

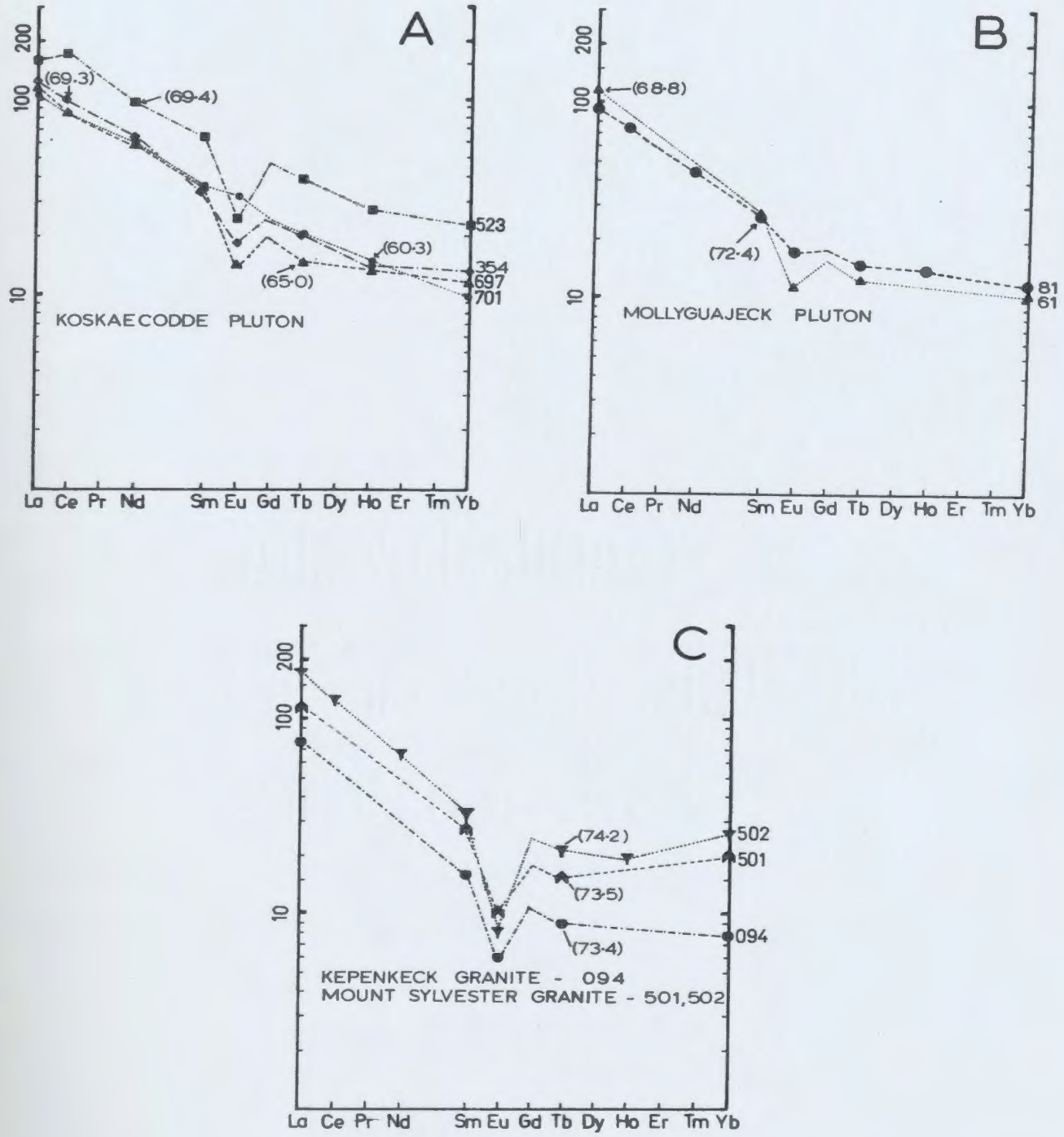

Figure 54: REE patterns from the northwestern granitoids. Chondrite normalized using values of Taylor and Gorton (1977). Samples analyzed by INAA.

respectively) and are slightly enriched in the heaviest REES compared to sample 701. Sample 354 is also slightly enriched in the light REES compared to 701. Sample 523 (69.4 SiO_2) has Eu/Eu* = 0.45 and is enriched in both LREE and HREE compared to 701.

The patterns for samples 61 (72.4% SiO_2) and 81 (69.3% SiO_2) from the Mollyguajeck Pluton have negative Eu anomalies of 0.53 and 0.75 respectively and are similar to the pattern for sample 697 from the Koskaecodde Pluton (Fig. 54).

The low total REE content of the Koskaecodde and Mollyguajeck plutons, relative to the Ackley Granite Suite is illustrated in Figure 53. Sample 523 has highest REE and is significantly enriched in La and Yb relative to the other samples from the Koskaecodde Pluton.

6-2-2 Discussion

The REE patterns in the Mollyguajeck and Koskaecodde plutons are similar. This supports the interpretation from petrographic, major and trace element data that these two granodiorite-granite plutons have a similar petrogenetic history.

The changes in the REE patterns are not directly related to the degree of differentiation as indicated by the silica content or by the Thornton-Tuttle Differentiation Index (see Dickson, 1983). This is illustrated by the variability in total REE content compared to the SiO_2 content of the samples. A Spearman rank correlation matrix of the 6

samples for which REE are available also shows no significant covariations with the REE and most major oxides, the exception being Eu which has a negative covariation with SiO_2 and a strong positive covariation with the Ca-Femic oxides (including P_2O_5 and TiO_2). Gromet and Silver (1983) have shown that in granodiorite, the bulk of the HREE occur in sphene, and the LREE reside in apatite. Thus variations in concentration and origin of these accessory minerals may account for the observed variations in the Koskaecodde and Mollyguajeck plutons. Apatite and sphene are generally euhedral indicating early crystallization.

6-3 REES IN THE ACKLEY GRANITE SUITE

6-3-1 Results

Sample 94 from the Kepenkeck Granite (Fig. 54) has the lowest total REE concentration (Fig 53) in an unmineralized granite analyzed from the Ackley Granite Suite and has Eu/Eu* = 0.22. The two other samples (#501 and #502) analyzed from the northwestern granitoids belong to the southern part of the Mount Sylvester Granite and have REE patterns (Fig. 54) which are similar to those from the Tolt and Hungry Grove granites (Fig. 55). Samples 501 and 502 have negative Eu/Eu* = 0.46 and 0.28 respectively. These two samples have slightly higher Total REE content (especially HREE; see Fig. 53) than do the granodioritic plutons and the Kepenkeck Granite.

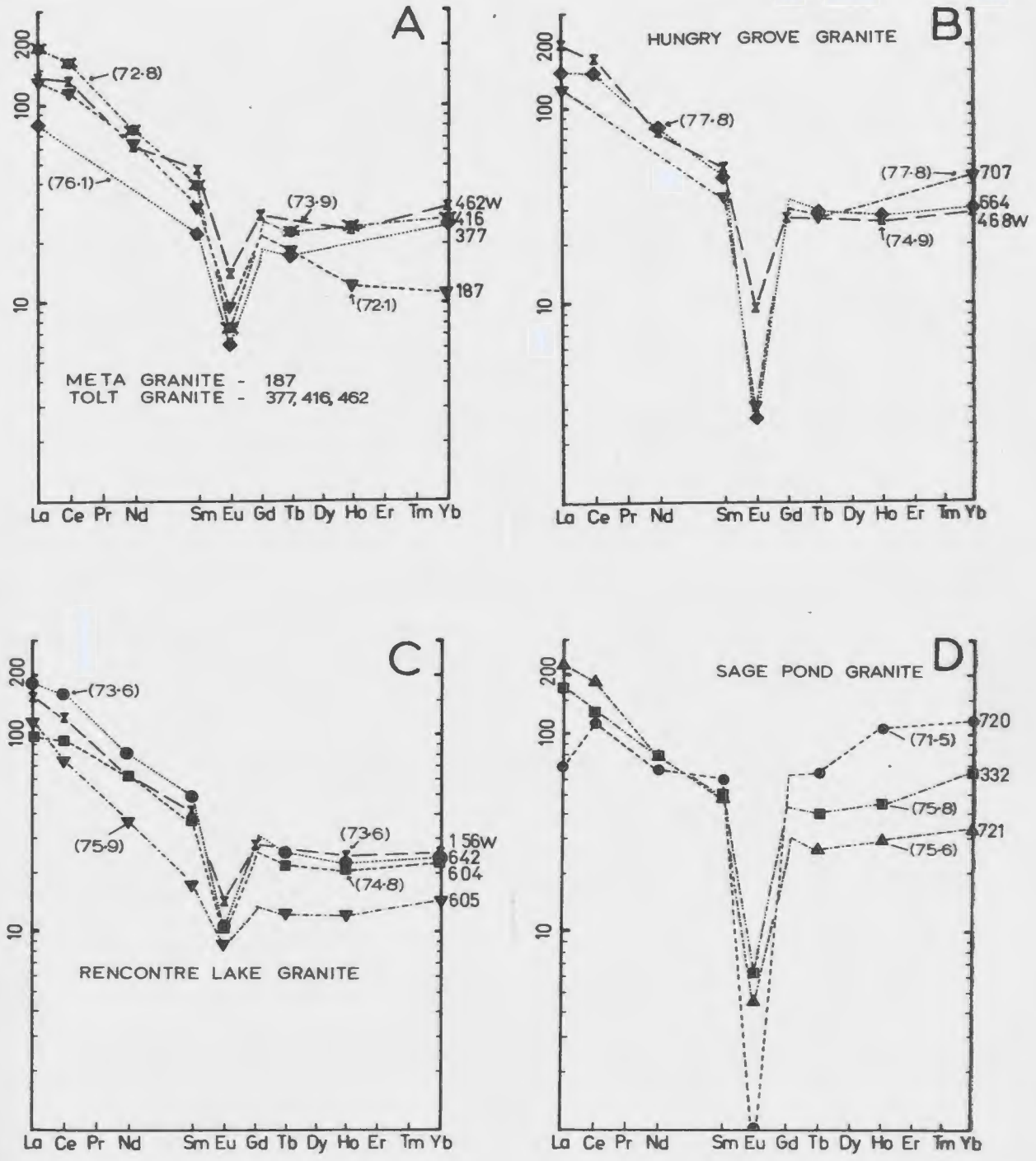

Figure 55: REE patterns from the southeastern Ackley Granite Suite. Chondrite normalized using values of Taylor and Gorton (1977). All samples analyzed by INAA. W - analyses of Whalen (1983).

The Meta Granite is represented by the analysis of sample 187 (Fig. 55). This sample has approximately median values for LREE, low values for HREE and highest La/Yb ratios (Fig. 57) compared to other granites from the southeast. It also has moderate negative Eu/Eu* = 0.37.

REE patterns from the Tolt Granite (samples 462, 416, 377) and from sample 468 from the Hungry Grove Granite are similar, with moderate negative Eu/Eu* varying from 0.24 to 0.40 (Fig. 55). Sample 664 from the Hungry Grove Granite has a similar REE pattern but has a much larger negative Eu anomaly (= 0.07). These samples, along with the samples from the Mount Sylvester Granite, all exhibit a moderate enrichment in heaviest REE and a higher total REE concentration relative to the granodioritic plutons. Sample 664 also has high LIL concentrations and is included in the trace element enrichment trend which culminates at mineralization. Sample 707 has both elevated HREE, a large negative Eu anomaly (= 0.10) and is geochemically specialized. Samples 332, 720 and 721 from the Sage Pond Granite have similar LREE and elevated HREE, compared to the relatively unspecialized samples from the Hungry Grove and Tolt granites (Fig. 55). These samples also have a large negative Eu anomaly (0.14, 0.01, and 0.12 respectively) similar to sample 664 and 707. There is no systematic variation of REE between the Sage Pond Granite and the other granites with major elements. However, the samples from the Sage Pond Granite are all relatively enriched in LIL elements and depleted in Ba and Sr. Sample 720, from the Sage Pond Granite, has elevated values for MREE and HREE, highest value for Yb (Fig. 53) and the largest negative Eu anomaly. This sample is partly sericitized and kaolinized, with high K_2O (7.17%) and AL_2O_3 (15.5%), relatively low SiO_2 (71.5%) and highest concentrations of Rb, Y, Nb, Th and U.

In contrast to the Sn-mineralized Sage Pond Granite, samples 156, 642 and 604 (Fig. 55), from the Mo-mineralized Rencontre Lake Granite have smaller negative Eu anomalies (= 0.42, 0.27 and 0.34 respectively), similar LREE, and slightly lower HREE, when compared to the unspecialized Tolt and Hungry Grove granites. Sample 605 (see Fig. 50 for location) which has the lowest total REE and the smallest Eu anomaly (= 0.60) is heavily chloritized.

6-3-2 Discussion

The low total REE content of sample 94 supports the whole-rock data (Al_2O_3 and Sr in particular) which indicates that the Kepenkeck Granite is petrogenetically distinct from the other granitoid rocks in the study area.

The similarity in REE patterns of samples 501 and 502 from the Mount Sylvester Granite and patterns from the Tolt and Hungry Grove granites supports the results of the discriminant function analysis reported in Chapter 5. These results correlate the southern part of the Mount Sylvester Granite with the Hungry Grove Granite.

The covariation of the REE with respect to the other geochemical variables is presented in Appendix E-3. The HREE have neither negative or positive covariations with Zr and Ce and have negative covariations with P_2O_5 and TiO_2. This suggests that crystallization of zircon, allanite, apatite or sphene may not be the the cause of enrichment of the REE and the other LIL elements. These features contrast sharply with

the LREE (excluding Sm) which have weak covariations (0.5 at the 90% level) with the other variables and do not exhibit significant inter-REE covariations. Thus the controls over the distribution of the LREE are different than those of the HREE. The lack of covariations suggests that simple fractionation involving the main silicate phases in the granite (all of which should create positive covariations of the REE) do not control the REE distribution. The strong positive covariations between HREE and the LIL elements suggest that all of these 'peralkaline' elements are essentially incompatible with respect to the main crystal phases in the granite.

In conclusion, the Koskaecodde and Mollyguajeck Plutons, the Kepenkeck Granite and the rest of the Ackley Granite Suite exhibit significantly different REE patterns which suggest different petrogenetic histories. In addition, there is a general trend to elevated HREE concentrations with geochemically specialized rocks associated with the tin-tungsten mineralization in the Sage Pond Granite and this trend is emphasized by an abrupt drop in Eu content of the granite. There are significant differences between the Rencontre Lake and Sage Pond granites, with three patterns in the former comparable to unspecialized granite from the Tolt and Hungry Grove granites and one depleted in all REES.

6-4 REES AT THE MOLYBDENITE PROSPECTS

6-4-1 Introduction

The REE patterns from the molybdenite prospects (Figure 56) were obtained from three sources. REE data for samples 6 and 98 were published along with whole rock geochemical analyses by Whalen (1983); the other samples were analyzed at MUN. Powders for analysis from samples 7, 14, and 120 were taken from the sample-powder library at MUN (thesis samples of Whalen, 1976) and whole rock analyses and sample descriptions are listed in Whalen (1976). Powders from samples 1160 to 1163 were obtained from the Analytical Laboratory at the Newfoundland Department of Mines and Energy, and whole rock analyses and sample descriptions have been published by Dickson (1983).

6-4-2 Results

The molybdenite prospects collectively have lower LREE concentrations and most samples have lower HREE concentrations than the presumed parent Rencontre Lake Granite. The Eu anomalies are variable with values ranging from 0.10 to 1.03 and there is a marked depletion in the Middle REE (MREE), particularly in Gd and Er, with reference to the regional granite patterns.

At the Ackley City prospect, samples 6 and 98 are described as aplite by Whalen (1983) and show comparable patterns to sample 605 from the Rencontre Lake Granite. These patterns are depleted relative to samples 156, 642 and 604 from the Rencontre Lake Granite and to other

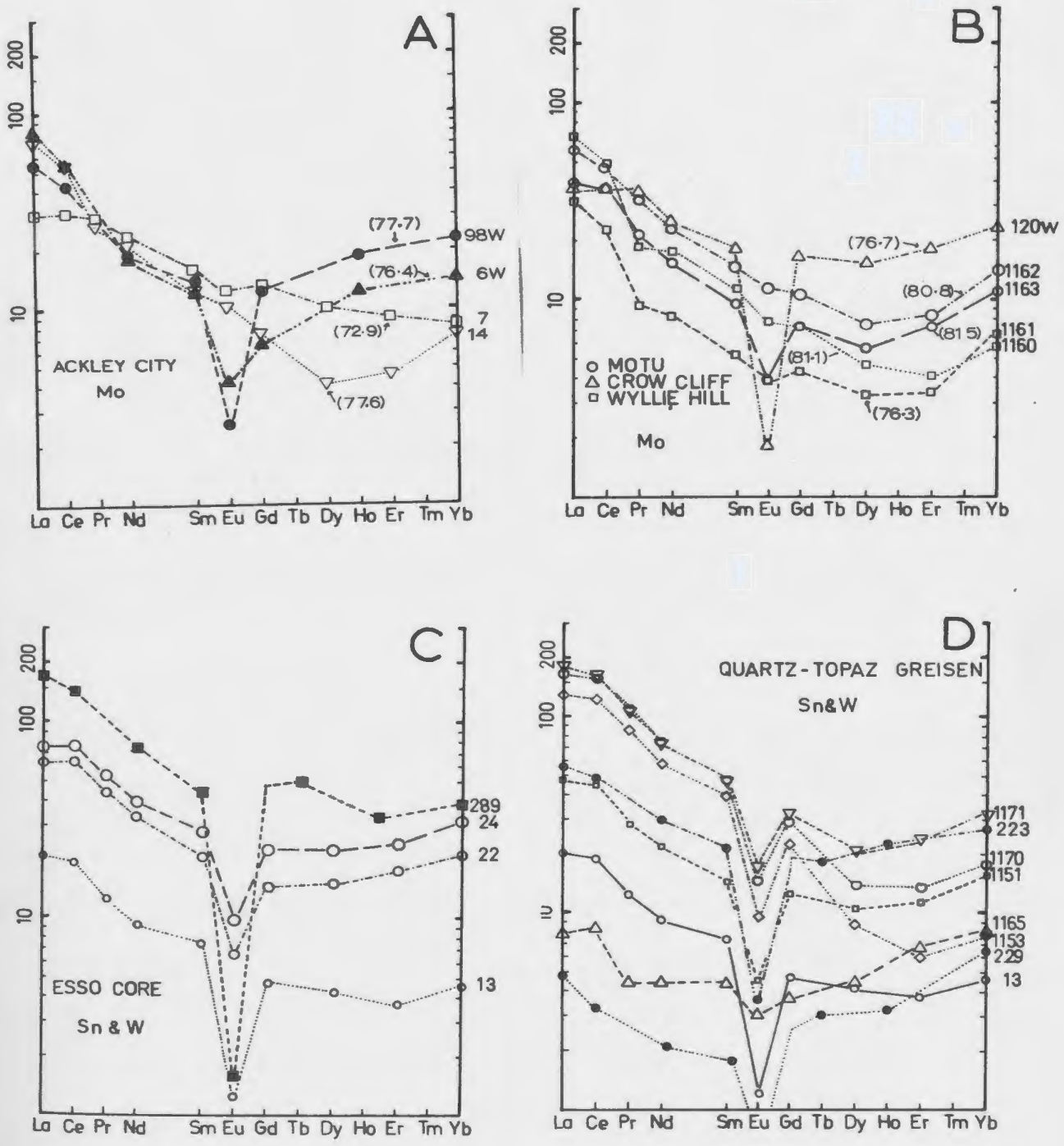

Figure 56: REE patterns from the mineralized areas in the southern Ackley Granite Suite. Chondrite normalized using the values of Taylor and Gorton (1977). Solid symbols - INAA data. Open symbols - XRF analyses. W - analyses from Whalen (1983).

samples from the southern Ackley Granite Suite. Samples 7 and 14 are described as granite-pegmatite and show relative depletion of TREE (total REE) and loss of the Eu anomaly (= 0.87 and 1.03 respectively).

The samples from the Motu prospect (1162 and 1163) are fine grained and contain minor rosettes of molybdenum. These samples are strongly depleted in MREE relative to the regional samples from the Rencontre Lake Granite and have Eu/Eu* = 0.89 and 0.47 respectively.

Sample 120 is a fine grained granite near the pegmatite at Crow Cliff. It has depleted LREE compared to the Rencontre Lake Granite, more normal HREE when compared to the Motu samples and a relatively large negative Eu/Eu* = 0.10.

Samples 1160 and 1161 from the Wyllie Hill prospect consist of slightly bleached fine-grained granite with minor disseminated molybdenite and pyrite. These samples show physical evidence for hydrothermal alteration, have a characteristic U-shaped REE pattern, the same low negative Eu anomaly (= 0.81), and exhibit the greatest amount of depletion in HREE of the samples from the molybdenum prospects.

The samples from the Motu and Wyllie Hill prospects have very high-silica contents, as also reported by Whalen (1976).

6-4-3 Discussion

In the samples from the molybdenite prospects, where miaroltic and

pegmatite features are common, the U-shaped REE patterns are thought to result from crystallization of the silicate phases in the presence of a separate fluid phase (Hanson, 1978; Taylor and Fryer, 1983). Comparable genetic histories are suggested for the four main molybdenite prospects by the similarity in REE patterns and this supports Whalen's (1976, 1980, 1983) interpretations that the different styles of mineralization are part of a continuum of processes. Detailed examination of the REE patterns from the prospects (Fig. 56) and comparison of these to the patterns from the Rencontre Lake Granite (Fig. 55) suggest that three stages of alteration can be recognized.

The first indications of alteration (Stage 1) are demonstrated by samples 98 and 120 which do not contain sulphide mineralization or visible signs of alteration. These are probably the least altered rocks analyzed from the molybdenite prospects and exhibit a relative depletion of LREE and a slight increase in the Eu anomaly (from 0.27 to 0.42 in the parent Rencontre Lake Granite to 0.10 in sample 120). Stage 2 is illustrated by samples 1162 and 1163 which contain minor molybdenite. These show depletion in all REES and also a large decrease in the size of Eu/Eu* (from 0.1 to values of 0.47 and 0.89). Sample 6 may be from an intermediate stage with low LREE and intermediate values for HREE and Eu/Eu*. Stage 3, illustrated by the Wyllie Hill samples, is the continued relative depletion of total REES, while the characteristic U-shape is maintained and Eu/Eu* changes from weakly negative to slightly positive (samples 1160, 1161). This latter stage is accompanied by silicification and minor sericitization.

6-5 REES ASSOCIATED WITH QUARTZ-TOPAZ GREISEN

6-5-1 Introduction

REE patterns from greisens and from granite adjacent to greisen in the Sage Pond area are shown in Figure 56. Samples 13, 22, 24, 223, 229 and 289 were collected by the author and samples 1151, 1153, 1165, 1170 and 1171 form part of the sample set analyzed by Dickson (1983). The locations of the analyzed samples are shown in Figure 46.

6-5-2 Results

Sample 289 is a relatively fresh, fine grained granite, adjacent to an isolated quartz-topaz greisen vein on surface. It has REE concentrations similar to those of the Sage Pond Granite and trace element-enriched portions of the Hungry Grove Granite (Fig. 55). Samples 13, 22 and 24 were collected from Esso drill core. Sample 24 is a fresh fine-grained, miarolitic granite, located 1 m from a 2 m wide quartz-topaz greisen vein within a swarm of greisen veins (Plate 31). This sample exhibits depletion of all REE, a U-shape and a relative decrease in the Eu anomaly (from 0.1 to 0.39). Sample 22 is a sericite-rich greisen marginal to one of the quartz-topaz veins (see Plate 22) and has a pattern similar to 24 with lower REE concentrations. Sample 13 is a quartz-topaz greisen and exhibits extreme depletion in all REES and $Eu/Eu^* = 0.2$.

REE patterns from various samples of quartz-topaz greisen are also presented in Figure 56. All of the samples are characterized by lower

HREE and a smaller Eu anomaly than samples from the Sage Pond Granite. No systematic correlation has been observed between REE and major oxide or trace element concentrations (including F). The samples from the larger Esso (#13) and Anesty (#229 and 1165) greisen bodies show the greatest depletion of total REE in the analyzed quartz-topaz greisen although there is no apparent direct relationship between the REE concentrations and the Sn and W concentrations of the analyzed samples.

6-5-3 Discussion

The features noted above indicate that the loss of REES from the host granite is spatially (<5 m) restricted to the areas of abundant greisenization or fluid activity. The intermediate stage of the alteration process is reflected by samples 22 and 24 and results in a U-shaped REE pattern.

The association between total REE depletion and quartz-topaz greisen which contains significant concentrations of Sn has also been noted at the East Kemptville tin deposit in Nova Scotia by Chatterjee and Strong (1983).

6-6 SUMMARY AND DISCUSSION OF REE BEHAVIOR

6-6-1 Magmatic Signatures

The observed REE patterns (Fig. 57) are characteristic of those in many high-silica granitic systems (Fig. 58). A straight negative slope with a weak to moderate negative Eu anomaly is characteristic of many of

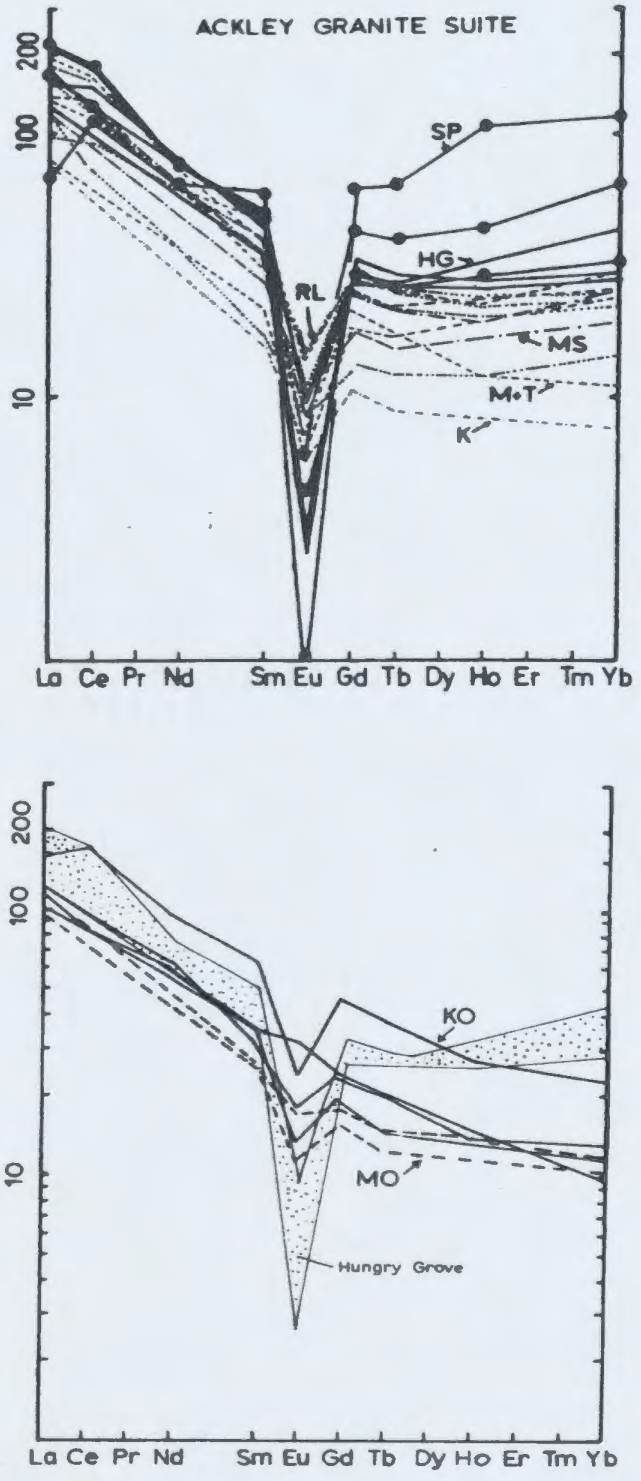

Figure 57: Summary of REE patterns from regional samples. SP - Sage Pond; HG - Hungry Grove; RL - Rencontre Lake; MS - Mount Sylvester; M - Meta; T - Tolt; K - Kepenkeck; KO - Koskaecodde; MO - Mollyguajeck. Stippled area - data from Hungry Grove Granite.

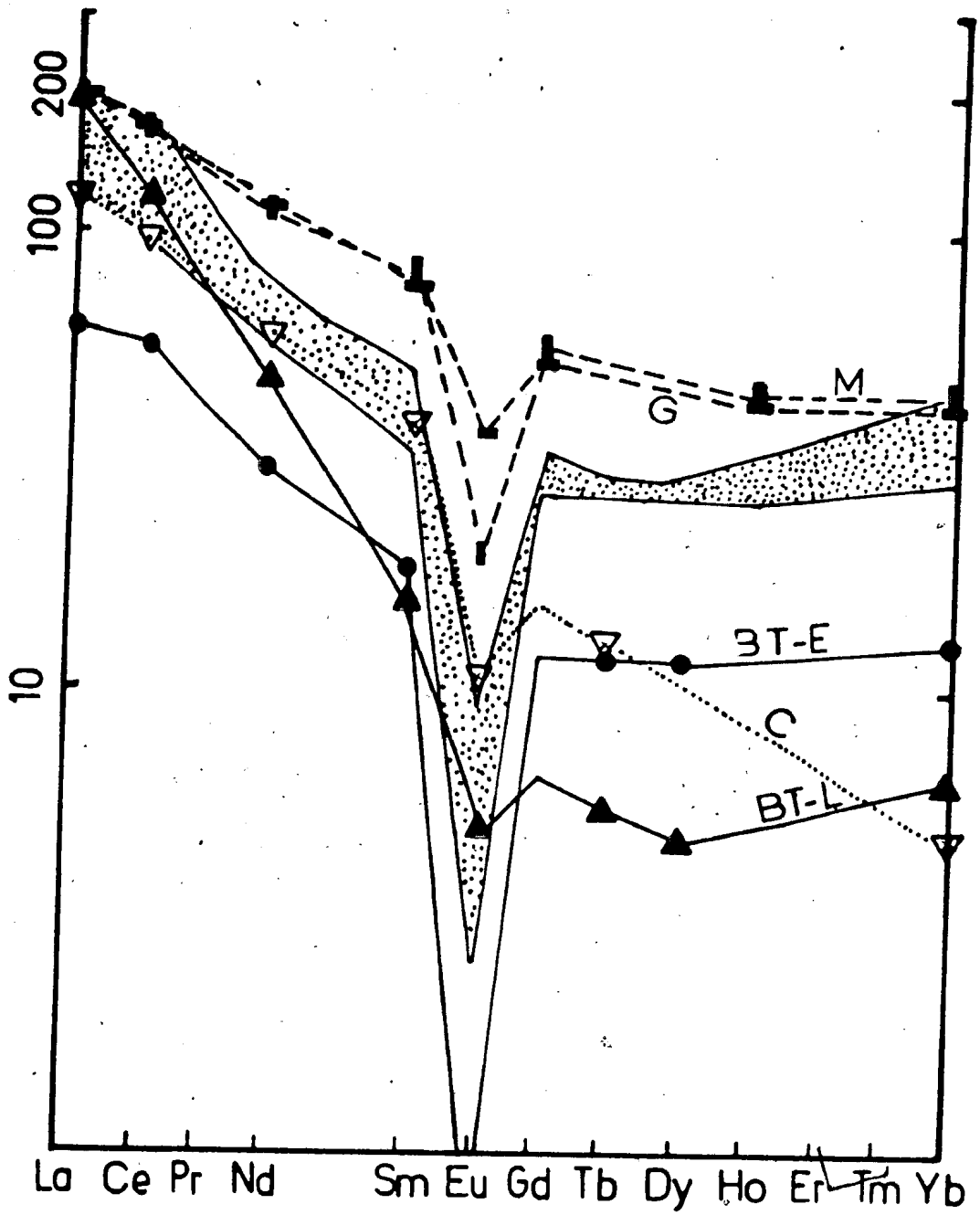

Figure 58: Comparison of REE patterns of selected high-silica systems to those from the Hungry Grove Granite. Stippled area = Hungry Grove Granite. M and G are averages of the Mumballo and Gabo 'A-type' granites (Collins et al., 1982). C is average of 5 samples from the Cornubian Granites (Alderton et al., 1980). BT-E and BT-L are early and late Bishop Tuff (Hildreth, 1979).

the S- and I-type systems as shown by the Cornubian Granites (Alderton et al., (1980), South Mountain Batholith (Muecke and Clarke, 1981) and by the calc-alkaline granitoid rocks of Peru (cf. Atherton and Sanderson, 1985). The anorogenic post-tectonic granites commonly exhibit a slight U-shape due to enrichment in HREE as shown by the A-type granites on Figure 58 (Collins et al., 1982), similar systems in the Mount Pleasant area of New Brunswick (Taylor et al., 1985), the Quartz Hill area of Alaska (Hudson and Arth, 1983), and the Proterozoic rapakivi granites studied by Weibe (1978). High-silica peralkaline granites show moderate to extreme enrichment of the HREE (cf. Taylor and Fryer, 1983). Similar U-shaped patterns with weak to strong negative Eu anomalies are present in some anorogenic high-silica volcanic systems such as the Bishop Tuff (Hildreth, 1979; Fig. 58) and topaz-bearing rhyolites (Huspeni et al., 1984).

Within the study area, the relative concentrations of REES demonstrate the independent genetic evolution of the Koskaecodde and Mollyguajeck plutons, the Kepenkeck Granite and the rest of the Ackley Granite Suite. These REE patterns emphasize the regional chemical consistencies in the southern Ackley Granite Suite and demonstrate that the HREE are concentrated along with other LIL trace elements. Europium is strongly depleted in a large halo surrounding the known mineralization in the Sage Pond Granite. The differences in LIL element behavior between the Rencontre Lake Granite and the Sage Pond Granite are also mirrored by the REE behavior since the former is not markedly enriched in HREE nor depleted in Eu.

Comparison of the various REE patterns from the Ackley Granite Suite show that the U-shape, or relative enrichment, of the HREE results from magmatic processes (i.e. independent of hydrothermal processes) during differentiation of the magma system (assuming sample 187 and 720 are genetically related). This feature was also observed in the Bishop Tuff (Hildreth, 1979).

6-6-2 Hydrothermal Signatures

Taylor and Fryer (1983) have recently reviewed the behavior of REE in hydrothermal systems and the following selected points are summarized from them. Flynn and Burnham (1978) determined experimentally that the REE do not partition significantly into simple aqueous solutions. However, they indicate that in Cl^--dominated aqueous systems, the LREE preferentially partition into the fluid phase, thus causing a LREE-depeleted pattern in the parent rock. Flynn and Burnham (1978) and Taylor and Fryer (1983) also suggest that the presence of other anionic species such as CO_3^{2-} or F^- in the aqueous fluid will alter the silicate-aqueous fluid partition coefficients such that the HREE are preferentially depleted from the parent rock. Conversely, redeposition of the mobilized REE may have the opposite effects with LREE enriched in Cl^--dominated systems and HREE enriched in CO^{2-}-dominated systems. In weakly acid F^--dominated aqueous systems, the stability of REE fluoro-complexes at lower fluoride concentrations ($< 10^{-3}$ M) has a maximum at Yb (Bilal et al., 1979; Bilal and Becker, 1979). Bandurkin (1961) also recognized that the stability of these fluoro-complexes in the fluid phase is enhanced by the prescence of Al^{3+}, a condition restricted to

those fluids producing phyllic and argillic alteration (Guilbert and Jewell, 1974; Taylor and Fryer, 1983; Strong et al., 1984).

The molybdenite mineralization in the Rencontre Lake area is accompanied by a decrease in total REE and a marked decrease in middle REE. The widespread pegmatite and miarolitic cavities indicate that a fluid phase was present during crystallization, and the decrease in MREE can be interpreted to result from silicate-aqueous fluid equilibra. The observed REE patterns in the mineralized areas at Rencontre Lake can thus be explained by assuming that crystallization and possible high-temperature hydrothermal alteration of the Rencontre Lake Granite took place in the presence of a fluorine-dominated aqueous fluid. Alternatively a fluid containing both Cl^- and CO_2 may have been present. The largest depletions are noted at Wyllie Hill where sericite alteration is visible and a larger fluid-rock ratio may be responsible for the greater amount of REE depletion. Leaching of the HREE and MREE would not affect the concentration of bivalent Eu and the observed decrease in the size of the Eu anomaly would result.

Samples 6 and 98 from the Ackley City prospect were used by Whalen (1983), in conjunction with sample 468, to assist in modelling crystal-liquid fractionation processes throughout the Ackley Granite Suite. Comparison of the REE patterns from the Ackley City prospect with the regional patterns for the Rencontre Lake Granite (Fig. 55) indicate that samples 6 and 98 (Fig. 56) are relatively depleted in all REE. The REE plutons have been modified by a fluid phase and therefore do not result directly from crystal fractionation.

The REE pattern for sample 605, located approximately 1 km north of the Wyllie Hill prospect, is also interpreted to have resulted from silicate-fluid interaction. This indicates that the hydrothermal systems in the Rencontre Lake Granite were of moderate dimensions.

The characteristic U-shaped depletions noted in the altered granite and greisens in the Sage Pond area may also be interpreted to result from leaching in the presence of a low-fluoride aqueous phase. The relative decrease in the Eu anomaly compared to the regional samples from the Sage Pond Granite, however, cannot be explained by continued leaching of the other REE, and must involve some redeposition of Eu from the hydrothermal fluids. These hydrothermal alteration processes are restricted to the greisen bodies and their immediate proximity. The presence of hematite in the greisen may indicate higher fluid fO_2 than in the magnetite-bearing parent granite, perhaps enhancing the stability of Eu in the greisen. However, this would imply a distinct difference in the behavior of Eu in the aplite-pegmatite and the greisen environments.

Feldspar, and in most samples muscovite, has been completely destroyed during the formation of the quartz-topaz greisen. Thus the implication of the interpretation that the changes in the REE concentrations result from a leaching process indicates that the REES reside in refractory accessory minerals (possibly sphene). Gromet and Silver (1983) showed that the bulk of the whole rock REE content of granodiorite is resident in apatite and sphene. Alternatively, the alteration process may have caused complete local redistribution of the REE between the old and new mineral phases without significant changes

in the bulk REE content. The depletion of REE in the larger greisen may simply reflect a more efficient leaching of the postulated REE-bearing refractory phases in areas where the hydrothermal fluids have been ponded at high temperatures. Alternatively, larger volumes of fluid have passed through.

CHAPTER 7 - RB-SR and $^{40}AR/^{39}AR$ STUDIES

7-1 INTRODUCTION

The Ackley Granite Suite provides an opportunity to evaluate temporal relationships of the distinct styles of mineralization to their host granites. Geochronological studies assist in determining the areal extent and cooling history of the magmatic system, and Rb-Sr studies provide some information on source rock variation. Fourteen new Rb-Sr and thirteen new $^{40}Ar/^{39}Ar$ analyses are presented.

Recent geochronological studies of mineralized granitoid plutons in the Appalachian - Caledonian Orogen indicate variable time intervals between pluton emplacement and mineralizing episodes (Strong, 1985). For example, Seal et al. (1985) have shown that magmatism and hydrothermal activity (Sb, W, Au), at Lake George, New Brunswick were essentially contemporaneous, while Halliday (1980), Jackson et al. (1981) and Bray and Spooner (1983) have documented a protracted period of hydrothermal activity for the Cornubian Sn-W province of southwest England. Zentilli and Reynolds (1985) have suggested that Sn-bearing greisens in the East Kemptville deposit of Nova Scotia were formed 60 Ma after emplacement of the host South Mountain Batholith.

7-2 PREVIOUS GEOCHRONOLOGICAL STUDIES

Published ages from the study area (Fig. 59) include three conventional K-Ar biotite ages (recalculated using the decay constants

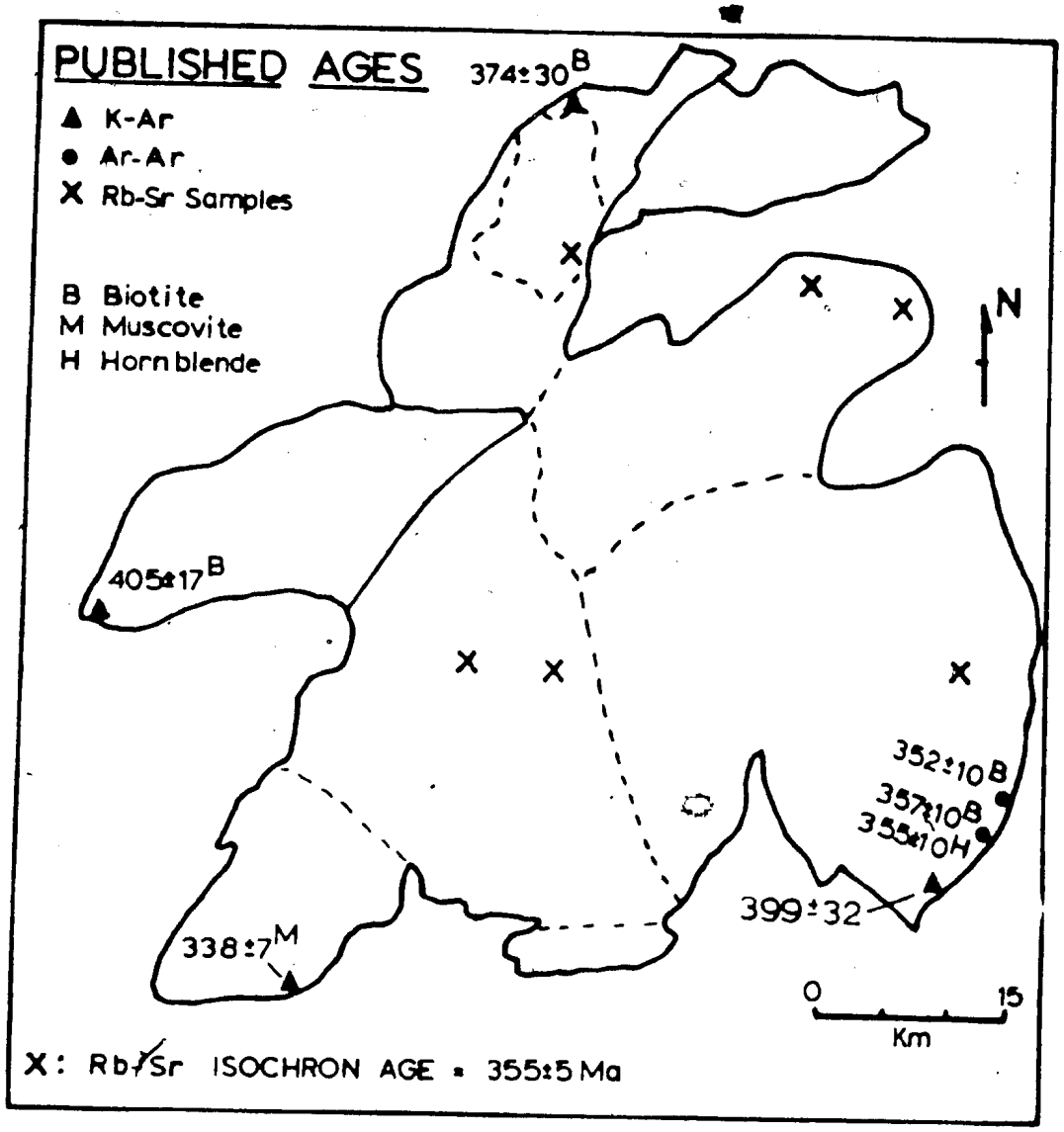

Figure 59: Summary of published radiometric ages from the study area. Internal solid lines are boundaries of Koskaecodde and Mollyguajeck plutons. Dashed lines are internal boundaries of the Ackley Granite Suite.

recommended by Steiger and Jaeger, 1977) of 374 ± 30 Ma (Lowden, 1961), 399 ± 32 Ma (Leech et al., 1963) and 405 ± 17 Ma (Wanless et al., 1972). There are large errors on these ages such that they cannot be used to differentiate possible units within the granitoids.

Bell et al. (1977) reported an Rb-Sr isochron age of 355 ± 5 Ma (2 sigma; recalculated using $\lambda = 1.42 * 10^{-11}$ yr^{-1}). These data were obtained from six samples from different granitoid units which were not recognized in the study area at that time. Five of the samples were from the Tolt, Meta and Hungry Grove granites and one sample was from the Kepenkeck Granite. The implication of this age is that all of the granitoid rocks in the study area (their Ackley City Granite) represent a single cooling event and a single magmatic system.

A K-Ar date of 338 ± 7 Ma was reported by Whalen (1980) on hydrothermal muscovite from the Ackley City molybdenite prospect in the Rencontre Lake Granite. This age was considered by Whalen to be in agreement with the previously reported age of Bell et al. (1977) and was thought to represent the age of crystallization of the granite and its contained mineralization.

Three $^{40}Ar/^{39}Ar$ spectra from biotite and a biotite-hornblende pair were obtained by Dallmeyer et al. (1983). The samples were located at the eastern margin of the Tolt Granite and the spectra gave integrated ages of 352, 357 and 355 Ma respectively (all ± 10 Ma) which were interpreted to represent the approximate age of emplacement and subsequent rapid cooling of the granite. These ages are similar to the

Rb-Sr age reported by Bell et al. (1977) and are younger than a conventional K-Ar age reported from the eastern margin (Fig. 59; Leech et al., 1963).

7-3 WHOLE ROCK RB-SR GEOCHRONOLOGY

7-3-1 Introduction

The Rb-Sr isotopic system and its application to geological problems has been reviewed by Faure (1977). Details of the analytical techniques are provided in Appendix B. The locations of fourteen whole rock samples analyzed to provide information on possible source and age variations in the study area are shown on Figure 60, along with the locations of the 6 samples analyzed by Bell et al. (1977). The Rb and Sr concentrations and Sr-isotope ratios are summarized in Table 17. Samples were selected on the basis of absence of chlorite alteration in thin section.

7-3-2 Results

Results of weighted least squares regression analyses are shown in the accompanying Figures for combinations of the new data along with the data of Bell et al. (1977). Errors are quoted are at the 1 sigma level. The regressed lines on most of the plots have a mean square of weighted deviates (MSWD) greater than 2 and are errorchrons as defined by Brooks et al. (1972). Nevertheless, there are significant variations in the indicated ages and the initial $^{87}Sr/^{86}Sr$ ratios between the northwestern granitoids and the granites from the southeast.

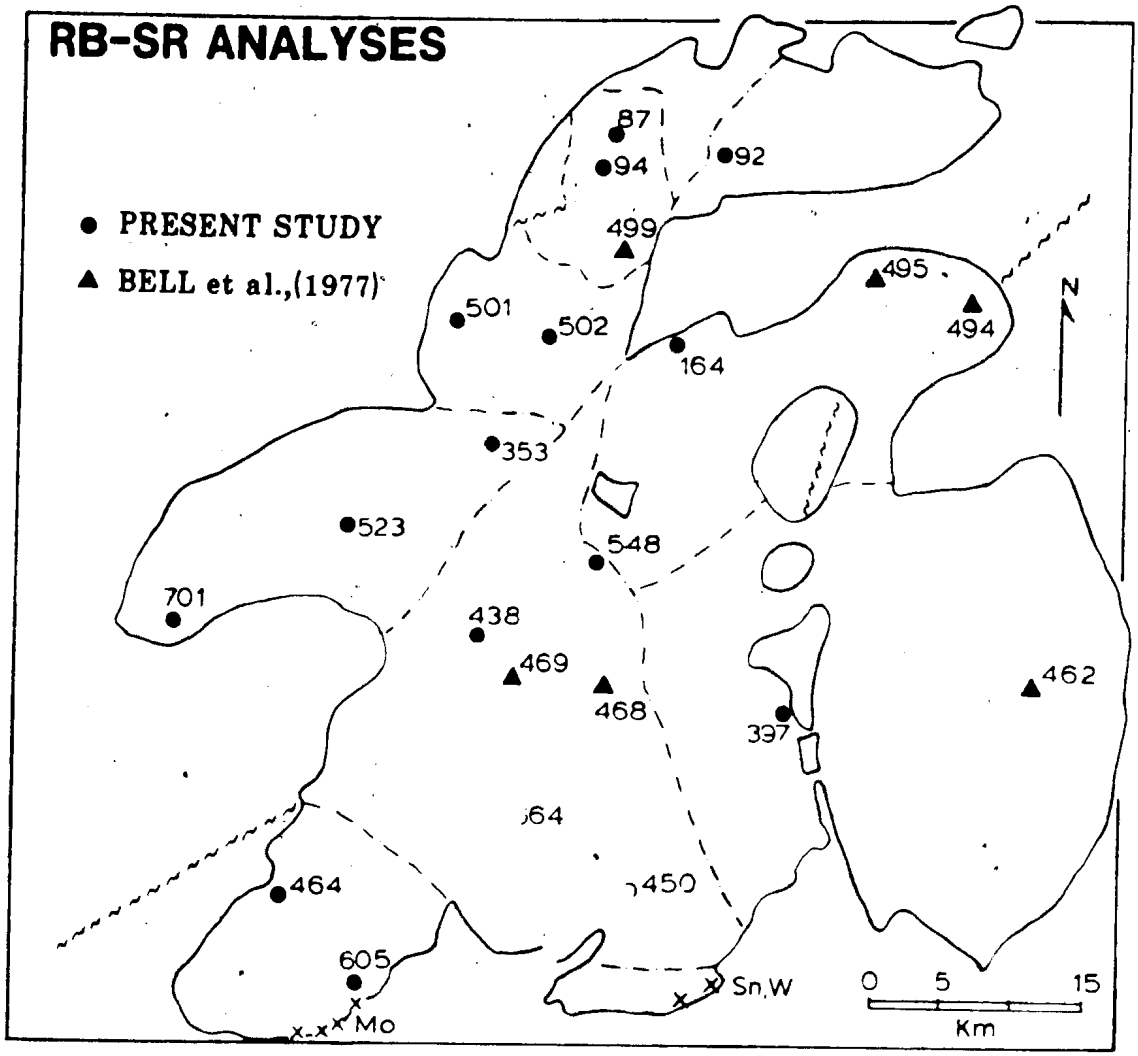

Figure 60: Locations of samples analyzed for Rb and Sr isotopic content. Dot-dash lines are internal boundaries of the Ackley Granite Suite.

Table 17: Rb-Sr isotope data. Sample location on Figure 60.

Sample	Rb	Sr	$^{87}Rb/^{86}Sr$	$^{87}Sr/^{86}Sr$
87	235.3	263.8	2.585	0.71888
92	192.9	277.5	2.015	0.72172
94	245.5	253.6	2.805	0.72028
164	186.0	162.6	3.316	0.72298
353	283.4	116.4	7.079	0.75151
397	311.6	65.6	13.844	0.77647
438	257.1	182.1	4.094	0.72757
464	150.1	99.4	4.377	0.72733
501	312.8	109.7	8.29	0.74819
502	322.6	82.6	11.36	0.76371
523	214.5	172.9	3.600	0.73148
605	241.8	65.6	10.720	0.76095
701	164.8	316.8	1.507	0.71819
Bell et al. (1977)				
CD 462	214	75	8.3	0.7479
468	294	35	24.5	0.8280
469	250	24	31.1	0.8618
494	248	84	8.5	0.7493
495	220	74	8.6	0.7497
499	212	344	1.78	0.7135

All data from the northwestern granitoids are plotted on Figure 61A. This sample grouping gives an age of 359.5 Ma, which is meaningless since it has a large error of 57.9 Ma and a MSWD of 522. However, the samples plot as two trends. Hornblende-bearing samples (92, 353, 523 and 701) from the Koskaecodde and Mollyguajeck plutons form the upper and steeper line and samples from the Kepenkeck and Mount Sylvester granites (87, 94, 499, 501 and 502) form the lower trend.

Hornblende-bearing samples from the Koskaecodde and Mollyguajeck plutons give a reasonably acceptable age of 426.9 ± 12.1 Ma with an MSWD of 6.3 and an initial strontium ratio of 0.7092 (Fig. 61B).

The combined samples from the Mount Sylvester and Kepenkeck granites have an indicated age of 370.4 ± 15 Ma, a large MSWD of 19 and an initial strontium ratio of 0.7049 (Fig. 62A). This is an unacceptable age due to the large MSWD. A line through the 2 sample points from the Mount Sylvester Granite gives an age of 356 Ma and an initial strontium ratio of 0.706. The 3 muscovite-bearing samples (Fig. 62B) from the Kepenkeck Granite give an indicated age of 465.9 ± 3.6 Ma with an MSWD of 0.05 and an initial strontium ratio of 0.7017. This latter line is the only isochron from the new data set, but the very low initial strontium ratio indicates anticlockwise rotation of the isochron, possibly due to subsolidus mobility of Sr or Rb. Alternatively, it is possible that incomplete homogenization of Sr-isotopic ratios from variable sources (cf. Juteau et al., 1984), resulted in the low initial strontium ratio. The low initial ratio indicates that this isochron is unacceptable with respect to age and initial ratio.

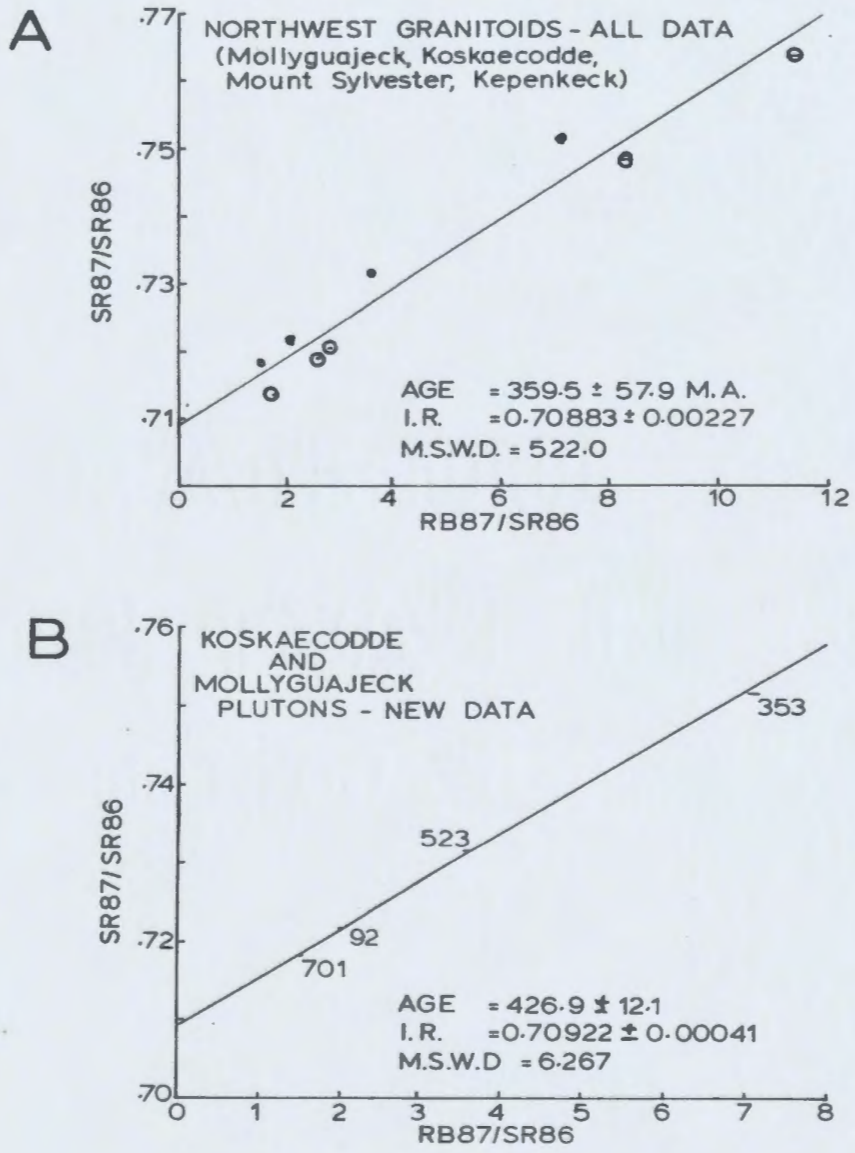

Figure 61: A: Isochron plot of all data from the northwest granitoids.
B: Isochron plot of data from the Koskaecodde and Mollyguajeck plutons.

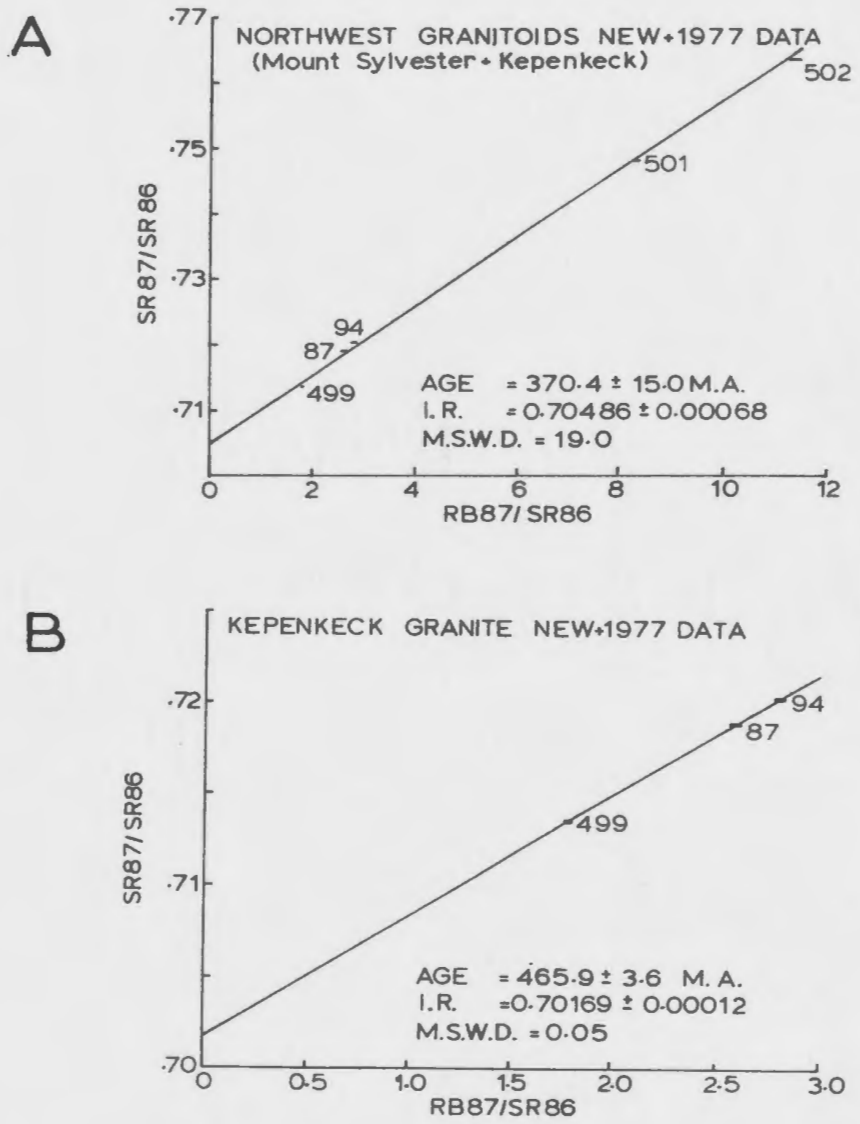

Figure 62: A: Isochron plot of data from the Mount Sylvester and Kepenkeck granites.
B: Isochron plot of data from the Kepenkeck Granite.

The 5 new analyses from the southeast granites provide an errorchron age of 357.6 ± 11.8 Ma with an initial strontium ratio of 0.7063 and MSWD of 9.9 (Fig. 63A). This is comparable to the isochron (indicated age of 348.5 + 1.9 Ma with an MSWD of 0.27 and an initial strontium ratio of 0.7070) obtained by regression of a line through the 5 data points of Bell et al. (1977) from the southeast granites (Fig. 63B). Combining the new data and the data of Bell et al. (1977) results in an errorchron age of 353.2 ± 4.7 Ma (1 sigma), an initial strontium ratio of 0.7063 and an MSWD of 4.2 (Fig. 63C). This latter age is taken to be the most acceptable Rb-Sr age for the southeast Ackley Granite Suite, and the age and initial ratio obtained from the two samples from the Mount Sylvester Granite also plot on this line. If a 2 sigma error is used to regress the 10 data points, the age error is doubled to 9 Ma and the MSWD is reduced to 2.4 such that the regressed line can essentially be considered an isochron.

7-3-3 Discussion of Rb-Sr Data

The data from the Koskaecodde and Mollyguajeck plutons support the petrological and geochemical observations which indicate that they are distinct from the Ackley Granite Suite. These plutons have a Middle Silurian (Wenlock) Rb-Sr age of 426.9 + 12 Ma, using the time scale of Harland et al. (1982). Samples from the southern Ackley Granite Suite give a Lower Carboniferous (Tournaisian-Visean), Rb-Sr age of 353 + 5 Ma (Harland et al., 1982). These dates would indicate that the Ackley Granite Suite is approximately 60 to 80 Ma younger than the Koskaecodde and Mollyguajeck plutons.

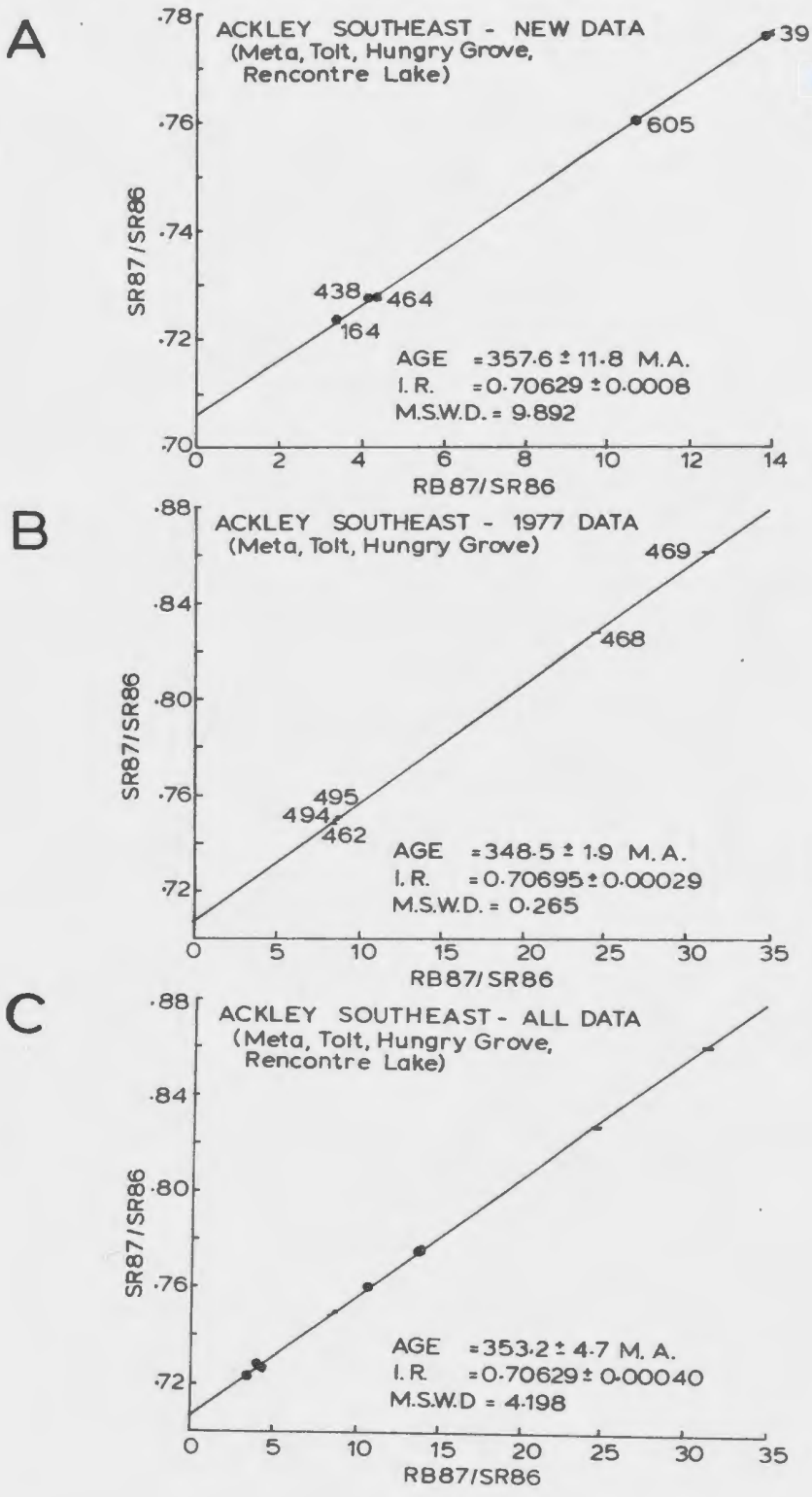

Figure 63: Isochron plots of data from the southeast Ackley Granite Suite.
A: New data from the Meta, Tolt, and Hungry Grove granites.
B: Data from Bell et al., 1977.
C: All data from the southeast Ackley Granite Suite.

The initial $^{87}Sr/^{86}Sr$ ratio of the hornblende-bearing granodiorites is 0.7092 which indicates either a relatively enriched, possible mid-crustal source for these rocks, or alternatively, a large amount of contamination of mantle-derived magma with relatively evolved, radiogenic, crustal material. This value is comparable to that for the Mount Peyton Suite ($^{87}Sr/^{86}Sr$ = 0.7091; Bell et al, 1977) and lies at the higher and younger end of the spectrum of initial ratios presented for the calc-alkaline plutonic rocks of the central Andes (McNutt et al., 1985) and of the Mesozoic plutonic rocks of California (Kistler and Peterman, 1973). These higher ratios occur on the continental or inboard side of the orogen. However, systematic areal variations in Sr-isotope ratios have not been documented for the plutonic rocks in Newfoundland (Strong, 1980).

In the Ackley Granite Suite, the initial ratio of 0.7063 indicates a relatively depleted, possibly lower crustal or upper mantle source for the southern granites. The fact that the data from the southeast granites ($\approx$ 2100 km^2) plot essentially on an isochron, suggests that the Sr-isotopic ratios were homogenized during the magmatic event. This may reflect a homogenous source, or homogenization in a magma chamber in the source region of the granite, or homogenization in the high-level Ackley magma chamber prior to crystallization of the granite. The disturbance, or inhomogeneity of the Rb-Sr system in the Kepenkeck Granite unfortunately prevents comparison of the initial ratios with the rest of the Ackley Granite Suite.

7-4 $^{40}AR/^{39}AR$ GEOCHRONOLOGY

7-4-1 Introduction

Ages were obtained from 8 biotite, 4 muscovite and one hornblende mineral separates, by the total fusion $^{40}Ar/^{39}Ar$ dating technique (Merrihue and Turner, 1966; Dalrymple and Lanphere, 1971). The samples were irradiated together in the reactor at McMaster University, Ontario (see Berger and York, 1979; Archibald et al., 1983) and were fused and analyzed by Dr. D. Kontak (see Kontak, 1985) at Queen's University, Ontario.

7-4-2 Results

The analytical results are presented in Table 18 and Figure 64. The error presented with the data has been calculated to include the error in the J-value in order to compare the data to previous results. The error for the J-value can be omitted for internal comparison of data since all the samples were irradiated together and this results in a reduction of the error in the age date by approximately 50%. The two oldest ages, 410.4 + 4.4 Ma and 392.5 + 7.6 Ma were obtained from magmatic biotites belonging to the Koskaecodde and Mollyguajeck plutons respectively. These ages are significantly older than the ages obtained from the Ackley Granite Suite which range from 378.4 + 4.8 Ma to 366.9 + 3.9 Ma.

Magmatic biotites separated from the Ackley Granite Suite provided the following ages:

Table 18: ^{40}Ar - ^{39}Ar total fusion ages (Refer to Figure 64).

Samp. No.[a]	$(^{40}Ar/^{39}Ar)m^b$	$(^{37}Ar/^{39}Ar)m^b$	$(^{36}Ar/^{39}Ar)c^c$	^{40}Ar rad. (%)	Age ± 2 (Ma)
7040237[b]	16.023	0.00223	0.00558	95.99	368.4 ± 4.2
221168[m]	16.579	0.00355	0.00368	93.82	371.3 ± 4.5
7040214[m]	17.008	0.00486	0.00494	91.71	371.4 ± 5.4
220257[b]	21.881	0.02182	0.01112	70.95	368.8 ± 9.6
220548[b]	16.006	0.00222	0.01800	95.99	367.7 ± 4.3
7040397[m]	16.229	0.00207	0.00027	96.30	373.5 ± 4.0
220664[b]	16.084	0.00258	0.00893	95.38	367.3 ± 4.2
220523[b]	17.691	0.00114	0.03665	98.10	410.4 ± 4.4
220087[b]	15.835	0.00176	0.04718	96.78	366.9 ± 3.9
220087[m]	16.323	0.00158	0.00089	97.17	378.4 ± 4.8
220464[b]	16.473	0.00307	0.09378	94.66	372.3 ± 4.8
220464[m]	16.018	0.00238	4.3112o	97.91	374.7 ± 3.8
220092[b]	17.070	0.00121	0.05326	97.84	392.5 ± 7.6
JL-90-3[b]	20.465	0.00265	0.00317	96.09	451.7
JL-90-2[b]	20.081	0.00209	0.00616	96.84	451.7
JL-90-1[b]	20.619	0.00358	0.00483	94.78	451.7

a b = biotite; m = muscovite; h = hornblende

b measured ratios

c corrected for decay of ^{37}Ar during and after irradiation.

$_{37} = 1.975 \times 10^{-2}$ day $^{-1}$.

J = 0.01455 for all Ackley samples and 0.014 for standard

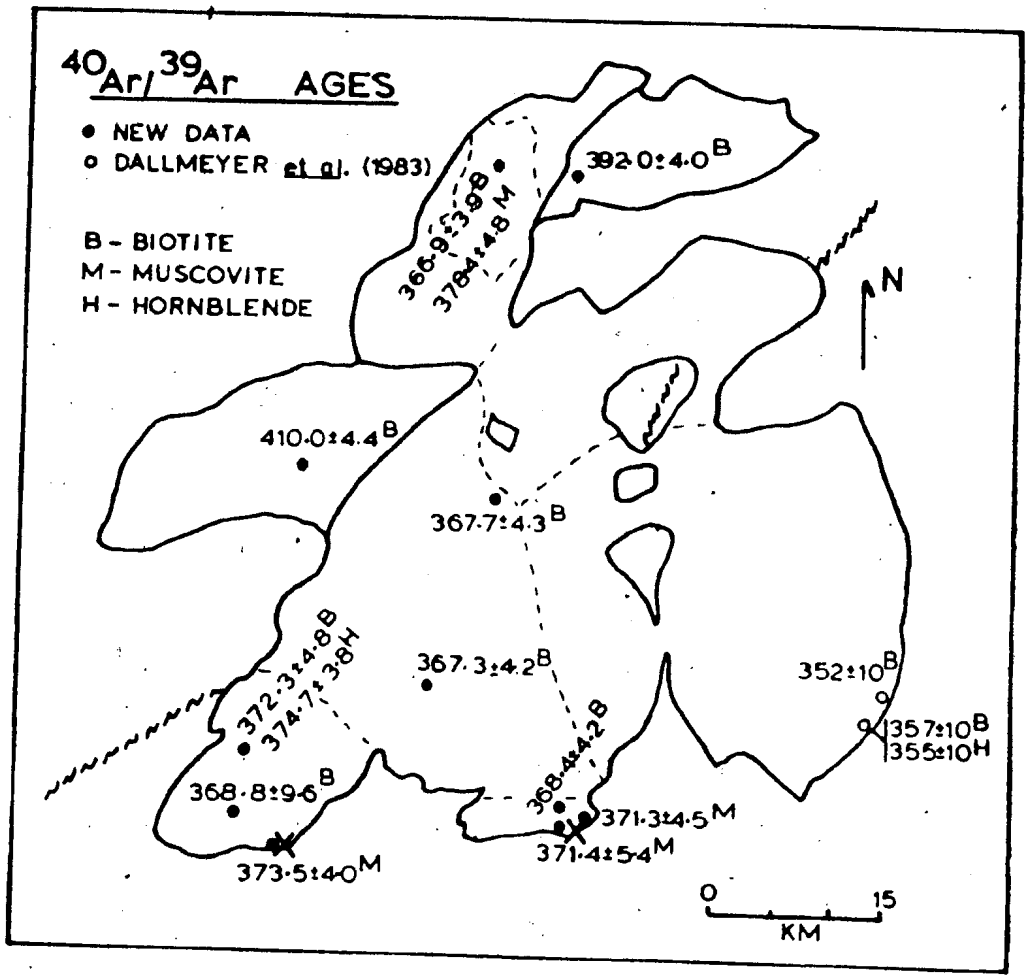

Figure 64: Sample locations, and Ar^{40}-Ar^{39} ages. Dashed lines are internal boundaries of the Ackley Granite Suite.

Kepenkeck Granite	- 366.9 ± 3.9 Ma
Hungry Grove Granite	- 367.7 ± 4.3 Ma
"	- 367.3 ± 4.2 Ma
Sage Pond Granite	- 368.4 ± 4.2 Ma
Rencontre Lake Granite	- 368.8 ± 9.6 Ma
"	- 372.3 ± 4.8 Ma.

These ages are statistically indistinguishable from each other, although ommision of the error for the J value may imply a slightly older age for one sample from the Rencontre Lake Granite. This latter sample also provided an almost identical age of 374.7 ± 3.8 Ma from hornblende.

A muscovite separate was analyzed from the Kepenkeck Granite sample and gave an age of 378.4 + 4.8 Ma, which is significantly older than the age obtained from coexisting biotite. The muscovite may be of primary magmatic origin, although a hydrothermal origin is also possible (see Chapter 3), and the Rb-Sr system is disturbed in this area.

Hydrothermal muscovite from the Ackley City prospect gave an age of 373.5 + 4.0 Ma. Hydrothermal muscovite from quartz-topaz greisen at the Anesty prospect and from an outcrop located 1 km east of the Anesty prospect, gave almost identical ages of 371.4 + 5.4 Ma and 371.3 + 4.5 Ma respectively. These ages are again indistinguishable from each other and from the ages of the magmatic minerals in their host rocks.

All of the above data demonstrate that the Ackley Granite Suite and its contained mineralization are contemporaneous. The similar ages from

the hornblende-biotite pair in the Rencontre Lake Granite and from the hydrothermal muscovite indicate very rapid cooling in this area since the closing temperatures of these minerals ranges from 500 to less than 300°C (Purdy and Jager, 1976; Jager, 1979; Harrison and McDougall, 1980; Harrison, 1981). Rapid cooling of the eastern part of the Tolt Granite was also indicated by the mineral ages obtained by Dallmeyer et al. (1983). In contrast, there is a slight discordance in ages between coexisting muscovite and biotite in the Kepenkeck Granite (378 and 367 Ma respectively). The different argon blocking temperatures for muscovite (ca. 350°C) and biotite (250-300°C) possibly indicate a slower rate of cooling of 5°C/Ma.

7-4-3 Discussion of $^{40}Ar/^{39}Ar$ Data

The ages of ~410 and 392 Ma obtained from the Kepenkeck and Mollyguajeck plutons suggest that emplacement and crystallization of these granitoids occurred in the Late Silurian to Early Devonian, (time scale of Harland et al. 1982). These ages must be considered as minimum dates since partial degassing of the minerals in response to the intrusion of the younger Ackley Granite Suite may have occurred. The Upper Silurian age of 410 + 4.4 Ma may be a better approximation of the earlier event since it is further removed from the later granites. This age is in agreement with the Rb-Sr whole rock isochron age of 427 + 12 Ma obtained from the same plutons, and both ages support the geochemical and petrological evidence which differentiates these granitoids from the Ackley Granite Suite.

The Ackley Granite Suite gives Middle-Late Devonian ages (Harland et al., 1982) of 369 to 378 Ma. Discordant muscovite-biotite ages in the Kepenkeck Granite give an indicated cooling rate of 5°C/Ma and suggest a relatively deeper level of intrusion (and hence slower cooling) in this area. In contrast, hornblende-biotite pairs indicate rapid cooling and thus high level of emplacement of the Rencontre Lake and Tolt granites. This rapid cooling in the south is consistent with the textural evidence (variable fine to coarse grain size, miarolitic cavities, aplite). The data suggest that cooling through the biotite blocking temperature was essentially 'instantaneous' in the Ackley Granite Suite and the rapid cooling may suggest that magma emplacement and crystallization occurred during a relatively short time span. This short time span is unlikely to exceed the range in the observed ages of 5 million years since there would probably be a greater age-variation due to differences in cooling history and crystallization of granite if the magma was maintained at high crustal levels for longer periods of time.

The Rb-Sr isotopic system in the Kepenkeck Granite appears to have been disturbed, which may also indicate that the $^{40}Ar/^{39}Ar$ system in the granite was disturbed. Consequently, it is entirely possible that the $^{40}Ar/^{39}Ar$ ages of 366 and 378 Ma in the Kepenkeck Granite reflect a high temperature hydrothermal event related to emplacement of the other granites of the Ackley Granite Suite. However, the gravity data (Fig. 3) suggest that the Kepenkeck Granite is contiguous with the rest of the Ackley Granite Suite; lacking further information, the $^{40}Ar/^{39}Ar$ ages are tentatively interpreted to represent post-intrusive cooling ages.

The similar ages obtained from the Ackley Granite Suite and its contained mineralization are in agreement with the magmatic associations proposed for the genesis of these deposits (Whalen, 1976, 1980, 1983; Dickson, 1983; Tuach, 1984a) and temporally confirm the physical correlation of lithogeochemical trends and mineralization. The hydrothermal systems responsible for the alteration and mineralization were relatively short-lived compared to those systems documented in the Cornubian batholith (Halliday, 1980; Jackson et al., 1982; Bray and Spooner, 1983). In the Cornubian batholith, it is possible that long lived hydrothermal system, overprinted mineralization and devolatification textures related to magma crystallization.

7-5 PREVIOUS AND NEW AGES - A COMPARISON

The $^{40}Ar/^{39}Ar$ ages of the Ackley Granite Suite (369-378 Ma) are at or above the limits of overlap in error with the previously published ages of 355 + 10 Ma (Bell et al., 1977; Dallmeyer et al., 1983) and are older than the Rb-Sr ages reported above. These features may be significant and may indicate a protracted low temperature cooling history such that the Rb-Sr system closed approximately 15 Ma later than the $^{40}Ar/^{39}Ar$ system. This interpretation implies that subsolidus recrystallization of alkali feldspar continued to low temperatures in the presence of aqueous fluids. It is possible, but considered unlikely, that the low temperature ($< 250°C$) hydrothermal event relates to a magmatism around 355 Ma, as suggested by the $^{40}Ar/^{39}Ar$ ages from the eastern part of the Tolt Granite.

The ages presented in this thesis are in agreement with the K-Ar age of 405 ± 17 Ma (Wanless et al., 1972) obtained from biotite from Koskaecodde Pluton (and the new ages from the Ackley Granite Suite are within the large error-range of the K-Ar ages presented by Lowden (1961), and Leech et al. (1963). The K-Ar age of 338 + 7 Ma presented by Whalen (1980) is significantly younger than the new $^{40}Ar/^{39}Ar$ ages and, assuming the data are valid, may indicate a later low temperature event involving either fluid activity or argon loss.

CHAPTER 8 OXYGEN ISOTOPES

8-1 INTRODUCTION

The application of oxygen isotope data to the study of granitic rocks and associated hydrothermal mineral deposits has been reviewed by Taylor (1978, 1979). Information can be obtained from these data about the possible source of the granitic magma, the extent of subsolidus silicate-fluid reactions during cooling of the pluton and the nature of the fluid involved in these subsolidus reactions. Oxygen isotope data are particularly useful in evaluating the extent of magmatic versus meteoric fluid involvement in mineralizing systems. Additional information may be obtained concerning the evolutionary history of these mineralizing fluids and the temperatures of mineral deposition. The objectives of this study were to investigate possible magma-source variations, and to delineate the nature and extent of subsolidus fluid interaction with the granites with special reference to the mineralized areas.

Twenty three whole rock samples from throughout the study area were analyzed for oxygen isotope composition, and quartz and feldspar mineral separates were analyzed from 17 of those samples. These samples were selected to test for possible variation due to source-signature and large scale subsolidus reactions. Composite samples of the Gander and Avalon terranes were also prepared and analyzed in order to test for isotopic inter-relationships between host rock and granite. Two samples of miarolitic quartz were analyzed to evaluate possible variations in

oxygen isotope composition between quartz in the host granite and quartz precipitated from hydrothermal fluids in the miarolitic cavities. Thirty seven mineral separates were obtained and analyzed from 9 samples from the prospects to investigate the fluid regimes involved in mineralization.

The analyses were performed by Dr. R. Kerrich at the University of Western Ontario. Details on sample preparation, analytical method, accuracy and precision are summarized in Appendix B.

8-2 REGIONAL ^{18}O VARIATION

8-2-1 Results

The data are presented in Table 19. In general, granitoids in the northwest are characterized by higher $\delta\,^{18}O$ whole-rock than the granites in the southeast (Fig. 65A). However, data in Table 19 reveal that some quartz-feldspar (q-f) fractionations are disturbed from the primary magmatic trend given by Δ q-f = + 1.0 ± 0.5 per mil (Fig. 66A), indicating that the whole rock values are the result of primary magmatic and secondary subsolidus signatures. Quartz is resistant to oxygen isotope exchange at temperatures of less than 600°C, whereas feldspars readily undergo retrograde isotopic re-equilibration down to 150°C (Clayton et al., 1968; Taylor and Forrester, 1979; Criss and Taylor, 1983; Giletti and Yund, 1984). Accordingly, $\delta\,^{18}O$ quartz is used as an estimator of primary whole rock composition, where $\delta\,^{18}O_{wr} = \delta\,^{18}O$ quartz - 1 (cf. Taylor, 1968). This approach is endorsed by the observation that quartz $\delta\,^{18}O$ values cluster tightly within individual

Table 19: The Oxygen isotope composition of whole rocks and mineral separates.

Unit Description	Sample Number	wt.% SiO_2	$\delta^{18}O$ wr	$\delta^{18}O$ qz	$\delta^{18}O$ ksp	$\delta^{18}O$ mu	$\delta^{18}O$ bi/ch	q-k	q-mu	q-bi
Koakaecodde										
Granite	506	74.6	8.6	10.6	8.3			+2.3		
Granite	523	69.4	10.0	10.7	9.8			+0.9		
Granite	697	65.0	9.7	10.5	9.8			+0.7		
Granite	701	60.3	9.3	-						
Kepenkeck										
Granite	178	75.5	9.1	9.5	8.2			+1.3		
Granite	84	73.4	9.2	9.8	8.3			+1.5		
Granite	89	70.7	8.6	9.1	7.8			+1.3		
Tolt										
Granite	363	97.8	7.8	7.3	7.7			-0.4		
Granite	268	74.7								
Granite	397	73.4	8.1							
Granite	23	69.3	5.9	9.0	6.3			+2.7		
Microlitic Quartz	370			7.4						
Hungry Grove										
Granite	732	79.3	8.1	7.9	8.6			-0.7		
Granite	268	74.7	9.4	8.6	10.0			-1.4		
Granite	438	73.1	10.1	8.9	12.2			-2.3		
Granite	443	71.4	8.2	8.5	7.9			+0.6		
Microlitic Quartz	450			8.0						
Meta										
Granite	111	79.8	9.3							
Granite	187	72.1	7.9	8.3	8.0			+0.3		
Granite	188	69.8	8.3	8.8	8.2			+0.6		
Rencontre Lake										
Granite	252	78.2	7.1							
Granite	605	75.9	6.5	5.8	7.5			-1.7		
Granite	604	74.8	6.6							
Granite	266	70.3	6.1	6.7	5.5		1.4ch	+1.2		5.3
Granite-AC	369*	-	7.0	7.2	6.9	5.5	1.7bi	+0.3	1.7	5.5
Pematite-AC	361*	-	6.6	7.6	6.2			+1.4		
Aplite±Mo-AC	344A*	-	5.8	6.9	5.0	1.9	3.0ch	+1.9	5.0	
Mu-greisen±Mo-A	349*	-	-	6.2	4.4	2.8		+1.8	3.4	
Stockwork py-WH.	378A*	-	-	8.3	5.2	3.8		+3.1	4.5	
Pegmatite-CC	461*	-	5.6	6.8	4.8			+2.0		

Table 19: (Cont.d)

Unit Description	Sample Number	wt.% SiO_2	$\delta^{18}O$ wr	$\delta^{18}O$ qz	$\delta^{18}O$ ksp	$\delta^{18}O$ mu	$\delta^{18}O$ bi/ch	q-k	q-mu	q-bi
Sage Pond										
Granite (regional)	716	77.8	8.6							
	332	75.8	8.3	8.5	8.1		3.5bi	-0.2		5.0
Granite-E	284*		6.3	6.4	6.0	3.5m[1]	1.9bi	+0.4		2.9
						2.9m[2]				3.5
Topaz greisen-E (900 ppm Sn)	170*		6.3	6.4		4.9m[1]				1.2
						2.9m[2]				3.2
Topaz greisen-AR (1 ppm Sn)	220*			7.9		4.5m[1]				3.4
						4.0m[3]				3.9
Gander Composites										
Regional	G1		12.6							
Marginal	G2		9.3							
Roof Pendant	G3		7.2							
Deformed Intrusives	G4		8.7							
Avalon Composites										
Metasediment	A1		4.7							
Roof Pendants	A2		5.6							
Volcanic	A3		4.5							

wr - whole rock; qz - quartz; ksp - alkali feldspar; mu - muscovite; bi - biotite; chl - chlorite; Mo - molybdenite; Sn - tin; AC - Ackley City prospect; WH - Wylie Hill prospect; CC - Crow Cliff prospect; E - Esso prospect; AR - Aneaty Ridge; G - granite sample.

Samples with an * were collected by J. Tuach in 1983; the other samples are from the regional collection of Dickson (1983).

See text for explanation of superscripts in muscovite column.

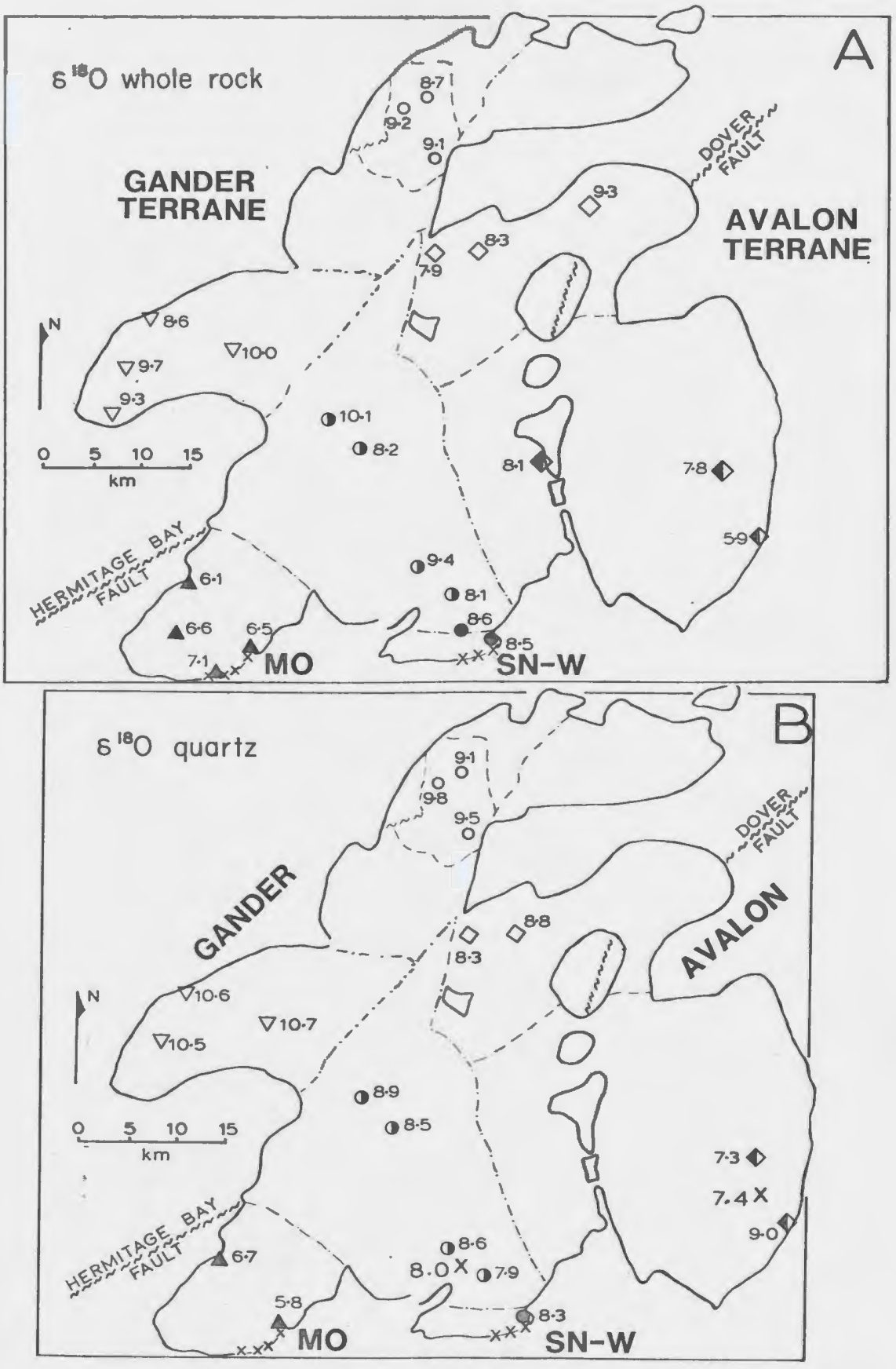

Figure 65: Oxygen isotope compositions of granite samples. Symbols as on Figure 17 or Figure 63.
A: Whole Rock.
B: Quartz. x - miarolitic quartz.

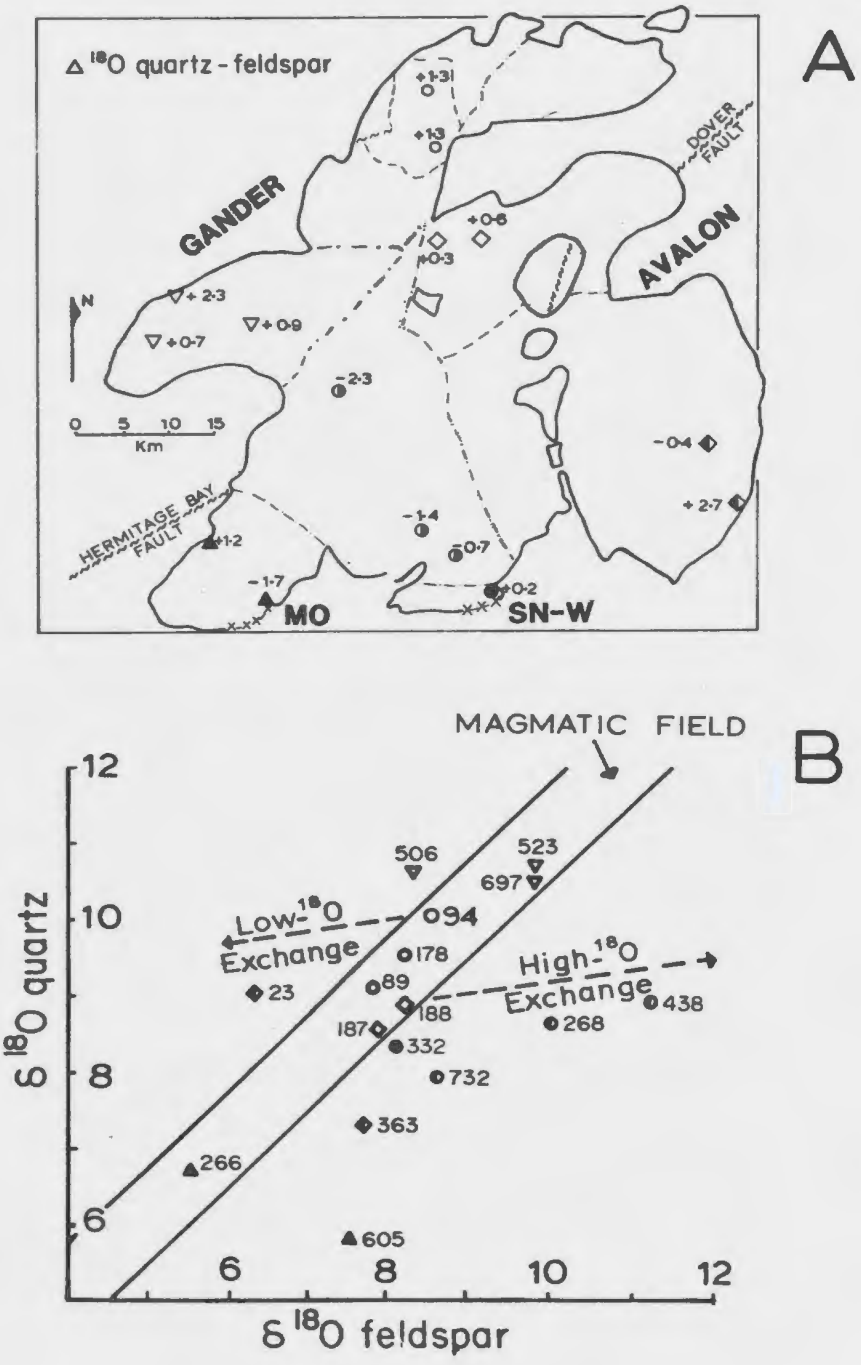

Figure 66: A: Oxygen isotope fractionation between quartz and feldspar.
B: Plot of the oxygen isotope compositions of coexisting quartz and feldspar.

lithological units whereas whole rock and feldspar are more dispersed, reflecting excursions about the magmatic quartz-feldspar trend (Fig. 66).

The Koskaecodde Pluton has $\delta^{18}O$ quartz = 10.6 ± 0.1 (1σ) and these are the highest values in the granitoids from the study area. The Ackley Granite Suite has average $\delta^{18}O$ quartz values (per mil; 1σ) as follows:

Kepenkeck	-	9.5 ± 0.3
Meta	-	8.5 ± 0.3
Tolt	-	8.1 ± 1.2
Hungry Grove	-	8.5 ± 0.5
Sage Pond (Sn-bearing)	-	8.5 ± 0.3
Rencontre Lake (Mo- bearing)	-	6.2 ± 0.6

The Kepenkeck Granite has the highest $\delta^{18}O$ quartz in the Ackley Granite Suite. The $\delta^{18}O$ quartz values from the Hungry Grove, Sage Pond and Meta granites can be considered to be isotopically homogeneous, with no significant inter-unit variations. The Rencontre Lake Granite has significantly lower $\delta^{18}O$ quartz (per mil) composition. Thus the estimated $\delta^{18}O$ whole rock compositions are as follows:

Koskaecodde	-	9.1
Kepenkeck	-	8.5
Hungry Grove, Meta, Tolt, and Sage Pond granites	-	7.5
Rencontre Lake	-	5.2

The composite of metasedimentary rocks from the Gander Terrane collected from the Trans Canada Highway is considered to be representative of the regional Gander Terrane rocks and possesses a whole rock oxygen isotope composition of 12.6 per mil. The composite of samples peripheral to the granitoids of the study area has an oxygen isotope composition of 9.3 per mil and the composite of samples of Gander Terrane rocks in roof pendants in the Ackley Granite Suite has a value of 7.3 per mil. (Table 19). The trend to lower $\delta^{18}O$ is ascribed to the incursion of ^{18}O-depleted meteoric waters accompanying intrusion of the plutons in the study area. In contrast, the Avalon Terrane is characterized by uniformly low $\delta^{18}O$, with peripheral metasedimentary composites 4.7 per mil, peripheral metavolcanics 4.5 per mil, and roof pendants 5.6 per mil (Table 19). A reconnaisance study of quartz-feldspar on rocks from within the Avalon Terrane has failed to identify significant fractionations (R. Kerrich, personal communication, 1985) and this low $\delta^{18}O$ signature is interpreted to be an inherent feature of Avalon Terrane rocks.

A composite of deformed granitoid intrusive rocks from the Eastern Meelpaeg and North West Brook complexes (Table 19) has a $\delta^{18}O$ whole rock value of 8.7 per mil, within the range of isotopically "normal" felsic plutonic rocks (cf. Taylor, 1978). This value is slightly higher than the value for the Gander Terrane lithologies in roof pendants.

Most samples from the study area plot in the field of normal granites on Figure 66B. Two samples (23 and 506) located near the margin of the plutonic rocks in the study area have relatively large positive

quartz-feldspar values and are displaced to the left of the magmatic field. Many of the samples from the southeastern Ackley Granite Suite have negative $\Delta^{18}O$ quartz-feldspar values and are displaced to the right of the magmatic field. In addition, there is an apparent trend of increasingly negative $\Delta^{18}O$ quartz-feldspar values from the area of tin mineralization in the Sage Pond Granite, towards the northern part of the Hungry Grove Granite (Fig. 66).

8-2-2 Source as Indicated by ^{18}O Variation

In the magmatic environment, the variability of $\delta^{18}O$ value of primary melts is thought to reflect the oxygen isotope composition of source regions due to the low magnitude of inter-mineral or mineral-melt fractionations at elevated temperatures. Melts originating in the mantle tend to possess tightly constrained primary compositions reflecting mantle uniformity with respect to $\delta^{18}O$ (Taylor, 1968; Kyser et al., 1981, 1982), whereas those generated in crustal regions dominated by metasedimentary or altered volcanic rocks may acquire elevated values due to prior interaction of source rocks with the hydrosphere. Taylor (1978) suggests that normal granites have $6 \leq {}^{18}O$ whole rock ≤ 10 and that values in excess of 8 per mil require a crustal component in the source region. Consequently, most of the samples are within the range of normal granites. The estimated whole rock values for the Koskaecodde Pluton (9.1 per mil) and the Kepenkeck Granite (8.5 per mil) are indicative of a significant crustal component in the genesis of these granites. In contrast, the estimated whole rock $\delta^{18}O$ value for the Hungry Grove, Meta, Tolt, and Sage Pond Granites (7.5 per mil)

indicates derivation of these rocks from a crustal igneous source which has not interacted with the hydrosphere, or from a mantle source.

The Koskaecodde Pluton exhibits petrographic and chemical features of I-type plutons, yet its oxygen isotope signature is that of a crustally derived S-type pluton (O'Neil and Chappell, 1977). The relative oxygen isotope signatures of the more aluminous Kepenkeck Granite and the rest of the Ackley Granite Suite conform to the normal relationships between oxygen isotopes and chemical-source parameters as described by O'Neil and Chappell (1977).

Magmatic processes have been recognized to increase primary $\delta^{18}O$ values by as much as 1.3 per mil during differentiation (Taylor, 1978; Muehlenbachs and Byerly, 1982). The data from the Ackley Granite Suite are from evolved granitic bodies. Therefore, the oxygen isotope compositional differences between the Kepenkeck Granite and the other granites cannot be related to such a process. In addition, the $\delta^{18}O$ values from the less evolved Koskaecodde Pluton are higher, indicating real differences in source-signature.

The Rencontre Lake Granite has an estimated magmatic whole rock value of $\delta^{18}O = 5.2$. This estimate is below the normal field of magmatic rocks (Taylor, 1978). Low- $\delta^{18}O$ volcanic rocks have been described by Hildreth et al. (1984) from the Yellowstone Plateau Volcanic Field. These low values were ascribed to the magmatic assimilation of meteoric waters during caldera collapse prior to final emplacement and crystallization of the volcanic rocks.

Alternatively, assimilation of low- $\delta^{18}O$ country rocks at the magmatic stage may result in low- $\delta^{18}O$ magmatic values (Taylor, 1978). Depletion by assimilation of country rock with an measured whole rock values of 4.7 and 5.6 per mil (Avalon composites), from an estimated 'normal' value of 7.5, to a value of 5.2 per mil would require total melting of the intruded rock with only minor primary magmatic input. Comparison of major and trace element data from the Rencontre Lake Granite and its host rocks does not suggest extensive assimilation. The mechanism of lowering the $\delta^{18}O$ value in the Rencontre Lake Granite by assimilation of meteoric water during eruption and caldera collapse is preferred. The tight grouping of $\delta^{18}O$ quartz within individual granitoid units throughout the study area also argues against high-level assimilation or melting of the country rock.

Within the Ackley Granite Suite, the isotopically heavier Kepenkeck Granite ($\delta^{18}O$ = 8.5 per mil) intruded the higher- ^{18}O Gander Terrane ($\delta^{18}O$ = 9.3 to 12.6), whereas the rest of the Ackley Granite Suite, possessing lower $\delta^{18}O$ occurs predominantly within the relatively lower- ^{18}O Avalon Terrane. This relationship raises the possibility that the Kepenkeck Granite and the remainder of the Ackley Granite Suite inherited their isotopic (and chemical) characteristics from partial melts of material isotopically comparable to the Gander and Avalon terranes respectively. The high $\delta^{18}O$-signature of the Koskaecodde Pluton would likewise suggest a Gander Terrane source.

The analyses of the composite samples provides the best available estimator of bulk $\delta^{18}O$ for specified lithologies of the two terranes.

Such values may not be representative of equivalent rocks at greater depth and may also have been modified by isotopic exchange with near surface meteoric waters accompanying granite intrusion.

The value of $\delta^{18}O = 12.6$ obtained from the regional composite of Gander metasediments is within the range of isotope composition for metasediments. However, both metasediments and metavolcanics of the Avalon Terrane have extremely low $\delta^{18}O$ relative to any plausible primary precursors and it is clear that these lithologies have experienced a history of $\delta^{18}O$ depletion. Quartz and feldspar fractionations in Avalon rocks do not indicate exchange with an external low-^{18}O aqueous reservoir, and accordingly, it is likely that the ^{18}O-depleted character of the Avalon Terrane existed prior to intrusion of the Ackley Granite Suite. This low signature may be related to Precambrian Pan-African intrusive activity, a deduction supported by the observation that the granite itself, specifically the eastern domain, does not record significant negative Δ quartz-feldspar.

Although there is a general correspondence between $\delta^{18}O$ of the granitoid rocks and the terranes which they intruded, the source-magma fractionation would be -0.3 to -3.6 per mil for the Gander Terrane, as against +2.4 per mil for the Avalon Terrane (Table 18). The gross correspondence of $\delta^{18}O$ granite with source terrane may signify a source rock control on magma compositions. However, the differences in sign and scale of source-magma fractionations imply that the estimated terrane values are unreliable and the most likely source of error is the estimated low $\delta^{18}O$ for the Avalon Terrane.

This study has been orientated towards identifying an 'Avalon' isotopic signature in the southeastern Ackley Granite Suite. The arguments presented above do not preclude the possibility that the granites of the Ackley Granite Suite with $\delta^{18}O$ between 6 and 8 per mil originated from a mantle source.

8-2-3 Regional Subsolidus Fluids

It has been shown that for most igneous rocks emplaced within 7-10 km of the terrestrial surface, oxygen isotope exchange occurs during incursion of external fluid reservoirs, which act to disturb the primary magmatic signatures. (Taylor, 1968, 1978; Taylor and Forrester, 1979; Gregory and Taylor, 1981; Criss and Taylor, 1983). In general, low-^{18}O meteoric waters tend to deplete magmatic rocks relative to primary values, whereas evolved formation brines or marine waters at low temperatures (Wenner and Taylor, 1976) and subsolidus exchange with CO_2 (Higgins and Kerrich, 1982) shift rocks to higher- $\delta^{18}O$ values. Feldspar is preferentially exchanged relative to quartz, and departures from magmatic quartz-feldspar fractionations of $+1.0 \pm 0.5$ per mil indicate subsolidus exchange with external fluid reservoirs.

The samples from the Koskaecodde Pluton and from the Kepenkeck Granite plot in the field of magmatic values on Figure 69. Consequently, possible subsolidus interaction of fluids with an extraneous oxygen isotope reservoir cannot be recognized. Both of these units exhibit abundant textural and petrographic evidence for subsolidus reactions. The fluids responsible for these alterations may therefore have been of

magmatic origin, as opposed to low to intermediate temperature meteoric fluids. In addition, the lack of evidence for low temperature fluid interaction may indicate a relatively deep level of emplacement in the crust, below the level of extensive, meteoric, hydrothermal activity.

In the southern Ackley Granite Suite, quartz in miarolitic cavities has a $\delta^{18}O$ close to that of quartz in contiguous granite (Fig. 65B). This indicates that crystallization of the miarolitic quartz occurred at near-solidus temperatures in the presence of magmatic fluids exsolved from the granite. A corollory to the correspondence of $\delta^{18}O$ quartz from cavities and granite is that participation of a significant component of an external aqueous reservoir in miarolitic growth can be ruled out.

Sample 506 from the Koskaecodde Pluton and sample 23 from the Tolt Granite are located within 50 meters of the external intrusive contact and are shifted to the left of the magmatic field. This feature is interpreted to result from exchange with an external reservoir of low-^{18}O meteoric water during cooling of the Granites.

In the southeastern granites, most samples are shifted to the right of the magmatic trend, by up to + 4 per mil. This shift is evident throughout the Tolt and Hungry Grove granites, as well as in all rocks analyzed from the Sage Pond Granite, and in one of two samples from the Rencontre Lake Granite (Fig. 65B). Shifts to the right of the magmatic trend are attributed to exchange with a relatively restricted volume of meteroic fluid which collapsed into the carapace of the cooling

granite (very low water/rock ratio). These fluids became increasingly enriched in $\delta^{18}O$ due to progressive exchange with the granite as they penetrated deeper into the carapace. The observed maximum shift to the right of the magmatic trend occurs in sample 438 which has a $\delta^{18}O$ feldspar value of 11.2 per mil. This value may have been generated by exchange of feldspar with a fluid ranging in composition from $\delta^{18}O$ = + 4 at 250°C to $\delta^{18}O$ = - 2 at 150°C. Alternatively, low temperature fluids of magmatic ongin may be derived from depth.

A halo of secondary muscovite (Fig. 13), and an increase in coarseness and amount of perthite occurs towards the southern contact at Sage Pond. These features could be interpreted to result from interaction of the carapace with an encroaching meteoric system but the observed quartz-feldspar fractionations are opposite to those expected. Enrichment of feldspar relative to quartz may also indicate the presence of a saline aqueous reservoir. However, this conflicts with the interpretated presence of a non-saline depleted meteoric reservoir responsible for regional depletions in the Gander Terrane and in the margins of the granites. Alternatively, the shifts to the right of the magmatic trend could by ascribed to preferential subsolidus exchange with heavier- $\delta^{18}O$ fluids such as CO_2. For example Allard (1979) presented $\delta^{18}O$-CO_2 values in gases emitted from a volcanic fissure of 7.8 to 8.2 per mil and values of 15.9 to 20.8 per mil in gas exsolved from lava flows. These high positive $\delta^{18}O$ values would permit high temperature exchange at low fluid/rock ratios and would require passage of a flux of CO_2 through the granite from deeper in the crust, or from the mantle. There is little evidence to support this suggestion.

The wide range of observed shifts in $\delta^{18}O$ feldspar throughout the granite is in common with other studied examples of granitic rocks that have experienced variable degrees of exchange with aqueous fluids (Taylor, 1971; Wenner and Taylor, 1976).

8-3 ^{18}O VARIATION IN MINERALIZED AREAS

8-3-1 Results

The data from the mineralized areas are summarized in Figure 67 and listed in Table 19. Data are presented (Fig. 67) from both the Rencontre Lake Granite which is described as a molybdenite mineralizing system and from the southern Hungry Grove and Sage Pond granites, described as a tin mineralizing system. Within the two mineralized areas or systems, the data from the regional granites is plotted on the left and data from mineralized and/or altered samples is plotted on the right. This arrangement permits rapid comparison of the oxygen isotope signatures between, and within the mineralizing systems.

8-3-1-1 Rencontre Lake Area: The $\delta^{18}O$ quartz values of 5.2 to 7.6 per mil at the molybdenite prospects (Fig. 67A) are comparable to those in the host-Rencontre Lake Granite (5.8 to 6.7 per mil). These estimated initial whole rock $\delta^{18}O$ values are at the lower limit of, or below, normal magmatic values (Taylor, 1978).

Sample 369 of granite from the Ackley City molybdenite prospect, plots in the field of magmatic quartz-feldspar fractionation (Fig. 67B) along with regional sample 266. Samples 349 (coarse muscovite greisen)

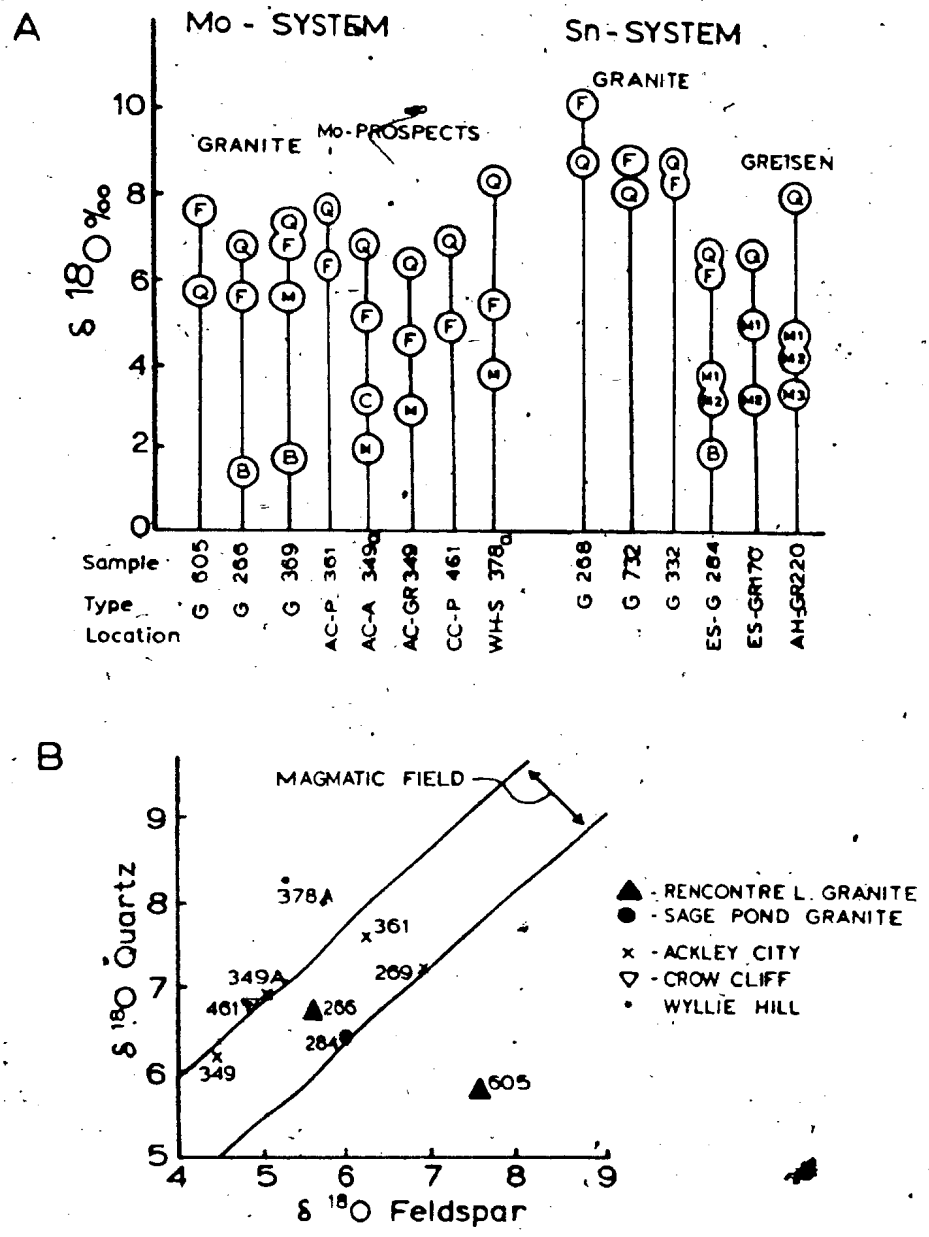

Figure 67: Oxygen isotope composition of silicates from the Rencontre Lake and Sage Pond areas.
A: Comparison of data from prospects to data from host granites.
B: Plot of the oxygen isotope compositions of coexisting quartz and feldspar.

and 361 (pegmatite) from the Ackley City prospect also plot in magmatic trend (Fig. 67B). Sample 461 of pegmatite from the Crow Cliff prospect and sample 349A of aplite from the Ackley City prospect plot slightly to the left of the magmatic trend indicating minor exchange with low- $\delta^{18}O$ fluids. Sample 378A from the Wyllie Hill prospect is a sericitized, fine grained granite containing stockwork mineralization and has a Δquartz-feldspar value = 3.1 per mil.

In the Rencontre Lake Granite, the Δ feldspar-biotite values of 5.3 and 5.5 per mil from samples 266 and 369 respectively, indicate temperatures of biotite crystallization in excess of 700°C, assuming equilibrium. The Δ quartz-muscovite value of 1.7 per mil from sample 369 also indicates a temperature of crystallization in excess of 700°C.

Samples 349A, 378A, and 461 plot to the left of the field of magmatic Δ quartz-feldspar (Fig. 67B), indicating reaction of the samples with low- $\delta^{18}O$ fluids. Therefore, fractionations between quartz and other mineral species in these samples do not represent temperatures of equilibrium crystallization. Neither is there any indication of equilibration between feldspar and muscovite. The indicated equilibrium temperature for Δ quartz-muscovite from sample 349 is around 460°C, but the indicated equilibrium temperature for Δ feldspar-muscovite is 250 to 270°C, again suggesting disequilibrium in the sample. Therefore, while the relatively high $\delta^{18}O$ values from muscovite and biotite suggest moderate to high crystallization temperatures in the mineralized areas, they do not provide reliable temperature estimates.

8-3-1-2 Sage Pond Area: Sample 284 (granite collected from drill core at the Esso prospect) plots in the magmatic quartz-feldspar field (Fig. 67, and sample 284 and 170 (greisens) from the Esso prospect are depleted by 1.5 to 2.2 per mil relative to other greisen samples and to regional samples from the Sage Pond Granite.

Two varieties of muscovite were separated from samples 284 and 170 and three different muscovites were obtained from sample 220. The fractionations of quartz-M1, quartz-M2 and quartz-M3, assuming equilibrium, may relate to temperature and compositional variables.

In the Sage Pond Granite, sample 332 is displaced to the right of the magmatic quartz-feldspar trend (Fig. 66B) indicating that the observed mineral fractionations may not represent magmatic equilibrium values. The quartz-biotite fractionation indicates a crystallization temperature in excess of 700°C. A comparable high temperature is indicated from sample 284 by the quartz-biotite value of 5.4 per mil, but Δ quartz-muscovite (two separate varieties of muscovite) indicate temperatures of 520 and 455°C and Δ feldspar-muscovite indicates temperatures around 150°C. Therefore, the mineral assemblages present are not equilibrium assemblages.

The presence of equilibrium assemblages cannot be established in samples 170 and 220 of quartz-topaz greisen. However, quartz-muscovite fractionations give temperature estimates from 370°C (M2, sample 220) to 490°C (M2, sample 170), with one muscovite variety (M1, sample 284) indicating an unlikely temperature in excess of 800°C.

8-3-2 Discussion of ^{18}O Variation in Mineralized Areas

In the Rencontre Lake area, the estimated $\delta^{18}O$ whole rock and mineral fractionation values between quartz, feldspar, biotite, chlorite and muscovite, indicate that the bulk of the mineralizing fluids were derived from a magmatic reservoir at high temperatures. The $\delta^{18}O$ quartz values indicate that both the host granite and the rocks at the prospects equilibrated with the same magmatic reservoir. Sample 378A shows evidence of low temperature alteration with an external low- $\delta^{18}O$ aqueous reservoir and this agrees with the observations that the Wyllie Hill prospect has low-temperature 'porphyry' affinities. Smaller shifts to the left of the magmatic trend exhibited by samples 461 and 349A also indicate minor exchange with low- $\delta^{18}O$ fluids.

Comparable high temperature fluids are indicated in the Sage Pond area. However, the prospects have relatively lower estimated $\delta^{18}O$ values compared to the regional granite samples, indicating that high temperature incursion of low- ^{18}O meteoric fluids may have occurred. Equilibrium conditions for oxygen isotope exchange between the different mineral species were not established in many samples and estimated temperatures probably represent minimum values.

The data from the prospects do not indicate extensive involvement of low temperature ($< 300°C$) meteoric fluids in the genesis of the mineralizing systems (cf. Taylor, 1979), a feature in agreement with available data from other comparable systems. For example, the estimated $\delta^{18}O$ whole rock values for granites associated with Climax-type

deposits range from 8.2 to 8.8 per mil (Stein and Hannah, 1985) and are heavier than estimated values of 6.9 to 7.6 per mil from the Hungry Grove and Sage Pond granites, and distinctly heavier than estimated values of 5.1 to 6.1 per mil in the Rencontre Lake Granite. Devono-Carboniferous plutons associated with mineralization in the Mount Pleasant area of New Brunswick have $\delta^{18}O$ whole rock values ranging from 8.0 to 8.9 per mil (Taylor et al., 1985).

CHAPTER 9 - FLUID INCLUSION STUDIES

9-1 INTRODUCTION

Roedder (1979, 1984), Eadington and Wilkins (1980) and Hollister and Crawford (1981) have recently reviewed the techniques and problems involved in the study of fluid inclusions, including the application of these techniques to the identification of ore forming fluids and the physical conditions of mineral deposition.

In the Ackley Granite Suite, fluid inclusions are abundant in quartz-topaz greisen, quartz veins, pegmatites, and in miarolitic cavities. However, most inclusions are less than 10 micrometers in diameter and consequently are rarely suitable for detailed study (and photography). In particular, the small size made determination of phase-changes during freezing runs difficult to impossible. Nevertheless, some conclusions as to the nature of the subsolidus and mineralizing fluids in the Ackley Granite Suite are offered which may serve as a basis for more detailed studies.

A total of 83 polished thin sections were examined and 40 were found to have suitable inclusions to permit heating and freezing studies. A description of techniques and equipement is presented in Appendix B. A brief description of samples and a summary of the data obtained are presented in Appendix G.

9-2 RESULTS

9-2-1 Regional Samples

Fluid inclusions from quartz crystals in miarolitic cavities were studied in several samples from the southern parts of the Ackley Granite Suite (Fig. 68). Most inclusions were less than 10 micrometers in diameter. Nevertheless, many of these inclusions appear to be of primary origin and consist predominantly of liquid and 10-20% vapour (L+V), co-existing with vapour-only (V) inclusions.

Several large L+V inclusions with a uniform proportion of 20% V were observed in a beryl crystal from a small quartz pocket (30 cm * 10 cm) approximately 2 km southeast of Big Blue Hill Pond (Fig. 68). In addition, several samples of quartz vein material from the Franks Pond molybdenum occurrence located approximately 5 km north of Rencontre Lake (Fig. 68) contain two-phase L+V inclusions.

Heating-freezing studies were performed on 14 inclusions and heating-only on another 36 inclusions from these regional samples. Only 4 samples from miarolitic quartz permitted heating-freezing studies and an additional 4 samples were subject to heating studies.

Homogenization temperatures ranged from less than 70 up to 410°C (Fig. 69), with a possible mode in the range at 340 to 390°C. The inclusions from the Franks Pond quartz veins had a homogenization temperature of 80 to 260°C.

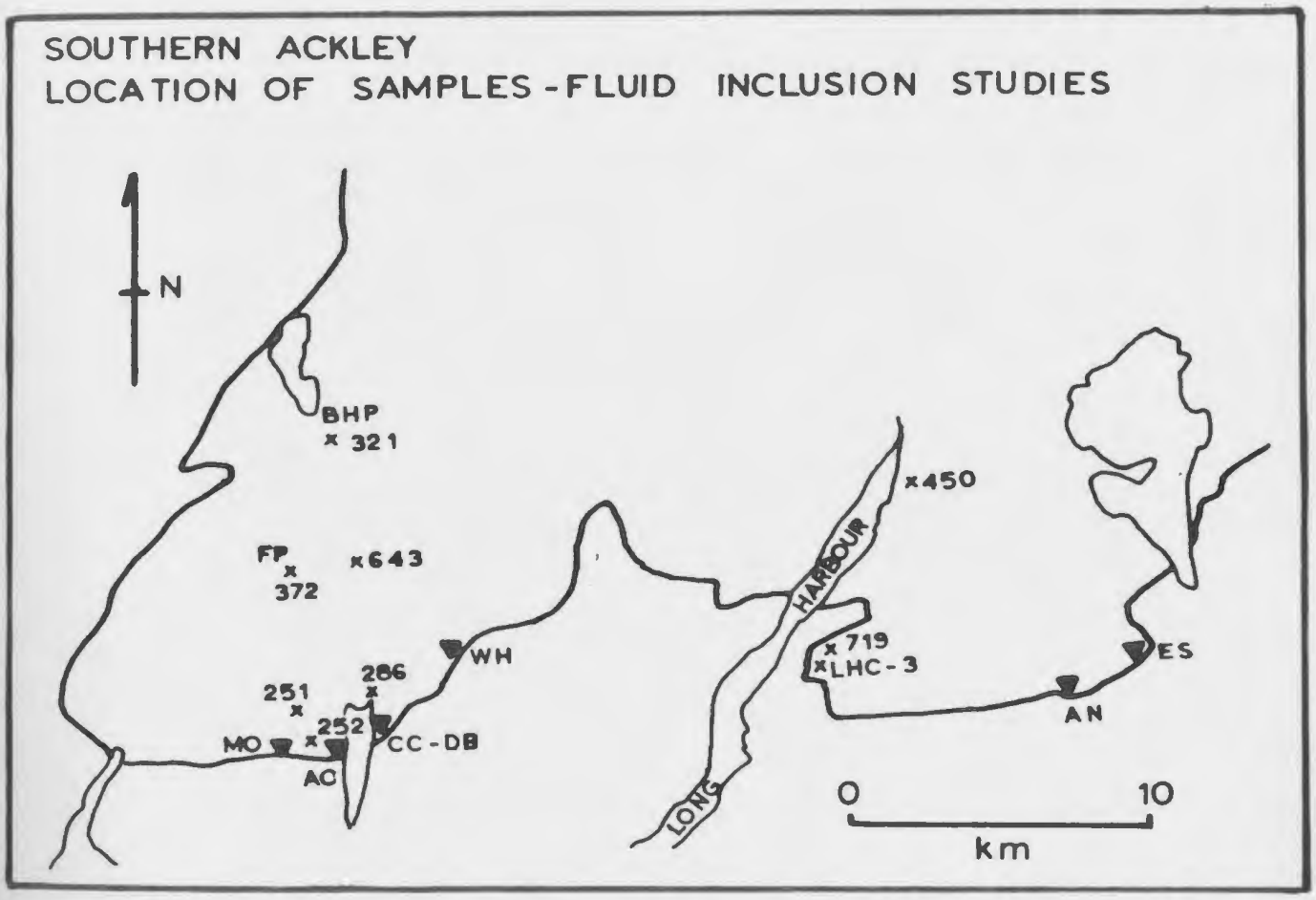

Figure 68: Location of samples used for fluid inclusion studies. Numbers refer to regional samples. Inverted triangles are significant prospects. ES - Esso; An - Anesty; WH - Wyllie Hill; CC-DB - Crow Cliff - Dunphy Brook; AC - Ackley City; MO - Motu; FP - Franks Pond; BHP - Big Blue Hill Pond. A detailed sample location map for the Sage Pond area is presented in Figure 46.

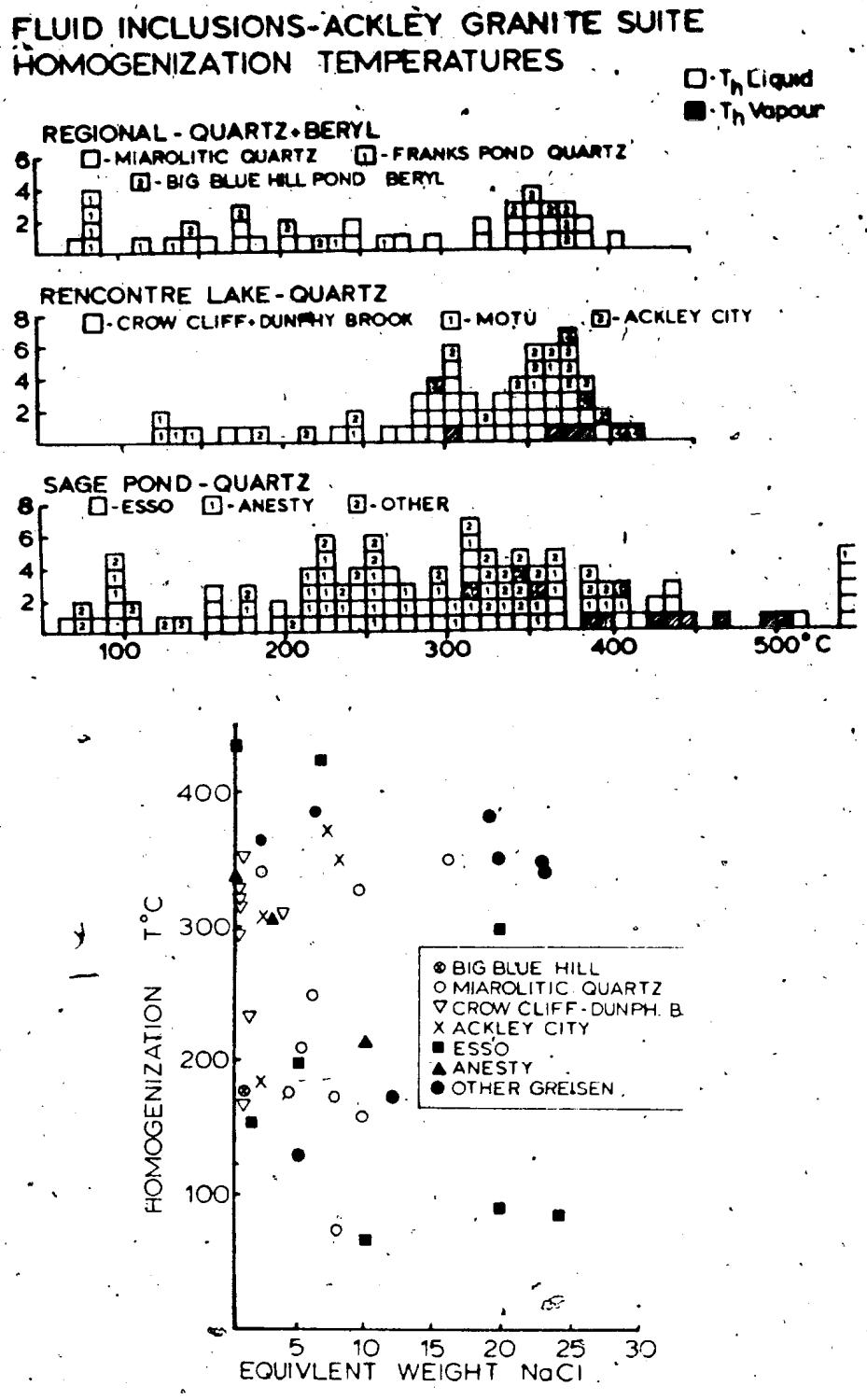

Figure 69: Homogenization temperatures of fluid inclusions from the Ackley Granite Suite.

Freezing runs on most of inclusions provided final melt temperatures between 0 and -13.6°C (Fig. 70A). These temperatures indicate an equivalent weight percent NaCl in the fluid of less than 17.5, with most samples containing less than 10% equivalent wt. % NaCl. Inclusions from the Franks Pond quartz veins and one inclusion from miarolitic quartz had lower final melt temperatures down to -30°C and commenced melting (eutectic) at temperatures down to -55.7°C (Fig. 70B).

9-2-2 Rencontre Lake Molybdenite Prospects

Twenty-five samples of vein and pegmatite material were examined from the molybdenite prospects. Samples from the Wyllie Hill prospect did not contain inclusions of suitable size for heating-freezing studies. Samples from the Motu, Crow Cliff-Dunphy Brook and Ackley City prospects contain abundant small inclusions and rare large inclusions. Most inclusions are similar to those from the regional miarolitic cavities (Plates 30, 31). However, small solid (S) cubes of halite occur along with vapor and liquid (L+V+S) in rare, isolated inclusions. Possible double rings suggesting the presence of minor CO_2 were observed in several inclusions from samples 646 and CC-1. These rings are very narrow and it is difficult to differentiate them from optical effects.

Primary V+L inclusions homogenize to both liquid and vapor between 275 and 400°C with most homogenizing between 350 and 400°C (Fig. 69). Several runs were made in which homogenization occurred to both liquid and vapour within a 10 degree interval in coexisting inclusions within the same field of view.

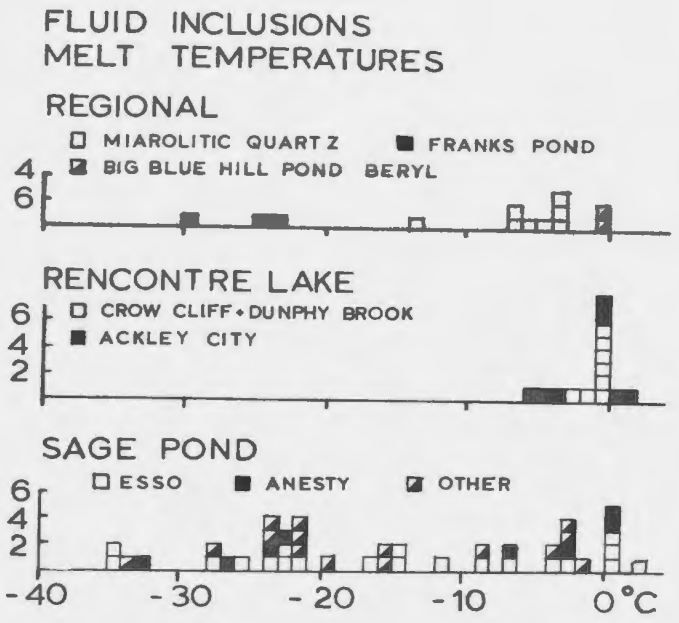

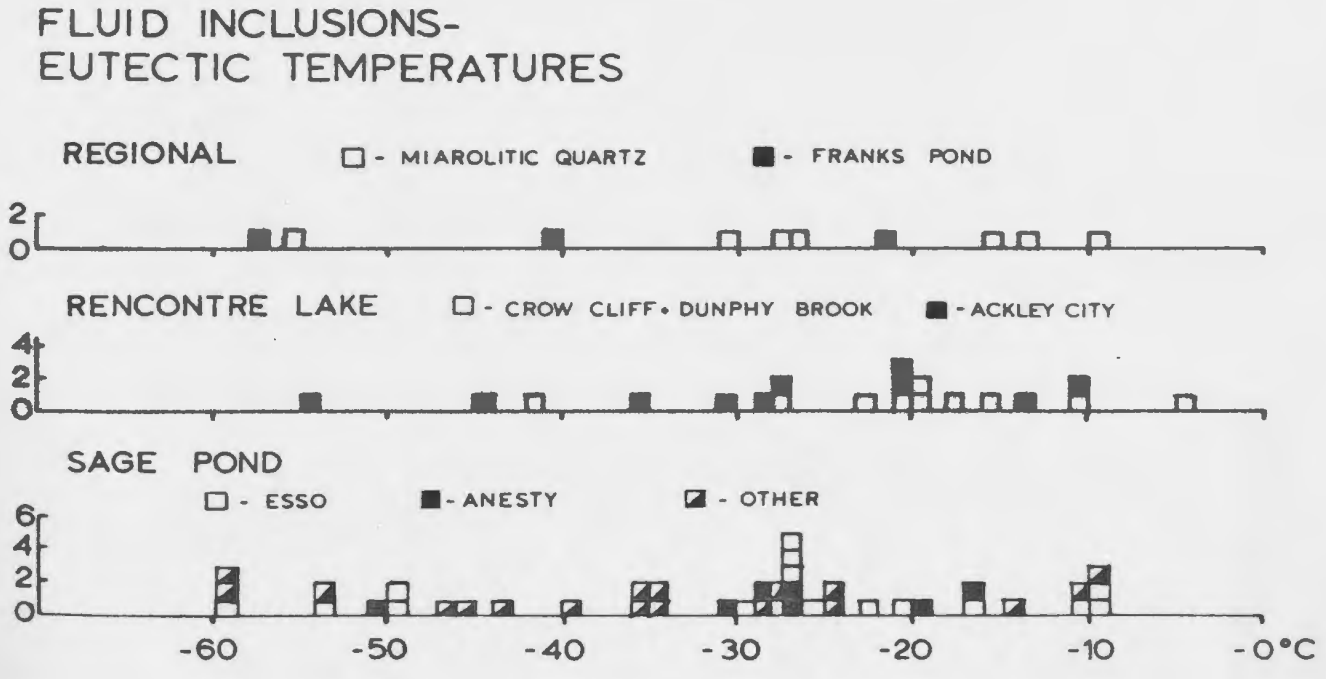

Figure 70: A: Final melt.
B: Eutectic temperatures of fluid inclusions from the Ackley Granite Suite.

A

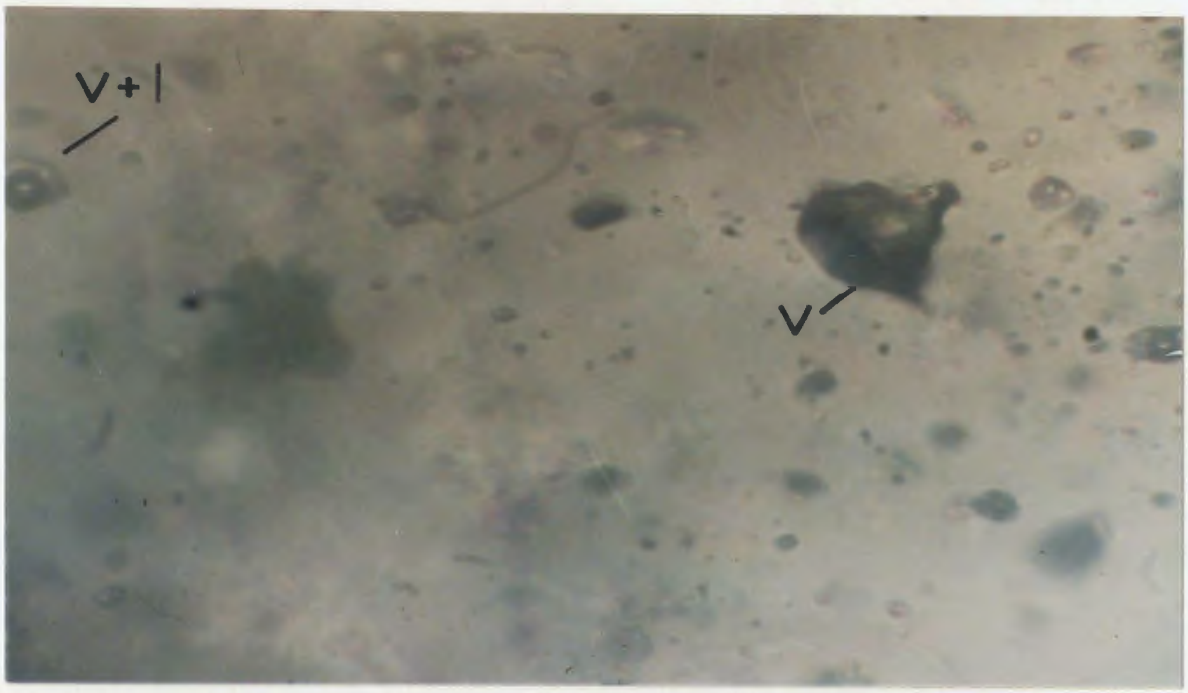

B

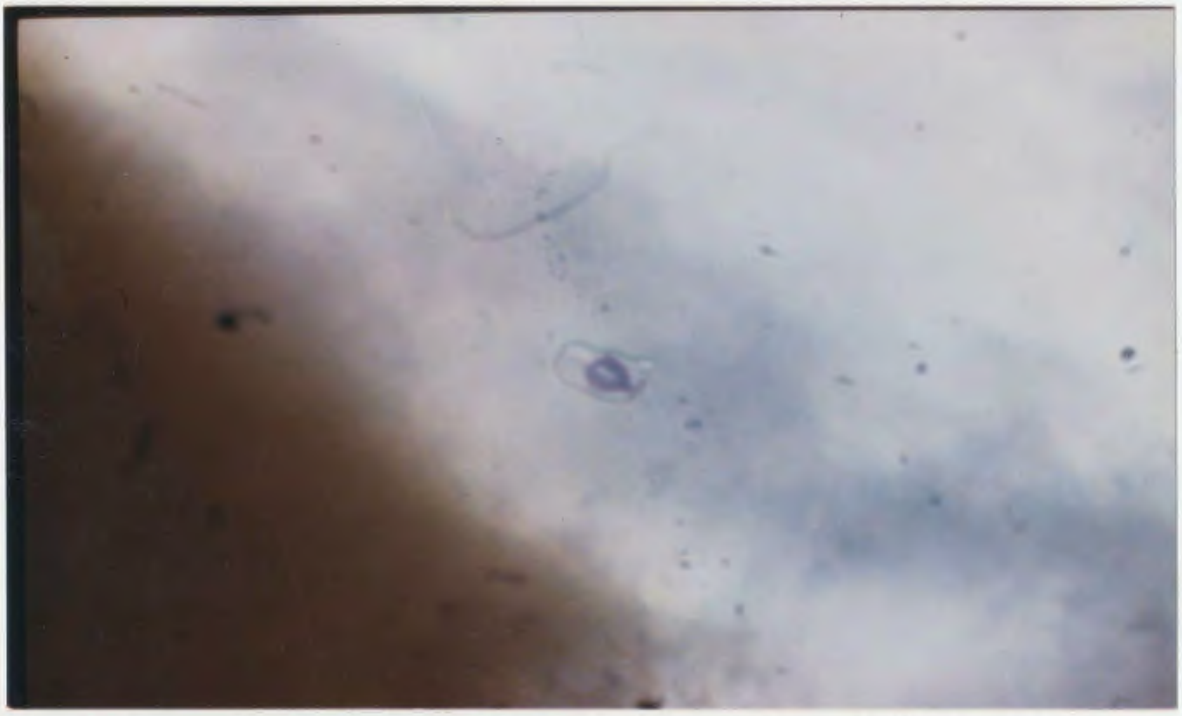

Plate 30: Fluid inclusions in quartz from the Rencontre Lake molybdenite prospects.
A: Vapour filled inclusion ($\approx 20\mu$) with smaller V+L and V inclusions in background. JT-393. Dunphy Brook.
B: V+L inclusion ($\approx 15\mu$). JT-370. Ackley City.

A

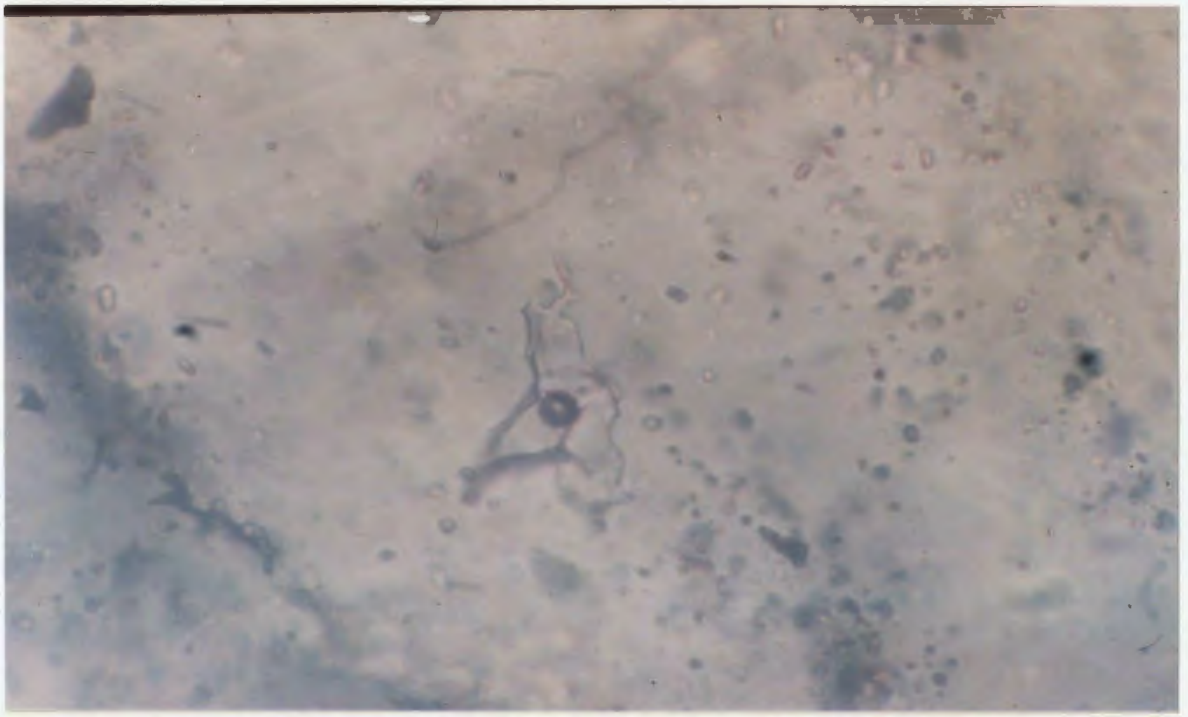

B

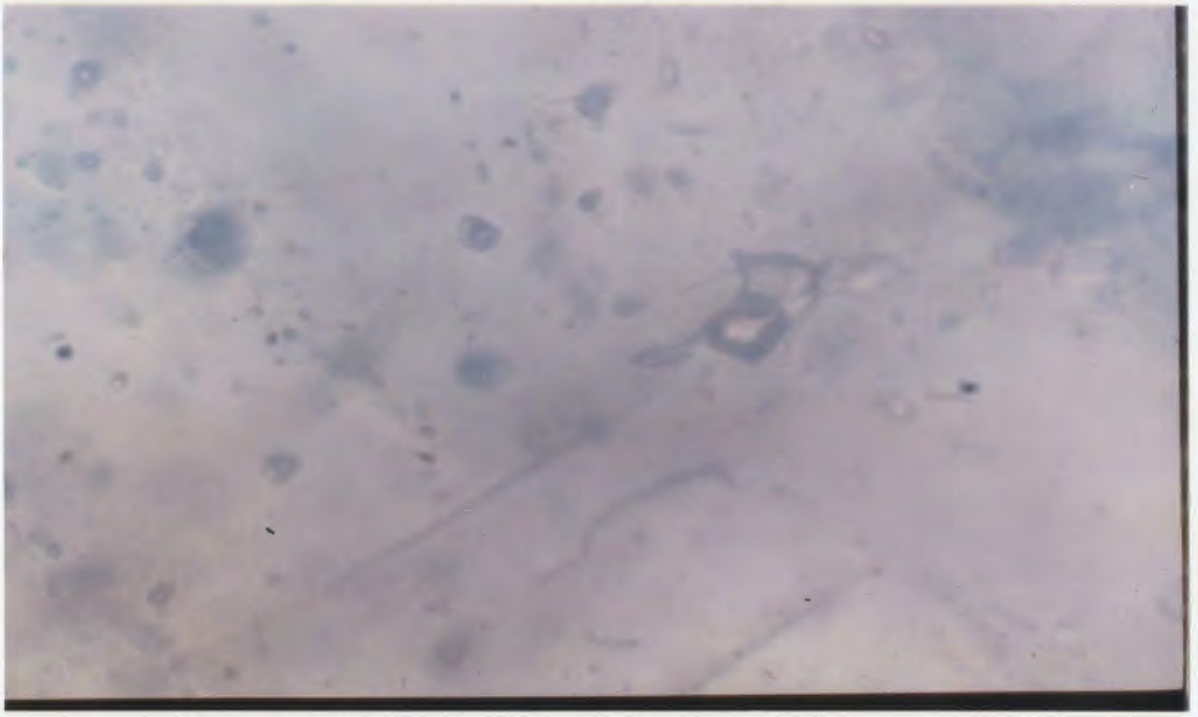

Plate 31: Fluid inclusions in quartz from the Rencontre Lake molybdenite prospects.
A: Irregular V+L inclusion (≈30μ) surrounded by abundant small V+L inclusions. CC-1. Crow Cliff.
B: V+L inclusion (≈25μ) with smaller V+L inclusions. CC-1. Crow Cliff.

A

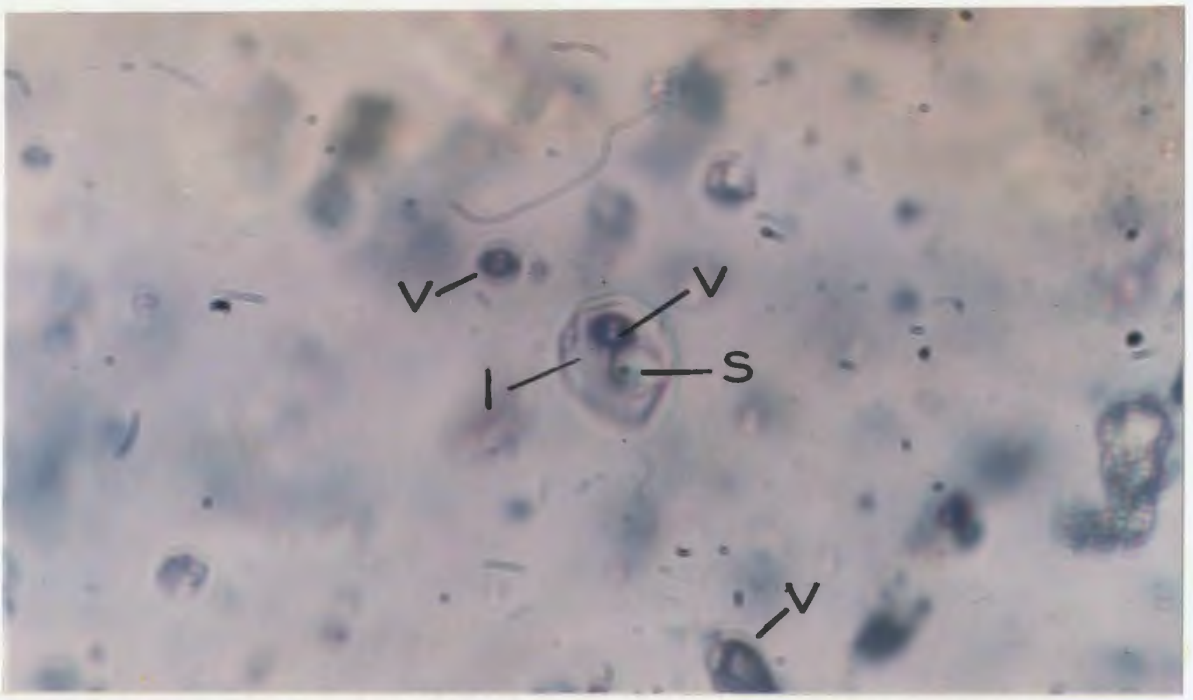

B

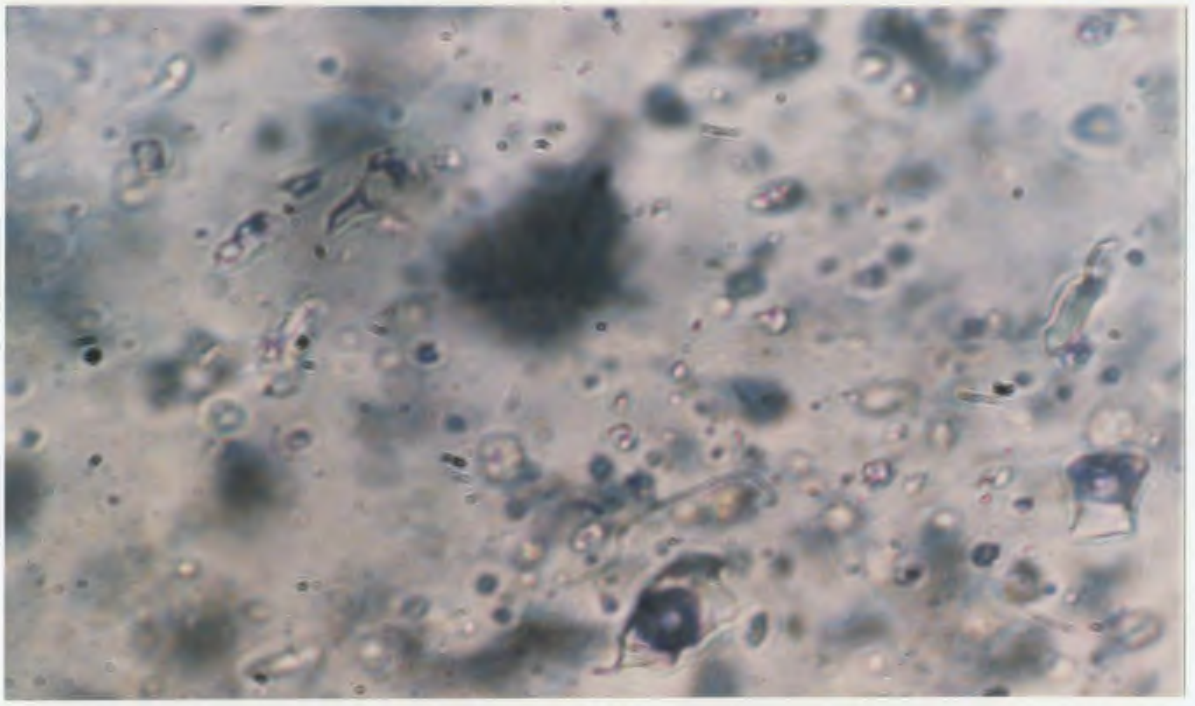

Plate 32: Fluid inclusions in quartz from the Sage Pond greisen.
A: V+L+S inclusion (15μ) with negative quartz outline. Note V inclusion at top of photo.
B: Abundant V+L, V+S+L and V inclusions. Largest inclusion 15μ.

A

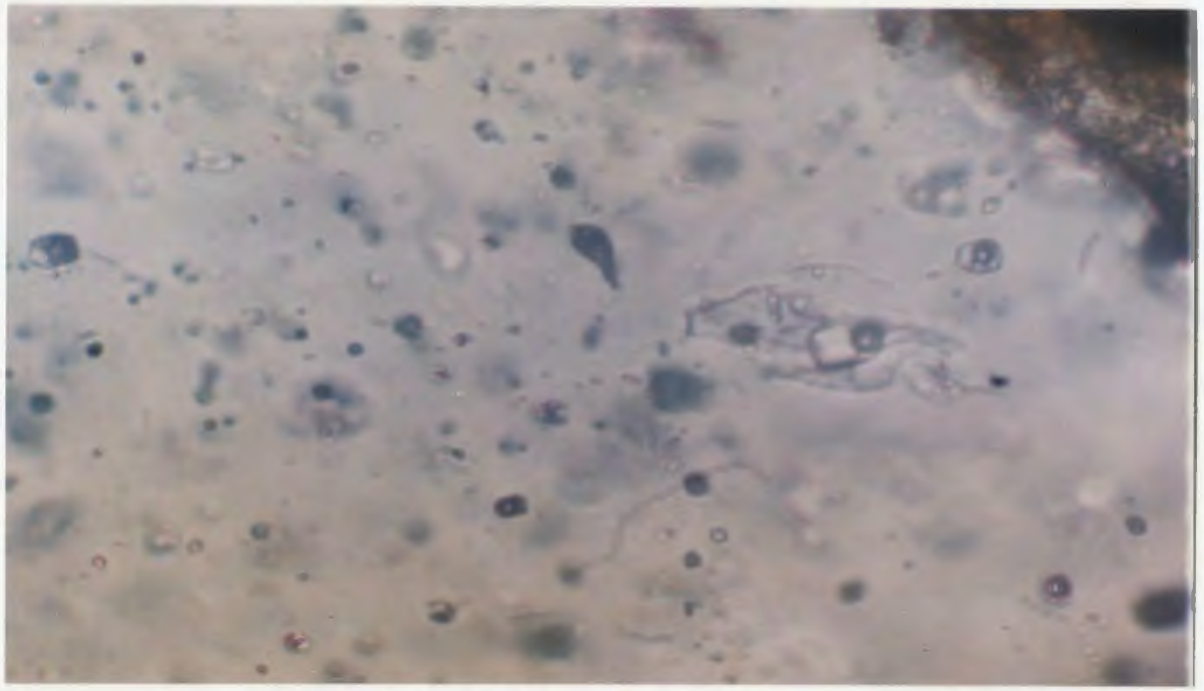

B

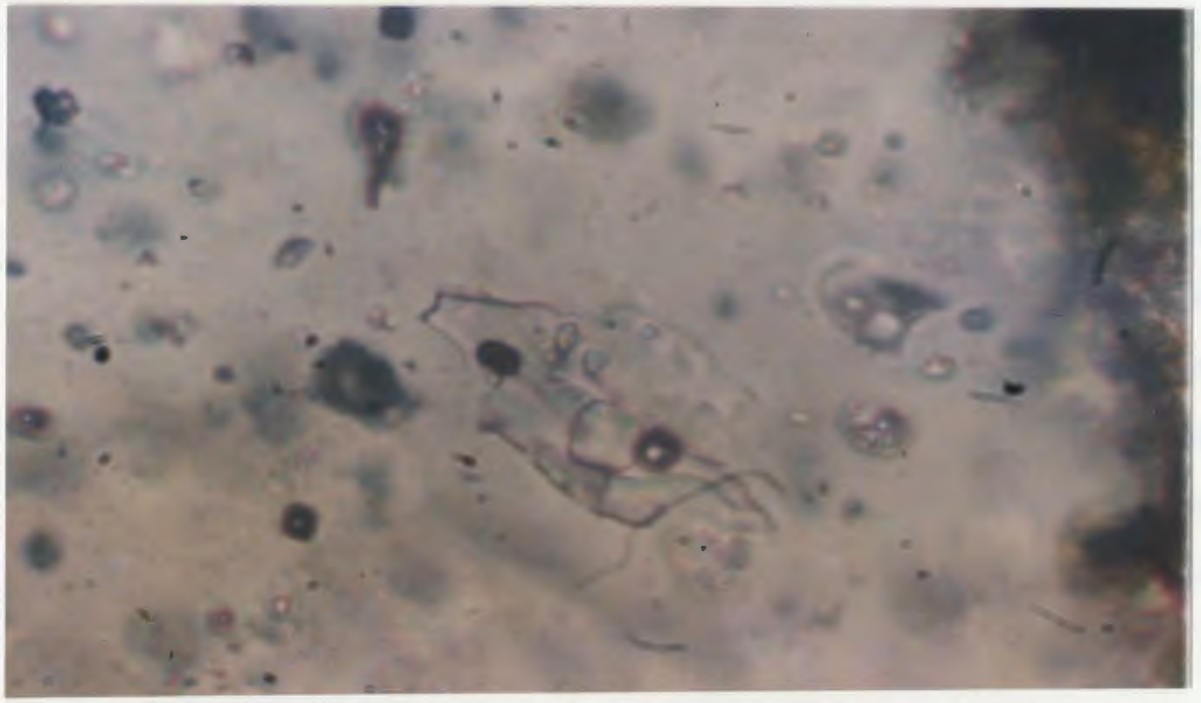

Plate 33: Fluid inclusions in quartz from the Sage Pond greisen. JT-138. Esso greisen.
A: Large (≈40μ) irregular inclusion with a minimum of 3 solid phases. Note variability of smaller inclusions in background.
B: Enlargement of inclusion in A showing dark red subhedral solid phase and rounding of edges of other solid phases. Again note variability of inclusions.

Freezing experiments gave final melting temperatures above -7°C (Fig. 70A), with most above -1°C. These indicate low salinity fluids with less than 10% equivalent wt. % NaCl. Final melt temperatures above 0°C were recorded from 2 inclusions. Temperatures down to -20.8°C were recorded for beginning of melt from the Ackley City prospect and down to -21.9°C from the Crow Cliff-Dunphy Brook prospect. The available data from the Motu, Ackley City, and Crow Cliff-Dunphy Brook molybdenite prospects are similar.

9-2-3 Sage Pond Greisens

Forty samples of quartz-topaz greisen from the Sage Pond area were examined. In contrast to the inclusions from the Rencontre Lake area, co-existing inclusions in quartz grains from the greisen are extremely variable from solid (S) to liquid (L) to vapour (V) only (Plates 32, 33). Up to 5 solid phases are observed. Abundant small inclusions are present, most are less than 10 micrometers in diameter. Negative quartz outlines are common (Plates 32, 33). Many of the larger inclusions have necked subsequent to their formation (Plates 32, 33) and therefore provide unreliable data. Small inclusions are also present in topaz and locally in fluorite. However, none were large enough to provide significant data.

With respect to possible multi-stage alteration and mineralization, the author can only quote Hall et al. (1974; page 894):

> "we have been unable to associate any distinctive type or variety of inclusion with a particular intrusion, stage of molybdenite, or alteration".

This statement applies to the different greisen veins and to different greisen types in the Sage Pond area.

The daughter minerals in the inclusions are isotropic and most have a cubic habit, indicating the predominance of NaCl or KCl. Tabular, rhombic, hexagonal, acicular and platy minerals are also common and may be sulphates or carbonates. In many inclusions, the daughter minerals have slightly rounded corners and a subhedral shape (Plates 32, 33). The rounded crystals suggest that many of the inclusions exchanged with an external aqueous reservoir after formation and are secondary. A variety of small (less than 1 micrometer), red, translucent crystals are common (see Plate 34), with hexagonal, platy, acicular, tabular and irregular shapes. These are probably hematite, although rutile and cassiterite may also occur. Thin double rings were noted in isolated inclusions in several samples and suggest the presence of minor CO_2, and rare inclusions were noted with up to 20% CO_2.

Inclusions with primary features gave a wide range of homogenization temperatures (Fig. 69) between 50 and greater than 500°C (the upper range of the heating stage) with most samples homogenizing between 200 and 400°C. Coexisting vapour-rich inclusions were seen to homogenize to both liquid and vapour within a 20°C temperature range.

Freezing studies (Fig. 70B), showed that some aqueous L+V+S and L+V inclusions began melting at temperatures as low as -60°C and had final melt temperatures below -21°C. Five inclusions had a final melt temperature above 0°C with one inclusion melting at 3°C. A wide range in salinity is indicated (Fig. 70) with some inclusions containing up to 70 wt. % equivalent NaCl.

A double ring in a single inclusion from sample 123A indicates the presence of CO_2. This inclusion had a eutectic temperature of -55.4°C and homogenized to vapour at 25°C, continuing the presence of CO_2. The inclusion decrepitated on heating at 224°C.

9-3 DISCUSSION

9-3-1 Rencontre Lake Area

The data from the molybdenite prospects indicate that quartz pegmatite and associated molybdenite formed in the presence of a low salinity fluid. Local salinity increase may be the result of boiling. The data lie on and near the critical point for low salinity fluids (critical point for pure water = 221.19 bars and 374.15°C). Therefore the fluids in the Rencontre area could have been trapped at undetermined, but higher, supercritical temperatures and pressures. The presence of pegmatite and the style of mineralization in this area, suggest closed depositional conditions under lithostatic pressure. An assumption that the fluids were boiling would suggest a minimum depth of formation of 800 to 1000 meters. This seems an unrealistically high level.

9-3-2 Sage Pond Area

The co-existence of such a wide range of inclusion-types again suggests that the fluids responsible for greisen formation were boiling. Detailed studies of inclusions in quartz from quartz-topaz greisen in New South Wales, Australia (Eadington, 1983), and from the Climax deposits, Colorado (Hall et al., 1974) have yielded comparable results and Eadington (1983) suggests that quartz trapped secondary inclusions throughout hydrothermal activity, making identification of primary and secondary inclusions difficult to impossible. Temperature and pressure estimates cannot be made on the available data from the Sage Pond area.

9-3-3 Composition and Variability of Fluids

The low eutectic temperatures and final melt temperatures below -21°C indicate that significant proportions of species other than Na^+ are present in the fluids involved in the formation of miarolitic quartz and the mineral prospects. Carbon dioxide vapour-liquid rings were not observed in these samples. The eutectic in the system $NaCl-CaCl_2-MgCl_2-H_2O$ is at -57°C (Crawford, 1981) and is above the recorded eutectic temperatures in two inclusions. However, it is suggested that Mg^{2+} and Ca^{2+} are important constituents of the fluids. This conclusion is consistent with the formation of Mg-rich hydrothermal muscovite (greisen) and secondary fluorite (plus calcite at Ackley City) from the fluids.

The final melt temperatures above 0° may reflect the presence of CO_2-clathrate in isolated fluid inclusions at the prospects (Higgins, 1979; Burruss, 1981a, b) and are consistent with the observation of rare double rings reflecting liquid H_2O - liquid CO_2 - vapour CO_2 inclusions. The extent of involvement of CO_2 in metal transport cannot be evaluated. Carbon dioxide-rich fluids are also suggested by the presence of calcite at the Ackley City prospect.

A significant contrast exists between the fluids considered to be responsible for mineralization in the Sage Pond area and those in the Rencontre Lake area. The fluids in the Sage pond area were highly saline and possibly boiled either periodically or continuously, while the fluids in the Rencontre Lake area had a uniform low-salinity composition and possibly boiled during precipitation of the quartz in pegmatites and veins.

The data from the different prospects in the Rencontre Lake area are similar, as are data from different greisens in the Sage Pond area. These features may reflect the internal homogeneity of processes which occurred in the two areas.

The similarity of fluid inclusions in regional samples and those from the magmatic-molybdenite prospects may suggest that they formed from a comparable fluid which was evolved directly from the magma during crystallization. This in turn suggests that the more complex fluids preserved in the hydrothermal greisen deposits resulted from reaction with country rock during fluid transport and migration along restricted

channelways. The trace element enrichment in the granites associated with the greisen deposits may have resulted in the partitioning of a greater concentration of Na, K, Mg, Cl, F, etc. into the fluid phase (see Flynn and Burnham, 1978). Alternatively, the physical evidence for a greater amount of aqueous fluid in the Rencontre Lake Granite compared to the Sage Pond Granite, may suggest that there was a relative dilution effect of the evolved fluids in the former area.

CHAPTER 10 - THE ACKLEY MAGMATIC/METALLOGENIC SYSTEM

10-1 INTRODUCTION

The objectives of this Chapter are to explore the nature of the Ackley Magmatic/Metallogenic System (AMMS) which formed the Ackley Granite Suite and its associated mineral deposits. The Koskaecodde and Mollyguajeck plutons have been shown to be temporally independent from the Ackley Granite Suite and are therefore excluded from the discussion.

10-2 MAGMA SOURCE

The relatively low initial $^{87}Sr/^{86}Sr$ of 0.7063 and the estimated ^{18}O whole rock values of 6.9 to 8.0 per mil in the Hungry Grove, Meta, Tolt, Rencontre Lake and Sage Pond granites indicate a relatively unevolved, possibly lower crustal source. Alternatively, the granites may have originated in the upper mantle, and the strontium and oxygen isotopic signatures may have resulted from crustal contamination. The reasonable MSWD indicates that the source region was homogenous with respect to the initial strontium ratios, or that vigorous convection and mixing occurred in a magma chamber either at depth or in the Ackley magma chamber. Minor heterogeneity is evident from the ^{18}O quartz values.

The Kepenkeck Granite has a low initial Sr ratio (0.7017) which probably reflects post-emplacement mobilization of Sr or Rb. The estimated initial oxygen isotope ratio of 8.6 per mil requires a

significant sedimentary component in the source region.

The association of the high- $\delta^{18}O$ Gander Terrane with the higher-^{18}O Kepenkeck Granite and the low- $\delta^{18}O$ Avalon Terrane with the rest of the lower- $\delta^{18}O$ Ackley Granite Suite may also reflect the nature of the source regions. While it is fully recognized that the surface rocks may have no relationship to rocks at depth, it is possible that melting of the relatively inhomogeneous, predominantly metasedimentary rocks, of the Gander Terrane could give rise to the aluminous, high- $\delta^{18}O$ granites with inhomogeneous initial strontium ratios, while melting of a plutonic and volcanic-rich source analogous to the Avalon Terrane could result in more homogenous isotopic ratios. Thus a direct melting relationship between the Gander Terrane and the Kepenkeck Granite and between the Avalon Terrane and the rest of the Ackley Granite Suite is postulated to have resulted from a lower crustal thermal event which transected the boundary between the Avalon and Gander tectono-stratigraphic terranes. These observations are in harmony with the concept of I- and S-type source terranes formulated by Chappell and White (1974), although their terminology would not strictly apply.

The overlap of the geochemical and isotopic signatures which are characteristic of the AMMS in the Avalon Terrane onto the Gander Terrane implies that the magma from the Avalon Terrane source-rocks flowed into the Gander Terrane. Alternatively, the Dover-Hermitage Bay Fault zone may be a steep southeast facing thrust and Avalon source rocks occur under the Gander Terrane.

10-3 EMPLACEMENT OF THE ACKLEY GRANITE SUITE

10-3-1 Introduction

A fundamental problem relating to the study of large plutonic bodies is the room problem (Read, 1957). In other words, how does the magma chamber develop? The alternatives are displacement of country rocks upwards, downwards, sideways, or in situ melting and assimilation.

In the case of high level, cross cutting plutons such as the Ackley Granite Suite, the geological, chemical and isotopic features indicate that assimilation or in situ melting are unlikely, leaving the alternative that magma is derived from depth and emplacement was by displacement. The sharp geological contacts with country rocks and the cross cutting attitudes of the contacts indicate that sideways, or forceful displacement of the country rock does not occur. In many cases where the roof zones of areally extensive and thick, high level, post-tectonic batholiths are intermittently exposed (cf. Cornubian Batholith), the geological relationships indicate a stratigraphic continuity across the upper surface of the pluton which precludes extensive upwards displacement. Thus downwards displacement of the country rocks would appear to be the most likely mechanism of emplacement.

Models for the emplacement of large granitoid bodies from their source region into the upper crust have been discussed by Pitcher (1979) and Hildreth (1981), amongst others. These authors invoke low density contrasts between magma and host rock and envisage a process of

diapirism and coalescence of diapirs at high crustal levels to form the large plutonic bodies. Bridgewater et al. (1974) convincingly demonstrated that crustal downwarping occurred under the large rapakivi granites of Greenland. Cauldron subsidence (Anderson, 1936) is also seen as a mechanism of emplacement of high level plutons and multiple cauldron subsidence to permit extensive high level magma chambers has been documented in parts of the Andes (Bussell, 1985; Bussell and Pitcher, 1985). Lineaments, or major fault zones are commonly seen as lines of crustal weakness which permit ascent and emplacement of granites into the upper crust (Leake, 1978; Pitcher 1979)

Examination of the contoured Bouguer gravity plot presented in Figure 3 (Miller, 1986a) and reproduced below, offers some insight to the mechanism and tectonic controls of emplacement of the AMMS, and high level granites in general.

10-3-2 Geophysical Surveys

A relatively detailed gravity survey over the study area was recently completed (Miller, 1986a). A contoured plot of Bouguer anomalies showing the location of the data stations and the outline of the plutonic rocks is presented in Figure 71. Preliminary modelling by Miller, using a constant density contrast of 0.1 g/cm^3 has provided estimates of granite thickness, and these are also indicated on Figure 71. The magnitudes of the gravity anomalies agree with those obtained by Weaver (1967) in the regional gravity survey of Newfoundland.

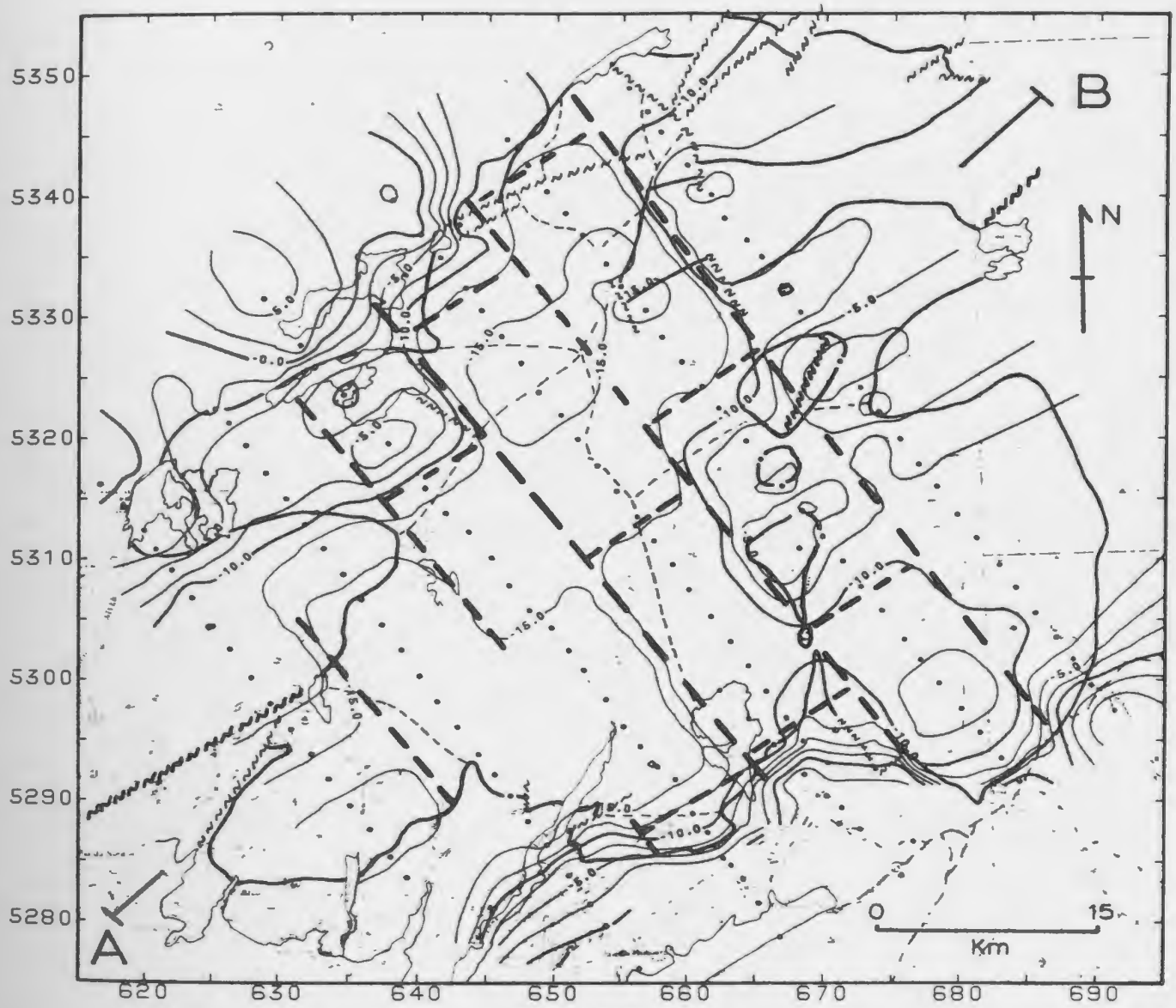

MAP 85-58

ACKLEY BATHOLITH GRAVITY SURVEY

BOUGUER CONTOURS

Figure 71: Computer contoured plot of Bouguer gravity anomalies in the study area (Miller, 1986a). Dots are data stations. Thick dashed lines are interpreted linear structures.

The boundary of the Ackley Granite Suite as currently exposed is generally marked by a steep gravity gradient and rapid increase in Bouguer gravity values. This feature suggests that the outer contact in these areas is steep. Subsurface granitic bodies may be present to the southwest and to the north.

The contour map shows considerable additional topography or gravity variation within the granite and it is reasonable to assume that this topography reflects changes in depth to the floor of the granite from the current erosion surface, ie. changes in the present thickness of the granite. The axis of the largest negative gravity anomaly, which presumably reflects the thickest granite, extends in a north-south direction across the trace of the Dover-Hermitage Bay Fault and across the geochemical and isotopic boundary to the west of this trace. These observations support the interpretations that large parts of the Ackley Granite Suite may represent a single magma chamber and that emplacement of the magma chamber occurred after movement on the Dover-Hermitage Bay Fault had ceased (Blackwood and O'Driscoll, 1976). There is a separate gravity-low anomaly over the Tolt Granite. However, the true relationship between the these main anomalies may be masked by gravity effects related to the large roof pendants which separate the two areas. The largest Bouguer anomalies occur in the south of the Ackley Granite Suite, associated with areas of mineralization.

Superimposed on, or at least complementing the main north-south trend, are a set of parallel northwest trends (Figure 71) with an approximate separation of 10 km which are present in both the Avalon and

Gander Terranes. These trends are defined by steep contour gradients which are interpreted to represent internal subvertical walls within the magma chamber.

It might be argued that the northwest trends are an artifact of the sample distribution and the contour package. However, new gravity data collected on northeast lines has confirmed the presence of the northwest linears (Miller, personal communication, 1986). Furthermore, the northwest gravity trends are parallel to and essentially in the same location as, strong northwest linear features defined by second derivative analysis (4 km spacing) of the total field magnetic data over the study area (Fig. 72). The total field magnetic data from the 1:50,000 scale magnetic series published by the Geological Survey of Canada was digitized and processed using a procedure described by Miller and Weir (1982) and these processed data were then used to compute the second derivatives (Henderson and Zietz, 1968). In addition, Miller (personal communication, 1986) has confirmed the location of the northwest lineaments by modelling the magnetic data. Therefore, the combined evidence from gravity and magnetic data indicate that the northwest trends are real and that they exercised considerable control on the subsurface shape of the Ackley Granite Suite.

There is also an implied sense of sinistral movement displayed by the northwest trends (Fig 71). These northwest trends are not apparent from the regional geology maps in the immediate vicinity of the Ackley Granite Suite, nor are they readily apparent from the 1:250,000 scale total field magnetics maps (Fig. 73), suggesting that sinistral faulting

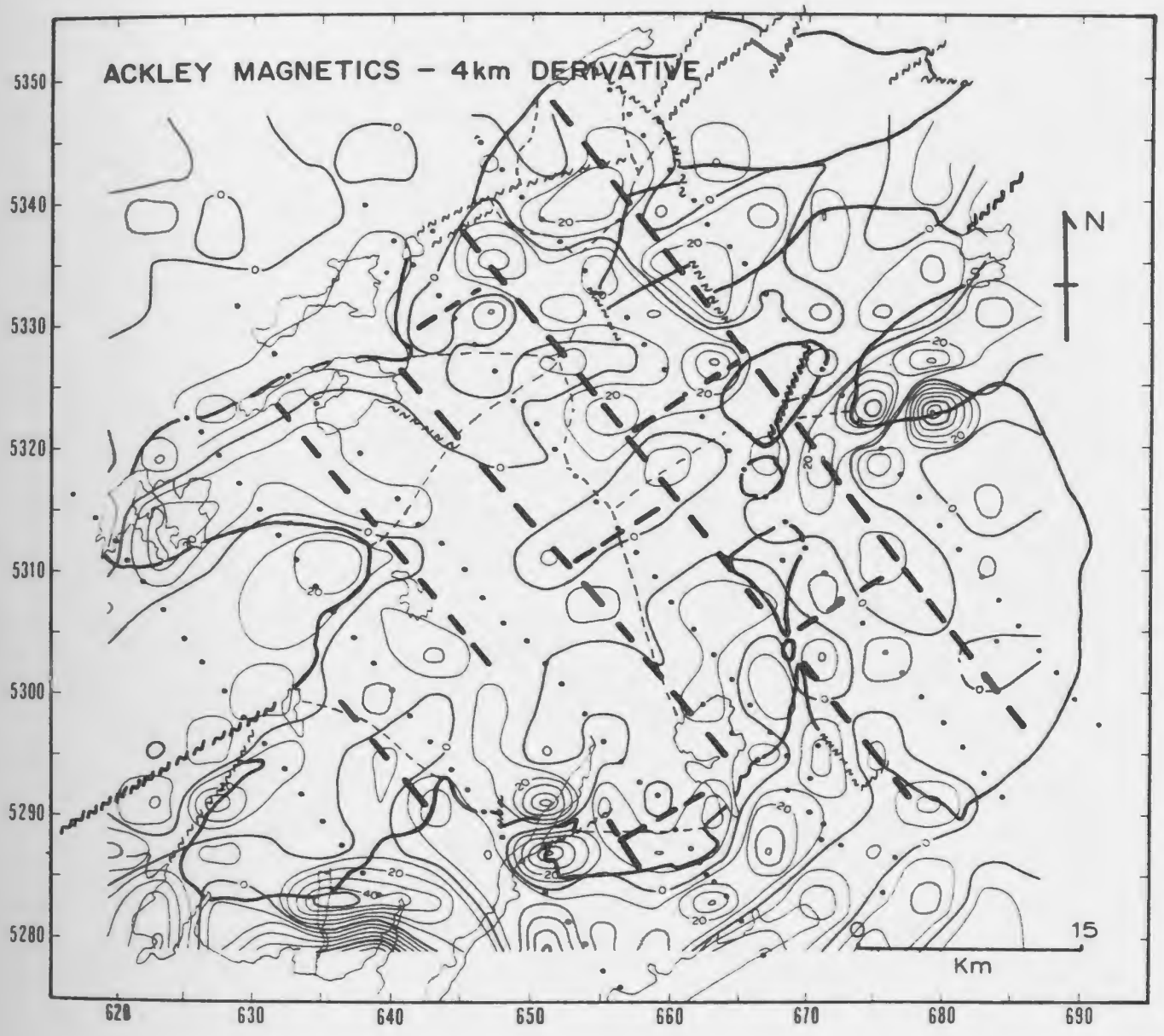

Figure 72: Plot of contoured second derivative (4 km) magnetic patterns from the study area (Miller, 1987, In Press). Thick dashed lines are interpreted linear structures shown on Figure 71.

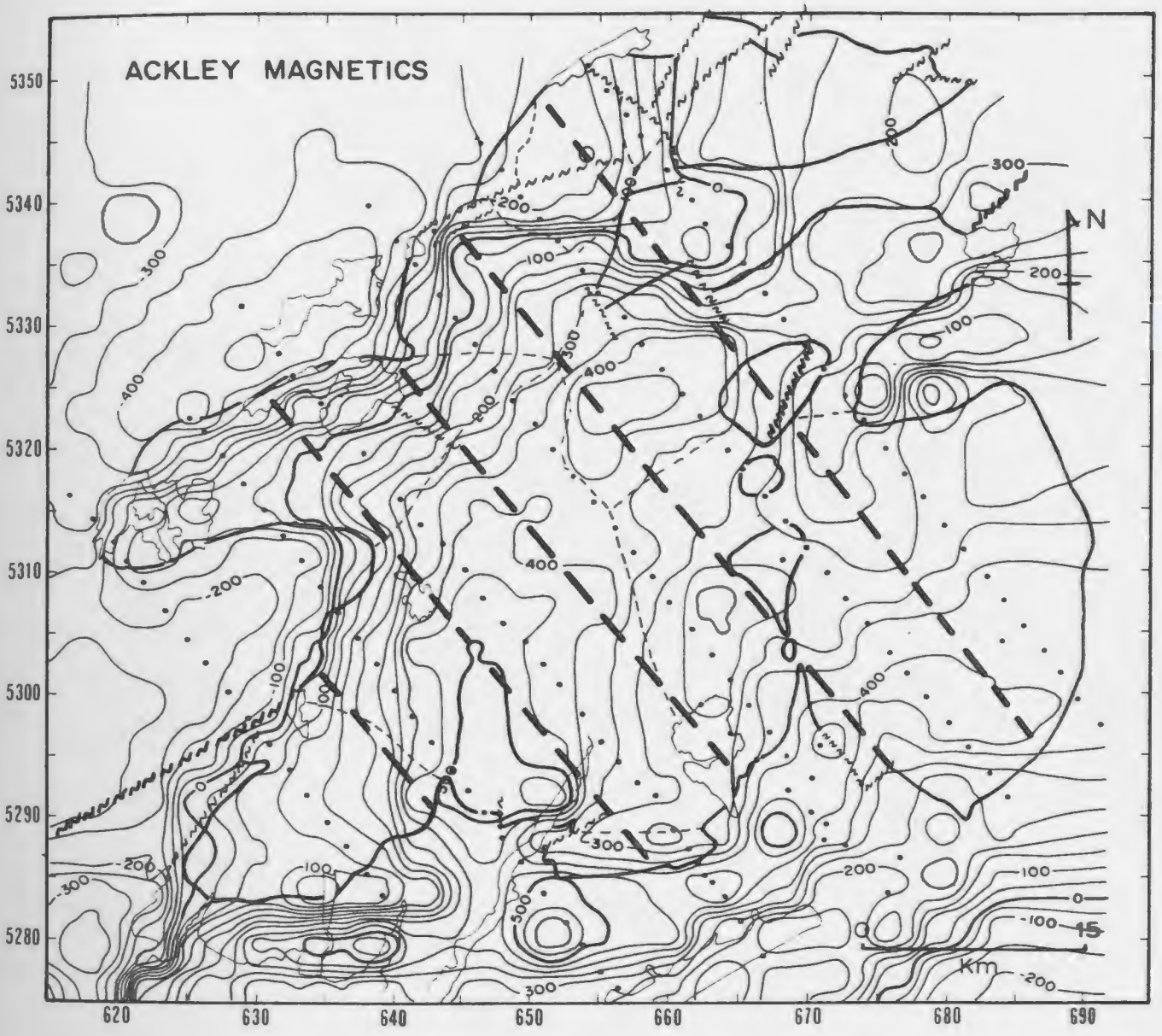

Figure 73: Summary of total field magnetic patterns in and around the study area (Miller, 1987, In Press). Thick dashed lines are interpreted linear structures from Figure 71.

is not a significant structural feature in the area. This implies that the pattern of sinistral movement suggested by the block pattern is a result of the relative vertical movements of blocks to different depths and does not result from movement along strike slip faults.

10-3-3 Emplacement Model

The northwest trending gravity anomalies can be interpreted to represent internal subvertical walls at the base of the magma chamber. These walls must have developed in response to faulting or fracturing of the upper crust prior to, or during emplacement of the magma. The preferred interpretation is that the AMMS developed in the upper crust due to the downwards displacement of large parallel crustal blocks with approximate plan dimensions of 10 by 20 km. The inferred process is here termed 'megablock stoping'.

The north-south anomaly, representing the deepest part of the Ackley Granite Suite, is interpreted to represent the axis of the major crustal displacement and must also represent the axis of the major thermal event which led to emplacement of the granites. Displacement of magma from a postulated melt zone in the lower crust upwards around the downward-stoping blocks probably occurred in response to an east-west regional tensional regime (possibly related to opening of the Atlantic Ocean) and to buoyancy differences resulting from relatively cold crustal blocks overlying hot, relatively siliceous melts at depth.

Considerable density contrast is envisaged between the magma (2.2 g/cc) and the intruded rocks (2.7 to 2.9 g/cc). This contrast would be sufficient to cause an excess lithostatic pressure (buoyancy force) of approximately 1 Kb in a 20 km column of rock. The total pressure acting to return magma to the top of the rock column in a 10 * 20 km area (megablock) from a magma chamber at its base is approximately $3 * 10^8$ N. This pressure may be sufficient to overcome frictional forces between blocks and resistance to flow caused by possible high viscosity of relatively silicic magma. The viscosity of the silicic magma is difficult to estimate. It is envisaged that a high temperature heat source can cause extensive to total melting of crust at temperatures above the granite liquidus (cf. 900 to 1000°C) and may form a granitic magma with relatively low viscosity, permitting rapid flow through available conduits. High viscosity in silicic magmas with low volatile content may be a feature that is restricted to surficial or near surficial environments at relatively low temperatures.

Schematic sections (Figure 74) show the possible mechanism of emplacement of the AMMS. The depth from surface to the roof of the pluton is inferred from studies by Whalen (1981), and Dickson (1983), from the presence of narrow thermal aureoles, and from the presence of miarolitic cavities and aplitic phases in the southern outcrops of the granite. The depth to the floor of the magma chamber and hence the assumed vertical extent of the stoped blocks is taken from preliminary calculations based on the gravity and magnetic data (H. Miller, personal communication, 1986).

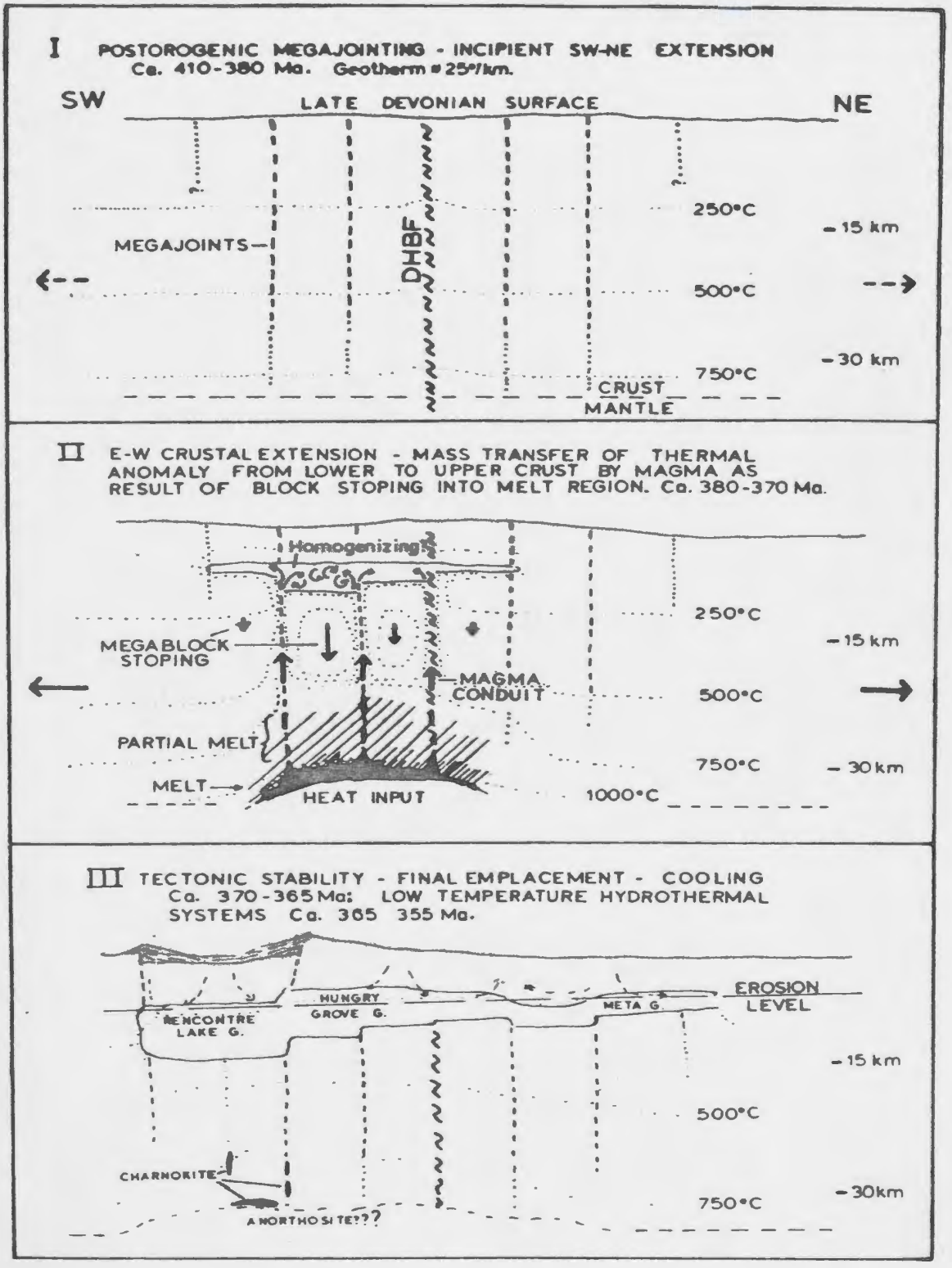

Figure 74: Schematic drawings of postulated mechanism of intrusion of the Ackley Granite Suite. A-B line of section shown in Figure 71. Caldera speculative (see later discussion). Dotted lines are estimated isotherms.

It is assumed that the magma chamber obtained a state of isostatic- or buoyancy-stability with overlying intruded rocks. The scale and style of emplacement is similar to that described by Bridgewater et al. (1974), for the rapakivi granites in Greenland. However, block stoping to permit magma emplacement was in this case more important than crustal downwarping and it is possible the downwarping described by Bridgewater et al. (1974) may result from frictional drag caused by downward displacement of crustal blocks. The boundaries of the Ackley Granite Suite are not defined by lineaments. Therefore, some secondary expansion of the magma chamber outside the confines of the downward moving blocks must have occurred.

Bridgewater et al. (1974) and Emslie (1980) postulated that a series of stacked, mushroom-shaped, magma chambers developed in the crust to permit emplacement of the Proterozoic rapakivi-anorthosite suite. These authors suggested that graben-type faults and structures may develop above each chamber permitting emplacement of magma to a higher crustal level and eventually onto the surface in graben or caldera basins. This may be a reasonable model for the development of the AMMS. However, it will be argued below that the primary structural controls over emplacement and shape of the AMMS relate to orogen-scale fractures which penetrate the total thickness of the crust.

The mechanism of emplacement proposed is different from the commonly accepted processes of diapirism and coalescence of diapirs at high crustal levels to form the large plutonic bodies (Pitcher, 1979; Hildreth, 1981). However, control of magma uprise by parallel fractures

or faults is comparable to that envisaged by Shaw (1980) and Hildreth (1981). Cauldron subsidence is another common mechanism of emplacement (Bussell and Pitcher, 1985). It is possible that the proposed mechanism of megablock stoping is dominant in the middle to upper crustal region while cauldron subsidence and caldera collapse may take place in the upper crust.

10-3-4 Speculations on the Tectonic Controls on Magmatism

The Ackley Granite straddles the Dover-Hermitage Bay Fault which implies a direct relationship between movement on the Fault and the tectonic controls over emplacement. Possible antithetic structural relationships may be envisaged between the fault and the northwest and north-south trends. However, the gravity patterns along with the geological relationships indicate that emplacement of the Ackley Granite post-dated movement on the Dover-Hermitage Bay Fault.

Northwest-trending topographic, structural and geophysical features are present throughout Newfoundland (Weaver, 1967; Hibbard, 1983; see Fig. 82) in rocks of all ages from Proterozoic Grenville gneiss to the Carboniferous sediments, and are present in the three main tectonostratigraphic terranes in Newfoundland (Humber, Dunnage and Avalon; Williams and Hatcher, 1983). The Bonne Bay - Placentia Bay Lineament (Swanson and Brown, 1962; Scott, 1980) extends from Bonne Bay, through the Buchans area, to Fortune Bay on the southeast coast of Newfoundland and is the most prominent northwest-trending feature. It is defined by changes in geology, gravity, magnetic, and topographic

trends. Detailed gravity surveys show the presence of northwest trends (usually coincident with magnetic trends) in the northwest Gander (Miller and Weir, 1982; Miller, 1986a), St-Mary's-Conception Bay (Miller, 1986b), Trinity Bay (Miller et al., 1985) Deer Lake Basin (Miller and Wright, 1984) and St. Georges Basin areas (Miller, personal communications, 1986). These lineaments have a separation of approximately 10 to 15 km. Thus the linear trends with an amplitude of 10 km, defined by gravity in the study area, are part of a regional tectonic trend which cuts all of the dominant northeast Paleozoic trends in Newfoundland.

North-trending topographic, geophysical and structural trends are also common in Newfoundland (Weaver, 1967; Hibbard, 1983). However, north-trending structures are less well defined than the northwest structures. The Late Silurian Skull Lake Syenite (Kean and Jayasinghe, 1982) and the peralkaline, Carboniferous, St. Lawrence Granite have a linear north-trending outcrop pattern, which cuts the normal tectonic trend. Both of these plutons are high level and post-tectonic. Emplacement of the St. Lawrence Granite was controlled by north and by northwest lineaments (Teng and Strong, 1975).

Thus the hypothesis is that emplacement of post-tectonic plutons after the end of the Acadian Orogeny was controlled by orogen-scale (cf. Tapponier and Molnar, 1976; Strong, 1980) fracture sets or megajoints. Periodic relaxation in an east-west direction caused localized thermal pulses into, and melting of, the lower crust. East-west extension and northwest megajoints permitted emplacement into the upper crust.

Devonian-Carboniferous, post-tectonic, biotite granites in Newfoundland, commonly with A-type or anorogenic affinities (Strong, 1980; Wilton, 1985; Tuach et al. 1986; Chorlton and Dallmeyer, 1986) appear to occur in association with major tectonic breaks. It is possible that the Dover-Hermitage Bay Fault and other major structures had a fundamental influence over the generation of these plutons, possibly as a line of weakness to the mantle which permitted an increase of thermal and possible fluid activity at the base of the crust (cf. Leake, 1978; Thompson et al., 1984).

10-4 THE MAGMA CHAMBER

10-4-1 Size and Shape

The Ackley Granite Suite occupies an area of approximately 2,400 km^2. The thickness estimates of granite modelled from the gravity and magnetic data by H. Miller (personal communication, 1986) are summarized on Figure 3 and indicate an approximate volume of 8000 km^3. This is a minimum estimate for the volume of magma in the AMMS since significant erosion of granite may have occurred in the northern and western parts of the exposed area.

The radiometric ages indicate that most of the granites cooled 'instantaneously' within the error limits of the ^{40}Ar-^{39}Ar dating technique (± 5 Ma). The geochemical and isotopic characteristics throughout the southern granites indicate a continuity of magmatic processes across geological boundaries which have been identified on the basis of texture and mineralogy. Statistical analysis of the chemical

data also indicates that the boundaries of the Hungry Grove, Meta and Tolt granites are artifacts of the crystallization history of a single large magma chamber rather than the result of intrusion of separate magma pulses or phases. This concept may also include the Kepenkeck Granite in the north which appears to be related to the same thermal event.

There is some independence in the trace element behavior between the Rencontre Lake Granite and the rest of the AMMS. However, this is thought to result predominantly from variations in high level magmatic processes (see below). The similarities in major element patterns and the continuity of the gravity patterns attest to the close genetic relationship between the two areas.

The data are consistent with a model which invokes filling of a large magma chamber through separate underlying conduits. Undetected differences in age of crystallization between the member granites, and possible differences due to shifts in the axis of the major deep crustal or mantle thermal event, may have given rise to some of the observed variations. For example, it is possible that the Tolt Granite to the east of the north-trending line of roof pendents represents a slightly younger and independent pulse of magma and that the Kepenkeck Granite may be independent. However, the AMMS is thought to have developed in response to a relatively short lived tectonic and thermal event in this part of the Appalachian Orogen.

10-4-2 Pressures and Temperatures

The precise physical conditions of emplacement of the AMMS remain enigmatic. The presence of relatively fine grained miarolitic varieties of granite in the south and the southerly trending chemical gradients suggest that the AMMS is eroded to a deeper level in the northern part of the Hungry Grove Granite and in the Tolt and Meta granites. The gravity data also indicate thinner granites in the latter areas relative to the southern part of the Hungry Grove Granite and the Rencontre Lake Granite. However, thickness of preserved granite may be independent of the paleosurface. Finally, the narrow thermal aureoles in the country rocks adjacent to granites along the southern contact indicate a high crustal level of emplacement.

Whalen (1980) suggested that the increase in degree of fractionation towards the contact in the Rencontre Lake area resulted from in situ differentiation of a granitoid magma with a near minimum melt composition in the system quartz-albite-orthoclase-water at P_{H_2O} (total) between 0.5 and 1 kb. Dickson (1983) presented a similar argument for data from the Hungry Grove, Meta, Tolt, Rencontre Lake and Sage Pond granites.

Analogies with modern high-silica volcanic fields which are thought to be underlain by large active magma chambers suggests a depth to the roof of the chamber of 5 to 10 km (Hildreth, 1981; Hill et al., 1985; Boden, 1986). Depth estimates for the formation of Climax-type ore systems associated with small stocks which may represent 'pimples' on

the surface of larger underlying batholiths range from 1 to 3 km (White et al, 1981). Assuming that the Sage Pond greisen system represents conditions in the lower parts of the Climax-type system, estimated depth of formation is in the range of 3 to 5 km.

Muscovite from the Kepenkeck Granite has a significant Fe and Mg component and may be of primary origin. Experimental studies combined with thermodynamic considerations has led Miller et al. (1981) and Anderson and Rowley (1981) to suggest a minimum depth of formation of 9.6 to 11.5 km for celadonitic muscovite. Therefore, the available pressure estimates also indicate that the AMMS is exposed at deeper levels to the north.

The magma must initially have been undersaturated in water to permit its emplacement at shallow depths (Burnham, 1967, 1979; Brown and Fyfe, 1969; Strong, 1980). Excess water is indicated by the presence of miarolitic cavities, pegmatites, and gas breccias. The water saturation is commonly considered to result from differentiation and/or crystallization in the upper portions of the magma chamber.

Temperature estimates are also elusive. Hematite-ilmenite pairs suitable for application of the Fe- Ti-oxide geothermometer (Buddington and Lindsay, (1964) were not found, and fO_2 has not been determined, thus preventing use of the phlogopite-annite geothermometer (Eugster and Wones, 1965). Le Bel (1979) proposed a geothermometer based on the Ti

content of biotite. However, the data from the study area show a wide range of temperatures of crystallization between 800 and 300°C and the data for individual granitoid bodies do not cluster or form realistic patterns. A major assumption of these proposed geothermometers is that the relative variation in absolute temperatures determines the compositional gradients in the magma. This seems rather unlikely. It is probable that temperature gradients influence the development and magnitude of compositional gradients. Consequently, the compositional gradients in the study area may be intrepreted to represent magmatic temperature gradients (cf. Volkov and Gorbacheva, 1980). However, if cooling and crystallization is a dynamic feature related to progressive heat loss to deeper levels in the magma chamber, the temperature recorded by the mineral may not be representative of the temperature of formation of the compositional gradients, nor the final solidus temperature of crystallization.

Estimated temperatures of crystallization of phenocrysts in high-silica ash flows range from 650 to 900°C based on the Fe- Ti-oxide geothermometer (cf. Hildreth, 1979; Boden, 1986). Experimental studies (cf. Dingwell, 1985; Manning and Pichivant, 1985) show that the granite liquidus and solidus is depressed to 650°C in the presence of F, B, and Li, and that silicate melts can persist to temperatures of 550°C for appropriate volatile-rich compositions. Homogenization temperatures from primary fluid inclusions in topaz (Eadington, 1983) indicate a trapping temperature of 500 to 620°C (Eadington, 1983; Kinnard et al., 1985). The presence of griesen and the fluorine-rich composition indicate that the final solidus temperature of the AMMS in the southern part was in the

range 600 to 700°C while higher temperatures may be expected in the north. This study placed no constraints on the temperature of emplacement of the AMMS into the upper crust.

10-4-3 Chemically Zoned Magma Chamber

In the preceding chapters, the argument was presented that coarse grained varieties of granite in the northern part of the Hungry Grove Granite and in the eastern part of the Tolt Granite, when compared to fine grained, miarolitic varieties in the Rencontre Lake and Sage Pond granites, indicate a deeper level of erosion in the north and east. Sharp physical boundaries have not been observed between the different granites of the Ackley Granite Suite and the geochemical and gravity gradients trend across the gradational contacts between the member granites. Furthermore, REE, Rb-Sr, ^{40}Ar-^{39}Ar and oxygen isotope data independently demonstrate an internal homogeneity between the Hungry Grove, Meta, Tolt, Rencontre Lake and Sage Pond granites. These features are consistent with the concept that Ackley Granite Suite and associated mineral deposits were generated and emplaced through large scale processes operating to form an extensive magma chamber. The element enrichment/depletion trends, and the size of the Ackley Granite Suite suggest that these rocks represent a frozen, geochemically stratified, magma chamber analogous to those modelled by Hildreth (1979) as a precursor to large volume (> 100 km^3) high-silica ash flows (see Fig. 7).

The analogy with the physical model of the magma chamber envisaged by Hildreth (1979, 1981) is remarkable. The geochemical trends which culminate in the Sage Pond area are readily interpreted as reflecting a vertical geochemical gradient. These trends, the greater variability and higher concentrations of the incompatible elements, and lower concentrations of Ba and Sr, at above 74% SiO_2, are consistent with the concept of a high-silica 'enriched' roof zone.

Superimposed on the general geochemical trends are the steeper geochemical gradients adjacent to the mineralized areas at Rencontre Lake and Sage Pond, which are interpreted to reflect magmatic differentiation processes focussed at the walls of the AMMS. These are compatible with the suggestion by Hildreth (1981, p. 101):

> "an ascending chemical boundary layer probably forms a low-density counterflow and rises slowly along the walls .... and helps to enrich the growing roof zone in such volatiles".

The larger cellular patterns of less silicic compositions observed in the element distribution plans (Figs. 31 to 38) might represent areas of upwelling via convection cells in the main magma chamber, while areas of lower silica adjacent to the margins of the AMMS might represent areas of magma replenishment from below. Assuming that the Kepenkeck Granite was a part of the AMMS, possible convection was not on a scale large enough, or did not last long enough, to destroy the contrasts with the rest of the AMMS. The homogeneity of the initial strontium ratios

may support the argument for vigorous convection and mixing in the southern AMMS.

10-4-4 Speculations on The Results of Eruption

The Rencontre Lake Granite shows similarities to the Hungry Grove, Tolt, Meta and Sage Pond granites, particularly in major element concentrations and mineralogical and textural features. However, there are also significant differences which require explanation. The Rencontre Lake Granite has relatively low values for the incompatible elements, lowest fluorine values, and enrichment/depletion trends are less extreme at the granite margins. The estimated $\delta^{18}O$ values are below the normal magmatic range and are lower than the values for the remainder of the Ackley Granite Suite but Δ Q-F values are magmatic. Chlorite alteration of the mafic minerals is a common feature in the Rencontre Lake Granite and is rare in the rest of the southern AMMS. Mineralizing fluids were less saline and molybdenum (as opposed to tin and tungsten) is the element of economic interest.

In the Yellowstone Plateau Volcanic Field, silicic flows which post-dated caldera collapse exhibit depletion of $\delta^{18}O$ quartz ranging from 1 to 6 per mil relative to more normal magmatic values in extensive ash flows (Huckleberry Ridge Tuff, Mesa Falls Tuff and Lava Creek Tuff), which accompanied caldera collapse (Hildreth et al., 1984). Caldera collapse occurred at intervals of 0.7 and 0.6 Ma. Post-collapse volcanism records a temporal recovery towards pre-collapse isotopic values. Hildreth et al. (1984) suggested that the depletions resulted

from contamination of the magmatic system by meteoric water during periods of explosiwe activity which sustained access and mixing of water with the magma.

The Rencontre Lake Granite can be considered to represent a frozen magma chamber which was in the process of recovering from caldera collapse. Mixing of meteoric water with the magma could account for the lower $\delta^{18}O$ in this area. In addition, the abundant physical evidence for saturation of the magma with water is readily explained by post-emplacement H_2O ingestion and the requirement for saturation due solely to postemplacement fractionation of an anhydrous parent would not be necessary.

The concept that the Rencontre Lake Granite was quenched as it was undergoing a process of post-collapse recovery can explain other features of this granite. The absence of steep and highly evolved incompatible element trends can be explained by loss of the upper magma layer during eruption. The more erratic element distributions in the Rencontre Lake Granite relative to the Hungry Grove and Sage Pond granites (e.g. Ba, Sr, Y) can be explained by turbulence in the magma chamber due to caldera collapse and the weak trends observed are those which form during the initial attempt of magma chamber to re-attain equilibrium. The higher element covariations could be related to the fact that the differentiation processes were extremely active after collapse in an attempt to regain equilibrium in the magma chamber. Upwelling of the more mafic areas may result from the turbulence due to eruption and collapse. Partitioning of fluorine into the volatile phase

and its loss to the magma system, may have occurred during caldera collapse, with the addition of excess water post-dating this event. Minor fluorite mineralization at the Rencontre Lake Prospects therefore relates to the magma recovery process and not to the regional geochemical patterns in the Rencontre Lake Granite. In addition, it is possible that the medial trace element concentrations in the Tolt and Meta granites reflect intermediate to late stages in the post-collapse recovery process.

Thus the relative immaturity of the Rencontre Lake Granite when compared to the Sage Pond Granite is possibly due to dynamic features of the magmatic-volcanic cycle. Alternative explanations are (i) different source rocks or (ii) other, more evolved granites had a longer emplacement and fractionation history. There is no evidence for different source rocks, and the lower oxygen isotope ratios are not explained and the ambiguities in the behavior of water and fluorine are more difficult to reconcile using an emplacement model.

10-5 FRACTIONATION PROCESSES

10-5-1 Introduction

The similarity of geochemical trends frozen in the AMMS to those inferred for the Bishop Tuff magma chamber (Hildreth, 1979, 1981) implies a similarity of processes. The following discussion will attempt to evaluate the possible mechanisms of chemical fractionation using the data presented from the Ackley Granite Suite.

One of the fundamental requirements of a chemical fractionation model is to explain the differences in behavior of the trace elements above and below the 74% SiO_2 level. These differences in both scatter and degree of enrichment/depletion of elements were illustrated by the Harker diagrams and by the factor analysis. By definition, Factor 1 (major elements) is independent of Factor 2 (trace elements), which implies different processes.

10-5-2 High-Level Crustal Melting and Assimilation

The available geochemical data from the host rocks to the Ackley Granite Suite (Whalen, 1976; Chapter 5) indicate that assimilation and element exchange of the country rock cannot produce the observed trends in the AMMS. The values for incompatible trace elements in the country rock are too low and the values for the compatible elements are too high. There is no evidence for partial melting of the country rocks adjacent to the AMMS and partial melting at depth would still require emplacement and geochemical fractionation to produce the observed trends.

10-5-3 Crystal/Melt Fractionation

Trends like those observed in the Ackley Granite Suite have generally been attributed to crystal-melt fractionation accompanied by filter pressing (McCarthy and Hasty, 1976). Whalen (1983) modelled crystal-melt fractionation in the Ackley Granite using selected data from his study area and a selected sample located 20 km to the north from the Hungry Grove Granite (the REE pattern from the Rencontre Lake

Lake area used by Whalen (ibid.) to model crystal liquid fractionation indicates that the REES have been depleted by magmatic fluids). Whalen's (ibid) conclusions were that crystal-liquid fractionation with large melt/crystal partition coefficients could produce the observed variations.

Published melt/crystal partition coefficients for the REE in feldspars from high-silica systems (Hanson, 1980) indicate that the melt should be enriched in all REE during crystal-liquid fraction, assuming that feldspars were the main fractionating phase. This is not the case since the LREE do not show a consistent trend. The possibility that fractionation and removal of hornblende at depth may contribute to observed trends cannot be evaluated. However, hornblende is absent from much of the exposed granite and therefore does not directly contribute to generation of the observed geochemical trends. The possibility of producing the observed REE patterns by fractionating accessory minerals remains, but fractionation of accessory minerals is unlikely to produce the observed behavior in highly incompatible elements such as Rb, Nb and Ta. In addition, Gromet and Silver (1983) argue that the bulk of the REE reside in accessory phases such as sphene and apatite which form early in the crystallization sequence; REES are therefore unlikely to serve as a good fractionation index in the granitic environment.

The differences in behavior of the trace elements above and below 74% SiO_2 would require either a sudden change in bulk partition coefficients in the upper portion of the AMMS, or the appearance of new phases for both fractionation and accumulation. It is possible that the

former could happen, e.g. due to melt depolymerization and complexing of elements of high ionic potential (Watson, 1979; Hess, 1980). There is no evidence for the fractionation of minerals which would be necessary to bring about the observed chemical variations.

Much of the southern exposures of the Ackley Granite Suite are equigranular and textures do not suggest cumulate processes. Rather, the textures are considered to represent rapid quenching of alkali feldspar and possibly quartz in response to loss of fluid pressure. Furthermore, it is unlikely that a process of separation of residual liquid could produce such consistent geochemical patterns over such a large area, or the enrichment and depletion patterns adjacent to the magma chamber walls. Therefore, a simple process of crystal-liquid fractionation cannot explain the observed features in Ackley Granite Suite.

10-5-4 Volatile Transfer

Burnham (1967) has demonstrated that a number of elements of interest would be partitioned into a volatile phase coexisting with the melt, especially in the presence of Cl, and it is reasonable to suggest that such a process operated in the AMMS. Such a suggestion is especially attractive with the abundance of physical evidence for the separation of a volatile phase in the southern parts of the AMMS, i.e. where the incompatible elements are most enriched. Nevertheless, in the Hungry Grove and Sage Pond granites, these enrichments and volatile textures are the end-products of smooth trends over a much larger area, where the physical evidence for volatiles is not present.

REE concentrations do not indicate widespread separation of a volatile phase during crystallization, but indicate that volatile activity is concentrated in areas of known mineralization. It is also difficult to explain how magmatic devolatilization could produce the extreme depletion of Ba and Sr. These elements substitute for K and Ca in the silicate phases and are unlikely to partition strongly into possible fluid phases. An upward flow of volatiles and incompatible elements would require a downwards migration of Ba and Sr unless these elements were removed from the system completely.

Volatile activity is not considered to be a viable mechanism to explain the overall geochemical trends in the AMMS, although partitioning of ore elements and fluorine into, and deposition from, a fluid phase was necessary to form the mineral prospects. Volatile exsolution was a result of, rather than a cause of, magmatic concentration mechanisms in the magma chamber.

Subsolidus hydrothermal alteration features include albitization, perthite formation, chlorite alteration of biotite in the Rencontre Lake Granite, and minor muscovite alteration in the Sage Pond and Hungry Grove granites. Visual evidence of alteration is absent except for an area of less than 1 km^2 around the Wyllie Hill prospect. The magmatic oxygen isotope signature of mineralization and adjacent granite preclude transfer of elements below a temperature of 350°C. Arguements against volatile transfer of elements in the AMMS are also applicable to high temperature subsolidus transfer amd there is no evidence to indicate that Bu and Sr were removed from the system by a subsolidus fluid phase.

10-5-5 Liquid-State Diffusion

As the evidence does indicate that the AMMS was a layered magma chamber like that envisaged by Hildreth (1979) with a high-silica cap overlying a less silicic magma, it could be that his proposed fractionation model of liquid-state thermogravitational diffusion (TGD) is the most acceptable one for the AMMS, a suggestion also made by Whalen (1983). This model invokes temperature-induced element-diffusive gradients in the high-silica stagnant roof zone above a vigorously convecting magma chamber, with supply of elements to the static zone aided by convection in the main magma chamber. This process is difficult to evaluate and has been opposed from both experimental (Lesher et al., 1982) and theoretical (Michael, 1983) perspectives.

Transport of elements across an interface with a static high-silica roof zone may have occurred by diffusion and may account for the differences in element concentrations above and below 74% SiO_2. The steep trace element gradients in the mineralized areas are also in agreement with aspects involving chemical specialization at the walls of the magma chamber (Hildreth, 1981).

10-5-6 Convective Fractionation

Convective fractionation (Rice, 1981; Sparks et al., 1984) is defined as "any fractionation process involving convection of fluid away from crystals". Sparks et al. (1984) suggested that as crystals grow in a closed system they locally deplete the adjacent fluid in the denser

compositions, and that the resulting less dense fluid would rise convectively and accumulate at the top of the system. In a magma system, the less dense material would essentially consist of the felsic components (commonly interpreted to represent "petrogeny's residua system"; Bowen, 1956), along with the LIL elements. The 'residua' components would retain their identity and remain separate from the main magma chamber due to the low chemical diffusivity and density contrasts. These authors emphasize that such a process would be particularly effective at the walls of the magma chamber where cooling is fastest, and would allow for effective fractionation of crystals at the boundary layer to produce major changes in the resulting liquid which then migrates upwards along the boundary.

This hypothesis removes one of Hildreth's (1979) major objections to crystal fractionation, ie. the necessity to remove unreasonably large proportions of crystals. Michael (1983) pointed out that fractionation of 65 to 70% of the observed phases could explain the variations in the Bishop Tuff (e.g. extreme Ba and Sr depletion). Sparks et al. (1984) show that sidewall crystallization and crystallization in the lower regions of the magma chamber could provide a physical and chemical mechanism of fractionation.

The convective fractionation model of Sparks et al. (1984) could be self-enhancing in that magma in the zone of crystallization would become progressively depleted in Ba and Sr and enriched in LIL elements. Later, least dense material to rise to the top of the magma chamber would be the most evolved, accounting for observed zonations

and the contrasts in element behavior around 74% SiO_2. In the case of the AMMS, the geochemical trends in the mineralized areas would represent areas of uprise of low density enriched liquids. The low density residual could also be depolymerized (Hess, 1980), thus enhancing its eventual stability at the top of the system. The local abundance of feldspar in the less silicic compositions in the AMMS might represents areas of crystallization at the base or along the lower walls of the magma system.

In the southern parts of the Hungry Grove Granite and in the Sage Pond Granite, highest silica values are spatially separated from the highest incompatible element values. This suggests that concentration of the SiO_2 and these trace elements was in part independent, or more probably that a process of segregation occurred at the roof of the magma system. For example, diffusion of the trace elements to the margins of the chamber may have been superimposed on the main segregation process, or silica enrichment through magmatic or volatile processes may occur towards the roof of the system while the trace element enrichment processes may be more effective along the margins of the system.

It is concluded that a process of convective fractionation (Sparks et al., 1984) coupled with the physical model presented by Hildreth (1979, 1981) can adequately explain the chemical and physical aspects of the zonations in the AMMS.

10-6 THE MINERALIZING PROCESS

From a metallogenic viewpoint, the geochemical trends in the AMMS can be considered to represent large magmatic systems which ultimately evolved to form Mo-bearing deposits in the Rencontre Lake Granite and Sn-W bearing deposits in the Sage Pond Granite. The culmination of the chemical trends at the areas of most significant mineralization, together with the magmatic oxygen isotope signature of the host granite and of the alteration associated with the mineralization, indicates that the minerals of economic interest and the fluids which caused their formation originated in the AMMS. In addition, the mineralizing processes may have operated most efficiently at the margins of the magma chamber to form deposits with similar morphology. The contemporaneity of mineralization and the host granite is also indicated by the ^{40}Ar-^{39}Ar ages. Segregation of Sn and Mo therefore originated in the AMMS.

It is envisaged that mineralization was formed through a combination of primary ore element concentration in the carapace and and at the walls of the magma chamber, followed by further concentration and deposition of ore elements by fluids directly evolved from a quenching magma. The fluids were commonly ponded at the walls and roof of the chamber. Crystallization of the magma at slightly deeper levels may have provided additional fluids and metals to the mineralized areas. It is again emphasized that the chemically evolved, mineralized granites are not considered as late differentiates. Rather, they are formed along with the main granite batholith, and crystallization may even precede that in the main chamber. The high-temperature, magmatic, oxygen isotope

signatures indicate that extensive meteoric circulation was not an important aspect of the mineralizing process.

Patterns of variation in mineralogy, texture and major element trends (plus Ba and Sr) are identical in both areas, indicating that the large scale petrogenetic processes which led to the spatially separated Mo and Sn-W deposits were similar (i.e. convective fractionation dominated by crystallization of K-feldspar and plagioclase at depth). Therefore, controls over the final product (ie. Sn or Mo) were developed late in the magmatic evolution of the AMMS.

Fluid inclusion studies indicated that compositions of the fluids associated with mineralization may be similar, but that fluids in the greisen veins are considerably more saline than those from the molybdenite deposits. Accurate estimates of temperature and pressure of fluid entrapment cannot be made. However, minimum trapping temperatures above 370°C are common.

The association of topaz and fluorite with the greisen and the enrichment of fluorine in the host granite at Sage Pond indicate the importance of fluorine to the Sn-W mineralization process. In contrast, the relative lack of fluorine in the Rencontre Lake area is reflected by the absence of topaz, trace amounts of fluorite associated with mineralization, and the relative geochemical immaturity of the Rencontre Lake Granite. Therefore, it is probable that the differences in mineralization relate directly to the observed chemical features in the host granites. For example, fluorine may have been unavailable in the

Rencontre Lake Granite for transport and concentration of Sn-W by fluorocomplexes, while Mo may be complexed by Cl-rich aqueous phases (Tingle and Fenn, 1984; Candela and Holland, 1984). Molybdenite deposition might also reflect lower fO_2 in the Rencontre Lake Granite (as suggested by the whole rock ferric/ferrous oxide ratios) or higher fS_2 as compared to the Sage Pond area. It has been suggested that fluorine escaped into the vapour phase, and water was added to the magma system, during eruption and caldera collapse in the Rencontre Lake area. This suggestion implies that physical aspect of the magmatic-volcanic cycle are important controls over mineralization.

10-7 HYPOTHETICAL MODEL OF THE AMMS

A conceptual model of the AMMS is presented in Figure 75 and incorporates the features discussed in the previous sections along with those shown in Figure 74. The upper diagram (75A) has vertical exaggeration and shows sidewall crystallization and trace element enrichment patterns towards the chamber walls and roof in the Sage Pond and Hungry Grove granites at silica levels greater than 74%. Deeper level of erosion is thought to have occurred towards the north. The lower diagram (75B) approximates true scale; the large convection cells are hypothetical.

The heat source depicted in Figure 76B is modelled after the basaltic input (mafic underplating) envisaged by Hildreth (1981). It is also possible that the heat source was generated in the anorogenic environment by uprise of mantle material in an extensional environment

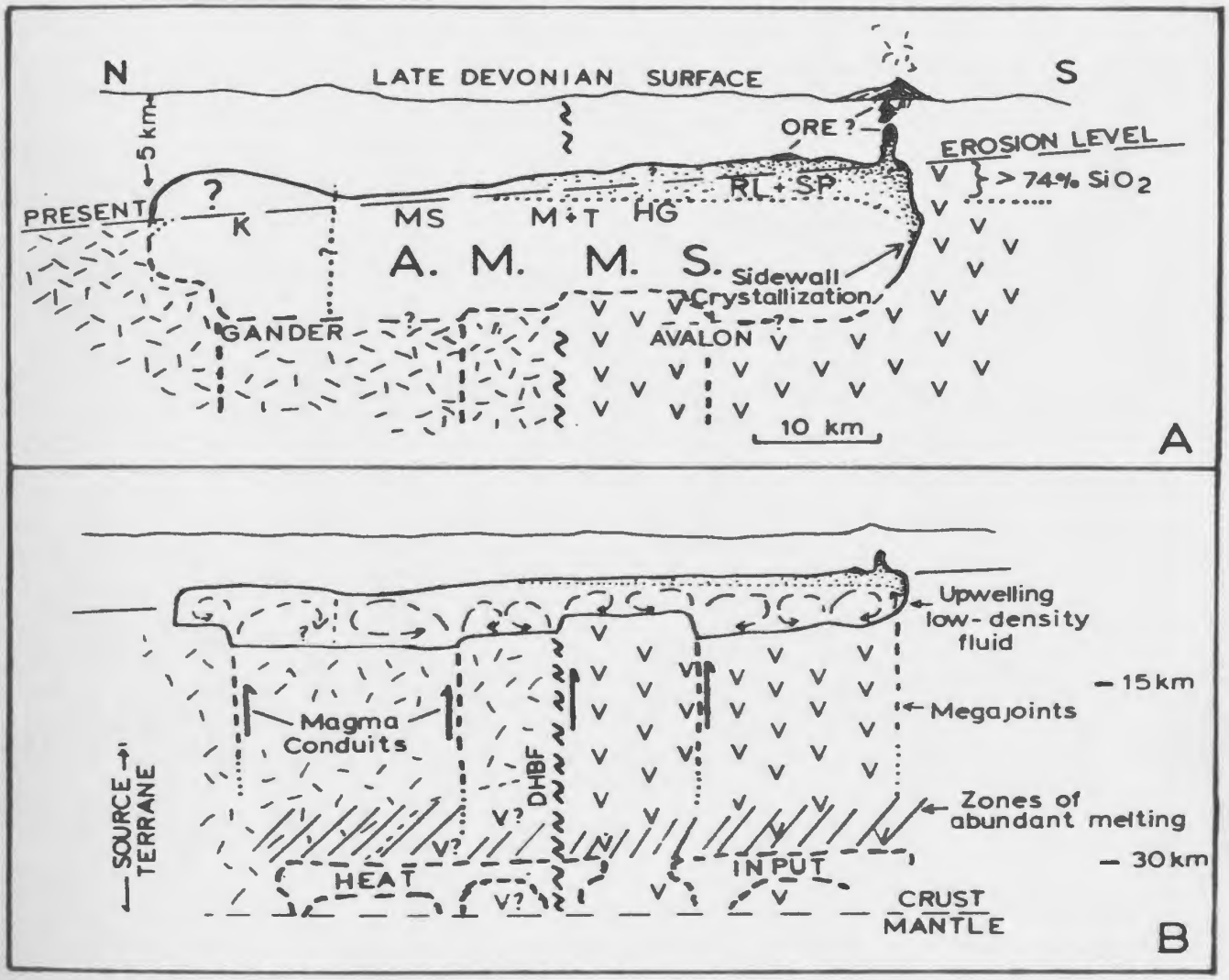

Figure 75: A: Model of the Ackley Magmatic/Metallogenic system. K-Kepenkeck, MS - Mount Sylvestor, M - Meta, T - Tolt, RL - Rencontre Lake, SP - Sage Pond. Stippled area is high-silica zone.
B: Model at same vertical and horizontal scale showing downward stoping of crustal blocks and upward movement of magma (arrows) along megajoints. Zone of melting inferred near crust/mantle interface. Convection cells inferred in main magma chamber.

(cf. Thompson et al., 1984); the possibility of mantle input to the chemistry of the AMMS cannot be evaluated on the basis of the current data.

10-8 SUBSOLIDUS HISTORY

In the southeastern granites, ubiquitous perthite textures, which coarsen southwards, attest to the presence of pervasive subsolidus hydrothermal systems throughout the AMMS. This conclusion is supported by the secondary muscovite in the Sage Pond and Hungry Grove granites and chlorite in the Rencontre Lake Granite.

The available $^{40}Ar/^{39}Ar$ ages from biotite-hornblende pairs are identical. Thus significant age differences between cooling through the blocking temperature of hornblende to biotite (ca. 500 to less than 300°C) (Purdy and Jager, 1976; Jager, 1979; Harrison and McDougall, 1980; Harrison, 1981) cannot be recognized. The Rb-Sr ages are approximately 15 Ma younger than the $^{40}Ar/^{39}Ar$ ages. Rb is presumed to reside predominantly in alkali feldspar which is subject to recrystallization down to 150°C, and it has been suggested in Chapter 7 that cooling through the temperature interval 300-150°C may have occurred over 15 Ma. Widespread deviation of the Δ quartz-feldspar values from normal magmatic values has been attributed to water-rock equilibration in large, low temperature, low- $\delta^{18}O$, meteoric hydrothermal systems which developed in the cooling granite. Postulated large scale meteoric hydrothermal systems may have developed during the low temperature interval of relatively slower cooling.

The subsolidus textural features focus on mineralized areas, which implies a direct relationship between the subsolidus systems and the mineralization processes. However, oxygen isotope signatures of the mineralized systems are high-temperature and dominantly magmatic. It is suggested that these magmatic oxygen isotope signatures were preserved because of rapid cooling below the blocking temperature for feldspar exchange (150°C) at the granite margins. Low temperature meteoric systems could have been most extensively developed in the central portions of the south eastern granites where cooling may have been slower. Consequently the subsolidus crystallization is a relatively high temperature event.

The spatial correlation of subsolidus recrystallization textures with the mineralized portions of the magma chamber are considered to reflect the probabilty that the largest volume of high temperature magmatic fluids passed through the roof zone. These textures are independent of the amount of deviation from the magmatic trend shown by the Δ quartz-feldspar values, supporting the conclusion that the low temperature systems were not involved in mineralization.

CHAPTER 11 - DISCUSSION AND CONCLUSIONS

"All cases are unique and very similar to others"

T. S. Elliot

11-1 DISCUSSION

11-1-1 The Equilibrium State of the System and Controls on Metallogeny

Implicit in the model presented above are the evolutionary or dynamic aspects of the AMMS. These suggest that with slow cooling through time, the system ultimately evolves to a chemical and density layered, stable configuration, with the quartzo-feldspathic components and incompatible elements concentrated in the roof zone of the magma chamber (cf. Hildreth, 1979. 1981).

The progression to an equilibrium state can be interrupted by cooling across the solidus, or by pressure quenching across the solidus due to loss of vapour. Alternatively, as has been suggested for the Rencontre Lake Granite, catastrophic events such as caldera collapse and eruption could interfere with the equilibrium configuration, and may ultimately lead to solidification. These catastrophic events may be due to volatile oversaturation in the roof of the system, thus the process is self-destructive.

Most of the large, high-silica ash flows that have been adequately studied are chemically zoned, as are many of the high-silica granitoid

plutons (cf. Hildreth, 1981; Boden, 1986) lending credence to the universality of the process of zonation in high-silica systems.

The inferred relationship between Mo mineralization and less mature, water saturated magma, and between Sn-W mineralization and chemically mature, anhydrous magma, also implies an evolutionary process related to the development of the magma system, with Mo mineralization preceding fluorine rich Sn-W mineralization. As the system develops and as fluorine and incompatible element concentrations build up in the roof zone, a greater tendency to produce Sn-rich greisen deposits can be expected. This temporal relationship is also indicated in the classic Climax-type environment where the Mo-W ore shells are cut by later topaz-rich Sn veins (White et al, 1981) and at the Mount Pleasant deposit in New Brunswick (Kooiman, et al., 1984). Climax-type systems also show the effects of excess water by the abundance of breccia pipes associated with molybdenite mineralization. The magma system may also become progressively more anhydrous if H_2O is lost from the magma chamber, either through eruptive or diffusive processes.

Thus there would appear to be significant temporal and physical controls over the primary mineralizing process in high-silica magmas which are essentially related to the degree of maturity of the chemically zoned system. It is envisaged that F ± B ± Li enrichment in a water-undersaturated magma may eventually lead to the formation of topaz-tin-bearing granites and to topaz-tin-bearing rhyolite when the LIL-rich magma is erupted. Burt and Sherridan (1985) and Taylor et al. (1985) emphasize the physical and possibly genetic differences between

the topaz bearing high-silica systems, Climax-type systems, and associated plutonic rocks. However, the similarities are more compelling to this author. Taylor et al. (1985) report the presence of adjacent biotite granites and topaz granites from the Mount Pleasant area which are presumably petrogenetically related to the larger, 'A-type', St. George Batholith (Whalen, 1986). The observations from the AMMS are applicable to this discussion since minor topaz is present in granites adjacent to the larger greisen veins in the Sage Pond area, confirming the direct genetic association. Undoubtably, there are additional chemical and volatile controls which serve to partition the elements of economic interest.

The crystallization history of the granite body will also affect the apparent relationship between the different intrusive phases. For example, a chilled carapace may be intruded by either less evolved or more evolved magma which subsequently freezes. However, the general assumption that the most evolved granite is the youngest intrusive phase requires careful consideration due to the dynamics and the temporal variation in maturity of the cooling magmatic-volcanic system. While the preserved mineralization discussed in this thesis is focussed at the margins of the magma chamber, other areas (cf. Cornubian Batholith; Stone and Exley, 1985) indicate extensive mineralization in cupolas on the upper surface of the magma chamber. This may relate to fluid and economic-element accumulation at the upper surface of the magma system which locally may be aided by the internal topography of crystallized carapaces in the system.

The geochemical and oxygen isotope evidence indicates that ore metals are derived from the magma, and the scale of the process envisaged can readily convert parts per billion in the magma to ore grades and tonnages at the roof of the magma chamber. Therefore, trace element signatures of source rocks may not be a critical factor. However, LIL-element enriched source rocks would undoubtably enhance mineralizing processes and depress the solidus, thus permitting emplacement of the magma to very high crustal levels, as elaborated in the model of Strong (1981).

11-1-2 Mineralization and Thickness of the Magma Column

The negative bouguer gravity anomalies indicate that the chemically evolved granites in the Rencontre Lake and southern part of the Hungry Grove granites are thickest. These areas are also the locale of the mineral deposits. Gravity studies in other large mineralized plutons show a similar relationship.

This relationship may partly reflect the fact that the roof facies will be preferentially preserved in areas of shallow erosion. Such an interpretation is possible for the Ackley Granite Suite, since the available evidence does suggest that deeper levels are exposed to the north and east. The relationship between thicker high-silica granites and the strong trace element enrichment/depletion trends may therefore suggest a depth or pressure control over the fractionation process. Perhaps depolymerization and volatile complexing is retarded at greater depths, causing large deposits to occur at high crustal levels.

An alternative interpretation is that the thickness of the magma column relates strongly to the ability to produce zoned high level systems. Thus a thicker fractionation column would result in a greater concentration of incompatible elements at the roof.

11-1-3 Classification of the AMMS

Dickson (1983) considered the northwestern granitoids to be petrogenetically distinct and less evolved than the southeastern granites which show a relatively greater degree of differentiation. He noted that the Koskaecodde and Mollyguajeck plutons have calc-alkaline affinities and that the other granites do not. The southeastern granites have alkaline affinities (Peacock, 1931). Dickson (1983) noted that most of the AMMS may be considered as I-type (Fig. 76), while the Kepenkeck Granite has some characteristics representative of S-type plutons. Whalen (1980) noted also that the granites in the Rencontre Lake area may be classified as I-type and in 1983 noted that these rocks are similar to anhydrous, alkaline, anorogenic, A-type plutons described by Loiselle and Wones (1979).

All of the samples from the southeastern granites and the samples from the Kepenkeck Granite plot in the field of A-type plutons on the Ga-Al_2O_3 discriminant diagram and most samples plot in the A-type field on the Na_2O-K_2O plot (Fig. 77; White and Chappell, 1983). Figure 78 shows the regional geochemical data summarized on a trace element discriminant diagram constructed by Winchester and Floyd (1977). The data from the southern granites, particularly the Rencontre Lake and

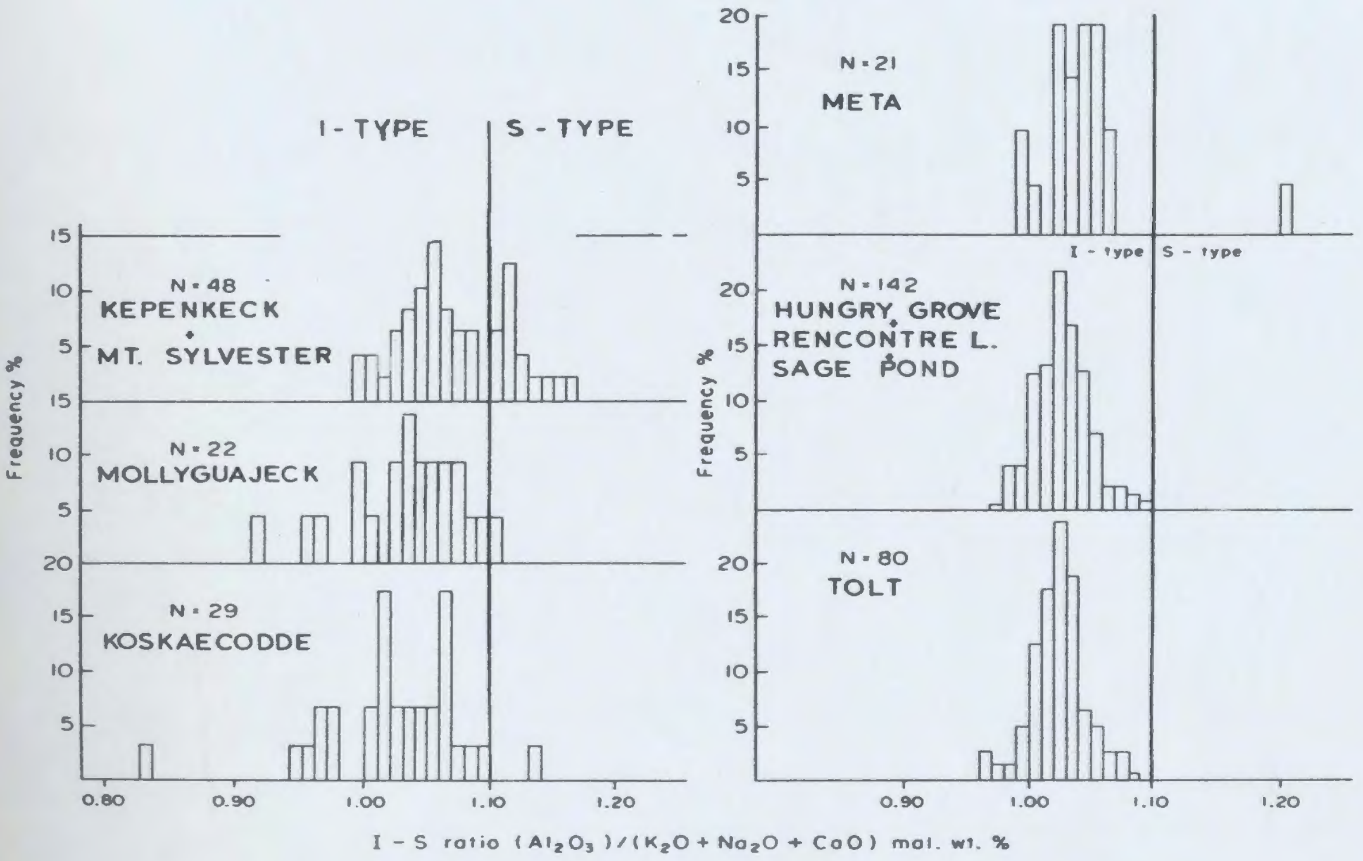

Figure 76: Histograms of ratios of Al_2O_3 / (K_2O + Na_2O + CaO) mol. wt % in the study area. Ratio < 1.0 - metaluminous, > 1.0 - peraluminous (Shand, 1950). Ratio < 1.1 - I-type, > 1.1 - S-type (Chappell and White, 1974). From Dickson (1983).

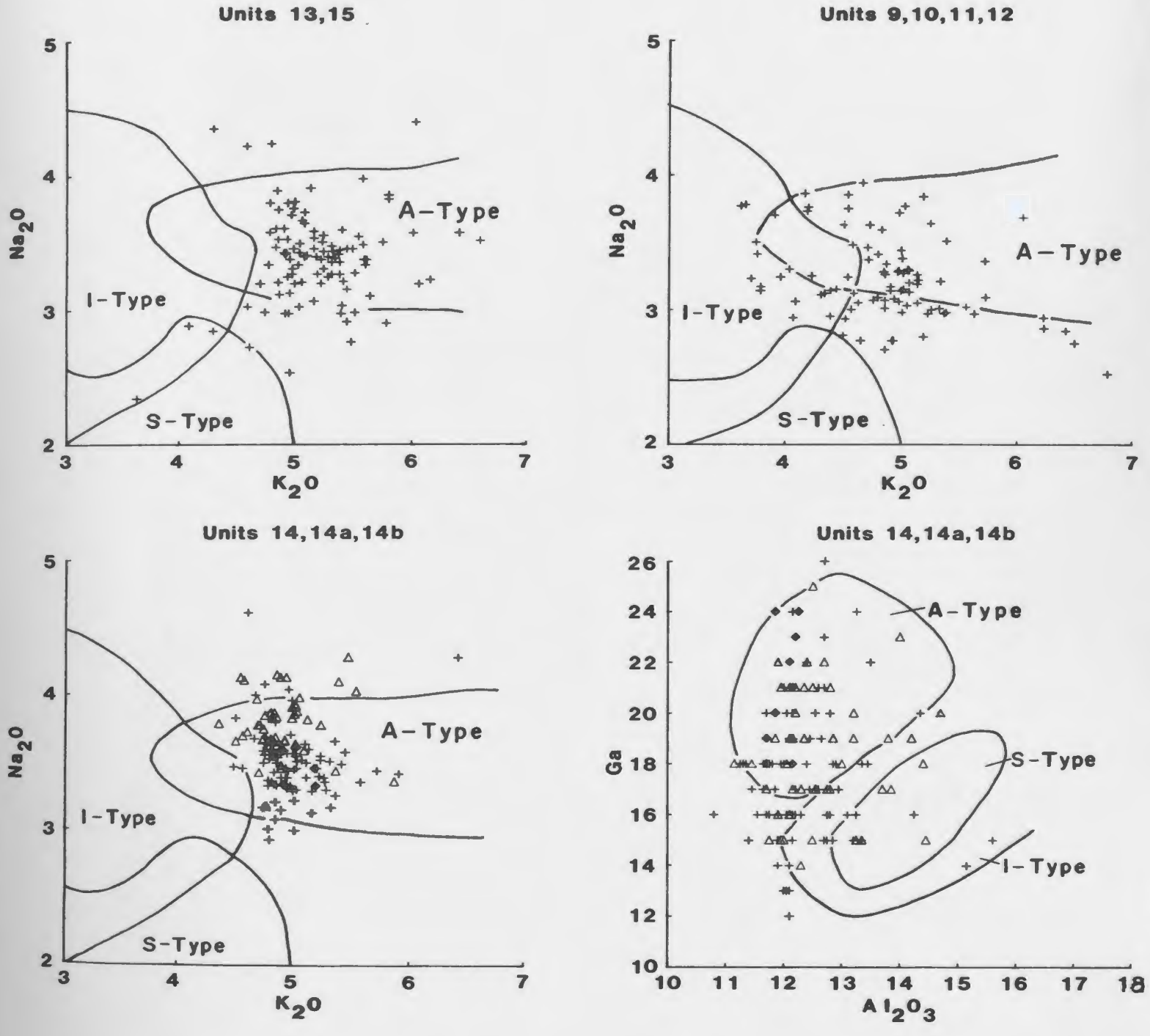

Figure 77: Na_2O versus K_2O diagrams and a Ga versus Al_2O_3 diagram showing fields of I-, S-, and A-type granites. After White and Chappell (1983). 9 - Koskaecodde, 10 - Mollygaujeck, 11 - Mount Sylvester and Kepenkeck, 13 - Tolt, 14 Hungry Grove, 14A (open triangles) - Rencontre Lake, 14B (solid diamonds) - Sage Pond, 15 - Meta.

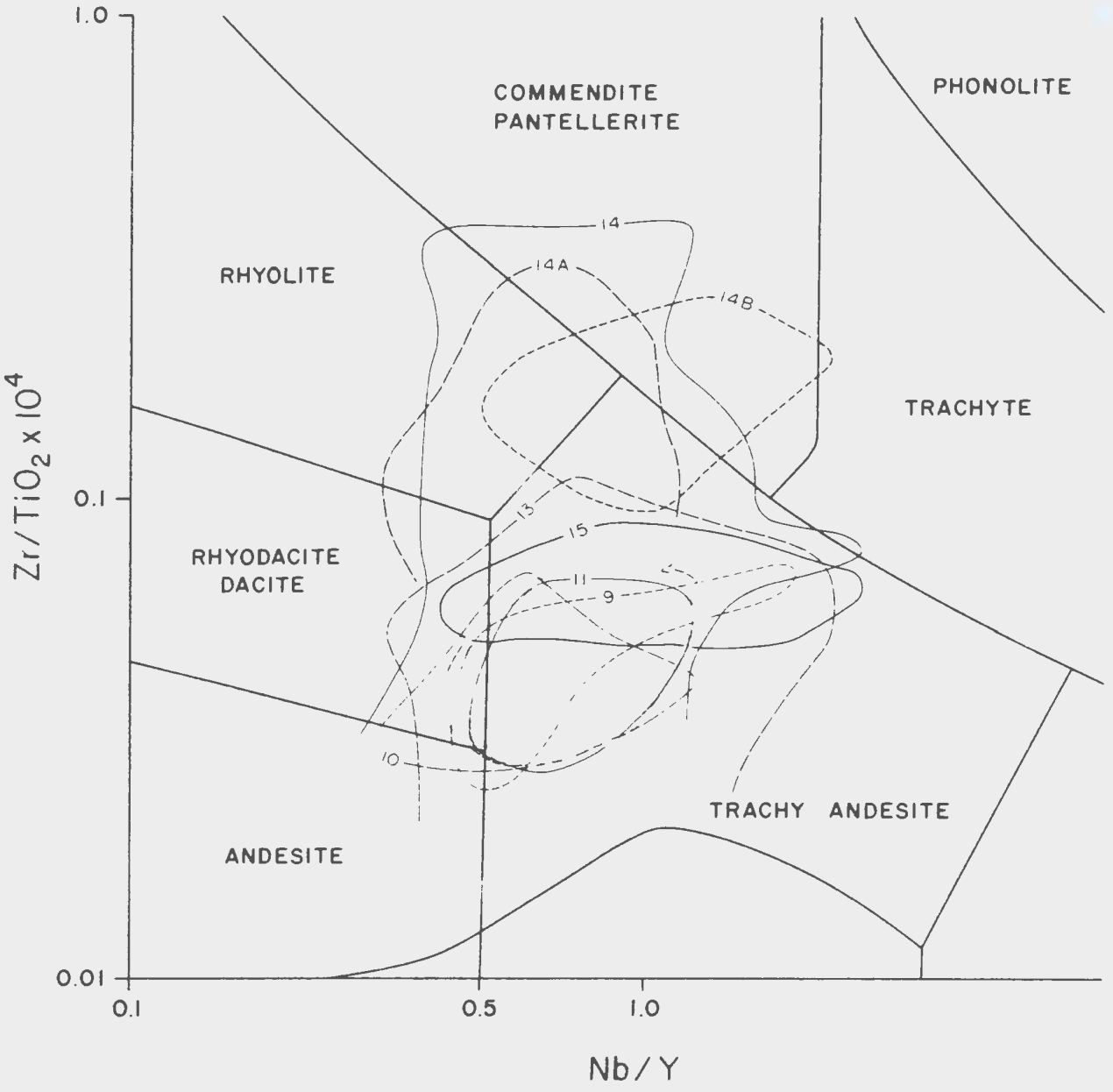

Figure 78: Plot of $Zr/TiO_2 * 10^4$ against Nb/Y for data from the study area. 9 - Koskaecodde, 10 - Mollyguajeck, 11 - Mount Sylvester + Kepenkeck; 13 - Tolt, 14 - Hungry Grove; 14A - Rencontre Lake; 14B - Sage Pond; 15 - Meta. Field boundaries are those of Winchester and Floyd (1977).

Sage Pond granites, show a slight overlap into the commendite field. These diagrams suggest an evolutionary trend towards peralkalinity in the most evolved parts of the Ackley Granite Suite.

Most samples from the study area plot in the field of Within Plate Granites (WPG) on the Nb-Y diagram (Fig. 79A; Pearce et al., 1984) assuming that the geological setting precludes an Ocean Ridge Granite (ORG)-environment for the study area. The Rb-Y+Nb diagram is the best discriminator (Fig. 80A), with most samples plotting in the field of WPG and samples from the Koskaecodde and Mollyguajeck plutons plotting in the field of Volcanic Arc Granites (VAG). The Ta-Nb diagram (Fig. 79B) shows an overlap between the WPG, ORG, VAG and also has one sample each from the Mollyguajeck, Kepenkeck and Mount Sylvester plutons in the field of Syn-Collision Granites (SYN-COLG). Finally, the data plot in both the fields of SYN-COLG and WPG on the Rb-Yb+Ta discriminant diagram (Fig. 80B). In conclusion, the plots indicate (somewhat ambiguously) that the Ackley Granite Suite has the chemistry of a post-tectonic WPG, with some components of a syn-COLG. The more mafic samples plot in the field of VAG and syn-COLG.

The high K_2O content and the elevated values of U and Th in the southeastern Ackley Granite Suite classify these rocks as High Heat Production granites (cf. Halls, 1985). Granites enriched in these elements have potential for hydrothermal power generation.

The geochemical features described above demonstrate an anorogenic signature to the southeasten granites of the Ackley Granite Suite.

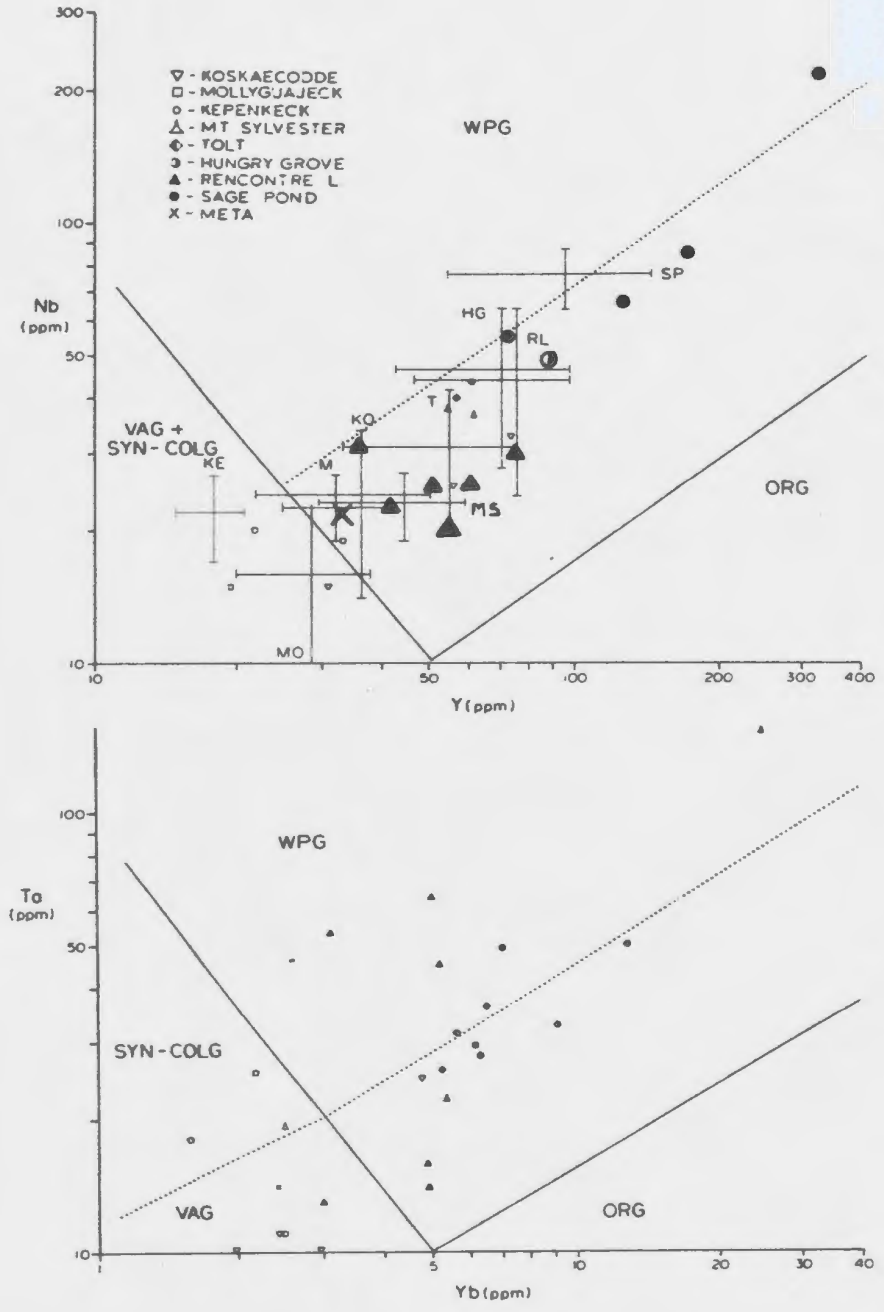

Figure 79: Discriminant diagrams. WPG - Within Plate Granites; SYNCOLG - Syn-Collision Granites; VAG - Volcanic Arc Granites; ORG - Oceanic Ridge Granite. After Pearce et al. (1984).
A: Nb versus Y. + is mean plus one standard deviation for units identified by abbreviations (see Figure 57). Data from Table 8.
B: Ta versus Yb.

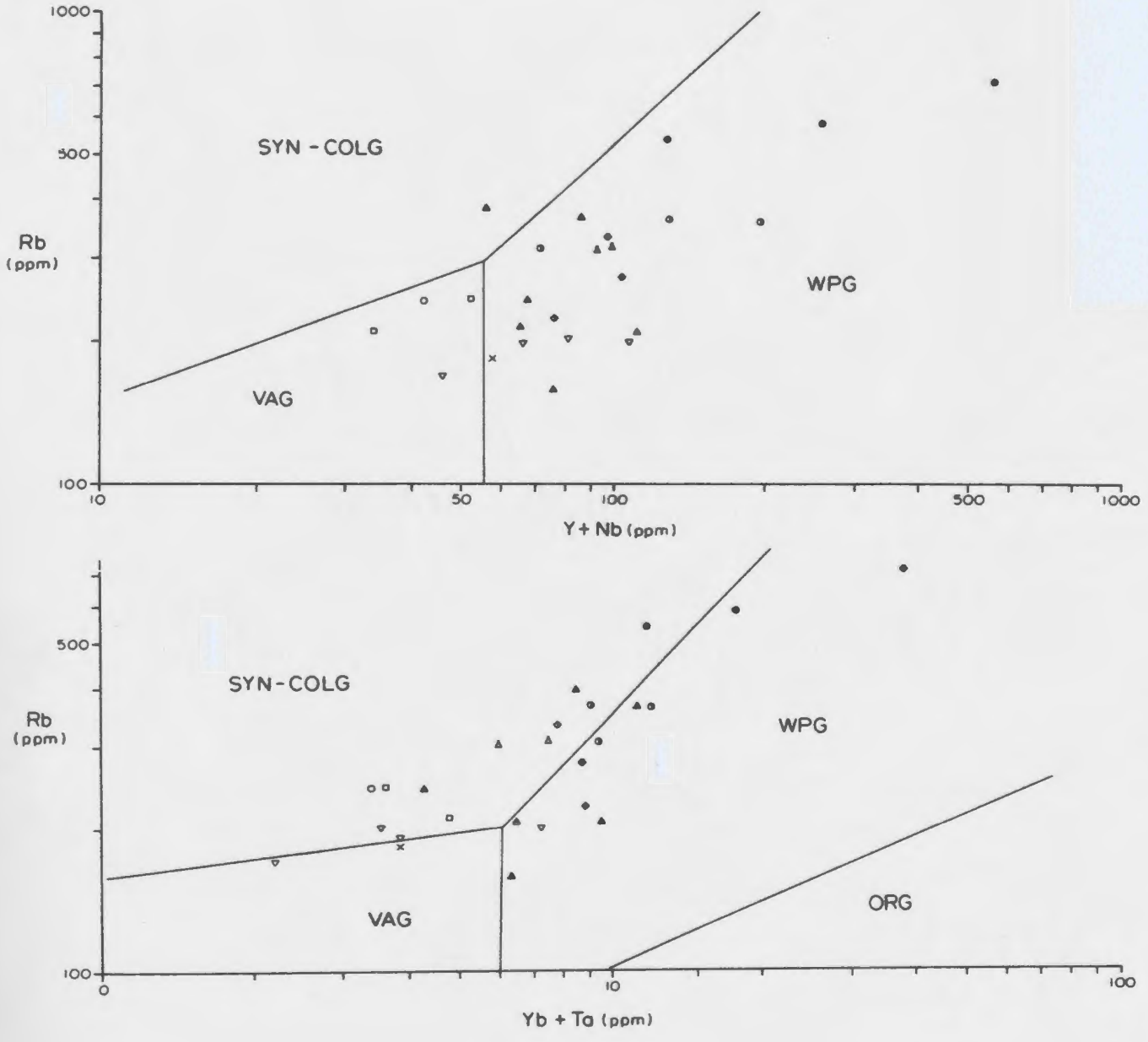

Figure 80: Discriminant diagrams. Symbols and abbreviations on Figure 79. After Pearce et al. (1984).
A: Rb versus Y+Nb.
B: Rb versus Yb+Ta.

However, geological information is necessary to interpret the data. While the Ackley Granite Suite exhibits A-type affinities, it is questionable whether this description is an improvement on the petrological classification of alkali-feldspar granite.

11-1-4 Metallogenesis and Other Granitic Systems

The question arises whether the convective fractionation process is applicable to the genesis of granophile deposits asociated with S-type or aluminous granites. Unfortunately, detailed studies comparable to those in the AMMS are not currently available and direct comparison is not possible.

Tischendorf (1977) divided the granites related to mineral deposits in the Erzgebirge into an Older and Younger complex. The younger complex was further divided into intermediate and chemically specialized granites. The implications are that there is a genetic progression from less evolved to highly evolved mineralized granite. Data from deep drill holes have shown that there is a vertical chemical gradient underlying mineralized areas with least specialized rocks at the bottom of the hole.

The geochemistry of the peraluminous, South Mountain Batholith (SMB) in Nova Scotia has been discussed in some detail by Chatterjee et al. (1983). This batholith is host to the recently discovered East Kemptville tin deposits which are located in a lobe of specialized granite on the generally steep contact of the granite with the country

rocks (Richardson et al., 1982), again implying an important sidewall component to magmatic-metallogenic development of this deposit. Data from the SMB are summarized in Table 1 and Fig. 2.

A plot of Rb versus K_2O for data from the SMB is presented in Figure 81 and there is a clear distinction between specialized and non-specialized granites. Also shown on this diagram are the data from various units of the study area, along with data from the granites adjacent to the greisen veins in the Sage Pond area. Although none of the regional samples from the study area reach the low background K/Rb ratio seen for the SMB specialized granites, data from the Sage Pond Granite tend towards those ratios. Data for samples adjacent to the greisen veins overlap, and fill the gap between specialized and non-specialized granites of the SMB. Thus data taken in isolation from the SMB suggests separate processes or origins, whereas comparison to the data from the AMMS indicates a continuity of processes. This feature along with the gross chemical similarities shown in Table 16, Figures 29 and 30 and the physical aspects of the East Kemptville deposits indicate that the same processes that were active in generating the AMMS were responsible for mineralization in the South Mountain magmatic system.

The author is unaware of systematic chemical data from the Cornubian Batholith which may be of relevance to this problem. However, the physical aspects of mineral deposition from a magmatic system are abundant in the form of tourmaline-breccia pipes and stockscheider. Extensive secondary alteration and mobilization may have obscured many of the magmatic signatures of deposition in this area.

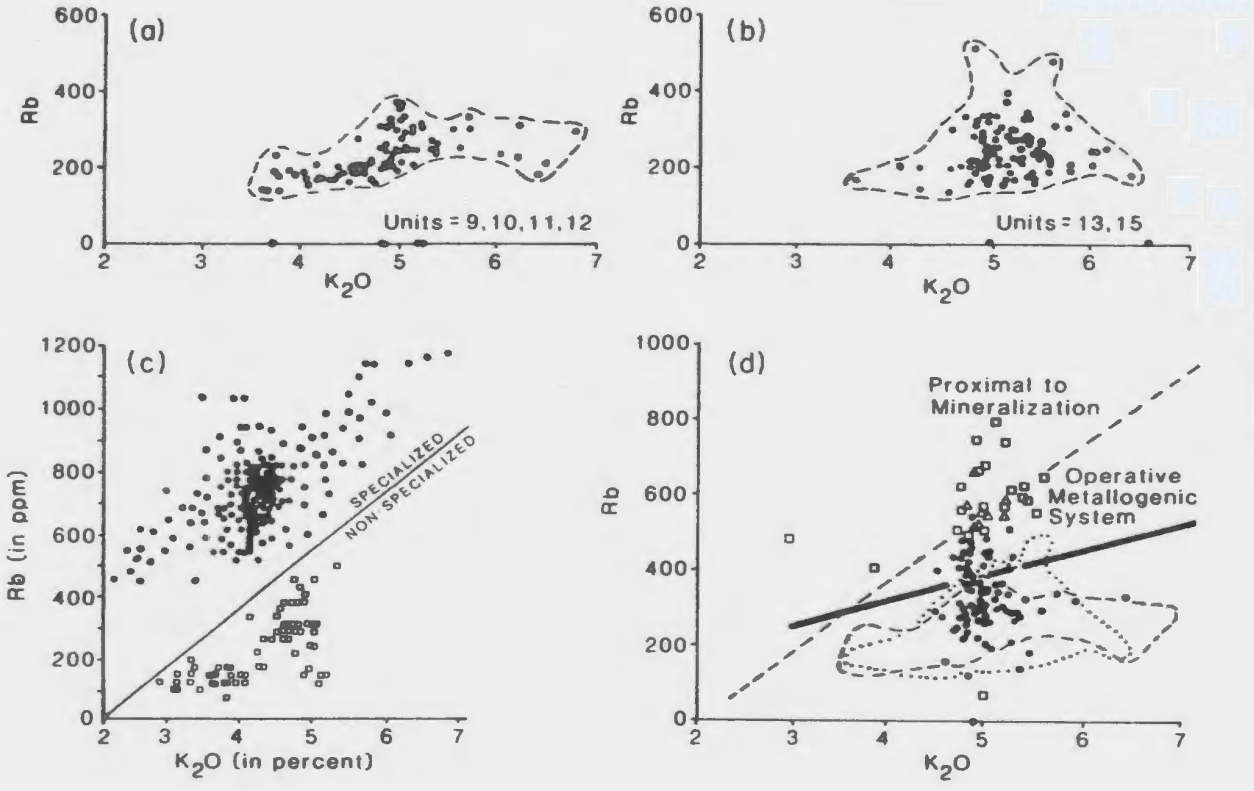

Figure 81: Plot of Rb versus K_2O in the Ackley Granite Suite (a,b,d) and those from the South Mountain Batholith (c) associated with the East Kemptville tin deposit (from Chatterjee et al., 1983). In d, dots are data from the Hungry Grove, Sage Pond and Rencontre Lake granites; data fields are those shown in a and b, straight dashed line is specialized/non-specialized boundary of Chatterjee et al. (1983) shown in c, open squares are samples within 1 km of the Sn-W greisen at Sage Pond, open triangles are samples collected adjacent to mineralization at Rencontre Lake, heavy line is suggested boundary for specialized and non-specialized rocks of the Ackley Granite Suite.

The inferred lower crustal or mantle influenced source for the AMMS differs significantly from that of the peraluminous 'S-type' SMB where the protolith is thought to be mid-crustal sedimentary sequences (Muecke and Clarke, 1981). The processes responsible for primary granitoid related mineralization may therefore operate independently of source composition in high-silica granite systems. An important requirement may be the development of a magma chamber at intermediate to high crustal levels and the thermal and tectonic stabilization of that magma chamber for a sufficient time interval to permit the magmatic-metallogenic process to occur. For this reason, attempts to apply source-related schemes to either classification or metallogenic interpretations of granitoid rocks, e.g. with the suggestion that Mo mineralization is associated with I-type and Sn with S-type (eg. Beckinsale, 1979) are not considered to be generally applicable.

Hildreth (1979, 1981) and Mahood and Hildreth (1983) suggested that magmatic processes of trace element and ore element enrichment also operate in peralkaline magma chambers and may generate peralkaline magmas. These processes precede any volatile activity and metasomatic alteration and may be the reason for the volatile enrichment. Similar conclusions were reached by Drysdall et al. (1985), from a study of Zr-Nb-Y mineralized granites in Saudi Arabia.

11-1-5 The Rapakivi Connection

The similarity in size, shape and mode of emplacement between the AMMS and Proterozoic, anorogenic, rapakivi granites (Bridgewater et al.,

1974) has already been noted and the geochemical signatures of these granites (Weibe, 1978; Emslie; 1978, Morse, 1982), and metallogeny (Haapala, 1985), are similar to those of the Ackley Granite Suite such that a common genetic history is implied. In the AMMS, rapakivi textures were noted in some samples from the Tolt, Meta and Hungry Grove granites. The Proterozoic rapakivi granites have a range of major oxide and trace element concentrations comparable to the Ackley Granite Suite and to A-type granites in general (Haapala, 1985), with a mineralogical range from hornblende-biotite granite, to rapakivi granite, to biotite granite, to topaz-bearing biotite granite. Mineral deposits typically consist of greisen-associated and pegmatite-aplite type granophile element concentrations. Total REE concentration are similar to those in the southern AMMS (Weibe, 1978) and show almost identical Eu depletions and relative enrichments in HREE. Changes to larger Eu anomaly and increasing HREE are associated with mineralized granites (Haapala, 1985).

The rapakivi granites are spatially associated with anorthosite massifs and related K-rich monzonite, mangerite and charnockite (Bridgewater et al. 1974; Emslie, 1978, 1985). Charnockites, which are confined to granulite facies terranes, are high-silica rocks and may have comparable major oxide and trace element concentrations to rapakivi granites. Information on the origin of the anorthosite massifs and of the related rocks may therefore provide insight to the genetic history of the high-silica systems such as the AMMS.

11-1-6 A Distinct Igneous Province in Newfoundland?

Distinctive, Devonian-Carboniferous, post-tectonic, alkali-feldspar, biotite bearing, high-silica granites in southern and eastern Newfoundland are identified in Figure 82 (Tuach and Miller; In preparation). These granites all show similarity of texture, mineralogy and composition to the southeastern Ackley Granite Suite (Strong et al., 1974; Strong, 1980; Wilton, 1985; Chorlton and Dallmeyer, 1986, Poole et al., 1985; Furey, 1985; Furey and Strong, 1986; O'Brien et al., 1986; Tuach, unpublished data). The Strawberry and Isle Aux Morts Brook granites have provided a whole-rock Rb-Sr age of 362 ± 15 Ma (Wilton, 1985) and biotite from the Chetwynd Granite has provided an $^{40}Ar/^{39}Ar$ age of 372 ± 5 Ma (Chorlton and Dallmeyer, 1986). These ages are similar to those from the southern Ackley Granite Suite (Chapter 8).

It is suggested that the cross-cutting alkali granites form an igneous province related to a thermal-magmatic pulse which resulted in Rb-Sr and ^{40}Ar-^{39}Ar ages between 375 and 350 Ma. Other post-tectonic plutons such as Kepenkeck Granite, the Middle Ridge Granite (Bell et al., 1977) and the Ironbound Syenite (Chorlton and Dallmeyer, 1986) may have been generated in the same igneous event.

11-1-7 Magma-Source Considerations

The controls on the genesis of the large high-silica systems must be related to the consistent, post-orogenic, continental, tectonic setting. Previous discussion concerning the Ackley Granite Suite

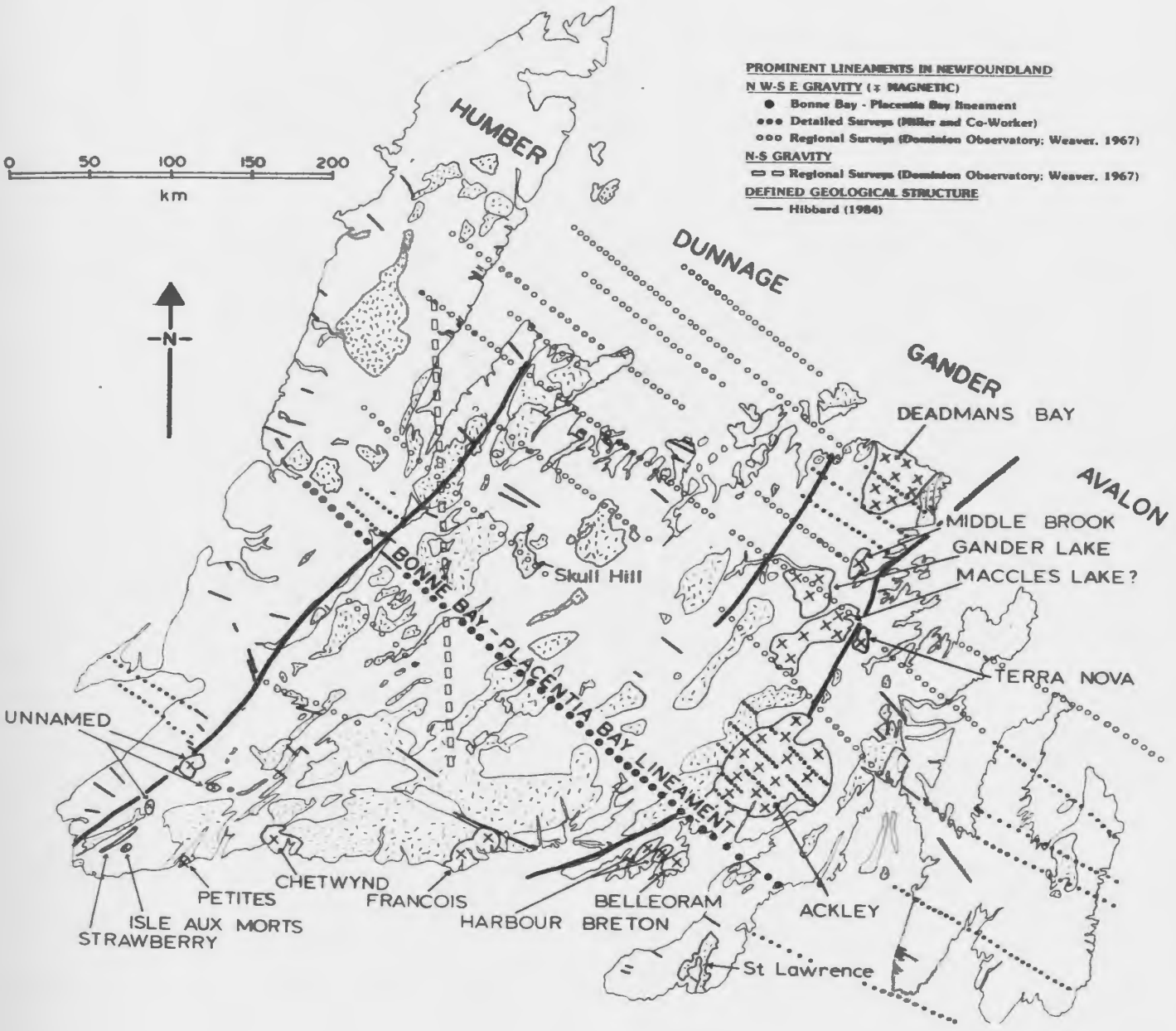

Figure 82: Distribution of granitoid rocks (hatched and crosses), Newfoundland, showing location of Devono-Carboniferous alkaline anorogenic granites (crosses). Also shown are locations of northwest geophysical lineaments (from Tuach and Miller, in preparation).

focussed on the local features in relationship to the Dover-Hermitage Bay Fault zone. However, the similarity of the alkali-granites in the Late Devonian-Early Carboniferous igneous province in Newfoundland (Fig. 82) provides further insight to the problem. These plutons occur in the Avalon, Gander and Dunnage terranes. This implies: 1) all granite systems evolve to comparable high-silica compositions, or 2) the lower crustal source is consistent throughout the Dunnage, Gander and Avalon terranes, or 3) there is a considerable contribution of granitic material to the magma systems from a much larger mantle reservoir.

The first alternative is not realistic since considerable variety in high-silica systems can develop (Table 16). An ultimate source from a homogenous lower crust may be possible. However, a lower crustal source which has previously undergone melting (Loiselle and Wones, 1979; Collins et al., 1982; Stein, 1985) and has produced comparable granites over such a large area also seems unlikely since it would require almost identical geological histories for the different terranes. Partial melting of a larger, homogenous, enriched mantle source, with variable crustal contamination (cf. Thompson et al., 1984), possibly accompanied by metasomatic transport of elements from the mantle into the lower crust (Bailey, 1980) may provide a more realistic origin for these alkali-feldspar granites.

It has been suggested that the anorthosite-rapakivi granite suite was formed by partial melting of the upper mantle and lower crust (Haapala, 1985) or that the granites represent melting of the lower crust caused by uprise of mantle-derived mafic magmas (Emslie, 1985).

Resolution of the source problem with respect to anorogenic granites requires much further work. A comparative study of the anorogenic granites in southern and eastern Newfoundland may provide further insights.

11-1-8 Implications for Mineral Exploration

In the Ackley Granite Suite, the observed geochemical trends which culminate at mineralization imply that it is possible to predict the direction to significant mineral deposits. The secondary enrichment trends of incompatible elements to higher and more variable values which are superimposed on the main magmatic trends reflect the mineralization process, and can possibly be recognized at lower threshold levels. This is demonstrated in Figure 81 which shows a field representing the operative metallogenic system in addition to the field of specialized samples proximal to mineralization. Samples plotting in the operative field would illustrate that the granite system was fertile and a detailed search for associated specialized plutons may be warranted. Regional negative gravity anomalies may indicate areas of thickest granite, where specialized, roof zone facies are most likely to occur.

From a detailed exploration perspective, it has been shown that highest Rb and lowest Ba and Sr values occur immediately adjacent to the mineralized greisen and aplite-pegmatite bodies. This provides a powerful directional indicator for the location of such deposits. While major elements, F, U and Th, along with other incompatible elements (including the HREE) provide useful regional guides to the possible

presence of granophile mineralization, they are not as effective in locating precisely the target of economic interest.

The low F content of the Rencontre Lake Granite agrees with experimental evidence indicating that Mo is not necessarily transported by fluoro-complexes (Tingle and Fenn, 1984; Candela and Holland, 1984). This indicates that regional fluorine anomalies are not necessarily correlated with molybdenite mineralization and may not reflect the presence of significant Mo.

On a regional scale, the alkaline granites which are shown on Figure 82, and which are included in the Upper Devonian-Lower Carboniferous igneous province suggested above, have potential to host Climax-type and granophile mineral deposits. The most significant analogy in the Appalachians, is the Mount Pleasant deposit in New Brunswick (Taylor et al., 1985). In Newfoundland, most of these granites host minor fluorite and molybdenite mineralization (Strong et al., 1974; Chorlton, 1983; Wilton, 1984; Poole et al., 1985; Furey, 1985; Furey and Strong, 1986; O'Brien et al., 1986).

The high LIL content of these granites enhances their ability to rise to high crustal levels (Strong, 1980, 1981). This in turn enhances the possibility of generating hydrothermal systems in the surrounding country rocks and provides an environment favourable for the generation of epithermal gold-silver deposits. Indeed, the common association of F, B, W, Mo, Sb, etc. with epithermal systems suggests such a relationship, and is the norm rather than exception (cf. Berger

and Eimon, 1983). Therefore, areas surrounding the high-level anorogenic granites and particularly structures intruded by or associated with the granites, provide a favourable gold-silver exploration target.

11-2 CONCLUSIONS

1) Petrological, geochemical and isotopic criteria indicate that the study area (the Ackley Granite of Dickson, 1983) consists of two distinct post-tectonic biotite-bearing granitoid suites. Two separate calc-alkaline granodiorite-granite plutons, occupying 450 km^2, occur at the western and northeastern extremities of the study area and have been named the Koskaecodde Pluton and Mollyguajeck Pluton respectively. The remainder of the study area has been renamed the Ackley Granite Suite (2,415 km^2) and consists of high-silica granites (sensu stricto) with a predominance of alkali granites.

2) The calc-alkaline Koskaecodde and Mollyguajeck plutons contain microcline and have minor hornblende in the more mafic compositions. Biotite has a Fe/Fe+Mg ratio of 0.45 to 0.49 and chlorite alteration of biotite is ubiquitous. An Rb-Sr age of 427 ± 12 Ma is essentially in agreement with an $^{40}Ar-^{39}Ar$ age of 410 ± 4 Ma. suggesting a Middle to Upper Silurian age (Harland et al., 1982). An initial strontium ratio of 0.7092 and estimated $\delta\,^{18}O$ whole rock ratios of 9.5 to 9.7 per mil, indicate a significant crustal component in the genetic evolution of the plutons.

3) The Ackley Granite Suite has been subdivided into 7 member granites which are slightly modified from the units of Dickson (1983). Muscovite-biotite bearing granite to the northwest of a line joining the Koskaecodde and Mollyguajeck plutons has been called the Kepenkeck Granite and possible associated biotite granite has been named the Mount

Sylvester Granite. Southeast of this line, biotite-granites have been named the Hungry Grove, Meta, Tolt, Rencontre Lake and Sage Pond granites based on their textural appearance. The Rencontre Lake and Sage Pond granites, occur in the south, host significant aplite-pegmatite Mo deposits and greisen Sn-W deposits respectively, and represent roof zone facies of the Ackley Granite Suite.

Perthitic orthoclase is the dominant feldspar and perthite textures coarsen southwards. Minor Fe-rich hornblende occurs in the most mafic compositions, and biotite shows a range of Fe/Fe+Mg ratios from 0.43 to 0.96. The highest ratios (annite) occur in proximity to the mineralized areas. Chloritic alteration of biotite is ubiquitous in the Rencontre Lake Granite, in comparison to a weak sericite alteration halo around the greisen deposits in the Sage Pond Granite.

Most of the high-silica granites in the Ackley Granite Suite have anorogenic 'A-type' affinities with moderate to low alumina and relatively high alkali and incompatible element content. The Kepenkeck Granite has relatively higher alumina content and correspondingly lower alklai content compared to the rest of the Ackley Granite Suite, and shows characteristics of sedimentary derived granites (S-type).

An Rb-Sr age of 358 ± 12 Ma is in agreement with a previously published Rb-Sr age of 349 ± 2 Ma (Bell et al., 1977) and previous $^{40}Ar-^{39}Ar$ ages of about 355 ± 10 Ma (Dallmeyer et al., 1983). New $^{40}Ar-^{39}Ar$ data from throughout the Ackley Granite Suite provide ages of around 370 ± 5 Ma. The initial strontium ratio of 0.7063 from the

southern Ackley Granite Suite and the estimated $\delta^{18}O$ whole rock value around 7.5 per mil in much of this area indicate a lower crustal source for these granites. An initial strontium ratio of 0.7017 from the Kepenkeck Granite indicates source inhomogeneity or secondary fluid activity, although the estimated $\delta^{18}O$ ratios 8.1 to 8.9 indicate a mid-crustal sedimentary source.

4) The petrographic, chemical, isotopic, and gravity signatures of the Ackley Granite Suite do not define the trace of the Dover-Hermitage Bay Fault zone which separates the Gander and Avalon tectonostratigraphic terranes. There is a tentative correlation between higher- $\delta^{18}O$, predominantly sedimentary rocks of the Gander Terrane and a sedimentary source for the high- $\delta^{18}O$ Kepenkeck Granite and between lower- $\delta^{18}O$, predominantly volcanic rocks of the Avalon Terrane and lower $\delta^{18}O$ values in the granites intruding the Avalon Terrane such that a direct correlation may be construed. The signatures indigenous to the Avalon Terrane overlap the Gander Terrane by a distance of 10 to 15 km and indicate that the Dover-Hermitage Fault is steeply dipping to the northwest, or that magma derived from the Avalon Terrane flowed into the Gander Terrane. These data confirm that movement ceased on the Fault prior to intrusion of the Ackley Granite Suite.

5) The Ackley Granite Suite is steep sided, and varies from 2-8 km thick. A north-south keel of thicker granite crosses the Dover-Hermitage Bay Fault at a moderate angle, indicating that the thermal event responsible for magmatic intrusion was independent of the Fault, and resulted from east-west, post-orogenic extension. Emplacement to high

crustal levels may have occurred by a process of megablock stoping, or foundering, of crustal blocks to lower crustal levels and, tectonic controls over the stoping process may relate to a system of orogen scale, post-orogenic megajoints.

6) The $\delta^{18}O$ quartz values from the mineral prospects in the Ackley Granite Suite are similar to those in the host granites. These oxygen isotope data indicate that the mineral deposits formed from magmatic fluids at magmatic temperatures, with possible minor lower temperature meteoric incursions at a stockwork deposit in the Rencontre Lake area. $^{40}Ar-^{39}Ar$ ages from secondary muscovite associated with mineralization in the Rencontre Lake and Sage Pond areas, are statistically indistinguishable from the ages of their host granites. These data indicate a contemporaneity of magmatic and mineralization processes.

Fluid inclusion studies indicate that the fluids which formed the aplite-pegmatite Mo deposits had a low salinity (< 5% Eq. wt. % NaCl). These fluids have a homogenization temperature of 350-400°C and may have originated at higher temperatures. In contrast the fluids from the Sage Pond greisens were extremely saline and have homogenization temperatures from 100 to 550°C. Many of the latter inclusions may have necked down or reequilibrated during subsequent cooling, and low eutectic temperatures indicate the presence of Ca and Mg in the fluids.

7) Analysis of the map distribution of major oxides and trace elements reveals systematic chemical variations in the Ackley Granite Suite which

culminate at the areas of mineralization in the Rencontre Lake and Sage Pond granites. These patterns are interpreted to indicate that the southern Ackley Granite Suite, and in particular the Hungry Grove and Sage Pond granites, represent a frozen equivalent to the density and geochemically stratified magma chambers which have been modelled by Hildreth (1979) as producing large-volume, high-silica, geochemically stratified ash flows.

8) The model of convective fractionation proposed by Sparks et al. (1984) accounts well for the observed enrichment of the roof zone of the magma chamber in LIL elements and the depletions in Ba and Sr, and also explains the geochemical trends which are locally concentrated at the steep walls of the magma chamber. Marginal and roofwards enrichments of the LIL eventually led to volatile exsolution and transport to form the Sn-W-bearing greisens in the Sage Pond Granite. The chemical trends show greater variability and greater degrees of enrichment or depletion at above 74% SiO_2, supporting the concept of magma depolymerization and volatile element complexing in the upper regions of the magma chamber. Diffusion processes such as those discussed by Hildreth (1979, 1981) may also have contributed to the element enrichment and depletion trends. The mineralized areas are spatially associated with the thickest parts of the granites indicating that depth of the magma column may be an important factor controlling element zonation.

9) The Rencontre Lake Granite has depleted magmatic $\delta^{18}O$ values of 4.7 and 5.8 per mil which are interpreted to result from incursion of meteoric water to the magma chamber. These depletions together with low

fluorine values, abundant physical evidence of water saturation, disturbed major and trace element contour trends and lower incompatible element concentrations, when compared to the remainder of the Ackley Granite Suite, suggest that Rencontre Lake Granite represents a portion of the Ackley Magmatic Metallogenic System which crossed the solidus, (ie. underwent resurgent boiling), while undergoing a period of postcaldera-collapse recovery.

10) High-silica magmatic systems continually mature to a chemical, and density stratified, equilibrium state, with the volatile and ore elements concentrated at the roof of the system. Variations in the metallogenic process in high-silica systems may relate to the dynamic and temporal state of maturity of the system. Topaz-bearing granites and rhyolites are seen as the end product of the process. A temporal relationship is also implied which suggests that aplite-pegmatite associated Mo mineralization should precede Sn-W-bearing greisen mineralization. Different sources are not considered to be important to the generation of the differing styles of mineralization.

11) Important practical considerations to mineral exploration are the unidirectional enrichments of the incompatible elements, and depletions in Ba and Sr. The most effective tracer elements being Rb, Sr, and perhaps Ba. Fluorine may not be a reliable tracer element for molybdenite mineralization.

REFERENCES

Abbey, S.
1980: Studies in "Standard Samples" for use in the general analyses of silicate rocks and minerals. Part 6. 1979 Edition of "useable" values. Geological Survey of Canada, Paper 80-14, 30 pages.

Allard, P.
1979: $^{13}C/^{12}C$ and $^{34}S/^{32}S$ ratios in magmatic gases from ridge volcanism in Afar. Nature, Volume 282, pages 56-58.

Allman-Ward, P.
1985: Distribution of uranium and thorium in the western lobe of the St. Austell Granite and the effects of alteration processes. In High Heat Production (HHP) Granites, Hydrothermal Circulation, and Ore Genesis. Edited by C. Halls, The Institution of Mining and Metallurgy, London, England, pages 437-458.

Anderson, E.M.
1936: The dynamics of formation of cone sheets, ring dikes, and cauldron subsidences. Proceedings of the Royal Society of Edinburgh, Volume 56, pages 128-157.

Anderson, F.D.
1965: Belleoram, Newfoundland. Geological Survey of Canada, Map 8-1965.

Anderson, F.D. and Williams, H.
1970: Gander Lake West Half, Newfoundland. Geological Survey of Canada, Map 1195A.

Anderson, J.L. and Rowley, M.C.
1981: Synkinematic peraluminous and associated metaluminous granites, Whipple Mountains, California. Canadian Mineralogist, Volume 19, pages 83-101.

Alderton, D.H.M., Pearce, J.A. and Pitts, P.J.
1980: Rare earth mobility during granite alteration: Evidence from southwest England. Earth and Planetary Science Letters, Volume 49, pages 149-165.

Archibald, D.A., Glover, J.K., Price R.A., Farrar. E. and Carmichael, D.M.
1983: Geochronology and tectonic implications of magmatism and metamorphism, southern Kootney arc, southeastern British Columbia. Part 1: Jurassic to mid-Cretaceous. Canadian Journal of Earth Sciences, Volume 20, pages 1891-1913.

Arthaud, F. and Matte, P.
1977: Late paleozoic strike-slip faulting in southern Europe and northern Africa: Result of right-lateral shear zone between the Appalachians and the Urals. Geological Society of America, Bulletin, Volume 88, pages 1305-1320.

Atherton, M.P., McCourt, W.J., Sanderson, L.M. and Taylor, W.P.
1979. The geochemical character of the segmented Peruvian Coastal Batholith and associated volcanics. In Origin of Granite Batholiths: Geochemical Evidence. Edited by M.P. Atherton and J. Tarney. Shiva Publishing Limited, Orpington, England, pages 45-64.

Atherton, M.P. and Sanderson, L.M.
1986: The chemical variation and evolution of the super-units of the segmented Coastal Batholith. In Granitoid Batholiths and Related Magmatism in Peru: Magmatism at a Plate Edge: The Peruvian Andes. Edited by W.S. Pitcher, M.P. Atherton, E.J. Cobbing and R. Beckinsale. Blackie and Sons, Glasgow, pages 208-227.

Bailey, D.K.
1980: Volcanism, earth degassing and replenished lithosphere mantle. Philisophical Transactions of the Royal Society of London, Series A297, pages 309-322.

Bandurkin, G.A.
1961: Behaviour of the rare earths in fluorine-bearing media. Geochemistry, Volume 61, pages 159-167.

Barr, D.A., Fox, P.E., Northcote, K.E. and Preto V.A.
1976: The alkaline suite porphyry deposits - A summary. In Porphyry Deposits of the Canadian Cordillera. Edited by A. Sutherland-Brown. Canadian Institute of Mining and Metallurgy, Special Volume 15, pages 359-367.

Barth, T.F.W.
1959: Principles of classification and norm calculation of metamorphic rocks. Journal of Geology, Volume 67, pages 135-152.

1961: A final proposal for calculating the mesonorm of metamorphic rocks. Journal of Geology, Volume 70, pages 497-498.

Bates, R.L. and Jackson, J.A.
1980: Glossary of Geology, second edition, American Geological Institute, McGraw Hill, 749 pages.

Beane, R.E.
1982: Hydrothermal alteration in silicate rocks, southwestern North America: In Advances in Geology of the Porphyry Copper Deposits, southwestern North America. Edited by S.R. Titley. University of Arizona Press, pages. 117-137.

Beckinsale, R.D.
1979: Granite magmatism in the tin belt of southeast Asia. In Origin of Granite Batholiths: Geochemical Evidence. Edited by M.P. Atherton and J. Tarney. Shiva Publishing Limited, Orpington, England, pages 33-44.

Bell, K., Blenkinsop, J. and Strong, D.F.
1977: The geochronology of some granitic bodies from eastern Newfoundland and its bearing on Appalachian evolution. Canadian Journal of Earth Sciences, Volume 14, pages 456-476.

Berger, B.R. and Eimon, P.I.
1983: Conceptual models of epithermal silver-gold deposits. In Cameron volume on Unconventional Mineral Deposits. Edited by W.C. Shanks. American Institute of Mining, Metallurgical and Petroleum Engineers, New York, pages 191-205.

Berger, G.W. and York, D.
1979: 40Ar/39Ar dating of multicomponent magnetizations in the Archean Schelly Lake Granite, northwestern Ontario. Canadian Journal of Earth Science, Volume 16, pages 1933-1941.

Bilal, B.A., Herrman, F. and Fleischer, W.
1979: Complex formation of trace elements in geochemical systems I. Potentiometric study of fluoro-complexes of rare earth elements in fluorite bearing model systems. Journal of Inorganics and Nuclear Chemistry, Volume 41, pages 347-350.

Bilal, B.A. and Becker, P.
1979: Complex formation of trace elements in geochemical systems II. Stability of rare earth fluoro-complexes in fluorite bearing model systems of various ionic strengths. Journal of Inorganic and Nuclear Chemistry, Volume 41, pages 1607-1618.

Blackwood, R.F.
1985: Geology of the Facheaux Bay map area. Newfoundland Department of Mines and Energy, Mineral Development Division, Report 85-4, 56 pages.

Blackwood, R.F. and O'Driscoll, C.F.
1976: The Gander - Avalon Zone boundary in southeastern Newfoundland. Canadian Journal of Earth Sciences, Volume 13, pages 1155-1159.

Boden, D.R.
1986: Eruptive history and structural developmant of the Toquima caldera complex, central Nevada. Geological Society of America Bulletin, Volume 97, pages 61-74.

Bowen, N.L.
1956: The evolution of the igneous rocks. Princeton University Press, Dover Publications, 332 pages.

Bradley, D.A.
1962: Gisborne Lake and Terrenceville map areas, Newfoundland. Geological Survey of Canada, Memoir 321, 56 pages.

Bray, C.J. and Spooner, E.T.C.
1983: Sheeted vein Sn-W mineralization and greisenization associated with economic kaolinization, Goonbarrow china clay pit, St. Austell, Cornwall, England: Geologic relationships and geochronology. Economic Geology, Volume 78, pages 1064-1089.

Bridgewater, D., Sutton, J. and Watterson, J.
1974: Crustal folding associated with igneous activity. Tectonophysics, Volume 21, pages 57-77.

Brooks, C., Hart, S.R. and Wendt, I.
1972: Realistic use of two-error regression treatments as applied to rubidium-strontium data. Reviews of Geophysical and Space Sciences, Volume 10, pages 551-577.

Brown G.C. and Fyfe, W.S.
1970: The production of granitic melts during ultrametamorphism. Contributions to Mineralogy and Petrology, Volume 27, pages 310-318.

Buddington, A.F. and Lindsay, D.H.
1964: Iron-titanium oxide minerals and synthetic equivalents. Journal of Petrology, Volume 5, pages 310-357.

Burnham C.W.
1967: Hydrothermal fluids at the magmatic stage. In Geochemistry of Hydrothermal Ore Deposits. Edited by H.L. Barnes. Holt, Rinehart and Winston, New York, pages 34-76.

1979: Magmas and hydrotheral fluids. In Geochemistry of Hydrothermal Ore Deposits. Edited by H. L. Barnes. Second edition, John Wiley and Sons, New York, pages 71-136.

Burnham, C.W. and Ohmoto, H.
1980 Late-stage processes of felsic magmatism. Mining Geology Special Issue, Volume 8, pages 1-11.

Burns, J.G.
1981: Report on reconnaisance geochemical survey, Ackley project, Newfoundland: Placer Development Limited. Newfoundland Department of Mines and Energy, File 1M/199, 9 pages.

1982: Report on exploration of the Ackley Granite during 1981: Placer Development Limited. Newfoundland Department of Mines and Energy, File 1M/198, 5 pages.

Burruss, R.C.
1981a: Analysis of equilibria in C-O-H-S fluid inclusions. In Fluid Inclusions: Applications to Petrology. Edited by L.S. Hollister and M.L. Crawford. Mineralogical Association of Canada, Volume 6, pages 39-74.

1981b: Analysis of phase equilibra in C-O-H-S fluid inclusions. In Fluid Inclusions: Applications to Petrology. Edited by L.S. Hollister and M.L. Crawford. Mineralogical Association of Canada, Volume 6, pages 75-100.

Burt, D.M.
1981: Acidity-salinity diagrams - Application to greisen and porphyry deposits. Economic Geology, Volume 76, pages 832-843.

Burt, D.M. Sheridan, M.F., Bikum, J.V. and Christiansen, E.H.
1982: Topaz rhyolites - distribution, origin, and significance for exploration. Economic Geology, Volume 77, pages 1818-1836.

Bussel, M.A.
1985: The centered complex of the Rio Huaura: A study of magma mixing and differentiation in high level chambers. In Granitoid Batholiths and Related Magmatism in Peru: The Andean Plate Margin. Blackie and Sons, Glasgow, pages 128-155.

Bussel, M.A. and Pitcher, W.S.
1985: The structural controls of batholith emplacement. In Granitoid Batholiths and Related Magmatism in Peru: The Andean Plate Margin. Edited by W. S. Pitcher, M. P. Atherton, E. J. Cobbing, and R. D. Beckinsale. Blackie and Sons, Glasgow, pages 167-176.

Butler, A.J. and Davenport, P.H.
1979a: Fluorine distribution in lake sediment in the Fortune Bay area, central Newfoundland. Mineral Development Division, Newfoundland Department of Mines and Energy, Open File Nfld. 966.

1979b: Lake sediment geochemical survey of the Fortune-Trinity Bay area, Newfondland. Mineral Development Division, Newfoundland Department of Mines and Energy, Open File Nfld. 1002.

Candela, P.A. and Holland, A.D.
1983: The partitioning of copper and molybdenum between silicate melts and aqueous fluids. Geochimica et Cosmochimica Acta, Volume 48, pages 373-380.

Chappell, B.W. and White, A.J.R.
1974. Two contrasting granite types. Pacific Geology, Volume 8, pages 173-174.

Chatterjee, A.K., Strong, D.F. and Muecke, G.K.
1983: A multivariate approach to geochemical distinction between tin specialized and uranium specialized granites of southern Nova Scotia. Canadian Journal of Earth Sciences, Volume 20, pages 420-430.

Cherry, M.E. and Trembath, L.T.
1978: The pressure quench formation of rapakivi texture. Contributions to Mineralogy and Petrology, Volume 68, pages 1-6.

Chorlton, L.B.
1980: Geology of the La Poile River area (110/16), Newfoundland. Newfoundland Department of Mines and Energy, Mineral Development Division, Report 80-3, 86 pages.

Chorlton, L.B. and Dallmeyer, R.D.
1986: Geochronology of early to middle Paleozoic tectonic development in the southwest Newfoundland Gander Zone. Journal of Geology, Volume 94, pages 67-90.

Clayton, R.N. and Mayeda, T.K.
1963: The use of bromine pentafluoride in the extraction of oxygen from oxides and silicates for isotopic analyses. Geochimica and Cosmochimica Acta, Volume 27, pages 43-52.

Clayton, R.N. Muffler, L.P.J. and White, D.E.
1968: Oxygen isotope study of calcite and silicates of the Ranch River No. 1 Well, Salton Sea geothermal field, California. American Journal of Science, Volume 266, pages 968-979.

Chorlton, L.B.
1980: Geology of the La Poile River area (110/16), Newfoundland. Newfoundland Department of Mines and Energy, Mineral Development Division, Report 80-3, 86 pages.

Chorlton, L.B. and Dallmeyer, R.D.
1986: Geochronology of early to middle Paleozoic tectonic development in the southwest Newfoundland Gander Zone. Journal of Geology, Volume 94, pages 67-90.

Clayton, R.N. and Mayeda, T.K.
1963: The use of bromine pentafluoride in the extraction of oxygen from oxides and silicates for isotopic analyses. Geochimica and Cosmochimica Acta, Volume 27, pages 43-52.

Clayton, R.N. Muffler, L.P.J. and White, D.E.
1968: Oxygen isotope study of calcite and silicates of the Ranch River No. 1 Well, Salton Sea geothermal field, California. American Journal of Science, Volume 266, pages 968-979.

Collins, W.J., Beams, S.D., White, A.J.R. and Chappell, B.W.
1982: Nature and origin of A-type granites with particular reference to southeastern Australia. Contributions to Mineralogy and Petrology, Volume 80, pages 189-200.

Colman-Sadd, S.P.
1976: Geology of the St. Albans map area, Newfoundland (1M/13). Mineral Development Division, Newfoundand Department of Mines and Energy, Report 76-4, 19 pages.

Colman-Sadd, S.P., Dickson, W.L., Elias, P. and Davenport, P.H.
1981: Whole rock analytical data, statistical printouts and maps of plutonic rocks and selected country rocks from southeastern Newfoundland. Mineral Development Division, Newfoundland Department of Mines and Energy, Open File Nfld. 1157, 6 pages.

Crawford, M.L.
1981: Phase equilibra in aqueous fluid inclusions. In Fluid Inclusions: Applications to Petrology. Edited by L.S. Hollister and M.L. Crawford. Mineralogical Association of Canada, Volume 6, pages 75-100.

Criss, R.E. and Taylor, H.P.
1983: An 180/160 and D/H study of Tertiary hydrothermal systems in the southern half of the Idaho Batholith. Geological Society of America Bulletin, Volume 94, pages 640-633.

Currie, K.L.
1985: An unusual peralkaline granite near Lac Brisson, Quebec-Labrador. In Current Research, Part A, Geological Survey of Canada, Paper 85-1A, pages 73-80.

Dallmeyer, R.D., Hussey, E.M., O'Brien, S.J. and O'Driscoll, C.F.
1983: Chronology of tectonothermal activity in the western Avalon Zone of the Newfoundland Appalachians. Canadian Journal of Earth Sciences, Volume 20, pages 355-363.

Dalrymple, G.B. and Lanphere, M.A.
1971: $^{40}Ar/^{39}Ar$ technique of K-Ar dating: a comparison with the conventional technique. Earth and Planetary Science Letters, Volume 12, pages 300-308.

Davenport, P.H., Tuach, J. and Dickson, W.L.
1984: Computer aided analysis of lithogeochemical data from Newfoundland granites and its role in mineral exploration. In Current Research, Mineral Development Division, Newfoundland Department of Mines and Energy, Report 84-1, pages 254-256.

Davidson, A.
1978: The Blackford Lake Intrusive Suite: An Aphebian alkaline plutonic complex in the Slave Province, Northwest Territories. In Current Research, Part A, Geological Survey of Canada, Paper 78-1A, pages 119-127.

de Albuquerque, C.R.
1975: Partitioning of trace elements in co-existing biotite, muscovite, and potassium feldspar of granitic rocks, northern Portugal. Chemical Geology, Volume 16, pages 89-108.

Deer, W.A., Howie, R.A. and Zussman, J.
1962: Rock forming minerals, Volume 1. Lowe and Brydone, Norfolk, England, 333 pages.

De Paolo, D.J.
1981: Trace element and isotopic effects of combined assimilation and fractional crystallization. Earth and Planetary Science Letters, Volume 53, pages 189-202.

Dickson, W.L.
1980: Geology of the Ackley Granite, eastern Newfoundland. Mineral Development Division, Newfoundland Deparment of Mines and Energy, Map 80-197.

1982: The southern contact of the Ackley Granite, southeast Newfoundland; location and mineralization. In Current Research, Mineral Development Division, Newfoundland Department of Mines and Energy, Report 82-1, pages 99-108.

1983: Geology, geochemistry, and mineral potential of the Ackley Granite and parts of the North West Brook and Eastern Meelpaeg Complexes, southeastern Newfoundland (parts of map areas 1M/10, 11, 14, 15, 16; 2D/1, 2, 3, and 7). Mineral Development Division, Newfoundland Department of Mines and Energy, Report 83-6, 129 pages.

Dickson, W.L., Elias, P. and Talkington, R.W.
1980: Geology and geochemistry of the Ackley Granite, southeast Newfoundland. In Current Research, Mineral Development Division, Newfoundland Department of Mines and Energy, Report 80-1, pages 110-119.

Dickson, W.L. and Howse, A.F.
1982: Geochemistry of whole rock and stream sediment samples from two mineralized areas of the Ackley Granite: Rencontre Lake and Anesty Hill molybdenite-cassiterite prospects. Mineral Development Division, Newfoundland Department of Mines and Energy, Open File Nfld. 1M/203, 6 pages.

Dingwell, D.B.
1985: The structure and properties of fluorine-rich silicate melts: Implications for granite petrogenesis. In Granite Related Mineral Deposits. Edited by R.P. Taylor and D.F. Strong. Canadian Institute of Mining and Metallurgy, Extended Abstracts, Halifax, pages 72-81.

Drummond, A.D. and Godwin, C.I.
1976: Hypogene Mineralization - An empirical evaluation of alteration and zoning. In Porphyry Deposits of the Canadian Cordillera. Edited by A. Sutherland-Brown. Canadian Institute of Mining and Metallurgy, Special Volume 15, pages 52-63.

Drysdall A.R., Jackson, N.J., Ramsay, C.R., Douch, C.J. and Hackett, D.
1984: Rare element mineralization related to Precambrian alkali granites in the Arabian Shield. Economic Geology, Volume 69, pages 1366-1377.

Eadington, P.J.
1983: A fluid inclusion investigation of ore formation in a tin mineralized granite, New England, New South Wales. Economic Geology, Volume 78, pages 1204-1221.

Eadington, P.J. and Wilkins, R.T.W.
1980: The origin, interpretation and chemical analysis of fluid inclusions in minerals. CSIRO Division of Mineralogy, Technical Communication, Volume 69, 44 pages.

Einaudi, M.T., Meinert, L.D. and Newberry, R.J.
1981: Skarn deposits. Economic Geology, Seventy-fifth Anniversary Volume, pages 317-381.

Emslie, R.F.
1978: Anorthosite massifs, rapakivi granites and late Precambrian rifting of North America. Precambrian Research, Volume 7, pages 61-98.

1980: Geology and petrology of the Harp Lake Complex, central Labrador: An example of Elsonian magmatism. Geological Survey of Canada, Bulletin 293, 136 pages.

1985: Proterozoic anorthosite massifs. In The Deep Proterozoic Crust in the North Atlantic Provinces. Edited by A.C. Tobi and L.R. Touret. NATO ASI Series C, Volume 158, pages 39-60.

Eugster H.P. and Wones, D.R.
1962: Stability regions of the ferruginous biotite, annite. Journal of Petrology, Volume 3, pages 82-125.

Faure, G.
1977: Principles of isotope geology. John Wiley and Sons, New York, 464 pages.

Flynn, R.T. and Burnham, C.W.
1978: An experimental determination of rare earth partition coefficients between a chloride containing vapour phase and silicate melts. Geochimica et Cosmochimica Acta, Volume 42, pages 682-701.

Fryer, B.J.
1977: Rare earth evidence for changing Precambrian oxidation states. Geochimica et Cosmochimica Acta, pages 361-367

Furey, D.J.
1985: Geology of the Belleoram Pluton, southeast Newfoundland. In Current Research, Part 1A. Geological Survey of Canada, Report 85-1A, pages 151-156.

Furey, D.J. and Strong, D.F.
1986: Geology of the Harbour Breton Complex, Newfoundland. In Current Research, Part 1A. Geological Survey of Canada, Report 86-1A, pages 461-464.

Giletti, B.J. and Yund, R.A.
1984: Oxygen diffusion in quartz. Journal of Geophysical Research. Volume 89, pages 4039-4046.

Grant, J.N., Halls, C., Avila, W. and Avila, G.
1977: Igneous geology and the evolution of hydrothermal systems in some sub-volcanic tin deposits of Bolivia. In Volcanic Processes in Ore Genesis. Edited by I.G. Gass. The Institution of Mining and Metallury, Special Volume 7, pages 117-126.

Gregory, R.T. and Taylor, H.P.
1981: An oxygen isotope study of Cretaceous oceanic crust, Samail Ophiolite, Oman: Evidence for seawater-hydrothermal circulation at mid ocean ridges. Journal of Geophysical Research, Volume 86, pages 2737-2755.

Gromet, L.P. and Silver, L.T.
1983: Rare earth element distributions among minerals in a granodiorite and their petrogenetic implications. Geochimica et Cosmochimica Acta, Volume 47, pages 925-939.

Guilbert, J.M. and Lowell, J.D.
1974: Variations in zoning patterns in porphyry ore deposits. Canadian Institute of Mining and Metallurgy, Volume 67, pages 99-109.

Haapala, I.
1985: Metallogeny of the Proterozoic rapakivi granites of Finland. In Granite Related Mineral Deposits. Edited by R.P. Taylor, and D.F. Strong. Canadian Institute of Mining and Metallurgy, Extended Abstracts, Halifax, pages 123-131.

Hall, W.E., Friedman, I. and Nash, J.T.
1974: Fluid inclusion and light stable isotope study of the Climax molybdenum deposits, Colorado. Economic Geology, Volume 69, pages 884-901.

Halliday, A.N.
1980: The timing of early and main stage ore mineralization in southwest Cornwall. Economic Geology, Volume 75, pages 752-759.

Halls, C.
1985: High Heat Production (HHP) Granites, Hydrothermal Circulation, and Ore Genesis. The Institution of Mining and Metallurgy, London, England, 593 pages.

Hamilton, W.
1969: Mesozoic California and the underflow of Pacific mantle. Geological Society of America Bulletin, Volume 80, pages 2409-2429.

Hanmer, S.
1981: Tectonic significance of the northeastern Gander Zone, Newfoundland: An Acadian ductile shear zone. Canadian Journal of Earth Sciences, Volume 18, pages 120-135.

Hanson, G.N.
1978: The application of trace elements to the petrogenesis of igneous rocks of granitic composition. Earth and Planetary Science Letters, Volume 38, pages 26-43.

1980: Rare earth elements in petrogenetic studies of igneous systems. Annual Review Earth and Planetary Sciences, Volume 8, pages 371-406.

Harland, W.B., Cox, A.V., Llewellyn, P.G., Pickton C.A.G. and Walters, R.
1982: A geologic time scale. Cambridge University Press. 131 pages.

Harrison, T.M.
1981: Diffusion of ^{40}Ar in hornblende. Contributions to Mineralogy and Petrology, Volume 78, pages 324-331.

Harrison, T.M. and McDougall, I.
1980: Investigations of an intrusive contact, northwest Nelson, New Zealand - I: Thermal, chronological and isotopic constraints. Geochimica et Cosmochimica Acta, Volume 44, pages 1985-2003.

Henderson, R.G. and Zeitz, I.
1968: The computation of second vertical derivatives of geomagnetic fields. In Mining Geophysics. Edited by T.A. Hansen, W.E. Keinrichs, R.C. Holmer, R.E. MacDougall, G.R. Rogers, J.S. Sumner and S.H. Ward. Society of Exploration Geophysicists, Volume II, Theory, pages 606-614.

Henley R.W. and McNabb, A.
1978: Magmatic vapour plumes and groundwater interaction. Economic Geology, Volume 73, pages 1-20.

Hess, P.C.
1980: Polymerization models for silicate melts. In Physics of Magmatic Processes. Edited by R.B. Hargraves. Princeton University Press, pages 3-48.

Hibbard, J.
1983: Geology of the Island of Newfoundland, Preliminary version. Newfoundland Department of Mines and Energy, Mineral Development Division, Map 83-106.

Hibbard, M.J.
1965: Origin of some alkali feldspar phenocrysts and their bearing on petrogenesis. American Journal of Science, Volume 263, pages 245-261.

1979: Myrmekite as a marker between aqueous and post-aqueous phase saturation in granitic systems. Geological Society of America, Bulletin, Part 1, Volume 90, pages 1047-1062.

Higgins, N.C.
1979: Theory, methods and application of fluid inclusion research. Geological Association of Canada, Newfoundland Section, Short Course Notes, 42 pages.

Higgins, N.C. and Kerrich, R.
1982: Progressive ^{18}O depletion during CO_2 separation from a carbon dioxide-rich hydrothermal fluid: Evidence from the Grey River tungsten deposit, Newfoundland. Canadian Journal of Earth Sciences, Volume 19, pages 2247-2257.

Hildreth, E.W.
1979: The Bishop Tuff: Evidence for the origin of compositional zonation in silicic magma chambers. Geological Society of America Special Paper 180, pages 43-76.

1981: Gradients in silicic magma chambers: Implications for lithostatic magmatism. Journal of Geophysical Research, Volume 86, pages 10153-10192.

Hildreth, E.W., Christiansen, R.L. and O'Neil, J.R.
1984: Catastrophic isotopic modification of rhyolitic magma at times of caldera subsidences, Yellowstone Plateau Volcanic Field. Journal of Geophysical Research, Volume 89. No. B10, pages 8339-8369.

Hill, D.P., Wallace, R.E. and Cockerham, R.S.
1985: Review of evidence on the potential for major earthquakes and volcanism in the Long Valley - Mono Crater - White Mountains regions of eastern California. Earthquake Research, Volume 3, pages 551-574.

Hill, J.D. and Thomas, A.
1983: Correlation of two Helikian peralkaline granite-volcanic centres in central Labrador. Canadian Journal of Earth Sciences, Volume 20, pages 753-763.

Hine, R., Williams, B.W., Chappell, B.W. and White, A.J.R.
1978: Contrasts between I- and S-type granitoids of the Koscuisko Batholith. Journal of the Geological Society of Australia, Volume 25, pages 219-234.

Hollister, L.S. and Crawford, M.L.
1981: Fluid Inclusions: Applications to Petrology. Mineralogical Association of Canada, Volume 6, 304 pages.

Hudson, T. and Arth, J.G.
1983: Tin granites of the Seward Peninsula, Alaska. Geological Society of America Bulletin, Volume 94, pages 768-790.

Huspeni, J.R., Kesler, S.E., Ruiz, J., Tuta, Z., Sutter, J.F. and Jones, L.M.
1984: Petrology and geochemistry of rhyolites associated with tin mineralization in Northern Mexico. Economic Geology, Volume 79, pages 87-105.

Ishihara, S.
1977: The magnetite series and the ilmenite series granitic rocks. Journal of Mining Geology, Volume 27, pages 293-305.

Jacobsen, R.R.E., Macleod, W.N. and Black, R.
1958: Ring complexes in the younger granite province of northern Nigeria. Geological Society of London, Memoir 1, 72 pages.

Jackson, N.J., Halliday, A.N., Sheppard, S.M.F. and Mitchell, J.G.
1982: Hydrothermal activity in the St. Just Mining district, Cornwall, England. In Metallization Associated with Acid Magmatism. Edited by A.M. Evans. J. Wiley and Sons, New York, pages 137-179.

Jackson, N.J., Drysdall, A.R. and Stoeser, D.B.
1985: Alkali granite related Nb-Zr-REE-U-Th mineralization in the Arabian Shield. In High Heat Production (HHP) Granites, Hydrothermal Circulation, and Ore Genesis. Edited by C. Halls. The Institution of Mining and Metallurgy, London, England, pages 479-488.

Jahns, R.H. and Burnham, C.W.
1969: Experimental studies of pegmatite genesis. I. A model for the derivation and crystallization of granitic pegmatites. Economic Geology, Volume 64, pages 843-864.

Jager, E.
1979: Introduction to geochronology. In Lectures in Isotope Geology. Edited by E. Jager and J.C. Hunziker. Springer-Verlag, Berlin, pages 1-12.

Jenness, S.E.
1963: Terra Nova and Bonavista map areas, Newfoundland: Geological Survey of Canada, Memoir 327, 184 pages.

Juteau, M., Michard, A., Zimmerman, J.L. and Albarede, F.
1984: Isotopic heterogeneities in the granitic intrusions of Monte Caparine, Elba Island, Italy and dating concepts. Journal of Petrology, Volume 25, Part 2, pages 532-545.

Kean, B.F. and Jayasinghe, N.
1982: Geology of the Badger map area (12A/16), Newfoundland. Newfoundland Department of Mines and Energy, Mineral Development Division, Report 81-2, 37 pages.

Kennedy, M.J. and McGonigal, M.H.
1972: The Gander Lake and Davidsville Groups of northeastern Newfoundland: New data and geotectonic implications. Canadian Journal of Earth Sciences, Volume 9, pages 452-459.

Kinnaird, J.A., Batchelor, R.A., Whitley, J.E. and MacKenzie, A.B.
1985: Geochemistry, mineralization and hydrothermal alteration of the Nigerian high heat producing granites. In High Heat Production (HHP) Granites, Hydrothermal Circulation and Ore Genesis. Edited

by C. Halls. The Institution of Mining and Metallurgy, London, pages 169-195.

Kistler, R.W. and Peterman, Z.E.
1973: Variations in Sr, Rb, K, Na and initial $^{87}Sr/^{86}Sr$ in Mesozoic granitic rocks and intruded wall rocks in central California. Geological Society of America, Bulletin 84, pages 3489-3512.

Kleeman, J.D.
1985: Origin of disseminated wolframite-bearing quartz-topaz rock at Torrington, New South Wales, Australia. In High Heat Production (HHP) Granites, Hydrothermal Circulation, and Ore Genesis. Edited by C. Halls. The Institution of Mining and Metallurgy, London, England, pages 197-202.

Kontak, D.J.
1985: The magmatic and metallogenic evolution of a craton-orogen interface: The Cordillera de Carabaya, Central Andes, S.E. Peru. Ph.D. Thesis, Queens University, Kingston, Ontario, 714 pages.

Kooiman, G.J.A., Mcloed, M.J. and Sinclair, W.D.
1984: The porphyry W-Mo deposit and associated Sn and polymetallic zones in the Fire Tower Zone, Mount Pleasant, New Brunswick. Geological Society of America, Abstracts with Programs, Volume 16, page 565.

Kyser, T.K., O'Niel, J.R. and Carmichael, I.S.E.
1981: Oxygen isotope thermometry of basic lavas and mantle nodules. Contributions to Mineralogy and Petrology, Volume 77, pages 11-23.

1982: Genetic relations among basic lavas and ultramafic nodules: Evidence from oxygen isotope compositions. Contributions to Mineralogy and Petrology, Volume 81, pages 88-102.

Leake, B.E.
1978: Granite Emplacement: The granites of Ireland and their origin. In Crustal Evolution in Northwestern Britain and Adjacent Regions. Edited by Bowes and B.E. Leake. Seel House Press, Liverpool, pages 221-248.

Leech, G.B., Lowden, J.A., Stockwell, C.H. and Wanless, R.K.
1963: Age determinations and geological studies (including isotopic ages) - Report 4. Geological Survey of Canada, Paper 63-17, page 21.

Lenthall, D.H. and Hunter, D.R.
1977: The geochemistry of the Bushveld Granites in the Potgietersus tin-field. Precambrian Research, Volume 5, pages 359-400.

Lesher, C.E., Walker, D., Candela, P. and Hayes, J.F.
1982: Soret fractionation of natural silicate melts of intermediate to silicic composition. Geological Society of America, Abstracts with Programs, Volume 14, page 545.

Loiselle, M.C. and Wones, D.R.
1979: Characteristics and origin of anorogenic granites. Geological Society of America, Abstracts with Programs, Volume 11, page 468.

Lowden, J.A.
1961: Age determinations by the Geological Survey of Canada, Report 2, isotopic ages. Geological Survey of Canada, Paper 61-17, page 85.

Mahood, G.A. and Hildreth, W.
1983: Nested calderas and trapdoor uplift at Pantalleria; Strait of Sicily. Geology, Volume 11, pages 722-726.

Manning, D.A.C.
1981: The effect of fluorine on liquidus phase relationships in the system Qz-Ab-Or with excess water at 1 Kb. Contributions to Mineralogy and Petrology, Volume 76, pages 206-215.

Manning, D.A.C. and Pichivant, M.
1985: Volatiles and their bearing on the behavior of metals in granitic systems. In Granite Related Mineral Deposits. Edited by R.P. Taylor and D.F. Strong. Canadian Institute of Mining and Metallurgy, Extended Abstracts, Halifax 1985, pages 184-187.

McCarthy, T.S. and Hasty, R.A.
1976: Trace element distribution patterns and their relationship to the crystallization of granitic melts. Geochimica et Cosmochimica Acta, Volume 40, pages 1351-1358.

McConnel, J.
1984: Follow-up geochemistry over three mineralized and metalliferous granitoids in south-central Newfoundland. Mineral Development Division, Newfoundland Department of Mines and Energy, Open File Nfld. 1429, 41 pages.

McGonigal, M.H.
1973: The Gander and Davidsville Groups: Major tectonostratigraphic units in the Gander Lake area, Newfoundland. Unpublished M.Sc. Thesis, Memorial University of Newfoundland, St. John's Newfoundland, 152 pages.

McKenzie, C.B.
1981: Wyllie Hill property examination. Unpublished Report, RioCanex Limited, 3 pages.

McNutt, R.H., Crocket, J.H., Clark, A.H., Caelles, J.C., Farrar, E., Haynes, S.J. and Zentilli, M.
1985: Initial $^{87}Sr/^{86}Sr$ ratios of plutonic and volcanic rocks of the central Andes between latitudes 26° and 29° south. Earth Planetary Science Letters, Volume 27, pages 305-313.

Merrihue, G. and Turner, G.
1966: Potassium-argon dating by activation with fast neutrons. Journal of Geophysical Research, Volume 71, pages 2853-2857.

Michael, P.J.
1983: Chemical differentiation of the Bishop Tuff and other high-silica magmas through crystallization processes. Geology, Volume 11, pages 31-34.

Miller, H.G.
1986a: Gravity surveys in insular Newfoundland. In Current Research. Newfoundland Department of Mines and Energy, Mineral Development Division, Report 86-1, pages 251-256.

1986b: A reophysical interpretation of the onshore and offshore geology of the southern Avalon Zone, Newfoundland. Canadian Journal of Earth Sciences, (in press).

1987: Geophysical studies of the Ackley Granite and the northern Gander Terrane, Newfoundland. Newfoundland Department of Mines and Energy, Mineral Development Division. Report In Press.

Miller, H.G. and Weir, H.C.
1982: The northwest Gander Zone: A Geophysical Interpretation. Canadian Journal of Earth Sciences, Volume 19, pages 1371-1381.

Miller, H.G. and Wright, J.A.
1984: Gravity and magnetic interpretation of the Deer Lake Basin, Newfoundland. Canadian Journal of Earth Sciences, Volume 21, pages 10-18.

Miller, H.G., Goodacre, A.K., Cooper, R.V. and Halliday, D.
1985: Offshore extensions of the Avalon Zone of Newfoundland. Canadian Journal of Earth Sciences, Volume 22, pages 1163-1170.

Miller, C.F., Stoddard, E.F., Bradfish, L.J. and Dollase, W.A.
1981: Composition of plutonic muscovite: Genetic implications. Canadian Mineralogist, Volume 19, pages 25-34.

Mittlefehldt, D.W. and Miller, C.F.
1983: Geochemistry of the Sweetwater Wash Pluton, California: Implications for "anomalous" trace element behavior during differentiation of felsic magmas. Geochimica et Cosmochimica Acta, Volume 47, pages 109-124.

Muecke, G.K. and Clarke, D.B.
1981: Geochemical evolution of the South Mountain Batholith, Nova Scotia: Rare earth element evidence. Canadian Mineralogist, Volume 19, pages 133-145.

Muehlenbachs, K. and Byerly, G.
1982: ^{18}O enrichment of silicic magmas caused by crystal fractionation at the Galapagos spreading center. Contributions to Mineralogy and Petrology, Volume 79, pages 76-79.

Mutschler, F.E., Wright, E.G., Ludington S. and Abbot, J.T.
1981: Granite molybdenite systems. Economic Geology, Volume 76, pages 874-897.

Nie, N.H., Hull, C.H., Jenkins, J.G., Steinbrenner, K. and Bent, D.H.
1975: Statistical package for the Social Sciences, Second Edition. McGraw Hill, New York, 675 pages.

Nockolds, S.R.
1947: The relation between chemical composition and paragenesis in the biotite micas of igneous rocks. American Journal of Science, Volume 245, pages 401-420.

Nolan, F.J.
1969: Report on the Rencontre East molybdenite deposits, Newfoundland. Norlex Mines Limited, Montreal. Newfoundland Department of Mines and Energy, File 1M11/(120), 19 pages.

North American Commission on Stratigraphic Nomenclature
1983: North American stratigraphic code. American Association of Petroleum Geologists Bulletin, Volume 67, pages 841-875.

O'Brien, S.J., Nunn, G.A.G. and Dickson, W.L.
1980a: Terrenceville (1M/10), Newfoundland. Mineral Development Division, Newfoundland Department of Mines and Energy, Map 80-199.

1980b: Gisborne Lake (1M/15), Newfoundland. Mineral Development Division, Newfoundland Department of Mines and Energy, Map 80-200.

O'Brien, S.J., Wardle, R.J. and King, A.F.
1983: The Avalon Zone: A Pan-African terrane in the Appalachian Orogen of Canada. Geological Journal, Volume 18, pages 195-222

O'Brien, S.J., Nunn, G.A.G., Dickson, W.L. and Tuach, J.
1984: Geology of the Terrenceville (1M/10) and Gisborne Lake (1M/15) map area, southeast Newfoundland. Mineral Development Division, Newfoundland Department of Mines and Energy, Report 84-4, 54 pages.

O'Brien, S.J., Dickson, W.L. and Blackwood, R.F.
1986: Geology of the central portion of the Hermitage Flexure area, Newfoundland. In Current Research, Newfoundland Department of Mines and Energy, Mineral Development Division, Report 86-1, pages 189-208.

O'Driscoll, C.F. and Hussey, E.H.
1978: Sound Island (1M/16), Newfoundland. Mineral Development Division, Newfoundland Department of Mines and Energy, Map 78-63.

Olade, M.A.
1980: Geochemical characteristics of tin-bearing and tin-barren granites, northern Nigeria. Economic Geology, Volume 75, pages 71-82.

O'Neil, J.R. and Chappell, B.W.
1977: Oxygen and Hydrogen isotope relations of the Berridale Batholith. Journal of the Geological Society of London, Volume 133, pages 559-571.

O'Sullivan, J.
1982: Report on geochemical and geological surveys carried out on Licences 1797-1804 inclusive, for the period June to October, 1981. Esso Minerals Canada Limited. Newfoundland Department of Mines and Energy, File 1M/196, 17 pages.

1983: Assessment report on trenching and diamond drilling carried out on Licence 2281 during September to December, 1982. Esso Minerals Canada Limited. Newfoundland Department of Mines and Energy, File 1M/207, 13 pages.

Peacock, M.A.
1931: Classification of igneous rock series. Journal of Geology, Volume 39, pages 54-67.

Pearce, J.A., Harris, N.B.W. and Tindle, A.G.
1984: Trace element discriminant diagrams for the tectonic interpretation of granitic rocks. Journal of Petrology, Volume 25, Part 4, pages 956-983.

Pitcher, W.S.
1979: The nature, ascent and emplacement of granitic magmas. Journal of the Geological Society of London, Volume 136, pages 627-662.

1983: Granite type and tectonic environment. In Mountain Building Processes. Edited by K.J. Hsu. Academic Press, London, N.Y., pages 19-40.

Pollard, P.J. and Taylor, R.G.
1985: Tin deposits: Exploration modelling and target generation. James Cook University of North Queensland, 170 pages.

Poole, J.C., Delaney, P.W. and Dickson, W.L.
1985: Geology of the Francois Granite, south coast of Newfoundland. In Current Research. Newfoundland Department of Mines and Energy, Mineral Devlopment Division, Report 85-1, pages 145-154.

Purdy, J.W. and Jaeger E.
1976: K-Ar ages of rock-forming minerals from the central Alps. Memoirs of the Institute of Geology and Mineralogy, University of Padua, Italy, Volume 30, 37 pages.

Read, H.H.
1957: The granite controversy. Thomas Murby and Co., London, 430 pages.

Rice, A.
1981: Convective fractionation: A mechanism to provide cryptic zoning (macrosegregation), layering, crescumulates, banded tuffs and explosive volcanism in igneous processes. Journal of Geophysical Research, Volume 86, Number B1, pages 405-417.

Richardson, J.M.G., Spooner, E.T.C. and McAuslan, D.A.
1982: The East Kemptville tin deposit, Nova Scotia: An example of a large tonnage, low grade, greisen-hosted deposit in the endocontact zone of a granite batholith. In Current Research 1B. Geological Survey of Canada, Paper 82-1B, pages 27-32.

Ricketts, J. and Baumgarner, J.
1954: Report on field examinations in Newfoundland. American Zinc Company of Tennessee. Newfoundland Department of Mines and Energy, File 1M/42.

Roedder, E.
1979: Fluid inclusions as samples of ore fluids. In Geochemistry of Hydrothermal Ore Deposits. Edited by H.L. Barnes. Holt, Rinehart and Winston, New York, pages 684-737

1984: Fluid inclusions. In Reviews in Mineralogy, Volume 12. Edited by P.H. Ribbe. Mineralogical Society of America, 664 pages.

Saunders, P.
1980: Assessment report on geological and geochemical surveys in the Hungry Grove Pond area, Newfoundland. Newfoundland Department of Mines and Energy, File 1M14/(185), 100 pages.

Scott, S.D.
1980: Geology and structural control of Kuroko-type massive sulphide deposits. In The Continental Crust and its Mineral Deposits. Edited by D.W. Strangeway. Geological Association of Canada, Special Paper 20, pages 705-721.

Seal, R.R., Archibald, D.A., Clark, A.H. and Farrar, E.
1985: K-Ar evidence for Pre-Devonian orogeny, Lake George area, Frederickton Trough, S.W. New Brunswick. Geological Association of Canada, Program with Abstracts, Volume 10, page A55.

Seedorf, E.
1985: Cyclic development of hydrothermal mineral assemblages related to multiple intrusions at the Henderson porphyry molybdenum deposit, Colorado. In Granite Related Mineral Deposits. Edited by R.P. Taylor and D.F. Strong. Canadian Institute of Mining and Metallurgy, Extended Abstracts, Halifax, pages 226-235.

Shand, S.J.
1950: Eruptive rocks, fourth edition. John Wiley and Sons, New York, 489 pages.

Shaw H.R.
1980: The fracture mechanisms of magma transport from the mantle to the surface. In Physics of magmatic Processes. Edited by R.B. Haywares. Princeton University Press, pages 201-264.

Shaw, H.R., Smith, R.L. and Hildreth, E.W.
1976: Thermogravitational mechanisms for chemical variations in zoned magma chambers. Geological Society of America, Abstracts with Programs, Volume 8, page 1102.

Sillitoe, R.H., Halls, C. and Grant, J.N.
1975: Porphyry tin deposits in Bolivia. Economic Geology, Volume 70, pages 913-927.

Sorensen, H.
1974: The alkaline rocks. John Wiley and Sons, New York, 622 pages.

Sparks, R.S.J., Huppert, H.E. and Turner, J.S.
1984: The fluid dynamics of evolving magma chambers. Philisophical Transactions of the Royal Society of London, Volume A310, pages 511-534.

Steiger, R.H. and Jaeger, E.
1977: Subcommission on Geochronology: Convention on the use of decay constants in geo- and cosmo-chronology. Earth and Planetary Science Letters, Volume 36, pages 359-362.

Stein, H.J.
1985: Genetic traits of Climax-type granites and molybdenite mineralization, Colorado Mineral Belt. In Granite-Related Mineral Deposits. Edited by R.P. Taylor and D.F. Strong. Canadian Instititute of Mining and Metallurgy, Extended Abstracts, Halifax 1985, pages 242-247.

Stein, H.J. and Hannah, J.L.
1985: Movement and origin of ore fluids in Climax-type systems. Geology, Volume 13 pages 469-474.

Stone, M. and Exley, C.S.
1985: High heat production granites of southwest England and their associated mineralization: A review. In High Heat Production (HHP) Granites, Hydrothermal Circulation, and Ore Genesis. Edited by C. Halls. The Institution of Mining and Metallurgy, London, England, pages 437-458.

Streckeisen, A.
1976: To each plutonic rock its proper name. Earth Science Reviews, Volume 12, pages 1-23.

Strong, D.F.
1980: Granitoid rocks and associated mineral deposits of eastern Canada and western Europe. In The Continental Crust and its Mineral Deposits. Edited by D.W. Strangeway. Geological Association of Canada Special Paper 20, pages 741-769.

1981: Ore deposit models - 5. A model for granophile mineral deposits. Geoscience Canada, Volume 8, pages 155-161.

1985: Mineral deposits associated with granitoid rocks of eastern Canada and western Europe: A review of their characteristics and their depositional controls by source rock compositions and late-stage magmatic processes. In Granite-Related Mineral Deposits. Edited by R.P. Taylor and D.F. Strong. Canadian Institute of Mining and Metallurgy, Extended Abstracts, Halifax 1985, pages 248-257.

Strong, D.F., Dickson, W.E., O'Driscoll, C.F. and Kean, B.F.
1974: Geochemistry of eastern Newfoundland granitoid rocks. Mineral Development Division, Newfoundland Department of Mines and Energy, Report 14-3, 140 pages.

Strong, D.F. and Hanmer, S.K.
1981: The leucogranites of southern Brittany: Origin by faulting, frictional heating, fluid flux and fractional melting. Canadian Mineralogist, Volume 19, pages 163-176.

Strong, D.F., Fryer, B.J. and Kerrich, R.
1984: Genesis of the St. Lawrence fluorspar deposit as indicated by fluid inclusion, rare earth element and isotopic data. Economic Geology, Volume 79, pages 1142-1158.

Strong, D.F. and Chatterjee, A.K.
1985: A review of some chemical and mineralogical characteristics of granitoid rocks hosting Sn, W, U, Mo deposits in Newfoundland and Nova Scotia. In High Heat Production (HHP) Granites, Hydrothermal Circulation, and Ore Genesis. Edited by C. Halls. The Institution of Mining and Metallurgy, London, England, pages 489-516.

Sutherland-Brown, A.
1976: Morphology and Classification. In Porphyry Deposits of the Canadian Cordillera. Edited by A. Sutherland-Brown. Canadian Institute of Mining and Metallurgy, Special Volume 15, pages 44-51.

Swanson, E.A. and Brown, R.L.
1962: Geology of the Buchans orebodies. Canadian Institute of Mining and Metallurgy, Volume 55, pages 618-626.

Swinden, H.S. and Dickson, W.L.
1981: Mt. Sylvester (2D/13), Newfoundland. Mineral Development Division, Newfoundland Department of Mines and Energy, Map 81-7.

Tapponier P. and Molnar, P.
1976: Slip-line field theory and large scale continental tectonics. Nature, Volume 264, pages 319-324.

Taylor, D. and Van Leeuwen, D.
1980: Porphyry deposits of southeast Asia. Mining Geology Special Issue, Volume 8.

Taylor, H.P.
1968: The oxygen isotope geochemistry of igneous rocks. Contributions to Mineralogy and Petrology, Volume 19, pages 1-71.

1971 Oxygen isotope evidence for large scale interaction between meteoric groundwaters and Tertiary granodiorite intrusions, western Cascade Range, Oregon. Journal of Geophysical Research, Volume 76, pages 7855-7874.

1978: Oxygen and hydrogen isotope studies of plutonic granitic rocks. Earth and Planetary Science Letters, Volume 38, pages 177-210.

1979: Oxygen and hydrogen isotope relationships in hydrothermal mineral deposits. In Geochemistry of Hydrothermal Ore Deposits. Edited by H.L. Barnes. John Wiley and Sons, New York, pages 236-277.

Taylor, H.P. and Forrester, R.W.
1979: An oxygen and hydrogen isotope study of the Skaergaard intrusion and its country rocks: A description of a 55 m. y.-old fossil hydrothermal system. Journal of Petrology, Volume 20, pages 355-419.

Taylor, S.R. and Gorton, M.P.
1977: Geochemical application of spark source mass spectography III. Element sensitivity, precision and accuracy. Geochimica et Cosmochimica Acta, Volume 41, pages 1375-1380.

Taylor, R.G.
1979: Geology of tin deposits. Elsevier, New York, 543 pages.

Taylor, R.P.
1979: Topsails igneous complex: Further evidence of middle Paleozoic epeirogeny and anorogenic magmatism in the northern Appalachians. Geology, Volume 7, pages 488-490.

Taylor, R.P. and Fryer, B.J.
1983: Rare earth element lithogeochemistry of granitoid mineral deposits. Canadian Institute of Mining and Metallurgy Bulletin, Volume 76, pages 74-80.

Taylor, R.P. and Strong, D.F.
1985: (Editors) Granite-related mineral deposits. Canadian Institute of Mining and Metallurgy, Extended Abstracts, Halifax, 289 pages.

Taylor, R.P., Sinclair, W.D. and Lutes, G.
1985: Geochemical and isotopic characterization of granites related to W-Sn-Mo mineralization in the Mount Pleasant area, New Brunswick. In Granite-Related Mineral Deposits. Edited by R.P. Taylor, and D.F. Strong. Canadian Institute of Mining and Metallurgy, Extended Abstracts, Halifax, pages 265-273.

Teng, H.C. and Strong, D.F.
1975: Geology and geochemistry of the St. Lawrence Granite and associated fluorspar deposits, southeast Newfoundland. Canadian Journal of Earth Science, Volume 13, pages 1374-1385.

Thompson, R.N., Harrison, M.A., Hendry, G.L. and Parry, S.J.
1984: An assessment of the relative roles of crust and mantle in magma genesis: an elemental approach. Philisophical Transactions of the Royal Society of London, Volume A310, pages 549-590.

Thor[illegible]n, C. P. and Tuttle, O. F.
1960: Chemistry of igneous rocks, I: Differentiation Index. American Journal of Science, Volume 258, pages 664-684.

Tindle, A.G. and Pearce, J.A.
1981: Petrogenetic modelling of an in-situ fractional crystallization in the zoned Loch Doon Pluton, Scotland. Contributions to 'Mineralogy and Petrology,' Volume 78, pages 196-207.

Tingle, T.N. and Fenn, P.M.
1984: Transport and concentration of molybdenum in molybdenite systems: Effects of fluorine and sulphur. Geology, Volume 12, pages 156-158.

Tischendorf, G.
1977: Geochemical and petrographic characteristics of silicic magmatic rocks associated with rare-element mineralization. In Mineralization Associated with Acid Magmatism. Edited by M. Stemprock, L. Burnol, and G. Tischendorf. Geological Survey of Czechoslovakia, Prague, pages 41-96.

Trueman, D.L., Peterson, J.C. and Smith, D.G.W.
1985: The Thor Lake, N.W.T. rare-metal deposit. In Granite-Related Mineral Deposits. Edited by R.P. Taylor and D.F. Strong. Canadian Institute of Mining and Metallurgy, Extended Abstracts, Halifax, pages 279-284.

Tuach, J.
1984a: Metallogenic studies of granite associated mineralization in the Ackley Granite and Cross Hills Plutonic Complex, Fortune Bay area, Newfoundland. Current Research, Part A, Geological Survey of Canada, Paper 84-1A, pages 499-504.

1984b: Tin analyses from whole rock samples of the Ackley Granite and Cross Hills Plutonic Complex, southeast Newfoundland. Mineral Development Division, Newfoundland Department of Mines and Energy, File 1M/211, 10 pages.

1984c: Tungsten analyses from topaz greisen veins, and the economic significance of lithogeochemical trends in the Ackley Granite. Mineral Development Division, Newfoundland Department of Mines and Energy, File 1M/214, 12 pages.

Tuach, J., Davenport, P.H., Dickson, W.L. and Strong, D.F.
1986: Geochemical trends in the Ackley Granite, southeast Newfoundland: Their relevance to magmatic/metallogenic processes in high-silica granitoid systems. Canadian Journal of Earth Sciences, Volume 23, pages 747-765.

Vernon, R.H.
1984: Microgranitoid enclaves in granites: Globules of hybrid magma quenched in a plutonic environment. Nature, Volume 309, pages 438-439.

1986: K-feldspar megacrysts: Phenocrysts, not porphyroblasts. Earth Science Reviews, Volume 23, pages 1-63.

Volkov, V.N. and Gorbacheva, S.A.
1980: Composition of rock forming biotite and the variation in crystallization conditions in a vertically zoned pluton. Geochemistry International, Volume 17, pages 75-79.

Wanless, R.K., Stevens, R.D., Lachance, G.R. and Delabio, R.N.
1972: Age determinations and geological studies, K-Ar isotopic ages, Report 10. Geological Survey of Canada, Paper 71-2, page 94.

Watson, E.B.
1979: Zircon saturation in felsic liquids. Experimental results and applications to trace element geochemistry. Contributions to Mineralogy and Petrology, Volume 70, pages 407-419.

Weaver, D.F.
1967: A geological interpretation of the Bouguer anomaly field of Newfoundland. Dominion Observatory Canada Publication, Volume 35, 5 pages.

Weibe, R.A.
1978: Anorthosite and associated plutons, southern Nain complex, Labrador. Canadian Journal of Earth Sciences, Volume 15, pages 1326-1340.

Wenner, D.B. and Taylor, H.P.
1976: Oxygen and hydrogen isotope studies of a Precambrian granite-rhyolite terrain, St. Francois Mountains, southeast Missouri. Geological Society of America Bulletin, Volume 87, pages 1587-1598.

Westra, G. and Keith, S.B.
1981: Classification and genesis of stockwork Mo deposits. Economic Geology, Volume 76, pages 844-873.

Whalen, J.B.
1976: Geology and geochemistry of molybdenite showings of the Ackley Granite, Fortune Bay, Newfoundland. Unpublished M.Sc. thesis, Memorial University of Newfoundland, St. John's, 267 pages.

1980: Geology and geochemistry of the molybdenite showings of the Ackley City Batholith, southeast Newfoundland. Canadian Journal of Earth Sciences, Volume 17, pages 1246-1258.

1983: The Ackley City Batholith, southeastern Newfoundland: Evidence for crystal versus liquid state fractionation. Geochimica et Cosmochimica Acta, Volume 47, pages 1443-1457.

1986: A-type granites in New Brunswick. In Current Research, Part A. Geological Survey of Canada, Paper 86-1A, pages 297-300.

White, A.J.R.
1979: Sources of granite magmas. Geological Society of America, Abstracts with Programs, Volume 11, page 539.

White, A.J.R., Beams, S.D. and Cramer, J.J.
1977: Granitoid types and mineralization with special reference to tin. In Plutonism in Relation to Volcanism and Metamorphism. Edited by N. Yamada. International Geological Correlation Program, 7th Circum-Pacific Plutonism Project Meeting, Toyoma, Japan, pages 89-100.

White, A.J.R. and Chappell, B.W.
1983: Granitoid types and their distribution in the Lachlan Fold Belt, southeastern Australia. Geological Society of America, Memoir, Volume 159, pages 21-34.

White, D.E.
1939: Geology and molybdenite deposits of the Rencontre Lake area, Fortune Bay, Newfoundland. Unpublished Ph.D. thesis, Princeton University, 119 pages.

1940: The molybdenite deposits of the Rencontre Lake area, Newfoundland. Economic Geology, Volume 35, pages 967-995.

White, W.H., Bookstrom, A.A., Kamilli, R.J., Ganster, M.W., Smith, R.P., Ranta, D.E. and Steininger, R. C.
1981: Character and origin of Climax-type molybdenum deposits. Economic Geology, Seventy-fifth Anniversary Volume, pages 270-316.

Williams, H.
1971: Geology of the Belleoram map area (1M/11), Newfoundland. Geological Survey of Canada, Paper 70-65, 39 pages.

1967: Geology, Island of Newfoundland. Geological Survey of Canada, Map 1231A.

Williams, H. and Hatcher, R.D., Jr.
1983: Appalachian suspect terranes. Geological Society of America, Memoir 158, pages 33-53.

Wilton, D.H.C.
1984: Metallogenic, tectonic and geochemical evolution of the Cape Ray Fault Zone, with emphasis on electrum mineralization. Unpublished Ph.D. thesis, Memorial University of Newfoundland, 618 pages.

1985: Tectonic evolution of southwestern Newfoundland as indicated by granitoid petrogenesis. Canadian Journal of Earth Sciences, Volume 22, pages 1080-1092.

Winchester, J.A. and Floyd, P.A.
1977: Geochemical discrimination of different magma series and their differentiation products using immobile elements. Chemical Geology, Volume 20, pages 325-313.

Wyllie, P.J.
1977: Crustal anatexis: An experimental review. Tectonophysic, Volume 43, pages 41-71.

Zentilli, M. and Reynolds, P.H.
1985: $^{40}Ar/^{39}Ar$ dating of micas from the East Kemptville tin deposit, Yarmouth County, Nova Scotia. Canadian Journal of Earth Sciences, Volume 10, pages 1546-1548.

APPENDIX A: NOMENCLATURE OF THE GRANITOID ROCKS

The objectives of this section are to propose nomenclature and to redefine existing units in accordance with the recommendations of the North American Commission on Stratigraphic Nomenclature (NACSN, 1983).

History of Nomenclature and Defined Areas

John W. Ackley was a mining engineer who supervised exploration efforts in the Rencontre Lake area during the late thirties (White, 1939, 1940). The exploration camp on the west side of Rencontre Lake was named Ackley City in his honour and subsequently the adjacent mineral deposit became known as the Ackley City prospect.

The name Ackley Batholith was first used by White (1939, 1940) to describe the biotite granites and alaskite in the Rencontre Lake to Long Harbour River area. Granitic rocks in the Gisborne Lake and Terrenceville map areas were included by Bradley (1962), and granitic rocks as far north as Fogo in northern Bonavista Bay were included in the batholith by Jenness (1963). Further definition of the Ackley Batholith in the Belleorum map area was made by Anderson (1965) and by Williams (1971). Granitic rocks in the Gander Lake (west half) map area were assigned to the Ackley Batholith by Anderson and Williams (1970).

The Ackley Batholith (see Figs. 1 and 2) as delineated on the geological compilation map of the Island of Newfoundland by Williams (1967), provided a geographic basis for work reported by Strong et al.

(1974) and by Whalen (1976, 1980, 1983). Strong et al. (op. cit.), used the names Ackley Batholith and Ackley City Batholith in their report. Whalen (op. cit) has used the name Ackley City Batholith throughout his work. Bell et al. (1977) refer to the Ackley City Batholith and to the Ackley City Granite. Clearly, the term Ackley should have precedence over Ackley City.

Dickson (1983) divided the area outlined by Williams (1967) into three main plutonic units, which he named the North West Brook Complex, the Eastern Meelpaeg Complex and the Ackley Granite (Fig. 2). He defined the Ackley Granite as consisting predominantly of medium to coarse grained, uniform to porphyritic, massive biotite granite. The North West Brook and the Eastern Meelpaeg complexes are strongly foliated granitoids and metasedimentary rocks of diverse composition. The North West Brook Complex is not bounded by the outline of the Ackley Batholith as shown by Williams (1967; dashed line boundary on Fig. 2), but continues along strike to the southwest and can be correlated with unnamed granitoids and metasedimentary rocks mapped by Colman-Sadd (1976). Dallmeyer et al. (1983) refer to the Ackley Granite as defined by Dickson (1983).

In addition to renaming and redefining the Ackley Batholith, Dickson (1983) subdivided his Ackley Granite into 10 separate subunits (Fig. 2) on the basis of mineralogy and texture (see Chapter 3).

Names to Abandon

Ackley has precedence over Ackley City (White, 1939, 1940) and all stratigraphic names using Ackley City should be abandoned.

The names ending in the term batholith should be abandoned for the following reasons: (i) A batholith is defined as an area of granitoid rocks larger than 100 km^2 (Bates and Jackson, 1980) and the name has different genetic implications for various workers; (ii) there is no provision for the term batholith in the recommended stratigraphic code for North America (North American Commission on Stratigraphic Nomenclature, 1983); iii) Ackley Batholith has been used to describe huge areas of granitoid rocks (Jenness, 1963) which are physically and probably genetically independent of the unit which is currently understood to represent the Ackley magmatic system.

Boundary Revision and Rank Elevation to Ackley Granite Suite

The work reported in this thesis has generally confirmed the subdivisions of the study area which were established by Dickson (1983), and has shown the need for minor revisions. Ackley is a well recognized and accepted name in the literature and should be retained. Accordingly, the Ackley Granite is elevated in rank to the Ackley Granite Suite to permit naming of the subunits.

There are significant geochemical, geochronological and geophysical differences within the Ackley Granite as defined by Dickson (1983), such

that the hornblende-bearing granodiorite to granite plutons in the western and northeastern extremities of the granite (The Koskaecodde and Mollyguajeck plutons, Fig. 2) may be unrelated to the thermal and magmatic pulse which was responsible for generation of the granites in the remainder of the study area. The boundaries of the Ackley Granite Suite are revised from those of the Ackley Granite (Dickson, 1983) to exclude these granodiorite-granite plutons (Fig. 2).

The Ackley Granite Suite is now defined as an area of predominantly post-tectonic, biotite-bearing, anorogenic granites (sensu stricto; Streckeisen, 1976), which exhibit sharp and discordant intrusive contacts with the country rocks. These granites appear to have been generated in a large thermal and magmatic event which has been dated by K-Ar, ^{40}Ar-^{39}Ar and Rb-Sr systematics to have occurred between 350 and 375 Ma.

Except where noted, internal contacts between granites of the Ackley Granite Suite are approximate, since outcrop is commonly poor and confined to isolated low-lying ridges. In areas with abundant outcrop, internal contacts are diffuse and gradational.

New Names

Granites of the Ackley Granite Suite: Names for the members of the Ackley Granite Suite are presented in Figure 2 and in Table 1. Unit descriptions, unit numbers, and their boundaries are generally those of Dickson 1983). However, unit 12 is thought to be composite and best

assigned to other units (see below). Further boundary revisions may be necessary in future.

The Mount Sylvester Granite is named after Mount Sylvester in the northeastern part of the Ackley Granite Suite. Additional outcrop areas are present to the north of the Kepenkeck Granite defined below. This granite was formerly referred to as unit 11A and consists of gray, massive, coarse grained biotite granite.

The Kepenkeck Granite is a new name for unit 11B which is located in the northern part of the Ackley Granite Suite to the east of Kepenkeck Lake. It consists of gray, massive, medium grained, porphyritic, biotite-muscovite granite. Dickson (1983) noted that there is a coincident aeromagnetic low associated with this granite and that it may represent a separate pluton which has intruded the Mount Sylvester Granite.

The Tolt Granite is equivalent to unit 13, and is the eastern member of the Ackley Granite Suite. This area was initially named the Tolt Facies of the Ackley Granite by Dickson et al. (1980), after a prominent hill in its northern extremity. It consists of pink, coarse grained, porphyritic, massive, biotite granite with minor areas of medium grained, equigranular, biotite granite. The outcrops exposed on the Burin Peninsula highway (Route 210), at the eastern margin of the granite, are atypical of much of the Tolt Granite and the Ackley Granite Suite in that they are relatively mafic and contain hornblende.

The Hungry Grove Granite is named after Hungry Grove Pond. It consists of pink, coarse grained, equigranular, biotite granite and is located in the central and eastern part of the Ackley Granite Suite (unit 14). The southeastern half of unit 12 has chemical, petrological and isotopic characteristics which indicate that the rocks are equivalent to unit 14, and consequently these rocks are included in the Hungry Grove Granite.

Separate outcrop-areas of fine grained, variably textured granite in the Rencontre Lake area and in the Sage Pond area were described as unit 14A by Dickson. There are significant geochemical and possibly genetic differences between the two areas, despite an overall similarity in physical appearance and two separate names are required. The Rencontre Lake Granite is located in the southwest part of the Ackley Granite Suite and is named after Rencontre Lake at its southern margin. It is predominantly a pink to orange, fine to medium grained, miarolitic biotite granite. Abundant fine grained aplite, and local pegmatite patches and occasional stockscheider may be present towards the southern contact and the significant molybdenite prospects are present at the southern contact. In the northwestern part of this unit, the rocks contain relatively less silica (70 to 72% versus 72 to 78%) and may contain minor hornblende. Variably textured fine grained rocks between Long Harbour and Gisborne Lake are named The Sage Pond Granite, after Sage Pond, and host massive, quartz-topaz greisen. The Sage Pond Granite grades northwards to the coarse grained Hungry Grove Granite.

The Meta Granite refers to pink, medium grained, equigranular to coarse grained, porphyritic, biotite granite, formerly called unit 15. The granite is located in the east-central part of the Ackley Granite Suite and is named after Meta Pond. Very few outcrops are present in this area.

Granodiorite-Granite Plutons: The Koskaecodde Pluton refers to coarse grained, massive, porphyritic, biotite-hornblende granodiorite with subordinate granite (unit 9). The Pluton is located to the west of the Ackley Granite Suite in the Koskaecodde Lake area. Granodiorite and granite previously included in the northern half of unit 12 have been assigned to this Pluton.

The Mollyguajeck Pluton refers to rocks located to the northeast of the Ackley Granite Suite, formerly assigned to unit 10, which are comparable to the Koskaecodde Pluton. Part of the contact between the Mollyguajeck Pluton and the Aokley Granite Suite is shown by Dickson (1983) as a north-trending fault and the entire contact may be faulted. The nature of the contact between the Koskaecodde Pluton and the Ackley Granite Suite is less obvious and requires further work to permit accurate definition.

APPENDIX B

SUMMARY OF SAMPLE PREPARATION TECHNIQUES, ANALYTICAL TECHNIQUES, PRECISION AND ACCURACY.

B-1 Sample Collection and Preparation

B-2 Microprobe Techniques.

B-3 Major and Trace Element Analyses (Dickson, 1983)

B-4 Instrumental Neutron Activation Analyses (Rare Earth Elements, As, Co, Cs, Hf, Sb, Sc, Ta, Th, and U)

B-5 Thin Film XRF Analyses (Rare Earth Elements)

B-6 Rb-Sr Analyses

B-7 $^{40}Ar/^{39}Ar$ Analyses

B-8 Oxygen Isotope Analyses

B-9 Fluid Inclusion Techniques

B-1 SAMPLE COLLECTION AND PREPARATION

The regional rock sampling program was conducted by Dickson (1983) on a 2 x 2 km square grid following a technique outlined by R.G. Garrett of the Geological Survey of Canada. Numerous cells could not be sampled due to lack of outcrop, and details of the project are provided by Dickson (1983). Approximately 2 kg of sample were collected as fresh chips from outcrop using a sledgehammer, and a fresh, fist-sized sample was collected from each sample site. The chips were reduced to less than 5 mm in a jaw crusher, and approximately 100 g were powdered to -300 mesh with a ceramic disk pulverizer in preparation for analyses. Each hand sample was slabbed, a thin section was prepared, and half was assigned to a reference collection maintained by the Department of Mines and Energy in St John's. The analytical data is listed in Dickson (1983), and is available from the Newfoundland Department of Mines and Energy on request.

Samples of granite collected by the current author from the Sage Pond area were of similar size and were prepared in the same manner. The outcrops of greisen are severely weathered and difficulty was encountered in obtaining fresh material. The lithology of the greisen in drill core is variable and large contiguous samples of an individual greisen-type were unavailable since much of the cored material was sent for assay.

B-2 MICROPROBE TECHNIQUES

Quantitative electron microprobe analyses of minerals in polished thin sections were performed at the Earth Science Department of Memorial University. In all samples, the largest and best formed crystals were analyzed. A three spectrometer JEOL JXA-50A automated electron microprobe microanalyser with Krisel control through a PDP-11 mini-computer was used for the analyses. Operating conditions were an accelerating voltage of 15 Kv, a beam current around 0.022 microamps, a beam diameter of 1-2 micrometers, and a counting rate of up to 60,000 with a default time of 30 seconds. The alpha correction program was used for the analyses.

Acceptable analyses totalled between 98 and 102% for non-hydrous silicate phases. The analyses of the hydrous silicates were monitored by frequent reanalyses of the standards, and were used if the values for the standard were acceptable. Precision is estimated to be within 5% and accuracy to be within 10%. The similarity of values obtained from biotite from repeat analyses within grains, and between grains in the same sample, (Appendix C) testify to the validity of the data presented. In addition, there is good agreement between microprobe analyses and AA-whole rock analyses of biotite separates (see Table 6).

A Hitachi S-570 scanning electron microscope with a solid state backscatter detector, and a Trachor Northern 5500 energy-dispersive X-ray analyser was used to assist in mineral identification. Accelerating voltage was 15 kv.

B-3 MAJOR AND TRACE ELEMENT ANALYSES

B-3-1 Analytical Techniques

Most major elements, Li, Mo, total Fe as Fe_2O_3, and Sn were determined by atomic absorption spectrometry, FeO by titration, P_2O_5 was analyzed colourimetrically, S, CO_2, and H_2O+ were analyzed using infrared detection apparatus, F was determined by the ion-selective electrode technique, U by neutron activation analyses, and other trace elements by X-ray fluorescence. Loss on ignition was determined by heating samples in a muffle furnace to 1100°C for 2 hours and measuring weight loss.

The X-ray fluorescence analyses were performed on pressed pellets at the Earth Science Department of Memorial University using a Phillips 1450 X-ray fluorescence spectrometer with a rhodium tube. U concentration was determined by Atomic Energy of Canada Limited and all other analyses were performed at the Department of Mines and Energy Laboratory in St. John's. The atomic absorption analyses were performed on a Varium Model 875 atomic absorption spectrometer with digital readout.

B-3-2 Detection Limits, Accuracy and Precision

Estimates of analytical detection limits, accuracy and precision with reference to international standards were presented by Dickson (1983). The accuracy and precision of the major elements is estimated to be within 2%. Only those trace elements with an estimated accuracy and precision of ± 5% were used in this thesis. Values for Cu, Ni and Cr were at and near the detection limit and are not considered useful. Results for La and Ce were poor and were therefore omitted from the current discussion.

B-4 INSTRUMENTAL NEUTRON ACTIVATION ANALYSES

Instrumental Neutron Activation Analyses were performed on 20 samples for the rare earth elements and for As, Co, Cs, Hf, Sb, Sc, Ta, Th, U, and W. This work was done by Dr. R.P. Taylor at the University of Montreal.

B-5 THIN FILM X-RAY FLUORESCENCE TECHNIQUES

Rare earth element analyses were carried out on 14 samples at Earth Science Department of Memorial University, using the thin film X-ray fluorescence technique developed by Fryer (1977). In this method, 1-2 gm of sample was leached using HF, and the resulting solution was passed through an ion exchange column. The REE were eluted by 2N HCl, H_2SO_4 was added to remove Ba, and the solution was dried on ion exchange paper. This paper was then analyzed on the X-ray fluorescence spectrometer.

The data are accurate within ± 10% or 0.1%, whichever is greater.

B-6 Rb/Sr ANALYSES

Rb/Sr analyses were carried out on 14 samples in the Department of Earth Sciences at Memorial University. Replicate Rb and Sr analyses, sufficient to provide a precision of approximately ± 0.3% on the Rb/Sr ratio, were obtained using standard whole rock pressed pellet X-ray fluorescence techniques (computer controlled Phillips PW1450). The estimated 2σ error for Rb and Sr concentrations is ± 1%.

Aliquots of each sample were dissolved in HF-HClO4 mixtures in teflon beakers, and Sr was separated by standard ion exchange methods. The separated Sr was loaded as the phosphate on single\Ta filaments, and analysed for its isotopic composition on a Micromass 30B thermal ionization mass spectrometer. Data acquisition and filament current was computer controlled. The intensity of the ^{88}Sr beam was maintained between 1 and 2 volts (Gain 1), and collected in a Faraday 'cup' detector.

Data were fitted to isochrons using the regression method of York (1969), with modifications from Brooks et al. (1972). The decay constant recommended by Steiger and Jager (1977), $\lambda^{38}Rb = 1.42 * 10\text{-}11\ yr^{-1}$, was used for computation.

B-7 $^{40}AR/^{39}AR$ DATING

The analyses were performed by Dr. D. Kontac. The $^{40}Ar/^{39}Ar$ dating technique (Merrihue and Turner, 1966) has been described in detail by Dalrymple and Lanphere (1971).

Pure mineral separates were prepared from 11 samples from throughout the study area using conventional magnetic separation and heavy liquid techniques. Samples were double wrapped in aluminum foil and together with three mineral age standards (JC-90) were irradiated for 60 hours at 2 MWH in the McMaster University reactor. (see Berger and York, 1979 and Archibald et al., 1983). After irradiation and removal from the sample holder, mineral separates were loaded into

tantalum containers, and subject to an 18 hour bake-out at 250°C. Samples were then fused in a stainless steel turret system, and analyzed using the mass spectrometer at Queens University. Details of data collection and reduction, along with correction procedures for interfering isotopes, are given by Kontak (1985).

The J values for the monitors and the $^{40}Ar/^{39}Ar$ ages have been calculated using expressions given by Dalrymple and Lanphere (1971), and the decay constants and isotopic abundances recommended by Steiger and Jager (1977); all errors are quoted at the 95% confidence level. The J values for the monitor range from 0.014466 to 0.014629 (mean of 0.014551-0.505%) in a random fashion, which indicates that there was no systematic variation in the flux gradient within the reactor.

The errors presented with the data include the calculated error in the J value; ommision of this factor from the error calculation would approximately half the uncertainty in age. The maximum errors have been presented to allow absolute comparison of the results to previous data. Ommission of the error in the J value is valid for internal comparison of the data since all the samples were irradiated together.

B-8 OXYGEN ISOTOPE ANALYSES

The preparation, and oxygen isotope analysis, of 23 samples from the study area were performed at the University of Western Ontario by Dr. R. Kerrich. Oxygen was extracted from minerals with bromine pentafluoride and quantatively converted to CO_2 prior to mass

spectrometric analysis (Clayton and Mayeda, 1963). Isotope data are reported as $\delta^{18}O$ in per mil relative to SMOW (Standard Mean Ocean Water). The overall reproducibility of $\delta^{18}O$ whole rock values has averaged -0.16 per mil (1σ). Analysis of NBS-28 gives 9.8 per mil.

Fractionations or differences in $\delta^{18}O$ among minerals are quoted as, defined as:

$$\alpha_{A-B} = 1000 \ln_{A-B} \sim \delta_A - \delta_B$$

where α is the fractionation factor for the coexisting minerals A and B.

Mineral separates were prepared using conventional magnetic separation and heavy liquid techniques. Quartz was isolated from quartz-feldspar mixtures by digestion of the latter in H_2SiF_6. The quartz-feldspar mixtures were reacted with BrF_5 first at 250°C and subsequently at 600°C to oxidize quartz. $\delta^{18}O$ values obtained from quartz separates and independently from the high temperature reaction were generally within ± 0.2 per mil.

Composite samples were prepared by thoroughly mixing 2 g powders of selected samples listed below. The regional Gander sample was collected by Dr. D. F. Strong and was made up of a composite of 6 powdered hand specimens of schistose metasedimentary rocks collected from the Gander Group at 5 km intervals along the Trans Canada Highway.

Samples used to make up composites[1] representing country rock lithologies are listed below:

GANDER COMPOSITES

G-1	Regional	Metasediments	Collected by D.F. Strong at 5 km intervals on Trans Canada Highway.
G-2	Marginal	Metasediments	220648, 220589, 220341, 220110, 220505, 220530.
G-3	Roof Pendant	Granite	220131, 220194, 220197
G-4	Deformed Intrusives	Granite	220141, 220722, 220656, 220234, 220223

AVALON COMPOSITES

A-1	Marginal	Metasediment	220120, 220455, 22020 JT-106B 220134, 220220
A-2	Roof Pendant	Schist	220115, 220392, 220594 220399
A-3	Marginal	Volcanic rocks	1940302, 1940295, JT-65, JT-487

[1] Samples preceded by 220 from collection of L. Dickson. Samples preceded by 1940 from collection of S. O'Brien.

B-9 FLUID INCLUSION TECHNIQUES

Doubly polished wafers were prepared for optical examination of fluid inclusions. Relative phase volumes in the fluid inclusions were estimated from optical study. Heating and freezing of the fluid inclusions were performed in the Earth Science Department of Memorial University using a Chaixmeca heating-freezing stage. Ideally, temperature measurements with this stage are possible within ± 0.2°C, but the small size of the inclusions lead to errors in the order of 1 degree for freezing, and 0.5°C for freezing temperatures. Inclusions were not heated above a temperature 500°C.

APPENDIX C

REPRESENTATIVE ELECTRON MICROPROBE ANALYSES OF MINERAL PHASES

APPENDIX C-1: Representative electron microprobe analyses and structural formula of feldspar.

SAMPLE NO.	7040024	7040024	7040024	1220087
No Anal.	1	1	2	1
Type	K-Perthite	Na-Lamellae	Plag	K-Perthite
Major oxide (weight percent).				
SiO_2	65.90	72.02	72.44	65.91
Al_2O_3	17.40	19.79	19.73	19.03
FeO_t	0.07	0.11	0.04	0.03
CaO	0.00	0.00	0.28	0.00
Na_2O	0.62	12.28	10.86	1.02
K_2O	14.73	0.11	0.21	15.77
TOTAL	98.73	104.35	103.57	101.86
No. of cations on the basis of 32 oxygens.				
Si	12.216	12.059	12.151	11.946
Al	3.803	3.907	3.902	4.067
Fe	0.011	0.015	0.006	0.005
Ca	0.000	0.000	0.050	0.000
Na	0.223	3.987	3.533	0.359
K	3.484	0.024	0.045	3.647
Mole proportions.				
Ab	6.01	99.41	97.37	8.95
Or	93.99	0.59	1.24	91.05
An	0.00	0.00	1.39	0.00

APPENDIX C-1: (Cont.d)

SAMPLE NO.	1220087	1220087	7040232		7040237
No Anal.	-1	1	5		2
Type	Plag-core	Plag-Rim	Plag		Plag
Major oxide (weight percent).			$\bar{x}$	$\bar{s}$	
SiO_2	66.05	67.94	70.59	0.74	66.87
Al_2O_3	22.39	20.72	19.64	0.33	20.21
FeO_t	0.01	0.03	0.04	0.03	0.03
CaO	2.30	0.48	0.39	0.29	0.07
Na_2O	10.68	11.80	12.54	0.46	11.62
K_2O	0.28	0.18	0.18	0.10	0.32
TOTAL	101.81	101.36	103.52	0.59	99.87
No. of cations on the basis of 32 oxygens.					
Si	11.443	11.776	11.974		11.775
Al	4.574	4.235	3.928		4.196
Fe	0.001	0.004	0.006		0.004
Ca	0.427	0.089	0.071		0.132
Na	3.588	3.996	4.125		3.968
K	0.062	0.040	0.039		0.072
Mole proportions.					
Ab	88.01	96.85	97.41		95.11
Or	1.52	0.97	0.92		1.72
An	10.47	2.18	1.67		3.17

APPENDIX C-1: (Cont.d)

SAMPLE NO.	1220257	1220438	1220438	1220438
No Anal.	2	1	1	1
Type	Plag	Orthoclase	Plag-Core	Plag-Rim
Major oxides (weight percent).				
SiO_2	66.71	64.79	65.09	68.98
Al_2O_3	20.64	18.94	22.29	18.87
FeO_t	0.09	0.10	0.18	0.09
CaO	1.47	0.06	2.59	1.53
Na_2O	11.33	1.91	10.19	10.56
K_2O	0.48	13.91	0.80	0.13
TOTAL	100.75	99.88	101.21	100.20
No. of cations on the basis of 32 oxygens.				
Si	11.674	11.919	11.387	12.038
Al	4.259	4.108	4.598	3.883
Fe	0.013	0.015	0.026	0.013
Ca	0.276	0.012	0.486	0.286
Na	3.845	0.681	3.457	3.574
K	0.107	3.265	0.179	0.029
Mole proportions.				
Ab	90.94	17.21	83.88	91.90
Or	2.54	82.49	4.33	0.74
An	6.52	0.30	11.78	7.36

APPENDIX C-1: (Cont.d)

SAMPLE NO.	1220450	1220450	1220464	1220464
No.Anal.	1	1	1	2
Type	Plag-core	Plag-Rim	K-Perthite	Plag
Major oxide (weight percent).				
SiO_2	67.54	71.64	67.41	65.97
Al_2O_3	20.03	18.65	18.51	21.66
FeO_t	0.03	0.08	0.08	0.13
CaO	0.48	0.23	0.07	2.22
Na_2O	11.98	11.33	3.58	10.43
K_2O	0.15	0.18	11.88	0.83
TOTAL	100.50	102.10	101.61	101.40
No. of cations on the basis of 32 oxygens.				
Si	11.826	12.215	12.068	11.512
Al	4.135	3.749	3.907	4.457
Fe	0.004	0.011	0.012	0.019
Ca	0.090	0.042	0.013	0.415
Na	4.068	3.746	1.243	3.529
K	0.034	0.039	2.714	0.185
Mole proportions.				
Ab	97.05	97.88	31.31	85.47
Or	0.80	1.02	68.36	4.48
An	2.15	1.10	0.34	10.05

APPENDIX C-1: (Cont.d)

SAMPLE NO.	1220523	1220523	1220523	1220548
No. Anal.	1	1	1	1
Type	Microcline	Plag-Core	Plag-Rim	Perthite
Major oxide (weight percent).				
SiO_2	66.71	57.76	61.57	66.36
Al_2O_3	17.78	26.04	24.05	19.44
FeO_t	0.03	0.18	0.06	0.07
CaO	0.00	8.96	6.49	0.04
Na_2O	0.24	5.95	8.81	2.52
K_2O	14.96	0.17	0.21	12.99
TOTAL	99.71	99.07	101.23	101.41
No. of cations on the basis of 32 oxygens.				
Si	12.222	10.430	10.864	11.934
Al	3.841	5.544	5.004	4.122
Fe	0.005	0.027	0.009	0.011
Ca	0.000	1.734	1.227	0.008
Na	0.085	2.084	3.015	0.879
K	3.497	0.039	0.047	2.981
Mole proportions.				
Ab	2.38	54.03	70.28	22.72
Or	97.62	1.02	1.10	77.08
An	0.00	44.96	28.61	0.20

APPENDIX C-1: (Cont.d)

SAMPLE NO.	1220548	1220664	1220664	1220664	1220701
No.Anal.	2	1	1	2	2
Type	Plag	K-Perth.	Na-Lamellae	Plag	Microcline
Major oxide (weight percent).					
SiO_2	65.76	66.93	68.41	67.45	65.27
Al_2O_3	22.42	19.23	21.39	21.43	18.86
FeO_t	0.12	0.01	0.00	0.03	0.07
CaO	2.62	0.02	1.25	1.39	0.00
Na_2O	10.30	1.87	11.57	11.15	0.92
K_2O	0.44	14.05	0.48	0.48	15.71
TOTAL	102.02	102.25	103.21	102.06	101.02
No. of cations on the basis of 32 oxygens.					
Si	11.415	11.987	11.674	11.640	11.944
Al	4.589	4.061	4.304	4.360	4.069
Fe	0.017	0.001	0.000	0.004	0.011
Ca	0.487	0.004	0.229	0.257	0.000
Na	3.467	0.649	3.829	3.731	0.326
K	0.097	3.211	0.105	0.106	3.668
Mole proportions.					
Ab	85.57	16.81	92.00	91.14	8.17
Or	2.41	83.09	2.51	2.58	91.83
An	12.03	0.10	5.49	6.28	0.00

APPENDIX C-1: (Cont.d)

SAMPLE NO.	1220701	1220701	1220701	
No.Anal.	1	1	12 Anal-7 Grains	
Type	Plag-Core	Plag-Rim	Plag.	
Major oxide (weight percent).			$\bar{x}$	$\bar{s}$
SiO_2	58.06	59.22	59.63	1.03
Al_2O_3	27.05	26.58	25.35	1.28
FeO_t	0.05	0.09	0.11	0.05
CaO	8.54	7.62	7.53	0.77
Na_2O	7.38	7.82	7.76	0.45
K_2O	0.08	0.07	0.11	0.04
TOTAL	101.30	101.54	100.59	1.41
No. of cations on the basis of 32 oxygens.				
Si	10.301	10.451	10.593	
Al	5.659	5.531	5.334	
Fe	0.007	0.013	0.016	
Ca	1.624	1.441	1.440	
Na	2.539	2.676	2.686	
K	0.018	0.016	0.025	
Mole proportions.				
Ab	60.73	64.75	64.70	
Or	0.43	0.38	0.60	
An	38.84	34.87	34.70	

APPENDIX C-2: Electron microprobe analyses[1] and structural formulae of biotite.

Sample No.	1220015	1220023	1220087	1220089	1220092
No. Anal.	2	2	2	3	2
Major oxides (weight percent).					
SiO_2	37.68	37.48	36.48	36.37	38.21
TiO_2	3.93	3.50	2.25	3.01	3.20
Al_2O_3	11.85	12.19	16.91	16.91	14.02
FeO_T	23.98	23.83	18.94	18.19	18.88
MnO	0.48	0.67	0.82	0.64	0.41
MgO	9.27	9.21	8.64	9.71	11.97
CaO	0.00	0.02	0.00	0.00	0.00
Na_2O	0.07	0.05	0.10	0.09	0.04
K_2O	8.89	8.68	9.42	10.03	8.61
TOTAL	96.18	95.63	93.55	94.98	95.33
No. of cations on basis of 22 oxygens.					
Si	5.826	5.822	5.661	5.560	5.776
Al^{iv}	2.160	2.178	2.339	2.440	2.224
Al^{vi}	-	0.055	0.755	0.608	0.275
Ti	0.457	0.409	0.263	0.346	0.364
Fe	3.101	3.096	2.458	2.326	2.387
Mn	0.063	0.088	0.108	0.083	0.053
Mg	2.136	2.133	1.998	2.212	2.697
Cu	-	0.003	-	-	-
Na	0.021	0.015	0.03	0.027	0.012
K	1.754	1.721	1.865	1.956	1.661
X_{ANN}	0.59	0.59	0.55	0.51	0.47

1 Mean ($\bar{x}$) and standard deviation ($\bar{s}$) are given for samples with more than three analyses.

2 Partially chloritized - best total selected for presentation.

APPENDIX C-2: (Cont.d)

Sample No.	1220099	1220138[2]	1220165	1220178
No. Anal.	1	1	2	2
Major oxides (weight percent).				
SiO_2	37.66	33.38	39.18	37.45
TiO_2	2.46	2.43	2.77	2.77
Al_2O_3	14.59	14.47	12.77	16.50
FeO_T	19.24	20.28	17.68	18.09
MnO	0.45	0.45	0.83	0.63
MgO	12.23	12.47	13.29	10.05
CaO	0.01	0.08	0.00	0.08
Na_2O	0.02	0.12	0.13	0.09
K_2O	9.70	7.00	9.13	8.43
TOTAL	96.44	90.75	95.79	94.01
No. of cations on basis of 22 oxygens.				
Si	5.682	5.372	5.889	5.704
Al^{iv}	2.318	2.628	2.111	2.296
Al^{vi}	0.278	0.118	0.152	0.667
Ti	0.279	0.294	0.313	0.317
Fe	2.428	2.730	2.223	2.304
Mn	0.058	0.061	0.106	0.081
Mg	2.750	2.992	2.978	2.281
Cu	0.002	0.014	-	0.013
Na	0.006	0.037	0.038	0.027
K	1.867	1.438	1.751	1.638
X_{ANN}	0.47	0.48	0.43	0.50

2 Partially chloritized.

APPENDIX C-2: (Cont.d)

SAMPLE NO.	7040231		7040237		1220257(2)	1220266
No. Anal.	4		5		1	3
	Major oxides (weight percent).					
	$\bar{x}$	$\bar{s}$	$\bar{x}$	$\bar{s}$		
SiO_2	39.36	1.21	37.55	0.96	32.33	37.05
TiO_2	1.50	0.32	1.82	0.02	1.20	3.38
Al_2O_3	19.92	0.26	18.53	0.17	16.63	11.60
FeO_T	20.32	1.77	24.00	0.61	31.69	27.35
MnO	1.29	0.09	1.52	0.06	1.58	0.69
MgO	0.82	0.04	1.24	0.24	2.82	7.38
CaO	0.00	0.01	0.02	0.01	0.05	0.05
Na_2O	0.17	0.08	0.18	0.05	0.12	0.12
K_2O	8.76	0.18	8.29	0.17	5.84	8.00
TOTAL	92.36	0.61	93.18	0.28	92.26	95.67
	No. of cations on basis of 22 oxygens.					
Si	6.127		5.929		5.396	5.845
Al^{iv}	1.873		2.071		2.604	2.155
Al^{vi}	[illegible]783		1.379		0.668	0.003
Ti	0.176		0.216		0.151	0.401
Fe	2.646		3.170		4.424	3.609
Mn	0.170		0.203		0.223	0.092
Mg	0.190		0.292		0.701	1.735
Ca	-		0.003		0.009	0.008
Na	0.051		0.055		0.039	0.037
K	1.740		1.670		1.244	1.615
X_{ANN}	0.93		0.92		0.86	0.68

2 Partially chloritized.

APPENDIX C-2: (Cont.d)

SAMPLE NO.	1220288	1220331	1220353		1220363
No. Anal.	3	2	9		2
Major oxides (weight percent).					
			$\bar{x}$	$\bar{s}$	
SiO_2	37.02	36.93	37.16	0.97	36.88
TiO_2	3.88	2.17	3.59	0.15	3.56
Al_2O_3	11.80	16.36	13.16	0.38	12.96
FeO_T	25.11	25.30	19.30	0.35	27.01
MnO	0.66	1.10	0.56	0.10	0.81
MgO	8.79	3.23	12.13	0.30	6.06
CaO	0.01	0.01	0.03	0.02	0.00
Na_2O	0.15	0.12	0.10	0.04	0.16
K_2O	8.20	8.44	8.03	0.48	9.46
TOTAL	95.63	93.68	94.06		96.93
No. of cations on basis of 22 oxygens.					
Si	5.784	5.905	5.717		5.772
Al^{iv}	2.174	2.095	2.283		2.228
Al^{vi}	-	0.989	0.105		0.163
Ti	0.456	0.261	0.415		0.419
Fe	3.282	3.384	2.484		3.536
Mn	0.087	0.130	0.073		0.107
Mg	2.047	0.770	2.782		1.414
Ca	0.002	0.002	0.005		-
Na	0.045	0.037	0.030		0.049
K	1.635	1.722	1.576		1.889
X_{ANN}	0.62	0.81	0.47		0.71

APPENDIX C-2: (Cont.d)

SAMPLE NO.	1220397	1220429	1220438	1220443	1220450
No Anal.	2	3	2	3	2
Major oxides (weight percent).					
SiO_2	38.79	38.89	38.36	36.81	38.18
TiO_2	3.89	3.38	3.82	3.24	2.25
Al_2O_3	11.59	11.67	12.18	12.28	15.01
FeO_T	22.28	22.46	20.22	25.34	24.81
MnO	0.71	0.80	0.69	0.72	1.27
MgO	9.42	10.40	10.16	8.26	4.70
CaO	0.00	0.00	0.05	0.00	0.01
Na_2O	0.27	0.08	0.11	0.18	0.18
K_2O	9.06	8.08	8.79	8.12	8.87
TOTAL	96.02	95.76	94.74	95.00	95.46
No. of cations on basis of 22 oxygens.					
Si	5.957	5.954	5.925	5.796	5.946
Al^{iv}	2.043	2.046	2.075	2.204	2.054
Al^{vi}	0.056	0.06	0.143	0.077	0.702
Ti	0.449	0.389	0.444	0.384	0.264
Fe	2.862	2.876	2.612	3.338	3.232
Mn	0.092	0.104	0.090	0.096	0.168
Mg	2.156	2.373	2.339	1.939	1.137
Ca	-	-	0.008	-	0.002
Na	0.08	0.024	0.033	0.055	0.054
K	1.775	1.578	1.732	1.632	1.763
X_{ANN}	0.57	0.55	0.53	0.63	0.74

APPENDIX C-2: (Cont.d)

SAMPLE NO.	1220456	1220464	1220506	1220523	
No. Anal.	1	2	3	4	
Major oxides (weight percent).				$\bar{x}$	$\bar{s}$
SiO_2	40.42	37.35	37.86	36.88	0.65
TiO_2	3.31	3.64	3.94	3.55	0.51
Al_2O_3	11.71	11.62	12.82	13.80	0.31
FeO_T	22.59	30.05	19.20	19.50	0.53
MnO	0.72	0.53	0.77	0.66	0.07
MgO	10.22	4.73	11.21	11.22	0.24
CaO	0.00	0.04	0.02	0.02	0.03
Na_2O	0.07	0.08	0.13	0.15	0.10
K_2O	8.30	8.01	8.36	8.06	0.52
TOTAL	97.34	96.05	94.31	93.89	1.04
No. of cations on basis of 22 oxygens.					
Si	5.803	5.929	5.816	5.696	
Al^{iv}	1.982	2.071	2.184	2.304	
Al^{vi}	0.000	0.104	0.137	0.209	
Ti	0.357	0.435	0.455	0.412	
Fe	2.441	3.990	2.467	2.519	
Mn	0.088	0.071	0.100	0.086	
Mg	2.187	1.119	2.567	2.583	
Ca	0.000	0.007	0.003	0.003	
Na	0.019	0.025	0.039	0.045	
K	1.520	1.622	1.639	1.588	
X_{ANN}	0.53	0.78	0.49	0.49	

APPENDIX C-2: (Cont.d)

SAMPLE NO.	1220542	1220548	1220557	1220560	1220603
No. Anal.	1	2	1	1	1
Major oxides (weight percent).					
SiO_2	38.19	38.13	36.29	37.48	35.53
TiO_2	3.21	2.54	3.63	3.45	0.00
Al_2O_3	12.47	12.37	12.96	12.04	19.35
FeO_T	24.36	24.05	28.11	23.03	25.26
MnO	0.75	0.88	0.72	0.77	1.09
MgO	8.46	8.18	5.21	9.27	0.66
CaO	0.00	0.00	0.00	0.00	0.05
Na_2O	0.14	0.17	0.01	0.33	0.25
K_2O	8.75	8.07	7.93	8.45	6.77
TOTAL	96.33	94.38	94.86	94.82	88.96
No. of cations on basis of 22 oxygens.					
Si	5.611	5.978	5.463	5.585	5.880
Al^{iv}	2.160	2.022	2.300	2.116	2.120
Al^{vi}	0.000	0.265	0.000	0.000	1.656
Ti	0.355	0.300	0.411	0.387	-
Fe	2.694	3.154	3.185	2.583	3.497
Mn	0.093	0.117	0.092	0.097	0.153
Mg	1.853	1.912	1.169	2.059	0.163
Ca	0.000	-	0.000	0.000	0.009
Na	0.040	0.052	0.003	0.095	0.080
K	1.640	1.614	1.523	1.607	1.430
X_{ANN}	0.59	0.62	0.73	0.56	0.96

APPENDIX C-2: (Cont.d)

SAMPLE NO.	1220604	1220664	1220694	1220697	1220701	
No. Anal.	1	2	2	1	8	
Major oxides (weight percent).					$\bar{x}$	$\bar{s}$
SiO_2	33.82	35.66	36.05	36.66	37.13	0.59
TiO_2	2.79	2.69	2.62	3.81	3.12	0.30
Al_2O_3	11.63	15.54	13.27	12.88	14.16	0.41
FeO_T	29.75	30.32	26.07	18.84	19.40	0.52
MnO	1.16	1.00	0.77	0.48	0.37	0.08
MgO	4.30	1.79	5.72	11.56	11.48	0.38
CaO	0.12	0.01	0.02	0.05	0.01	0.01
Na_2O	0.04	0.17	0.16	0.07	0.06	0.03
K_2O	6.14	8.23	8.29	8.45	8.67	0.20
TOTAL	89.79	95.40	95.40	92.84	94.51	
No. of cations on basis of 22 oxygens.						
Si	5.777	5.720	5.832	5.729	5.711	
Al^{iv}	2.223	2.280	2.168	2.271	2.289	
Al^{vi}	0.119	0.659	0.363	0.102	0.279	
Ti	0.358	0.325	0.319	0.448	0.361	
Fe	4.250	4.068	3.528	2.462	2.462	
Mn	0.168	0.136	0.106	0.064	0.048	
Mg	1.095	0.428	1.379	2.693	2.632	
Ca	0.022	0.002	0.003	0.008	0.002	
Na	0.013	0.053	0.050	0.021	0.018	
K	1.338	1.684	1.711	1.685	1.702	
X_{ANN}	0.80	0.90	0.72	0.48	0.49	

APPENDIX C-2: (Cont.d)

SAMPLE NO.	1220716	1220732
No. Anal.	2	1
Major oxides (weight percent).		
SiO_2	40.43	36.96
TiO_2	1.39	2.44
Al_2O_3	19.39	15.85
FeO_T	17.45	24.10
MnO	1.05	1.64
MgO	4.05	4.99
CaO	0.02	0.01
Na_2O	0.26	0.23
K_2O	8.12	8.32
TOTAL	92.26	94.54
No. of cations on basis of 22 oxygens.		
Si	6.166	5.801
Al^{iv}	1.834	2.199
Al^{vi}	1.652	0.734
Ti	0.159	0.288
Fe	2.226	3.164
Mn	0.136	0.218
Mg	0.921	1.167
Ca	0.003	0.002
Na	0.077	0.070
K	1.580	1.666
X_{ANN}	0.71	0.73

APPENDIX C-3: Electron microprobe analyses and structural formula of chlorite.

SAMPLE NO.	1220087	1220138	1220257	1220268	1220286
No. Anal.	1	1	1	1	2
Major oxides (weight percent).					
SiO_2	26.80	29.62	23.15	28.25	27.13
TiO_2	0.06	0.06	0.04	0.16	0.71
Al_2O_3	19.44	16.67	20.75	16.78	16.79
Fe_T	25.09	24.31	41.69	30.18	34.87
MnO	0.87	0.59	2.61	0.55	0.84
MgO	13.52	16.97	0.68	9.32	5.90
CaO	0.00	0.02	0.00	0.09	0.10
Na_2O	0.01	0.00	0.00	0.06	0.03
K_2O	0.00	0.00	0.00	0.37	0.15
TOTAL	85.79	87.25	88.92	85.79	86.51
No. of cations on the basis of 28 oxygens.					
Si	5.465	6.226	5.350	6.256	6.129
Al^{iv}	4.674	3.884	4.831	3.925	4.052
Al^{vi}	-	0.000	0.822	0.455	0.420
Ti	0.008	0.008	0.006	0.026	0.120
Fe	3.851	4.274	8.058	5.589	6.588
Mn	0.150	0.105	0.511	0.103	0.160
Mg	4.109	5.317	0.234	3.076	1.586
Ca	-	0.005	-	0.021	0.024
Na	0.004	-	-	0.025	0.012
K	-	-	-	0.104	0.043
X_{fe}	0.48	0.45	0.97	0.65	0.77

APPENDIX C-3: (Cont.d)

SAMPLE NO.	1220331	1220438	1220456	1220560	1220571
No. Anal.	2	1	1	1	1
Major oxides (weight percent).					
SiO_2	26.14	27.83	32.80	27.45	26.43
TiO_2	0.37	0.00	0.32	0.04	0.34
Al_2O_3	19.30	16.73	16.97	21.15	17.50
Fe_T	34.65	25.45	26.75	30.48	39.64
MnO	1.41	0.71	0.86	0.80	0.29
MgO	2.88	15.54	15.18	10.33	4.53
CaO	0.11	0.15	0.18	0.04	0.00
Na_2O	0.08	0.13	0.00	0.00	0.01
K_2O	0.79	0.13	0.04	0.04	0.11
TOTAL	85.74	86.45	92.92	90.33	88.85
No. of cations on the basis of 28 oxygens.					
Si	5.992	5.964	6.128	5.377	5.435
Al^{iv}	4.189	4.217	3.738	4.804	4.243
Al^{vi}	1.027	0.008	0.000	0.081	0.000
Ti	0.063	-	0.044	0.006	0.052
Fe	6.643	4.561	3.762	4.493	6.135
Mn	0.273	0.128	0.136	0.132	0.051
Mg	0.983	4.963	4.226	3.016	1.388
Ca	0.026	0.034	0.035	0.008	-
Na	0.035	0.053	-	-	0.004
K	0.231	0.035	-	0.010	0.029
X_{fe}	0.87	0.48	0.47	0.60	0.81

APPENDIX C-3: (Cont.d)

SAMPLE NO.	1220603	1220604	1220697
No. Anal.	1	2	2
Major oxides (weight percent).			
SiO_2	26.05	24.22	26.05
TiO_2	0.01	0.06	0.02
Al_2O_3	17.23	18.39	19.11
Fe_T	40.94	39.13	23.80
MnO	0.49	0.93	0.75
MgO	1.10	5.08	17.00
CaO	0.07	0.02	0.04
Na_2O	0.18	0.01	0.02
K_2O	0.23	0.01	0.02
TOTAL	86.34	87.88	87.70
No. of cations on the basis of 28 oxygens.			
Si	6.113	5.549	5.528
Al^{iv}	4.069	4.632	4.653
Al^{vi}	0.698	0.336	0.129
Ti	0.002	0.010	0.004
Fe	8.035	7.498	4.225
Mn	0.098	0.180	0.134
Mg	0.384	1.734	5.378
Ca	0.017	0.005	0.008
Na	0.081	0.004	0.007
K	0.068	0.003	0.005
X_{fe}	0.95	0.81	0.44

APPENDIX C-4: Electron microprobe analyses and structural formula of hornblende from the Ackley Granite.

SAMPLE NO.	1220015	1220092	1220099	1220-138-1	1220-138-2
No. Anal.	2	2	3	1	2
Major oxides (weight percent).					
SiO_2	45.21	46.57	45.43	45.96	51.23
TiO_2	1.32	0.96	1.43	1.39	0.18
Al_2O_3	7.09	7.54	8.03	8.00	4.11
FeO_T	21.84	16.35	16.61	16.71	14.57
MnO	1.08	0.55	0.69	0.71	0.06
MgO	8.09	11.90	11.23	11.30	14.45
CaO	10.43	11.66	11.19	10.86	12.18
Na_2O	1.75	1.09	1.28	1.45	0.56
K_2O	0.97	0.74	0.94	0.85	0.30
TOTAL	97.81	97.36	97.02	97.24	98.33
No. of cations on the basis of 23 oxygens.					
Si	6.947	6.963	6.865	6.901	7.478
Al^{iv}	1.053	1.037	1.135	1.099	0.522
Al^{vi}	0.232	0.293	0.296	0.307	0.186
Ti	0.153	0.108	0.163	0.157	0.020
Fe	2.807	2.045	2.099	2.099	1.779
Mn	0.141	0.070	0.088	0.090	0.007
Mg	1.853	2.652	2.529	2.529	3.144
Ca	1.718	1.868	1.812	1.747	1.905
Na	0.521	0.316	0.375	0.422	0.159
K	0.190	0.141	0.164	0.167	0.056
X_{fe}	0.60	0.44	0.45	0.45	0.36

APPENDIX C-4: (Cont.d)

SAMPLE NO.	1220464	1220678	1220701
No. Anal.	3		1
Major oxides (weight percent).			
SiO_2	43.74	46.00	46.39
TiO_2	1.17	1.32	0.89
Al_2O_3	7.11	7.89	8.30
FeO_T	28.00	16.02	17.67
MnO	1.34	0.55	0.57
MgO	4.31	11.58	10.84
CaO	10.09	11.25	9.79
Na_2O	2.14	1.06	0.99
K_2O	0.98	0.92	0.95
TOTAL	98.89	95.76	96.47
No. of cations on the basis of 23 oxygens.			
Si	6.876	6.721	7.007
Al^{iv}	1.124	1.279	0.993
Al^{vi}	0.194	0.080	0.485
Ti	0.138	0.145	0.101
Fe	3.682	1.762	2.232
Mn	0.178	0.068	0.073
Mg	1.010	2.522	2.440
Ca	1.700	1.761	1.585
Na	0.652	0.300	0.290
K	0.197	0.172	0.183
X_{fe}	0.79	0.41	0.48

APPENDIX C-5: Electron microprobe analyses and structural fromulae of 'muscovite-sericite'.

SAMPLE NO.	7040024[1]	1220087	1220089	7040214[2]	7040232[1]
No. Anal.	2	1	1	1	2
Major oxides (weight percent).					
SiO_2	45.62	48.53	45.69	46.91	47.21
TiO_2	0.56	0.89	1.25	0.06	0.37
Al_2O_3	20.56	31.97	30.49	32.41	25.65
FeO_T	9.30	3.83	3.75	3.24	6.66
MnO	0.46	0.00	0.04	0.06	0.28
MgO	4.67	1.05	0.82	0.12	2.13
CaO	0.01	0.00	0.00	0.00	0.00
Na_2O	0.29	0.45	0.43	0.21	0.20
K_2O	9.46	7.83	9.98	9.04	9.67
TOTAL	91.05	94.55	92.45	92.07	92.18
No. of cations on the basis of 22 oxygens.					
Si	6.694	6.421	6.349	6.414	6.671
Al^{iv}	1.306	1.579	1.653	1.556	1.329
Al^{vi}	2.251	3.409	3.342	3.694	2.945
Ti	0.062	0.089	0.131	0.006	0.039
Fe	1.141	0.381	0.436	0.372	0.787
Mn	0.057	0.001	0.005	0.007	0.034
Mg	1.021	0.207	0.170	0.025	0.449
Ca	0.002	0.000	-	-	-
Na	0.083	0.155	0.116	0.056	0.055
K	1.771	1.322	1.769	1.585	1.744
X_{fe}	0.53	0.65	0.72	0.94	0.64

[1] Granite samples in close proximity (<200 m) to mineralization.
[2] Greisen.

APPENDIX C-5: (Cont.d)

SAMPLE NO.	7040285A[2]	7040289[2]	1220178	1220331	1220332
No. Anal.	1	1	1	2	1
Major oxides (weight percent).					
SiO_2	49.49	47.70	48.26	49.38	48.19
TiO_2	0.18	0.09	0.50	0.16	0.21
Al_2O_3	24.85	30.32	29.65	25.50	25.47
FeO_T	4.10	4.13	5.17	6.66	7.07
MnO	0.09	0.24	0.03	0.43	0.22
MgO	4.05	0.09	1.52	1.98	2.36
CaO	0.00	0.02	0.01	0.01	0.00
Na_2O	0.08	0.11	0.26	0.12	0.16
K_2O	9.32	9.35	8.54	8.87	9.13
TOTAL	92.16	92.02	93.94	93.12	92.82
No. of cations on the basis of 22 oxygens.					
Si	6.858	6.598	6.492	6.842	6.738
Al^{iv}	1.142	1.402	1.508	1.158	1.262
Al^{vi}	2.918	3.543	3.194	3.007	2.936
Ti	0.019	0.009	0.051	0.017	0.022
Fe	0.475	0.478	0.523	0.772	0.827
Mn	0.011	0.028	0.003	0.050	0.026
Mg	0.836	0.019	0.305	0.409	0.492
Ca	-	0.003	0.001	0.001	-
Na	0.021	0.030	0.068	0.032	0.043
K	1.648	1.650	1.466	1.568	1.629
X_{fe}	0.36	0.96	0.63	0.65	0.63

[2] Greisen.

APPENDIX C-5: (Cont.d)

SAMPLE NO.	1220363	1220697	1220716	1220732
No. Anal.	1	2	1	1
Major oxides (weight percent).				
SiO_2	46.47	45.57	42.65	46.86
TiO_2	0.11	0.14	1.21	0.24
Al_2O_3	26.69	25.58	21.97	26.69
FeO_T	6.35	5.05	12.20	6.57
MnO	0.01	0.00	0.63	0.25
MgO	1.38	2.08	3.49	1.28
CaO	0.00	0.00	0.03	0.00
Na_2O	0.25	0.18	0.30	0.20
K_2O	9.80	9.37	9.35	8.58
TOTAL	91.16	93.01	91.84	90.71
No. of cations on the basis of 22 oxygens.				
Si	6.630	6.679	6.331	6.669
Al^{iv}	1.370	1.321	1.669	1.331
Al^{vi}	3.119	3.099	2.176	3.147
Ti	0.012	0.015	0.135	0.026
Fe	0.758	0.619	1.515	0.782
Mn	0.001	-	0.079	0.030
Mg	0.293	0.454	0.772	0.272
Ca	-	-	0.005	0.000
Na	0.069	0.051	0.086	0.055
K	1.784	1.752	1.771	1.558
X_{fe}	0.72	0.58	0.66	0.74

Microfiche on following page (420) cannot be reproduced.

Unreproduced microfiche entitled:

Appendix III, Report 83-6

Field, majors, trace and norms.

Page 420: la microfiche ne peut être reproduite.

L'en-tête de cette microfiche est:

Appendix III, Report 83-6

Field, majors, trace and norms.

APPENDIX D

MAJOR AND TRACE ELEMENT ANALYSES

APPENDIX D-1: Major and trace element composition of granites in the study area. Reproduced from Dickson (1983).

APPENDIX D-2: Major and trace element composition of samples of fine to medium grained, equigranular, weakly porphyritic granite in the Sage Pond area. All samples preceded by Department of Mines and Energy code 7040.

Sample No.	114	116	117	119	175
Oxide (wt.%)					
SiO_2	77.2	77.3	77.2	77.7	81.0
Al_2O_3	11.70	11.65	11.15	12.15	9.10
Fe_2O_3	.27	.52	.30	.91	.08
FeO	.54	.60	.51	.43	.38
MgO	.06	.10	.07	.03	.05
CaO	.07	.12	.06	.03	.10
Na_2O	2.88	2.76	3.24	3.99	2.61
K_2O	5.42	5.38	4.72	2.95	3.94
TiO_2	.17	.13	.16	.11	.16
MnO	.03	.04	.02	.08	.03
P_2O_5	.02	.01	.02	.01	.01
LOI	.66	.95	.64	1.00	.68
TOTAL	99.0	99.6	98.1	99.4	98.1
H_2O	.43	.64	.46	.87	.47
S	.03	.03	.02	.04	.00
CO_2	.12	.22	.10	.12	.25
Element (g/t)					
Li	69	78	69	34	52
Be	9	5	8	4	11
F	1568	1511	1284	887	304
V	2	5	5	4	5
Zn	18	32	21	47	18
Ga	22	18	20	24	15
Rb	587	591	504	482	393
Sr	5	7	3	5	11
Y	31	63	54	53	33
Zr	0	0	0	0	0
Nb	69	69	67	107	49
Ag	0.1	.1	.1	.1	.1
Ba	25	57	35	8	52
Pb	16	21	15	9	15
Th	55	56	56	54	49
U	8	9	6	.	5

APPENDIX D-2: (Cont.d)

Sample No.	178	187	207	214	215
Oxide (wt.%)					
SiO_2	76.5	77.5	78.0	75.5	75.1
Al_2O_3	12.20	11.95	11.65	12.45	12.25
Fe_2O_3	.05	.31	.02	.18	.62
FeO	.79	.57	.50	.69	.51
MgO	.06	.08	.02	.04	.03
CaO	.23	.13	.17	.41	.52
Na_2O	3.43	3.45	3.80	3.90	3.72
K_2O	5.51	5.19	3.87	4.94	4.90
TiO_2	.17	.19	.12	.16	.12
MnO	.03	.03	.02	.03	.02
P_2O_5	.02	.01	.08	.02	.02
LOI	.64	.59	.66	.75	.91
TOTAL	99.6	100.0	98.9	99.1	98.7
H_2O	.36	.44	.50	.42	.45
S	.24	.01	.01	.01	.00
CO_2	.14	.12	.09	.09	.07
Element (g/t)					
Li	68	77	23	87	123
Be	9	10	7	15	6
F	1113	348	746	2060	4127
V	5	6	3	5	3
Zn	17	17	15	15	11
Ga	21	19	22	22	24
Rb	553	569	407	666	747
Sr	11	6	4	3	4
Y	61	66	49	111	145
Zr	0	0	0	0	0
Nb	77	79	81	95	99
Ag	.10	.20	.10	.10	.10
Ba	20	32	33	0	2
Pb	33	19	36	23	7
Th	82	69	36	92	88
U	9	9	14	13	8

APPENDIX D-2: (Cont.d)

Sample No.	231	232	237	238	248
Oxide (wt.%)					
SiO_2	76.3	74.4	74.5	76.7	78.0
Al_2O_3	12.85	12.50	12.25	12.30	11.60
Fe_2O_3	.84	.21	.13	.71	.42
FeO	.00	.53	.72	.00	.51
MgO	.03	.03	.03	.03	.08
CaO	.14	.54	.42	.23	.20
Na_2O	4.02	3.83	3.99	3.98	3.44
K_2O	5.09	5.19	4.99	4.75	4.82
TiO_2	.14	.15	.11	.14	.20
MnO	.05	.03	.03	.04	.04
P_2O_5	.01	.03	.02	.01	.03
LOI	.69	.89	.55	.53	.53
TOTAL	100.2	98.3	97.7	99.4	99.8
H_2O	.35	.44	.31	.44	.46
S	.00	.00	.01	.01	.01
CO_2	.11	.03	.10	.08	.07
Element (g/t)					
Li	225	109	134	44	35
Be	8	8	9	5	12
F	2171	4335	3004	1653	950
V	3	7	3	4	7
Zn	16	16	16	19	29
Ga	24	23	19	24	20
Rb	794	740	680	622	490
Sr	4	12	4	5	16
Y	49	55	101	53	69
Zr	0	0	0	0	0
Nb	94	107	89	89	51
Ag	.10	.10	.10	.10	.10
Ba	0	26	0	0	64
Pb	18	17	23	45	21
Th	72	79	84	88	55
U	12	5	19	10	5

APPENDIX D-2: (Cont'd)

Sample No.	249	281	282	283	284
Oxide (wt.%)					
SiO_2	77.7	75.5	76.7	75.9	76.3
Al_2O_3	11.90	12.10	11.85	12.05	11.50
Fe_2O_3	.64	1.25	.99	.90	.18
FeO	.53	.00	.00	.00	.65
MgO	.10	.07	.08	.06	.07
CaO	.21	.41	.49	.30	.49
Na_2O	3.28	3.23	3.16	3.18	3.54
K_2O	4.99	5.25	5.58	5.39	4.76
TiO_2	.21	.20	.20	.19	.19
MnO	.03	.02	.02	.02	.03
P_2O_5	.03	.02	.02	.03	.02
LOI	.66	1.22	.79	1.09	.77
TOTAL	100.3	99.3	99.9	99.1	98.5
H_2O	.56	.	.43	.61	.39
S	.01	.00	.07	.52	.03
CO_2	.06	.00	.04	.05	.11
Element (g/t)					
Li	50	86	88	114	101
Be	11	34	7	10	15
F	1454	3838	4231	3338	3893
V	8	5	5	4	4
Zn	22	18	17	19	17
Ga	18	23	20	23	20
Rb	505	614	647	624	558
Sr	17	7	8	9	9
Y	89	97	86	95	109
Zr	0	0	0	0	0
Nb	58	70	67	72	63
Ag	.10	.10	.10	.10	.10
Ba	88	43	38	70	25
Pb	23	14	11	9	13
Th	59	77	71	68	88
U	9	22	8	14	17

APPENDIX D-2: (Cont.d)

Sample No.	292	294
Oxide (wt.%)		
SiO_2	76.2	76.3
Al_2O_3	11.95	11.75
Fe_2O_3	.03	.04
FeO	.88	.80
MgO	.07	.08
CaO	.55	.56
Na_2O	3.40	3.60
K_2O	5.00	4.98
TiO_2	.21	.20
MnO	.02	.02
P_2O_5	.03	.02
LOI	.94	.88
TOTAL	99.3	99.2
H_2O	.49	.45
S	.10	.08
CO_2	.06	.10
Element (g/t)		
Li	111	95
Be	33	27
F	5064	4752
V	5	7
Zn	13	18
Ga	21	19
Rb	66	569
Sr	8	9
Y	139	112
Zr	0	0
Nb	72	78
Ag	.10	.10
Ba	26	16
Pb	10	13

APPENDIX E

CORRELATION COEFFICIENTS

Appendix E-1: Table of Spearman non-parametric correlation coefficients (x 100) for oxides and elements of samples from the Rencontre Lake Granite (N = 46). Correlation coefficients at less than the 90% confidence level are omitted.

	SiO_2	Al_2O_3	Fe_2O_3	FeO	MgO	CaO	Na_2O	K_2O	TiO_2	MnO
SiO_2										
Al_2O_3	-81									
Fe_2O_3	-42	46								
FeO	-70	71								
MgO	-68	77	46	63						
CaO	-75	88	43	79	82					
Na_2O	-62	77	31	71	45	73				
K_2O	-45	59	29	28	57	48	.			
TiO_2	-75	84	53	67	94	85	52	61		
MnO	-72	70	60	48	79	68	51	36	83	
P_2O_5	-68	79	44	61	82	79	53	59	83	76
LOI	.	.	.	.	20	.	.	.	.	23
Li	.	.	.	23	.	.	34	32	.	.
Be	.	-22	.	-22	-34	-28	.	-40	-37	.
F	-45	34	.	62	34	41	37	.	38	35
V	-56	49	27	57	51	56	41	34	51	40
Zn	-51	36	41	37	39	50	22	23	44	53
Ga	.	.	.	.	.	.	36	27	.	.
Rb	55	-60	-40	-60	-66	-67	-39	-49	-73	-48
Sr	-70	73	39	58	78	79	39	64	82	68
Y	.	.	-20	.	.	.	.	-48	-19	.
Zr	-74	72	30	79	65	84	60	39	74	56
Nb	43	-45	-25	-26	-57	-41	.	-47	-57	-36
Mo	-25	27	.	29	.	22	.	23	27	.
Sn	30	-40	.	-27	-53	-45	.	-40	-50	-40
Ba	-70	71	35	60	76	78	41	60	81	62
Pb	39	-35	.	45	-40	-41	-33	.	-40	-25
Th	52	-53	-31	-42	-63	-53	-22	-60	-63	-39
U	57	-67	-39	-57	68	63	-42	61	68	45

Appendix E-1: (Cont.d)

	MnO	P_2O_5	LOI	Li	Be	F	V	Zn	Ga	Rb	Sr
P_2O_5		LOI									
LOI	.		Li								
Li	.			Be							
Be	-32		23		F						
F	32		31	.		V					
V	54		.	.	42		Zn				
Zn	43		.	.	22	.		Ga			
Ga	.		31	.	45	.	.		Rb		
Rb	-54		.	54	-36	-55	-38	.		Sr	
Sr	77		.	-35	39	72	55	.	-76		
Y	.		22	.	.	-25	.	21	29	31	
Zr	70		.	-25	47	68	58	.	70	83	
Nb	-34		.	36	-26	-37	.	.	72	-60	
Mo	.		.	.	.	.	.	.	-23	22	
Sn	-54	27	.	34	.	-42	.	.	35	-54	
Ba	74	.	.	-35	38	71	56	.	-74	97	
Pb	-31	.	.	25	-34	-49	.	.	69	-47	
Th	-50	.	.	44	-25	-59	-34	.	78	-73	
U	-61	.	25	49	.	-49	-21	.	64	-63	

Appendix E-1: (Cont.d)

Sr	Y								
Y		Zr							
Zr	.		Nb						
Nb	44	-35		Mo					
Mo	.	32	.		Sn				
Sn	.	-36	37	.		Ba			
Ba	-25	86	-56	25	-52		Pb		
Pb	.	-53	60	.	41	-48	-41	Th	
Th	47	-55	79	.	50	-74	-41		U
U	33	-54	50	-19	53	-64	43	79	

Appendix E-2: Table of Spearman non-parametric correlation coefficients (x 100) for oxides and elements of samples from the Hungry Grove and Sage Pond granites (N = 96). Coefficients at less than the 90% confidence level are omitted for clarity.

	SiO_2	Al_2O_3	Fe_2O_3	FeO	MgO	CaO	Na_2O	K_2O	TiO_2	MnO
SiO_2										
Al_2O_3	-78									
Fe_2O_3	-37	22								
FeO	-51	56	-25							
MgO	-69	67	20	69						
CaO	-62	68	.	72	78					
Na_2O	-34	57	17	19	.	28				
K_2O	-26	27	.	.	15	.	-23			
TiO_2	-72	62	27	64	89	73	.	20		
MnO	-52	62	.	67	62	65	30	.	63	
P_2O_5	-68	67	24	64	80	75	18	.	82	62
LOI	-30	27	17	20	25	18	19	.	15	20
Li	16	.	-20	.	-15	.	.	-18	-25	15
Be	22	-28	.	-34	-38	-31	.	-17	-36	.
F	.	.	.	.	.	14	13	14	.	.
V	-44	41	35	22	40	35	20	.	39	26
Zn	-22	34	16	25	22	26	41	-17	.	34
Ga	18	.	.	.	-15	-16	29	-31	-28	.
Rb	47	-42	-32	-38	-49	-48	.	-14	-53	-18
Sr	-57	45	38	33	62	48	.	.	60	26
Y	34	-33	-24	.	-38	-32	.	-22	-37	.
Zr	-42	34	36	23	37	33	15	.	35	24
Nb	41	-38	-26	-24	-44	-42	.	-18	-47	.
Mo	.	.	.	.	.	.	.		.	.
Sn	20	.	-22	.	-20	-13	17		-31	.
Ba	-54	42	40	29	58	43	.		53	24
Pb	47	-33	-37	-16	-37	-34	.		-47	-16
Th	44	-42	-26	-41	-50	-46	.		-51	-25
U	55	-46	.	-45	-52	-44	.	-18	56	-28

Appendix E-2: (Cont.d)

MnO	P_2O_5										
P_2O_5		LOI									
LOI	.		Li								
Li	-23	.		Be							
Be	-32	20	41		F						
F		16	31	31		V					
V	41	18	16	30	20		Zn				
Zn	22	23	.	-13	.	53		Ga			
Ga	-21	.	38	24	24	.	27		Rb		
Rb	-53	.	54	63	31	47	22	39		Sr	
Sr	62	.	36	-46	-30	70	42	-37	-70		Y
Y	42	.	37	39	37	34	.	43	53	-51	
Zr	38	14	.	19	.	58	43	.	-38	64	-15
Nb	-50	.	39	45	35	44	.	47	71	-62	65
Mo	.	.	.	.	14	.	.	.	.	.	.
Sn	-26	.	24	32	13	-18	.	29	28	-31	.
Ba	57	14	-28	-40	-20	69	46	-23	-60	95	-45
Pb	-45	.	39	36	14	-44	.	38	50	-49	35
Th	-56	.	37	43	31	-48	-25	38	50	-50	35
U	-62	.	39	62	39	-50	-17	32	73	-67	56

Appendix E-2: (Cont.d)

Y	Zr							
Zr		Nb						
Nb			Mo					
Mo				Sn				
Sn	-16	28			Ba			
Ba	66	-52		-27		Pb		
Pb	-42	47		36	-41		Th	
Th	-42	47		36	-41	39		U
U	-21	66		15	-64	40	72	

Appendix E-3: Table of Spearman non-parametric correlation coefficients (x 100) for oxides and elements (including REEs) of samples from the Hungry Grove, Sage Pond, Tolt, Meta, and Southwest Mount Sylvester Granites (N = 11 for most correlations; N = 9 for correlations with W). Correlations at less than the 90% confidence level are omitted for clarity.

Sample Numbers = 220187, 220332, 220377, 220416, 220462, 220468, 220501, 220502, 220664, 220707, 220720, 220721

	SiO_2	Al_2O_3	Fe_2O_3	FeO	MgO	CaO	Na_2O	K_2O	TiO_2	MnO
SiO_2										
Al_2O_3	-89									
Fe_2O_3	-80	74								
FeO	.	.	.							
MgO	-44	.	52	70						
CaO	.	.	.	79	82					
Na_2O	-60	77	43	.	.	.				
K_2O	.	.	.	-62	-57	-55	.			
TiO_2	.	.	.	85	84	82	.	-72		
MnO	-53	59	.	52	58	.	44	-60	75	
P_2O_5	-80	69	61	56	74	60	.	-46	63	56
LOI	.	.	.	.	47	.	.	.	45	.
H_2O^+	-72	70	73	56	79	55	44	-60	63	61
S	.	.	.	.	.	.	51	-57	.	.
CO_2	.	.	.	.	.	.	.	.	.	.
Li	43	-73	.	.	.	.	-73	.	.	-46
Be	.	.	.	-49	.	.	.	.	-45	-43
F	50	-61	.	.	.	.	-53	.	.	-71
V	-61	54	52	82	86	85	.	-59	85	60
Zn	.	.	.	47	.	.	52	-69	56	68
Ga	.	.	.	-53	-83	-59	46	.	-61	.
Rb	.	.	.	-85	-86	-83	.	75	-94	-76
Sr	-76	75	60	58	79	61	.	-62	74	77
Y	.	.	.	-77	-87	-75	.	47	-80	-62
Zr	-82	68	69	.	.	.	48	.	.	.
Nb	.	.	.	-59	-75	-61	.	82	-78	-75
Mo	.	.	.	.	.	.	.	.	.	.
Sn	.	.	.	-81	-65	-67	.	77	-82	-71
Ba	-44	.	.	73	95	77	.	-71	91	69
Rb	45	.	.	-61	-72	-51	.	61	-66	-61
La	.	.	.	.	.	.	.	-61	.	.
Ce	.	.	.	.	.	-64	.	.	.	.
Nd	67	-55	.	.	.	.	.	.	.	.
Sm	.	.	.	-74	-63	-76	.	.	-67	.
Eu	.	.	.	57	81	61	.	-71	81	64
Tb	.	.	.	-73	-82	-75	.	56	-73	-64
Ho	.	.	.	-81	-86	-78	.	81	-90	-72
Yb	.	.	.	-78	-84	-73	.	63	-87	-74
Lu	.	.	.	-76	-86	-74	.	61	-86	-72
As	-71	89	.	.	.	.	77	.	.	.
Co	-87	95	87	79	92	81	.	-69	93	81
Cs	43	-56	.	.	.	.	.	.	.	-51

Appendix E-3: (Cont'd)

	SiO_2	Al_2O_3	Fe_2O_3	FeO	MgO	CaO	Na_2O	K_2O	TiO_2	MnO
Hf	.	.	.	.	.	.	41	47	-42	.
Sb	.	.	.	.	.	.	45	.	.	.
Sc	-75	53	49	61	70	63	.	.	76	56
Ta	.	.	.	-77	-69	-70	.	66	-77	-63
Th	.	.	.	-79	-77	-69	.	55	-84	-74
U	.	.	.	-81	-72	-50	.	60	-78	-76
W	.	-54	.	.	.	.	-70	.	.	-67

Appendix E-3: (Cont.d)

	MnO	P_2O_5	LOI	H_2O^+	S	CO_2	Li	Be	F	V	Zn
P_2O_5											
LOI	.										
H_2O^+	82	44									
S	.	.	.								
CO_2	51	.	.	-43							
Li	.	.	.	.	.						
Be	.	.	.	.	.	.					
F	.	.	.	.	.	72	.				
V	84	42	86	.	.	.	.	.			
Zn	.	.	57	.	.	.	-46	.	49		
Ga	-60	.	-49	.	-57	.	.	.	-60	.	
Rb	-66	.	-69	.	.	.	59	.	-84	-59	
Sr	94	.	88	.	.	.	.	-49	86	45	
Y	-65	.	-58	.	.	.	-51	.	-77	.	
Zr	54	.	54	.	.	.	45	.	54	.	
Nb	-60	.	-64	-46	.	.	44	.	-66	-60	
Mo	.	58	.	.	.	.	.	59	.	.	
Sn	-70	.	-63	-48	.	.	.	.	-80	-54	
Ba	76	42	77	.	.	.	.	.	86	49	
Pb	-84	.	-61	.	-58	.	.	.	65	.	
La	.	45	.	.	.	.	.	.	.	51	
Ce	.	.	.	.	.	.	.	.	.	.	
Nd	-67	.	.	.	.	.	.	.	-58	.	
Sm	-44	.	.	.	.	.	67	.	-57	.	
Eu	62	49	66	.	.	.	.	.	68	.	
Tb	-66	.	-44	.	.	.	50	.	-67	.	
Ho	-67	.	-85	.	.	.	76	.	-86	-81	
Yb	-65	.	-59	.	.	.	54	.	-77	-45	
Lu	-67	.	-60	.	.	.	52	.	-76	-42	
As	64	.	.	68	.	.	.	-65	.	.	
Co	76	.	71	.	59	52	.	-52	83	.	
Cs	.	.	.	.	.	76	46	55	.	.	
Hf	.	.	.	.	.	.	.	.	.	.	
Sb	.	.	.	54	.	.	.	.	.	.	
Sc	77	47	66	.	42	.	.	.	82	.	
Ta	-56	.	-53	.	.	.	54	.	-72	-47	
Th	-55	.	-49	.	.	.	66	.	-70	-49	
U	51	.	-66	.	.	.	42	.	-71	-60	
W	.	.	.	.	.	61	.	83	.	.	

Appendix E-3: (Cont.d)

Zn	Ga										
Ga		Rb									
Rb	64		Sr								
Sr	-58	-79		Y							
Y	89	87	-71		Zr						
Zr	.	.	42	.		Nb					
Nb	66	83	77	78	.		Mo				
Mo	.	.	.	.	.	.		Sn			
Sn	53	82	-79	75	.	85	59		Ba		
Ba	-80	-88	83	-86	.	-88	.	-81		Pb	
Pb	71	73	-81	72	.	70	57	71	-77		La
La	.	.	.	.	.	.	.	.	.	.	
Ce	.	.	.	.	.	.	.	.	.	.	.
Nd	.	.	-62	.	.	.	.	.	.	.	.
Sm	70	76	-48	86	.	62	.	67	62	60	.
Eu	67	74	72	64	.	82	.	-72	90	-71	.
Tb	89	81	-68	95	.	87	.	71	-85	81	.
Ho	67	98	-83	90	.	96	.	89	-93	74	.
Yb	82	91	77	96	.	89	.	87	-90	76	.
Lu	85	91	77	97	.	89	.	84	-91	77	.
As	.	.	66	.	77	.	.	.	.	.	.
Co	-60	-95	81	-70	76	-66	.	-59	79	-66	.
Cs	.	.	-46	.	.	.	.	.	.	.	.
Hf	63	43	.	58	60	75	61	62	-56	-55	.
Sb	.	.	.	.	.	.	.	.	.	.	.
Sc	45	-62	71	-54	72	.	.	-56	71	-57	.
Ta	69	83	-69	87	.	89	45	92	-81	65	.
Th	78	89	-66	96	.	81	.	80	-82	69	.
U	67	80	-64	80	.	74	.	77	79	62	.
W	.	.	.	.	.	.	.	.	.	.	.

Appendix E-3: (Cont.d)

La	Ce										
Ce		Nd									
Nd	65		Sm								
Sm	.	.		Eu							
Eu	.	58	.		Tb						
Tb	.	.	93	-81		Mo					
Ho	.	50	88	-75	96		Yb				
Yb	.	.	83	-59	92	99		Lu			
Lu	.	.	81	-67	94	95	99		As		
As	.	.	.	.	.	.	.	.		Co	
Co	.	.	.	79	-61	.	-66	-67	.		Cs
Cs	.	67	.	.	.	.	.	.	.	-57	
Hf	.	.	50	-59	76	68	62	64	.	.	.
Sb	.	.	.	.	.	.	.	.	.	.	.
Sc	.	-60	.	60	-44	-60	-50	-56	.	88	.
Ta	.	.	84	-46	-60	-50	-56	90	.	-52	.
Th	.	.	71	-69	90	93	83	86	.	-69	46
U	.	.	43	-76	76	78	68	69	.	-62	.
W	.	.	.	.	.	.	.	.	-89	.	.

Appendix E-3: (Cont.d)

Cs	Hf						
Hf		Sb					
Sb	.		Sc				
Sc	.	.		Ta			
Ta	62	.	.		Th		
Th	59	.	-58	72		U	
U	.	.	-58	57	.	86	W
W	.	.	.	.	.	.	

APPENDIX F

INNA ANALYSES AND XRF - REE ANALYSES

Trace element and rare earth element data. W - INAA from Whalen (1983), X-XRF data, I - INAA data.

Sample No.	6	7	14	98	120
Source	W	X	X	W	X
Sc	2.60	.	.	2.10	.
Co	.	.	.	.	.
As	.	.	.	.	.
Sb	.	.	.	.	.
Cs	3.80	.	.	3.50	.
La	29	9.53	21.97	19	11.28
Ce	38	25.42	44.14	35	29.13
Pr	.	3.41	3.08	.	4.15
Nd	8.00	13.81	12.64	12.00	14.82
Sm	2.50	3.14	2.39	2.80	3.89
Eu	.30	.91	.74	.19	.13
Gd	1.70	3.40	2.00	3.20	4.39
Tb	.	.52	.34	.	.76
Dy	.	3.38	1.34	.	5.13
Ho	.90	.71	.	1.40	.80
Er	.	1.97	1.02	.	3.94
Yb	3.10	1.75	1.56	5.00	4.94
Lu	.54	.51	.	.89	.
Hf	3.70	.	.	6.20	.
Ta	5.30	.	.	6.40	.
W	.	.	.	.	.
Th	40.00	.	.	69.00	.
U	26.00	.	.	20.00	.
Rock type/ Location	Aplite Ackley City	Pegm. Ackley City	Peg. Ackley City	Aplite Ackley City	Gran. Crow Cliff

APPENDIX F: (Cont.d)

Sample No.	156	462	468	220061	220081
Source	W	W	W	I	I
Sc	4.40	4.20	1.50	5.40	7.81
Co	.	.	.	22.53	66.12
As	.	.	.	2.58	.
Sb	.	.	.	.42	.70
Cs	6.90	5.50	6.60	15.40	10.60
La	49	42	69	36.5	28.5
Ce	91	107	133	.	63.5
Pr	.	.	.	.	.
Nd	40.00	42.00	48.00	.	26.90
Sm	8.10	9.00	9.70	5.43	5.50
Eu	1.06	1.08	.70	.82	1.25
Gd	7.30	7.40	7.00	.	.
Tb	.	.	.	.61	.74
Dy	.	.	.	.	.
Ho	1.80	1.80	1.90	.	1.04
Er	.	.	.	.	.
Yb	5.20	6.50	6.10	2.17	2.50
Lu	.82	1.00	.93	.33	.36
Hf	6.10	5.70	4.90	4.42	4.01
Ta	4.50	3.60	2.90	2.63	1.11
W	.	.	.	.	.
Th	27.20	25.00	40.00	19.20	19.80
U	5.40	3.10	5.60	5.05	5.09
Rock type/ Location	Gran. Rencon. Lake	Tolt Gran.	Hungry G.Gran.	Molly. Plut.	Molly. Plut.

APPENDIX F: (Cont.d)

Sample No.	220094	220187	220332	220354	220377
Source	I	I	I	I	I
Sc	4.29	4.25	2.93	7.91	2.24
Co	2.61	2.56	.45	6.85	.82
As	2.01	.	.	.	.29
Sb	.34	1.20	.33	.61	.16
Cs	10.70	3.46	8.24	6.15	4.72
La	24.1	42	53.7	37.3	25.3
Ce	.	97	103.2	82.6	.
Pr	.	.	.	.	.
Nd	.	37.60	45.90	38.30	.
Sm	3.14	6.03	9.75	7.27	4.40
Eu	.43	.69	.44	1.37	.44
Gd	.	.	.	.	.
Tb	.44	.91	1.96	1.00	.84
Dy	.	.	.	.	.
Ho	.	.91	3.27	1.02	.
Er	.	.	.	.	.
Yb	1.59	2.43	12.90	2.91	5.20
Lu	.24	.36	2.05	.45	.80
Hf	3.17	5.78	6.59	4.86	4.25
Ta	1.82	1.36	5.05	1.03	2.64
W	1.66	.	5.74	1.74	2.23
Th	13.20	23.30	64.10	22.50	28.30
U	5.78	3.35	10.10	4.16	5.66
Rock type/ Location	Kep. Gran.	Meta Gran.	Sage P. Gran.	Kos. Gran.	Tolt Gran.

APPENDIX F: (Cont.d)

Sample No.	220416	220501	220502	220523	220604
Source	I	I	I	I	I
Sc	5.39	4.13	3.75	10.80	1.99
Co	3.16	2.36	2.17	8.90	.97
As	.62	.66	.	.	.
Sb	.17	.32	.55	1.00	.53
Cs	5.81	8.06	5.87	13.00	3.27
La	62.2	36.6	54.8	49.30	31.1
Ce	134.6	.	101.9	137.30	78.0
Pr	.	.	.	.	.
Nd	46.50	.	39.20	56.50	36.30
Sm	7.82	5.38	6.72	12.60	7.21
Eu	.56	.75	.59	1.79	.75
Gd	.	.	.	.	.
Tb	1.13	.75	1.05	1.93	1.09
Dy	.	.	.	.	.
Ho	1.83	.	1.41	2.00	1.56
Er	.	.	.	.	.
Yb	5.61	4.08	5.34	4.72	4.92
Lu	.89	.63	.85	.69	.80
Hf	7.08	5.71	4.89	9.21	5.89
Ta	3.08	1.95	2.18	2.50	1.57
W	1.09	1.29	4.16	.	.73
Th	30.70	28.60	35.00	25.50	20.70
U	4.18	3.28	5.88	4.03	4.43
Rock type/ Location	Tolt Gran.	Mt.Syl. Gran.	Mt.Syl. Gran.	Kos. Gran.	Ren.L. Gran.

APPENDIX F: (Cont.d)

Sample No.	220605	220642	220664	220697	220701
Source	I	I	I	I	I
Sc	3.92	3.63	1.81	11.00	16.70
Co	.80	1.34	.17	9.31	16.00
As	.	.42	.	2.3	1.1
Sb	.43	.15	.97	.27	.10
Cs	4.53	3.33	7.26	4.37	4.80
La	36.3	57.8	47.4	34.70	33.1
Ce	59.7	134.4	121.8	75.30	69.3
Pr	.	.	.	.	.
Nd	21.70	54.30	47.00	35.30	36.80
Sm	3.45	9.55	8.72	6.78	7.34
Eu	.63	.77	.19	1.03	2.48
Gd	.	.	.	.	.
Tb	.61	1.25	1.46	.71	1.01
Dy	.	.	.	.	.
Ho	.86	1.62	1.98	.95	1.13
Er	.	.	.	.	.
Yb	3.00	4.97	6.33	2.48	2.07
Lu	.59	.86	1.05	.33	.30
Hf	3.31	6.19	6.21	6.07	6.00
Ta	1.31	1.44	2.81	1.08	.06
W	.	.	1.26	.57	1.0
Th	24.70	19.10	36.90	11.90	7.60
U	5.44	3.48	4.57	1.75	1.84
Rock type/ Location	Ren. Gran.	Ren.L. Gran.	Hun. G.Gran.	Kos. Plut.	Kos. Plut.

APPENDIX F: (Cont.d)

Sample No.	220707	220720	220721
Source	I	I	I
Sc	.96	2.41	2.00
Co	.56	.	.
As	.39	1.9	.16
Sb	.20	.84	.35
Cs	6.38	5.01	6.84
La	38.7	21.9	71.8
Ce	.	92.5	150.2
Pr	.	.	.
Nd	.	39.50	46.80
Sm	7.03	11.70	9.32
Eu	.22	.01	.32
Gd	.	.	.
Tb	1.37	3.07	1.29
Dy	.	.	.
Ho	.	7.94	2.14
Er	.	.	.
Yb	9.30	28.40	7.00
Lu	1.48	5.15	1.05
Hf	6.76	12.70	6.35
Ta	3.29	15.20	4.75
W	2.83	.61	12.00
Th	62.80	79.30	60.40
U	12.10	31.10	8.51
Rock type/ Location	Hun. G.Gran.	Sage P. Gran.	Sage P. Gran.

APPENDIX F: (Cont.d)

Sample No.	221151	221153	221160	221161	221162
Source	X	X	X	X	X
Sc	.	.	.	.	.
Co	.	.	.	.	.
As	.	.	.	.	.
Sb	.	.	.	.	.
Cs	.	.	.	.	.
La	14.92	40.84	22.03	9.9	18.38
Ce	37.34	97.99	39.87	18.9	36.60
Pr	3.31	9.76	2.13	1.07	3.82
Nd	13.06	33.89	10.20	4.91	13.72
Sm	2.90	7.49	2.26	1.03	2.89
Eu	.34	.72	.55	.28	.82
Gd	3.26	5.89	1.89	1.11	2.82
Tb	.60	.76	.55	.30	.75
Dy	3.36	2.86	1.50	1.07	2.49
Ho	.38	.	.	.18	.50
Er	2.44	1.26	.87	.73	1.79
Yb	3.24	1.66	1.24	1.48	2.99
Lu	.	.	.	.	.
Hf	.	.	.	.	.
Ta	.	.	.	.	.
W	.	.	.	.	.
Th	.	.	.	.	.
U	.	.	.	.	.
Rock type/ Location	Q-T Gres. Turner Pond	Q-T Gres. Anesty Ridge	Bleach-Gran. Wyllie Hill	Bleach-Gran. Wyllie Hill	Gran. Motu

APPENDIX F: (Cont.d)

Sample No.	221163	221165	221170	221171	7040013
Source	X	X	X	X	X
Sc	.	.	.	.	.
Co	.	.	.	.	.
As	.	.	.	.	.
Sb	.	.	.	.	.
Cs	.	.	.	.	.
La	12.31	2.46	52.25	56.85	6.89
Ce	28.94	6.82	128.75	136.17	15.69
Pr	2.46	.52	12.27	12.73	1.45
Nd	9.31	2.55	43.28	43.85	5.47
Sm	1.91	.85	8.77	9.07	1.46
Eu	.29	.23	1.06	1.23	.09
Gd	1.90	.98	7.52	7.89	1.25
Tb	.24	.25	1.41	1.62	.09
Dy	1.89	1.37	4.53	6.81	1.37
Ho	.31	.35	.06	.35	.19
Er	1.58	1.45	2.90	5.07	.79
Yb	2.30	1.57	3.68	6.38	.96
Lu	.	.	.	.	1.10
Hf	.	.	.	.	.
Ta	.	.	.	.	.
W	.	.	.	.	.
Th	.	.	.	.	.
U	.	.	.	.	.
Rock type/ Location	Gran. Turner Pond	Q-T Gres. Anesty	Q-T Gres. Anesty Ridge	Q-T Gres. Anesty Ridge	Q-T Gres. ESSO

APPENDIX F: (Cont.d)

Sample No.	7040022	7040024	7040223	7040229	7040289
Source	X	X	I	I	I
Sc	.	.	1.30	1.80	5.50
Co	.	.	111.60	83.60	1.60
As	.	.	1.10	1.20	6.40
Sb	.	.	.08	.05	.07
Cs	.	.	5.00	.09	9.30
La	19.28	23.51	17.4	1.47	54.1
Ce	50.66	61.48	39.1	2.85	123.3
Pr	5.08	6.26	.	.	.
Nd	18.08	22.95	17.70	1.30	44.30
Sm	3.96	5.59	4.40	.35	8.60
Eu	.46	.72	.26	.06	.11
Gd	3.80	5.74	.	.	.
Tb	.80	1.27	.90	.15	2.43
Dy	4.87	7.21	.	.	.
Ho	.75	1.23	1.63	.25	2.52
Er	3.79	5.26	.	.	.
Yb	4.34	6.51	5.76	1.34	7.55
Lu	.	.	.77	.15	1.03
Hf	.	.	4.70	6.80	7.30
Ta	.	.	13.10	13.70	7.90
W	.	.	1083.00	798.00	1380.00
Th	.	.	16.30	4.80	78.10
U	.	.	4.20	2.90	18.60
Rock type/ Location	Ser. Gres. ESSO	Sage P. Gran. ESSO	Q-T Gres. Anesty Ridge	Q-T Gres. Anesty	Q-T Gres. ESSO

APPENDIX G: Fluid Inclusion Data. FI - Fluid inclusion. Vis. Melt - temperature of first visible melt (eutectic); Tm - liquidus temperature; ThV - temperature of homogenization to vapour; ThL - temperature of homogenization to liquid; ThS_1, ThS_2, ThS_3 - melting temperatures of solid phases; Decrep. - temperature of decrepitation of fluid inclusion.

Crow Cliff - Dunphy Brook area

Sample No.	Location	Description	FI Type %V	%L	%S	Freezing Vis. Melt	Tm	Heating ThV	ThL	ThS_1	ThS_2	ThS_3	Decrep.
CC 1	Crow Cliff	Quartz from pegmatite	30	70		-19.2	-0.3		338.5				
			20	80		-16	-0.6		352				
			25	75					358.5				
			5	94	1				380	429			429
JT-393	Dunphy Brook	Quartz from pegmatite	20	80		- 4.2	-0.1		298.7				
			80	20				300					
			10	90					278.0				
			30	70					342.1				
			15	85					319.2				
			30	70					373.7				
			25	70					289.5				
			10	90					293.7				
			5	95					176.5				
JT-461	Crow Cliff	Quartz from pegmatite	5	95		-17.2	-0.3		322.4				
						- 6.2			331.0				
EGM 643	Crow Cliff	Quartz from pegmatite	10	20		too small							
EGM 646	Dunphy Brook	Quartz from pegmatite	15	85					309.1				
			20	80					313.0				
			15	85					336.3				
			19	80	1				303.2	240			
			9	90	1				291.0	240			
			20	80					286.9				
			4	95	1	-10.3	-0.8		169.4				
			15	85		-18.5	-2.1		310.1				
			50	50					364.2				
			30	70					288.0				
EGM 628	500m North of Dunphy Brook	Quartz in miarolitic cavities	10	90					398.0				
			10	90					370.0				
			10	90					352.0				
			10	90		-16.0			266.4				
			5	95		-21.9	-0.8		233.5				
			50	50					340.0				
			35	65									400

APPENDIX G:(cont'd)

Dunphy Brook - Wyllie Hill - Motu - Ackley City

Sample No.	Location	Description	FI Type %V %L %S	Freezing		Heating					
				Vis. Melt	Tm	ThV	ThL	ThS_1	ThS_2	ThS_3	Decrep.
EGN 628	500m North of Dunphy Brook	Miarolitic quartz in aplite	5 95				307.3				
			15 85				348.3				
			15 85				358.5				
			40 60			378.8					
			25 75			365.0					
			15 85				369.6				
			15 85				302.0				
			10 90			387.9					
EGN 626	Wyllie Hill	Quartz vein		too small							
JT 378	Wyllie Hill	Quartz eyes in microgran.		too small							
JT 378A	Wyllie Hill	Altered granite		too small							
JT 380	200 m North of Wyllie Hill	Quartz vein		too small							
JT 336	Motu	Granite north of showing	25 75				293.9				
			5 95				120.0				
			40 60				362.0				
			2 98				130.0				
			5 95				122.8				
			5 95				142.0				
			50 50				355.1				
EGN 631	Ackley City	Quartz in fine gr. gran.		too small							
EGN 632.	Ackley City	Quartz in pegmatite		too small							
EGN 640	Ackley City	Quartz in musc. greisen		too small							
JT 349	Ackley City	" " " "		too small							
JT 351	Ackley City	Quartz in quartz-calcite vein	10 90				356.1				
			20 80	-13.4	- 4.5		371.2				390
			75 25								
			10 90				321.8				

APPENDIX G:(cont'd)

Ackley City

Sample No.	Location	Description	FI Type %V %L %S	Freezing Vis. Melt	Freezing Tm	Heating ThV	Heating ThL	Heating ThS_1	Heating ThS_2	Heating ThS_3	Decrep.
JT 351	Ackley City	Quartz-calcite vein	30 70				346.8				396
			20 70								
			10 90				246				390
			60 40								
JT 352	Ackley City	Quartz vein, Mo blebs		too small							
JT 354	Ackley City	Quartz in pegmatite with aplitic margin	20 80	-10.9	- 0.1		lost				
			25 75	-20.8	- 5.4		350.0,3				
			30 70				375.4				
			20 80				377.8				
JT 360	Ackley City	Quartz with Mo in vugs		too small							
JT 361	Ackley City	Quartz in pegmatite		too small							
JT 362	Ackley City	Quartz in vugs		too small							
JT 369	Ackley City 200 m North	Quartz vein	30 60	- 6.0	- 3.0		306.0				
			30 70			405.0					
			30 70				387.6				
			20 80			410.0					
			50 50			385.0					
			40 60			395.0					
			15 85				215.4				
JT 370	Ackley City 200 m NW	Quartz vein		too small							
JT 371A	Ackley City 250 m NW	Quartz vein	10 90		1.4		184.7				
			50 50				366.2				
			20 80				394.1				
			30 70				373.5				

APPENDIX G:(cont'd)

Big Blue Hill Pond area - Franke Pond - Long Harbour area

Sample No.	Location	Description	FI Type %V %L %S	Freezing		Heating					
				Vis. Melt	Tm	ThV	ThL	ThS_1	ThS_2	ThS_3	Decrep.
JT - 329	SE end Big Blue Hill Pond	Beryl in quartz-beryl pod	2 98	- 6.6	0.6		176.2				
			1 99	-20.4	- 0,0		144.2				
			2 98				210.0				
			70 30				375.2				
			40 60				350.0				
			50 50				361.5				
			40 60				343.2				
			10 90				226.2				
			55 45				373.6				
			55 45				371.5				
		quartz strained									
JT - 352	Franke Pond	Quartz in pegmatite	1 99	-66.1	-29.6		84.2				
			1 99	-41	-23.9		89.2				
			1 99	-58	-24.6		89.7				
			1 99				88.8				
			3 97				112.7				
			3 97				131.1				
			30 70				264.2				
			25 75				245.0				
JT - 373	Franke Pond	Quartz vein with Mo		too small							
LHC - 3	Long Harbour area	Miarolitic quartz	20 80				322.2				
			20 80				374.7				
			20 80								380
122251	Long Harbour area			too small							
122252	Long Harbour area	Miarolitic quartz	40 60	-55.7	-13.6		350				
			5 95				348				
			10 90				290				
			30 70				359				
			15 85				383				
			25 75				382				
			20 80			394					
			45 55				401				

APPENDIX G:(cont'd)

Long Harbour area - Esso Core/Trenches

Sample No.	Location	Description	FI Type %V %L %S	Freezing		Heating					
				Vis. Melt	Tm	ThV	ThL	ThS_1	ThS_2	ThS_3	Decrep.
122286	Long Harbour area	Microlitic quartz	10 90	-10	-6.1		327.7				
			10 90	- 7	-3.8		248.0				
122370	Long Harbour area	" "	5 95	-30.8	-4.8		74				280
			10 90								240
			10 90	-14.7	-1.2		340.5				
			15 85				368.0				
			5 95				360.5				
			5 95	-26.0	-3.2		175				
122450	Long Harbour area	" "	5 95	-13.2	-6.2		151.9				
			5 95	-27.6	-4.8		173.2				
			5 95	-15.4	-3.7		209.2				
112643	Long Harbour area	" "	5 95				243.3				
			5 95				273.0				
			5 75 20				182.8				
112719	Long Harbour area	" "	25 75				354.6				
			10 90				217.3				
JT - 12	DDH AG-3 at 35.3 feet	Quartz in greisen	2 94 4	-50	-34.9		107	115			
			10 80 10	-49.5	-34.3		244.8	101			438.7
			1 90 5				97.2	210			
			15 60 25	-30	-23.6		365	7400			400
			5 94 1				264	7430			430
			20 80	-26	-22.6		348.7				
JT - 13	DDH AG-3 at 29.0 feet	" " "	5 90 5				551	261.2			
			5 90 5				551	380			
			5 95				486.4				
			5 95				551				
			1 79 20					350			491
			50 50								385
			2 96 2	-44.8	-27.1						
			2 98	-60	-4.8						
			10 80 10				600	128.8	336.8		
			30 70				430.4	343			

APPENDIX G:(cont'd)

Esso Core/Trenches (cont'd)

Sample No.	Location	Description	FI Type XV XL XS	Freezing Vis. Melt	Freezing Tm	Heating ThV	Heating ThL	Heating ThS_1	Heating ThS_2	Heating ThS_3	Decrep.
			50 50				517.7				
			2 98	-26.2	- 8.3						380.6
			1 99	-28	- 6.6		66.5				
			1 77 22				166.7	344.9			
			80 20								285.5
JT - 14	DDH AG-3 at 17.0 feet	Quartz in Greisen	20 20 60				282	360			458
			10 30 60				215.2	155	359		450
			5 85 10				198	238			
			10 40 50				366	181	370		390
			10 90				233				330
			80 20					450			
			5 60 35				153.3	156.8	347.4	376.1	500
			15 85								460
			55 45			350					
JT - 15	DDH AG-3 at 36.0 feet	" " "		too small							
JT - 16	DDH AG-3 at 30.0 feet	" " "		too small							
											390
JT - 17	DDH AG-3 at 45.5 feet	" " "	5 95	-25.1	-14.8		297.8				437
			5 95				290				
			2 90 8				150.6	277.1			
			50 50			464					
			30 70				411.9				
			5 95	-10.8	- 3.1		197.5				
			5 95				221.6				
			5 80 15				402.0				500
			75 25			490					
			60 40			500					
JT - 22	DDH AG-5 at 25.5 feet	" " "		too small							
JT - 23	DDH AG-5 at 50.0 feet	Quartz in sericitic gres.	10 30 60				269	190	438		
JT - 25	DDH AG-5 at 57.0 feet	Quartz in kaolin-greisen		too small							
JT - 26	DDH AG-5 at 200.0 feet	Quartz vein in granite		too small							

APPENDIX G:(cont'd)

Esso Cores/Trenches - Aneaty Greisen

Sample No.	Location	Description	FI Type %V %L %S	Freezing Vis. Melt	Freezing Tm	Heating ThV	Heating ThL	Heating ThS_1	Heating ThS_2	Heating ThS_3	Decrep.
JT - 156	Trench 25	Quartz in greisen	5 95	-14.5	0.3		244.3				
			5 95				355.0				
			5 95				271				
			60 40			445					
			20 80				313.7				
			50 50			420					
			10 80 10	- 9	0		268.6				
			40 60				321.2				
JT - 163	Trench 55	" " "	2 95 3	-32.5	-21.9		84.6	14.4	126.2	373.4	
			2 97 1	-32	-15.8		92				
			49 50 1	-22.2	-11.9			180			490.7
JT - 168	Trench 15	" " "		too small							
JT - 169	Trench 35	" " "	2 98	-10	0.8		153.4				
			5 85 10				224.3	302.5	379		391
			5 90 5				267.5				
			30 70	-17	- 4		424				
			2 83 15				248	333.1			
			2 96 2				177.2	342			
			50 50	-20.2	0.1	435					
221165	Aneaty Main Greisen	Quartz in greisen	15 65 20				297.8	62.6	306.9		476
			10 80 10				291.2	190.8			
			15 70 15				255.8	270.6			
			10 80 10				311.0				
JT - 138	Aneaty Main Greisen	" " "	20 70 10	-40	-22.2		650	404.6	558		
			2 78 20	-46.9	-26		300				490
			20 78 2	-36	-23.2		360				
			10 75 15	-46.7	-32.0		406	270.3			
JT - 226	Aneaty Main Greisen	" " "	15 85	-20	0.2		338.2				
			90 10			316					
			20 80				311.6				
			10 90				315.6				
			10 90				368.2				

APPENDIX G:(cont'd)

Anesty Greisen Cont'd

Sample No.	Location	Description	FI Type %V %L %S	Freezing		Heating					
				Vis. Melt	Tm	ThV	ThL	ThS_1	ThS_2	ThS_3	Decrep.
			40 60			406					
			75 25			382.7					
			60 40			394.3					
			2 98	-30.5	0.0						
			25 75	-28.7	- 3.4		306.9				
			10 90				179.1				
			2 98				274.2				
			2 95 3				212.6	280.5			
			10 40 50				224.1	147.4	282		
			15 55 35				254.5	158.3	315	320	
			10 40 50				220	109.8	313.6		
			10 50 40				232.2	162	318.5		
			5 95	-16.9	0.3		214				
			10 40 50				229.5	129	320		
			10 70 20				222	301			
JT - 229	Anesty Main Greisen	Quartz in greisen		too small							
JT - 224	Anesty Main Greisen	Quartz in sericitic greis.	5 94 1				358.4				
			20 80				397.5				
			10 75 15				326.4	232.9			
			15 70 15				284.8	292.0			
			40 40 20					261.8			460
JT - 224 C	Anesty Main Greisen	" " " "	10 70 20				398.9	175			
			10 70 20				381	100			
			2 96 2	-54.8			95				
			15 85				310				
			20 80				328.4				
			5 95				90				
JT - 204 A	Anesty Main Greisen	Quartz in layered greis.		too small							
JT - 204 B	Anesty Main Greisen	" " " "		too small							
JT - 136	Anesty Main Greisen	Quartz vein with Mo	10 75 15				273.6	96	294.6		
			10 75 15				259.8	122	291.0		
			5 75 15				251.5	312.2	366.4		
			15 85				350				

APPENDIX G:(cont'd)

Sage Pond - General area

Sample No.	Location	Description	FI Type %V %L %S	Freezing Vis. Melt	Freezing Tm	Heating ThV	Heating ThL	Heating ThS_1	Heating ThS_2	Heating ThS_3	Decrep.
221153	West of Sage Pond	Quartz in sericitic gran.	5 80 15				226	201.2	297		
			10 80 10	-54	-27.6		341.5				448
			10 40 50				251.1	143.3	320		
			10 40 50				251.4	157.4	372.5		
			2 75 23				128.4	59	308.5	350.2	458.5
			10 60 30	-26.2	-21		349.6		458.5		458.5
JT - 147	West of Sage Pond	Quartz in greisen		too small							
JT - 224				too small							
JT- 224A				too small							
JT - 245	Anesty Hill	Quartz vein		too small							
JT - 245A	Anesty Hill	Quartz in greisen	1 90 9				76	485			
			2 78 20					348.2			424
JT - 252B	North of Rabbit Pond	Quartz in pegmatite	5 85 10	-35.6	-23.2		200				360
			30 70	-31.9	-21.5						453.7
			75 25	-28.8	-23.7						640
			5 65 30	-21	-19.2						420
			80 10 10								530
JT - 253		Quartz vein	20 80	- 3	- 1.1		365.5				380
			30 60 10	-43	-33.3						550
			25 75	-10.4	- 3.8		387.8				
JT - 118	South of Crow Pond 1+18N	Quartz fluorite vein		too small							
JT - 123A	South of Crow Pond 2+40N	Quartz in greisen	2 8 85	-55.4							224
			9 90 1	-27.4	- 8.2		174.3				
JT - 160	South of Crow Pond 8+60N	" " "	30 70	-25	-15.0		384.9				
			80 20			355					
			75 25			349					
			10 90	-35	-15.6		352.4				
			5 95				338				

APPENDIX G:(cont'd)

Sage Pond area

Sample No.	Location	Description	FI Type %V %L %S	Freezing Vis. Melt	Freezing Tm	Heating ThV	Heating ThL	Heating ThS_1	Heating ThS_2	Heating ThS_3	Decrep.
			10 90				322.9				
			5 95				329.4				
JT - 161	South of Crow Pond 1+80N	Quartz in greisen		too small							
JT - 193				too small							
JT - 195				too small							
JT - 209A	Southeast Sage Pond	" " "	5 90 5	-34.2	- 4.2						399
			5 95	- 9.2	3.3		130.5				
			40 60					285			399
			5 90 5				249.5	110	393.9		
JT - 209D	Southeast Sage Pond	Quartz in pegmatite	2 96 2	-59.4	-38.5		98	105			
			2 94 2				104.8	75	105		
			2 96 2				78	120			
			5 75 20				335.2	340	431.5		
JT - 211	Southeast Sage Pond	Quartz in greisen	30 70	-29	-21.2		347				470
			30 70				319.5				
			5 80 15				238.5	320			